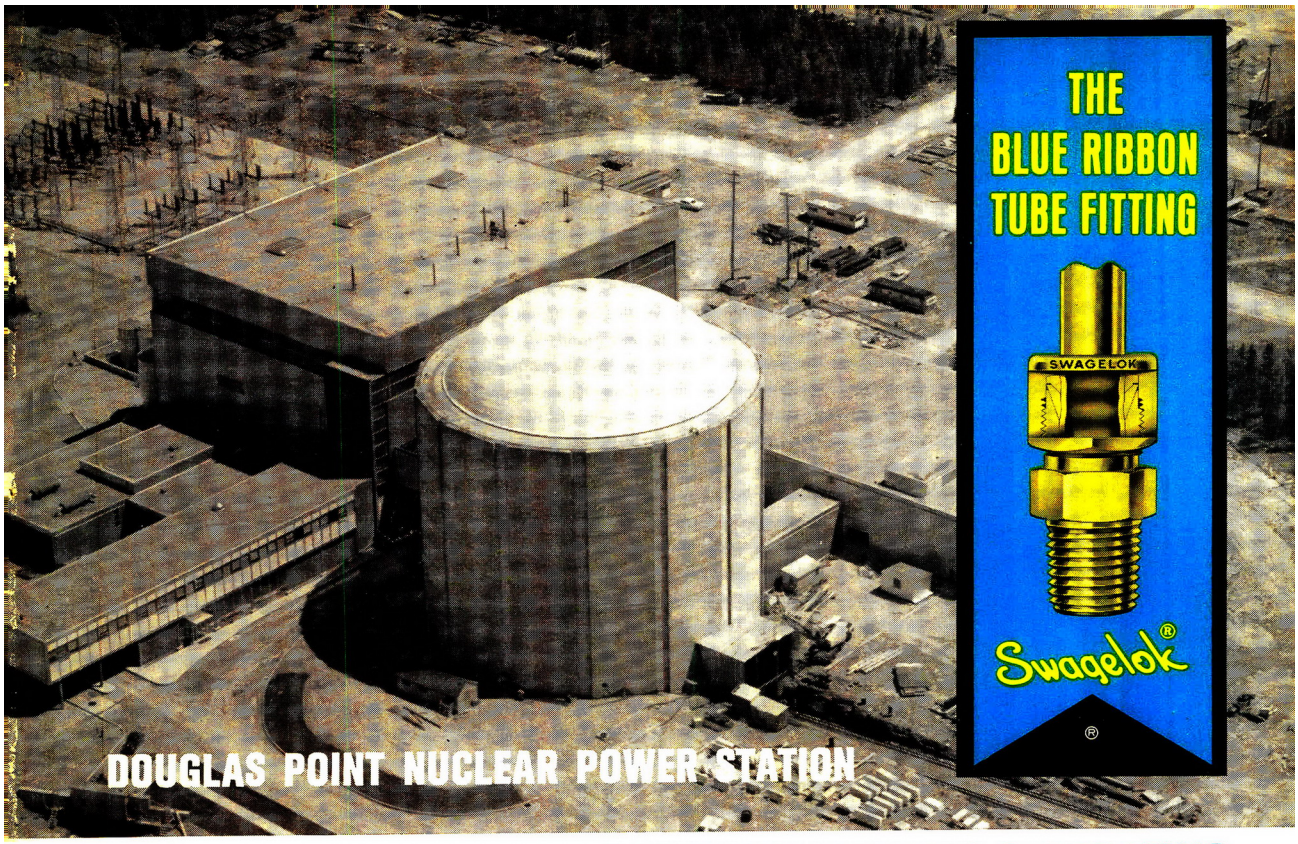

CANADA'S FIRST, FULL SCALE NUCLEAR ELECTRIC GENERATING STATION USES Swagelok® TUBE FITTINGS

Douglas Point is a 200 Mw Nuclear Power Station. It is being constructed by the Canadian Government through its Nuclear Research and Development Agency, Atomic Energy of Canada Limited.

One of the most outstanding features of this power station is that continuous refueling will be conducted while the reactor is on load.

The purpose of on power fueling is to reduce unit energy costs through continuous operation with no down time for refueling. The fueling machines must operate at 585°F. with pressures of 1500 psig. so that trouble free operation with positive performance in all phases is important.

SWAGELOK Tube Fittings are used in fueling machines and instrumentation applications in the Douglas Point Station.

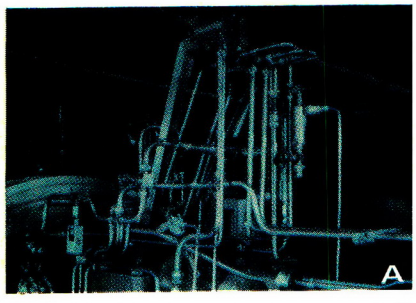

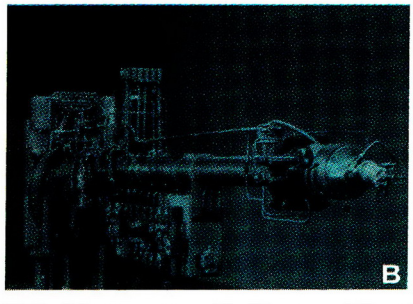

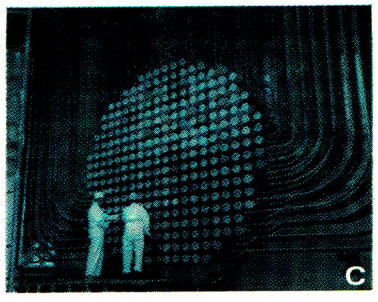

A. *Stainless Steel SWAGELOK Tube Fittings in refueling machine.* **B.** *Fueling machines, operated by remote control, permit on-power refueling.* **C.** *20′ Diameter calandria, main vessel in reactor structure, has 306 ports for loading and unloading fuel.*

© 1966 by Crawford Fitting Company/all rights reserved

CRAWFORD FITTING COMPANY • 29500 SOLON ROAD • SOLON, OHIO 44139
CRAWFORD FITTINGS (CANADA) LTD. • ONTARIO, CANADA.

EM-Reagents are products of E. Merck A.G., Darmstadt, West Germany

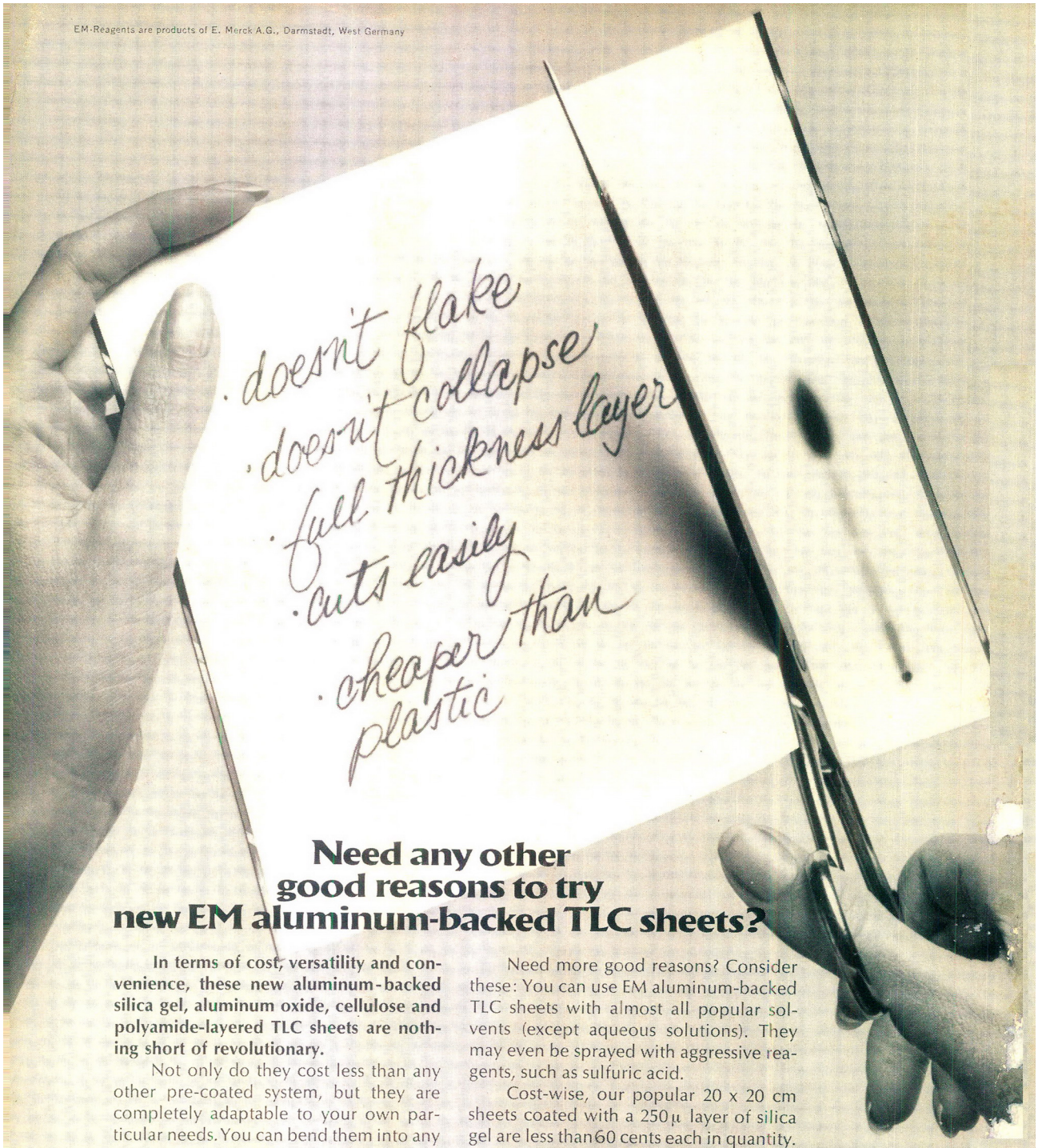

Need any other good reasons to try new EM aluminum-backed TLC sheets?

In terms of cost, versatility and convenience, these new aluminum-backed silica gel, aluminum oxide, cellulose and polyamide-layered TLC sheets are nothing short of revolutionary.

Not only do they cost less than any other pre-coated system, but they are completely adaptable to your own particular needs. You can bend them into any shape you wish, cut them to any size you require, even punch them for easy filing. To develop, just stand them in a tank (they require no special support and will not collapse). These sheets also have a thick, abrasion-resistant layer that will not flake, permitting stacking and compact packaging.

Need more good reasons? Consider these: You can use EM aluminum-backed TLC sheets with almost all popular solvents (except aqueous solutions). They may even be sprayed with aggressive reagents, such as sulfuric acid.

Cost-wise, our popular 20 x 20 cm sheets coated with a 250 μ layer of silica gel are less than 60 cents each in quantity.

Doesn't this sound like the kind of TLC sheet you've always hoped for? If it does, we'd be happy to send you a free sample (and our catalog).

Just write: EM-Reagents Division, Brinkmann Instruments, Cantiague Road, Westbury, N.Y. 11590.

A DIVISION OF
BRINKMANN

JUNE 1969

ANALYTICAL CHEMISTRY



ANALYTICAL CHEMISTRY IN THE MARINE SCIENCES 22A

New...at TRACOR.



Dual Headed Flame Photometric Detector for Simultaneous Three-Way Response! (P,S and normal FID mode)

The Melpar FPD has been further improved with the addition of an optional second photometric channel. A single hydrogen-rich flame is used for simultaneous observation of phosphorus and sulfur emissions plus ionization response with a standard target. Careful calculation of response ratios can assist in the absolute identification of P and S containing compounds. The new detector is based on the dual detector described in Anal. Chem. 40, 1448, (1968) by M.C. Bowman and M. Beroza.

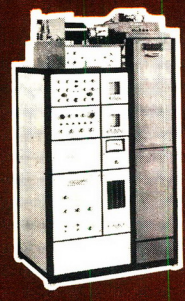

FPD . . . already established for hundreds of analyses:

- PESTICIDES
- PETROLEUM FRACTIONS
- AIR POLLUTION
- NATURAL GAS
- FLAVORS
- PHOSPHOLIPIDS

Now operable at 250°C to bring a new dimension to more analyses.

For most successful operation, the FPD should be used with an all-glass system—such as **"the ultimate chromatograph:"** The MICRO TEK MT220.

For further information, contact TRACOR, Inc., Analytical Instruments, 6500 Tracor Lane, Austin, Texas 78721. Phone: (512) 926-2800

The Detectors Make the Difference... TRACOR®

AA-132

Circle No. 71 on Readers' Service Card

Circle No. 105 on Readers' Service Card →

At $5500, the new L3-40 is the outstanding value in the low and intermediate speed range. It combines the heart of an ultracentrifuge with the acceleration and convenience of a centrifuge. At low speeds, it gobbles up material like bacteria and cells two liters at a time. At top speeds, it generates a wrenching 272,000g of force to spin down viruses and subcellular particles.

The L3-40 has: vacuum and refrigeration systems; super-quiet operation (you literally can't hear it running in the lab); complete operator protection including an ultracentrifuge barrier ring; large rotor chamber to hold the full line of Beckman rotors including the new zonals; and it's convertible to 50,000 rpm should your needs change.

Can you think of anything we've missed? If so, it's probably described in our brochure. For a copy, return the coupon below.

Beckman® INSTRUMENTS, INC.

INTERNATIONAL SUBSIDIARIES: AMSTERDAM; CAPE TOWN; GENEVA; GLENROTHES, SCOTLAND; LONDON; MEXICO CITY; MUNICH; PARIS; STOCKHOLM; TOKYO; VIENNA

New Beckman L3-40. It just obsoleted every centrifuge in the 15,000 to 40,000 rpm range.

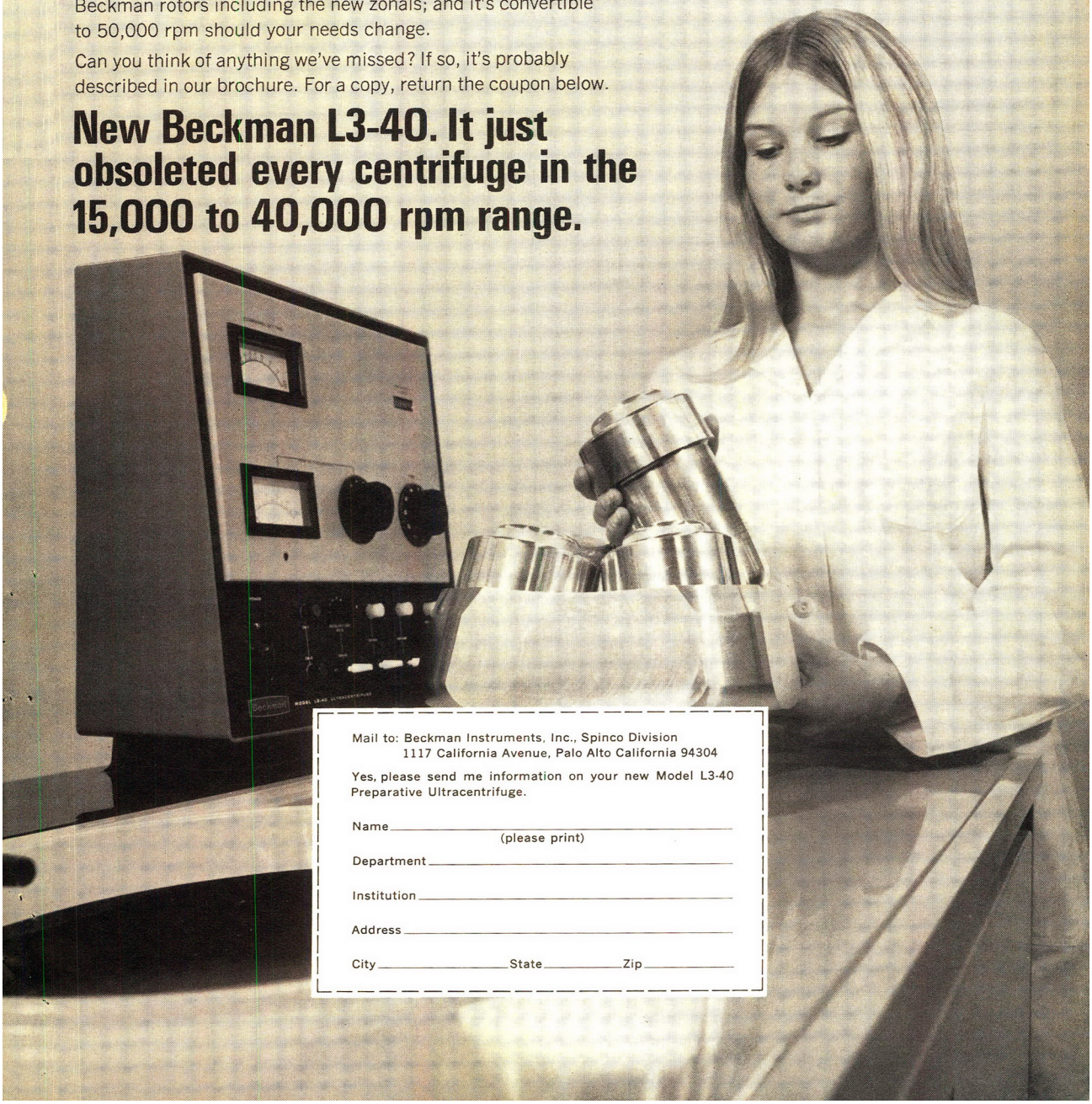

Mail to: Beckman Instruments, Inc., Spinco Division
1117 California Avenue, Palo Alto California 94304

Yes, please send me information on your new Model L3-40 Preparative Ultracentrifuge.

Name _____
(please print)

Department _____

Institution _____

Address _____

City _____ State _____ Zip _____

VOLUME 41, NO. 7 JUNE 1969

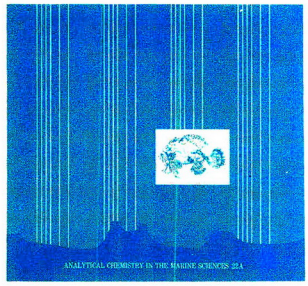

This Month's Cover. Laser devices are used to map the ocean bottom and to plot three-dimensional maps of "clouds" of plankton in water at considerable depth. The role of analytical chemistry and instrumentation in marine science is discussed in the Report for Analytical Chemists, page 22 A.

© Copyright 1969

by the American Chemical Society

MANUSCRIPT REQUIREMENTS published in December 1968 issue, page 2269, outlines scope and copy requirements to be observed in preparing manuscripts for consideration. Manuscript (4 copies) should be submitted to ANALYTICAL CHEMISTRY, 1155 Sixteenth St., N.W., Washington, D. C. 20036.

The American Chemical Society assumes no responsibility for the statements and opinions advanced by contributors to its publications. Views expressed in the editorials are those of the editors and not necessarily represent the official position of the American Chemical Society.

1969 Subscription Rates

	1 yr.	2 yr.	3 yr.
Members, domestic and foreign	$ 4.00	$ 7.00	$10.00
Nonmembers, domestic and Canada	5.00	9.00	12.00
Nonmembers, foreign except Canada	15.00	27.50	40.00

Postage: Canada and Pan-American Union, $2.50; foreign, $3.50. Single copies: current, $2.00 except Annual Reviews and Laboratory Guide issues, $3.00 each. Postage: Canada and Pan-American Union, $0.15; foreign, $0.20. Rates for back issues and volumes are available from Special Issues Sales Dept., 1155 Sixteenth St., N.W., Washington, D. C. Claims for missing numbers will not be allowed if received more than 60 days from date of mailing plus time normally required for postal delivery of journal and claim. No claims allowed because of failure to notify the Subscription Service Department of a change of address or because copy is "missing from files."

Published monthly with Review Issue added in April and a Laboratory Guide in July by the American Chemical Society, from 20th and Northampton Sts., Easton, Pa. 18042; Executive Offices, Editorial Headquarters, and Subscription Service Department, 1155 Sixteenth St., N.W., Washington, D. C. 20036; Advertising Office, 430 Park Ave., New York, N.Y. 10022. ANALYTICAL CHEMISTRY and other ACS periodicals are available on microfilm. For information write to: MICROFILM, Special Issues Sales, American Chemical Society, 1155 Sixteenth St., N.W., Washington, D.C. 20036.

Second class postage paid at Easton Pa.

CHANGE OF ADDRESS: Notify Subscription Service Department, American Chemical Society, 1155 Sixteenth St., N.W., Washington, D. C. 20036. Such notification should include both old and new addresses, with ZIP code numbers, and be accompanied by mailing label from a recent Issue. Allow four weeks for change to become effective.

ANCHAM

ANALYTICAL CHEMISTRY

Contents

REPORT FOR ANALYTICAL CHEMISTS

Robert B. Fischer discusses the special contributions analytical chemistry and instrumentation can make to the exploitation of marine resources **22 A**

NEWS

Professor Ronald Belcher wins the SAC's third Gold Medal; Dr. Velmer Fassel receives the 1969 SSP Award. Scientific meetings are scheduled **49 A**

BOOK REVIEWS

Books on electrochemistry of oxygen, molecular crystals, chemical applications of spectroscopy, and practical chromatography (French) are reviewed by Jaroslav Kuta, J. D. H. Donnay, James D. Winefordner, and E. sz. Kovats and M. Ballenegger, respectively. **67 A**

EDITORS' COLUMN

The health of the analytical instrumentation industry here and abroad is considered on the basis of studies made by the Organization for Economic Cooperation and Development **81 A**

FEATURED LABORATORY

Nalco Chemical Company's research laboratory in Chicago is deeply involved in pollution control and water treatment **84 A**

INSTRUMENTATION

A. Boksenberg, a physicist from University College London, describes a new technique for reading spectral information. The method is illustrated in vacuum ultraviolet spectrometry **87 A**

EDITORIAL

The education of nonscientists in science presents some problems in view of the increased complexity of modern science and the rapid pace of developments **873**

Author Index **6 A**

Briefs **11 A**

Calendar of Events **54 A**

New Chemicals **115 A**

Future Articles **130 A**

Manufacturers' Literature **117 A**

New Products **99 A**

Readers' Information Service **95 A**

Scheduled Technical Courses **52 A**

Evaluating Dispersion in Gel Permeation Chromatography. Axial Dispersion of Polymer Molecules in Packed Beds of Nonporous Glass Beads. *R. N. Kelley and F. W. Billmeyer, Jr.* 874

Versatile Reciprocal Time Computer for Reaction Rate Methods. *S. R. Crouch* 880

Computer-Assisted Gas–Liquid Chromatography. *H. M. Gladney, B. F. Dowden, and J. D. Swalen* 883

Computer Characterization of Chromatographic Peaks by Plate Height and Higher Central Moments. *Eli Grushka, M. N. Myers, P. D. Schettler, and J. C. Giddings* 889

Quantitative Interpretation of Semilogarithmic Gas Chromatographic Data. *R. L. Wade and S. P. Cram* 893

Cyanolysis and Spectrophotometric Estimation of Trithionate in Mixture with Thiosulfate and Tetrathionate. *D. P. Kelly, L. A. Chambers, and P. A. Trudinger* 898

Determination of Piperazine Rings in Ethyleneamines, Poly(Ethyleneamine), and Polyethylenimine by Infrared Spectrometry. *H. L. Spell* 902

Spectrophotometric Studies of Iron(II) Complexes of Pyridyl Benzodiazepin-2-ones. *J. D. Sabatino, O. W. Weber, G. R. Padmanabhan, and B. Z. Senkowski* 905

Coulometric Titration of Microgram Amounts of Americium at the Conducting Glass Electrode. *R. C. Probst* 910

Adsorption of Organic Molecules at a Carbon Paste Electrode. *E. P. Meier and J. Q. Chambers* 914

Optimizing Concentration Determinations in the Presence of Maxima and Catalytic and Kinetic Waves Using the Vibrating Dropping Mercury Electrode. *R. E. Cover and J. G. Connery* 918

Kinetic Waves in Systems Containing Cobalt(II) and Cysteine-Like Compounds. Polarographic Catalytic Hydrogen Waves in Acid Solutions of Mercaptoanilines in Presence of Cobalt(II) or -(III). *I. M. Kolthoff and P. Mader* 924

Kinetic Waves in Systems Containing Cobalt(II) and Cysteine-Like Compounds. Adsorption Phenomena in the Cystamine–Cobalt(II) System in Borax Medium. *P. Mader and I. M. Kolthoff* 932

A Unified Treatment of Electrolysis at an Expanding Mercury Electrode. *K. B. Oldham* 936

Temperature Profiles of Turbulent Hydrogen Diffusion Flames Used in Atomic Fluorescence Spectrometry. *R. Smith, C. M. Stafford, and J. D. Winefordner* 946

Determination of Arsenic by Atomic Absorption Spectrometry with an Electrodeless Discharge Lamp as a Source of Radiation. *Oscar Menis and T. C. Rains* 952

Simultaneous Determination of Trace Elements in Platinum by Isotope Dilution and Spark Source Mass Spectrometry. *Robert Alvarez, P. J. Paulsen, and D. E. Kelleher* 955

Ultra-Trace Determination of Oxygen and Carbon by Charged Particle Activation Analysis. *H. L. Rook and E. A. Schweikert* 958

Notes

Separation and X-Ray Spectrographic Determination of Microgram Quantities of Arsenic in Copper-, Iron-, and Nickel-Base Alloys. *K. E. Burke and M. M. Yanak* 963

An Improved Flux-Fusion Technique for X-Ray Emission Analysis. *D. A. Stephenson* 966

Potentiometric Titrations of Sulfate Using an Ion-Selective Lead Electrode. *J. W. Ross, Jr., and M. S. Frant* 967

Nuclear Magnetic Resonance Analysis of Rubber Vulcanizates. *D. W. Carlson and A. G. Altenau* 969

Determination of Total Paraffins, Monochloroparaffins, and Polychloroparaffins by the Fluorescent Indicator Adsorption Method. *T. A. Washall* 971

ห้องสมุด กรมวิทยาศาสตร์
2 2 ก.ค. 2512

Klett

Photometers

Klett-Summerson Photoelectric Glass Cell Colorimeter

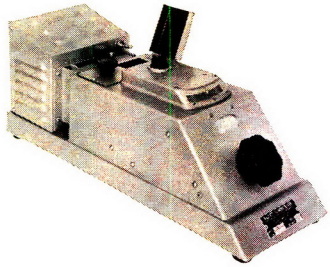

No. 900-3

The Klett Fluorimeter

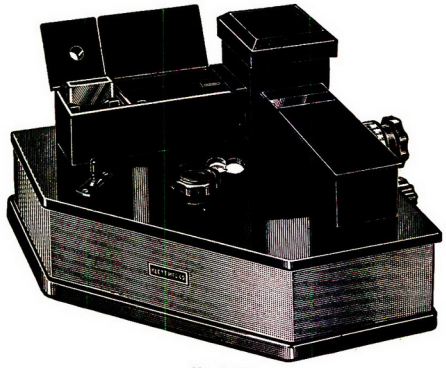

No. 2070

Designed for the rapid and accurate determination of thiamin, riboflavin, and other substances which fluoresce, in solution. The sensitivity and stability are such that it has been found particularly useful in determining very small amounts of these substances.

KLETT SCIENTIFIC PRODUCTS

PHOTOELECTRIC COLORIMETERS • BIO-COLORIMETERS
COLORIMETER-NEPHELOMETERS • COLONY MARKER
• KLETT REAGENTS • GLASS CELLS

Klett Manufacturing Co., Inc.

179 EAST 87TH STREET, NEW YORK, N. Y.

Circle No. 45 on Readers' Service Card

Contributed Articles

Principles and Methods of External Photochemical Titrant Generation. *H. D. Drew and J. M. Fitzgerald* **974**

Determination of Amphetamine and Related Amines in Blood by Gas Chromatography. *R. B. Bruce and W. R. Maynard, Jr.* **977**

Determination of $E_{2}^{\circ} - E_{1}^{\circ}$ for Overlapping Waves in Stationary Electrode Polarography. *R. L. Myers and Irving Shain* **980**

Spectrophotometric Determination of Iron with 2-Pyridyl-2'-Hydroxymethane Sulfonic Acid. *E. E. H. Pitt and V. M. Stanway* **981**

Methods for the Isolation and Characterization of Constituents of Natural Products. A Periodic Acid Column Procedure for the Oxidation of Vic-Glycols, Epoxides, and α-Hydroxy Acids at the Micromole Level. *D. P. Schwartz, J. L. Weihrauch, and L. H. Burgwald* **984**

Correction. Resolution of Overlapping Bands. Functions for Simulating Band Shapes. *R. D. B. Fraser and Eikichi Suzuki* **935**

Correction. Rapid Separation by Carbon Number and Determination of Naphthene and Paraffin Content of Saturate Petroleum Distillates up to 185 °C. *J. V. Brunnock and L. A. Luke* **935**

Correction. An Analyzer for the Dynamic Microdetermination of Carbon, Hydrogen, Nitrogen, Sulfur, and Oxygen. *George Dugan and V. A. Aluise* **935**

Aids for Analytical Chemists

High-Stability Low-Noise Precision Spectrometer Using Optical Feedback. *H. L. Pardue and S. N. Deming* **986**

Electrolytic Dissolution of Tantalum, Niobium, and Other Refractory Metals. *A. Aladjem* **989**

Dielectric Percentage Saturation Detector. *E. J. Gelb and S. N. Steen* **990**

An Improved Procedure for Solid Scintillation Fluorography of Tritium-Labeled Compounds. *K. Randerath* **991**

our point of view!



No need to be without an expanded scale pH meter—it's only $40 more.

Photovolt's *Expander IV,* pH meter 112, is $395.00—only $40 more than most laboratory models.

Any range of four pH units can be expanded over the entire scale. This solid state unit is readable and reproducible to within 0.005 pH and accurate to within 0.01 pH. An expanded millivolt range, ± 140 mv, readable to 0.5 mv extends *Expander IV's* ability to all ion selective electrodes.

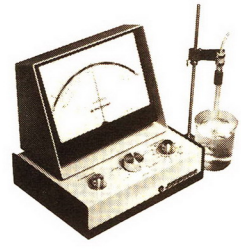

Expander IV is supplied with a single, fast, high-sensitivity electrode, but it also accepts all others, including ion selective and redox electrodes.

An output is available for Karl Fischer titrations, as well as a 10 mv recorder output.

Our point of view is that there is no longer any reason to be without an expanded scale pH meter. What's your point of view?

PHOTOVOLT CORPORATION *1115 Broadway, New York, N.Y. 10010 · (212) 989-2900*

Circle No. 113 on Reader's Service Card

New solid state viscometer for single or multiple checks.

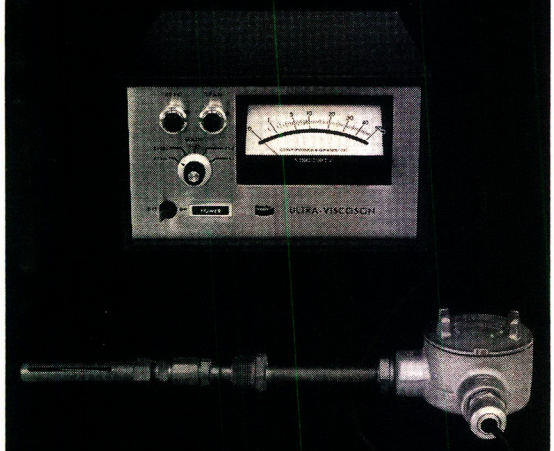

And a new bench mark for competitors.

New accuracy. New solid state reliability. New flexibility. That's the new Ultra-Viscoson Viscometer from Bendix. A multi-probe system lets you check out viscosities at various locations in the plant on the superbly accurate computer (it actually measures mathematical product of viscosity and density in four ranges: 0-50, -500, -5000 and -50,000 centipoises x grams/cc). A special probe permits operation in fluids up to 600° F. And for operation of standard potentiometric recorders or recorder controllers, a variable-output control allows a full-scale voltage from 0 to 100 millivolts. Sound like this new viscometer is all you could ask for? Ask for more information and see how right you are. The Bendix Corporation, Scientific Instruments and Equipment Division, 1775 Mt. Read Blvd., Rochester, N. Y. 14615.

Bendix

Circle No. 14 on Readers' Service Card

Author Index

Aladjem, A. 989
Altenau, A. G. 969
Alvarez, R. 955

Billmeyer, F. W., Jr. 874
Bruce, R. B. 977
Burgwald, L. H. 984
Burke, K. E. 963

Carlson, D. W. 969
Chambers, J. Q. 914
Chambers, L. A. 898
Connery, J. G. 918
Cover, R. E. 918
Cram, S. P. 893
Crouch, S. R. 880

Deming, S. N. 986
Dowden, B. F. 883
Drew, H. D. 974

Fitzgerald, J. M. 974
Frant, M. S. 967

Gelb, E. J. 990
Giddings, J. C. 889
Gladney, H. M. 883
Grushka, E. 889

Kelleher, D. E. 955
Kelley, R. N. 874
Kelly, D. P. 898
Kolthoff, I. M. 924, 932

Mader, P. 924, 932
Maynard, W. R., Jr. 977
Meier, E. P. 914
Menis, O. 952
Myers, M. N. 889
Myers, R. L. 980

Oldham, K. B. 936

Padmanabhan, G. R. 905
Pardue, H. L. 986
Paulsen, P. J. 955
Pitt, E. E. H. 981
Propst, R. C. 910

Rains, T. C. 952
Randerath, K. 991
Rook, H. L. 958
Ross, J. W., Jr. 967

Sabatino, J. D. 905
Schettler, P. D. 889
Schwartz, D. P. 984
Schweikert, E. A. 958
Senkowski, B. Z. 905
Shain, I. 980
Smith, R. 946
Spell, H. L. 902
Stafford, C. M. 946
Stanway, V. M. 981
Steen, S. N. 990
Stephenson, D. A. 966
Swalen, J. D. 883

Trudinger, P. A. 898

Wade, R. L. 893
Washall, T. A. 971
Weber, O. W. 905
Weihrauch, J. L. 984
Winefordner, J. D. 946

Yanak, M. M. 963

ANALYTICAL CHEMISTRY

A-page Reprints 1969

BIND important A-page material with original research papers

Volume 41 A-page reprints will include the Reports for Analytical Chemists, Instrumentation Columns, Book Reviews, Editors' Columns, and other features.

Orders may be placed now for delivery in January 1970

Price for set of A-page reprints is $3

Send name and address to ACS and reserve your set of A-page reprints

TO: Special Issues Sales
American Chemical Society
1155 Sixteenth St., N.W.
Washington, D.C. 20036

Bills will be mailed when reprints are available for distribution

Carbohydrate chromatography... now automatic!

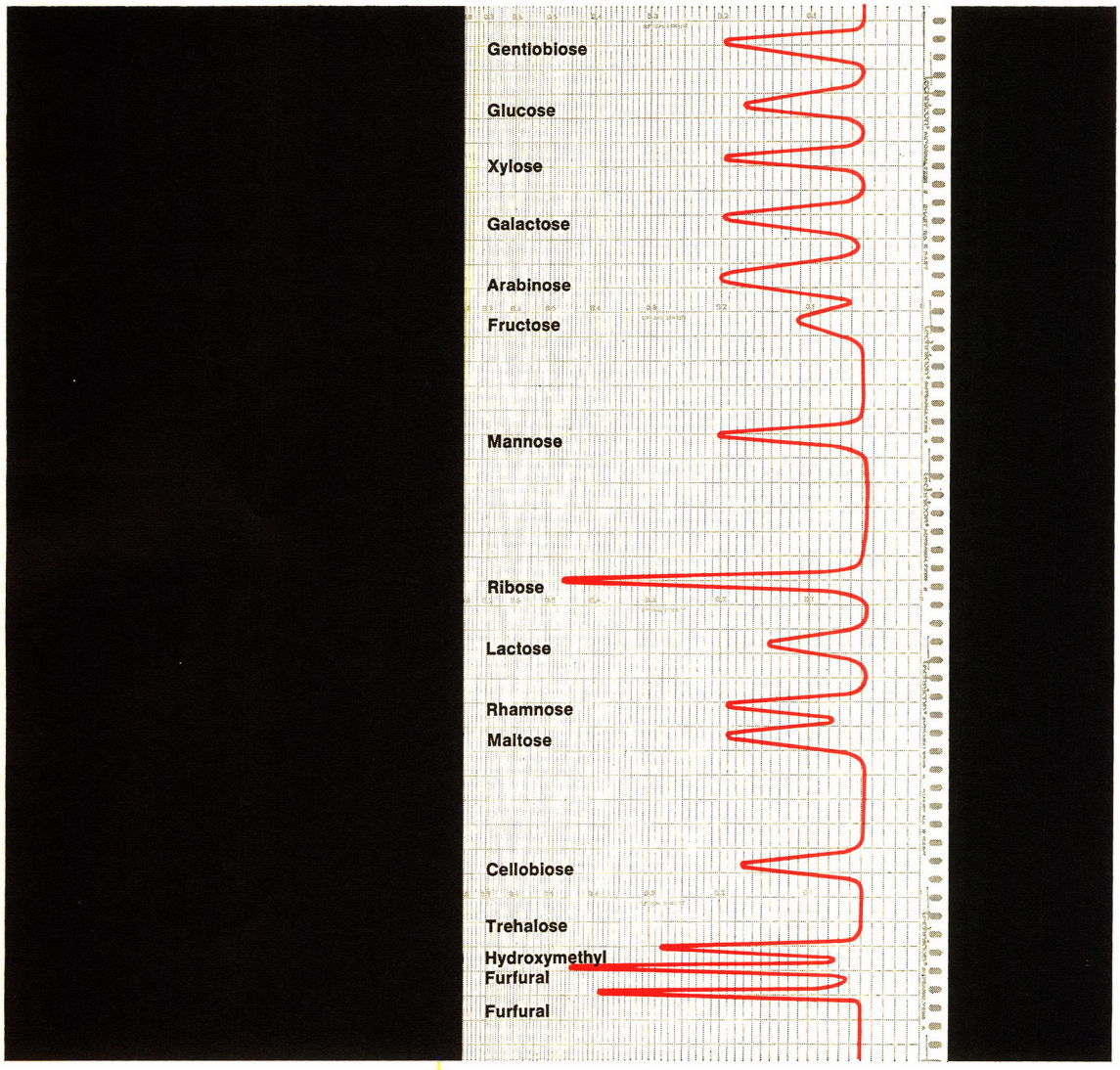

■ The 15-sugar chromatogram reproduced about one-sixth size above was produced on the new, automated Technicon® Sugar Chromatography System in 7½ hours. Notice that furfural, hydroxymethylfurfural, pentoses, hexoses, and disaccharides are well resolved.

■ This new system is uniquely sensitive (to 1 microgram of ribose, for example).

■ If the ability to quickly separate and quantitate a mixture of carbohydrates would help your work, please write for our 6-page booklet and a typical chromatogram.

TECHNICON CORPORATION • Tarrytown, New York 10591

T.M.

Circle No. 129 on Readers' Service Card

See ACS Laboratory Guide for All Products/Sales Office

Cut your field down to size.

The size of a mini-catalogue. A mini-catalogue of reprints of the world's foremost journals in the field of chemistry. Journals such as *American Chemical Society Journal, Journal of Organic Chemistry, Enzymologia,* and the *Journal of Physical Chemistry*. These reprints —like all Johnson reprints—are identical or similar in format to the originals.

In addition to volume numbers, years, and prices for individual volumes and cloth and paper bound sets, the mini-catalogue contains precis describing the editorial contents and objectives of each journal. For a *free* copy, simply mail the coupon. 23



111 Fifth Avenue, New York, N.Y. 10003

Please send me your *free* mini-catalogue Reprints of Journals in the Field of Chemistry.

Name_____

Address_____

_____

City_____ State_____ Zip_____

Circle No 5 on Readers' Service Card

Circle No. 53 on Readers' Service Card →

4-wide AEC compatible pulse height analyzer: $1995

BE SKEPTICAL.
INVESTIGATE.

The 555

NUCLEAR DATA INC

1330 E. GOLF ROAD, PALATINE, ILLINOIS 60067 PHONE 312/529-4600

NUCLEAR DATA, GMBH, FRANKFURT, GERMANY

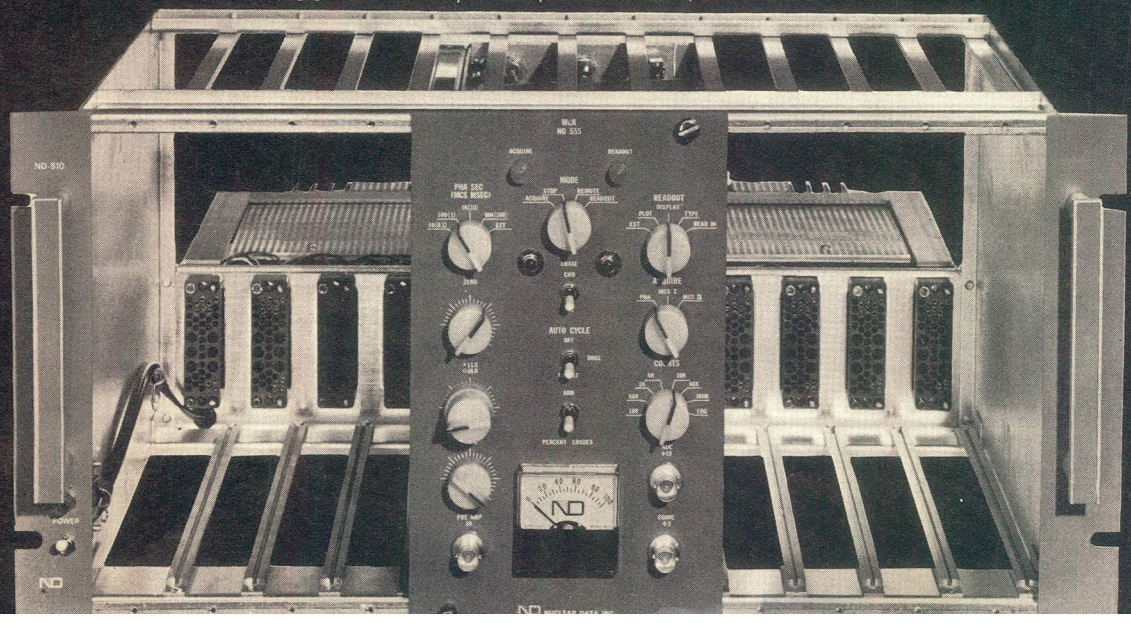

Why choose between economy and performance when you buy a balance ?

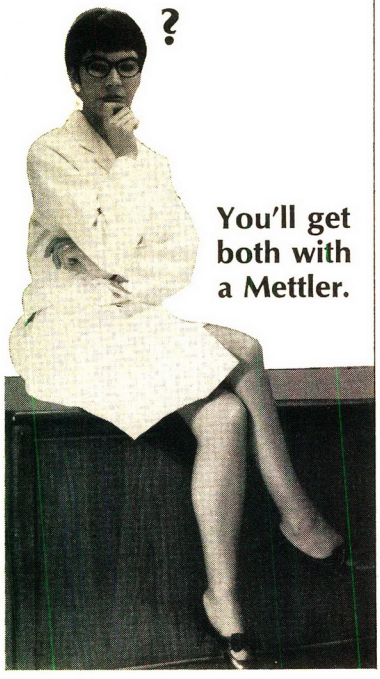

You'll get both with a Mettler.

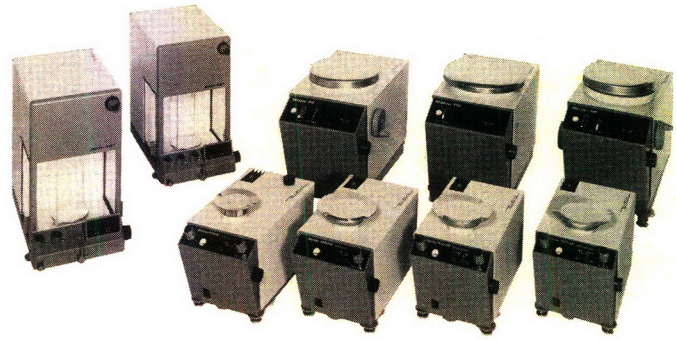

Want weighing performance, but worried about exceeding your budget? Here are 38 solutions to the balance buyer's dilemma. Mettler's 16 top-loading and 22 analytical balances.

SPEED + PRECISION = PERFORMANCE

Our top-loaders are tops when it comes to speed and weighing ease. Put the sample on the pan. Then read the weight. If you are filling a container to a target weight, Mettler's helpful filling guide shows the approximate weight on the pan throughout the filling . . . without interruptions.

Newest of the Mettler top-loaders is Model P162. It weighs up to 160 g with a precision of ±1 mg and features 10-g taring ability. Like other Mettler top-loaders, it provides digital and analog readout. Your new personnel will get the same precise results as the old hands in the department.

MANY TO CHOOSE FROM

Select the balance you need for your work from one of our top-loaders. We have one that weighs to 10 kg; another that takes arithmetic out of weight loss studies. Some automatically compensate for changes in level. All will carry out five types of weighings. Weighing unknowns. Checkweighing. Weighing-in. Batching. Weighing objects below the balance.

THE ECONOMICAL ANALYTICALS

One of the major features of all Mettler analytical balances is the impressive precision-capacity ratio. Take our low-cost Model H10. It weighs to 0.1 mg over the 0 to 160-g range. That's one part in 1,600,000.

You get two balances for the price of one with our Mettler Model H20. It combines the capacity of a macro analytical with the precision of a semi-micro. Some Mettler analyticals give an instant reading of the approximate weight on the pan. We call this feature preweighing.

WEIGHT WATCHING MADE EASY

With digital readout — standard on many Mettler analyticals — you'll weigh with unsurpassed speed, convenience and accuracy. A filling guide cuts your weighing-in time by 50 percent. Optical taring allows you to compensate for container weights.

Need clearly printed records of your weighings? Check our Models H10P and H20P which print out results on adhesive-backed paper. Then there's our sophisticated H20E electronic. As it weighs, it generates an analog signal which can be fed to compatible instrumentation such as recorders. The H20E can also be interfaced with computer or other control equipment to continuously monitor and keep weight changes within predetermined limits.

There are more: from our $550 basic balance that's ideal for classroom use to our $2,550 ultra-micro with ±0.1 microgram precision.

When is a Mettler NOT a balance?

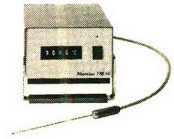

When it's our TM 15 digital platinum resistance thermometer. Portable and precise, it provides absolute accuracies up to ±0.15°C over the −20 to +300°C range. The sensors may be changed without recalibration and provide a linear output to other instruments.

For information or a demonstration of a Mettler balance or the new TM 15, write Mettler Instrument Corporation, 20 Nassau St., Princeton, N.J. 08540.

Mettler®

Circle No. 95 on Readers' Service Card

A C BRIEFS

Highlights
of Articles in
This Issue

Evaluating Dispersion in Gel Permeation Chromatography. Axial Dispersion of Polymer Molecules in Packed Beds of Nonporous Glass Beads

Experimental data are in good agreement with a theoretical model incorporating molecular and eddy diffusion, and velocity-profile effects as the major cause of axial dispersion.

R. N. KELLEY and F. W. BILLMEYER, Jr., Departments of Chemistry and Materials, Rensselaer Polytechnic Institute, Troy, N. Y. 12181

Anal. Chem., 41, 874 (1969)

Versatile Reciprocal Time Computer for Reaction Rate Methods

An all-electronic instrument is described which computes the reciprocal of time for use in reaction rate procedures. Rate measurements on synthetic signals and phosphate samples show the technique to be precise and accurate.

S. R. CROUCH, Department of Chemistry, Michigan State University, East Lansing, Mich. 48823

Anal. Chem., 41, 880 (1969)

Computer-Assisted Gas–Liquid Chromatography

The resolution of skewed overlapping peaks is accomplished by using a new line-shaped function and least-squares technique.

H. M. GLADNEY, B. F. DOWDEN, and J. D. SWALEN, International Business Machine Corp., Research Division, San Jose, Calif. 95144

Anal. Chem., 41, 883 (1969)

Computer Characterization of Chromatographic Peaks by Plate Height and Higher Central Moments

Moments characterize a peak completely and are related to parameters such as theoretical plate height and form of asymmetry such as peak tailing. A method for measuring moments is described.

ELI GRUSHKA, MARCUS N. MYERS, PAUL D. SCHETTLER, and J. CALVIN GIDDINGS, Department of Chemistry, University of Utah, Salt Lake City, Utah 84112

Anal. Chem., 41, 889 (1969)

Quantitative Interpretation of Semilogarithmic Gas Chromatographic Data

Column parameters and peak areas are calculated by treating Gaussian elution profiles as parabolas with floating-base line techniques.

R. L. WADE and S. P. CRAM, Department of Chemistry, University of Florida, Gainesville, Fla. 32601

Anal. Chem., 41, 893 (1969)

Cyanolysis and Spectrophotometric Estimation of Trithionate in Mixture with Thiosulfate and Tetrathionate

The method depends on the alkaline cyanolysis of thionates to yield thiocyanate which can be estimated colorimetrically. Factors affecting the reaction of thiosulfate, trithionate, and tetrathionate are described.

D. P. KELLY, L. A. CHAMBERS, and P. A. TRUDINGER, Baas Becking Geobiological Lab., Bureau of Mineral Resources, P.O. Box 378, Canberra City, A.C.T. 2601, Australia

Anal. Chem., 41, 898 (1969)

Determination of Piperazine Rings in Ethyleneamines, Poly(Ethyleneamine), and Polyethylenimine by Infrared Spectrometry

Quantitative knowledge of these molecular structures aids in their end use and in determining reaction conditions to produce the amines.

HARRY L. SPELL, The Dow Chemical Co., Texas Division, Freeport, Texas 77541

Anal. Chem., 41, 902 (1969)

Spectrophotometric Studies of Iron(II) Complexes of Pyridyl Benzodiazepin-2-ones

Molar absorpitivity and conditional formation constants of these complexes have been determined. Advantages of the benzodiazepin ligands over the dipyridyl type for the determination of Fe are discussed.

J. D. SABATINO, O. W. WEBER, G. R. PADMANBHAN, and B. Z. SENKOWSKI, Analytical Research Laboratories, Hoffman–La Roche Inc., Nutley, N. J. 07110

Anal. Chem., 41, 905 (1969)

Coulometric Titration of Microgram Amounts of Americium at the Conducting Glass Electrode

A conducting glass (tin oxide) electrode in carbonate electrolyte is used to quantitatively oxidize Am(III) to Am(V). Ten to 60 μg of Am can be coulometrically titrated.

R. C. PROPST, Savannah River Laboratory, E. I. du Pont de Nemours and Co., Aiken, S. C. 29801

Anal. Chem., 41, 910 (1969)

Adsorption of Organic Molecules at a Carbon Paste Electrode

Specific adsorption of an organic phosphate ester from aqueous acid solution is determined. The adsorbed species is uncharged and associated with the organic phase of the carbon paste electrode.

EUGENE P. MEIER and JAMES Q. CHAMBERS, Chemistry Department, University of Colorado, Boulder, Colo. 80302

Anal. Chem., 41, 914 (1969)

New!
Tri-Carb® Automatic Sample Oxidizer

Combusts 40 ^3H Samples an hour for Liquid Scintillation Counting

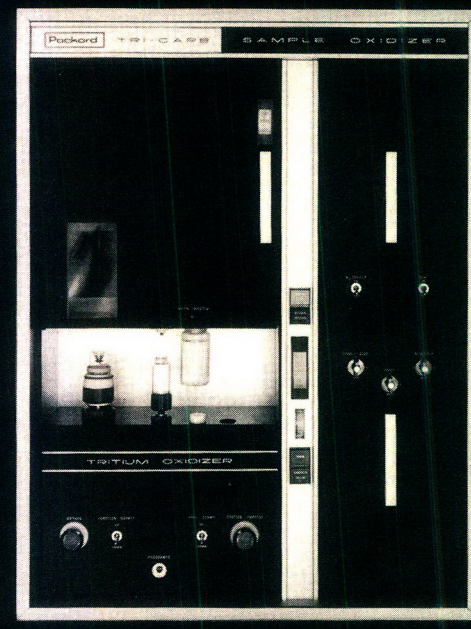

Packard

Say goodbye to time-consuming and troublesome methods of preparing tritium samples for liquid scintillation counting. The new Model 300 Tri-Carb Sample Oxidizer does the work automatically, at a rate that makes the method practical for virtually every experiment involving tritium as a tracer.

The Tri-Carb Sample Oxidizer provides recoveries of 97-99%+ for many materials, with routine achievement of 1% standard deviation. (This can be reduced to 0.3% in many cases, making the deviation essentially that resulting from dispensing errors and counting statistics.) Efficiencies of 80 to 95% of those obtained with a sealed, unquenched tritium toluene standard are achieved.

The new instrument, based on the pending Kaartinen* patents, combines the speed of closed system flame combustion with the advantage of unlimited tritium sample size. The only manual operations are positioning of the sample and counting vial, and pushbutton initiation and control of the combustion process. The balance of the cycle—including addition of scintillator—is carried out through automatic sequencing within the Sample Oxidizer.

Nitrogen purging is used to eliminate oxygen quenching, and because no manual handling is necessary during the cycle, the method is relatively insensitive to the operating skills of the user. Thus, a high degree of sample standardization is achieved.

For complete specifications write for Bulletin 300Q to the Packard Instrument Company, 2200 Warrenville Road, Downers Grove, Illinois 60515 or Packard Instrument International S.A., Talstrasse 39, 8001 Zurich, Switzerland.

*Niilo Kaartinen, Dept. of Physiology, University of Turku, Finland

A SUBSIDIARY OF AMBAC INDUSTRIES, INC. AMBAC

Circle No. 56 on Readers' Service Card

Optimizing Concentration Determinations in the Presence of Maxima and Catalytic and Kinetic Waves Using the Vibrating Dropping Mercury Electrode

Maxima for the first and second kind are suppressed at the VDME without the addition of surfactants. Catalytic and kinetic currents are minimized or eliminated.

RICHARD E. COVER and JAMES G. CONNERY, Department of Chemistry, St. John's University, Jamaica, New York 11432

Anal. Chem., 41, 918 (1969)

Kinetic Waves in Systems Containing Cobalt(II) and Cysteine-Like Compounds. Polarographic Catalytic Hydrogen Waves in Acid Solutions of Mercaptoanilines in Presence of Cobalt(II) or -(III)

The characteristics of the two catalytic hydrogen waves are studied and found to be quite different from those of Brdička waves.

I. M. KOLTHOFF and P. MADER, School of Chemistry, University of Minnesota, Minneapolis, Minn. 55455

Anal. Chem., 41, 924 (1969)

Kinetic Waves in Systems Containing Cobalt(II) and Cysteine-Like Compounds. Adsorption Phenomena in the Cystamine–Cobalt(II) System in Borax Medium

Traces of cobalt(II) completely suppress the current maximum and shift the cystamine wave to more negative potentials.

P. MADER and I. M. KOLTHOFF, School of Chemistry, University of Minnesota, Minneapolis, Minn. 55455

Anal. Chem., 41, 932 (1969)

Unified Treatment of Electrolysis at an Expanding Mercury Electrode

A general treatment is given of voltammetry at an electrode expanding with any power law. Stationary and DME electrodes are special cases. All degrees of reversibility are embraced.

KEITH B. OLDHAM, Science Center, North American Rockwell Corp., Thousand Oaks, Calif. 91360

Anal. Chem., 41, 936 (1969)

Temperature Profiles of Turbulent Hydrogen Diffusion Flames Used in Atomic Fluorescence Spectrometry

Temperature of H_2/Air, H_2/Ar/entrained Air, H_2/N_2O, and H_2/entrained Air flames supported on total-consumption nebulizer-burners are measured with an iridium—60% iridium–40% rhodium thermocouple.

R. SMITH, C. M. STAFFORD, and J. D. WINEFORDNER, Department of Chemistry, University of Florida, Gainesville, Fla. 32601

Anal. Chem., 41, 946 (1969)

Determination of Arsenic by Atomic Absorption Spectrometry with an Electrodeless Discharge Lamp as a Source of Radiation

Arsenic extraction into organic phase followed by a displacement reaction into aqueous phase and the use of total-consumption burner of Ar–H_2 flame eliminated background radiation interference.

OSCAR MENIS and T. C. RAINS, Analytical Chemistry Division, National Bureau of Standards, Washington, D. C. 20234

Anal. Chem., 41, 952 (1969)

Simultaneous Determination of Trace Elements in Platinum by Isotope Dilution and Spark Source Mass Spectrometry

The technique is applied to the simultaneous determination of Ag, Cu, Ni, Pb, and Pd in platinum. Results, ranging from 0.5 ppm for Ni and 14 ppm for Pb, are compared with those of the other methods.

ROBERT ALVAREZ, PAUL J. PAULSEN, and DANIEL E. KELLEHER, Spectrochemical Analysis Section, National Bureau of Standards, Washington, D. C. 20234

Anal. Chem., 41, 955 (1969)

Ultra-Trace Determination of Oxygen and Carbon by Charged Particle Activation Analysis

Analytical results are given for the nondestructive determination of oxygen in silicon in the parts-per-million to the parts-per-billion range.

HARRY L. ROOK and EMILE A. SCHWEIKERT, Activation Analysis Research Laboratory, Texas A&M University, College Station, Texas 77843

Anal. Chem., 41, 958 (1969)

Notes

Separation and X-Ray Spectrographic Determination of Microgram Quantities of Arsenic in Copper-, Iron-, and Nickel-Base Alloys

Arsenic at the 1–100 ppm level is separated from its matrix by precipitation with sodium hypophosphate. Tellurium is required as a carrier.

KEITH E. BURKE and MICHAEL M. YANAK, The International Nickel Company, Inc., Paul D. Merica Research Laboratory, Sterling Forest, Suffern, N. Y. 10901

Anal. Chem., 41, 963 (1969)

An Improved Flux-Fusion Technique for X-Ray Emission Analysis

Three lithium borate base fluxes were developed to decompose a variety of refractory materials. Graphite or vitreous carbon crucibles are used for fusions carried out at 1100°C.

D. A. STEPHENSON, Research and Development Laboratories, Corning Glass Works, Corning, N. Y. 14830

Anal. Chem., 41, 966 (1969)



Introducing Chromato-Prep,™ a low-cost, preparative liquid chromatograph that enables you to prepare gram quantities of high-purity single-species materials from nonvolatile or thermally unstable organic mixtures for identification, component concentration, or further analyses.

If you're involved in synthesizing new organic compounds; or isolating and identifying components of complex organic mixtures; or collecting purified material for analysis by UV, IR, or NMR; or any other investigations where you need high-purity, single species fractions, you'll appreciate the capabilities of the Waters Chromato-Prep.

The Chromato-Prep lets you separate just about anything having molecular weights up to several million (depending on the column and the packing materials used for the separation). Many samples can be run with just a single injection to obtain sufficient quantities for your studies. Where extremely high resolution is required, you can get it by adding our differential refractometer or UV photometer, a recorder, and a recycle system.

All at a very low cost.

For more information write to Waters Associates Inc., 61 Fountain Street, Framingham, Massachusetts, or call (617) 879-2000.

4317B

WATERS ASSOCIATES

Circle No. 73 on Readers' Service Card

Potentiometric Titrations of Sulfate Using an Ion-Selective Lead Electrode

A lead-sensing electrode serves as the end point indicator in direct titrations of sulfate ion with lead perchlorate. The method is practical to *ca.* $5 \times 10^{-5} M$ sulfate.

JAMES W. ROSS, Jr., and MARTIN S. FRANT, Orion Research, Inc., 11 Blackstone Street, Cambridge, Mass. 02139

Anal. Chem., 41, 967 (1969)

Nuclear Magnetic Resonance Analysis of Rubber Vulcanizates

Vulcanizates are dissolved in hot hexachlorobutadiene and run directly on the NMR without separating the carbon black. Calculated and found compounded formula for total amount of natural rubber, butadiene, and styrene were in close agreement.

DAVID W. CARLSON and ALAN G. ALTENAU, The Firestone Tire & Rubber Co. Central Laboratories, Akron, Ohio 44317

Anal. Chem., 41, 969 (1969)

Determination of Total Paraffins, Monochloroparaffins, and Polychloroparaffins by the Fluorescent Indicator Adsorption Method

The method is applicable to multicarbon range mixtures in the C_6–C_{16} range and to samples having wide variations in composition.

THOMAS A. WASHALL, ARCO Chemical Co., Research Division, Philadelphia, Pa.

Anal. Chem., 41, 971 (1969)

Principles and Methods of External Photochemical Titrant Generation

Titrant is prepared as needed by passing a photogenerator through a quartz tube irradiated by a low-pressure mercury arc. Effects of pump and lamp stability, flow rate, and length of photolysis zone are evaluated.

H. D. DREW and J. M. FITZGERALD, Department of Chemistry, Seton Hall University, South Orange, N. J. 07079

Anal. Chem., 41, 974 (1969)

Determination of Amphetamine and Related Amines in Blood by Gas Chromatography

The method is sufficiently sensitive and specific for determining amphetamine, methamphetamine, chlorphentermine, and fenfluramine in blood following oral administration of 5 mg of each drug.

ROBERT B. BRUCE and WILLIAM R. MAYNARD, Jr., A. H. Robins Co. Inc., 1211 Sherwood Avenue, Richmond, Va. 23220

Anal. Chem., 41, 977 (1969)

Determination of $E_2°$–$E_1°$ for Overlapping Waves in Stationary Electrode Polarography

Data have been calculated which make it possible to determine $E_2°$–$E_1°$ from experimentally measured values of E_{p}–$E_{p/2}$. The correlation is applicable only to reversible multistep charge transfer reactions.

R. LEE MYERS and IRVING SHAIN, Chemistry Department, University of Wisconsin, Madison, Wis. 53706

Anal. Chem., 41, 980 (1969)

Spectrophotometric Determination of Iron with 2-Pyridyl-2′-Hydroxymethane Sulfonic Acid

Conditions for the formation of a colored complex of iron with 2-pyridyl-2′-hydroxymethane sulfonic acid are investigated. Iron is determined spectrophotometrically in the range of 0.1–4 ppm.

E. E. H. PITT and V. M. STANWAY, Department of Chemistry and Metallurgy, Lanchester College of Technology, Coventry, England

Anal. Chem., 41, 981 (1969)

Methods for the Isolation and Characterization of Constituents of Natural Products. A Periodic Acid Column Procedure for the Oxidation of Vic-Glycols, Epoxides, and α-Hydroxy Acids at the Micromole Level

A convenient periodic acid oxidation procedure is reported for oxidation of susceptible structures in lipids at the micro- and submicromole level.

D. P. SCHWARTZ, J. L. WEIHRAUCH, and L. H. BURGWALD, Dairy Products Laboratory, Eastern Utilization Research and Development Division, Washington, D. C. 20250

Anal. Chem., 41, 984 (1969)

Aids for Analytical Chemists

High-Stability Low-Noise Precision Spectrometer Using Optical Feedback

HARRY L. PARDUE and STANLEY N. DEMING, Department of Chemistry, Purdue University, Lafayette, Ind. 47907

Anal. Chem., 41, 986 (1969)

Electrolytic Dissolution of Tantalum, Niobium, and Other Refractory Metals

ABRAHAM ALADJEM, Soreq Research Center, Yavne, Israel

Anal. Chem., 41, 989 (1969)

Dielectric Percentage Saturation Detector

E. J. GELB and S. N. STEEN, L. S. G. Industries Corp., P. O. Box 928, Valley Station, Wayne, N. J. 07470

Anal. Chem., 41, 990 (1969)

An Improved Procedure for Solid Scintillation Fluorography of Tritium Labeled Compounds

KURT RANDERATH, The John Collins Warren Laboratories of the Huntington Memorial Hospital of Harvard University at the Massachusetts General Hospital, Boston, Mass. 02114

Anal. Chem., 41, 991 (1969)

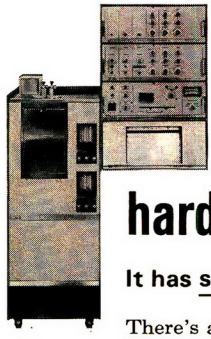

The gas chromatograph for hard-to-chromatograph materials

It has system detectability and linearity

There's a long list of materials that have always been hard-to-chromatograph: steroids, pesticides, vitamins, organo-metallics, polyfunctional industrial organic chemicals, to name the most common. The chromatographer who attempts to analyze these materials with an ordinary gc usually runs into two serious problems: inadequate *system* detectability and linearity. In plain English, he is unable to detect very small quantities (around the nanogram level) of these easily degradable materials; and, at higher concentrations, his gc does *not* respond proportionately to different amounts.

In the two plots reproduced here, we offer objective evidence that the HP Model 402 High-Efficiency GC possesses excellent system detectability and linearity. In the first place, the 402 easily detected trifluoperazine and testosterone chloroacetate, both hard-to-chromatograph materials, in the low nanogram range. Moreover, the 402's response is almost perfectly linear.

Neither of these *system* characteristics is likely to show up in the long list of specs that usually describe high-efficiency gc's. But you'd be well advised to make sure that your gc possesses them if you intend to handle hard-to-chromatograph samples. One sure way is to call the nearest HP sales office, or write for Bulletin 4020. Prices start at $4000.

Hewlett-Packard, Route 41, Avondale, Pennsylvania 19311. In Europe: 1217 Meyrin-Geneva, Switzerland.

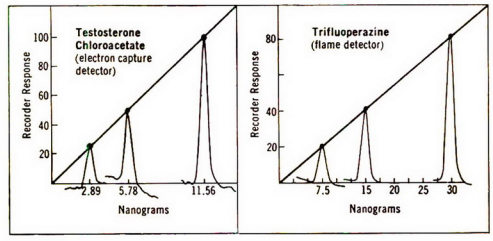

HEWLETT hp PACKARD

ANALYTICAL INSTRUMENTS

43906

Circle No. 106 on Readers' Service Card

WE MAKE THE WORLD'S FINEST NMR SAMPLE TUBE



. . . and we can prove it!

In high resolution NMR spectroscopy, four factors point to the importance of using sample tubes manufactured with *maximum precision:* (a) ease of spinning; (b) minimizing spinning side bands and, hence, some limited degree of sensitivity increase; (c) thin wall fabrication and a corresponding optimum filling factor; and (d) minimizing errors in resonance line positions when comparing lines simultaneously in separate samples.

Now, check the following table which shows the camber and wall thickness variation tolerances to which we manufacture the Wilmad Royal Imperial line of NMR sample tubes. These tolerances have been previously unheard of in the industry.

Cat. No.	Camber (Along 7" length)	DIMENSIONS IN INCHES		
		Wall Thickness Variation (I.D. to O.D.)	O.D.	I.D.
525-PP	0.001"	±0.001	0.195 0.196 (5 mm.)	0.1655 ±0.0005
526-PP	0.0005"	±0.001	0.195 0.196 (5 mm.)	0.1655 ±0.0005
527-PP	0.001"	±0.0005	0.195 0.196 (5 mm.)	0.1655 ±0.0005
528-PP	0.0005"	±0.0005	0.195 0.196 (5 mm.)	0.1655 ±0.0005

Wilmad Royal-Imperial 5 mm. NMR sample tubes give you *consistent optimum performance* in any spectrometer, but especially in the higher frequency ranges of units rated from 100 to 300 MHz. The tubes are manufactured of precision bore tubing and are highly polished for accurate spectral resolution. Buy your NMR sample tubes from the same supplier as the manufacturer of your spectrometer does . . . Wilmad.

NEW NMR CATALOG AVAILABLE

If you haven't received your copy of our new Bulletin 5006-1, write today and we'll send it to you by return mail.

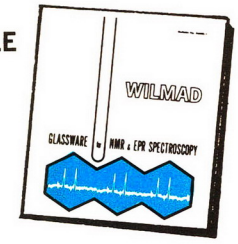

WILMAD GLASS COMPANY, INC.

Pioneer in Glass for NMR and EPR Spectroscopy

U.S. Route 40 and Oak Rd. • Buena, N.J. 08310 • Phone: (609) 697-3000

Circle No. 109 on Readers' Service Card

A point of view on

EASE OF OPERATION

When you tell a technician to "Count these samples," you want optimized counting. Without having to repeat a lot of instructions. You get what you want in our new Mark II™ Liquid Scintillation System.





MARK II



Circle No. 76 on Readers' Service Card

Now, when you send someone off to count your samples, you know it'll be done right. That's because all it takes to put the Mark II to work on *your* samples is the setting of the auto-program operating mode.

Remember, too, that every Mark II™ System accommodates up to 12 separate counting programs. One of them (or all 12 of them) can be yours, especially set up by you and locked-in for optimized counting of your samples.

Which means that you can be one of a dozen different users of a cooled, 300-sample Mark II. Or its only user, with up to 12 different kinds of samples. Either way, you always get top-of-the-line counting performance.

One of the secrets: A "program cap" that fits over the first vial in your batch of samples. It *automatically* picks your optimized counting program from among all the others.

Simple, easy operation. Plus unexcelled performance that you'll want to get the specs on. Find out more about the Mark II.

Call your Nuclear-Chicago sales engineer. Or write directly to us. 9-511

NUCLEAR-CHICAGO
A SUBSIDIARY OF G. D. SEARLE & CO.

2000 Nuclear Drive, Des Plaines, Illinois 60018, U.S.A.
Donker Curtiusstraat 7, Amsterdam W. The Netherlands
ALS-241

The tolerances are so close

on our 700 syringes that you are guaranteed accurate delivery of any rated quantity to within ± 1%... and you can repeat that delivery time after time within ± 1%. Made of 300 series stainless steel and alkali-resistant glass, each unit is tested to five atmospheres pressure. You can choose from seven models, from 5 ul to 500 ul, with a complete selection of needle styles and accessories.

Let us send you our new Catalog on syringes and related equipment. Write to: Hamilton Company, P.O. Box 307B, Whittier, Calif. 90608.

Repeatable Precision: Hamilton's 5 to 500 Microliter Syringes



HAMILTON

Circle No. 36 on Readers' Service Card

GUARANTEED AGAINST FLAKING!

PRE-COATED TLC MATERIAL
E. Merck (Darmstadt, Germany)

Whether you select the Brinkmann pre-coated *aluminum* sheets for thin layer chromatography procedures — or the pre-coated *glass* plates, they have this in common: Both have a thick, abrasion-resistant layer that will not flake and is guaranteed to arrive in good condition, and both come in the widest variety of sorbents available.

LOW-COST PRE-COATED ALUMINUM SHEETS AND ROLLS: Aluminum-backed pre-coated sheets are made in two sizes—5x20 cm or 20x20 cm . . . or on a continuous aluminum sheet roll 20x500 cm long. Because the aluminum backing is so thin (0.1 mm), the material can be cut with scissors to whatever size you wish, and may be punched for easy filing. Safe, easy to handle . . . no sharp edges. Little space is needed, as the sheets can be stacked one on top of the other. The material can be used with almost all popular solvents (except aqueous solutions) — even sprayed with aggressive reagents, such as sulfuric acid.

LOW-COST PRE-COATED GLASS PLATES: These plates are available with aluminum oxide, cellulose powder, silica gel and other sorbents, with or without fluorescent indicators . . . in sizes ranging from 5x10 cm to 20x30 cm. The surface is so stable that you can actually write on it. That's why these plates can be packed and shipped directly on top of each other in compact, convenient plastic containers. All conventional spray reagents, strong polar solvents, stains and charring techniques may be used.

Ask us for detailed information.

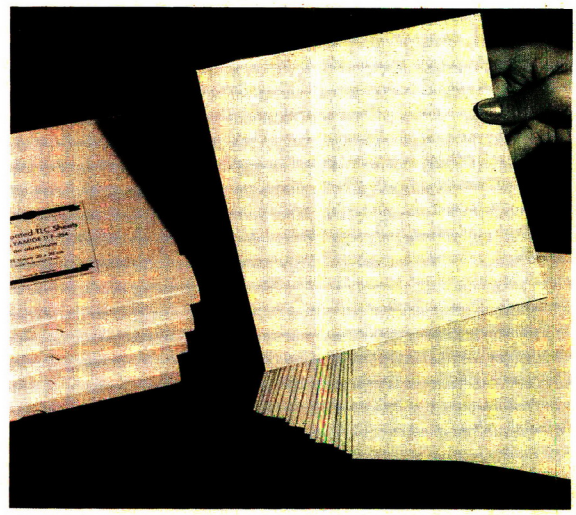

These aluminum-backed, pre-coated sheets won't flake, won't collapse. They're flexible and may be easily cut with scissors — yet they are sufficiently stable to be self-supporting in conventional TLC developing tanks.

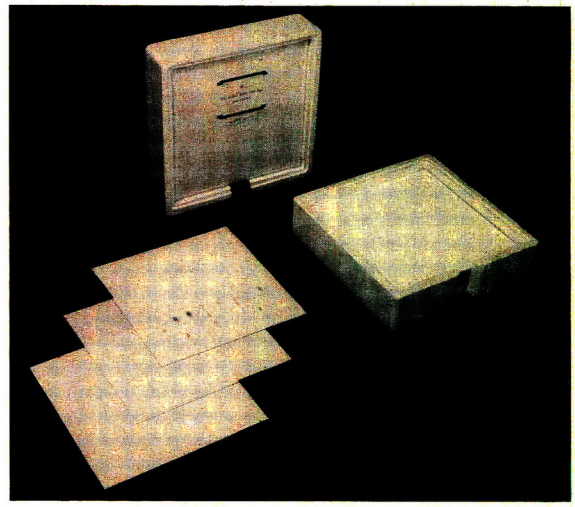

Pre-coated glass plates are also guaranteed against flaking. They come stacked in compact plastic containers — ready for use.

SCIENTIFIC GLASS APPARATUS CO., INC.
BLOOMFIELD, NEW JERSEY

LABORATORY . . .
♦ APPARATUS
♦ INSTRUMENTS
♦ CHEMICALS
♦ GLASSWARE

Branches: Boston 16 Mass. • Danbury Conn. • Elk Grove Village Ill. • Fullerton Calif. • Philadelphia 2 Penna. • Silver Spring Md. • Syracuse 2 N. Y.

Circle No. 65 on Readers' Service Card

See ACS Laboratory Guide for All Products/Sales Office

A BURNING QUESTION!

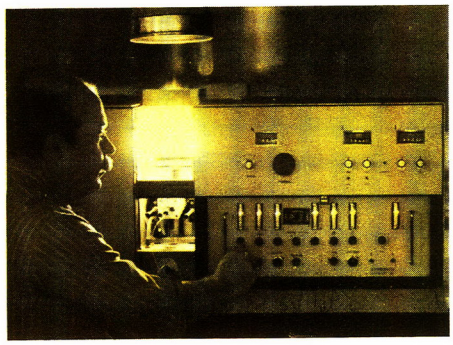

ATOMIC ABSORPTION OR FLAME EMISSION?

Some elements are best analyzed by atomic absorption - others including alkali metals, boron, uranium and the rare earths by flame emission. The IL Model 153 Absorption-Emission Spectrophotometer analyzes elements with either technique - simultaneously. No need to compromise. Dual channels of double beam spectroscopy permit determinations in the mode of analysis that produces the greatest precision with the utmost sensitivity.

This unique feature provides the ability to simultaneously read out two elements in concentration, or to determine a single element with an internal standard. The procedure insures the greatest possible analytical versatility, with maximum ease in sample handling.

Other exclusive features include a new AA Counter-Flo Jet Ⓣ Nebulizing System that enhances sensitivity and improves precision; completely automatic burner flame ignition with programmed fail-safe circuitry; push button controls for automatic baseline and calibration corrections, and an integral electronic test circuit for checkout of possible malfunctions. Simplified zone balance with independent currents for the six hollow cathode tubes help speed up analytical procedures. Totally solid-state, modular "in a drawer" electronics insure reliability. No other atomic absorption unit has so many of the "extras" built-in. No other instrument can give higher analytical precision, or faster, safer analyses.

Let us show you how this advanced Absorption-Emission Spectrophotometer can provide the best solution to your analytical problems. See for yourself the ease with which each sample can be evaluated and how much laboratory time can be saved without loss of sensitivity or accuracy. Ask us for a no-obligation demonstration. Or, for further information write for Data 153. Instrument leasing program details upon request.

INSTRUMENTATION LABORATORY INC.
113 HARTWELL AVE., LEXINGTON, MASS. 02173

OFFICES IN: ATLANTA • BALTIMORE • BOSTON • CHICAGO • CLEVELAND • DALLAS • DENVER DETROIT • HOUSTON • LOS ANGELES • NEWARK • NEW YORK • PHILADELPHIA • SAN FRANCISCO • ST. LOUIS • TRENTON • MONTREAL • TORONTO • VANCOUVER • ZURICH

Circle No. 41 on Readers' Service Card

ห้องสมุด กรมวิทยาศาสตร์

Analytical Chemistry in the Marine Sciences

Analytical chemists can play a key role in the future exploitation of marine resources, not only because of the central significance of chemical analysis and instrumentation in this field, but because of the analytical chemists' expertise in sampling, measurement, separation of chemical species, concentration techniques, processing and assimilating data, and their broad scientific knowledge and interests

by Robert B. Fischer, California State College, Dominguez Hills

Current advances in the basic and applied marine sciences are tremendously significant and exciting. It is virtually inevitable that even greater developments will occur, at an increasing rate, in the foreseeable future. The purpose of this Report is to review briefly some of the roles which analytical chemistry and chemical instrumentation are playing in these areas, particularly in the science and technology relating to the practical, economic exploitation of marine resources. We will not limit our concern to qualitative and quantitative determinations of chemical composition as such. Rather, we will include some considerations of sampling, separation, measurement, and the processing and interpretation of data obtained in measurement—all components within the overall analytical process.

As in many other currently active areas of scientific and technological endeavor, the output of technical literature is overwhelming. The June-July 1968 issue of the *Newsletter of the American Society for Oceanography* reported that the number of published articles in oceanographic science increased from 7,000 to 20,000 in the two-year period, 1965 to 1967, and that, in 1967, 700 journals were specializing in oceanographic information. In addition, of course, many relevant articles appear in other journals, including ANALYTICAL CHEMISTRY. Accordingly it has been necessary to be highly arbitrary in selecting the material for inclusion in this paper. It is intended that each item which has been selected be both interesting and significant, but there is certainly no intention to imply that there are not many other items which may be of equal or even greater importance. For example, very little will be said about pollution, an area in which relatively little is known of the physical, chemical, and biological interactions which occur, even though pollution has surely become one of the most crucially significant problem areas of modern times. Likewise, the tremendous reserves of oil and gas under the ocean floor will be omitted from discussion.

Analysis of Sea Water

Typical ocean waters contain twelve elements in solution in concentrations greater than one part per million (*1*). These elements range from chlorine at nearly two per cent and sodium at over one per cent, down through magnesium, sulfur, calcium, potassium, bromine, carbon, strontium, boron, and silicon, to fluorine at slightly over one part per million.

The ratios among these dissolved components are quite constant throughout most of the oceans. However, the absolute values vary considerably from place to place, both laterally and vertically. The constancy of these ratios of concentration among major dissolved components is not necessarily indicative of a static condition. More likely, a dynamic condition exists in which the rate at which a given component is introduced by runoff into the oceans is equalled by the rate of its deposition by sedimentation.

Twelve more elements are found in dissolved forms in average sea waters at concentrations of 0.6 to 0.01 part per million, and another nine elements at concentrations ranging down to 0.001 part per million (*1*). Unlike the more concentrated solutes, the ratios as well as the absolute values of the concentrations of these substances vary widely from place to place. Other elements have also been identified in sea waters; virtually every element must be present, at least in minute trace quantities.

The considerable quantities of experimental data upon which the preceding paragraphs are based consist directly, of course, of countless numbers of chemical analyses. The qualitative identifications and quantitative determinations have been performed over periods of many years, by many persons, using many analytical methods, in many

laboratories, on shipboard and in land-based laboratories. Colorimetric and titrimetric procedures have been predominant, but virtually all kinds of analytical methods and techniques have been found to be useful.

One of the most commonly encountered determinations is that of salinity, which is important as an overall indicator of salt content in oceanographic surveys. The salinity is determined most directly by titration of the halide by silver nitrate, using any of the conventional methods of end point indication (*2, 3*). Alternatively, salinity data are often obtained less directly by measurement of one or more associated parameters, such as electrical conductivity, density, and index of refraction. Unfortunately, the relationships of these parameters to each other and to actual salt content are not adequately established, nor are the effects of temperature and pressure upon these relationships. For example, data obtained from measurement by one method may be repeatable within 0.002% salinity, while the accuracy is good only within 0.02%; an accuracy more closely approaching the precision would be helpful for some purposes (*4*).

Others of the most important determinations are those of the micronutrients in sea water, especially phosphate, nitrate, and silicate.



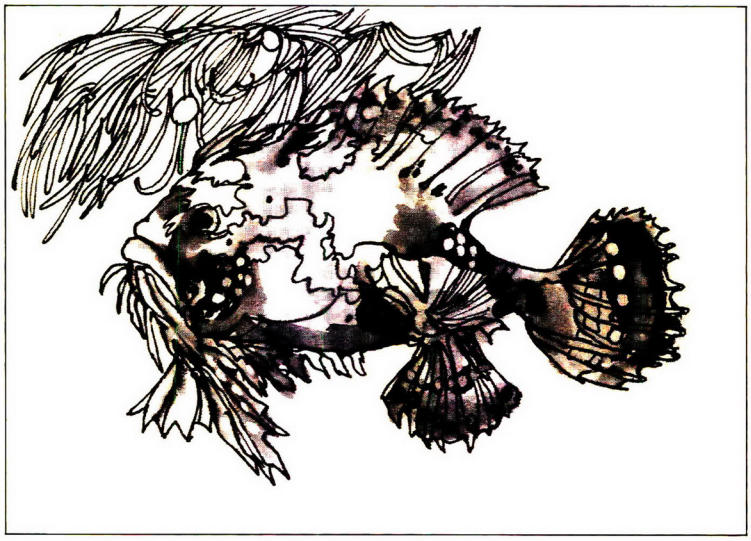

Plankton, which thrive in the presence of phosphates, attract fish. Thus, the presence of phosphates is indicative of fish. All three of these inorganic components are determined by modified forms of conventional colorimetric procedures (*2*): phosphate by conversion to "molybdenum blue," nitrate by reduction to nitrite and conversion to an azo dye, and silicate by conversion to silicomolybdic acid and then to its corresponding heteropoly acid for colorimetric measurement. A preliminary extraction with isobutanol is frequently necessary to render the phosphate procedure sufficiently sensitive for the concentrations found in sea water.

Among the many other analytical procedures which are of value are those of vitamin B_1, biotin, and vitamin B_{12}, for each of which an appropriate organism is introduced and allowed to incubate, sodium carbonate with ^{14}C is added, and measurement is made of the uptake of ^{14}C upon exposure to light (*2*).

Although these and other methods for the analysis of sea water are quite conventional in principle, special considerations are necessary because of the nature of the sample. For example, the blank for a colorimetric determination ideally should consist of sea water like the sample, except totally minus the desired constituent. This is impossible to provide, not only because of the overall variations in salinity, as already mentioned, but also because it is literally impossible to find any natural sea water which is totally lacking in any of the most frequently desired constituents. The method of standard additions is of much usefulness, but a more common procedure is to use a synthetic sea water as the reference standard. Unfortunately, several different standard sea waters have been proposed. Even more unfortunately, several different ones have been used as standards of comparison in chemical analyses.

Further improvements are needed in the development of equipment for rapid, automated analyses. The possibility of using a system such as the Technicon AutoAnalyzer is especially appealing. In one study of the use of this system for the determinations of phosphate, silicate, and nitrate (*5*), it was concluded that (*a*) the apparatus could be transported, quickly set-up and operated satisfactorily at sea, (*b*) twenty duplicate samples could be run per hour, as compared to three per hour by manual methods by an analyst working at top efficiency (a condition seldom found at sea!), and (*c*) both the precision and the accuracy were significantly better by the automatic method than by the manual methods.

Rapidity in obtaining analytical results is desirable not only for the sake of convenience, but more importantly because it permits on-the-spot decisions to be made as to further courses of action—and because it minimizes the danger of significant error due to changes occurring during storage of samples for subsequent analysis.

The development of ion selective electrodes is particularly significant. The science of marine chemistry has advanced to the point where it is concerned not only with concentrations and compositions, but also with the routes and mechanisms of reactions which occur in the oceanic environment. Further new knowledge must be based, in part, upon measurements of actual ionic species, activities, and activity coefficients. By means of measurements with a calcium electrode, for example, it was found that 84% of the calcium ion in a certain standard sea water exists as Ca^{+2}, the remaining 16% presumably being complexed with sulfate, carbonate, and bicarbonate; these values are in general agreement with predictions based upon prior thermodynamic concepts (*6*).

Economic Extraction of Dissolved Minerals

Only three of the inorganic solutes in sea water are now being extracted commercially on a large scale, salt, bromine, and magnesium (*7*).

It is to be expected that more of the dissolved minerals will be commercially extracted on a large scale in the future. Even though most components are very dilute, the facts remain that they are there and that the total quantities are tremendous (*1*). Furthermore, the mineral content of the ocean waters is continually being replenished, such as by run-off from rivers, at rates that exceed many-fold the rates at which man can remove them in the foreseeable future.

Processes have been developed already for the extraction of all major components and for many of the minor ones as well. Some of these processes have been well-proved in the laboratory, and technology has progressed to bring some of them close to the point of economic utility. Here is a broad area of active research and development in which analytical chemists must play central roles. Not only are chemical analyses needed, but of even more significance is the fact that the pro-

The Laser Story from Orlando Research

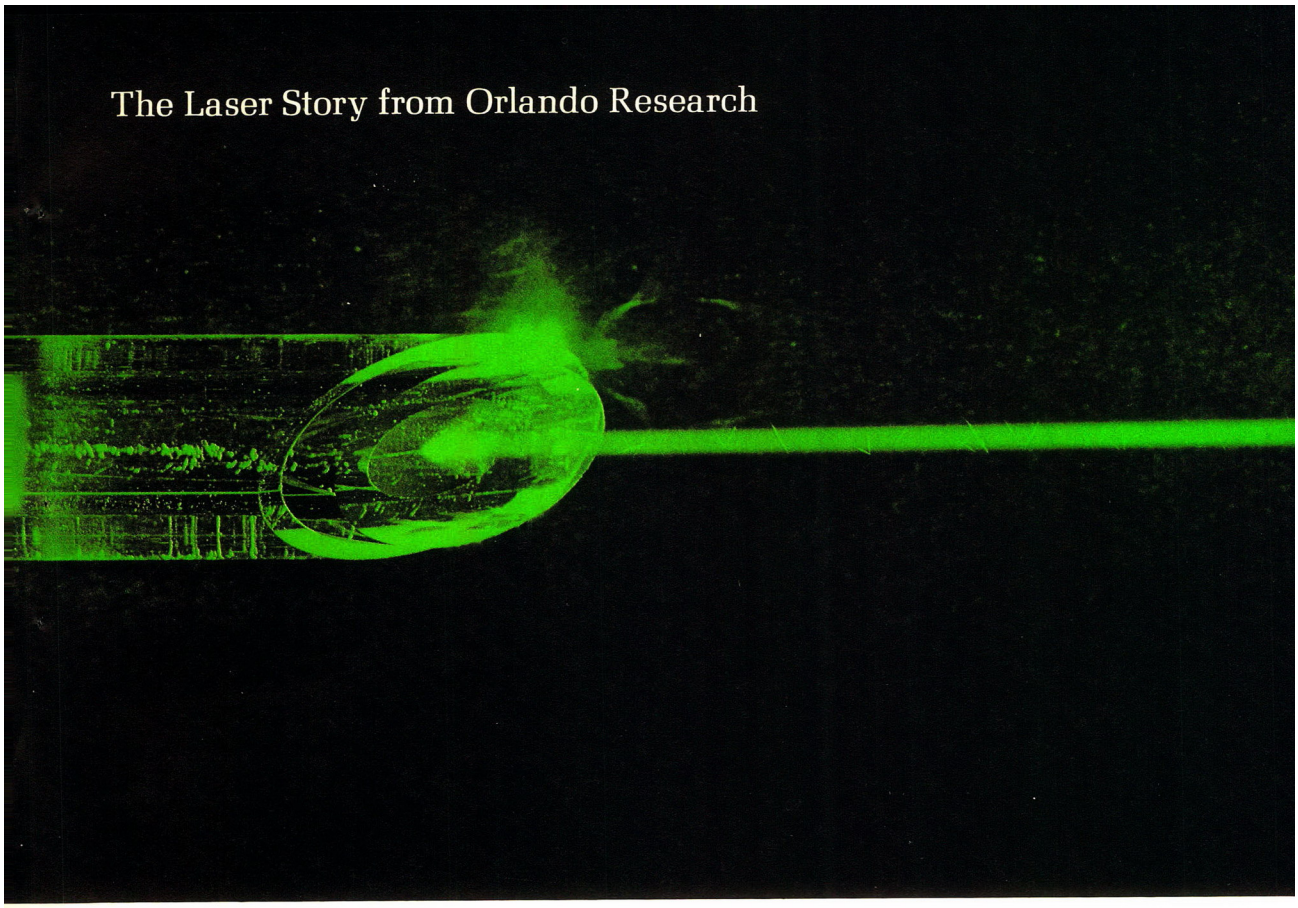

A MEASURABLY BETTER BEAM OUTPUT

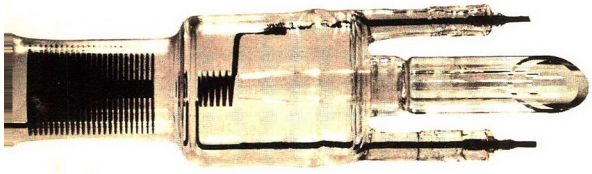

Orlando Research's patented secondary anode ion laser tube

Orlando Research makes the one ion laser that does not suffer decreased output due to tube erosion by the laser plasma. The patented **secondary anode,** positioned axially-concentric to the plasma stream, is biased positive with respect to the plasma. It confines plasma to a linear path and prevents stray-ion bombardment of the tube. Result: you get much better power stability over the life of the tube. Other features that make Orlando Research lasers last longer and yield better output include extra-heavy cathode design and absolutely no external gas-fill requirement. Write P. O. Box 13266, Orlando, Fla. 32806 today for our brochure that gives detailed specifications on all our CW ion lasers. They're measurably better.

ORLANDO RESEARCH CORPORATION

Circle No. 125 on Readers' Service Card

cedural and technological problems which must be overcome to make these processes economically feasible are basically scaled-up versions of the same kinds of problems of identification, separation, and concentration which are continually met and overcome by the analytical chemist. For example, uranium exists in sea water to the extent of about 0.003 part per million. A process has been developed for extracting this uranium by means of ion exchange in combination with tidal currents to cause the water to pass through the resin bed. Even though about 100 tons of sea water are required to yield one cent's worth of uranium, it is not unreasonable to predict that this may become an economically feasible means of meeting a significant fraction of the world's demand for this metal. It is probable that other metals can similarly be extracted commercially on an economic basis by use of other highly selective resins in the not-too-distant future. It is also interesting to note at this point that the possibilities of using tidal currents as sources of power are receiving continuing attention; however, technology is likely as advanced as far as is economically warranted at the present time.

Natural Enrichment of Dissolved Components

Some marine organisms serve to collect and to concentrate some of the trace components of ocean water. As examples, iodine is concentrated by sponges and seaweeds, iron by some sea snails, copper and zinc by some mollusks, and nickel by sponges and mollusks. It is highly possible that, if more basic knowledge could be gained as to the mechanisms by which these concentrating actions occur, the processes could be deliberately exploited in meaningful ways.

Within the last five years, three "hot brine pools" have been discovered deep in the center of the Red Sea. Numerous technical and popularized articles have appeared describing these regions of enriched concentrations of dissolved components (*8*). The largest of these pools, named the Atlantis, is at a depth of almost 2,000 meters, has a thickness of about 180 meters, extends over an area of about 8 miles by 4 miles, is at a temperature of about 45 °C., is about ten times more concentrated than normal sea waters in sodium, potassium, chlorine, and calcium, and contains some trace elements at concentrations ranging up to 50,000 times those found in average ocean waters. Among the analytical tools which played very extensive roles in the identification and characterization of these hot brine pools were atomic absorption spectroscopy and the electrobalance, the latter being particularly usable for quantitative weighings under shipboard conditions.

Sediments, which were collected from the ocean floor in the regions of these pools by dredging and by coring, are gel-like, which fact suggests that they were formed by precipitation. Analyses of these sediments, after drying, reveals the presence of iron, zinc, manganese, cobalt, cadmium, barium, and copper, mostly as oxides, in concentrations and quantities that are of commercial interest.

Another type of analytical determination which has proved to be useful in marine science, including the analyses of the Red Sea hot brine pools, is the determination of ^{18}O. In general, ocean waters are somewhat enriched in ^{18}O as compared to fresh waters, and highly saline waters are even more highly enriched in ^{18}O. However, the ^{18}O content of the Red Sea brines is even less than that of average sea water. This observation, along with several others, has led to the tentative explanation that these pools originated by discharge from the ocean floor. Possibly there is a rifting of rock in the ocean floor, with water going down and then returning back up, leaching the minerals as it goes. If this explanation is correct, these pools actually comprise continuous sources of salts and of heat. The economic potential of these pools is tremendous.

One of the resources being extracted from sea water on a commercial basis is pure water. The amounts being extracted have increased about 30% per year for each of the past ten years (*7*). The processes are of practical and potential interest, not only because of the pure water produced, but also

Still using your hands to fold filter paper?

If you are, stop. S&S has already done the job for you. They are called #560 folded analytical filter papers, and they're tear-proof.

Used for preparing Glucose, BUN or other protein-free filtrations, #560 folded cost only $1.83 per box of 100, 12½ cm diameter. Minimum order is $5.00.

#560 folded filter papers is just one more lab aid from S&S, manufacturers of:

1 Pure cellulose acetate for electrophoresis.
2 Collodion Bags for protein concentration.
3 Standard S&S 903 Paper for PKU tests.
4 Finest Filter Papers, Chromatography Papers.
5 Folded Filter Papers.

S&S the first name in filtration...
SCHLEICHER & SCHUELL
(603) 352-3810

Schleicher & Schuell, Inc.
Keene, New Hampshire 03431
Please send free information on circled items from above descriptions.
1 2 3 4 5
Name
Address
City
State Zip
AC669

Circle No. 64 on Readers' Service Card

Now Available . . .
Heath 701 Spectrophotometer

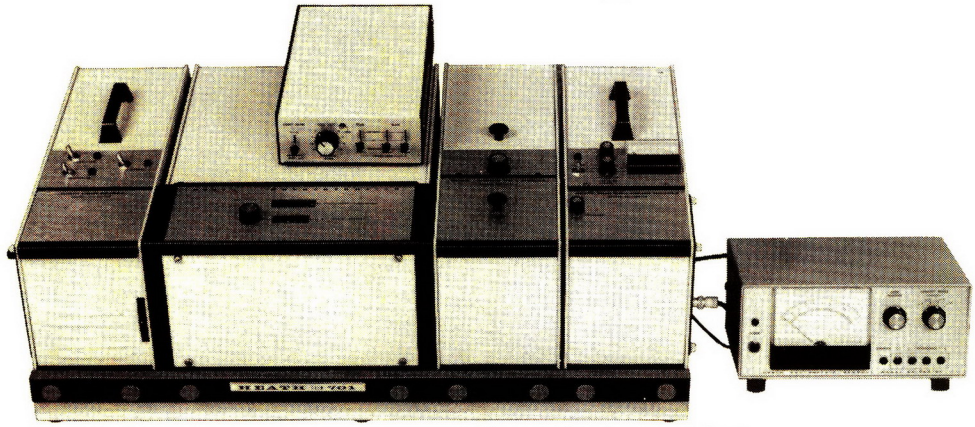

- **UV - Vis**
- **± 1 Å Accuracy**
- **Better than 1 Å Resolution**
- **Less than 0.1% Stray Light**
- **Linear Absorbance readout**
- **Interfaces directly with recorder and DVM**
- **Convertible to Atomic Absorption and Double Beam**
- **. . . $2500***

The new Heath/Malmstadt-Enke "701" UV-Visible Single-Beam Spectrophotometer is now ready for delivery. This instrument utilizes an original design based on the unique Heath/Malmstadt-Enke modular system. The "701" offers unequalled flexibility and versatility with excellent photometric accuracy and reproducibility for just $2500*.

NEW OPEN-ENDED CONCEPT. The "701" consists of modules locked together into a single unitized instrument by means of a self-aligning instrument base. Future conversion of the "701" into other spectrometric systems is easily possible by integrating the Monochromator and the Photomultiplier modules with other components. New modular units will be available soon expanding the system's capability to Atomic Absorption, Atomic Fluorescence, Flame Emission and Double Beam modes. The need for multiple instruments is eliminated and investment considerably reduced as there is no duplication of equipment.

HIGH PERFORMANCE. The "701" features a wavelength range of 1900 to 7000 Å. Level of stray light is extremely low: 0.05% average with less than 0.1% maximum between 2200 and 6000 Å. Wavelength accuracy is ± 1 Å, wavelength reproducibility is ± 0.2 Å, both constant throughout the wavelength range. System resolving power is better than 1 Å. Spectral bandwidth is continuously adjustable between 0.5 and 40 Å.

UNIQUE FEATURES. The "701" uses electronic digital stepped scanning which permits a greater number of accurate speeds than by mechanical means. The IC digital design allows for pulse-to-pulse synchronization of the wavelength scan with the recorder and other system modules. Remote control is built-in as the "701" is operated by a separate Control Unit. Provisions for external programming are also included.

CONVENIENT OPERATION. The unusually large light-tight sample cell compartment of the "701" is capable of holding a wide variety of cells from 0.1 to 10 cm. It allows accurate and reproducible positioning of four 1 cm cells. Space is provided for auxiliary equipment: temperature control devices, filters, stirrers, etc. The Photo-multiplier module is supplied with a 1P28A PM tube interchangeable for conventional side window as well as end-on window type tubes with special characteristics.

DESIGN OF THE "701". Locked on the EU-701-1 Instrument base are the following modules:

Light Source Module EU-701-50 producing UV, Vis and near IR radiation at very constant intensity from its Deuterium and Tungsten lamps. Power supply is included.
Monochromator EU-700 featuring Czerny-Turner f/7, 350 mm, 1180 lines/mm grating optical design with MgF_2 coated aspheric mirrors for maximum UV efficiency.
Sample Cell Module EU-701-11 accepting a wide range of special sample handling devices from micro-cells to vessels up to 5" diameter.
Photomultiplier Module EU-701-30 containing a 1P28A PM tube mounted in a double light-tight compartment with shutter. PM voltage from power supply can be adjusted between 150 and 1500 V and is externally programmable.
A set of seven filters for broad band wavelength discrimination is provided with the system.

READOUT OPTIONS. The standard analog readout is in % Transmittance and in Linear Absorbance over the spans of 0-1, 0-2 and 1-2 on the 6" meter of the Photometric Readout Module EU-703-31 which can also be used as an interface with a recorder or a DVM. An alternative log/linear recorder readout on a 10" chart is also available by using the EU-201V Multi-Speed Log/Linear Recording Photometer. The recorder is calibrated in the same linear Absorbance and Transmittance ranges plus three decades of scale expansion. Two or more readouts can be used for simultaneous direct readout and chart recording.

The "701" is especially useful for research in universities and in industry but is equally well suited for routine use in control laboratories. Its versatility and performance together with its very low price make the "701" the best value in UV-Vis Spectrophotometers.

Price of the "701" is $2500* with analog photometric readout, $2695* with log/linear recorder, $2245* without readout. Write for detailed information.

HEATH

HEATH COMPANY, Dept. 560-01 *a Schlumberger company*
Benton Harbor, Michigan 49022

☐ Please send detailed information "701" Spectrophotometer.

Name .....

Address .....

City .....State ..... Zip .....

Prices & specifications subject to change without notice.
* Mail order prices; F. O. B. factory. EK-275

Circle No. 121 on Readers' Service Card

Column Chromatography in Three Easy Lessons*



*Three Easy Prices Too! For Complete Information Send For Brochure CC31

Lesson No.1

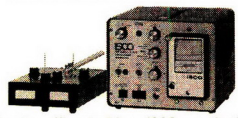

Monitor the effluent with an ISCO quantitative ultraviolet analyzer. Linear absorbance recording and single or dual-beam operation at 254 and 280 mμ are only a few of ISCO's exclusive features.

Lesson No.2

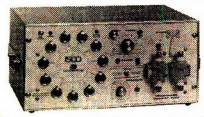

Any simple or complex elution gradient formed by combining two liquids can be dialed directly into the Dialagrad Programmed Gradient Pump. Program duration and pumping rates are easily adjusted over broad ranges.

Lesson No.3

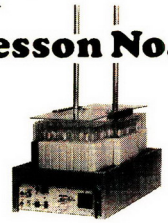

Collect the effluent in one of ISCO's two linear or four round fraction collectors. Prices range from $245.00 for the Model 270 to $850.00 for the Model 326. No after school sessions necessary when you use ISCO equipment.

INSTRUMENTATION SPECIALTIES CO., INC.
4700 SUPERIOR LINCOLN, NEBRASKA 68504
PHONE (402) 434-0231 CABLE ISCOLAB LINCOLN

Circle No. 42 on Readers' Service Card

because of the relatively concentrated brines which are discharged as the effluents.

General Oceanographic Surveys

Some of the physical and chemical properties which are most commonly measured in general oceanographic surveys are temperature, salinity, density, sound velocity, movements of ocean currents, magnetic field strengths, gravity, the presence of seismic tremors, and the depth and other characteristics of the ocean floor. Apart from some of the newer remote sensing methods (to be discussed later in this section), these measurements require the use of underwater sensors, some means of storing and retrieving the data, some means of converting the raw numbers into meaningful units, and the reduction of data into a usable format. In general, it may be stated that the rate of producing new data has exceeded the ability of manpower alone to process and to assimilate it. Accordingly, various types of computing equipment have become absolutely essential in modern oceanographic surveys.

The results of routine survey measurements, particularly when they are anomalous in any significant way, point to the desirability of further examination, including for example the collection of sediments and cores from the ocean floor for further analysis.

The ocean waters present a particularly hostile environment for electronic equipment which must be submerged in it. The temperature range is not unfavorable. Much more deleterious, however, are the facts that sea water is a good conductor of electricity, that it is highly conducive to corrosion, that it supports living organisms which can damage electronic devices and connecting cables, and that the high pressures at great depths present serious leakage problems. Interestingly enough, failures of underwater connectors have caused a disproportionate amount of the difficulties that have arisen through equipment failure in this hostile environment. Recent developments in solid-state electronics and in encapsulated circuitry have already proved to be of value, not only because of relatively small size and low power consumption, but also because of increased reliability. The over-all costs of an oceanographic cruise are so great that reliability of associated electronic equipment is very important—in fact, this is one area which even now is most seriously in need of considerable improvement.

Remote sensing from airborne bases is one of the general areas in which very exciting advances are now underway. [*Editors' note:* See J. A. S. Adams, *et al.*, ANAL. CHEM., 22A (May 1969)]. Let us refer briefly to specific examples. Prospecting for regions of abnormally high brine concentrations can be speeded up considerably by use of gamma ray detectors, based on the facts that ^{40}K is the major source of gamma rays in ocean waters, and that potassium is one of the major dissolved components which are found in reasonably constant ratios in all sea waters.

This concept has been extended in an instrument designed for airborne use by Texas Instruments, Inc. The total activity detected is separated by a multi-channel pulse height analyzer into contributions from uranium, the thorium series, and ^{40}K. Digital processing of the data provides an output which consists of iso-radiation contour maps showing the concentrations of each of the three components, their ratios, and the total count. This procedure makes possible the very rapid collection of considerable quantities of data over wide areas.

Remote temperature sensing by means of infrared radiation thermometers has proved to be especially valuable. Modern instrumentation typically employs a chopping device to permit repetitive comparison to a local object of precisely known and constant temperature, a thermistor bolometer as the detector, and the resultant development of an a-c signal the magnitude of which is a direct measure of the temperature of the area of the ocean relative to that of the standard (*9*). Continual readings are made and plotted as the area of interest is scanned. Only a thin top layer of the water, possibly about 20 microns thick, contributes directly to the mea-

surement. Wind and wave conditions typically influence the temperature of this thin layer by as much as 0.5 °C., even though the measuring system is inherently capable of a precision better by fivefold.

Wide area temperature surveys are of considerable practical value. As a single example, consider the herring industry, which is of much economic significance to Iceland. These fish feed in the zone of demarcation where the Atlantic and Polar Waters meet in the Norwegian Sea, and the exact location varies from year to year. In 1967, this region was so far from the mainland of Iceland that much of the harvest spoiled on the return trip. In 1968 an aerial system of remote temperature sensing was employed, by means of which it was possible to ascertain in twelve days the sea-surface temperatures around the entire island of Iceland out to a distance of 100 miles. The practical values are considerable, both in rapidly locating where the fish are and also in providing a basis for making appropriate arrangements for storage and transport back to the home base.

Mapping of the ocean bottom has been accomplished for twenty-five years primarily by sonar methods, in spite of the fact that the velocity of sound is dependent somewhat upon the temperature of the water and by other conditions which may not be constant nor even known. An interesting alternative system, the "laser range gate," has been developed by Electro-Optical Systems. A pulse of laser light replaces the sonar emission. The approximate time for this pulse to return from the ocean floor is calculated in advance, and the receiver "gate" is opened only briefly at this time, thus minimizing the background "noise" from other random reflections and scatterings.

Sonar systems to locate areas of high plankton density have been quite unsuccessful because of the fact that the sonar wavelengths so greatly exceed the typical sizes of plankton that the sonar scattering cross sections are virtually nil for most forms of plankton. Early attempts to use visible light, with its shorter wavelengths, have been largely unsuccessful because of such factors as poor transmission through sea water, background light from other sources, bioluminescent organisms, and so forth. Accordingly, conventional methods of "analyzing" directly for plankton consist of sampling with nets and bottles, necessarily limiting the analyses to very small volumes or regions at a time.

Once again, a new instrumental system employing laser light appears to be very promising. This device, called the "lidar," is essentially a device for radar-like plotting of three-dimensional maps of "clouds" of plankton in water at considerable depths. The lidar employs blue-green light, at 0.53 micron, which radiation is short enough for appreciable scatter from plankton and which penetrates water to a reasonable extent with minimal Rayleigh scatter from water molecules. This particular apparatus repetitively emits short pulses of high peak power at this sharply defined wavelength. The photomultiplier detecting system is coordinated with the emitted pulses, so as to minimize "noise" from other sources of light. The fact that laser light is coherent is not significant in this application.

The significance of this, and other newer methods of rapidly collecting masses of analytical data may be illustrated by the following statement which concludes an article on the lidar. "At a pulse repetition rate of 5,000 pulses per second and with one-meter resolution cells, it appears that in one minute of operation an airborne oceanographic lidar will sample more volume elements of the ocean than have been sampled by all the net-and-bottle, scattering meter, and transmissometer measurements to date. A good many surprises may be in store" (*10*).

A very versatile deep sea instrument capsule has been developed for the collecting of data on physical properties at or near the ocean floor (*11*). An unmanned, self-contained capsule is dropped to the ocean floor from a surface ship. For a predetermined period of time, ranging from days to months, data are automatically collected by appropriate sensors and recorded on

ACCURATE
MOISTURE
ANALYSIS

fibers • grains • semi-liquids • solids



Control costs and maintain consistent quality through accurate moisture analysis.

Dietert-Detroit Moisture Tellers are widely used in industry for research and analysis of foodstuffs, chemicals, fibers, foundry sands, soaps, tobacco, ceramics and similar materials. Complete range of models available.

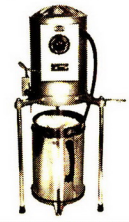

MODEL 278A-12 is equipped with two 8″ dia. x 12″ deep sample pans, to accommodate bulky samples such as wool.

HARRY W. DIETERT CO.
CONTROL EQUIPMENT
9330 Roselawn Avenue • Detroit, Michigan 48204
Telephone: 933-9790 (Area Code 313)

Please send Moisture Teller Catalog and prices.

Name_____
Company_____
Address_____
City_____ State_____

Circle No. 27 on Readers' Service Card

Separate amines easily, efficiently with

New Chromosorb* 103

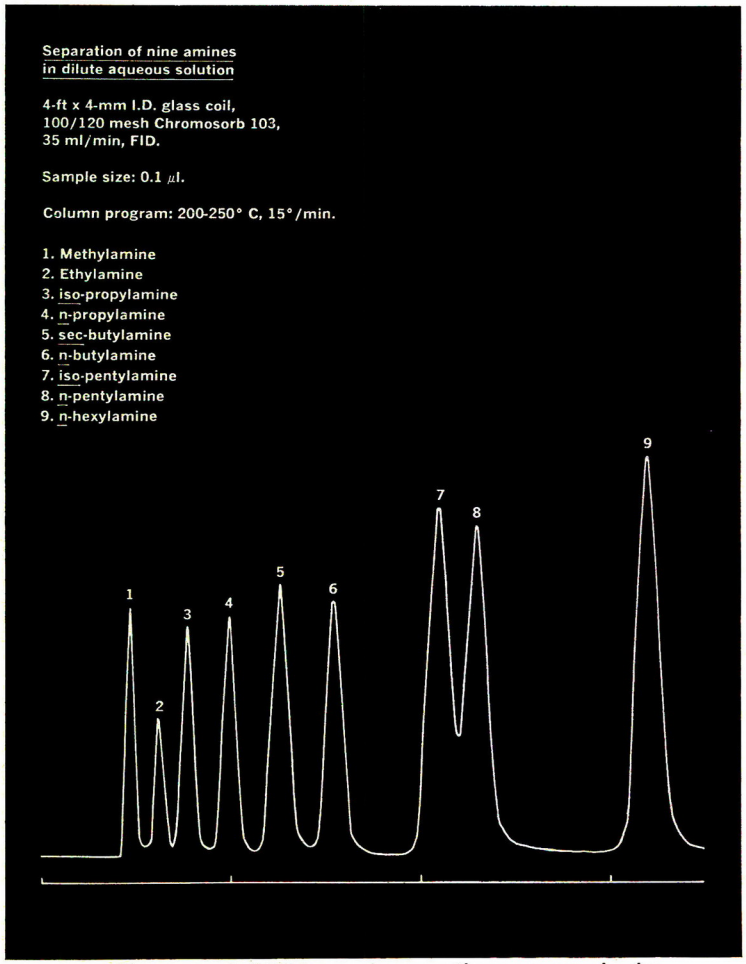

Chromosorb 103 is a polyaromatic porous resin developed by Johns-Manville as a solid-type support for the separation of amines and basic compounds.

Until now, amine separation has been both laborious and difficult. With new highly selective Chromosorb 103, it's fast and easy.

For more specific information, write for our bulletin FF-181. Johns-Manville, Box 290-C, Trenton, New Jersey.

Johns-Manville

*Chromosorb is a Johns-Manville registered trademark for its brand of products developed for use as support material or adsorbents for gas chromotography.

Circle No. 44 on Readers' Service Card

magnetic tape within the capsule. At the appropriate time, the capsule is returned to the surface by a command transmitted from the surface ship, the tapes are removed and the data processed as is appriate.

A variety of sensors can be employed. Among the applications already tried out are the measurement of deep sea tides by the recording of pressure fluctuations within one millimeter, the measurement of temperatures within a few millionths of a degree, and the measurement of water currents in the range of 0.1 to 10 centimeters per second.

Minerals on and below the Ocean Floor

General oceanographic surveys, some aspects of which have been mentioned, are often aimed in part at locating exploitable resources at and below the ocean floor. Detection methods, many of which employ virtually all of the general methods of analytical chemistry as well as geophysical and other types of study and information, are far ahead of the commercial exploitation of ocean bottom minerals. Many known deposits await either lower costs of "mining" or higher market price of the products before they will be exploited commercially on any large-scale basis. Nevertheless, there are some general areas in which improvements are needed in analytical procedures and methods, including, for example, more adaptation of analytical systems to shipboard operation, and more data on "normal" concentrations over more areas of the oceans in order that anything unusual can be more readily noted, and more rapid and complete access to the masses of such data which have already been collected by various governmental and private agencies.

One type of potentially exploitable mineral resource known to exist on the ocean floors consists of manganese nodules, ranging typically from one to 20 centimeters in diameter. Growth layers are often in evidence, frequently around some foreign nucleus such as a shark's tooth; this fact and related factors point clearly to formation by precipitation. It has been estimated that deep sea nodules are being con-

Introducing the NEW 1072 Signal Averaging Computer...

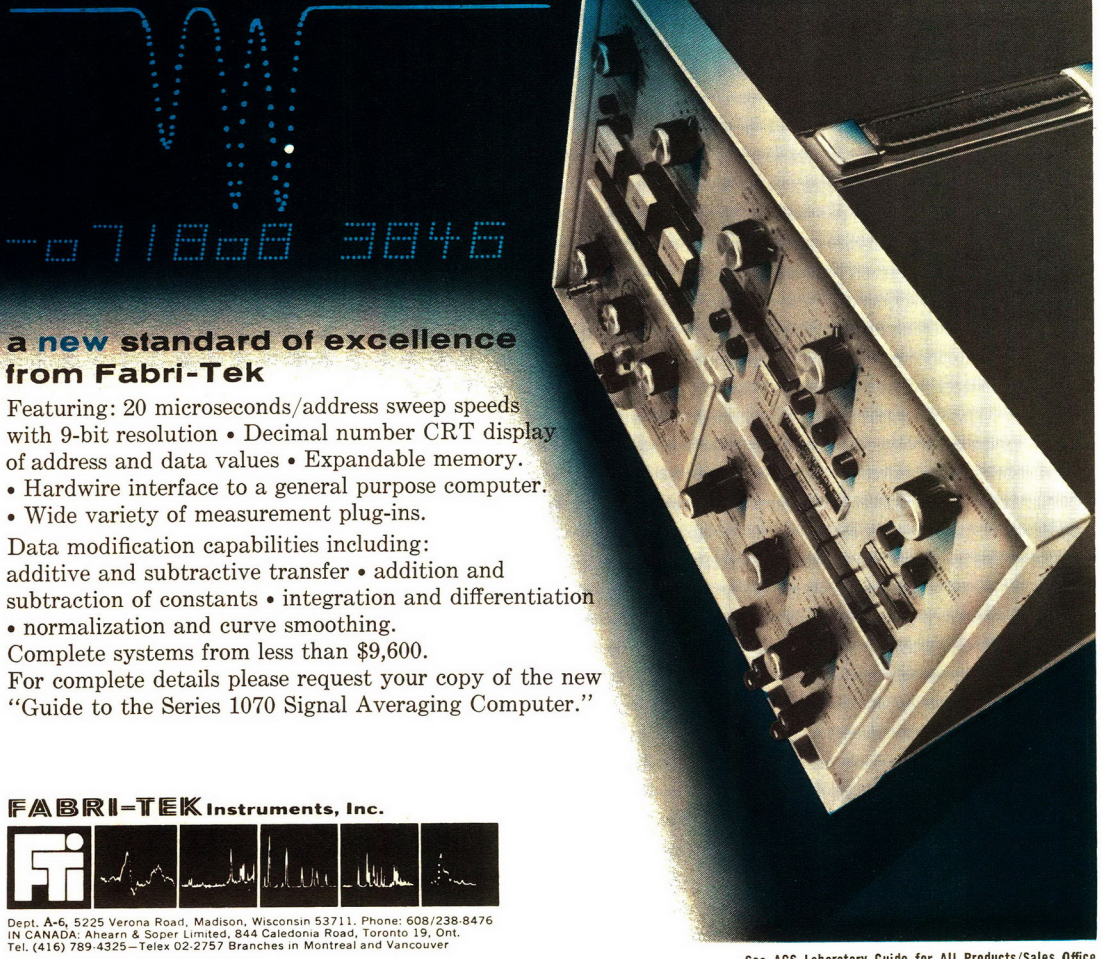

a new standard of excellence from Fabri-Tek

Featuring: 20 microseconds/address sweep speeds with 9-bit resolution • Decimal number CRT display of address and data values • Expandable memory. • Hardwire interface to a general purpose computer. • Wide variety of measurement plug-ins.

Data modification capabilities including: additive and subtractive transfer • addition and subtraction of constants • integration and differentiation • normalization and curve smoothing.

Complete systems from less than $9,600.

For complete details please request your copy of the new "Guide to the Series 1070 Signal Averaging Computer."

FABRI-TEK Instruments, Inc.

Dept. A-6, 5225 Verona Road, Madison, Wisconsin 53711. Phone: 608/238-8476
IN CANADA: Ahearn & Soper Limited, 844 Caledonia Road, Toronto 19, Ont.
Tel. (416) 789-4325—Telex 02-2757 Branches in Montreal and Vancouver

Circle No. 32 on Readers' Service Card

tinually deposited now at a rate such that, for example, the amount of nickel deposited annually is equal to the Free World consumption (*12*). If more knowledge could be obtained as to the origin of the nodules, it is conceivable that the natural process could be controlled and expanded to include other substances with economically beneficial results.

Typical chemical compositions of these nodules include manganese (24%), iron (14%), cobalt (0.35%), nickel (0.99%), and copper (0.53%). There is much variation from these typical values. The Westinghouse Astronuclear Laboratory has recently developed a new nondestructive technique based upon neutron activation for the rapid analysis of these nodules. At the present time, the recovery of these deposits for their manganese content is economically marginal. This condition could change markedly, however, particularly because most of the present commercial sources of manganese lie outside the United States and primarily in the eastern European nations.

More recently, during some routine sampling and analyses of sediments from the floor of Green Bay, large quantities of manganese pellets were found there as well (*13*). The pellets were mixed about half-and-half with sand. While the average manganese content, about 8 or 9%, is less than that of the manganese nodules found on the floor of the open oceans, the Green Bay deposits are readily accessible at depths of only 50 to 100 feet and, in addition, are solely within the continental United States.

Fisheries

Although analytical chemists more frequently use fishing as an avocation rather than as a part of their vocation, there are definite relationships between analytical chemistry and the fisheries industry. We have already noted the roles of nutrients and temperature in locating the presence of fish. A few more specific comments and illustrations may be of interest.

The methodology used in fish harvesting and processing has not changed over the last couple of decades nearly so markedly as has the



methodology in most other technical fields of endeavor, and it is reasonable to expect that analytical chemists and analytical chemistry can participate effectively in future efforts along these lines. Among the general areas in which improvements are conceivable are in better fish detection systems, in better preservation methods, and in the development and marketing of new fish-based products.

Fish protein concentrate, FPC, is a tasteless, white or slightly grayish flour with a minimum of 75% pure animal protein which is made by processing whole bodies of inexpensive, and often otherwise undesirable, fish—especially hake (*14*). Common processing procedures involve grinding up the whole fish and removing the water and lipids by solvent extraction. Much of the bone may also be removed, in order to reduce the fluoride content of the final product. Approximately 500 pounds of raw fish are required to yield 150 pounds of FPC.

The use of fish protein concentrate is already common in some countries, as an additive in many food products. There is now a very serious world-wide diet deficiency of protein, and there can be no reasonable doubt that a greatly expanded use of FPC could go far in meeting this need. The President's Panel on Oceanography has estimated that a small daily supplement of FPC could meet the world protein deficit for as little as two dollars per person annually.

There has been much objection in the United States to the use of FPC, particularly on the basis of psychological factors relating to the fact that whole fish are included. It was not until 1967 that the Federal Food and Drug Administration first approved the use of FPC for human consumption, and even then with the restriction that packaging be limited to units not exceeding one pound net weight. Strict analytical specifications were established, as is surely proper for any product intended for human consumption, which may be summarized briefly as follows:

- protein (N × 6.25) : 75% or more by a standard AOAC method
- moisture : less than 10% by weight of the final product
- fat : less than 0.5% by weight of the final product
- residual isopropyl alcohol (if used in the extraction process) : less than 250 parts per million
- residual ethylene dichloride (if

Only from Kimble one-stop shopping

Now, exclusively from Kimble, there's superbly crafted laboratory ware for your every requirement:

Kimble *reusable* glassware. Kimble *disposable* glassware. Kimble *reusable* plastic ware. Kimble *disposable* plastic ware.

. . . all available from your professional "supermarket"— your nearby laboratory supply house.

This unique Kimble advantage provides single-source convenience and economy. It's backed by the name that stands for quality in materials and craftsmanship, and innovative design leadership.

Simplify your next order for labware products — *glass* or *plastic; reusable* or *disposable* — specify Kimble!

Kimble
PRODUCTS by OWENS-ILLINOIS
Toledo, Ohio 43601

Circle No. 1 on Readers' Service Card



Here's a new instrument that makes Far Infrared routine and push-button easy.

Up until now, working with Far IR was a time-consuming task that meant working with non-standard equipment.

But Perkin-Elmer has changed that with the FIS-3, a new double-beam instrument designed specifically for the Far IR spectral region—one that will provide results on a routine, non-complicated basis.

For one thing there's no need to stand around and adjust knobs and dials constantly. The FIS-3 is made for the research scientist who wants to push the button and walk away to more important tasks while the instrument scans the entire FIR range from 400 to 30 cm^{-1} (25-333μ) automatically and unattended.

To insure that maximum system energy is available, the entire optical path is evacuated—water vapor can be efficiently and quickly removed from the entire instrument in just twelve minutes. This, of course, means that you get into operation faster and run more samples per unit operating time. If desired, the sample compartment can be purged with dry air, and the remainder of the instrument evacuated.

Spectra are conveniently presented on a preprinted chart. Presentation is unbroken, continuous, and at a constant scale factor over the entire range. All the information is immediately available, easy to read directly from the chart.

Another Far IR problem has been minimized—that of sampling other than ambient temperatures. The FIS-3's unique switch-selectable double chopping mode of operation ignores these sampling effects, provides undistorted band depths.

As part of our system-oriented approach we offer a complete line of liquid, solid and gas sampling accessories, many of them specially made for use in a vacuum environment. Several of them hold multiple samples, so you can make successive sample runs without disturbing the instrument's equilibrium.

It all adds up to a new standard instrument for the Far IR. Both routine and research grade spectra are now available from one instrument.

Write for the new and detailed brochure about this newest instrument from the leader in IR. Instrument Division, Perkin-Elmer Corporation, 702 Main Avenue, Norwalk, Connecticut 06852.

PERKIN-ELMER

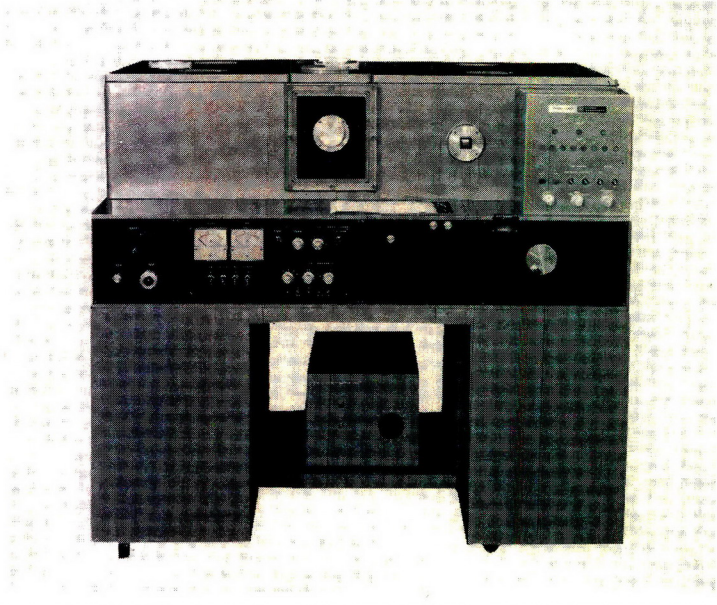

Circle No. 140 on Readers' Service Card

used in the extraction process) : less than 5 parts per million
fluoride : less than 100 parts per million
free of *E coli* and salmonella
"only faint fish odor and taste"

A specific recent development can serve to illustrate a very different type of innovation in instrumentation in the fisheries industry. One of the major limitations in the shrimp industry in the Gulf of Mexico is the fact that the shrimp burrow into the floor sands in the daytime, so are available for harvesting only when they come out to forage at night. In a rather elaborately designed and conducted research study, a means was found to make daytime harvesting feasible (*15*). An electrical device which repetitively emits brief pulses of electricity is dragged along a few feet ahead of the trawl net. The shrimp apparently are literally shocked up from their burrowing locations into positions where they are gathered by the trawl.

It was found that the daytime catch with the electro-trawl system was about equal to the normal nighttime catch. Interestingly enough, the catch at night was actually decreased by use of the electrical pulse system—conceivably the shrimp, which were already foraging around just above the bottom, were given sufficient warning by the electrical shock to get out of the way before the trailing net reached them!

Another area in which we can anticipate further developments involving analytical chemistry and the fisheries industry is in the area of inspection for health purposes of canned fish and fish products. As was pointed out in the August 1968, *Newsletter of the American Society for Oceanography,* there is now virtually no official inspection of anything, from the fishing vessel to the packaged products. Some laws do exist, of course, on both federal and state levels, but they generally do little more than call for "wholesomeness" with little or no provision for meaningful inspection and enforcement. A major effort was made in the 90th Congress to improve the situation with the introduction of HR 15155, the "Wholesome Fish Act." The health situation is so serious, potentially if not actually, that further developments are surely forthcoming. Just what form these regulations will take is not clear, but it is clear that they must be based quite directly upon the designation of analytical standards and analytical procedures to assure compliance with those standards.

Bioactive Marine Natural Products

It has been estimated that there are thousands of marine organisms known to contain toxic substances, that less than one per cent of these have been examined for their biological activities, and that the active agents have been determined in only about a dozen of these (*16*). It has further been claimed that not one industrial or government agency is making any systematic and continuous exploration of bioactive marine natural organisms (*17*). Thus this broad area presents a tremendous field for further research and development, and it is absolutely essential that analytical chemists and analytical chemistry must play central roles, as has been the case over the last few decades in other areas of natural product chemistry.

The possibilities of usefully applying drugs from the sea have long been recognized. For example, some Egyptian hieroglyphics of 2700 B.C. appear to show poisonous puffer fish, and Pliny (50 A.D.) recommended the use of ground up stingray barbs as a pain reliever for toothache.

Let us briefly mention a few more current reports, all of which must be considered now as strictly preliminary experimental observations and definitely not as established forms of treatment. The "red tide," which appears occasionally along the Pacific coastal beaches under certain weather and temperature conditions and which consists of single-celled plankton, not only can kill fish, but an antibiotic separated from it is effective in depressing respiration and in reducing blood pressure. An aqueous extract of certain sponges, diluted considerably, has inhibited the growth of staphylococcus, a scourge of hospitals. An extract from a hagfish has shown potential

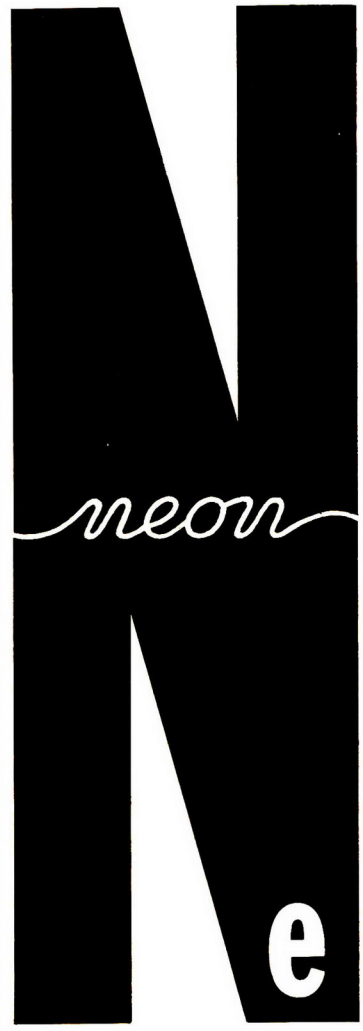

Neon. We have it for you pure and ultra pure. In a variety of pressures and containers.

For this year's catalog, write: Rare and Specialty Gases Dept., Airco Industrial Gases, 150 East 42nd Street, New York, N.Y. 10017.

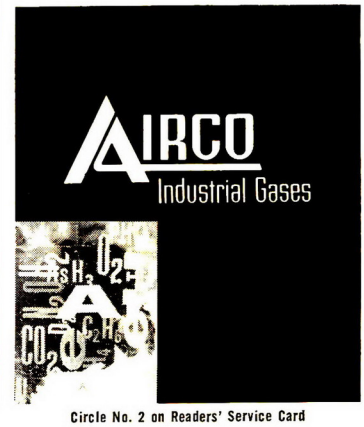

Circle No. 2 on Readers' Service Card

Now in bead form for chromatography of biologic substances...

Sephadex®

Ion Exchangers

Because of its advantages—stability and inertness—Sephadex has been used to produce a new class of ion exchangers: QAE-, DEAE-, CM- and SE-Sephadex. Since their introduction they have been used extensively, particularly in the biochemical and clinical field.

In the new bead form they will be more useful both for laboratory and manufacturing scale processes. Their spherical shape gives increased mechanical strength and leads to easier column packing. More uniform particles result in improved hydrodynamic properties.

All Sephadex Ion Exchangers have a high capacity and low nonspecific adsorption. They are available in two types that differ in porosity, thus offering flexibility for your specific requirements. Sephadex Ion Exchangers are of analytic grade purity and are produced under rigorous quality control, thus ensuring uniform products to give accurate and reproducible results.

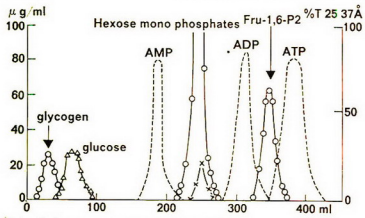

Model experiment with glycogen, glucose, sugar phosphates and adenosine phosphates on a column of DEAE-Sephadex A-25.

(From Biochim. Biophys. Acta 74 (1963) 588, by permission of the author)

Anion Exchangers

Type	Grade	Ionic Form	Capacity (meq/g)	Bed Volume[1] (ml/g)
QAE-Sephadex A-25	40-120μ	Cl^-	3.0 ± 0.4	5-8
QAE-Sephadex A-50	40-120μ	Cl^-	3.0 ± 0.4	30-40
DEAE-Sephadex A-25	40-120μ	Cl^-	3.5 ± 0.5	5-9
DEAE-Sephadex A-50	40-120μ	Cl^-	3.5 ± 0.5	25-33

Cation Exchangers

Type	Grade	Ionic Form	Capacity (meq/g)	Bed Volume[2] (ml/g)
CM-Sephadex C-25	40-120μ	Na^+	4.5 ± 0.5	6-10
CM-Sephadex C-50	40-120μ	Na^+	4.5 ± 0.5	32-40
SE-Sephadex C-25	40-120μ	Na^+	2.3 ± 0.3	5-9
SE-Sephadex C-50	40-120μ	Na^+	2.3 ± 0.3	30-38

1. In Tris—HCl buffer, pH = 8.3, ionic strength = 0.05.
2. In sodium phosphate buffer pH = 6, ionic strength = 0.06.

For additional technical information, including booklet on Sephadex Ion Exchangers, write to:

PHARMACIA FINE CHEMICALS INC.
800 Centennial Avenue, Piscataway, N. J. 08854
Pharmacia (Canada) Ltd., 110 Place Crémazie, Suite 412, Montreal 11, P.Q.

(Inquiries outside U.S.A. and Canada should be directed to PHARMACIA FINE CHEMICALS AB, Uppsala, Sweden.)

Circle No. 10 on Readers' Service Card

See ACS Laboratory Guide for All Products/Sales Office

usefulness in slowing down heart action as, for example, during open heart surgery. Some starfish and some sea urchins have yielded steroids which are chemically similar to digitalis, a potent cardiac drug. A substance derived from clams has exhibited some antitumor properties on mice.

It would seem that virtually all types of chemical, analytical, and bioanalytical techniques could profitably be employed in further research and development in the area of bioactive marine natural products, from fish and other types of marine organisms. One of the specific desiderata worthy of particular stress is that it would be highly desirable to study the various substances close to where they are found, rather than storing and shipping them to central research centers far from the sea and thus running the risk of change in their chemical and biological characteristics.

Kelp and other forms of marine algae, as well as fish, are possible sources of biologically active substances. One of the present author's colleagues, Professor Solomon Marmor, is currently heading an active research effort in this direction.

Education and Personnel

Academic curricula directly in the marine sciences invariably include regular course work in analytical chemistry. One goverment publication lists "typical requirements for undergraduate preparation leading to graduate study" in four sub-specialties—marine biology, oceanography, fisheries, and marine geology (*18*). In every one of these curricula, courses in qualitative analysis and in quantitative analysis are listed either as required or as recommended. Furthermore, it is not unusual to find that the laboratory work in some of the more advanced courses offered in marine science curricula bears much in common with courses in instrumental methods of analysis as offered in regular chemistry curricula.

It must be recognized and stressed that curricula and degrees directly in marine science are by no means the only educational avenues into careers in the marine sciences. In fact, a 1964 NSF survey of 2,650 persons in marine science and technology revealed that 616 held degrees in marine science; the remainder had degrees in the various basic disciplines. Other more recent estimates are generally consistent on a percentage basis. In brief, virtually every kind of science and technology which is ocean-based has its counterpart which is land-based; in other words, every "oceanology" field has a counterpart in "landology."

The first recommendation resulting from a California state study is that, "Education programs. . . stress the fundamental sciences and engineering in the education of marine scientists and engineers, who must first of all be competent in a basic academic discipline, secondarily in applications to oceans and to oceanic problems" (*19*). The same report, in projecting future manpower needs for that state, included a prediction that probably not more than 5% of the future manpower needs for industrial ocean-related scientists and technologists would be for persons whose major training is in ocean science and technology, the balance of the needs being for persons with heavy training in the basic fields of science and engineering. In fact, the importance of mathematics, physics, and chemistry is stressed heavily even for the education of fisheries biologists.

One of the main points of this entire paper is that analytical chemistry and analytical chemists are almost ideally suited for playing key roles in the future exploitation of marine resources, not only because of the central significance of the use of chemical analyses and instrumentation in gathering necessary data, but even more important because of the analytical chemist's expertise in such areas as sampling, measurement, separation of chemical species, concentration of trace components, processing and assimilating masses of data, and also because of his wide theoretical and practical scientific knowledge and interests.

The Complex Legal Situation

There are worldwide legal complications which underlie virtually all practical considerations relating

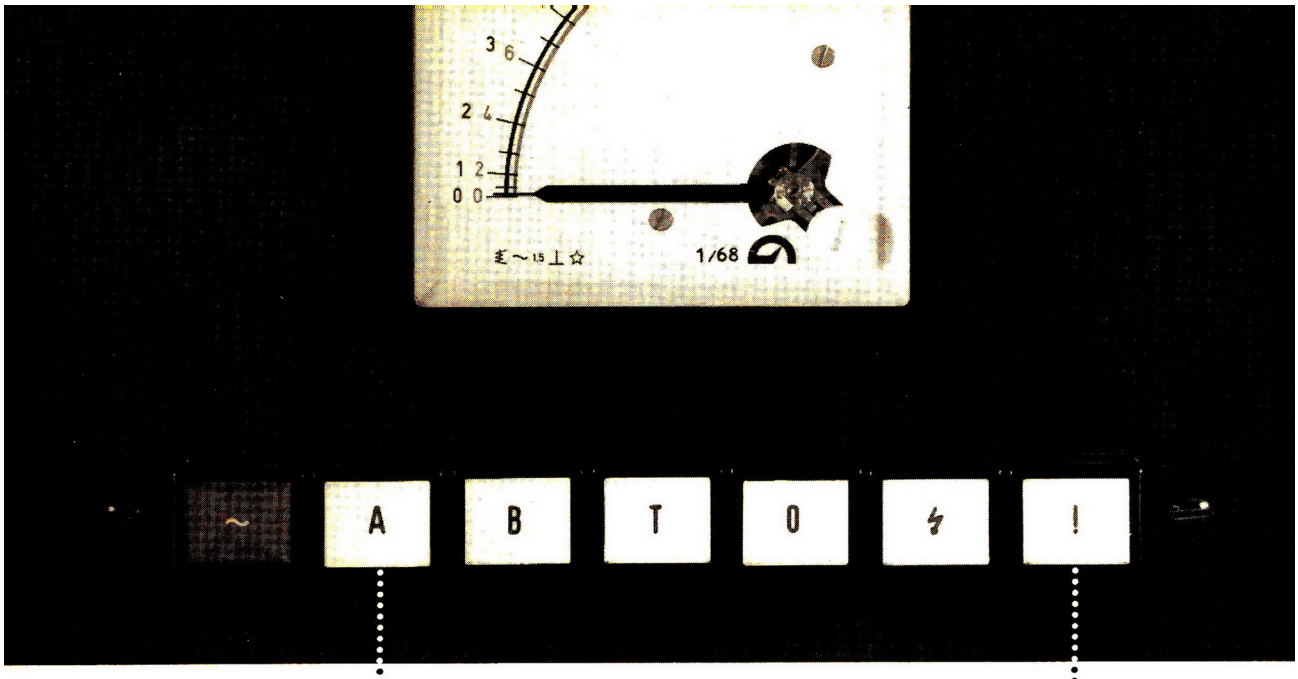

This button does all the work. Push it and . . .
It opens the shutter.
Exposes the film the proper length of time.
Closes the shutter.
Advances the film to the next frame.
Advances the frame counter.
Recocks the shutter ready for the next exposure.

This is the panic button. It flashes when . . .
You forgot to load the camera.
You've run out of film.
The film is torn.
You've reached the end of the roll.
You can't push button A while button ! is flashing.

Introducing the Photomicroscope II...

A tale of two buttons.

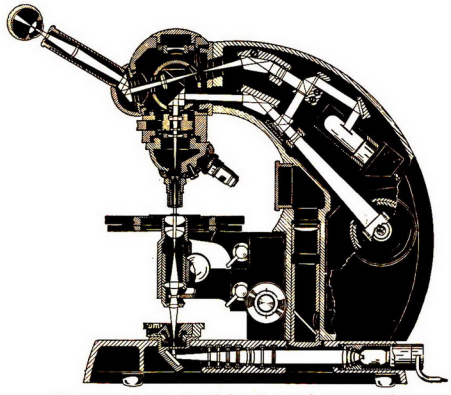

Cut-away view of the Zeiss Photomicroscope II.

What the other buttons do is give you added versatility. But there are more important things to talk about here.

Such as the stability between camera and microscope only an integrated system can offer.

Such as exposure times from 1/100 sec. to hours, if need be.

Such as automatic exposure control for all films rated from 2½ to 8000 ASA.

Such as a system specifically designed to take optimum advantage of the latest high speed color films.

Such as increased sensitivity for selected-area "spot" readings—particularly helpful for dark-field and fluorescence work.

Such as a whole lot more.

The new ZEISS Photomicroscope II makes photomicrography literally a snap—as easy as using any quality 35mm automatic amateur camera. But it's as professional an instrument as you can get.

For complete information, including what the other buttons do, write Carl Zeiss, Inc., 444 Fifth Avenue, New York, N.Y. 10018.

Nationwide service.

ZEISS

THE GREAT NAME IN OPTICS

CARL ZEISS
WEST GERMANY

ATLANTA, BOSTON, CHICAGO, COLUMBUS, DENVER, HOUSTON, LOS ANGELES, PHILADELPHIA, ST. LOUIS, SAN FRANCISCO, SEATTLE, WASHINGTON, D. C.

Circle No. 114 on Readers' Service Card

new ultra superior purity lets you see the past more clearly



Only Ultra Carbon offers four levels of purity to provide conditions needed for standard to critical evaluation. When your analysis requirements call for a low metallic blank level and samples are restricted to mgms.—whether it be for archaeological samples or aircraft engine contaminants—Ultra Carbon's new Ultra Superior Purity graphite can provide the sensitivity and precision needed. And for less critical evaluations, Ultra Carbon supplies three other purity levels: Ultra "F", the famed purity level that has led the industry for 25 years; Spectro-Tech, an intermediate purity level; and Standard, for routine metallurgical analysis. Write for more detailed descriptions of any of these products. Ultra Carbon Corporation, P.O. Box 747, Bay City, Michigan 48706.

Ultra "F", Spectro-Tech and Ultra are Registered Trade Marks of Ultra Carbon Corporation.

ULTRA CARBON®

Circle No. 72 on Readers' Service Card

to the economic exploitation of marine resources. Let us mention only one specific facet of the complexity of the legal siuation. The 1958 Geneva Convention on the Continental Shelf defined the continental shelf as "areas adjacent to the coast but outside the area of the territorial sea to a depth of 200 meters or, beyond that limit, to where the depth of the superjacent waters admits of the exploitation of the natural resources of the said area." In view of the latter part of this definition, and in view of the rapidly advancing technology, some of which has been mentioned in this paper, is there really any limit to the "continental shelf" to which any technologically advanced nation can claim jurisdiction? As is attested by frequent articles in the daily newspapers, these matters are of considerable practical importance in present-day international relations, and they are of very active concern in the United Nations.

As stated in a recent report to the President and to the Congress of the United States, this "nation's stake in the oceans is therefore an important part of its stake in the very future of man's world" (*20*). It is impossible, of course, to predict with certainty what this stake will be. It is clear, however, that analytical chemistry and analytical chemists will continue to play very vital roles in the ongoing development of the marine sciences and marine technology.

Literature Cited

(1) J. L. Mero, "The Mineral Resources of the Sea," Elsevier Publishing Co., Amsterdam and New York, 1965.
(2) J. D. H. Strickland and T. R. Parsons, "A Practical Handbook of Sea-Water Analysis," Fisheries Research Board of Canada, Ottawa (1968).
(3) D. F. Martin, "Marine Chemistry, Volume 1: Analytical Methods," Marcel Dekker Co., New York, 1968.
(4) "Navy/Marine Corps Research and Development Problems," Dept. of Navy, Washington (1967).
(5) N. R. Anderson and J. R. Jadamec, private communication (manuscript submitted to *Deep-Sea Research*).
(6) M. E. Thompson and J. W. Ross, Jr., *Science*, **154**, 1643 (1966).
(7) C. M. Shigley, *Ocean Industry*, **3**, 43 (November 1968).
(8) A. R. Miller, C. D. Densmore, E. T. Degens, J. C. Hathaway, F. T. Manheim, P. F. McFarlin, R. Pocklington, and A. Jakela, *Geochimica et Cosmochimica Acta* **30**, 341 (1966).
(9) M. Weiss, *Oceanology International*, (Sept.-Oct. 1968), page 44.
(10) G. Sorenson, and R. C. Honey, *Ocean Industry*, **3**, 51 (Oct. 1968).
(11) F. E. Snodgrass, *Science*, **162**, 78 (1968).
(12) *Chem. Eng. News*, **47**, 17 (Feb. 10, 1969).
(13) R. J. Harker, private communication (Dec. 17, 1968).
(14) R. R. Nunn, *Ocean Industry*, **3**, 47 (Nov. 1968) and **4**, 36 (Jan. 1969).
(15) N. L. Pease and W. R. Seidel, *Commercial Fisheries Review*, **29**, 58 (1969).
(16) R. E. Hillman, *Oceanology International*, (Sept.-Oct. 1967), page 33.
(17) L. F. Miloy, *Ocean Industry*, **3**, 74 (June 1968).
(18) "University Curricula in the Marine Sciences," Interagency Committee on Oceanography, for the National Council on Marine Resources and Engineering Development, Washington (1967).
(19) Subcommittee on Education and Research, Governor's Advisory Committee on Ocean Resources, Sacramento, California (1966).
(20) "Our Nation and the Sea." Report of the Commission on Marine Science, Engineering and Resources, Washington (1969).



***ROBERT B. FISCHER** is Dean of the School of Natural Sciences and Mathematics and Professor of Chemistry at the California State College, Dominguez Hills. Among several distinctive features of this fairly new institution is its stress upon interdisciplinary fields of study, including some course work and research in marine sciences. Prior to joining the original planning staff of this College, Dr. Fischer was for 15 years a member of the chemistry faculty of Indiana University. He has written numerous research articles and textbooks in several areas of quantitative analysis and chemical instrumentation, also being the co-author of two recent textbooks in quantitative chemical analysis.*

Bell & Howell introduces the first complete mass spectrographic analytical service for SOLIDS.

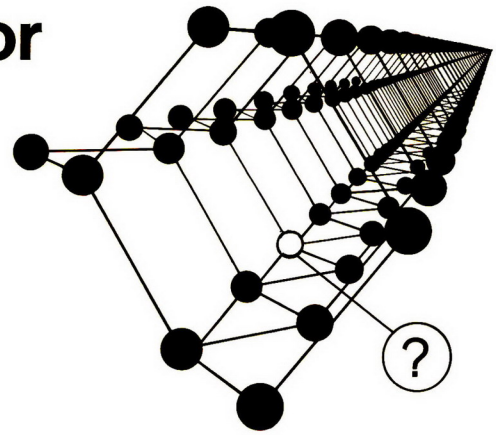

Mass spectrometry permits analysis of solids with detection limits as low as 0.0005 ppm with low sample consumption. Until recently this analysis has been economically limited to owners of highly sophisticated equipment.

Obviously, a service was needed that would cater to the needs of the "occasional" mass spectrometry user.

Bell & Howell was the logical one to offer it. They are the recognized leaders in the development of analytical techniques for mass spectrometry. And they possess the full range of equipment required to do the job. (The Analytical Instruments Division of Bell & Howell is the world's leading manufacturer of mass spectrometers.)

Result: a service capable of analyzing virtually *any* solid sample is now available to you at a *reasonable* cost.

For example, analytical costs are as low as a few dollars per impurity for impurities in the ppb range. Samples commonly contain between 30 to 40 impurities. Ultrapure materials such as those of semiconductor grade generally contain 10 to 15.

Typical materials which may be analyzed:

Semiconductors—All types, II-VI, III-V, Group IV and binary systems, epitaxial and thin films.

Metals—Virtually all metals.

Chemicals—Refractories, high resistivity, salts, rubber, plastic, solutions.

Biological Materials—Blood, urine, bone, etc.

Minerals—Glass, ores, rocks, tektites.

Miscellaneous—Wood, wool, cotton, other common materials.

You are welcome to visit our laboratories and participate in the analysis of your materials. Normal delivery is 2-3 weeks. Three-day service is also available at special rates.

ELECTRONIC MATERIALS DIVISION

BELL & HOWELL

360 SIERRA MADRE VILLA, PASADENA, CALIFORNIA 91109 ▪ (213) 796-9381

BELL & HOWELL

ELECTRONIC MATERIALS DIVISION
360 Sierra Madre Villa, Pasadena, California 91109

Please send me all the facts about your
New Mass Spectrometry Analytical Service.
I am also interested in:

☐ Gallium Arsenide crystals and other compound semiconductors

☐ X-Ray Diffractometry Service

NAME_____ COMPANY_____

ADDRESS_____ CITY_____

STATE_____ ZIP_____

AC

Circle No. 102 on Readers' Service Card

CSA approved!

heat desiccator interiors up to 250°C...safely!

Glas-Col heating mantle allows you to use your desiccator as a safe, efficient vacuum drying oven

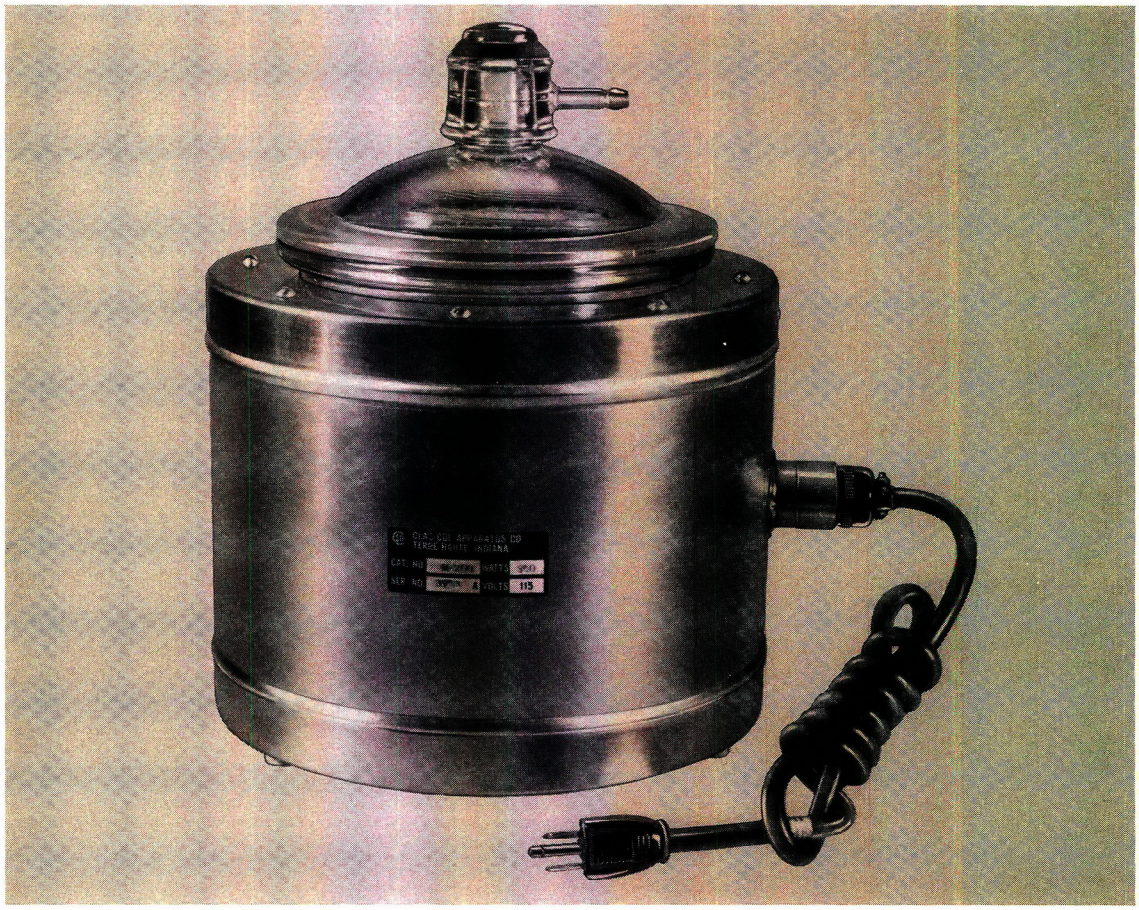

■ This Glas-Col heating mantle bears the Canadian Standards Association seal of approval for heating heavy-walled vessels used in vacuum drying of samples. For a small cost, it will convert your desiccator into a safe, efficient vacuum drying oven.

Its uniform heat minimizes chance of thermal strain to glass vessels. And it provides an effective shield in rare instances when vessels do collapse under high vacuum-high pressure conditions.

Glas-Col desiccator heating mantles have been used for years—safely, and with complete success.

CATALOG NUMBER	DESICCATOR FLANGE DIAMETER	WATTAGE	PRICE
TM-200	160mm	330w-115v	$45.00
TM-202	200mm	380w-115v	57.00
TM-204	250mm	380w-115v	65.00

GLAS-COL®
HEATING MANTLES

Glas-Col Apparatus Company
Dept. AC, 711 Hulman Street, Terre Haute, Indiana 47802
U.S. Patents 2,231,506; 2,739,220; 2,739,221; 2,282,078.

Circle No. 35 on Readers' Service Card

Circle No. 92 on Readers' Service Card →

Wouldn't it be great if someone designed a 160 g top-loader with 1 mg accuracy and all-digital readout?

Someone has. Sartorius.

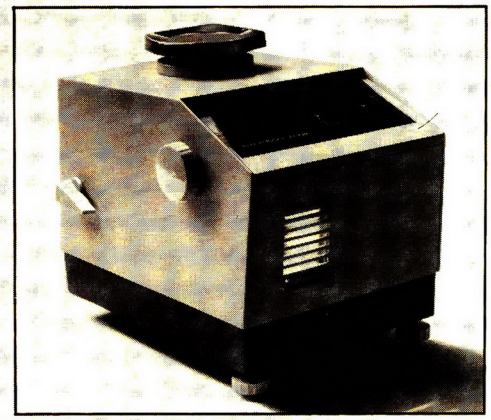

There are other top-loading balances with 160 g capacity, but none is as accurate and easy to read as the new Sartorius 2255... and none is as stable.

To eliminate interpolation error with 'between the line' results, the Model 2255 provides all-digital readout to 1 mg. To further insure accuracy, there is absolutely no discernible swing—this balance stays at the indicated weight. There's no need to squint, either. Its huge new optical scale is a pleasure to read, even under the most adverse lighting conditions.

At only $725, the above features alone would make the 2255 a great buy, but there are more. The Taramatic® single knob taring system and below-balance weighing accessories are included at no extra cost.

For research, quality control, student use, or any other application requiring 1 mg weighing accuracy at loads up to 160 g, this is the simplest, yet most advanced top-loading balance available.

Sartorius all-digital top-loaders also come with higher capacities. Our 40-page catalog describes them all. For your copy, just write: Sartorius Division, Brinkmann Instruments, Cantiague Road, Westbury, N.Y. 11590.

sartorius balances



The excellence of our manual spectrophotometer is automatic

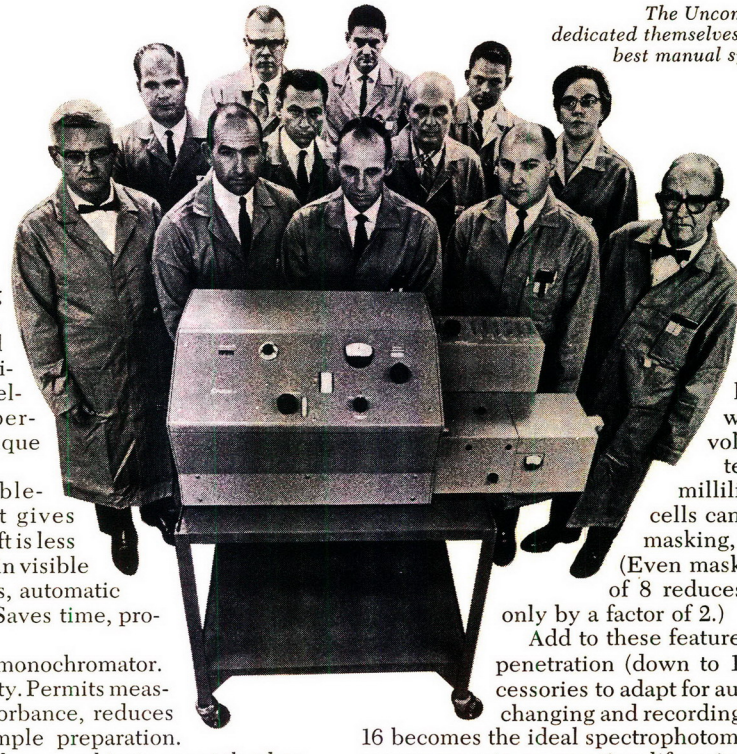

The Uncompromisers—They dedicated themselves to producing the best manual spectrophotometer. And did it.

And like our recording spectrophotometers, the CARY 16 manual instrument automatically achieves its excellence and reliable performance through unique design features.

First, take the double-beam photometer. It gives high zero stability (drift is less than 0.00016 abs/hour in visible range) and continuous, automatic blank compensation. Saves time, produces reliable data.

Next, the double monochromator. This insures light purity. Permits measurements at high absorbance, reduces errors, minimizes sample preparation. The CARY 16's the only manual instrument that has a double-beam, double monochromator system.

Then the photometric accuracy. It's the highest of any spectrophotometer made, manual or recording. 0.00024 absorbance near zero, 0.001 near 1 absorbance.

Finally, the exceptional beam geometry is particularly important where sample volumes are limited. Normally, 1 milliliter semi-micro cells can be used. With masking, micro cells. (Even masking by a factor of 8 reduces the S/N ratio only by a factor of 2.)

Add to these features the deep UV penetration (down to 1700Å) plus accessories to adapt for automatic sample changing and recording, and the CARY 16 becomes the ideal spectrophotometer for kinetic measurements or exacting life science studies, as well as for general analytical work.

A price list and catalog are yours for the asking. Write Cary Instruments, a Varian Subsidiary, 2724 South Peck Road, Monrovia, California 91016. Ask for Data File A709-69.

CARY 16

Circle No. 84 on Readers' Service Card

Circle No. 66 on Readers' Service Card →



With Baker-flex, charring means well done...not burned

A charred TLC plate doesn't have to look like the bottom of a frying pan, just because it's flexible. The new BAKER-FLEX™ flexible TLC sheet has ended all that. The Silica Gel IB and Aluminum Oxide IB sheets permit sulfuric acid charring . . . all BAKER-FLEX sheets utilize the normal visualization techniques you're familiar with. In other words, BAKER-FLEX products combine some of the best features of glass plates with the many advantages of flexible sheets. You get increased resolution and better definition on BAKER-FLEX, because its thicker adsorbent layer permits loading of two to eight times more sample than on any other flexible plate. These new sheets come in two sizes (5 cm x 20 cm and 20 cm x 20 cm) with eighteen different adsorbents, including fluorescents, so now you can use flexible sheets for more types of separations than ever before. And that's not all. BAKER-FLEX sheets are rugged, pre-coated, flexible, abrasion resistant, have a solvent-resistant substrate, can be cut to size and written on. If you would like more details, plus five each of four different flexible sheets (two of which can be charred) to try in your existing separation programs or in the development of new ones, just order the new BAKER-FLEX Selector Kit #1 (Comm. No. 4490), priced at $10, from your J. T. Baker distributor.

J.T.Baker CHEMICAL®

J. T. BAKER CHEMICAL COMPANY, PHILLIPSBURG, NEW JERSEY 08865

Ace High Vacuum Stopcock



- Rugged
- All Glass & Teflon

with new easy action plug!

New easy action plug adds real fingertip ease to the high performance of the rugged Ace high vacuum stopcock. The new plug is interchangeable and can be ordered separately for original 8194 vacuum stopcock barrels.

Ace high vacuum stopcock features smooth action semi-needle valve that permits fine adjustment of opening. "O" ring makes positive closure against glass seat. Reference marks on body and handle aid repetitive setting. The stopcock barrel is made of heavy walled glass. It can be used with corrosive gases, will withstand at least 30 lbs. internal pressure. All glass construction permits annealing. Write Ace for sizes, prices!

ACE GLASS INCORPORATED

Vineland, New Jersey

Louisville, Ky. Ludlow, Mass.

Circle No. 128 on Readers' Service Card

Circle No. 100 on Readers' Service Card →

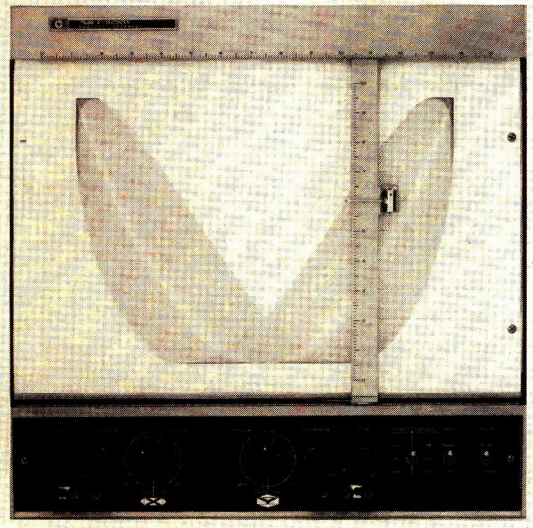

Industry Standards

These general-purpose XY recorders set new price/performance standards for users. Bold words, but we can prove them. We call them "general purpose" because they combine features and performance covering a broad range of user needs. And the price is down where everyone serious about recording XY data can afford them.

High performance: On both the 7035B (8½"x 11") and 7005B (11"x 17"), you get 20 in/sec slewing speed, five calibrated input ranges from 1 mv/in. to 10 V/in, with metric calibration optional; one megohm input impedance on all but the two most sensitive ranges; 0.2% accuracy full scale, with 0.1% linearity and resettability. Features: All the time-and field-tested HP features are standard, such as all-solid-state circuitry, exclusive electric paper hold-down, zener reference, electric pen lift, easy-load platen, rack/bench convertability, instant access for adjustment or maintenance. Price: A low $985 (7035B) and $1195 (7005B).

To check on how closely we meet your XY recorder standards, call your local HP field engineer. Or write Hewlett-Packard, Palo Alto, Calif. 94304; Europe: 1217 Meyrin-Geneva, Switzerland.

HEWLETT hp PACKARD

GRAPHIC RECORDERS

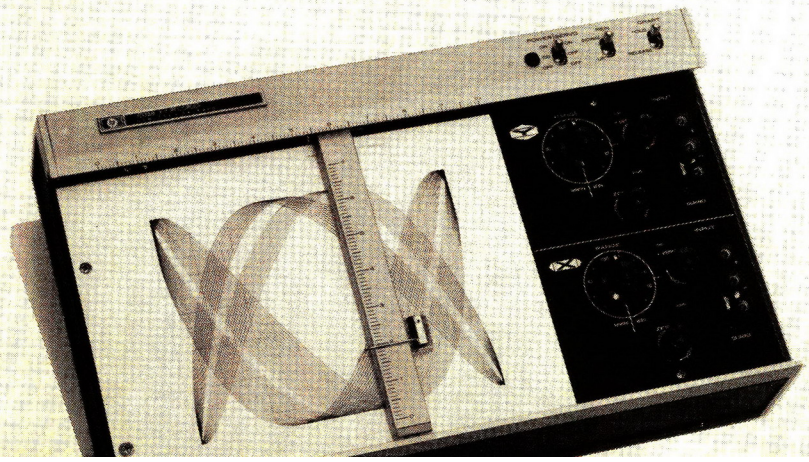

It pays to listen to everybody.

Like the time Danish physicist Dr. Niels Bohr let the air out of Professor Einstein's objection to the Heisenberg uncertainty principle. You may recall how the Professor postulated a box lined with perfect mirrors having an alarm clock inside, the entire device suspended from a balance.

The contrivance suggested the Heisenberg principle wouldn't work in a 4-dimensional universe. That had Dr. Bohr stumped. Until he recollected having listened to Einstein's theory making the rate of the clock a function of gravity and saw that the clock's rate of operation must depend on its position in the gravitational field of the earth.

" 'Twas sport to have the master hoist with his own petard."

We listen to everybody, too. We draw on the experience and know-how of The Radiochemical Centre at Amersham, England, and G. D. Searle & Co.

Now we're listening to you and learning more every day. Which is why we can serve you so well.

Which is just as satisfying as winning a joust with Professor Einstein.

Need technical assistance? Call our Customer Service Dept. in Des Plaines, Ill. We're all of us good listeners.

And send for our first edition.



how the great Dane helped old mc^2 box himself in

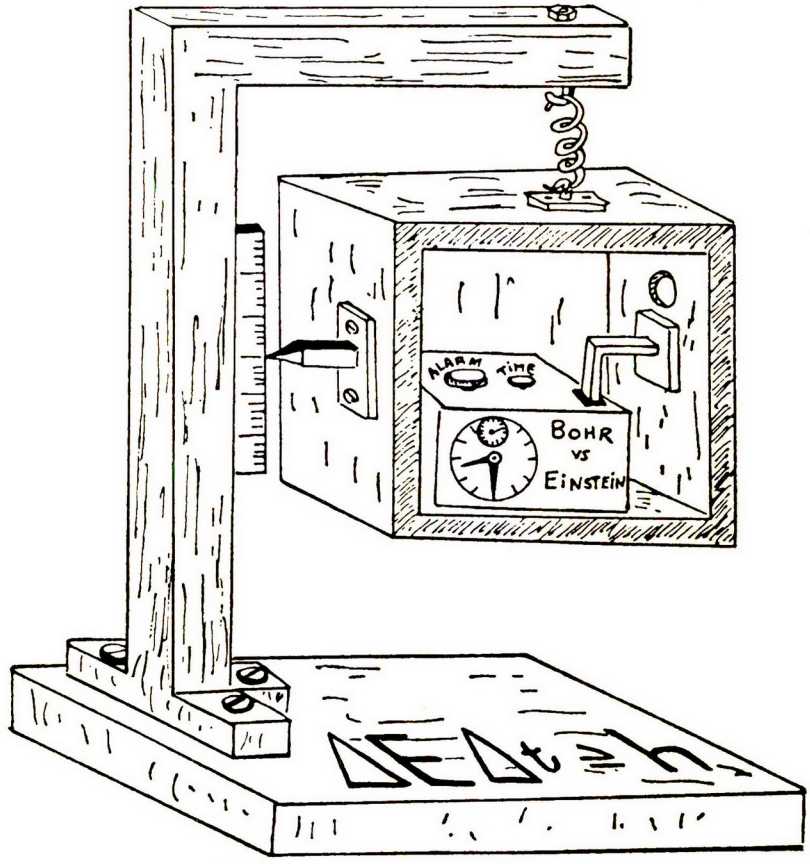

2000 NUCLEAR DRIVE, DES PLAINES, ILLINOIS 60018 TELEPHONE: (312) 296-1055

Amersham/Searle

AMERSHAM/SEARLE CORPORATION
AN ACTIVITY OF G. D. SEARLE & CO. AND THE RADIOCHEMICAL CENTRE

"From THIRTY YEARS THAT SHOOK PHYSICS by G. Gamow, illus. by G. Gamow, copyright 1966 by Educational Services, Inc., pub. by Doubleday & Co., Inc."

Circle No. 8 on Readers' Service Card

We announce a breakthrough in quantitative analysis of TLC · gel · paper · column chromatograms. Now we need your help.

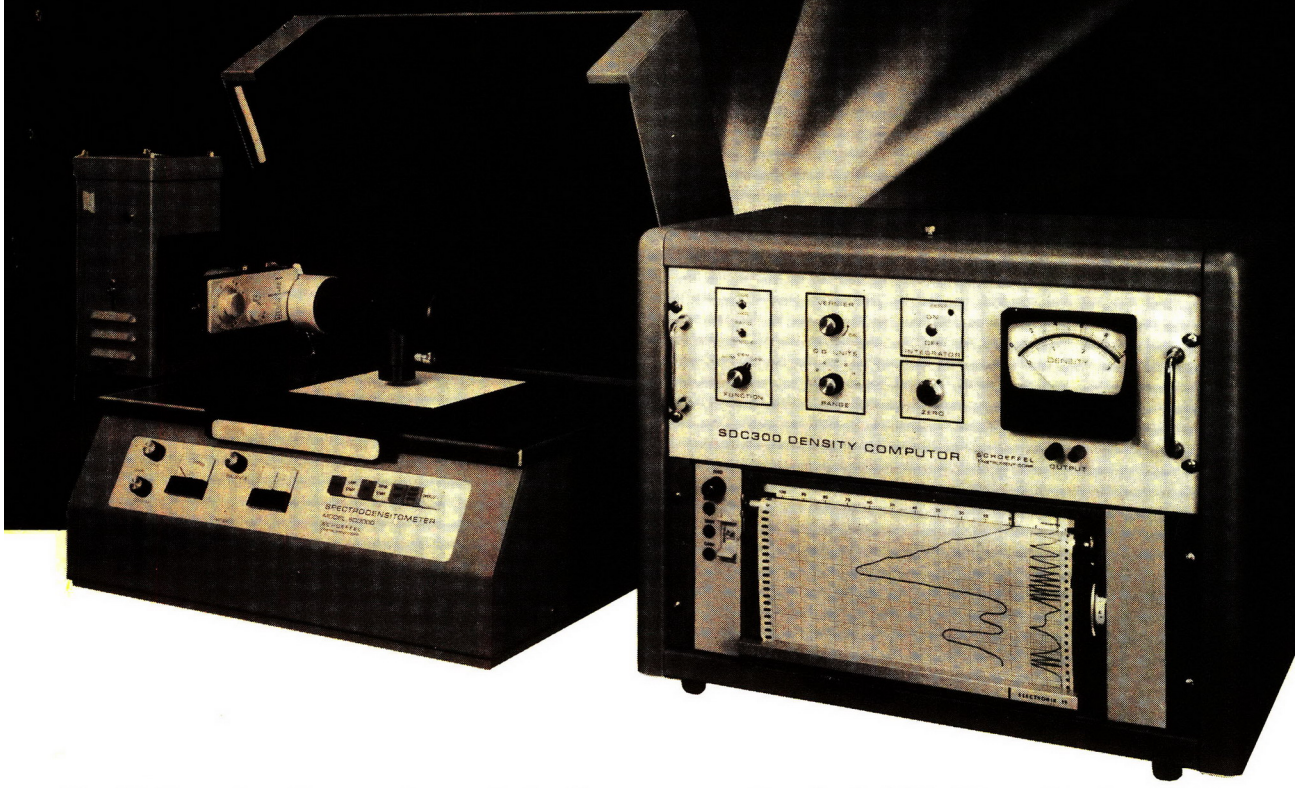

Quantitative, automatic, accurate, non-destructive, rapid and repeatable analysis of chromatograms is now practicable.

We announce the Schoeffel SD 3000 Spectrodensitometer. It is the state of the art in analysis and evaluation of TLC, gel, column, paper chromatograms and electrophoresis strips. The leading commercially available system capable of true quantitative evaluation. It is clearly and demonstrably superior to any other commercial system.

The SD 3000 is the only modular totally intercepting double-beam, ratio-recording, background discriminating instrument system. It is operable in transmission, reflectance and fluorescence as well as quenching modes. Spectral scanning is continuous at any wavelength from 200 to 700 mμ to 3 O.D. units. It does not commonly require chromatogram staining and can resolve overlapping zones otherwise invisible. The system can detect many substances, non-destructively, in sub-nanogram amounts.

With the SD 3000, chromatography takes a giant step toward becoming an exact science . . . With your help.

If you would like technical data, reprints describing use of the SD 3000 in quantitation of steroids, estrogens, etc. and/or a prompt and convincing demonstration please write or 'phone.
24 Booker St., Westwood, N. J. (201) 664-7263

SCHOEFFEL
LIGHT AND LIGHT MEASUREMENT

Circle No. 79 on Readers' Service Card

5 versatile L/I instruments for the research laboratory:

1. An amphibious tube rocker and roller. 2. An instant centrifuge. 3. The perfect pipet. 4-5. Automatic Repipets® and Dilutors.

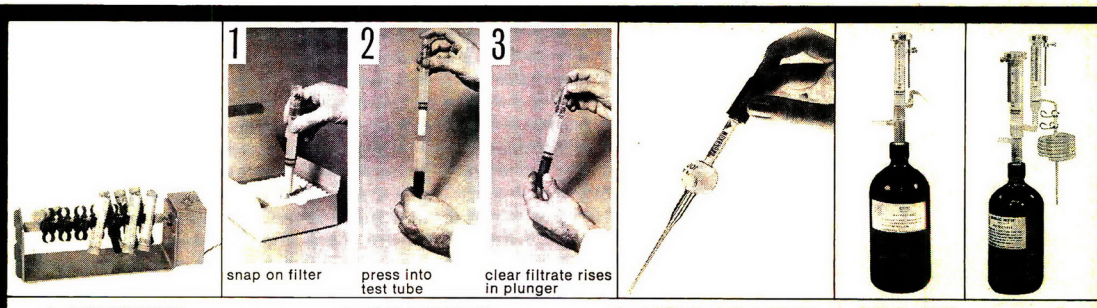

1. LABQUAKE™ 2. STAT-FILTER® 3. GRUNBAUM PIPETS 4. REPIPETS® 5. DILUTORS

1. L/I LABQUAKE™. A silent, small, submersible tube rocker and rotator for all sizes of tubes, ¼" to 1½" diameter. Occupies only 3½ x 8 x 4½ inches when fully loaded with 14 tubes. LABQUAKE has 28 tube positions altogether that accommodate clips to hold tubes of varying sizes. Adjustable bracket holds LABQUAKE fully or partially submerged in water bath. Use for thorough mixing of blood without cell damage (holds Vacutainers®); agitating during tissue, bacteria growth; preparing homogeneous dispersions of particulates for Coulter® and other particle monitors; cell trypsinization in tissue culture; enzymatic hydrolysis of steroids, and many other applications.

Price: LABQUAKE (patent pending), for 110-120 VAC, furnished with (14) 13 mm and (14) 16 mm clips, $59.50. Maximum capacity, 250 ml. Other clips may be substituted.

2. STAT-FILTER®. For instant filtration by high pressure or vacuum—in the palm of your hand. You get crystal clear filtrates within 3 seconds after precipitates form. All precipitates over 10 microns are retained with no possibility of remixing after separation. The versatile STAT-FILTER uses disposable polypropylene test tubes and plungers, making it suitable for **any** filtration. Inexpensive demonstration kits are available.

Price: Complete STAT-FILTER SYSTEM, including 3 plungers, 100 disposable polypropylene filters and test tubes, and 25 test tube closures, $38. Demonstration STAT-FILTER kit with 1 plunger, 10 filters, 7 test tubes and 3 closures, $9.00.

3. GRUNBAUM PIPETS (The Perfect Pipet). The versatile GRUNBAUM micro-pipet aliquots, dilutes, transfers, and stores reagents. It's the only pipet that can handle ether, alcohol, acetone, etc. It's self-adjusting, self-filling, non-dripping and self-cleaning (sample B washes out sample A). Guaranteed accuracy: 5 μl, ±3%; 10 and 20 μl, ±2%; 25 μl and larger, ±1%. Guaranteed reproducibility: 0.1% at 100 μl. Sizes stocked for immediate delivery: 1, 2, 3, 4, 5, 10, 15, 20, 25, 50, 75, 100, 150, 200, 250, 300, 400, and 500 μl. Other sizes on request.

Price: $6.

4.-5. Automatic REPIPETS® and Dilutors. These unique instruments pipet, dilute and dispense with a **guaranteed** accuracy of 1% and a reproducibility of 0.1%. PYREX® L/I REPIPETS and Dilutors are of one-piece fused glass construction with no connections—eliminating any chance for leaks. L/I's instruments fit directly on your reagent bottles, ½-ounce and larger. Any reagent can be handled, including concentrated acids, concentrated alkalies, and chlorinated hydrocarbons. All amber instruments are supplied for your labile reagents. L/I stocks REPIPETS and Dilutors in ½, 1, 5, 10, 20 and 50 ml sizes, adjustable from zero to full scale.

Prices: REPIPETS $52.50; Dilutors $99.50. Micro and Macro Teflon® tips included.

SPECIAL NOTICE. Effective immediately, telephone orders for 10 ml L/I REPIPETS and Dilutors will be shipped within 72 hours. Mail orders 1-2 weeks.

Order from Labindustries or your distributor.

LABINDUSTRIES

The Error Eliminators

1802A Second Street • Berkeley, California 94710

Phone (415) 843-0220 • Cable: LABIND, Berkeley, Ca. (USA)

Circle No. 120 on Readers' Service Card

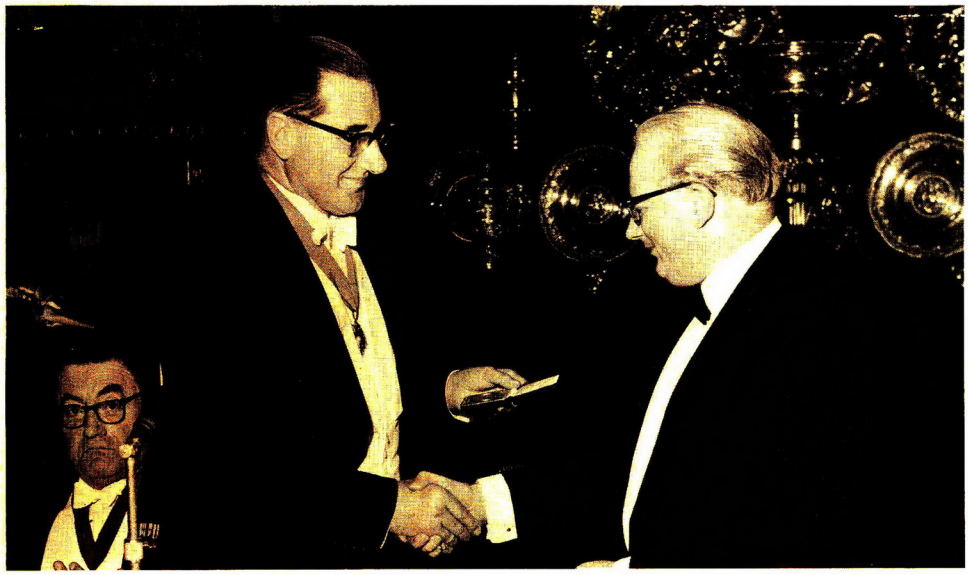

Ronald Belcher (right) of the University of Birmingham in England was presented with the third Gold Medal of the Society for Analytical Chemistry by A. G. Jones, President of the Society, March 7, at the Society's annual dinner

Ronald Belcher Wins Gold Medal

PROFESSOR RONALD BELCHER, winner of the third Gold Medal of the Society for Analytical Chemistry, was born in Nottingham in 1909. He began his scientific career at the University of Sheffield in the Department of Fuel Technology. After study in Austria under Hans Lieb in the Pregl Institute at Graz, he became a Leverhulme Research Fellow in 1940–41 and subsequently became a lecturer on microchemistry. In 1947 he joined Professor Harry Melville's staff at the University of Aberdeen as the lecturer in analytical chemistry and laid the foundation for his research school of analytical chemistry.

In 1949 he moved with Prof. Melville to the University of Birmingham where he has been active in analytical chemical research ever since. In 1959 he was made an honorary member of the Austrian Microchemical Society and began his work with the IUPAC. At Birmingham he built up a large research team pursuing work in microchemistry, organic reagents, titrimetry, complexometry, submicrochemistry, spectrophotometry, atomic absorption, gas chromatography, kinetics, etc. In 1959 he was appointed Professor of the first exclusive Chair of Analytical Chemistry in the U.K. The impact of Professor Belcher's group at Birmingham has had a profound effect of the development of analytical chemistry in the U.K., Europe, Asia, and the U.S.

Professor Belcher has published over 300 research papers, many reviews, and several editions of six or seven textbooks. He is a Past President of the International Union of Pure and Applied Chemistry's Analytical Division and is currently Vice-President of the Society for Analytical Chemistry.

The third Gold Medal honors Professor Belcher for his many contributions to analytical chemistry, not only in research, but also in influence in teaching and inspiring students to specialize in analytical chemistry.

How do you get the highest resolution **consistently** in ion exchange chromatography?

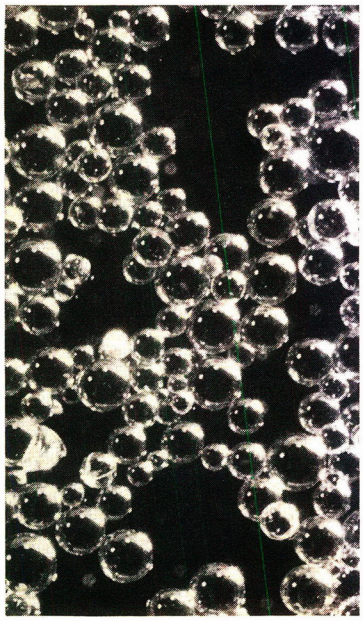

Only by using Bio-Rad AG® resins!

BIO-RAD AG resins represent the highest level of purity available for ion exchange chromatography.

AG resins are exhaustively purified and sized to specific ranges to assure sharp resolution and highest reproducibility. For example, the maximum iron content in AG-1 anion resin is 0.00005%.

For the full story on BIO-RAD and its role in ion exchange technology—including valuable data on Bio-Rex resins, specialty resins, resin selection, regeneration and applications—send for our general catalog, Price List T.

BIO-RAD Laboratories

Dept. A-6 • 32nd and Griffin Ave.
Richmond, California 94804

Circle No. 103 on Readers' Service Card
See ACS Laboratory Guide for All Products/Sales Office

27th Pittsburgh Diffraction Conference

The 27th Pittsburgh Diffraction Conference will be held November 5 through 7, 1969, at Mellon Institute, Carnegie-Mellon University, Pittsburgh, Pa. Papers on any aspect of diffraction, microscopy, small angle scattering, crystal physics, and chemistry, or related applications and instrumentation are being solicited. Abstracts of 400 words or less should be forwarded to the program chairman, John L. Bomback, U.S. Steel Corp., Fundamental Research Laboratory, Monroeville, Pa. 15146, before Sept. 8.

A symposium on ESCA, electron spectroscopy for chemical analysis, will be held Thursday, Nov. 6. Outstanding speakers will present invited papers on electrons produced by X-ray excitation, applications to metals, and molecular orbitals and Auger electrons. A special session on ultra structure of membranes by electron microscopy and X-ray diffraction is also planned.

Guest speaker for the Thursday evening meeting following the banquet is M. Kent Wilson, head of the chemistry section of the National Science Foundation.

Nominations for the Sidhu Award are requested in the form of one-page resumes of the candidate who must have made an outstanding contribution to the field of diffraction and be under 33 years of age. Nominations should be sent to the program chairman before July 1.

A confidential employment register will be maintained and employment opportunities are requested for posting. Please address inquiries to John H. Scott, U.S. Steel Research Center, Monroeville, Pa. 15146.



Velmer A. Fassel, Iowa State University and the Ames Laboratory, is shown receiving the 1969 Spectroscopy Society of Pittsburgh Award, March 5 in Cleveland, Ohio, during the Pittsburgh Conference on Analytical Chemistry and Applied Spectroscopy. The Award was presented by J. K. Scanlon (left) Chairman of the SSP and honors Dr. Fassel for his outstanding contributions to spectroscopy

ORNL Announces 13th Conference on Analytical Chemistry in Nuclear Technology

The 13th Conference on Analytical Chemistry in Nuclear Technology will be held in Gatlinburg, Tenn., Sept. 30 through Oct. 2, 1969, under the sponsorship of the Analytical Chemistry Division of Oak Ridge National Laboratory. All sessions of the meeting will be held in the Mountain View Hotel.

Papers, up to 25 minutes in length, are being solicited. Original, unpublished work in the following areas will be considered:

Analytical Chemistry for Fast Breeder Reactor Programs

Determination of major components, oxygen to metal ratios, trace impurities in fuels; analysis of alkali metal coolants for trace contaminants

Activation and Radiochemical Analysis

Nondestructive radionuclide analysis with lithium-drifted germanium detectors and computer applications; radioactive standards; analytical applications of nuclear techniques and devices

Automated Methods of Analysis

In process control; in environmental pollution; in bioanalytical and clinical applications.

Those interested in making contributions should submit an abstract of 200–500 words not later than June 20. The title, name of author, and estimate of time for presentation should accompany the abstracts.

All inquiries regarding this conference should be directed to L. J. Brady, Oak Ridge National Laboratory, P.O. Box X, Oak Ridge, Tenn. 37830.

Molecular Photochemistry

Marcel Dekker, Inc., 95 Madison Ave., New York, N. Y. 10016, has commenced publication of a new quarterly journal, *Molecular Photochemistry*. Volume 1, No. 1 appeared in January 1969. The purpose of this journal is to foster the interrelationships between photochemists and spectroscopists. Papers will describe original and fundamental researches in mechanisms of photochemical processes, structure–reactivity and spectral–reactivity relationships, structures of molecules in excited states, radiationless processes, and electronic energy transfer.

The Editor is A. A. Lamola, Bell Telephone Laboratories, Murray Hill, N. J. 07974. Regional editors are located in the U.S.S.R. and Japan. The subscription rate for the U.S. and other countries in the U.S. postal zone is $30 per volume; in Canada and other foreign countries, the rate is $37 per volume.

At last, a choice in low temperature ashing from

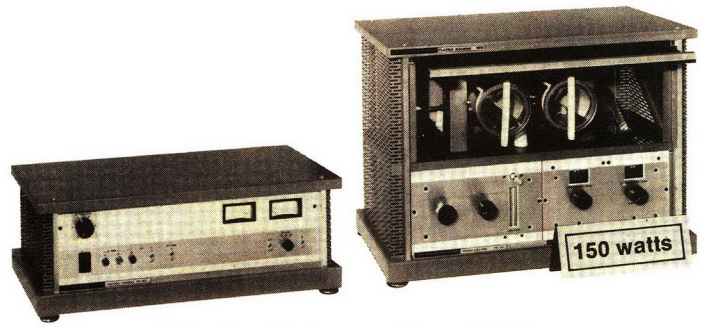

We've brought plasma machines within the reach of every laboratory — large or small. The new 150 watt IPC 1001 has two large ashing chambers that give you sample handling capacity up to 1.0 gram per hour.

to

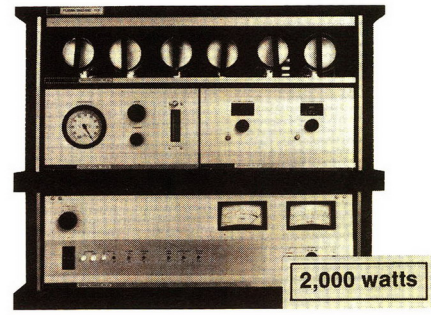

When you need faster, larger capacity ashing, IPC offers larger power units . . . 300, 1000, up to 2000 watts. Pick the IPC plasma machine that's right for you. Then, choose up to six ashing chambers. You'll be able to ash up to thirty 1-gram samples simultaneously . . . faster than 3.60 grams an hour.

Action of every IPC Plasma machine is so gentle that such fleeting elements as arsenic, selenium, and zinc aren't lost. And, there's no contamination from outside agents when ashing.

In addition to plasma machines, IPC offers a wide selection of plasma systems for R&D and production work. You can also choose from a complete line of accessories for faster ashing and easier sample handling.

If you need high speed, versatile, easy-to-operate plasma machines, we'll help you select the one that's right for you. **Write International Plasma Corporation, P.O. Box 4136, 25222 Cypress Avenue, Hayward, California 94544. Or, phone (415) 783-2067.**

IPC

Circle No. 43 on Readers' Service Card

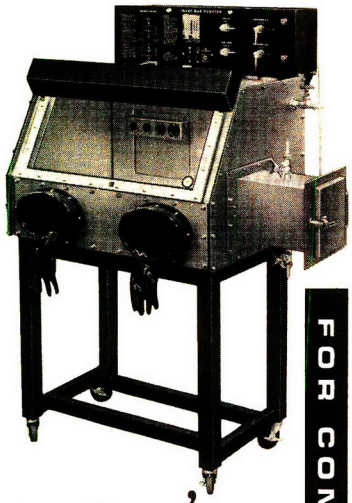

K·S·E's NEW FAMILY OF COMPACT INERT GAS PURIFICATION SYSTEMS provides a reliable and economical way to purify inert gases to levels of below 1 P.P.M. H_2O and O_2 the units are available in various configurations to meet requirements from casual laboratory applications to continuous production.

SALIENT FEATURES

- Stainless steel purification columns.
- Purge gas preheaters for rapid regeneration.
- 10,000 hours pump rating.
- Two to three weeks between regenerations.
- Regeneration heaters replaceable without tools or disassembly.
- Automatic purge control and N_2 removal modification kits are also available.
- Operates at ambient temperature.
- Purification column charge rated in excess of 5000 regeneration cycles.
- The entire volume of gas circulated is purified—none bypasses the purification column.
- Available from stock.

FOR COMPLETE INFORMATION WRITE OR CALL...

K·S·E DIVISION
KEWAUNEE SCIENTIFIC EQUIPMENT CORP. ADRIAN, MICHIGAN

4043 LOGAN ST.

Circle No. 88 on Readers' Service Card

Scheduled Courses in Analytical Techniques

Information is given in the following order: date, name of course, location of course, professional person(s) in charge of course, and/or sponsoring organizations and Contact (numbers in parentheses refer to addresses and telephone numbers given at the bottom of the list of scheduled courses).

June 2 to 6—3rd ISA Short Course on Process Analytical Instrumentation. Marriott Motor Hotel, Philadelphia, Pa. *Contact:* C. E. Borchers, Northwestern University, Evanston, Ill. 60201

June 4 to 6—Vacuum Instrumentation and Technology. Cleveland Engineering & Scientific Center, Cleveland, Ohio. *Contact:* O. G. Tex Hudson, Clark Goodman Supply, 1161 Brook Pk. Rd., Cleveland, Ohio 44109

June 7 to 8—Interpretation of Infrared Spectra. Philadelphia, Pa. Norman B. Colthup. ACS. *Contact (1)*

June 7 to 8—Computer Programs in Chemical Research. Pittsburgh, Pa. DeLos D. DeTar, D. E. DeTar. ACS. *Contact (1)*

June 8 to 27—Digital Computers in Chemical Instrumentation. Purdue University. *Contact:* S. P. Perone, Chemistry Dept., Purdue University, Lafayette, Ind. 47907

June 9 to 11—Use of Operational Amplifiers in Instrumentation. Oakland, Calif. McKee-Pedersen. *Contact:* Richard G. McKee, Mc-Kee-Pedersen Instruments, P.O. Box 322, Danville, Calif. 94526

June 9 to 13—Two Separate Courses: Infrared Interpretation, Part I; Gas Chromatography. Philadelphia, Pa. Sadtler Research. *Contact (2)*

June 9 to 13—Laser Raman Institute and Workshop. University of Maryland. *Contact:* Ellis R. Lippincott, Center of Materials Research, University of Maryland, College Park, Md. 20742

June 9 to 13—Fifth Annual X-Ray Spectrometry Clinic. State University of New York at Albany. *Contact:* Henry Chessin, State University of New York at Albany (SUNYA), Dept. of Physics, 1400 Washington Ave., Albany, N. Y. 12203

June 11 to 13—Basic Gas Chromatography. Springfield, N. J. Varian Aerograph. *Contact:* Tom Campbell, Varian Aerograph, 25 Route 22, Springfield, N. J. 07081

June 13 to 15—Spectrometric Identification of Organic Compounds. Milwaukee, Wis. Robert M. Silverstein, G. Clayton Bassler. ACS. *Contact (1)*

June 16 to 17—Chromatography Seminar. Sharon, Pa. Penn State. *Contact:* Penn State Continuing Education, Shenago Valley Campus, South Water Ave., Sharon, Pa. 16146

June 16 to 20—21–110 Mass Spectrometer. Monrovia, Calif. CEC/Analytical Instruments Div. *Contact (3)*

June 16 to 20—Summer Institute in Advanced NMR and Advanced Mass Spectroscopy. Stevens Institute of Technology. *Contact:* E. R. Malinowski, Stevens Institute of Technology, Hoboken, N. J. 07030

June 16 to 20—Theory and Interpretation in Mössbauer Spectroscopy. Catholic University, Washington, D. C. *Contact:* Leopold May, Dept. of Chemistry, Catholic University, Washington, D. C. 20017

June 17 to 20—Fractional Distillation. Hopatcong, N. J. Dimitrios Tassios. *Contact (4)*

June 17 to 21—Automation Analysis in Chemistry. St. Louis, Mo. *Contact:* Washington University, Box 1048, St. Louis, Mo. 63130. Tel: (314) 863-0100, Ext. 4779

June 17 to 27—Two Intensive Courses in Infrared Spectroscopy: June 17 to 21, Technique; June 23 to 27, Applications. MIT. Richard C. Lord, Dana W. Mayo. *Contact:* Director of the Summer Session, Rm. E19-356, Massachusetts Institute of Technology, Cambridge, Mass. 02139

June 18 to 26—Elements of Metallurgy. Toronto, Ontario. American Society for Metals. *Contact (5)*

June 22 to 27—Organic Polarography. Georgetown U., Washington, D. C. V. Horak. R. de Levie. *Contact (6)*

June 23 to 25—Chromatography Workshop. Hopatcong, N. J. Alan Fleischman. *Contact (4)*

June 23 to 27—Electronics for Scientists and Engineers. Hopatcong, N. J. Saul Ritterman. *Contact (4)*

June 23 to 27—Recent Advances in Separation Processes. UCLA. C. J. Huang. *Contact (7)*

June 23 to 27—Two Separate Courses: Mass Spectrometry; Management of Laboratory Services. Philadelphia, Pa. Sadtler Research. *Contact (2)*

June 25 to 27—Basic Gas Chromatography. San Francisco. Varian Aerograph, *Contact:* George Jordan, Varian Aerograph, 2700 Mitchell Dr., Walnut Creek, Calif. 94598

June 25 to 27—Statistical Data Evaluation Methods. Hopatcong, N. J. Thomas Hayton. *Contact (4)*

June 26 to 28—Chemical Microscopy. New York City. John A. Reffner. ACS. *Contact (1)*

July 6 to 7—Atomic Absorption Spectroscopy. Hanover, N. H. D. A. Keyworth, T. C. Rains, S. M. Pier. ACS. *Contact (1)*

July 7 to 11—X-Ray Techniques in the Industrial Laboratory. London, England. McCrone Research Institute. *Contact (8)*

July 7 to 11—Infrared and Raman Spectroscopy: Techniques, Theory, and Interpretation. UCLA. W. J. Lehman, H. J. Sloane. *Contact (7)*

July 7 to 11—Two Separate Courses: Infrared Interpretation, Part I; Gas Chromatography. Philadelphia, Pa. Sadtler Research. *Contact (2)*

July 7 to 18—Metallography. Metals Park, Ohio. American Society for Metals. *Contact (5)*

July 8 to 10—Chemistry Laboratory Instrumentation. Hopatcong, N. J. Nelson Alpert. *Contact (4)*

July 9 to 10—Gas Chromatography. Hanover, N. H. H. M. McNair, James Miller or R. S. Juvet, Jr. or W. E. Baitinger. ACS. *Contact (1)*

July 14 to 18—Fine Particle Measurements Workshop (4th Annual). Hopatcong, N. J. Merrill Jackson. *Contact (4)*

July 14 to 18—Industrial Use of the Polarizing Microscope. London, England. McCrone Research Institute. *Contact (8)*

July 14 to 18—Reflection Spectroscopy: Theory and Applications. UCLA. W. N. Hansen, T. B. Hirschfeld. *Contact (7)*

July 14 to 25—Electron and Light Microscopy. Cornell University. George G. Cocks, S. Breese, Jr. *Contact:* Julian C. Smith, Director of Continuing Education, College of Engineering, Cornell University, Ithaca, N. Y. 14850

July 16 to 18—Basic Gas Chromatography. Sydney, Australia. Varian Aerograph. *Contact (9)*

July 19 to Aug. 9—Research Instrumentation. Brooklyn Campus, Polytechnic Institute of Brooklyn. (Partially supported by NSF grants under its College Teacher Program; also open to industrial and academic scientists). *Contact:* Kenneth Jolls, Office of Special Programs, Polytechnic Institute of Brooklyn, 333 Jay St., Brooklyn, N. Y. 11201. Tel: (212) 643-4442 or 643-2266

July 21 to 25—Two Separate Courses: Thermoanalysis Workshop; Electronics and Analytical Instrumentation. Philadelphia, Pa. Sadtler Research. *Contact (2)*

July 22 to 26—Techniques of Infrared Spectroscopy. University of Minnesota. *Contact:* Dept. of Conferences and Institutes, Nolte Center for Continuing Education, University of Minnesota, Minneapolis, Minn. 55455

July 23 to 25—Basic Gas Chromatography. Melbourne, Australia. Varian Aerograph. *Contact (9)*

July 26 to 27—Interpretation of Infrared Spectra. New York City. Norman B. Colthup. ACS. *Contact (1)*

July 28 to Aug. 1—Chemical Interpretation of Infrared Spectra. University of Minnesota. *Contact:* Dept. of Conferences and Institutes, Nolte Center for Continuing Education, University of Minnesota, Minneapolis, Minn. 55455

July 28 to Aug. 1—Combined GC–MS–IR Analysis. Georgetown U., Washington, D. C. C. F. Hammer, P. C. Rankin. *Contact (6)*

Aug. 1 to 2—Thin-Layer Chromatography. Wilmington, Del. M. Karl Brandt. ACS. *Contact (1)*

Aug. 4 to 5—Gas Chromatography. Washington, D. C. H. M. McNair, James Miller or R. S. Juvet, Jr. or W. E. Baitinger. ACS. *Contact (1)*

Aug. 4 to 8—Ninth Annual Program in Infrared and Ultraviolet Absorption Spectroscopy. Arizona State University. *Contact (10)*

Aug. 4 to 8—Two Separate Courses: Techniques of Infrared Spectroscopy; IR and NMR of Heterocyclic Systems. Philadelphia, Pa. Sadtler Research. *Contact (2)*

Aug. 4 to 8—Combined GC–MS–IR Analysis. Georgetown U., Washington, D. C. C. F. Hammer, P. C. Rankin. *Contact (6)*

Aug. 7 to 9—Electroanalytical Chemistry. New York City. Irving Shain, Dennis H. Evans. ACS. *Contact (1)*

Aug. 11 to 15—Workshop on the Measurement of the Appearance of Properties of Materials. Marriott Twin Bridges Motor Hotel, Washington, D. C. *Contact:* Hunterlab, 9520 Lee Highway, Fairfax, Va. 22030

Aug. 11 to 15—Two Separate Courses: Infrared Interpretation, Part I; Gas Chromatography. Philadelphia, Pa. Sadtler Research. *Contact (2)*

Aug. 18 to 20—Fluorescence and Phosphorescence Spectrometry—Introduction. Hopatcong, N. J. G. G. Guilbault. *Contact (4)*

Aug. 18 to 20—Polarography. Hopatcong, N. J. Galen W. Ewing. *Contact (4)*

Aug. 18 to 20—Residual Gas Analyzer Spectra Interpretation. Monrovia, Calif. CEC/Analytical Instruments Div. *Contact (3)*

[1] Education Office, American Chemical Society, 1155 16th St., N. W., Washington, D. C. 20036. Tel: (202) 737-3337
[2] Sadtler Educational Division, Sadtler Research Laboratories, Inc., 3316 Spring Garden St., Philadelphia, Pa. 19104. Tel: (215) 382-7800
[3] Coordinator of Training and Technical Publications, Bell & Howell, 1500 S. Shamrock Ave., Monrovia, Calif. 91106
[4] Center for Professional Advancement, Saul Gordon Assoc., P.O. Box 66, Hopatcong, N. J. 07843. Tel: (201) 398-7110
[5] Ronald J. Seman, Metals Park, Ohio 44703. Tel: (216) 338-5151
[6] C. F. Hammer, Institute for Advanced Analytical Chemistry, Georgetown University, Washington, D. C. 20007. Tel: (202) 337-3300, Ext. 317
[7] University Extension, UCLA, 10851 Le Conte Ave., Los Angeles, Calif. 90024.
[8] Mrs. Miriam L. Fallert, McCrone Research Institute, 451 East 31st St., Chicago, Ill. 60616. Tel: (312) 842-7105
[9] David B. Smyth, Varian Pty., Ltd., 38 Oxley St., Crows Nest, Sydney, NSW, Australia
[10] Jacob Fuchs, Dept. of Chemistry, Arizona State University, Tempe, Ariz. 85281

Circle No. 11 on Readers' Service Card→

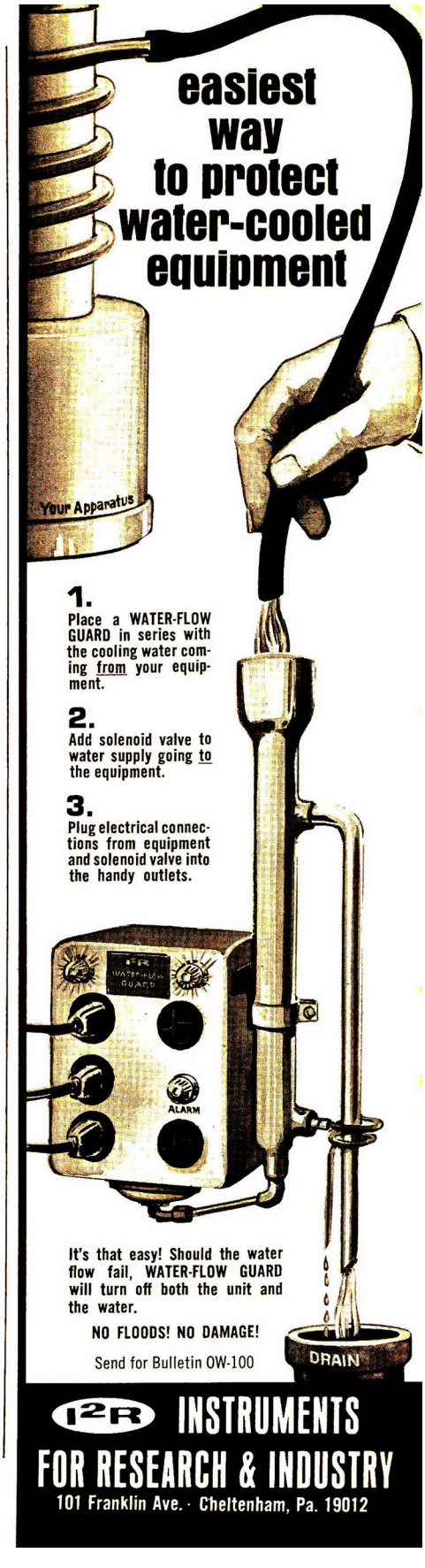

USE IT ANY WHERE, ANY TIME!

FERRETMETER

FOR PORTABLE ALLOY METAL SORTING

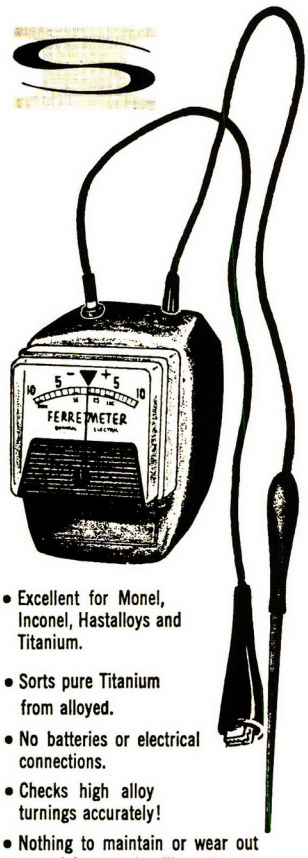

- Excellent for Monel, Inconel, Hastalloys and Titanium.
- Sorts pure Titanium from alloyed.
- No batteries or electrical connections.
- Checks high alloy turnings accurately!
- Nothing to maintain or wear out except inexpensive file probe.
- Perfect for steel warehouses and pipe sorting. Easily sorts look-alike alloys!

Write For FREE Brochure

STEELMET INC.

P.O. BOX 100, WILSON STATION, CLAIRTON, PENNA. 15025, U.S.A.
TELEPHONE (412) 462-8012
TELEX: 86-6132

Circle No. 67 on Readers' Service Card

CALENDAR OF EVENTS

June 4 to 6	**International Congress on Automated Analysis.** Conrad Hilton Hotel, Chicago, Ill. *Contact:* Jerome E. Golin, Technicon Corp., Ardsley, N. Y. 10502
June 5 to 6	**Third Great Lakes Regional ACS Meeting.** DeKalb, Ill. Includes Analytical Chemistry Sessions. *Contact:* Richard C. Bowers, Northern Illinois University, DeKalb, Ill. 60115
June 5 to 11	**Fifth International Meeting of Forensic Sciences.** Toronto, Canada. *Contact:* Frank L. Wilson, Dept. of the Attorney General, Parliament Bldg., Toronto 2, Canada
June 9 to 13	**Gordon Research Conference on Magnetic Resonance.** New Hampton, N. H. *Contact:* W. George Parks, University of Rhode Island, Kingston, R. I.
June 11 to 13	**ACS Analytical Chemistry Summer Symposium.** University of Georgia, Athens, Ga. Sponsors: Analytical Chemistry Division and ANALYTICAL CHEMISTRY. Subject: Modern Instrumental Techniques for Elemental Analysis. *Contact:* G. H. Morrison, Dept. of Chemistry, Cornell University, Ithaca, N. Y. 14850. Page 45 A, Apr.
June 12 to 13	**Vacuum Microbalance Techniques, Eighth Conference.** Wakefield (near Boston), Mass. *Contact:* W. W. Czanderna, Dept. of Physics, Clarkson College of Technology, Potsdam, N. Y. 13676
June 12 to 13	**24th Annual Northwest Regional ACS Meeting.** University of Utah, Salt Lake City, Utah. Includes Analytical Chemistry Sessions. *Contact:* Edward M. Eyring, Dept. of Chemistry, University of Utah, Salt Lake City, Utah 84112
June 22 to 27	**ASTM 72nd Annual Meeting.** Chalfonte-Haddon Hall, Atlantic City, N. J. *Contact:* American Society for Testing and Materials, 1916 Race St., Philadelphia, Pa. 19103
June 23 to 25	**4th IMEKO—Photon Detectors Symposium.** Hotel International, Prag. *Contact:* IMEKO Secretariat, Budapest, 5, P. O. B 457, Hungary
June 25 to 27	**14th Annual Symposium and Exhibition on the Art of Glassblowing.** Thruway Motor Inn, Albany, N. Y. Sponsor: American Scientific Glassblowers Society. *Contact:* Joseph W. Baum, 200 Highland Ave., Rensselaer, N. Y. 12144
June 26 to 27	**ASTM Committee E-15 on Analysis and Testing of Industrial Chemicals.** Franklin Motor Inn, Philadelphia, Pa. *Contact:* American Society for Testing and Materials, 1916 Race St., Philadelphia, Pa. 19103

Coming Events

July 13 to 19—VII International Congress of Clinical Pathology. Montreal, Canada. *Contact:* VII International Congress of Clinical Pathology, P. O. Box 8, Station "G," Montreal 18, Canada

July 14 to 16—Conference on Nonconventional Electron Microscopy. St. Catherine's College, Oxford, England. *Contact:* The Institute of Physics and The Physical Society, 47 Belgrave Square, London, S.W.1, England

July 14 to 18—International Conference on Atomic Absorption Spectroscopy. Sheffield, England. *Contact:* A.A.S. Conference Secretary, Society for Analytical Chemistry, 9/10 Savile Row, London, W.1, England. Page 43 A, May

July 15 to 18—Meeting on NMR Spectroscopy. Birmingham, England. *Contact:* The Chemical Society, Burlington House, London, W.1, England

July 16 to 18—Symposium on Surface Area Determination. University of Bristol. Sponsors: IUPAC, Society of Chemical Industry, School of Chemistry, University of Bristol. *Contact:* D. H. Everett, University of Bristol, Bristol BS8, 1TS, England

July 16 to 18—Fourth National Conference on Electron Microprobe Analysis. Huntington-Sheraton Hotel, Pasadena, Calif. *Contact:* A. A. Chodos, Geology Dept., California Institute of Technology, Pasadena, Calif. 91109

July 21 to 25—International Symposium on Analytical Chemistry. Birmingham, England. Sponsors: SAC and IUPAC. *Contact:* D. M. Peake, 61 Lodge Rd., Walsall, Staffordshire, England. Page 57 A, Aug.

July 28 to Aug. 1—28th ISA Research Conference on Instrumentation Science. Hobart & Wm. Smith College, Geneva, N. Y. *Contact:* N. E. Huston, University of Wisconsin, 1815 University Ave., Madison, Wis. 53706

Aug. 4 to 5—Eleventh Annual Rocky Mountain Spectroscopy Conference. Denver, Colo. *Contact:* H. N. Barton, Dow Chemical Co., P.O. Box 888, Golden, Colo. 80402

Aug. 4 to 7—International Conference on Raman Spectroscopy. Carleton University, Ottawa, Canada. *Contact:* J. A. Koningstein, Chemistry Dept., Carleton University, Ottawa, Canada

Aug. 6 to 8—Denver Conference on Applications of X-Ray Analysis. Albany Hotel, Denver, Colo. *Contact:* J. B. Newkirk, Denver Research Insti-

tute, University of Denver, Denver, Colo. 80210. Page 66 A, Apr.

Aug. 11 to 14—International Symposium on Electron and Nuclear Magnetic Resonance. Clayton, Australia. *Contact:* C. J. Coogan, CSIRO, Clayton, Victoria, Australia 3618

Aug. 11 to 15—Gordon Research Conference on Analytical Chemistry. New Hampton School, New Hampton, N. H. *Contact:* W. George Parks, University of Rhode Island, Kingston, R. I.

Aug. 13 to 27—8th International Congress and General Assembly of the International Union of Crystallography. State University of New York at Stony Brook, *Contact:* David Shoemaker, Dept. of Chemistry, Massachusetts Institute of Technology, Cambridge, Mass. Page 89 A, Feb.

Aug. 17 to 22—Annual Meeting American Association of Clinical Chemists. Denver, Colo. *Contact:* David A. Roethel, 1155 16th St., N.W., Washington, D. C. 20036

Aug. 17 to 24—3rd NMR Symposium. University of Toronto, Toronto, Ont. Sponsor: Physical Chemical Division (CIC) and University of Toronto. *Contact:* Chemical Institute of Canada, 151 Slater St., Ottawa 4, Ontario, Canada

Aug. 18 to 22—Gordon Research Conference on Separation and Purification. Colby Junior College, New London, N. H. *Contact:* W. George Parks, University of Rhode Island, Kingston, R. I.

Aug. 18 to 22—Gordon Research Conference on Ion Exchange. Kimball Union Academy, Meriden, N. H. *Contact:* W. George Parks, University of Rhode Island, Kingston, R. I.

Aug. 20 to 27—22nd International Congress of Pure and Applied Chemistry. Sydney, Australia. *Contact:* Chairman, Organising Committee, Box 2249U, GPO, Melbourne, Australia

Aug. 25 to 29—International Conference on Luminescence. University of Delaware. Sponsors: IUPAC and American Physical Society. *Contact:* R. B. Murray, Dept. of Physics, University of Delaware, Newark, Del. 19711. Page 55 A, June

Aug. 31 to Sept. 4—International Conference on Calorimetry and Thermodynamics. Warsaw, Poland. *Contact:* H. Kehiaian, Secretary, Organizing Committee, Institute of Physical Chemistry, Polish Academy of Sciences, P. O. Box 49, Warsaw 42, Poland

Sept. 2 to 6—24th Annual Symposium on Molecular Structure and Spectroscopy. Ohio State University. *Contact:* K. Narahari Rao, Dept. of Physics, Ohio State University, 174 W. 18th Ave., Columbus, Ohio 43210.

Sept. 7 to 12—158th National ACS Meeting. New York City. Includes Analytical Division Sessions. *Contact:* Fred McLafferty, Cornell University, Ithaca, N. Y. 14850

Sept. 8 to 13—Seventh International Congress of Clinical Chemistry. Geneva, Switzerland. *Contact:* VIIth International Congress of Clinical Chemistry, Palais des Expositions, 1211 Geneva 4, Switzerland.

Sept. 14 to 20—20th Meeting of Comité International de Thermodynamique et de Cinétique Electrochimiques (CITCE). Strasbourg, France. *Contact:* H. Tannenberger, Institut Batelle 7, route de Drize, 1227 Carouge, Geneva, Switzerland

Sept. 15 to 20—General Assembly of the Gesellschaft Deutscher Chemiker. Hamburg, Germany. *Contact:* GDCh, 6000 Frankfurt (M), Postfach 119075, Germany

Sept. 16 to 18—17th Detroit Anachem Conference. Detroit, Mich. *Contact:* Walter Wagner, Dept. of Chemistry, University of Detroit, Detroit, Mich. 48221. Page 43 A, May

Sept. 22 to 24—4th International Symposium on the Identification of Substances by Paper and Thin Layer Chromatography. Frascati, Italy. *Contact:* Karl Macek, c/o Istituto di chimica, Piazzale delle Scienze, Roma, Italy. Page 47 A, Mar.

Sept. 23 to 25—Eighth Annual Meeting ASTM Committee E-19 on Chromatography. Sheraton Hotel, Philadelphia, Pa. *Contact:* M. G. Bloch, Mobil Research & Dev. Corp., Paulsboro, N. J. 08066

International Luminescence Conference

The International Conference on Luminescence will be held at the University of Delaware, August 25 through 29, 1969. The Conference is cosponsored by the International Union of Pure and Applied Physics and by the American Physical Society, and is also supported by the Office of Naval Research, the National Science Foundation, the University of Delaware Research Foundation, and the DuPont Co. The scope of the conference includes all basic luminescent phenomena of both inorganic and organic materials, with some emphasis on interrelations between properties of these two classes of materials and between luminescence and other branches of molecular physics and solid-state physics. Fundamental experimental and theoretical research on luminescence, and not device technology, will be considered.

The organizing committee is composed of representatives from Russia, France, Germany, England, Poland, Netherlands, Japan, Hungary, and the United States.

The Conference will include both invited and contributed papers. All papers and discussions will be published collectively following the meeting.

Further information on this meeting is available from R. B. Murray, Dept. of Physics, University of Delaware, Newark, Del. 19711.

Industry Items

Block Engineering, Inc., 19 Blackstone St., Cambridge, Mass. 02139, has announced that Block Engineering and **Sadtler Research Laboratories, Inc.,**

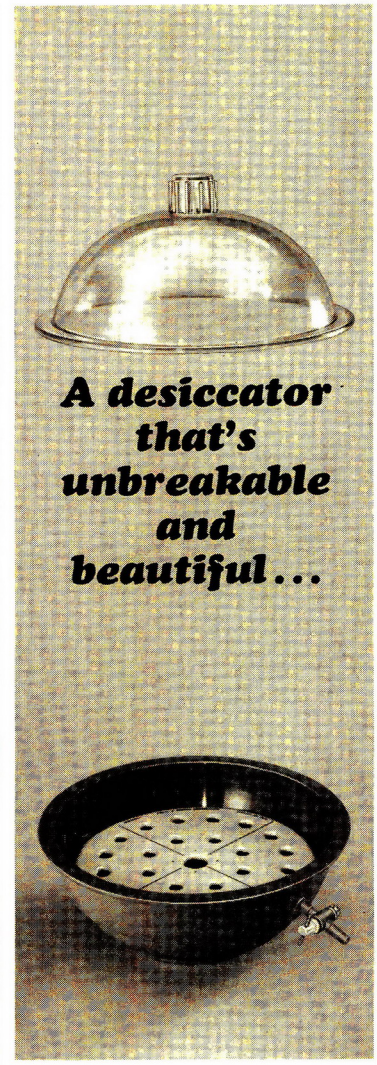

from the top of its transparent, distortion-free dome to the bottom of its blue-green base. That's why you'll be proud to own a new Nalgene® Vacuum Desiccator. Inside this spacious desiccator you can use our new ceramic-metal desiccator plate of Nucerite® or any other one you'd like.

When you specify Nalgene Labware, 20 years' leadership says you're right. Ask your Laboratory Supply Dealer for our new Catalog, or write Dept. 6806, Nalgene Labware Division, Rochester, N.Y. 14602.

NALGENE LABWARE DIVISION
NALGE
SYBRON CORPORATION

Circle No. 51 on Readers' Service Card

ASK MATHESON...

...why this new linear mass flowmeter outperforms other mass flowmeters

Linearity within 1%—that's the key to improved performance from this mass flowmeter. Featuring a new linear transducer, this flowmeter incorporates a major advancement in the successful Matheson flowmeter design. Having all the advantages of mass flow measurement—no temperature and pressure corrections necessary—the new linearity permits precision operation of remote data reduction equipment, totalizers and integrators without need to condition the output signal. Requires no moving parts, projections or sensing elements in the flow stream.



...to explain why you should consider Primary Standards if you analyze your own gas mixtures

Matheson Primary Standards have accuracies approaching that of the most sophisticated gas analysis equipment. Accuracies equal or exceed 1% of the component value . . . at concentrations above 2% the accuracy is ±0.02% *absolute*. Prepared by weight (the gas is actually weighed) on high load, high sensitivity analytical balances, Primary Standards have proven to be extremely dependable. They are a must for calibration applications in systems employing electronic digital integration . . . for process control instrument calibration where fractions-of-a-percent can save thousands of dollars.

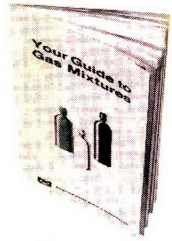

...how these micro-flow valves enable you to precisely control very low liquid or gas flows

Our recently patented Models 150 and 151 Micro-Flow Valves are recommended for control of very low flows of gases or liquids. Suggested applications are in mass spectrometry, gas chromatography and high vacuum systems. A flow as minute as 0.25 cc./min. of air can be controlled. A fine screw permits twenty turns in ½" of total stem travel.The overall range in flow for this valve is at least 1000 to 1. The unique design permits a relatively low price.

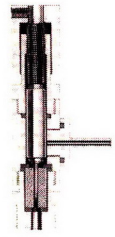

Ask Matheson *now*—Matheson offers the most complete gas service

MATHESON P. O. Box 85, East Rutherford, N. J. 07073

NAME

FIRM

ADDRESS

CITY STATE ZIP

Please send me "in depth" answers

- ☐ Matheson Linear Mass Flowmeter (Engineering Report)
- ☐ Matheson Primary Standards (Brochure)
- ☐ Models 150 & 151 Micro-Flow Valves (Engineering Report)
- ☐ Catalog 26

MATHESON GAS PRODUCTS

A Division of Will Ross, Inc., East Rutherford, N.J.; Cucamonga, Calif.; Gloucester, Mass.; Joliet, Ill.; LaPorte, Texas; Morrow, Ga.; Newark, Calif.; Whitby, Ont.

3-69G

Circle No. 123 on Readers' Service Card

News

3316 Spring Garden St., Philadelphia, Pa. 19104, have agreed to the merger of Sadtler into a wholly-owned subsidiary of Block. The merger, which has been approved by both companies' Boards of Directors, must be submitted to stockholders for approval. Block Engineering has also recently entered into an agreement to acquire **Dunn Analytical Instruments,** Silver Spring, Md., and has recently acquired **Basic Devices, Inc.**

Damon Engineering, Inc., 115 Fourth Ave., Needham Heights, Mass. 02194, announced agreement in principle for the acquisition of the following U.S. firms: **Lawndale Laboratory Co.** and **Rhodes-Medical Arts Laboratories,** Philadelphia; **Central Bioanalytical Laboratories, Inc.,** and **Pachter's Medical Laboratories, Inc.,** New York City; **Lyne Laboratories,** Boston; and **Kelso Medical Laboratory,** Washington, D. C. with additional facilities in Va., Md., and Nassau, Bahamas. In addition, Daman plans to acquire a 50% interest in **Instituto Analyzer Multiple Automatizada,** Buenos Aires. All the transactions are subject to appropriate corporate approval. These acquisitions mark the entry of Damon's Biomedical Sciences Division into biomedical testing. The laboratories propose to become an international network of clinical labs and related facilities to provide new and unique automated testing services. The laboratories will also function as a testing ground for instrumentation developed by Daman's medical instrumentation division, **International Equipment Co.**

Kollmorgen Corporation, 104 Lower Westfield Rd., Holyoke, Mass. 01040, has acquired 80% of **LERES (Laboratoires d'Etudes et de Realisations d'Equipements Scientifiques).** LERES makes transmission and reflectance spectrophotometers, which are sold under the names of SPILA and TRILAC, respectively. The new acquisition will become part of the Macbeth Color and Photometry Group of Kollmorgen.

Scientific equipment leasing has been expanded in a new plan announced by **Perkin-Elmer Corp.,** Norwalk, Conn., and **United States Leasing Corp.** The new program applies to company made analytical instruments including lasers and laser products and special instruments manufactured by Hitachi, Ltd., Japan, which are sold in the U. S. by P-E. The plan provides deposit-free, 100% financing of equipment costs including applicable sales taxes, transportation, and deliver and installation charges. Warrantees and guarantees remain fully effective and service contracts are established directly with P-E.

Circle No. 59 on Readers' Service Card→

Circulatory problems? Try Temptrol

If you are experiencing hot and cold spells with your lab circulators, Temptrol offers positive relief!

You can select the level of precise temperature control you need, the capacity you need, the temperature range you need.

Temptrol combination constant-temperature-baths-and-circulating-systems provide accurate temperature control both within their built-in baths and in separate instruments or baths through which the bath media is circulated. Baths and circulating systems may be used simultaneously or either may be used alone.

There are nine Temptrol models. Those equipped with a hydraulic thermostat achieve uniformity of ±0.5C or better and sensitivity of ±0.3C; those with a thermoregulator, uniformity of ±0.02C and sensitivity of ±0.1C. Pumping capacities range from 42.5 to 300 gal./hr. at 0 head.

Reservoir capacity range is: 1.25, 2.25 and 2.75 gallons, plus the Lo-Temptrol which is a 15 gallon capacity unit that cools to −30C.

Two versatile portable units, Stir-Pump and Porta-Temp, complete the Temptrol line. When used with the Precision Porta-Cool, the Porta-Temp converts any container into a low cost, wide range—0 to 90C—constant temperature bath and circulating system, giving you the advantages of the "bucking technique."

When putting your money into circulation, be sure it's in Temptrol. Get complete performance data on individual Temptrol units from your Precision Scientific Dealer or write us. Precision Scientific Co., 3737 W. Cortland St., Chicago, Ill. 60647.

PRECISION PS SCIENTIFIC

SUBSIDIARY OF GCA CORPORATION



Just because

it's hard to titrate, write, watch, and prepare samples, all at the same time:

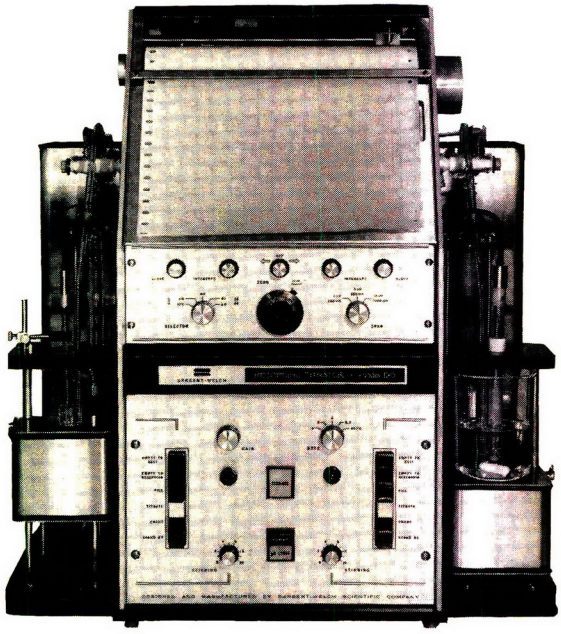

We give you

the Sargent-Welch Model DG Automatic Recording Titrator.

We give you, in fact, our *second-generation* automatic recording titrator. For dual pH or other potentiometric titrations. For plots of pH or e.m.f. vs. volume of titrant (and for first derivatives of such plots). Consider the DG's many advantages.

Consider first the time-saving value of the Model DG's *dual* titrating stations. While one station is in use, the second can be readied for following titrations. Using different reagents or concentrations. Virtually continuous, serial titrations of a large volume of samples. Pushbutton operation. Four fixed delivery rates *and* a variable rate controlled by curve slope for the best combination of speed in non-critical regions and accuracy at inflection points.

And burettes are quickly replaced *as a unit* for titrant changes. Burette stopcocks work automatically, too (no more forgotten, open settings). Stepper motor drives burettes and chart for precise, *electronic* synchronism without awkward mechanical linkages.

Next to be considered are the recording functions of the DG. Separate inputs for each titration station, with asymmetry and electrode-response adjustments for each input. Spans of 2, 5, and 10 pH (200, 500, and 1000 mv), with accuracy of 0.25% of full scale. Ten-turn zero adjustment *calibrated* to 0.01 pH or 1 mv. Pen response of 2 seconds (1.5 sec. *faster* than the DG's predecessor).

Also to be mentioned: An adjustable cam-and-microswitch that permits either (1) stopping the titration at predetermined endpoint or (2) operating the Model DG as a pH-stat. And optional automatic temperature compensation.

Finally, a look inside the DG. All solid-state circuitry. Standard 115/230-volt, 50-60 Hz operation.

The Model DG Automatic Recording Titrator—$3100. More details from your Sargent-Welch representative. Or write. 9-214

SARGENT-WELCH

Scientific instruments, apparatus, chemicals.
Sargent-Welch Scientific Company
4647 Foster Ave.; Chicago, Ill. 60630

Chicago/Anaheim/Birmingham/Cincinnati
Cleveland/Dallas/Denver/Detroit
Springfield, N.J./Toronto/Montreal/Vancouver

Circle No. 80 on Readers' Service Card

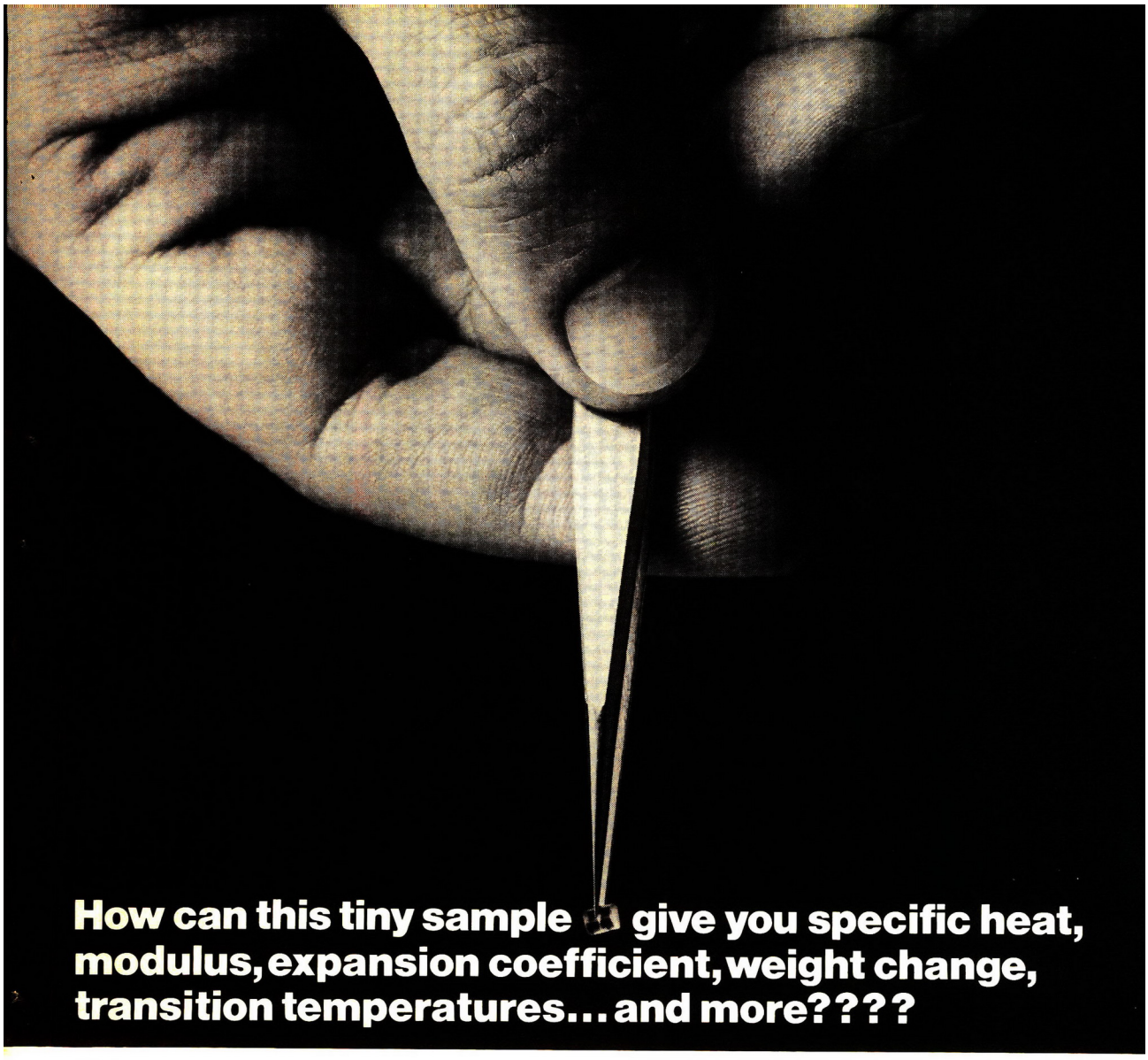

How can this tiny sample give you specific heat, modulus, expansion coefficient, weight change, transition temperatures... and more????

Read how Thermal Methods, the newest techniques of material characterization, offer you both quantitative and qualitative data and reproducible results.

Thermal Methods are unique techniques for identifying material characteristics. What you do is subject a milligram-size sample of material to precisely controlled temperature changes. Property changes measured by a specific transducer are recorded and can give you a world of information about the material.

More specifically, it can identify the material for you, show differences between chemically similar materials, and show thermal or mechanical history of the sample. The thermogram, the record of this response, is like a fingerprint: positive identification.

Thermal Methods can also give you information on the chemical behavior of materials. You can detect and measure polymerization of monomers and prepolymers. You can measure partial curing (B stage) of thermosetting resins.

And that's only the beginning. You can study chemical reaction kinetics in detail, such as rates of crystallization or polymerization.

You can study physical changes in detail such as sublimation, vaporization, fusion, crystal-crystal transitions, and first-order and second-order transitions (glass transitions). Also, changes in weight, volume, elastic and compressive moduli and creep phenomena.

And the best part of all this is that all these measurements are easy to make, analyses are fast (many taking less than ten minutes) and data are reproducible.

Du Pont offers the only complete Thermal Methods Laboratory including capabilities for Differential Thermal Analysis, Differential Scanning Calorimetry, Thermomechanical Analysis and Thermogravimetric Analysis.

We have a new bulletin describing the many applications of the Du Pont Thermal Methods Laboratory. For your free copy, write Du Pont, Room 7261-B Wilmington, Delaware 19898.

DU PONT REG. U.S. PAT. OFF. **Instruments**

Circle No. 89 on Readers' Service Card

Mettler automatic thermal instruments give you

1. melting and boiling points objectively
2. precise control in thermal microscopy
3. dropping points electronically

Melting and Boiling Points by the Numbers

1 Our melting/boiling point instrument, the Mettler FP-1, automatically runs melting and boiling point tests and displays results on its digital readout panel. All you do is (1) select a heating rate, (2) insert the sample, (3) press the "start" lever, (4) read the objective results to 0.1°C on the readout panel. You do not have to make subjective choices of the melting or boiling temperature, nor must you "eyeball" and apply corrections to mercury-in-glass thermometers.

Up to 50 mpd/hr

From 30 to 50 melting point determinations can be done per hour with the FP-1, depending on the heating rate. Any of five heating rates can be selected: 10°C/min for quick survey work; 1°, 2°, 3°C/min for routine tests or where a precision of 0.5°C is adequate, and 0.2°C/min for precise determinations to a reproducibility of ±0.1°C.

Take Three

You can make three melting point determinations simultaneously, thus identifying crystalline compounds by mixed melting point determinations in one rapid operation. Used with a standard time-base recorder, the Mettler FP-1 can provide curves showing changes in light transmission as sample temperature increases. This technique is useful in measuring melting ranges; in the construction of phase diagrams; and in analyzing the purity of compounds.

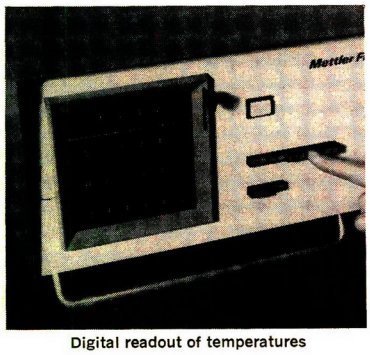

Digital readout of temperatures

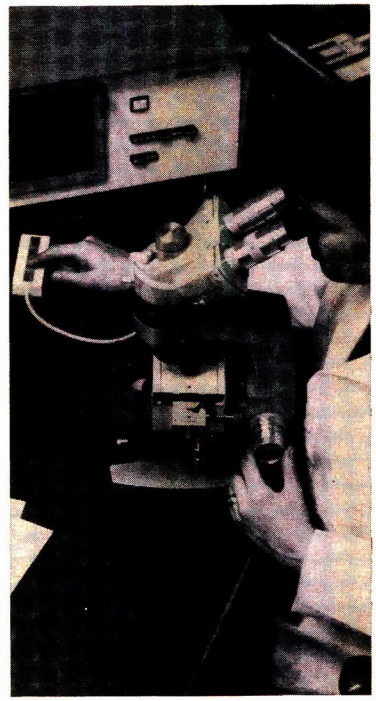

Pushbutton control of thermal events

Thermal Microscopy

2 For thermal microanalyses, attach the Mettler FP-2 to your microscope and take fingertip command of the thermal process. You never lose visual contact with the sample because the FP-2 has a pushbutton controller to increase, decrease or maintain sample temperature at a precise value. With the same controller you can record the exact temperature at which any three thermal events occur. These include beginning of melt, end of melt, phase change, or any of several conditions in the crystallization process. Temperatures are recorded in digital form on an indicator panel. The top digital indicator shows the temperature of the sample chamber. The indicators below it record the three individual temperature events you selected. These studies in thermal microscopy can be conducted at the same five heating rates available with the FP-1.

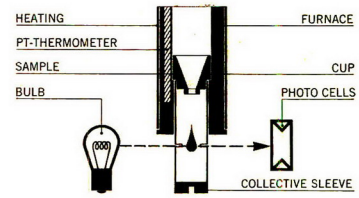

Determines dropping points electronically

Good at the First Drop

3 The Mettler FP-3 automatically determines dropping points of lubricating greases, ointments and edible fats in just a few minutes. The procedure conforms to the ASTM D-566 and D-2265 test specifications. When the first drop of grease to fall from a heated sample cup crosses a light beam, the dropping point is registered on the digital readout panel. The FP-3 is simple to operate: select desired temperature program, put sample cup in furnace and read dropping point. Up to 12 dropping point determinations can be conducted per hour over a temperature range of −20°C to +300°C. Heating rates are also selectable and include 0.2, 1.0, 2.0, 3.0 and 10.0°C/min rates. Accuracy of temperature indication at a heating rate of 0.2°C/min is ±0.1°C. Reproducibility (at 0.2°C/min) is ±0.2°C.

If you want to take the subjectivity out of your melting, boiling, or dropping point determinations, ask Mettler for FP-1 and FP-3 literature. Need precise control in your thermal microanalyses? Request literature on the Mettler FP-2. Or request a demonstration or trial in your own lab of these instruments. Write Mettler Instrument Corporation, 20 Nassau Street, Princeton, New Jersey 08540.

Mettler®

Circle No. 96 on Readers' Service Card

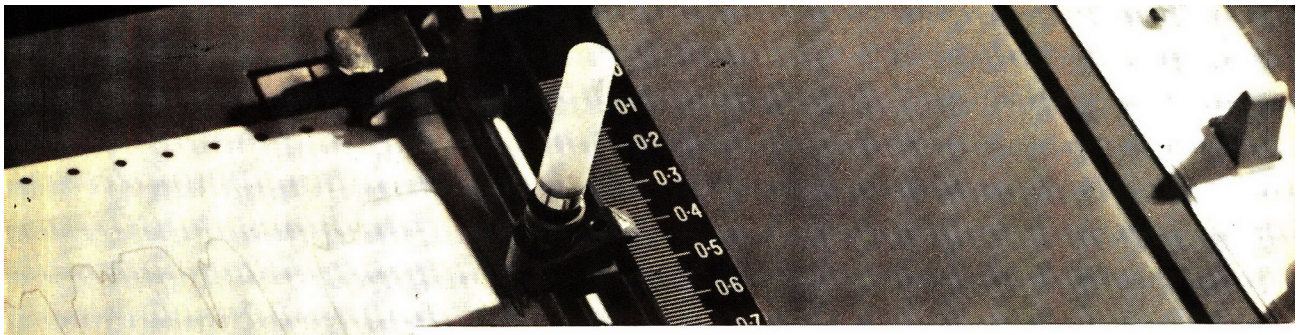

Perkin-Elmer offers you the most complete range of U.V. Spectrophotometers in the world!

One of them is ideal for your application. For instance, the new Model 402 scans from 190 to 850 nm in only two minutes and gives you built-in ordinate scale expansion, selectable wavelength limit switches, time drive and repetitive scanning, Flowchart recording, plus automatic multiple sampling to follow enzyme reactions. The Model 124 is a double-beam instrument with manual or recording operation, whilst the Model 139 has an extensive range of accessories for unsurpassed versatility. The Model 6/20 is robust and reliable, ideal for routine clinical use. The Model 450 has a double monochromator giving superb performance from 165 nm.
Get details from Perkin-Elmer Ltd, Beaconsfield, Bucks, England.
Tel: Beaconsfield 2571.
Telex 83257.

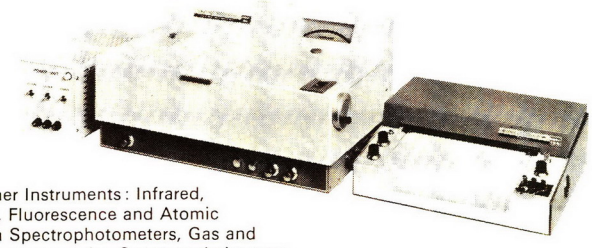

Perkin-Elmer Instruments: Infrared, Ultraviolet, Fluorescence and Atomic Absorption Spectrophotometers, Gas and Liquid Chromatographs, Spectropolarimeters, Elemental and Thermal Analysers, Mass and NMR Spectrometers.

PERKIN-ELMER

Circle No. 136 on Readers' Service Card

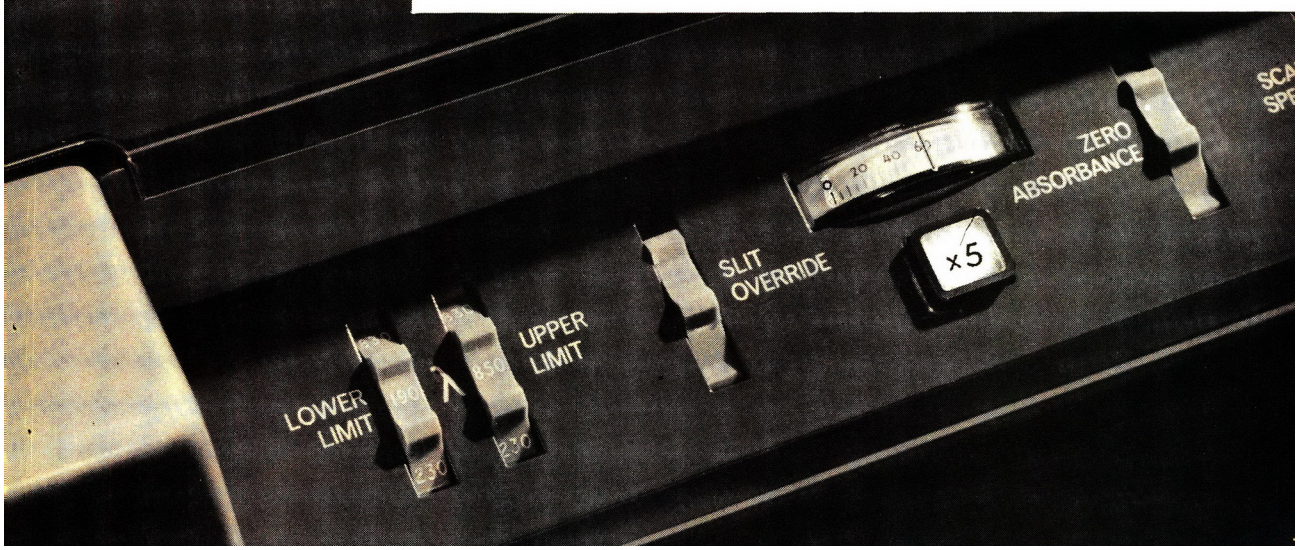

This NEW rotating electrode extends the operating capability of the Electroscan 30® Electroanalytical System. A wide potential range is provided by a variety of interchangeable electrode tips, such as: Boron Carbide, Vitreous Carbon, Nickel, Platinum, Gold, Platinum Wire, and Carbon Paste. It is available with fixed (30 rps) or variable (3-100 rps) rotational speeds.

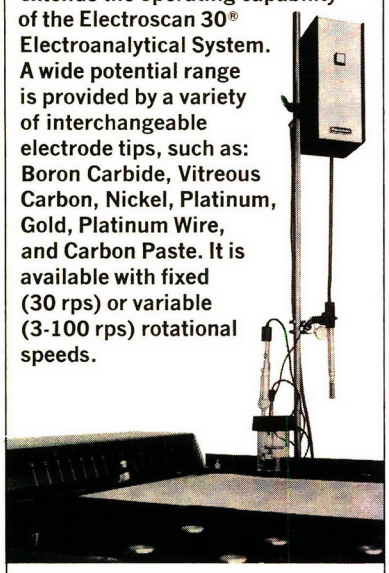

In electrochemical analysis... Beckman builds the Mind Free-er

Electroscan 30®: the most versatile self-contained electroanalytical system available. The advanced circuitry of this single instrument incorporates galvanostat and potentiostat modes of operation, a pH meter, and a 10-inch potentiometric recorder. It provides solutions to problems associated with organic and inorganic studies in research, education, and general analytical areas. Studies such as kinetics of electrode processes, rate constants, diffusion coefficients, and reaction mechanisms. The instrument's capability may be further extended by using any of a wide variety of accessories. Electroscan 30®: for a proven performer, it is the most "experimental" device going. For full details, contact your Beckman Sales Representative or write for Data File No. 9.

Beckman®
INSTRUMENTS, INC.
SCIENTIFIC INSTRUMENTS DIVISION
FULLERTON, CALIFORNIA • 92634

INTERNATIONAL SUBSIDIARIES: AMSTERDAM; CAPE TOWN; GENEVA; GLENROTHES, SCOTLAND; LONDON; MEXICO CITY; MUNICH; PARIS; STOCKHOLM; TOKYO; VIENNA

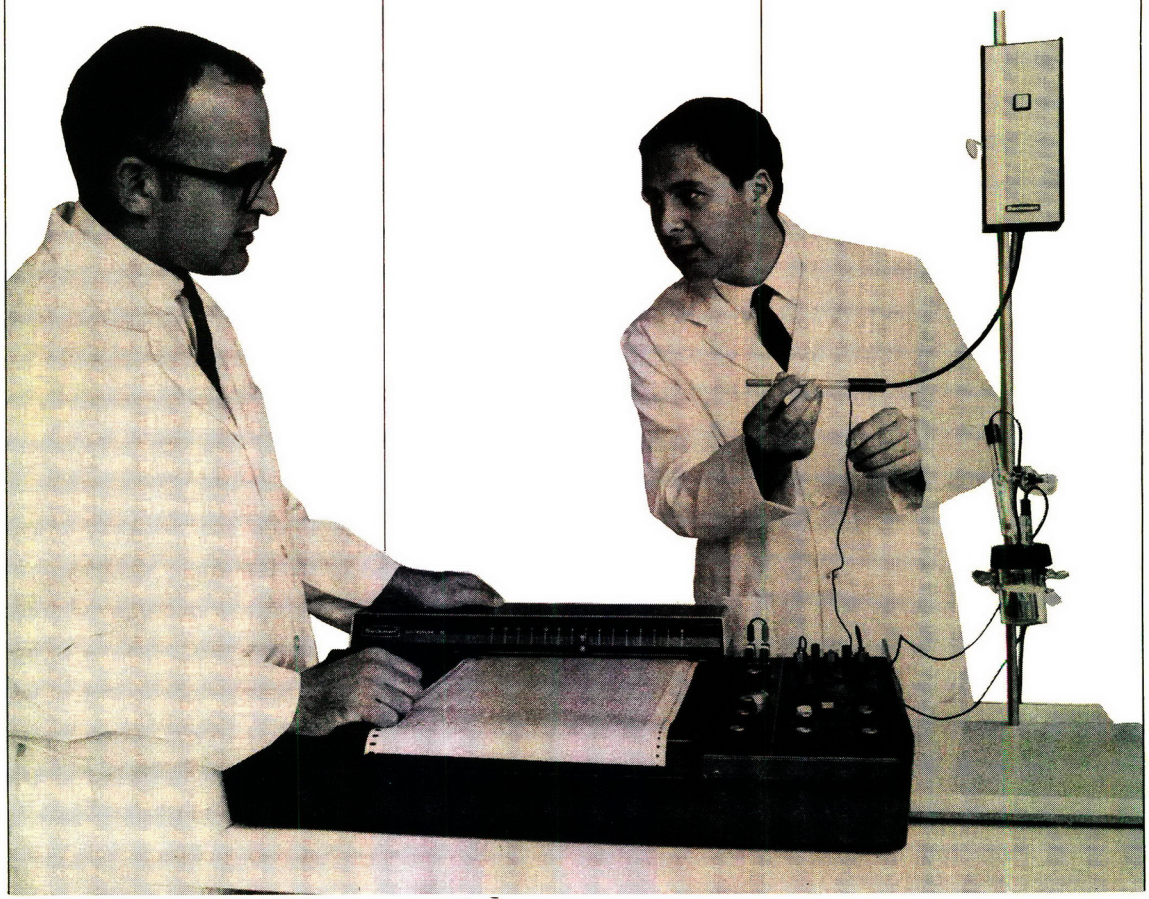

Circle No. 104 on Readers' Service Card

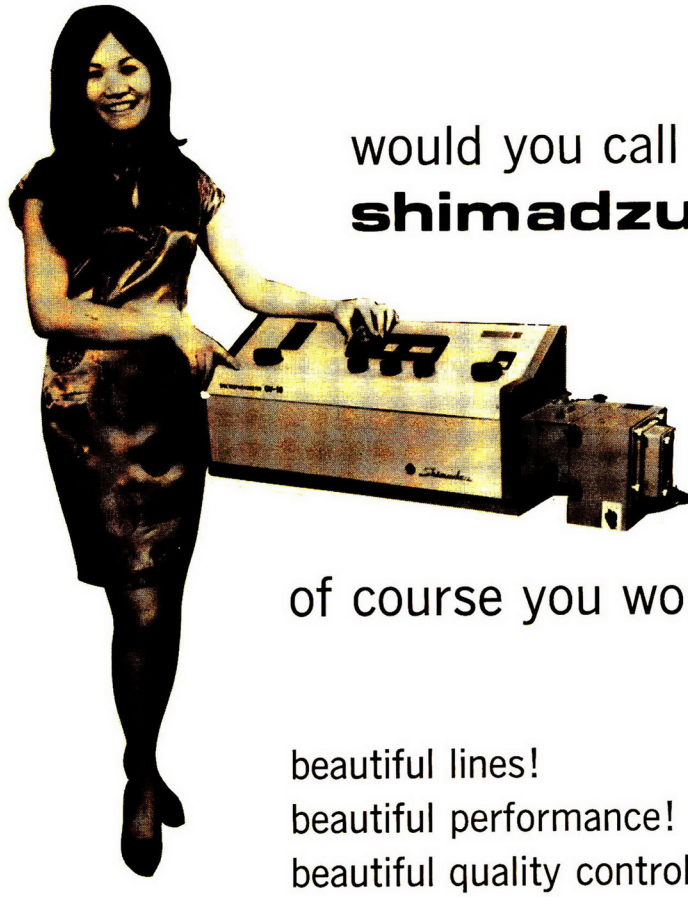

would you call **shimadzu** beautiful?

of course you would...

beautiful lines!
beautiful performance!
beautiful quality control!
a beautiful spectrophotomer!

Let's talk about beauty... in a spectrophotometer. And that brings us to the **shimadzu** QV-50.

Rarely does a piece of equipment perform completely as per manufacturer's specifications, and the QV-50 practically never needs servicing.

The expectations of all our users in the field were far exceeded. Range and accuracy are real. The QV-50 can expand either end of its readout from 0 to 10% and from 90% to 100% over the full scale.

shimadzu has internal beauty too. The enclosed monochromoter is a sealed unit (dirt and dust can't get in to affect optics and create stray light). As standard equipment, a set of thermospacers is supplied. We take this for granted, but no other instrument of its type has this as a standard feature. It also supplies a cell holder which will take from micro to 20mm. cuvettes.

The QV-50 power supply does not generate heat like its competition because of its partially transistorized construction. It will take a much greater range of accessory equipment than does any other single beam spectrophotometer of its type.

shimadzu 's a pioneer in the introduction of optical rotatory dispersion and circular and flow dichroism in single beam spectrophotometric instruments.

AND THE BEAUTY OF IT ALL? These important standards are now brought into your price range—$3500.

COSMOS SCIENTIFIC CO.

921 BERGEN AVE., JERSEY CITY, N.J. 07306 · (201) 925-1101

Distributed by: **Ace Scientific Supply Co.** Linden, New Jersey; **American Instrument Co., Inc.** Silver Spring, Maryland; **Preiser Scientific Co.** Charleston, West Virginia

Circle No. 24 on Readers' Service Card

See ACS Laboratory Guide for All Products/Sales Office

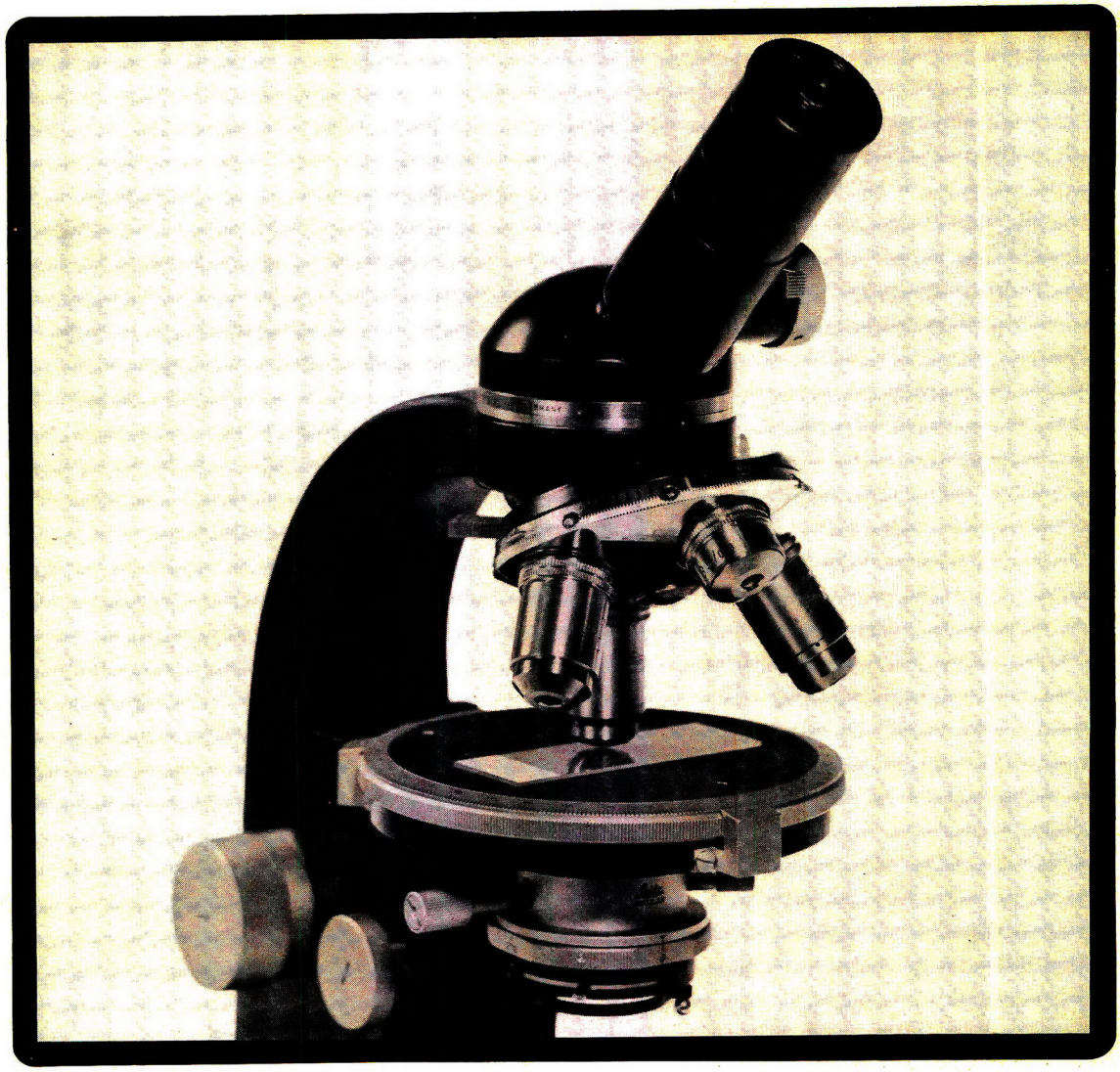

LEITZ SM-POL POLARIZING MICROSCOPE IN A CLASS BY ITSELF FOR THE EARTH SCIENCES

Why is the Leitz SM-POL fast becoming the standard classroom instrument for the advanced geology and chemistry student? It is a polarizing microscope of modern design that is simple to operate. It greatly facilitates development of student techniques in conoscopy, orthoscopy and other general applications in transmitted polarized light. And it is reasonably priced.

The Leitz SM-POL offers a built-in Bertrand lens and pinhole diaphragm in a 360° rotatable, inclined tube. Single-knob coarse and fine adjustment (never needs lubrication) and a particularly wide field of view simplify routine observation and identification. The basic instrument can be customized to suit institutional requirements, with a choice of interchangeable condensers, optical elements and illumination.

The Leitz SM-POL is probably the most popular teaching microscope in geology departments of leading universities. Write for further information on the SM-POL and its many uses in polarized-light microscopy. 63166

Leitz

E. LEITZ, INC., 468 PARK AVENUE SOUTH, NEW YORK, N. Y. 10016
Distributors of the world-famous products of Ernst Leitz G.m.b.H., Wetzlar, Germany—Ernst Leitz Canada Ltd.
LEICA AND LEICINA CAMERAS · LENSES · PROJECTORS · MICROSCOPES

Circle No. 112 on Readers' Service Card

One more reason to research the System T-60:

Computerized NMR spectroscopy

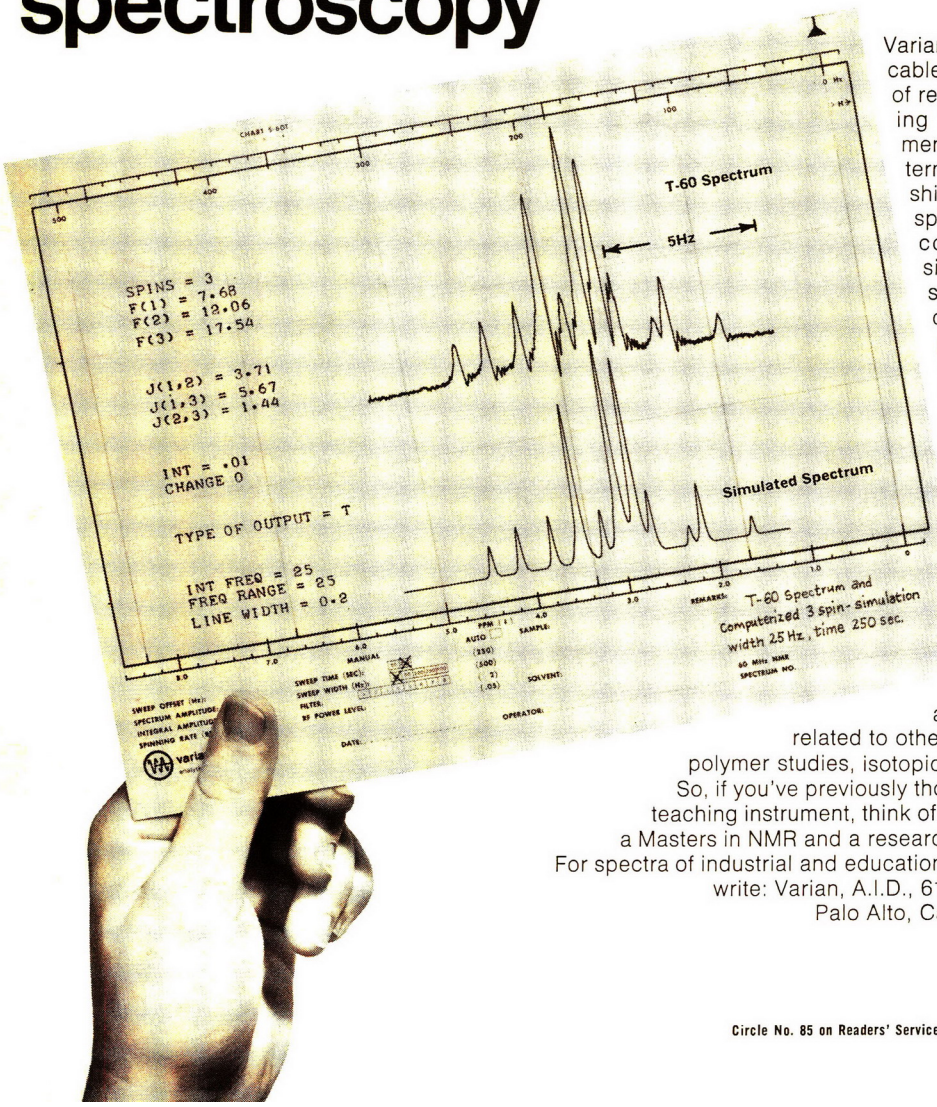

Varian's System T-60 carries impeccable credentials for a wide range of research work. The accompanying T-60 spectrum of an experimental sample has a complex pattern due to small relative chemical shifts of three protons which are spin coupled to each other. The computerized spectrum was simulated by a T-60/computer system from chemical shifts and coupling constants of this sample in less than five minutes. Compare it to the T-60 spectrum. You'll see that it's a good fit and confirms the assignments. You'll also see that the narrow sweep width (1Hz/cm), resolution (0.2 Hz), and spectrum stability of the T-60 were prerequisites for this analysis.

The System T-60, with or without computer, can be used for many other research problems. Also, inexpensive accessories allow you to do basic research related to other nuclei, quantitative analyses, polymer studies, isotopic substitutions. And on and on. So, if you've previously thought of the T-60 as a student-teaching instrument, think of it now as The Graduate — with a Masters in NMR and a research grant for you. For spectra of industrial and educational applications, write: Varian, A.I.D., 611 Hansen Way, Palo Alto, California, 94303.

varian
analytical instrument division

Circle No. 85 on Readers' Service Card

GILFORD UV & VIS SPECTROPHOTOMETERS

. . . . FLEXIBILITY TO MATCH YOUR GROWING NEEDS

OVER 300 READINGS PER HOUR . . . with the model 2443 RAPID SAMPLER

The Gilford vacuum operated rapid sampling system requires samples of only 0.5 ml and can process over 300 per hour. The cuvette remains in the measuring beam for both filling and cleaning, minimizing sample handling and cuvette breakage. Construction of chemically inert Kel-F permits the use of a wide variety of reagents.

With this increased productivity available, transcription time becomes a limiting factor. A permanent record of absorbance or concentration can be printed out automatically by adding the Gilford Model 410 Absorbance/Concentration Meter and Model 4006 Data Lister.

UV or VIS . . . STAINED OR UNSTAINED with the model 2410 LINEAR TRANSPORT

Separation of ribosomal RNA by gel electrophoresis has made a powerful technique available. The development of the Gilford Model 2410 Linear Transport permits you to scan such gels in the ultraviolet directly. You get increased accuracy with high resolution. The time consuming staining process is eliminated.

Unstained and stained materials may now be analyzed, as both ultraviolet and visible energy can be used. With the Model 2410 Linear Transport you will be able to handle materials such as polyacrylamide gel cyclinders and slabs, cellulose acetate membranes, and photographic emulsions.

RECORD 4 INDIVIDUAL REACTIONS WITH 12 POINTS PER REACTION EVERY 3 MINUTES . . . with the model 2441 AUTOMATIC POSITIONER

Your spectrophotometer equipped with the Gilford automatic sample handling system will produce more data than before, while maintaining the precise alignment demanded when using micro cuvettes. In the automatic mode up to 16 plot points, four per individual cuvette, can be recorded in one minute. The exclusive offset feature permits individual baseline adjustment for each cuvette position.

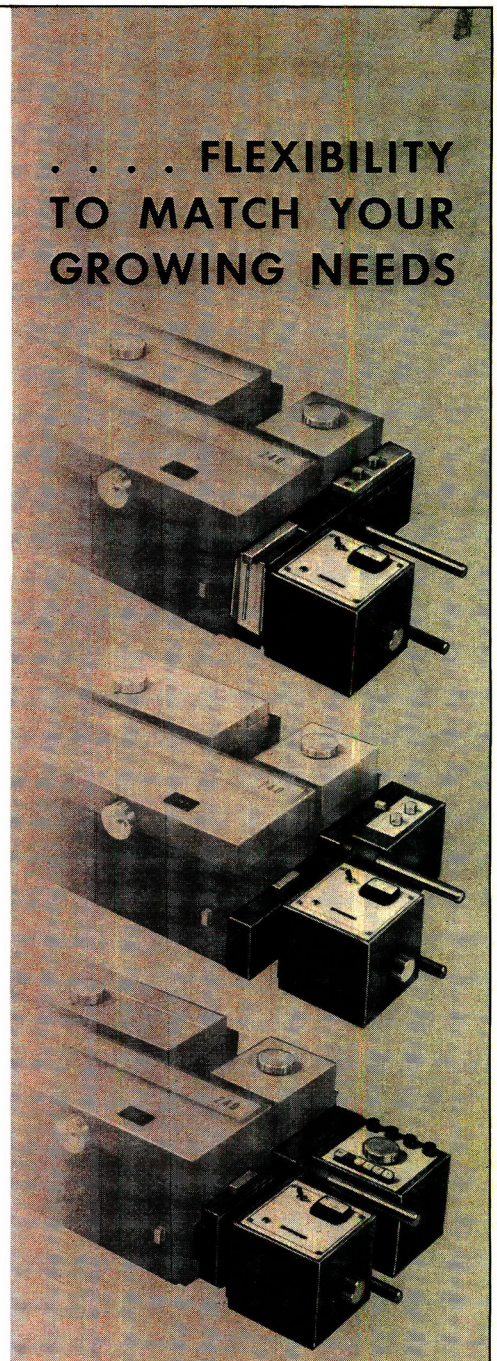

gilford®

Instrument Laboratories Inc.
Oberlin, Ohio 44074

All Gilford UV/VIS Spectrophotometers and most quality monochromators are readily adapted to use these accessories. Find out how easily and inexpensively these devices can be adapted to your present system. Call 216/774-1041 now, or write for Bulletin AC-69.

Circle No. 34 on Readers' Service Card

BOOK REVIEWS

Molecular Crystals: Their Transforms and Diffuse Scattering. José Luis and Marisa Amorós. xxi + 479 pages. John Wiley & Sons, Inc., 605 Third Ave., New York, N.Y. 10016. 1968. $22.50

Reviewed by J. D. H. Donnay, Faculty of Philosophy, Johns Hopkins University, Baltimore, Md. 21218

The authors, two crystal physicists, professors at Southern Illinois University, came to this country from the University of Madrid. Spain's drain was our gain as we acquired this renowned man-and-wife team! For over 15 years they have kept up an intense interest in diffuse X-ray scattering by crystals. This field represents stage III in the development of crystal-structure determination, the first two stages having dealt with (1) static atoms and (2) average thermal ellipsoids. The authors achieve the purpose of their book, which is to show how experimental data obtained from the diffuse scattering of molecular crystals can be analyzed to yield a better understanding of the dynamics of the crystal structure. Our present state of knowledge is the culmination of a long series of experimental investigations that began with Laue's observation that the falling-off of X-ray intensities with increasing glancing angle is due to atomic vibrations. The only recent book in English on diffuse reflections was that of Wooster (1962). The present monograph covers essentially the same ground as the authors' Spanish book of 1963, but the presentation has been completely reworked, reorganized, and greatly expanded. The authors' chief tool is their Difference Fourier Transform (DFT). They show, for instance in the case of anthracene, how this DFT function can be calculated directly from Bragg intensities measured at two temperatures, say 95 and 295 °K: the 2-dimensional temperature-difference Patterson function $\Delta P\ (xOz)$ is computed from intensity differences ($I_{95°-295°}$) of *HOL* reflections, and the needed coefficients of the series $I_{DFT}\ (x^*Oz^*)$ are the sampled values of ΔP. From the maxima of the DFT function, the tilt of the molecule and the coordinates of the atoms can be deduced. The theoretical treatment of scattering is explained with the indispensable mathematics "kept at the lowest possible level", the authors assure us. The book, the second volume in the Wiley series of Monographs in Crystallography, is presented by Professor M. J. Buerger, with a foreword by Dame Kathleen Lonsdale. It was written for crystallographers, but any physicist or chemist should enjoy most of it, particularly its spectacular figures—even though the reproduction of the Laue photographs is not as good as in the Spanish book and much detail of diffuse scattering has been lost. The text is marred by more misprints than I would have expected. An occasional hispanism tells us which country we have to thank for much of the beautiful work reported.

The Electrochemistry of Oxygen. James P. Hoare. xiv + 423 pages. John Wiley and Sons, Inc., 605 Third Avenue, New York, N. Y. 10016. 1968. $19.50

Reviewed by Jaroslav Kuta, J. Heyrovsky Polarographic Institute of the Czechoslovak Academy of Sciences, Prague, Czechoslovakia

Studies of oxygen evolution and reduction and of hydrogen overvoltage, which are the basic electrochemical reactions so important in plant electrolysis, storage batteries, etc., represent an enormous number of papers during the last 100 years. Besides their practical applications, the present knowledge of electrode kinetics is based on the investigation of these important reactions. The recent intensified research in fuel cells, storage batteries, and bioelectrochemical studies attracted still more interest in these fundamental reactions. One of these important topics—the electrochemistry of oxygen—is covered in a review monograph by an expert in this field, James P. Hoare. The author has succeeded in presenting an enormous amount of sometimes controversial material in a very readable and concise form. The book is very informative for all interested in the topic.

In the first third of the book, the author considers the reversible behavior of the oxygen electrode, its oxides on noble metals, and the kinetics of evolution and reduction of oxygen on inert electrodes. A rather comprehensive chapter includes the results obtained with electroanalytical methods and their applications in various fields of analytical chemistry. The second half of the monograph describes the electrochemical behavior of oxygen on active and porous electrodes and the role of oxygen in corrosion processes.

The organization of the book could cause certain difficulties for the reader. Some data on the electrochemical properties of oxygen for inert electrodes are hidden in the Chapter "Electroanalytical Chemistry" (partially elsewhere). In previous chapters, the data were organized according to the electrode material. This chapter could be also shortened by deletion of introductory pages dealing with principles of electroanalytical methods, inasmuch as these principles are well known to most chemists. More space could be devoted to some basic equations of electrode kinetics. Too brief a theoretical explanation may lead to the impression that the proposed mechanisms in the book are based solely on the Tafel slope ~ 0.12 V.

It would be better if the important numerical data scattered throughout the text were presented in tables. An unfortunate omission was a table containing the values of exchange currents and related parameters for the electrode kinetics on various metals. Also omitted was a list of important numerical data for studying the electrochemistry of oxygen, such as oxygen solubilities in the most commonly used electrolytes, diffusion coefficients, etc.

The number of errors in the text, in references or imprecise formulations, is relatively small—*e.g.*, on page 5, $\Delta G°$ should be $-\Delta G°$; on page 182, diffusion is also a kind of mass transfer; and Casopis, pages 69, 77, 397, is not the name of the author but means "Journal" in Czech.

Nevertheless, the stated objections and shortcomings do not diminish the value of the book. The book is clearly and intelligently written and contains many comments and critical remarks of an experienced scientist on the controversial data and explanations published in the literature.

As explained at the beginning, the book covers various aspects of the electrochemistry of oxygen and hence it will find many readers among electrochemists, analytical chemists, and workers in related areas.

Manuel Pratique de Chromatographie en Phase Gazeuse. Jean Tranchant, Editor. xi + 361 pages. Masson et Cie, 120 Boulevard Saint-Germain, Paris 6e, France. 1968. 80F

Reviewed by E. sz. Kováts and M. Ballenegger, Institut de Chimie-physique, Ecole Polytechnique Federale-Lausanne, Switzerland

The second edition of this excellent handbook is another demonstration that a group of specialists, together with an editor, can produce the most useful books for practice. The reader profits both from the experience of the authors and from the synthetic capability of the coordinator. In this case the editor himself is also a specialist and it is probably through his efforts that the nomenclature is quite uniform throughout the book.

This book is mainly intended for the practical chromatographer. This may be seen from the treatment of underlying theory: the derivations are short and emphasis is placed on the understanding and demonstration of the final equations, this being the easiest for the beginner. The reader finds at the end of each chapter a full list of references that are quite up to date.

After a short theoretical introduction (J. Tranchant), the second chapter (J. Tranchant) is devoted to isobar-isothermal chromatography; a short treatment of the theory precedes a discussion of the factors influencing column performance.

In the next chapter (J. Tranchant) the different programming techniques (programmed temperature and programmed pressure) are presented, discussed theoretically, and compared one with the other.

In the fourth chapter (J. Lebbe) construction details of the chromatographic apparatus are given. A short paragraph is devoted to the critical discussion of each individual part with the exception of columns and detectors, which are treated in the next two chapters.

The columns (A. Prévot) are presented in the classical way—*i.e.*, filled and open tubular columns separately. A detailed discussion is given about the support and the stationary phase, together with practical examples. Preparation of the column filling is described in a manner which is easy to execute. A separate paragraph is devoted to the solid stationary phase (adsorbant and modified adsorbant) and to the preparative column.

Two authors (N. Guichard and J. Buzon) describe and classify the detectors. Again, construction details are given. At the end of the chapter there



This product bears 10 successive coatings.

If they are not put down with utmost precision, the product doesn't work.

How well it does work is one of the great success stories of business history.

On hand at
any camera shop.

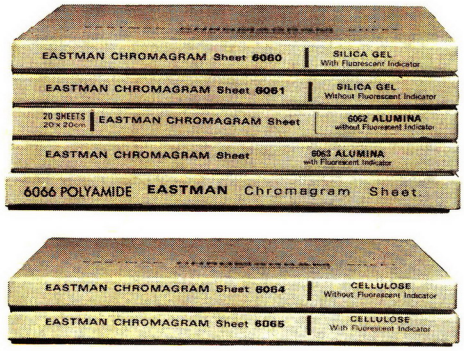

Permit use of two decades of paper chromatography work, yet give same speed and higher resolution than other cellulose-coated TLC media. Credit the purity of the cellulose with which we start and the way we purify it further and redistribute the particle size.

Same plant has to put only one layer on each of these.

Ought to be pretty dependable sheet for your thin-layer chromatography.

On hand at

B&A / CURTIN / FISHER / HOWE & FRENCH / NORTH-STRONG / SARGENT-WELCH / SHANDON / VAN WATERS & ROGERS / WILL

along with

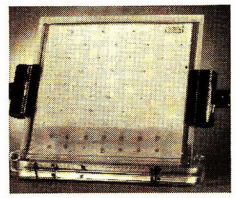

EASTMAN CHROMAGRAM Developing Apparatus, an easily assembled, fast-equilibrating chamber that saturates reproducibly with solvent vapor.

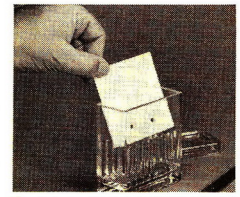

EASTMAN CHROMAGRAM Developing Jar, small and inexpensive, right for pre-testing and for the shorter migrations.

While thinking of TLC, send off a request for the detailed recipe book "EASTMAN TLC Visualization Reagents" to Eastman Kodak Company, Eastman Organic Chemicals, Rochester, N.Y. 14650.

Kodak

is a useful table for comparison of operating characteristics and for localization of the usual detector breakdowns.

The seventh chapter (J. Tranchant) deals with aspects of qualitative analysis. First, practical advice for choosing the type of column and achieving better separation with a given stationary phase is given. A comparative discussion of different systems of identification follows, together with the possibility of obtaining more structural information by the application of further analytical methods (direct coupling with the mass spectrograph and separate treatment of isolated substances).

The quantitative side of the problem is discussed in the next chapter (J. Lebbe): electronic and mechanic integrators, manual evaluation, use of standards, treatment of composite peaks, trace analysis, and finally precision and accuracy.

In the last chapter (J. Serpinet) numerous applications are described in detail.

The reviewers enthusiastically recommend this book also for college students.

Chemical Applications of Spectroscopy, Vol. IX, 2nd Rev. Ed., Part One. W. West, Editor. x + 486 pages. John Wiley and Sons, Inc., 605 Third Ave., New York, N. Y. 10016. 1968. $16.95

Reviewed by James D. Winefordner, Department of Chemistry, University of Florida, Gainesville, Fla.

The second edition of Volume IX, Part I of "Techniques of Organic Chemistry" has ably met a portion of the aim of its predecessor of 12 years ago—namely, to offer a sufficiently comprehensive account of the theory of spectra of organic compounds over the spectral range extending from the microwave to the ultraviolet region to allow the novice unfamiliar with the theory to obtain an introduction to spectra, but yet to cover the needs of the organic chemist engaged in spectroscopic studies. The first edition of Volume IX contained six chapters: Introductory Survey of Molecular Spectra; Microwave and Radiofrequency Spectroscopy; Theory of IR and Raman Spectra; Applications of IR and Raman Spectra to Elucidate Molecular Structure; Electronic Spectra in the UV–Visible Region which was divided into two parts, one on theory and one on application; and Fluorescence and Phosphorescence. The second edition has been completely rewritten and updated from the first edition and is now in several parts. Part I is devoted to only electronic absorption and emission spectra of or-

CURTIN

headquarters for HAMILTON precision syringes

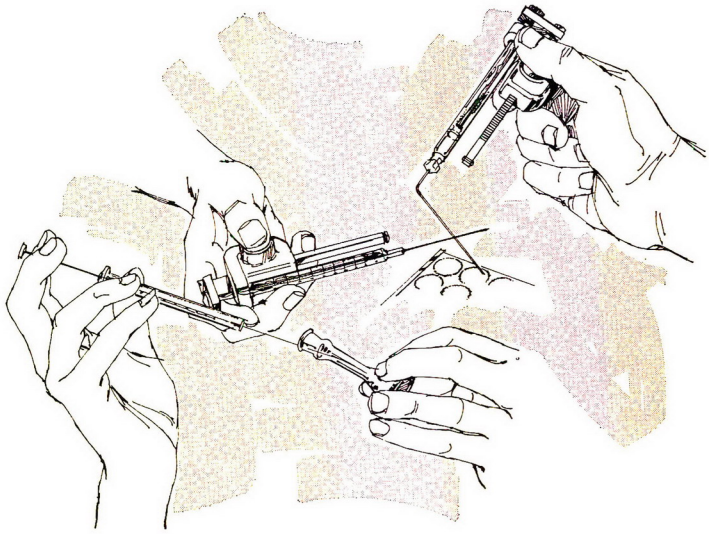

Microliter syringes, gas-tight syringes, filter syringes, medical type syringes, special purpose syringes such as back-fill, threaded plunger, solid sampler and Teflon syringes . . . there's even a Super-syringe. Whatever your needs are, there's a Hamilton syringe that can do the job. Hamilton syringes are accepted as the standard in precision measuring devices in laboratories all over the world. For unsurpassed accuracy, reproducibility and precision, try a Hamilton. For information, write . . . Curtin Scientific Company, P.O. Box 1546, Houston, Texas 77001.

CURTIN SCIENTIFIC COMPANY

SCIENTIFIC APPARATUS · CHEMICALS · LABORATORY FURNITURE

HOUSTON · TULSA · LOS ANGELES · NEW ORLEANS · ATLANTA · SAN FRANCISCO · DALLAS · PITTSBURGH · BOSTON
MIDLAND, MICH. · JACKSONVILLE · WASHINGTON · WAYNE, N. J. · ST. LOUIS · SEATTLE · MEXICO CITY · MONTERREY
GEO. T. WALKER DIVISION · MINNEAPOLIS, MINNESOTA

Circle No. 82 on Readers' Service Card

ganic compounds, (covers material in Chapters 1, 5, and 6 of the first edition) whereas Part II will be devoted exclusively to Microwave Molecular Spectra (covers material in Chapter 2 of the first edition). Other parts will treat IR and Raman spectroscopy, NMR, EPR, etc.

The Introductory Survey Chapter by W. West is so well written and sufficiently complete that it could serve as the theoretical portion of a course on spectrochemical methods of analysis. Dr. West covers the following comprehensive list of topics: spectroscopic units; the origin of pure rotational, vibrational–rotational, and electronic absorption and electronic luminescence spectra; the use of potential energy curves, particularly with respect to the Franck–Condon Principle, the Morse equation, predissociation and the general description of electronic states; intensities of transitions; and a fine discussion of applications of electronic absorption spectra to structure determination. This chapter alone warrants the purchase of this fine, well-edited book.

The remaining three chapters cover the general theory of electronic spectra (A. B. F. Duncan), the interpretation of electronic absorption spectra (R. T. Matsen, R. S. Becker, and D. R. Scott), and fluorescence and phosphorescence spectroscopy (R. S. Becker) in considerably greater depth than in the introductory chapter (W. West) and also in much greater detail than the corresponding material in the first edition. These chapters are well written and well edited and are designed for the more fundamental spectroscopist interested in structure analysis by means of electronic spectra. For example, the chapter by Dr. Duncan contains an excellent section on the use of group theory to determine molecular symmetry and selection rules. In addition, Dr. Duncan covers in considerable depth the principles of atomic spectra and the spectra of diatomic and polyatomic molecules. The final two chapters, which cover the interpretation of electronic absorption and emission (photoluminescence) spectra, contain sufficient theory, as well as the types of chromophors and fluorophors (and phosphors), to be complete within themselves. Although there is some overlap and repetition of the theoretical topics in the four chapters, each chapter is self-consistent and useful without the need to read all preceding chapters.

Despite the relatively high cost of this volume, this reviewer feels that all analytical chemists using molecular spectroscopy should have a copy of Part I (and all other parts if they compare with Part I) in their own library.

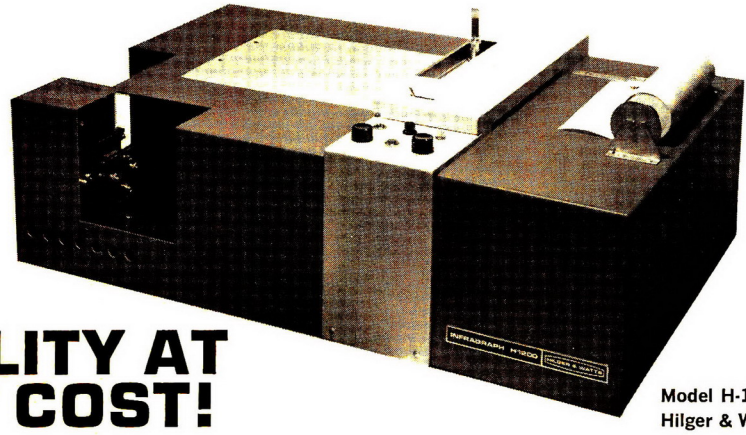

QUALITY AT LOW COST!

Model H-1200
Hilger & Watts Infragraph

THE MOST ATTRACTIVE BUY IN INFRARED SPECTROSCOPY

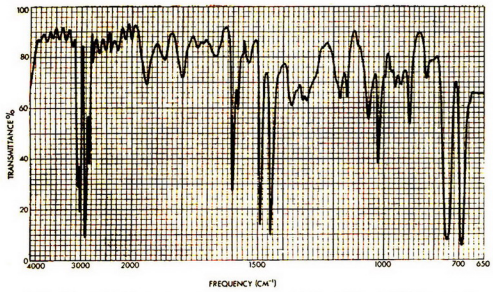

1½ min. polystyrene scan shows spectral quality at high speed comparable to expensive high-performance instruments

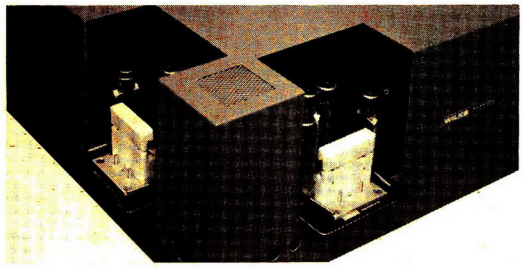

Sample- and reference-beam "corner design" offers enhanced freedom of accessory selection

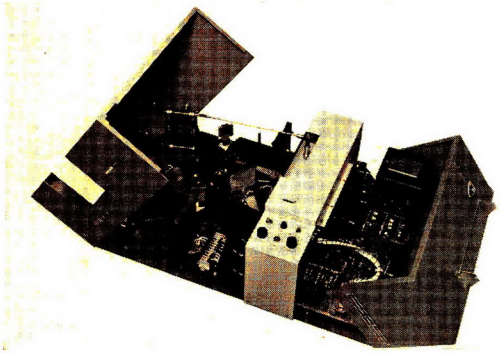

Fold-back covers permit "fingertip" accessibility for instruction and maintenance

BEST PRICED IR SPECTROPHOTOMETER
The new Hilger & Watts H-1200 Infrared Spectrophotometer, distributed exclusively in the United States by Wilks Scientific is not only the lowest priced instrument of its type available but offers versatility and performance provided only by much higher priced instruments.

FASTEST PRODUCTION OF SPECTRA
The Infragraph's outstanding capability of recording complete spectra with excellent resolution and low noise in less than 2 minutes, multiplies the output of useful data. One instrument does the work of several and saves investment for additional equipment.

BROADER ACCESSORY CAPABILITY
Separated sample and reference beam compartments in the Infragraph's unique optical arrangement increase double-beam accessory adaptability. The application-oriented and budget-minded investigator will welcome the Infragraph's accommodation of Wilks Scientific's complete line of standard and special IR accessories.

RUGGED AND RELIABLE
Rugged construction using quality components and solid-state electronics have produced excellent reliability records for the many instruments already installed in Europe. Service personnel and stocks of spare parts or supplies are available at Wilks Scientific to ensure uninterrupted operation.

INFRAGRAPH SPECIFICATIONS:
Spectral range: 4000 to 650 cm^{-1} (2½ to 15.4 microns)
Resolution: Better than 5 cm^{-1} at 1000 cm^{-1}
Abscissa Accuracy: 5 cm^{-1} from 2000 to 650 cm^{-1}
Repeatability: 2 cm^{-1}
Photometric Accuracy: 2% T Repeatability: 1% T
Scanning Speeds: 1½ to 20 min. continuously variable
Pen Response: 1 sec. full scale (noise level less than 1%)
Recording System: Flat bed, flow and single charts
Chart Presentation: Linear cm^{-1}, 9″ and 18″ abscissa
Time Drive: Transmittance recording at constant wavelength
Dimensions: 27½ x 17⅞ x 8½ inches. Weight: 81 pounds

INFRARED IS OUR BUSINESS

WILKS SCIENTIFIC CORPORATION

SOUTH NORWALK • CONNECTICUT 06856
TELEPHONE • (203) 838-4537

Circle No. 133 on Readers' Service Card

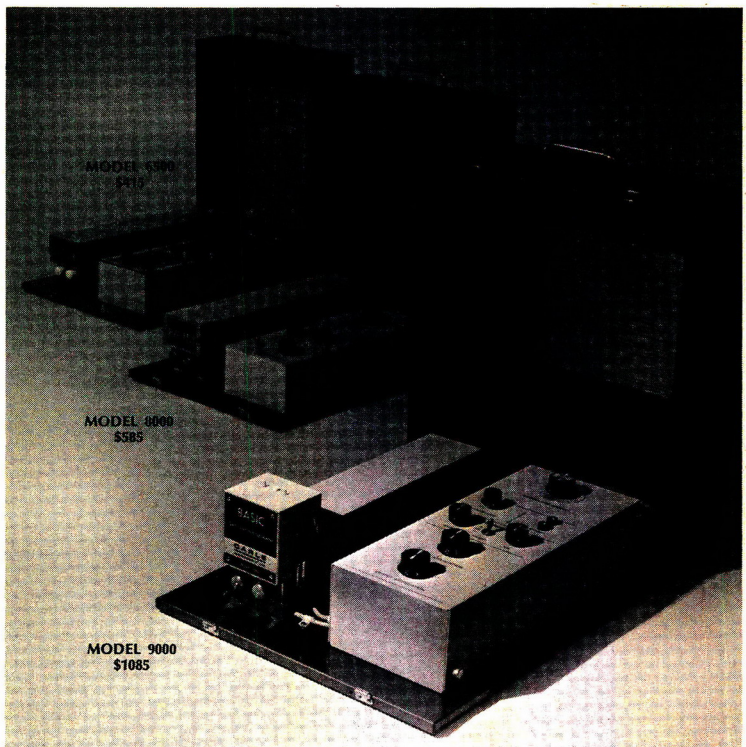

flame ionization sensitivity– a new basic solution

FID instrumentation is not new to gas chromatography. But the Carle Model 9000 Basic™ GC with Flame Ionization Detector is . . . in concept . . . in low cost design . . . and in rugged, reliable, and simplified performance.

Start with these key features:

- Advanced design differential hydrogen flame detector.
- 1 x 10^{-11} MOSFET solid state electrometer.
- Proven dual column, on column inlet system.

At $1085, this is an outstanding new instrument for high sensitivity gas chromatographic applications of organic and biochemical analysis, environmental pollution, or any area where hydrogen flame sensitivity is paramount.

The Model 9000 is the latest in the Carle family of widely accepted Basic™ Gas Chromatographs. Other models include:

MODEL 6500 – More than 750 of these units are in use throughout the world particularly in colleges and universities as an ideal instructional device.

MODEL 8000 – A unique solution to repetitive routine analysis, the Model 8000 frees high-cost research chromatographs for more difficult problems.

Write today for Data File 123 containing complete information on all three of these instruments.

CARLE

INSTRUMENTS, INC.

1141 East Ash Avenue, Fullerton, California 92631 (714) 879-9900

Circle No. 119 on Readers' Service Card

See ACS Laboratory Guide for All Products/Sales Office

New Books

Handbook of Biochemistry. Herbert A. Sober, Editor. The Chemical Rubber Co., 18901 Cranwood Parkway, Cleveland, Ohio 44128. 1968. $29

The results of current research in two fast-moving fields of science are set forth in the "Handbook of Biochemistry with Selected Data for Molecular Biology." The book consists almost entirely of tabular data, and care has been taken to assure a high degree of reliability in the data. Eleven sections make up the book: abbreviations and nomenclature; amino acids; peptides and proteins; carbohydrates; lipids; steroids, purines, pyrimidines, nucleotides, and oligonucleotides; nucleic acids; genetics and biology; physical and chemical data; and miscellaneous. Enclosed with each book is a four-color "chart of biochemical pathways," measuring 3×4 feet, which outlines the dynamic relationships that exist in intermediary metabolism and illustrates the interdependence of the various biochemical systems involved in energy storage and utilization, biosynthesis, and catabolism.

Reviews in Macromolecular Chemistry Vol. 3. George B. Butler and Kenneth F. O'Driscoll, Editors. viii + 422 pages. Marcel Dekker, Inc., 95 Madison Ave., New York, N. Y. 10016. 1969. $16.50

This is the book edition of the international publication of advances in high-polymer chemistry. It is published annually from the journal edition to make available a complete, durable, hardbound, fully-indexed publication. The book should be of interest to organic and physical chemists, biochemists, engineers, and all students and research workers in polymer chemistry and related fields.

Progress in Coordination Chemistry. Michael Cais, Editor. xxvii + 845 pages. American Elsevier Publishing Co., Inc., 52 Vanderbilt Ave., New York, N. Y. 10017. 1968. $45

Abstracts, not only of the scientific contributions presented during the Eleventh International Conference on Coordination Chemistry, held at Haifa and Jerusalem from September 8–18, 1968, but of all those submitted, are gathered together in this volume. The wide range of topics covered by the abstracts presents a picture of what is today the state of progress in coordination chemistry. They are: coordination compounds in homogeneous catalysis; photochemistry in coordination

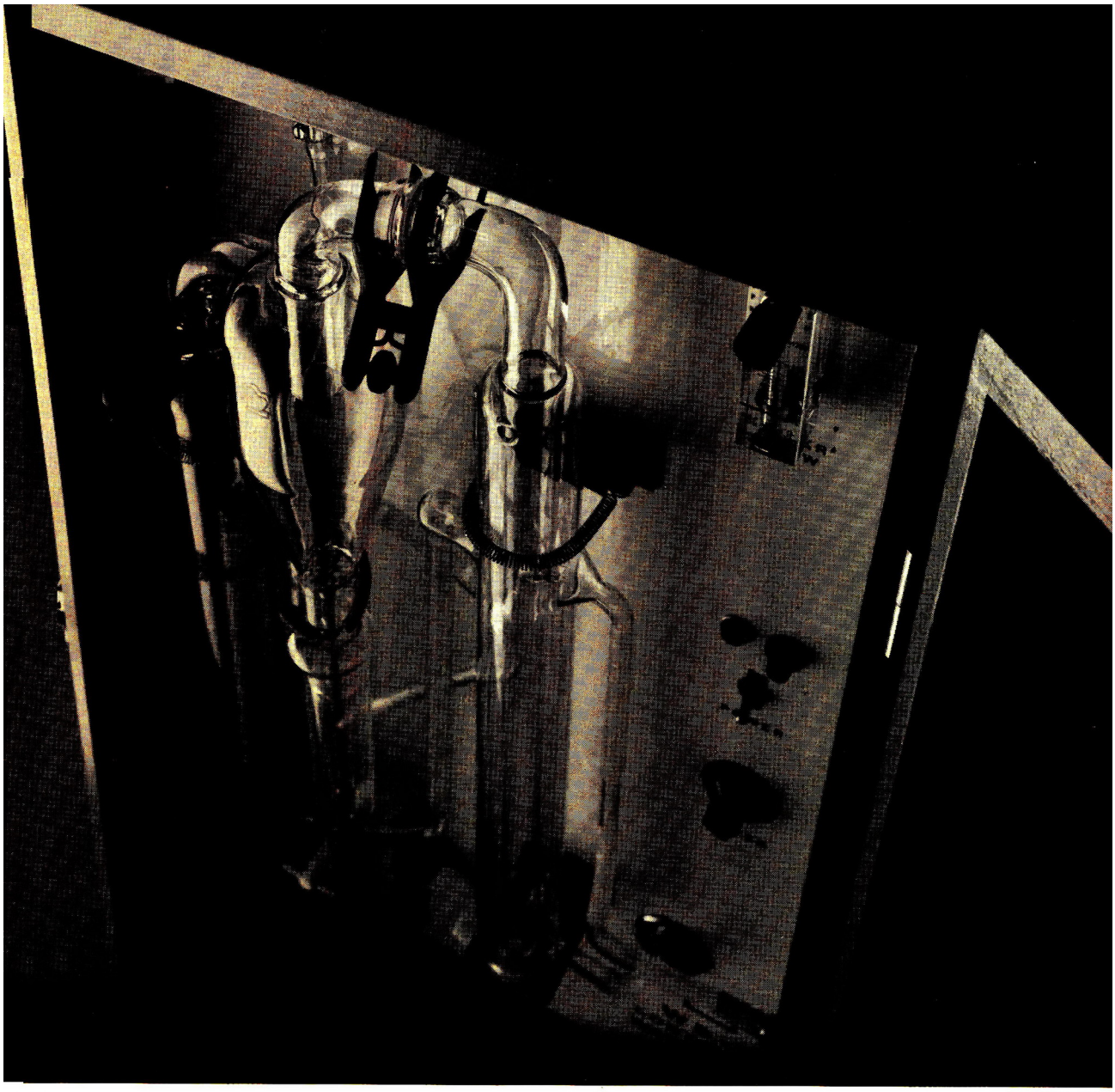

What price purity?

How much is a good laboratory still worth? (A still with an all glass and Teflon® system that produces distilled water of 2 million ohms purity and less than 0.3 ppm total solids from tap water and a 110 volt outlet.)

That's our definition of a good water still and we have one in our WS-2 Continuous Water Still—for a surprisingly low $395.

A redistillation kit can be added to satisfy the real purists (actually, the WS-2 makes better distilled water in a single pass than most other stills do with redistillation).

There are several ways we assure purity. For example: in the "cyclone separator" the long circular travel path together with two vapor direction changes scrub vapors and provide good refluxing and de-entrainment. Double venting removes volatile material and dissolved gases. Non-volatile contaminants are carried away in the cooling water drainage. Automatic pressure regulation prevents uneven operation and reduces distillate waste.

Depending on local water supplies, the WS-2 with redistiller can consistently achieve resistivity well in excess of 2 million ohms.

Besides high purity at low cost, the WS-2 gives you the reliability, durability, and advanced design of Kontes products: non-leaking joints, a rapid-start heater, and Teflon tubing and O-rings. If external water pressure drops too low, the still automatically shuts off and triggers both audible and visual alarms.

It's compact, portable, and easily cleaned without disassembly.

Normal output of distillate is 2 liters an hour.

If you've been looking for a low-cost, practical solution to the pure water problem, you couldn't find a better one than the WS-2. Contact your Kontes representative or write for more details.

® Trademark of Du Pont

KONTES
Vineland, New Jersey

Regional Distributors: **KONTES OF ILLINOIS,** Franklin Park, Illinois • **KONTES OF CALIFORNIA,** Berkeley, California

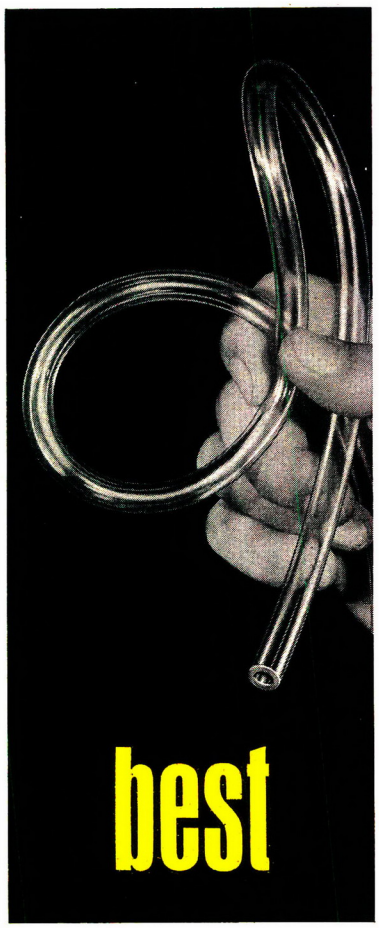

Day in and day out, the reliability, long life and versatility of Tygon flexible plastic Tubing proves over and over that it's your best laboratory tubing investment.

TYGON® TUBING

Crystal-clear
Flexible
Chemically inert
Non-oxidizing
74 standard sizes

At laboratory supply houses everywhere, or write Norton Plastics and Synthetics Division, Akron, Ohio 44309.

32-114

NORTON

PLASTICS & SYNTHETICS DIV.
FORMERLY U.S. STONEWARE INC.
AKRON, OHIO 44309

Circle No. 52 on Readers' Service Card

compounds; kinetics and mechanism of reactions of coordination compounds; synthesis, structure, and stereochemistry of coordination compounds; organometallic chemistry; coordination compounds in biochemistry; theories of bonding in coordination compounds; physical methods in coordination compounds; coordination compounds in solvent extraction; and coordination compounds in nonaqueous solvents.

Molecular Spectroscopy of the Triplet State. S. P. McGlynn, T. Azumi, and M. Kinoshita. xiii + 434 pages. Prentice-Hall, Inc., Englewood Cliffs, N. J. 07632. 1969. $16.95

This book represents a single-volume source to the principal publications in the field. Including extensive tables of data and bibliographies, it will be an aid for advanced students and research workers in physical chemistry, chemical physics, biochemistry, and biophysics who are engaged in this area of study. The early chapters provide a general coverage of the triplet state involvement in chemistry, physics, biology, biochemistry, and biophysics. These are followed by detailed handling of spinorbit coupling in all its physical manifestations in molecules. Much of this material has never before appeared in the literature of the field, and is of particular significance to readers interested in the areas of luminescence, photochemistry, photobiology, and weak intermolecular interactions. The final three chapters are concerned with spin–spin coupling. The development of spin-spin and spinorbit approaches to zerofield splitting studies is systematically and succintly developed here, and will be of particular interest to EPR spectroscopists and readers concerned with the disposition of energy among excited levels.

Comprehensive Index on API 44-TRC Selected Data on Thermodynamics and Spectroscopy. xvii + 507 pages. Thermodynamics Research Center, Department of Chemistry, Texas A & M University, College Station, Texas 77843. 1968. $14

The index which is composed of an alphabetical Compound Name Index and a Formula Index gives the location of all date reported in each of the six categories of both the API Research Project 44 and the TRC Data Project series of publications of numerical tables and spectral catalogs. This computer-generated index is designed primarily for use with data published by the API Research Project 44 and the TRC Data Project. Used alone, it will be of limited value.

(continued on page 77A)

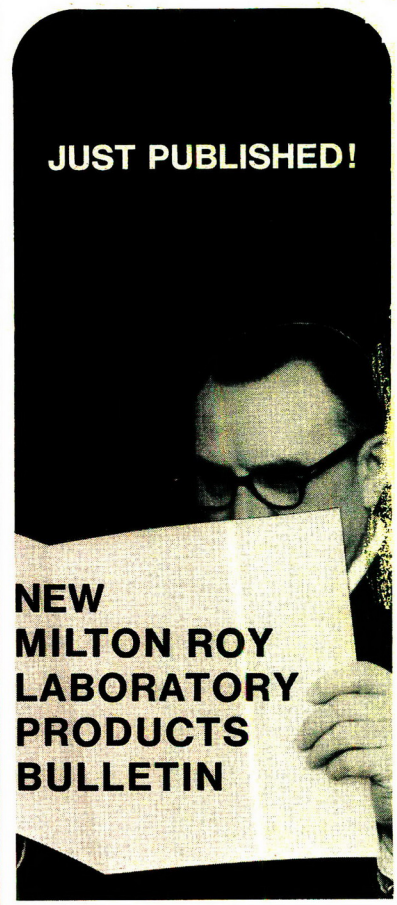

Ready now! A new, comprehensive bulletin describing Milton Roy's special line of products for use in gas or liquid chromatography and other critical laboratory applications. Helpful technical data on:

- **Hydrogen Generators**
- **Instrument Pumps**
- **Deuterium Generation**
- **Hydrogen Purifiers**
- **Low-capacity Controlled Volume Pumps**
- **Gas Analyzers**

Find out how these products can bring better performance and greater economy into your laboratory. Send today for your copy of the new bulletin. Write to Milton Roy Company, P.O. Box 12169, St. Petersburg, Florida 33733.

MILTON ROY COMPANY
ST. PETERSBURG, FLORIDA

Circle No. 50 on Readers' Service Card

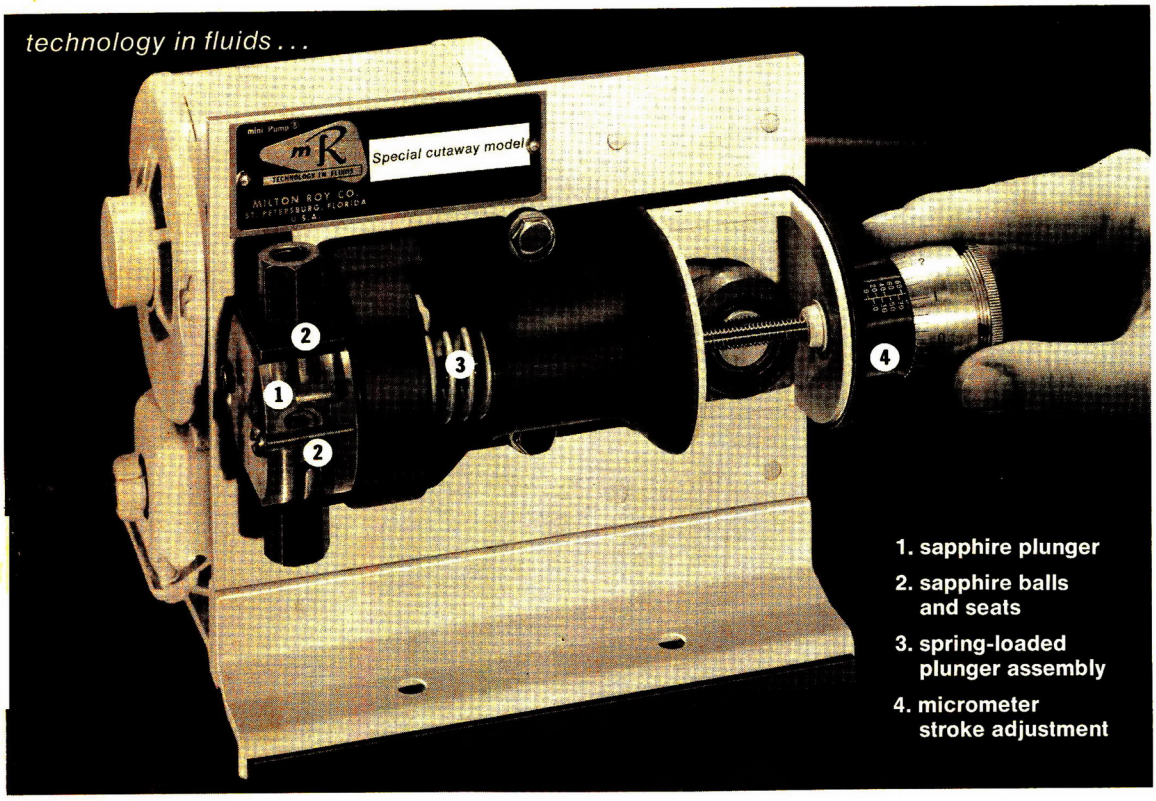

look into the advantages of the instrument miniPump® for liquid chromatography

Instrument miniPumps serve as critical components in many major-make analyzers for metering small volumes of liquids at pressures to 1000 psig with constant repetitive accuracy of ±0.3%.

Superior miniPump performance results from precise reciprocating action achieved with a unique spring-loaded plunger assembly actuated by a cam. Plunger travel is continuously adjustable with a micrometer stroke control that permits capacity changes as close as 0.2% of stroke.

For optimum pump service, single-crystal sapphires are used for the plunger and for the seats and balls in the double-ball check valves. The superfinished plunger will not distort, score, or corrode, and permits O-ring sealing to prevent contamination of the liquid being pumped. A special stainless steel alloy makes the entire liquid end highly chemical resistant. Use of dry, antifriction bearing surfaces results in oil-less operation.

Capacity ranges are from 16 to 460 milliliters/hour for the simplex models, duplex units available. Prices are only $348 for simplex models, $608 for duplex, F.O.B. Factory.

Check into all the advantages of the Instrument miniPump by writing today for Bulletin 25.002 to Milton Roy Company, P.O. Box 12169, St. Petersburg, Florida 33733. Plants also at Philadelphia, Pa.; Rochester, Minn.; Peterborough, Ontario; Runcorn-Cheshire, England. Sales and service offices worldwide.

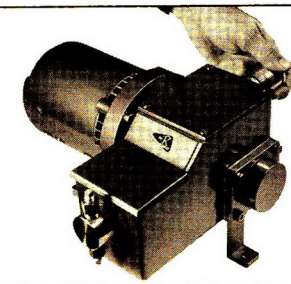

Milroyal D Controlled Volume Pump is another proven component for critical analyses applications. Laboratory capacities from 30 to 7150 ml/hour. Discharge pressures to 1000 psig (some models to 3000 psig). ±1.0% repetitive accuracy. Simplex and Multiplex models. Prices from $282, F.O.B. Factory. Ask for Bulletin 36.001.

MILTON ROY COMPANY
ST. PETERSBURG, FLORIDA

Circle No. 49 on Readers' Service Card

Why is the Jarrell-Ash

LASER RAMAN SYSTEM

THE BEST?

A. LOWEST SCATTERED LIGHT

The Jarrell-Ash Laser Raman System utilizes a new double Monochromator (vertically-stacked Czerny-Turner instruments) that produces stray light levels of less than 10^{-10}. This permits detection of very weak Raman spectra, especially important when it occurs close to the exciting line.

B. PERFECT TRACKING

Gratings of both monochromators are mounted on a common pivot to insure perfect tracking over the entire wavenumber range of the instrument. This allows sharply defined Raman spectra to be recorded even though it may occur as far as 3000 to 4000 cm^{-1} from the exciting line.

C. BETTER RESOLUTION

Utilizing twin, symmetrical Czerny-Turner optical paths, the double monochromator produces better resolution than any other comparable instrument. Maintaining extremely small included angles, coma is reduced to negligible proportions. The direction of the lower monochromator's optical path is reversed from that of the top. This eliminates "double dispersion" and provides higher energy through-put and higher resolution with a narrow exit slit.

D. ACCEPTS NUMEROUS COMMERCIAL LASERS

The Jarrell-Ash Laser Raman System can utilize many of the newly developed commercial lasers, e.g., the He-Ne, Kr, Ar and others that maintain constant, stable high intensity output. This allows great flexibility in exciting various samples.

E. LARGEST SAMPLE CHAMBER

The sample chamber features a working area 66 cm wide x 85 cm long x 60 cm high to permit use of even large Dewars for controlled temperature experiments.

F. FLEXIBLE OPTICAL PATH

The optical path offers high efficiency and flexibility. The use of Brewster angle-prisms to divert the laser beam, eliminates light loss due to reflection. Special lenses are employed to maintain intensity and control beam size. Provisions are made to direct the laser beam down through, straight through, or up into the sample.

G. POLARIZATION FEATURES

Polarization characteristics of the gratings are matched to those of the system. Special optics permit the plane of polarization of the laser beam to be altered accurately, an especially useful feature in semi-conductor, crystal and related studies.

An informative, descriptive bulletin on the 25-300 Laser Raman System is available on request. Direct requests to Jarrell-Ash Co.

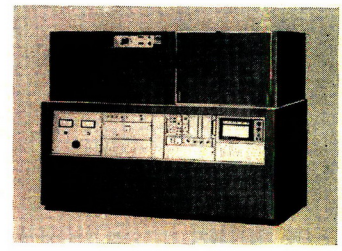

Jarrell-Ash
DIVISION OF FISHER SCIENTIFIC CO.

Jarrell-Ash Division/Fisher Scientific Company, 590 Lincoln Street, Waltham, Mass. 02154

PLANTS IN: Le Locle, Switzerland / Kyoto, Japan / **SALES OFFICES:** Burlingame and Costa Mesa, California / Dallas and Houston, Texas / Silver Spring, Maryland / Farmington, Michigan / Elmhurst, Illinois / Springfield, New Jersey / East Hartford, Connecticut / Port Credit, Ontario, Canada

Circle No. 86 on Readers' Service Card

Chemist's Guide: Basic Chemical and Physical Data. J. P. Jesson and E. L. Muetterties. iii + 43 pages. Marcel Dekker, Inc., 95 Madison Ave., New York, N. Y. 10016. 1969. Paperbound. $1.95

This book consists of physical and chemical data that are not easily accessible in a single source and which are of value to the student of chemistry and to the research chemist. Contents: General and magnetic constants — Energy conversions — Atomic radii, electronegativities, and ionization potential — Ionic radii — Spectrochemical, nephelauxetic, and π-acceptor series —Electrode potentials — Bond energies — Selected structural data — Bond dipole moments and polarizabilities — Electron affinities — Nuclear magnetic resonance data — Hammett substituent constants — Triplet excitation energies — Amino acids-DNA and genetic code — Character, correlation, and direct product tables — Coordination polyhedra — Atomic numbers, weights, and electronic configurations.

U. S. Government Publications

The following publications can be ordered from the U. S. Department of Commerce Clearinghouse for Federal Scientific and Technical Information, Springfield, Va., 22151. Prices for all documents are $3.00 each for paper copy and 65¢ for microfiche. All orders require prepayment by coupon, check, or money order.

Mössbauer Study of Dilute Alloys of Iron. (AR-680 952). A Lineberger. November 1968. 48 pages.

Studies magnetic ordering in alloys of iron and germanium and iron and tin by means of the Mössbauer effect. Mössbauer absorption spectra in a transmission geometry are used to measure changes in the hyperfine splitting due to certain numbers and locations of impurities.

Radiochemistry of Silicon [NAS-NS-3049 (Rev)]. D. R. Schink. November 1968. 81 pages.

Covers the following topics: nuclides of silicon (nuclear properties, production availability); chemistry of silicon as applicable to radiochemistry; safety practices; and radiochemical practices and counting techniques.

Anodic Polarization of Titanium and its Alloys in Hydrochloric Acid (AD-682 740). M. Levy and G. N. Sklover. November 1968. 15 pages.

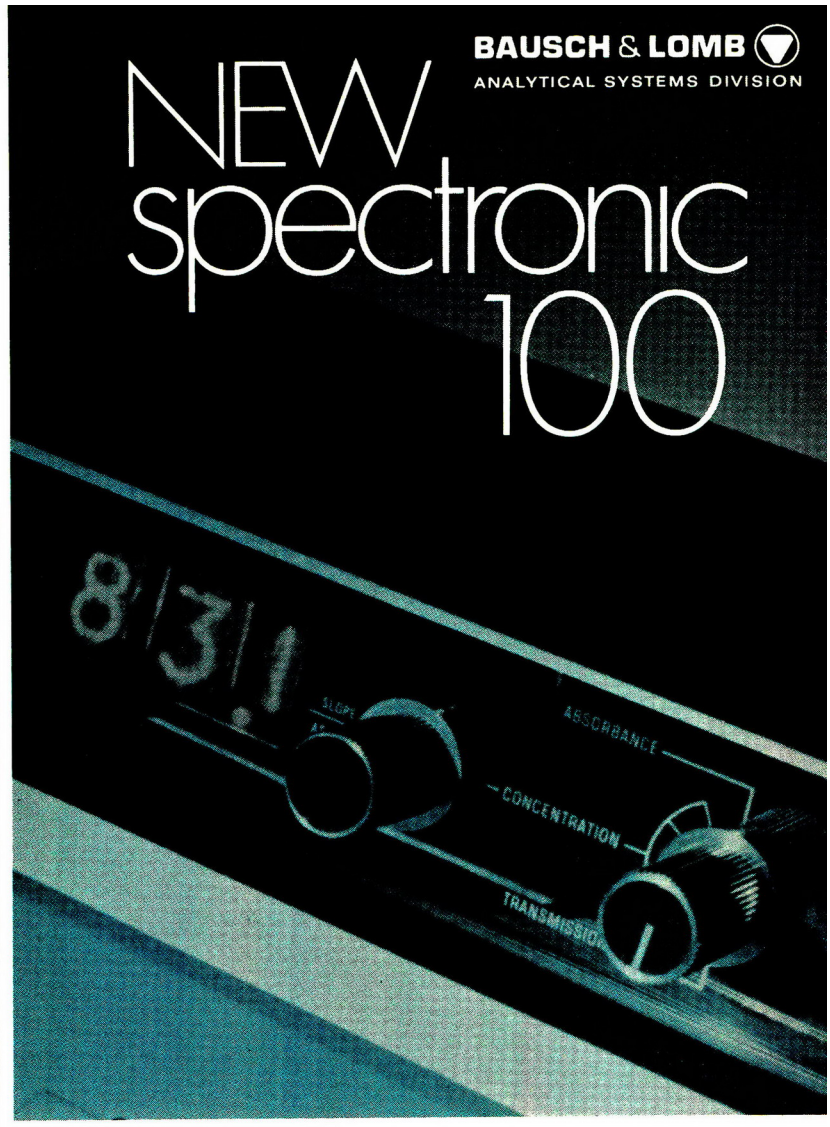

four place digital readout, three modes: linear T and A, plus concentration

The new Spectronic® 100 is one of the most versatile, yet accurate and reliable Spectrophotometers available in the medium price range. It provides the customer with maximum operational ease and instrument appeal as well as unprecedented measurement flexibility and versatility. It permits the analyst to read results in transmittance, absorbance, or absolute concentration units directly from single, multiple or microflow thru cells, using a digital Nixie tube display. BCD output is available from a 40 pin connector at the rear of the instrument enabling the user to quickly and conveniently use any one of a variety of recording or printout devices — analog or digital.

Wavelength range extends from 325nm-925nm, with a 8.0nm bandpass. Readout to four digits: in transmittance from 000.0-100.0%, in absorbance from 0.000 to 2.000A and in concentration from 0000-2000 with selectable positioning of the decimal point.

Reliability of the Spectronic 100 is demonstrated in the short term stability of better than 0.001A, and long term stability of less than 0.001A/hr., coupled with zero drift of less than 0.2% per day.

For more details, write for Catalog 33-6031. If you'd like to see one in your lab, we'll gladly arrange a demonstration. Contact Analytical Systems Division, Bausch & Lomb, 81018 Linden Avenue, Rochester, New York 14625.



Spectronic 100 Spectrophotometer

RS FOR THE ANALYSIS OF PESTICIDES RESIDUE

CARLO ERBA HAS DEVELOPED A SERIES OF SOLVENTS WHICH POSSESS A MAXIMUM RESIDUE OF THE ORDER OF 10^{-9}% OF INTERFERING SUBSTANCES (GLC e.c.d. EXPRESSED AS ALDRIN)

CARLO ERBA

DIVISIONE CHIMICA INDUSTRIALE - VIA IMBONATI 24 - 20159 - MILANO



Ion Exchange Analysis of Magnesium Alloys (AD-682 741). T. A. Ferraro. December 1968. 18 pages.

Uses a cation exchange–hydrochloric acid system to separate lithium, magnesium, and aluminum from each other, and an anion exchange–hydrochloric acid system to separate 0.1 to 20% zinc from magnesium. An improved chelometric method is presented for determination of the separated zinc.

Energy Levels and Intensities in the Solution Absorption Spectra of the Trivalent Lanthanides (ANL-7358). W. T. Carnall *et al.* March 1968. 94 pages.

Contains sections on the theory of lanthanide absorption spectra, experimental procedures and curve fittings, results of intensity correlations, and the use of intensity correlations to refine energy-level parameters.

Development of a Spectrographic Method for Determination of Low-Level Impurity Elements in Lead–Zirconate Lead–Titanate Mixtures (PB-128 163). N. A. Mirti and B. Shivak. 1968. 126 pages.

Bibliography of Laser Publications of Interest to Emission Spectroscopists (IN-1219). J. M. Baldwin (Ed.). October 1968. 23 pages.

Contains references in the following categories (1) laser beam interactions with gases and vapors, (2) action of laser beams upon matter initially present as a condensed phase, and (3) applications of lasers to spectrographic analysis.

Annual Cumulative Index (USGRDR) is now available. Published through the cooperative efforts of DDC and the Clearinghouse, the Index lists all reports announced in U. S. Government Research & Development Reports during 1968. Each entry gives subject field/group; a code denoting the journal containing an abstract of the report; and the price of the report if sold by the Clearinghouse. The six sections composing the Index are: Section 1, Personal Author; Section 2, Corporate Author; Section 3, Contract Number; Section 4 Accession Number; Section 5, Subject A–M; Section 6, Subject N–Z. Price is $3.00 per section.

BAUSCH & LOMB
ANALYTICAL SYSTEMS DIVISION

NEW spectronic 70

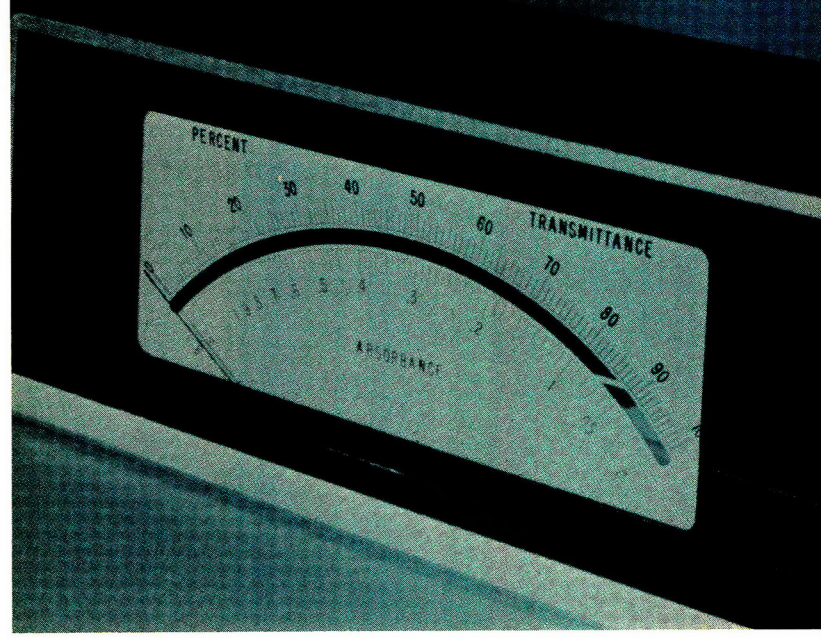

325-925nm range, 8nm bandpass high stability and reliability

The wide wavelength range of the new Spectronic® 70 is continuous. Phototubes and filters are automatically interchanged—no manual changing is required. Readout is in absorbance units and linear transmittance—on a large, mirror-scale meter. A fast optical system of an entirely new design combines fine accuracy and mechanical stability with easy operation. The all solid state electronics with the latest in integrated circuit technology assure high stability and reliability, and exceptional precision.

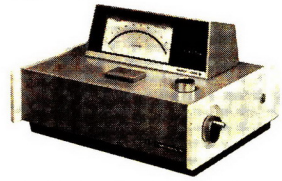

Spectronic 70 Spectrophotometer

Operation is extremely simple: set wavelength, adjust for 100% T or 0.0A with reference, introduce sample and read. An accessory outlet allows instant attachment of a variety of readouts including strip-chart recorders, digital readouts, the B&L Concentration Computer for direct concentration readings, and a digital voltmeter for Nixie tube display.

Unprecedented sampling flexibility permits use of cylindrical cells up to 50mm path length and rectangular cells—either semi-micro, short path or constant temperature cells.

For more details, write for Catalog 33-6030. If you'd like to see one in your lab, we'll gladly arrange a demonstration. Contact Analytical Systems Division, Bausch & Lomb, 60918 Linden Avenue, Rochester, New York 14625.

← Circle No. 6 on Readers' Service Card

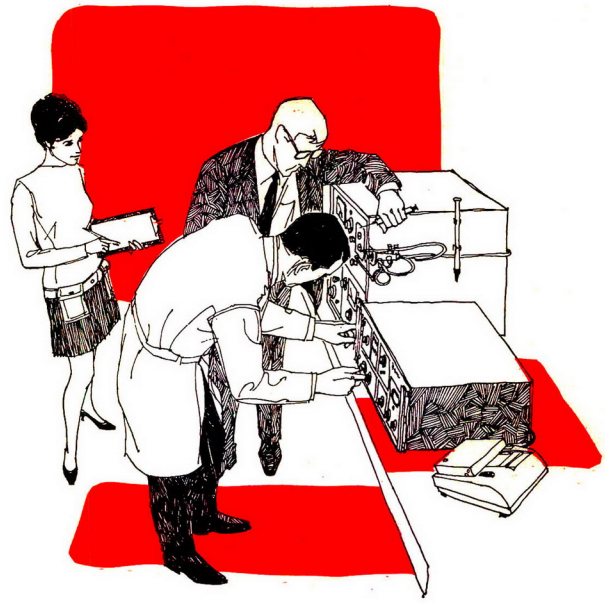

The only true test of any integrator is... on your gas chromatograph!

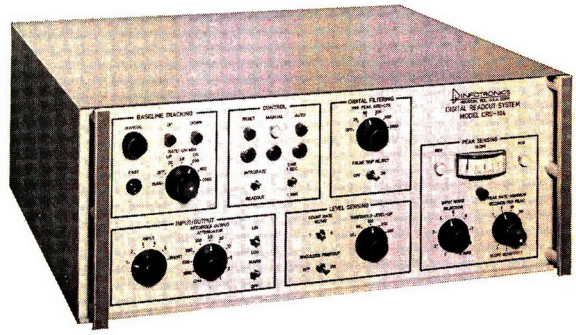

Put an Infotronics electronic digital integrator to work on your most difficult GC peaks... convoluted, drifty, noisy, or fused. See for yourself how precisely each peak is resolved and integrated automatically. We know you'll agree Infotronics integrators offer superior accuracy and overall performance. Test these features:

Test greater slope sensitivity. Carefully designed slope sensing and noise rejection systems enable you to handle **both** fast and gradually changing peaks with a single control set-up... once set, hands-off! Other integrators, even those offering dual slope sensitivity controls, cannot match the accuracy and ease-of-operation.

Test automatic baseline drift correction. Though the output signal from your GC drifts—they all do—our drift corrector detects and precisely corrects the error... hands-off, automatically.

Test sophisticated logic circuitry. Our integrators do more than simply count areas accurately. Our logic circuitry (including memory) distinguishes a true peak, or noise, or a shoulder peak. The integrator also approximates the area count for fused peaks... hands-off, automatically.

Test wide dynamic range. We know our integrators will match your GC detector across its full output range... without attenuation switching, because we offer wide dynamic range... 0 to 1 volt.

Test our experience. Eight years' spent in designing, manufacturing, and innovating in the field of digital integration gives us confidence we have the problem-solving, hands-off integrators. If you want to test one on your "worst case" run, contact Jim Cotton, Infotronics Corporation, 7800 Westglen, Houston, Texas 77042. Phone (713) 782-9770.

INFOTRONICS CORP.
7800 WESTGLEN • HOUSTON, TEXAS 77042
435

Circle No. 124 on Readers' Service Card

EDITORS' COLUMN

IN AMERICAN INDUSTRY there are few parallels to the remarkable growth of analytical instrument companies since the end of World War II. As America pressed deeper into the scientific age, the remarkable successes and vitality of a few of these companies became the envy of entrepreneurs throughout the world. Despite rumblings to the contrary, and a few notable exceptions, the analytical instruments business shows every evidence of continuing to be in a healthy, dynamic state. The role of scientific instrument makers and users will become even greater as America begins to grapple with the great problems associated with social reforms that will improve the common welfare in health and nutrition, housing, transportation, and environmental control.

Basic philosophies regarding the sale and use of analytical instruments differ somewhat from country to country, and there are particular differences between such large segments of the world market as the U. S. and Europe in general. Two years ago these differences were explored in an article by Dr. Jan Krugers [ANAL. CHEM., **39**, (1), 28A (1967)]. The essence of this report was that Europeans demand more versatility in their instruments and that in the past not enough attention has been given to sales organization.

These considerations, and others that should be of great interest to scientists and businessmen concerned with the future and problems of the scientific instruments business in the United States and abroad, are discussed in "Gaps in Technology—Scientific Instruments," published by the Organization for Economic Cooperation and Development. Great detail is given, in terms relative to the U. S., Europe, and Japan, to studies of the markets, production capacities, and growth rates of companies; as well, a wealth of information is pre-

This is the most powerful, yet easiest to use, calculating/computing system available. It's also the most versatile. You can create your own individualized system by selecting true building block modules from a family of peripheral devices larger than all competitive calculating products combined. Start with a basic 300 Series calculator if you like; add accessories as needs grow without worrying about compatibility, obsolescence, retraining or special program languages. The 370 will loop, branch, perform subroutines and manipulate arrays. You can have up to 480 steps of program storage and up to 64 separate data storage registers, also automatic typewriter or teletypewriter output, CRT graphic display and time-sharing basic keyboards for your associates.

The 370 solves these problems . . .

for Engineers and Scientists:
Inversion of 6 x 6 Matrices,
Roots of Equations,
Up to 7 Simultaneous Equations,
Fourier Analysis.

for Statisticians:
Mean, Variance and Standard Deviation,
2nd-order Regression Analysis,
Distributions such as:
Binomial, Normal Probability, etc.

And also:
General Nth-order Regression,
Multiple Regression,
Analysis of Variance,
Factorial Design.

These and many other highly-useful programs are furnished free in a 250 page program library. Three volumes of basic calculator programs and a two-volume 370 reference manual are also offered. Call now for complete details.

Solves problems ordinary calculators can't, full-scale computers shouldn't.

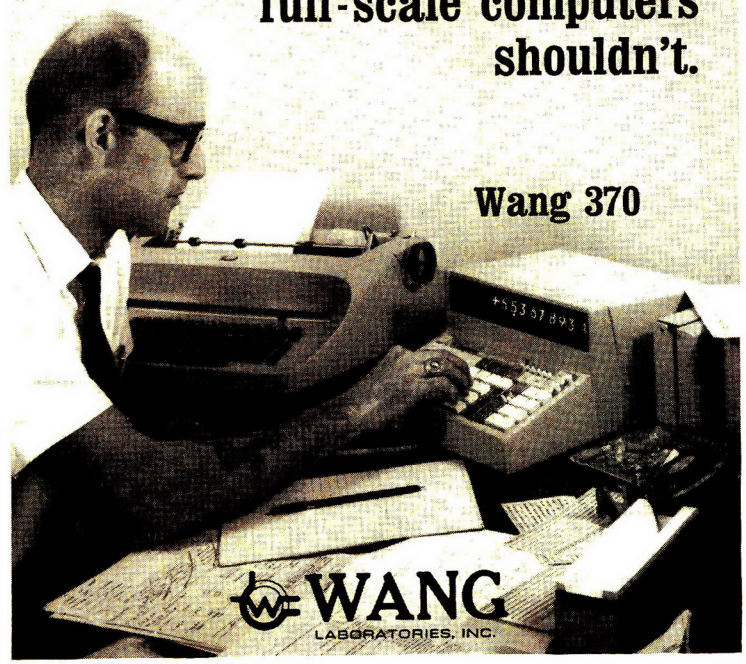

Dept. 6-Y 836 North St., Tewksbury, Massachusetts 01876 • Tel. 617 851-7311

Call today!

				(612) 881-5324	(714) 234-5651
(201) 272-7160	(301) 588-3711	(314) 727-0256	(505) 255-5775	(614) 488-9753	(716) 381-5440
(203) 288-8481	(301) 821-8212	(315) 463-9770	(512) 454-4324	(615) 523-8648	(717) 236-4782
(205) 881-5360	(303) 364-7361	(317) 631-0909	(513) 531-2729	(616) 454-4212	(805) 962-6112
(206) 525-2000	(304) 344-9431	(404) 633-6327	(515) 288-5991	(617) 851-7311	(808) 536-5359
(212) 682-5921	(305) 563-8458	(412) 366-1906	(516) 437-2500	(617) 542-7160	(813) 877-6590
(213) 776-2985	(305) 841-3691	(414) 442-0160	(517) 835-7300	(702) 322-4692	(816) 444-8388
(214) 361-7156	(309) 674-8931	(415) 692-0584	(518) 463-8877	(703) 595-6777	(817) 834-1433
(215) 642-4321	(312) 297-4323	(502) 426-1116	(601) 982-1721	(703) 359-6320	(918) 747-0018
(216) 333-6611	(313) 352-2144	(504) 729-6858	(608) 244-9261	(713) 668-0275	(919) 272-5683

Circle No. 115 on Readers' Service Card

Now . . . Analysis As Never Before On Chromatographic Media



WITH THE **Farrand**

VIS-UV CHROMATOGRAM ANALYZER

for UV and VISIBLE FLUORESCENCE SCANNING
FLUORESCENCE QUENCHING
UV and VISIBLE DENSITOMETRY

CHECK THESE FEATURES:

- ✓ **Unique 3 slit scanning system** averages non-uniform background for optimum sensitivity
- ✓ **Double beam ratio recording** for highest precision and accuracy
- ✓ **Double and single beam** facilities are standard
- ✓ **Two grating monochromators** provide highly efficient selection of wavelength
- ✓ **Interchangeable quartz/glass optics** provide maximum transmission throughout UV/visible range
- ✓ **Automatic digital** readout integration
- ✓ **21 speed strip chart recorder** standard in system
- ✓ **Sensitivity** to nanogram quantities on TLC plates

FOCI®
A product of
Farrand Optical Co., Inc.
New York, N.Y.

Direct inquiries to:

Farrand OPTICAL CO., INC. Commercial Products Division

535-A South 5th Avenue, Mount Vernon, New York 10550 (914) 668-9393 / Cable Address: FOCIUS NY

Circle No. 131 on Readers' Service Card

See ACS Laboratory Guide for All Products/Sales Office

sented that explores whether or not a technology gap really exists. Both "off-line" and "on-line" (process control) instruments are considered. "Off-line" instruments are broken down into analytical, electronic test, nuclear, and biomedical categories, along with optical and electron microscopes. This report is one of the OECD's series of "Gaps in Technology" that also embraces such topics as electronic components, computers, plastics, pharmaceuticals, and nonferrous metals.

Their basic findings, which are difficult to distill from the extensive tables and innumerable summaries, seem to indicate that for analytical instruments there is no fundamental disparity in technology underlying tht instruments themselves. Greater American participation in the world market has been as a result of better management—in particular, the ability to accurately predict future trends, coupled with shorter delivery times and better rapport with customers.

At the present time the American manufacturers appear to be more preoccupied with user-oriented problems (such as better sampling, and computer interfacing) than they are with basic design progress. This is not uncharacteristic of American development schemes. After all, the current crop of American automobiles offers little that was not available 15 years ago—technologically speaking. This does not mean that the American instrument makers are resting on their laurels—or that their vision of the future has been either bifurcated or myopic. Let us hope that the equivalents of the turbine engine or the air-lift car are at least on the drawing boards, and that the scientific underpinnings of the analytical instrument manufacturers will remain strong, yet flexible.

John K. Crum

Correction: The reference to a general article on holography in this column in May should read: *Endeavour*, **28**, 40 (January 1969).

Our Ad is not Perfect . . . . . but our CELLS are . . . . . and we have all types of

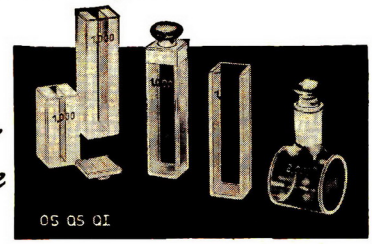

Standard . . . Flow-through . . .
Constant-temperature . . . . . .
Anaerobic . . Special design Cells.
SUPRASIL — INFRASIL — SPECIAL OPTICAL GLASS
(far uv-ir) (uv-ir) (near uv-visible)
Also available
ULTRAVIOLET LIGHT SOURCES
Deuterium Lamps
(30–60 watts — air cooled)
(150 watts — water cooled)
Mercury Vapor Lamps
Hollow Cathode Lamps
Power Supplies
Write for literature to
HELLMA CELLS, INC.
Box 544, Borough Hall Station, Jamaica, N. Y. 11424
Tel.: (212) 544-9534
Circle No. 94 on Readers' Service Card

No other pumps infuse fluids more uniformly, reproducibly, reliably

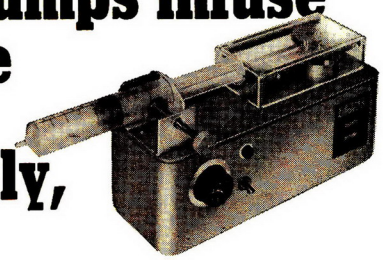

You can't beat syringe pumps for uniformity of flow, reproducibility, and their ability to handle fluids under clean, even sterile conditions. And Sage's line of more than 20 different pumps includes large and small capacity versions, discrete rate and infinitely variable rate models. Infusion/withdrawal models are available. There is even one, the new unlimited volume Model 220, which pumps continuously from a reservoir.

The Model 255-2 (shown above) permits you to dial any desired flow rate from 0.02 μl/hr to 98 ml/hr, holds single syringes up to 100 cc capacity or two syringes up to 50 cc (for double channel pumping). Other Series 255 pumps cover different rate ranges. Price $420. Other models from $160. Write or call for complete data.

SAGE INSTRUMENTS, INC.
Subsidiary of Orion Research Incorporated
230 Ferris Ave., White Plains, N.Y. 10603 ■ 914 949-4121
Circle No. 139 on Readers' Service Card

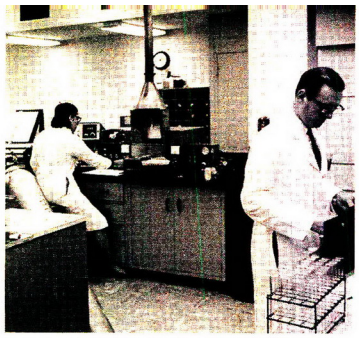

Complete emission-atomic absorption laboratory accurately detects and measures trace elements in samples

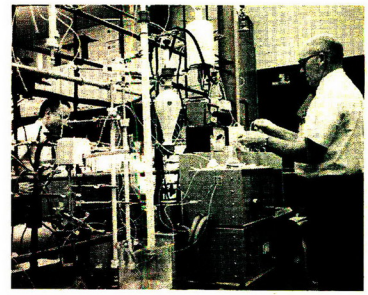

Chromatographic equipment separates compounds ranging from 10 to 10^8 molecular weights. Setups include gel, gas, thin layer, and column chromatographs

Nalco's Water Treatment Research Laboratory

Water pollution and treatment receive emphasis at Nalco's research center. The tools of analytical chemists—up-to-date instruments—aid in the search for solutions to the problems in industrial waste waters and process streams

FEATURED LABORATORY

Nalco Chemical Company's central research laboratory, Chicago, Ill., has completed a $2 million expansion which increases laboratory space by 50% to 84,000 square feet and permits doubling of the technical staff to almost 200. Key elements in the expansion are the organic chemistry, water analysis, and microbiology laboratories, all of which are heavily instrumented. The library and pilot plant research facilities were also increased substantially.

More than $700,000 in new instrumentation was added recently. New instruments include an electron microscope, NMR spectrometer, gas chromatography equipment, emission spectrograph, carbon analyzers, atomic absorption spectrophotometers, osmometers, and viscometric and light-scattering equipment. These instruments supplement the X-ray fluorescence, diffraction, infrared spectrometers, and similar instruments already on hand.

Nalco is a major supplier of polymer chemicals for treating industrial waste waters and process streams. Increasingly, it handles problems in industrial pollution control in which the laboratory gets heavily involved. Projects concerning pollution and water treatment problems encompass many industries including steelmaking (chemicals in spent liquor), small metalworking shops (cutting oils, suspended solids, and emulsified oils), paper (dissolved soluble organics), and chemicals (diverse problems).

Nalco also makes specialized chemicals used in petroleum production and refining, metal production and processing, papermaking, and other industrial and municipal applications.

Organizationally, the research center has four departments. The pilot plant and analytical services department is responsible for water analysis, compound analysis, organic analytical chemistry, and X-ray and electron microscope laboratories. There is also a corporate research department which is involved in new products and processes, and two departments to fill the needs of Nalco's operating divisions. One is concerned with pollution control, ion exchange, petroleum chemicals, and coagulant chemicals. The other concentrates on papermaking chemicals, boiler feedwater treatment, microbiology, and water stabilization.

Water treatment researchers attack pollution problems two ways: developing better treatment methods and materials, and trying to eliminate contaminants in industrial processes in the first place. An example of the latter approach is the development of nonchromate, nonphosphate corrosion inhibitors for cooling towers. According to L. David Moore, research director, the deeper you probe into the industrial process, the more efficient the solution becomes.

Much of the laboratory's actual work centers on developing, synthesizing, and analyzing high molecular weight polyelectrolytes. These are the basic chemical tools for separating solids from water by coagulation and flocculation.

One study at Nalco seeks simply to improve water sampling and analytical procedures—particularly for field analysis. Currently, all Nalco field men have custom designed test kits for extensive on-the-spot analysis of many components. One problem is that because of time and physical action, specimens can change character during shipment from the plant site to the laboratory. Nalco hopes to develop a more extensive sampling and testing kit to cover additional field situations and at the same time provide reliable data.

According to R. R. Burns, vice president of research, "Polution control isn't a single insurmountable problem, but a series of separate, solvable ones. Through research, the cost of pollution control has dropped to the point where many industries actually make a profit through reclamation of product. But the problems need to be solved one at a time. With this laboratory expansion we can take on more problems and find the answers faster."

Gel-permeation chromatography, used in medical research for years, is used at Nalco for studying water treatment chemicals. Because the gels needed for gel chromatography of water-soluble polymers are not commercially available, a technician synthesizes a batch

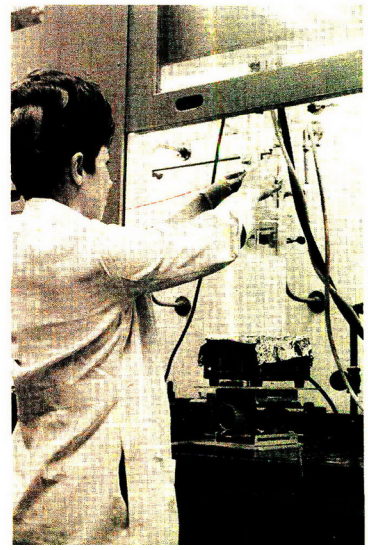



Membrane osmometry, viscometry, and light scattering are used to determine the molecular weights of polymers



IBM 1130 computer works on measurement of constituent levels. The computer rapidly handles large amounts of data

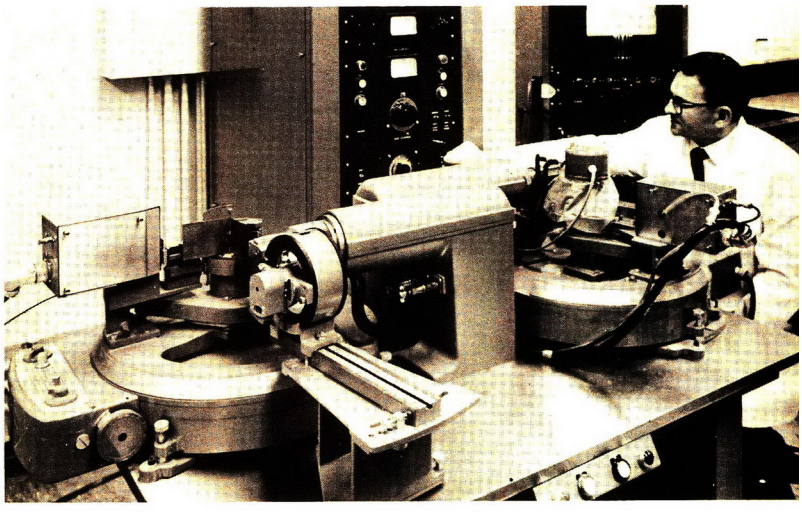

Dual-purpose X-ray diffraction-fluorescence unit aids in identification of water specimens brought to the laboratory for water treatment studies



Aha, the old computer-takes-the-gas trick.

Some people have no use for computers.

For them, DIGITAL has Computerpacks — special-purpose laboratory systems. For gas chromatography. For signal averaging. For pulse-height analysis. Each Computerpack is complete. With all the hardware, all the software, all the interfaces — everything needed to get the job done.

That's 9 to 5. After 5, well . . .

There's a computer inside. A real, live, all integrated-circuit, 4096-word core memory, FORTRAN-speaking, full general-purpose PDP-8/I. Nearby is the software that runs more than 4,000 PDP-8 installations around the world. Press a button and presto! There it is.

You can ignore the computer. But it'll still be there — just in case.

DIGITAL EQUIPMENT CORPORATION, Maynard, Massachusetts 01754, Telephone: (617) 897-5111 — Cambridge, Mass. • New Haven, Conn. • Rochester, N.Y. • New York City • Long Island, N.Y. • Princeton, Parsippany, N.J. • Washington, D.C. • Cocoa, Fla. • Atlanta • Knoxville, Tenn. • Huntsville • Philadelphia • Pittsburgh • Cleveland • Dayton • Chicago • Minneapolis • Ann Arbor • Houston • Dallas • Salt Lake City • Denver • Albuquerque • Los Angeles • San Francisco • Seattle. INTERNATIONAL, Ottawa • Toronto • Montreal • Edmonton • Reading • Manchester • Paris • Munich • Cologne • The Hague • Stockholm • Milan • Sydney • West Perth • Melbourne • Tokyo.

digital
COMPUTERS · MODULES

Circle No. 28 on Readers' Service Card

Advisory Panel

Jonathan W. Amy Jack W. Frazer
Glenn L. Booman Howard V. Malmstadt
Robert L. Bowman William F. Ulrich

A New Detector for Spectrometry

The use of this device in the vacuum ultraviolet is shown. However, the technique can feasibly be applied in other spectral regions and in mass spectrometry

by A. Boksenberg
Department of Physics, University College London

This article discusses a new technique for reading spectral information in the form of a spatial distribution of charge, at present under development in the Physics Department of University College London [A. Boksenberg, R. L. F. Boyd, J. C. Jones, *Nature*, **220**, 556 (1968)], that promises to be useful in ultraviolet spectrometry, mass spectrometry, and possibly other applications too.

A charge image is first recorded on the surface of an insulating layer by direct photoemission, photoconduction, or other means, according to the character of the information to be detected.

For example, to record a spectrum in the vacuum ultraviolet, an insulating photoemitter can be conveniently used in an otherwise conventional spectrograph; then the unbalanced positive charges that remain after the photon-induced surface emission of electrons, constitute the recorded image and this is a direct analog of the spectral pattern to which the layer is exposed.

To extract the information thus recorded, a reading process is employed that is basically similar to the charge measuring technique used in the vibrating reed (dynamic capacitor) electrometer, but here added mechanical sophistication is required for the measurement of charge images.

In the vibrating reed electrometer, a quantity of charge is determined by mechanically varying the value of an associated capacitor and measuring the resulting alternating current with a sensitive amplifier. In the new application described here, a charge image residing on the surface of a thin insulating layer backed by a grounded conducting plate is read out, element by element, by means of a fine, closely scanning, vibrating, conducting probe connected to a current amplifier, the direction of vibration being normal to the surface.

During the entire reading operation the surface of the layer is never touched by the probe, so the image remains intact and may repeatedly be read without detriment. But a more important consequence of nondestructive reading is that the probe can remain over each effective image element sufficiently long to enable the inherent charge level to be measured as accurately as desired by use of the narrow-band lock-in amplifier technique. In other words, the image can be read out without substantially degrading it with noise introduced in the reading process.

This is in direct contrast to the conditions obtaining in a conventional television camera tube—which uses electron beam readout—where the image is necessarily destroyed as it is read; a normal wide-band amplifier must then be used so the signal-to-noise advantage of a lock-in amplifier is lost. Nevertheless, this loss can be effectively reduced by intensifying the image before recording, although this is usually at the cost of considerable complexity and a severe limitation in dynamic range.

However, the real value of the new image detecting technique follows from the total avoidance of electron optics both in the reading and recording processes. This allows the image area to assume almost any desired extent and contour—as is true for photographic film—and makes the system particularly appropriate for use in spectrographic instruments where focal surfaces are often long and curved. In comparison, the need for accurately defined electric and magnetic fields for electron acceleration and focussing in image intensifiers and television camera tubes severely constrain the permissible geometrical extent of their sensitive areas.

Figure 1 shows, in schematic form, the various practical steps of the detection procedure for use in the vacuum ultraviolet. First, the image is recorded by exposing a highly insulating photoemitting layer through an open mesh held at a high positive potential relative to the conducting backplate. This mesh collects the emitted photoelectrons while recording and is subsequently drawn aside, or otherwise removed, for reading. In general, the storage layer is not homogeneous but consists of a dielectric spacer layer with a thin surface film of photoemitter, as indicated. Such a surface layer is not difficult to find for detection in the vacuum ultraviolet since many insulators are also efficient photoemitters in this region, notably the alkali halides. Probably the best of these is cesium iodide, having near unit quan-

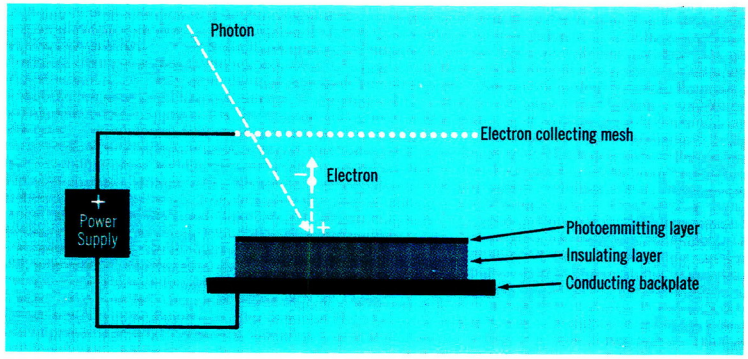

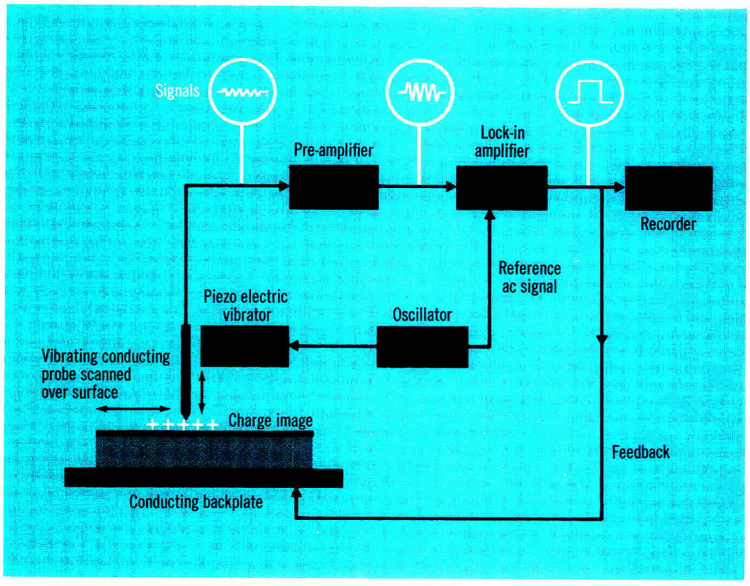

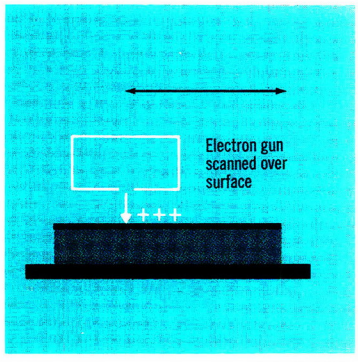

Figure 1. Schematic showing the practical steps in the detection procedure in the vacuum ultraviolet. Top: Recording the image; Middle: Reading the image; Bottom: Erasing the image

tum efficiency (the ratio of the numbers of emitted electrons to incident photons) over the range 10–1000 Å. In comparison, the appropriate photographic emulsions have efficiencies between one and two orders of magnitude lower.

Next, the reading process: since spectra essentially contain information in one dimension only, the scanning action can be correspondingly one-dimensional and the probe knife-edged in form and held normal to the dispersion direction.

To get a better understanding of the reading process, we define the image density in the vicinity of the probe at any instant as σ and the respective capacitances of the probe and the conducting backplate to an area a of surface beneath the probe $C_1(t)$ and C_2, the former being a function of time because of the impressed vibration. For simplicity, we neglect fringe effects and assume the potential difference between probe and backplate is zero. Then, if the instantaneous charge on $C_1(t)$ is $q_1(t)$ and the induced signal current is $i_1(t)$:

$$q_1(t) = \frac{C_1(t)\sigma a}{C_1(t) + C_2}$$

$$i_1(t) = \frac{d}{dt}[q_1(t)] = \frac{C_2\sigma a \dfrac{dC_1(t)}{dt}}{[C_1(t) + C_2]^2}$$

Thus, the signal current is periodic with the probe vibration and its amplitude is proportional to the surface charge density and to the rate of change of $C_1(t)$—i.e., to the frequency of vibration. Also, it can be shown that optimum signal generation occurs when C_2 and the mean value of $C_1(t)$ over one cycle are approximately equal.

The current is passed to a sensitive current pre-amplifier, then to a lock-in amplifier where phasing reference is provided by the vibrator oscillator, and finally to a recorder. The sensitivity of the system is such that a charge equivalent to a few tens of electrons can be detected with certainty using a vibration frequency of 10 kHz and a reading rate of ten image elements a second.

In practice, the probe is vibrated by means of a piezo-electric crystal operating near resonance. Scanning may be achieved by mounting the probe unit on a movable carriage which is borne against a reference surface accurately related to the surface of the storage layer. Alternatively, the probe unit may be fixed and the storage layer moved.

The spatial resolution of the system is naturally dependent both on the geometrical configuration of the probe and its mean separation from the sur-

Circle No. 60 on Readers' Service Card→

Resolve 10 Nanosecond Signals Buried In Noise

Complex repetitive waveforms are accurately resolved to 10 nanoseconds and recovered from noise in the new PAR™ High Resolution Boxcar Integrator. The Model 160 achieves signal recovery by time averaging a small portion of a coherent waveform over a large number of repetitions. Because the mean value of the noise approaches zero when averaged over many repetitions, the averaged output results only from the coherent content of the sampled portion of the waveform. To recover the entire waveform, the incremental portion being sampled and averaged is either manually or automatically scanned over the period of interest.

An optional digital storage module is available for maintenance of averaging accuracy in situations where the repetition rate of the investigated phenomenon is extremely low or to serve as an interface to peripheral data processing equipment.

Price of the Model 160 Boxcar Integrator is $3,250. For more information or to arrange a demonstration write Princeton Applied Research Corporation, P. O. Box 565, Princeton, New Jersey 08540 or call 609-924-6835.

PRINCETON APPLIED RESEARCH CORPORATION

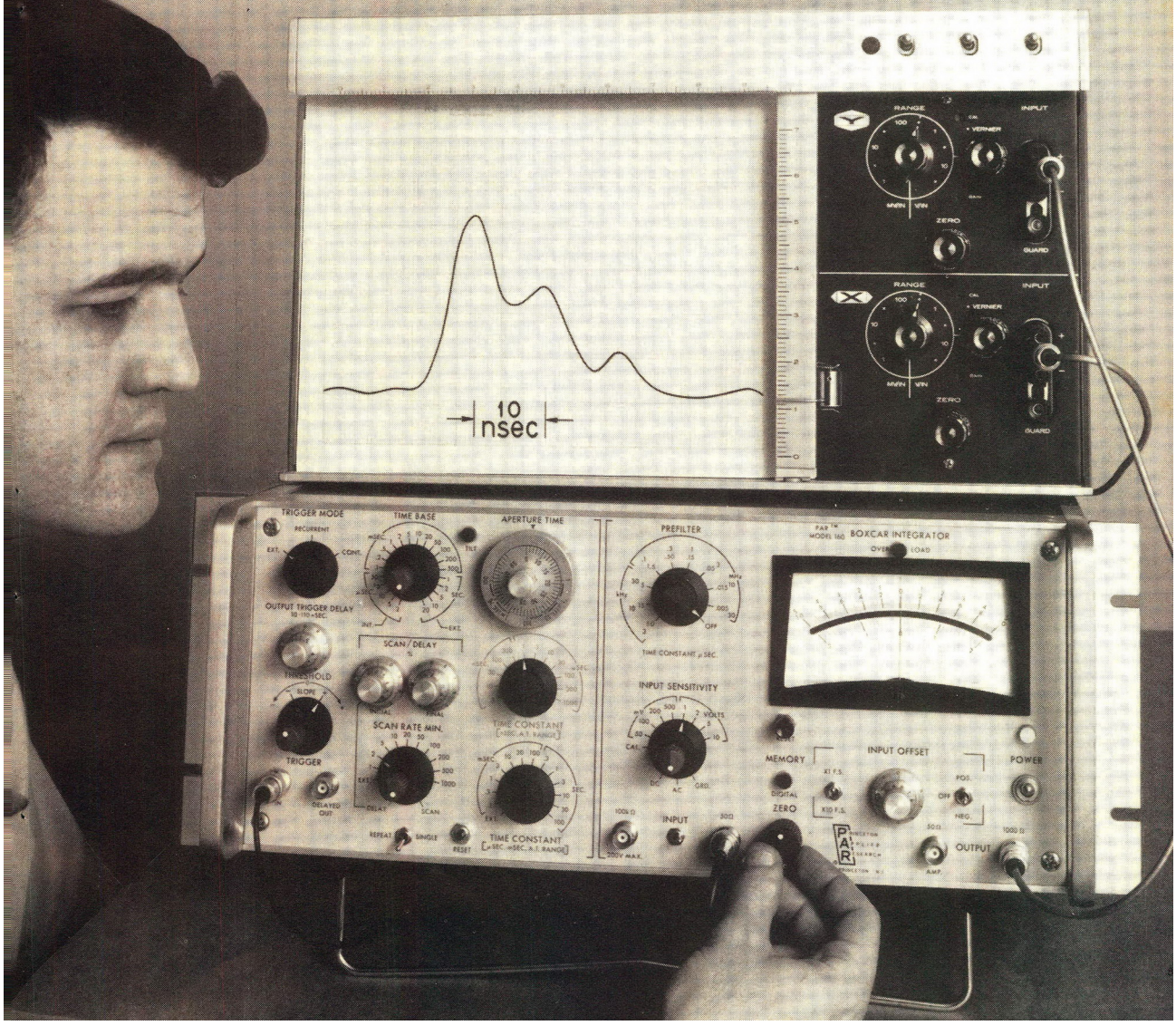

face. The probe width and mean separation both need to be in the region of 10 microns to achieve a resolution comparable to that obtainable photographically. Furthermore, the second harmonic component of the signal gives a better resolution than the first, since it is generated predominantly when the probe is closest to the surface during each vibration cycle. For optimum resolution performance, the probe must also be electrically blinkered by means of carefully designed guard electrodes—not shown in the diagram—in order to better confine its "view" to the region of the storage surface in its immediate vicinity.

To maintain the resolution—and therefore, the probe mean separation—constant over the whole of the scan for a nominal separation of only a few microns is a difficult mechanical undertaking but can be adequately achieved if aided by servo control. This also has the effect of stabilizing sensitivity, a feature which likewise becomes increasingly necessary with decreasing separation. Such servo action may be realized simply by applying a correcting bias to the piezoelectric vibrator to stabilize the mean separation and, if necessary, also controlling the vibrator drive oscillator to stabilize amplitude. One way of measuring the two parameters to be controlled is by the use of a conducting strip deposited along the edge of the storage surface and an overlaying subsidiary probe mounted on the vibrator. By maintaining a constant potential difference between them and measuring the first and second harmonic components of the resulting signal current, the mean separation and vibration amplitude can be uniquely determined. However, in applications where the passive mechanical performance of the system is adequate for resolution but not for maintaining a sufficiently constant sensitivity, the latter may be acceptably stabilized by the usual method of negative feedback, as shown in the diagram.

After reading, the image is erased for a fresh exposure by scanning it with a low velocity electron beam, a procedure that effectively replaces the electrons that were emitted from the surface during recording.

As a first commercial application of the image detecting system, work is proceeding to apply it in place of the photographic plateholder in a Hilger and Watts two-metre grazing incidence vacuum spectrograph (normally working in the range 5–950 Å), in collaboration with the U.K. Atomic Energy Authority, Hilger and Watts Ltd., and the U.K. National Research Development Corporation. The main advantages here to be gained over the use of film are: a high detecting efficiency, linearity of response, one to two orders of magnitude increase in dynamic range and an electronic readout that obviates the need to change exposed plates—obviously a great operational convenience for a vacuum instrument.

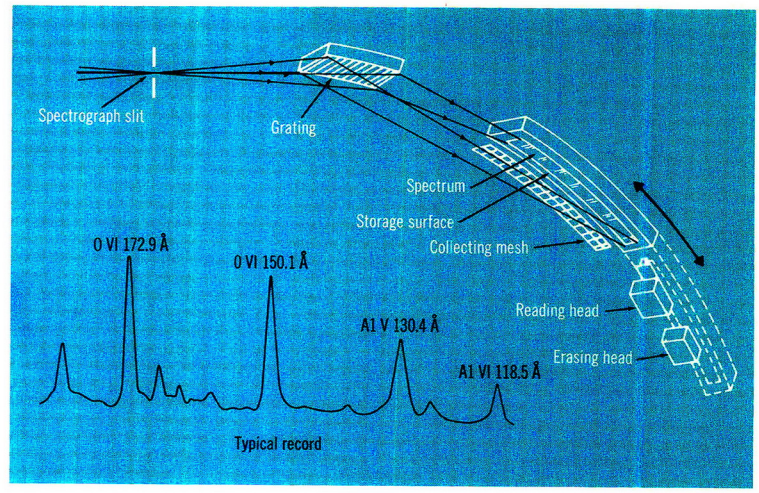

Figure 2. Vacuum spectrograph with image detector in place of photographic plateholder

The basic components of the experimental system are illustrated in Figure 2. As described above, the sequence of operations consists of (a) conversion of the ultraviolet spectrum image to a static charge image, (b) electromechanical readout and (c) erasure. In the current trials, the collecting mesh, reading and erasing heads are fixed and the storage layer, which is coated on to a large curved glass block, is moved to the collecting mesh for recording and then slowly scanned past the reading and erase heads at the completion of the exposure. The wavelength range covered in this trial instrument is 5–250 Å. A portion of a typical record obtained in preliminary and as yet unoptimized experiments is included in the figure and shows spectral features in the region 100–200 Å obtained with an air-filled flash tube source. The quality of the storage layer is such that it is possible to retain spectra as charge images for many days after exposure.

As an additional function, the exposure can be electronically controlled by appropriately gating the potential of the collecting mesh relative to the backplate to alternately inhibit and encourage photoemission as required (the backplate is a metallic film deposited on the glass support block before applying the storage layer). Although this in itself is probably an unnecessary complication, it does lead to an interesting extension of the basic detection technique, namely, in time-resolving transient spectral phenomena. This can be achieved by constructing a collecting mesh in the form of a number of longitudinal sections insulated from one another. During exposure, the applied potential is gated from negative to positive and back to negative for each in turn, thus recording the spectral information as a stack of adjacent time-staggered spectrum strips. To read the composite image, it is envisaged that the piezo-electric vibrator would contain a separate probe system for each spectrum strip.

The use of the reading technique for detection in other spectral regions is inherently more difficult than in the vacuum ultraviolet, largely because of problems associated with the use of suitable layers. In the near ultraviolet and optical regions, a photoconductive rather than photoemissive approach is currently being studied, the former being preferred since it avoids the inconvenience of a vacuum envelope not now needed optically.

Mass spectrometry is another possible area of interest for application of the technique. Here, ions conventionally separated and then received on an insulating layer could be directly read out without further processing. Alternatively, charge multiplication by secondary emission at the storage surface could provide a useful degree of intensification to aid in the detection of very low levels of impurities.

TRACE INORGANICS IN WATER

ADVANCES IN CHEMISTRY SERIES No. 73

Twenty-one papers from a symposium by the Division of Water, Air, and Waste Chemistry of the American Chemical Society, chaired by Robert A. Baker. Includes:

Five surveys on broad topics

- **Transport properties of electrolytes**
- **Anions in aqueous solution**
- **Effects of trace inorganics on the ice/water system**
- **Aluminum species in water**
- **The role of hydrous Mn and Fe oxides in fixation of metals in soils and sediments**

Eleven papers on analytical developments, such as:

- **Atomic absorption (3 papers)**
- **Atomic fluorescence**
- **Flame emission**
- **Neutron activation**

And five research reports.

396 pages with index Clothbound (1968) $12.50

Set of L.C. Cards free with library orders.

Other books in the ADVANCES IN CHEMISTRY SERIES on inorganic chemistry include:

No. 72 Mass Spectrometry in Inorganic Chemistry	**Cloth**	**(1968)**	**329 pages with index $12.00**
No. 71 Lanthanide/Actinide Chemistry	**Cloth**	**(1968)**	**359 pages with index $11.00**
No. 62 Werner Centennial	**Cloth**	**(1967)**	**661 pages with index $17.50**
No. 54 Advanced Propellant Chemistry	**Cloth**	**(1966)**	**290 pages with index $10.50**
No. 49 Mechanisms of Inorganic Reactions	**Cloth**	**(1965)**	**266 pages with index $10.00**
No. 42 Boron-Nitrogen Chemistry	**Cloth**	**(1964)**	**330 pages with index $10.00**
No. 39 Nonstoichiometric Compounds	**Paper**	**(1963)**	**253 pages with index $9.00**
No. 37 Reactions of Coordinated Ligands and Homogeneous Catalysis	**Paper**	**(1963)**	**255 pages $9.50**
No. 36 Free Radicals in Inorganic Chemistry	**Paper**	**(1962)**	**175 pages with index $7.50**
No. 32 Borax to Boranes	**Paper**	**(1961)**	**244 pages $8.00**
No. 21 Ozone Chemistry and Technology	**Cloth**	**(1959)**	**465 pages $10.00**
No. 19 Handling and Uses of Alkali Metals	**Paper**	**(1957)**	**177 pages $7.00**

All books postpaid on U.S. and Canada; plus 20 cents foreign and PUAS.

Order from: **SPECIAL ISSUES SALES**
DEPT. B
AMERICAN CHEMICAL SOCIETY
1155 SIXTEENTH STREET, N.W.
WASHINGTON, D.C. 20036

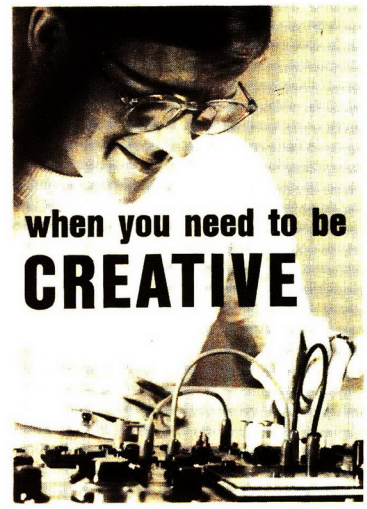

it helps to have instruments capable of performing a wide variety of tasks. The versatile **MP-System** gives you the basic building blocks common to most electronic instruments. Interconnect the precision modules with patch cords and they will perform most electro- and photometric instrument functions.*

NEED ASSISTANCE?
Our 114 page manual answers most questions. It contains detailed descriptions, practical applications and set-ups. A new lab manual by L. P. Morgenthaler explains operational amplifiers and their use in chemical instrumentation. In addition, the bi-monthly MPI **Applications Notes** keeps you up-to-date on **new** uses.

ECONOMICAL
Simplicity, solid state circuitry and good design have been combined to permit the lowest price consistent with high performance.

***coulometry, polarography, pH titrations, spectrophotometry, colorimetry, filter fluorometry, conductimetry, temperature measurement, etc.**

MPI

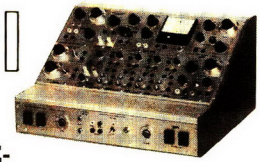

McKEE-PEDERSEN INSTRUMENTS
BOX 322, DANVILLE, CA 94526
Circle No. 46 on Readers' Service Card

Summer Sessions

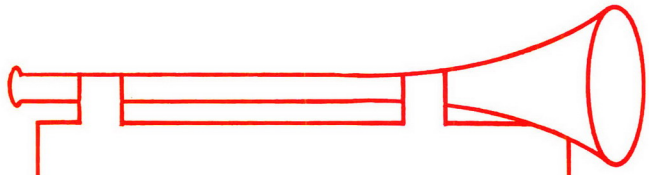

NEW ENGLAND SHORT COURSE FESTIVAL
Hanover, New Hampshire

Atomic Absorption Spectroscopy—July 6-7. Dr. Donald A. Keyworth, Theodore C. Rains, and Dr. Stanley M. Pier; two days; no textbook required; fee $70.

This course is primarily for chemists and technicians interested in the application of AAS to analysis and covers the fundamentals of atomic absorption theory as well as instrument designs. Comparison is made to flame emission and atomic fluorescence spectrometry. Topics include typical instrument component arrangements, methods of calibration and calculation, and sources of error in terms of spectral, flame, and chemical interferences. Specific applications will be drawn from typical industrial and clinical problems.

Gas Chromatography—July 9-10. Dr. Harold M. McNair and Dr. James Miller; two days; no textbook required; fee $65.

The objective of the course is to cover the basic aspects of gas chromatography. The course introduces basic instrument requirements, illustrates applications, defines nomenclature, and provides a background for using the technique. Included are examples of how to choose the proper columns and how to identify and quantitate peaks. The course will be of value to bench chemists, supervisors, technicians, and graduate and undergraduate students. It will also interest those working in nonchemical fields such as biological, agricultural, food sciences, and pollution.

Modern Organic Synthesis—July 12-13. Dr. Barry M. Trost and Dr. Edwin Vedejs; two days; no textbook required; fee $60.

This course is intended for individuals who are concerned with putting organic molecules together. It covers both the methods and tools of organic synthesis, with heavy emphasis on modern aspects of synthesis. Individual syntheses are selected which afford maximum exposure to a variety of concepts and tools. Research supervisors, bench chemists, and teachers will all benefit from the course.

This summer heralds several "firsts" for ACS Short Courses.

For the first time, Short Courses activity will continue full-scale during the summer months. The course locations are varied—from one coast to the other—from metropolitan centers to mountain resort areas. Many of the locations may suggest family vacations.

Also for the first time, the NEW ENGLAND SHORT COURSES FESTIVAL is being offered. Three ACS Short Courses will be given in succession on the Dartmouth College campus in Hanover, N.H. The three courses are among those that have been requested most often during the past year—"Atomic Absorption Spectroscopy," "Gas Chromatography," and "Modern Organic Synthesis." Dormitory space and recreational facilities will be available to Short Course registrants and their families.

Other "firsts" include premier sessions for three new Short Courses—"Chemical Microscopy" will be offered in New York City on June 26–28; "Modern Organic Synthesis," a festival course, will be offered in Hanover, N.H., on July 12–13; and "Applied Polymer Science" will be offered in Berkeley, Calif., on Aug. 14–16.

To register or to obtain complete information on any of the summer courses, convenient lodging, and student discounts, please write to Education Office, American Chemical Society, 1155–16th St., N.W., Washington, D.C. 20036. During the two-week period prior to a course, registration should be made by telephone: area code 202, 737-3337 ext. 258.

INDUSTRIAL CENTERS

Pittsburgh

Computer Programs in Chemical Research—June 7–8. Dr. DeLos F. DeTar and Carleton E. DeTar; two days; fee $90; required text, D. D. McCraken, "A Guide to FORTRAN IV Programming," Wiley, 1965, $5.00; sponsor, Pittsburgh Section in cooperation with Carnegie-Mellon University.

This course is devoted primarily to instruction in writing simple FORTRAN programs. It will interest those who need (1) to write programs to solve particular problems, (2) to use effectively programs obtained from other sources, and (3) to assess the capabilities of computers to judge the suitability of computer techniques for solving chemical problems. Programs of the type run and discussed may be found in "Computer Programs for Chemistry," D. F. DeTar, ed., Benjamin, 1968.

Milwaukee

Spectrometric Identification of Organic Compounds—June 13–15. Dr. Robert M. Silverstein and Dr. G. Clayton Bassler; two and one half days; fee $90; required text, R. M. Silverstein and G. C. Bassler, "Spectrometric Identification of Organic Compounds," 2nd ed., Wiley, 1967, $10; sponsor, Milwaukee Section.

The application of the combined information from UV, IR, NMR, and mass spectra to identification of organic compounds will be presented in lectures and problem sessions. The emphasis is on the interplay among the four complementary spectra. The course is primarily for organic chemists and requires a sound working knowledge of organic chemistry.

Wilmington area

Thin-Layer Chromatography—Aug. 1–2. M. Karl Brandt, Dr. Victor W. Rodwell, and Dr. Fredric M. Rabel; two days; fee $105; required text, J. Bobbitt, A. Schwarting, and R. Gritter, "Introduction to Chromatography," Reinhold, 1968, $4.00; sponsor, Delaware Section.

This course is directed toward those who have little or no knowledge of thin-layer chromatography. The emphasis is placed on techniques rather than theory. Laboratory sessions are included. The course will interest organic chemists, biochemists, practical analytical chemists, and, to some extent, inorganic chemists. Technicians, high school teachers, and graduate students, as well as practicing chemists, will benefit from the course.

EAST COAST CITIES

Philadelphia

Interpretation of Infrared Spectra—June 7–8. Norman B. Colthup; two days; fee $60; required text, N. B. Colthup, L. H. Daly, and S. E. Wiberley, "Introduction to Infrared and Raman Spectroscopy," Academic Press, 1964, $12; sponsor, Philadelphia Section.

The chief purpose of this course is to teach some elementary theory, with major emphasis on the interpretation of infrared spectra. Topics include: introductory theory of molecular vibrations and absorption of infrared radiation; origin of group frequencies and interaction and coupling effects; techniques used in obtaining infrared spectra; methods of making band assignments through selection rules, gas contours, and isotope effects; and interpretation of IR spectra of numerous organic compounds. The course will be of most value to organic chemists who have made some preliminary use of IR spectroscopy as a tool for the study of molecular structure. However, no previous IR experience is required.

New York City

Chemical Microscopy—June 26–28. Dr. John A. Reffner; three days; no textbook required; fee $80.

This course is intended for chemists and engineers with no formal training in microscopy. It emphasizes the basic principles of modern microscopy, especially ordinary light microscopy. Discussions of such special areas as polarized light, dark field, phase contrast, interference, fluorescence, and dispersion staining are also included. Transmission electron, scanning electron, and x-ray microscopy are discussed in terms of instrumentation and application.

Interpretation of Infrared Spectra—July 26–27. Norman B. Colthup; two days; fee $60; required text, N. B. Colthup, L. H. Daly, and S. E. Wiberley, "Introduction to Infrared and Raman Spectroscopy," Academic Press, 1964, $12.

For description of course, see Philadelphia.

Electroanalytical Chemistry—Aug. 7–9. Dr. Irving Shain and Dr. Dennis H. Evans; three days; no textbook required; fee $100.

This course is designed to provide a basic understanding of mass transfer, charge transfer, and kinetic processes in electroanalytical chemistry. Registrants should have at least a B.S. in chemistry and should be familiar with polarography at least at the level treated in typical instrumental analysis textbooks. All but highly advanced workers in the field of electroanalytical kinetics will benefit from the course.

Washington, D.C.

Gas Chromatography—Aug. 4–5. Dr. Harold M. McNair and Dr. James Miller; two days; no textbook required; fee $65; sponsor, Chemical Society of Washington.

For description of course, see Hanover, N.H.

WESTERN VACATION AREAS

Denver area

Molecular Orbital Theory—July 18–19. Dr. Howard E. Zimmerman and Dr. Reuben D. Rieke; two days; no textbook required; fee $65; sponsor, Colorado Section.

This course is designed to bring an organic chemist who knows no molecular orbital theory to the point where he can do simple calculations on organic molecules and to provide sufficient background to proceed to more sophisticated methods. The course shows how the calculations are done prior to the introduction of the theoretical background. Useful methods for simplifying the calculations are introduced, including a simple and gradual approach to group theory. Some applications of simple MO theory such as the application to correlation diagrams are presented. Students should know integral calculus, but extensive math background is not required.

Berkeley, Calif.

Applied Polymer Science—Aug. 14–16. Dr. Robert W. Lenz and Dr. Adi Eisenberg; three days; fee $80; required text R. W. Lenz, "The Organic Chemistry of Synthetic High Polymers," Wiley, 1967, $16; sponsor, California Section.

This course deals with the practical aspects of the synthesis of useful high molecular weight polymers, and with the measurement and interpretation of the physical and mechanical properties most important for their characterization and utilization. Theoretical aspects are tied in with practical problems and applications. Continuing emphasis is placed on the relations between synthesis, characterization, properties, and utility.

Thomas Melting Rate Programmer

for *Thomas*-Hoover Melting Point Apparatus

automatically controls temperature rise to comply with U.S.P. specifications



- ***eliminates subjective operator error***
- ***promotes inter-plant and inter-shift uniformity***

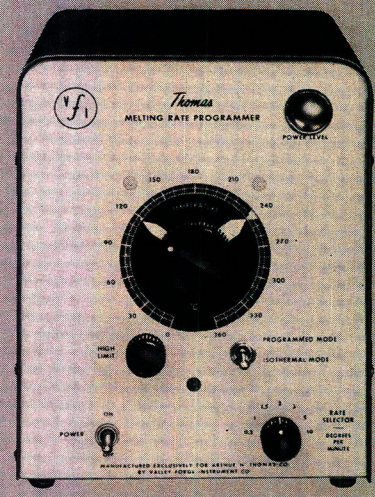

For automatically controlling rate of temperature rise in Thomas-Hoover Melting Point Apparatus. Ensures compliance with U.S.P. specifications for melting point determination on pharmaceutical products. Increases accuracy of m.p. determinations by eliminating subjective operator error in establishing and maintaining constant melting rate.

Frees analyst for other duties by making it unnecessary for him to remain at the instrument during bath warm-up. Assures inter-shift and inter-plant uniformity in technique and results. Usable with all Thomas-Hoover units now in service.

Specifications

Range 0 to 360°C.
Heating Rate Options ½, 1, 1½, 2, 3, 5 and 10 degrees per minute.
Heating Rate Accuracy within 1% of selected rate.
Installation. No modification of Thomas-Hoover unit is required. Platinum resistance thermometer probe mounts in standard melting bath unit. Plug-in harness completes necessary circuitry; no re-wiring required. Locking clamp secures autotransformer rotor at maximum input position.

Operation. Operator sets program starting point to a few degrees below, and high temperature limit to a few degrees above, the expected melting point. Programmer is switched to isothermal mode, desired heating rate is selected, and power switches are turned on. When bath reaches the selected program start point, the isothermal control maintains this temperature.

The operator, who has been free to perform other duties during the heat-up period, now switches unit to programmed mode, and begins observing sample. The bath temperature increases at the selected rate, as indicated by the advancing white pointer.

After recording the melting point the operator may permit the temperature to rise to the temperature preset as high limit, if samples of higher melting point are to be subsequently programmed. Alternatively, operator may return programmer to isothermal mode, reset the program start point, and allow the bath to cool to this point for repetition of the determination. Rate of temperature rise may be changed, stopped, or started, at any time during operation.

6406-R10. Programmer, as described. For 115 volts, 60 cycles, a.c. *Without Melting Point Apparatus* . . **800.00**
6406-R20. Ditto, for 115 volts, 50 cycles, a.c. **800.00**

Bulletin 155 sent upon request.

Thomas **ARTHUR H. THOMAS COMPANY**

Scientific Apparatus and Reagents

VINE STREET AT 3RD • P.O. BOX 779 • PHILADELPHIA, PA. 19105, U.S.A.

Circle No. 70 on Readers' Service Card

ANALYTICAL CHEMISTRY

June 1969, Vol. 41, No. 7

Editor: HERBERT A. LAITINEN

EDITORIAL HEADQUARTERS
Washington, D. C. 20036
1155 Sixteenth St., N.W.
Phone: 202-737-3337 Teletype WA 23

Managing Editor: John K. Crum

Associate Editors: Josephine Pechan, Virginia E. Stewart

Editorial Assistants: Eugenie C. Callaghan, Ana Sol de Gutiérrez

Contributing Editor: R. H. Müller

Production Staff—Washington:

Director of Design: Joseph Jacobs

Production Manager: Bacil Guiley

Art and Layout: Norman W. Favin

Production Staff—Easton, Pa.:

Associate Editor: Charlotte C. Sayre

Assistant Editor: Elizabeth R. Rufe

Advisory Board: Klaus Biemann, A. E. Cameron, Lyman Craig, Henry Freiser, John Funkhouser, Marcel Golay, D. R. Johnson, Joseph Jordan, D. W. Margerum, W. Wayne Meinke, R. A. Osteryoung, R. L. Pecsok, C. N. Reilley, A. Lee Smith, James D. Winefordner

AMERICAN CHEMICAL SOCIETY PUBLICATIONS

Director of Publications, Richard L. Kenyon

Director of Business Operations, Joseph H. Kuney

Publication Manager, Journals, David E. Gushee

Executive Assistant to the Director of Publications, Rodney N. Hader

Circulation Development Manager, Herbert C. Spencer

Assistant to the Director of Publications, William Q. Hull

REGIONAL EDITORIAL BUREAUS

NEW YORK, N. Y. 10017
733 Third Ave.

PHILADELPHIA, Pa. 19107
Philadelphia National Bank Building
Broad & Chestnut Streets

PITTSBURGH, Pa. 15219
530 William Penn Place

CHICAGO, Ill. 60603
36 South Wabash Ave.

CLEVELAND, Ohio 44114
1367 East Sixth St.

SAN FRANCISCO, Calif. 94104
57 Post St.

LOS ANGELES, Calif. 90005
422 South Western Ave.

HOUSTON, Texas 77002
514 Main Bldg.
1212 Main St.

FRANKFURT/MAIN, West Germany
32 Grosse Bockenheimerstrasse

LONDON, W. C. 2, England
27 John Adam St.

TOKYO, Japan
Iikura Central Building, 4th Floor
12 Iikura Kata-machi, Azabu
Minato-ku, Tokyo

WASHINGTON, D. C. 20036
1155 Sixteenth St., N. W.

Advertising Management

REINHOLD PUBLISHING CORP.
(for Branch Offices, see page 129 A)

For submission of manuscripts, see page 2 A.

Science Education for Nonscientists

THE TRADITIONAL APPROACH in American colleges and universities to assure some degree of familiarity with the methods and accomplishments of the physical sciences among nonscience majors has been to require a year's course in natural science during the first or second year of study. Some institutions have experimented with survey courses covering several sciences, while others have offered special courses in single sciences for nonscience majors.

A basic question is whether such students are best served by courses "in" science or "about" science. In past generations, a persuasive argument could have been presented to the effect that there is only a single structure of science, and therefore that it is illogical to present one kind of science course for scientists and another for nonscientists. But with the increasing complexity of modern science and with the quickened pace of its development, it is necessary to re-examine the validity of the traditional approach. In addition, it must be recognized that people who were educated in arts or humanities 10 or 20 years ago, and who received an adequate exposure to science at that time, most likely are hopelessly inadequate in their understanding of current science. Yet these very people are apt to be in positions of leadership in business and government, charged with the responsibility for making decisions affecting the welfare of science.

As for college courses in chemistry for nonscience majors, an article by Prof. William F. Kieffer, of the College of Wooster [*J. Chem. Educ.*, **45**, 550, September (1968)] is noteworthy in several respects. First of all, the course is offered at the junior or senior level, flaunting the custom of restricting nonmajor courses to the first two years. Second, the same course is offered regardless of the type of physical science course taken earlier. Third, advantage is taken of greater maturity and broader experience of the students to include the historical and philosophical background underlying scientific discoveries along with the science itself.

With respect to the education of nonscience professionals, the special courses instituted several years ago by Dr. W. W. Grigorieff of Oak Ridge Associated Universities deserve special mention. Being first organized to bring groups of University professors from nonscience fields together with scientists for several weeks of lectures and discussions about modern science, the program has shifted during the past two years toward noneducators—e.g., clergymen—and toward shorter courses. Encouraged by the success of this program, several universities have recently experimented with special short courses in a similar vein. Such experiments deserve careful study as guidelines for further progress in this important area of education.



Evaluating Dispersion in Gel Permeation Chromatography

Axial Dispersion of Polymer Molecules in Packed Beds of Nonporous Glass Beads

R. N. Kelley and F. W. Billmeyer, Jr.

Departments of Chemistry and Materials, Rensselaer Polytechnic Institute, Troy, N. Y. 12181

The causes of zone broadening in GPC columns can be attributed to free-stream dispersion (outside the gel) and broadening due to the permeation process itself. Free-stream dispersion in the absence of permeation was studied utilizing nonporous glass beads and solutes covering a wide range of diffusivity. The major variables examined were flow rate, solute diffusivity, and particle size and size distribution of the packing beads. The experimental data are in good agreement with the theoretical model previously proposed, which incorporates molecular diffusion, eddy diffusion, and velocity-profile effects as the major causes of axial dispersion. Particle segregation effects were shown to be relatively unimportant.

THE EFFICIENCY of a chromatographic process depends upon the nature and extent of the dispersive mechanisms operative in the packed bed. As a result of such processes, not all the molecules of a single solute species are eluted at the same time. This leads to a spread of elution or retention times about a mean, and determines the column efficiency. An understanding of the factors affecting the distribution of retention times is a prerequisite for the successful design of chromatographic columns and packed beds.

It has been established (*1–5*) that the gel permeation chromatography (GPC) separation is dependent upon the volumes of the solute molecules, but relatively little is known about the detailed mechanisms controlling the permeation process itself. Various models for predicting elution times in GPC have been proposed (*5–12*), and several approaches (*4, 12–21*) have been taken to evaluate peak broadening, which is probably the major factor limiting the accuracy with which molecular-size distributions can be determined by GPC at the present time. Our own approach (*14*) proposes that broadening during flow through a GPC column arises from free-stream dispersion effects plus mass transfer of solute molecules into and out of the pores (the permeation process). We feel that the detailed mechanisms controlling the permeation process can best be elucidated when the free-stream dispersion characteristics of macromolecular solutes are better understood.

Many of the concepts developed to explain chromatographic dispersion phenomena may be applied, in some part, to the GPC process, and many excellent reviews of dispersion in gaseous (*22–24*) and liquid (*25–28*) systems have been published.

Conventional studies of dispersion in liquid systems have usually employed conductivity devices for determining solute concentrations within or at the exit of a packed bed. Correspondingly, most data in the literature have been obtained for aqueous systems with ionic solutes. Comparatively few data are available for organic systems and almost none have been reported for high-polymer solute molecules. The recent development of a continuous recording differential refractometer, by Waters Associates, Inc., Framingham, Mass., has facilitated dispersion measurements with organic solvents and macromolecular solutes, and has made this investigation possible.

In this paper, the results of axial dispersion measurements using nonporous glass beads are presented and discussed in light of the approach previously described (*14, 15*). The main purposes of these axial measurements are to gain an understanding of the dispersion characteristics of macromolecules as compared to those of small molecules; to determine the major variables (mechanisms) affecting free-stream dispersion in GPC; and to establish whether our theoretical approach

(1) J. C. Moore, *J. Polym. Sci., Part A*, **2**, 835 (1964).
(2) J. C. Moore and M. C. Arrington, "The Separation Mechanism of Gel Permeation Chromatography: Experiments with Porous Glass Column Packing Materials," 3rd International Seminar on Gel Permeation Chromatography, Geneva, Switzerland, May 1966.
(3) H. Benoit, Z. Grubisic, P. Rempp, D. Decker, and J. G. Zilliox, *J. Chim. Phys.*, **63**, 1507 (1966).
(4) W. B. Smith and A. Kollmansberger, *J. Phys. Chem.*, **69**, 4157 (1965).
(5) E. F. Casassa, *J. Polym. Sci., Part B*, **5**, 773 (1967).
(6) J. Porath, *Pure Appl. Chem.*, **6**, 233 (1963).
(7) T. C. Laurent and J. Killander, *J. Chromatogr.*, **14**, 317 (1964).
(8) P. G. Squire, *Arch. Biochem. Biophys.*, **107**, 471 (1964).
(9) W. W. Yau and C. P. Malone, *J. Polym. Sci., Part B*, **5**, 663 (1967).
(10) W. W. Yau, H. L. Suchan, and C. P. Malone, *J. Polym. Sci., Part A-2*, **6**, 1349 (1968).
(11) J. B. Carmichael, *J. Polym. Sci., Part A-2*, **6**, 572 (1968).
(12) J. B. Carmichael, *Macromolecules*, **1**, 526 (1968).
(13) J. C. Giddings and K. L. Mallik, ANAL. CHEM., **38**, 997 (1966).
(14) F. W. Billmeyer, Jr., G. W. Johnson, and R. N. Kelley, *J. Chromatogr.*, **34**, 316 (1968).
(15) F. W. Billmeyer, Jr., and R. N. Kelley, *ibid.*, p 322.
(16) J. Coupek and W. Heitz, *Makromol. Chem.*, **112**, 286 (1968); W. Heitz and J. Coupek, "Column Efficiency in GPC," 5th International Seminar on Gel Permeation Chromatography, London, England, May 19–22, 1968.
(17) W. Heitz and W. Kern, *Angewandte Makromol. Chem.*, **1**, 150 (1967).
(18) J. G. Hendrickson, "Basic Gel Permeation Chromatography Studies VI. Peak Spreading Causes and Evaluation," 4th International Seminar on Gel Permeation Chromatography, Miami Beach, Fla., May 22–24, 1967.
(19) M. LePage, R. Beau, and A. J. deVries, *Polymer Preprints*, ACS Div. Polymer Chem., **8**, (2), 1211 (1967).
(20) L. H. Tung, *J. Appl. Polym. Sci.*, **10**, 375, 1271 (1966).
(21) J. J. Hermans, *J. Polym. Sci., Part A-2*, **6**, 1217 (1968).
(22) K. B. Bischoff, *Ind. Eng. Chem.*, **58**, 18 (1966).
(23) O. Levenspiel and K. B. Bischoff, *Adv. Chem. Eng.*, **4**, 95 (1963).
(24) G. W. Johnson, Ph.D. Thesis, Rensselaer Polytechnic Institute, Troy, N. Y., Feb. 1967.
(25) S. F. Miller and C. J. King, University of California Radiation Laboratory Report 11951, May 1965.
(26) A. Hennico, G. Jacques, and T. Vermeulen, University of California Radiation Laboratory Report 10696, March 18, 1963.
(27) T. K. Perkins and O. C. Johnston, *Soc. Petrol. Eng. J.*, **3**, 70 (1963).
(28) M. C. Hawley, Ph.D. Thesis, Michigan State University, 1964.

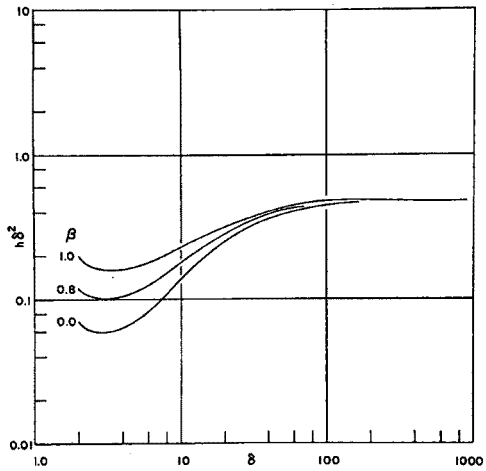

Figure 1. Variation of dispersion parameter ($h\delta^2$) with aspect ratio (δ) as a function of β for uniform packing

From Johnson (*24*); β = eddy diffusivity/(molecular diffusivity + eddy diffusivity)

adequately describes dispersion in such systems. With these goals achieved, permeation effects may be isolated from free-stream dispersion effects and studied independently.

THEORY

The theoretical-plate concept as expressed by the height equivalent to a theoretical plate (HETP) has proved to be extremely useful for evaluating the separation efficiency of chromatographic columns. Several theories have been proposed (*13, 21, 29–32*) to predict HETP in gaseous or liquid chromatographic systems. In general, it is postulated that

$$\text{HETP} = 2D/U + (\text{a mass transfer contribution}) \quad (1)$$

where D is an overall dispersion number and U is the average linear flow velocity. The assumptions and equations involved in deriving Equation 1 have been discussed in a previous paper (*14*).

Van Deemter (*29*) assumed that the dispersion number was composed of a longitudinal molecular-diffusion term and an eddy-diffusion term and that the mass-transfer contribution was a linear function of velocity. For some chromatographic systems, this approach did not correlate well with experimental results. It was to explain these deviations that Giddings developed his coupling theory (*30, 33*). In this theory, the eddy diffusivity is coupled in a nonadditive manner with the mobile-phase resistance to nonequilibrium mass transfer.

Another approach (*32*) which helps to explain the origin of coupling has been to extend van Deemter's theory by incorporating an additional term to account for velocity-profile effects caused by nonuniform velocity over the column cross section. A nonuniform velocity profile causes a spread in retention times whose magnitude is determined primarily by radial (transverse) diffusion. Johnson (*24*) applied this approach to gaseous systems and stated that a major portion of the observed broadening in liquid systems results from velocity-profile effects. Sie and Rijnders (*32*) found this approach valuable for describing band broadening in packed chromatographic columns for gaseous systems, and point out that it may also be useful in liquid chromatography. We have previously indicated (*14, 15*) the possible value of utilizing a velocity-profile approach to explain broadening in GPC.

Most chromatographic column-packing materials have a relatively wide particle-size range. During column packing, the particles can segregate, producing some cross sections having a small-particle-diameter packing and others having large-diameter packing. Such particle-size segregation, coupled with variations in packing density, presents variable resistance to the flowing fluid and leads to a nonuniform velocity profile. Because the column void fraction is greater near the wall, the flowing fluid encounters less resistance there, and the average velocity near the wall is correspondingly greater than in the center of the bed. Several investigators have reported this behavior (*24, 34–37*).

The overall longitudinal-dispersion number D is therefore assumed to be the sum of contributions from molecular diffusion, eddy diffusion, and velocity-profile effects operating in the column:

$$D = \underset{\text{molecular diffusion}}{\phi D_l} + \underset{\text{eddy diffusion}}{\lambda U d_p} + \underset{\text{velocity-profile effects}}{hR^2U^2/\bar{D}_r} \quad (2)$$

where $\phi = {}^2/_3$ is a tortuosity factor, D_l is diffusivity in the mobile-phase, $\lambda = {}^1/_{11}$ is a eddy-diffusion proportionality constant, d_p is the effective particle diameter, h is a velocity-profile constant, R is the column radius, and $\bar{D}_r$ is an average radial diffusivity. This form of the expression for the overall dispersion number was developed by Taylor (*38*) and Aris (*39*).

In cases where a mass transfer process such as adsorption or permeation is absent or negligible, as in the use of nonporous glass beads with suitable solute molecules, Equation 1 becomes:

$$\text{HETP} = 2\phi D_l/U + 2\lambda d_p + 2hR^2U/\bar{D}_r \quad (3)$$

The utility of this equation for describing mobile-phase dispersion in actual liquid chromatographic systems depends greatly on the evaluation of the average radial diffusivity $\bar{D}_r$ and the appropriate velocity-profile constant h for the experimental column used. Previous work (*24, 27, 32, 40*) has shown that the radial diffusivity is determined by radial gradients existing within the column which come about from both molecular-diffusion and eddy-diffusion processes.

(29) J. J. van Deemter, F. Zuiderweg, and A. Klinkenberg, *Chem. Eng. Sci.*, **5,** 271 (1956).
(30) J. C. Giddings, ANAL. CHEM., **34,** 1186 (1962).
(31) H. F. Walton, in "Chromatography," E. Heftmann, Ed., Reinhold Publishing Corp., New York, N. Y., 1961, p 299.
(32) S. T. Sie and G. W. A. Rijnders, *Anal. Chim. Acta*, **38,** 3 (1967).
(33) J. C. Giddings, ANAL. CHEM., **35,** 1338 (1963).
(34) R. Rhoades, Ph. D. Thesis, Rensselaer Polytechnic Institute, Troy, N.Y., 1963.
(35) C. E. Schwartz and J. M. Smith, *Ind. Eng. Chem.*, **45,** 1209 (1953).
(36) M. Morales, C. W. Spinn, and J. M. Smith, *ibid.*, **43,** 225 (1951).
(37) E. J. Cairns and J. M. Prausnitz, *ibid.*, **51,** 1441 (1959).
(38) G. I. Taylor, *Proc. Roy. Soc.*, **A219,** 186 (1953); **A223,** 446 (1954); **A225,** 473 (1954).
(39) R. Aris, *Proc. Roy. Soc.*, **A235,** 67 (1956).
(40) V. P. Dorweiler and R. W. Fahien, *Am. Inst. Chem. Eng. J.*, **5,** 139 (1959).

Table I. Packed Columns Used in This Study

Mesh range	Void fraction	Plates/ft[a]	Av particle diameter for Reynolds-number calculations, μ
40–45	0.39	150	385
80–100	0.36	475	163
100–120	0.38	650	137
120–140	0.39	1400	115
200–230	0.33	900	68
80–100/100–120 1/1 by volume	0.38	480	147
80–100/100–120/120–140 1/1/1 by volume	0.39	860	130

[a] Measured at 1 cc/min with cyclohexane solute and toluene solvent.

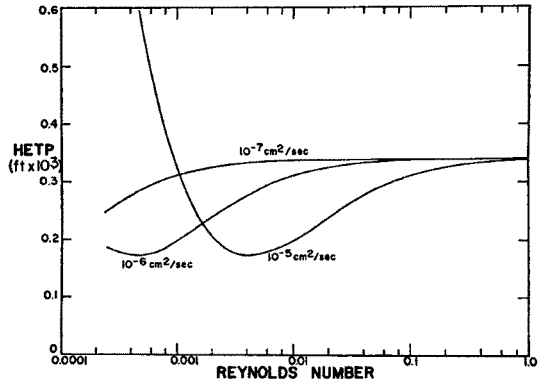

Figure 2. Theoretical variation of HETP with Reynolds number as a function of molecular diffusivity (cm²/sec)

Calculated using Equation 11, toluene data, 40-micron uniform particle diameter, 0.305 in i.d. column, and $h\delta^2$ taken from Figure 1

These in turn depend upon the variation of velocity across the column:

$$D_r(\rho) = \phi D_l + \lambda d_p U(\rho) \quad (4)$$

where ρ is a dimensionless radial position variable: $\rho = r/R$, where r is the actual radial position variable. From Equation 4, the average radial diffusivity is

$$\bar{D}_r = \phi D_l + \lambda d_p U \quad (5)$$

Sie and Rijnders (*32*) have pointed out that incorporation of this expression for $\bar{D}_r$ into the velocity-profile term of Equation 3 leads to a coupling which is very similar to that of Giddings (*30*). Such coupling assumes that molecular diffusion and eddy diffusion are independent.

By definition (*39*),

$$h = -2\int_0^1 \rho f_1(\rho)\int_0^{\rho} 1/\rho' f_2(\rho')\int_0^{\rho'} \rho'' f_1(\rho'')d\rho'' d\rho' d\rho \quad (6)$$

where ρ' and ρ'' are dummy integration variables, $f_1(\rho)$ is a velocity variation function, and $f_2(\rho)$ is a radial-dispersion variation function. Both $f_1(\rho)$ and $f_2(\rho)$ may be obtained directly from the velocity profile according to the relationships

$$f_1(\rho) = U(\rho)/(U - 1) \quad (7)$$

and

$$f_2(\rho) = D_r(\rho)/\bar{D}_r = 1 + \beta f_1(\rho) \quad (8)$$

where

$$\beta = \alpha/(\alpha + 1) \quad (9)$$

and

$$\alpha = \lambda U d_p/\phi D_l \quad (10)$$

Johnson (*24*) evaluated the velocity-profile constant h for packed beds with uniform packing as a function of aspect ratio (δ = column diameter/particle diameter) and β utilizing the basic definition given in Equation 6 and a modified theoretical velocity profile which extended the work of Rhoades (*34*) to include the radial variation of void fraction in a packed bed. The resulting data are plotted in Figure 1. Use of this graph permits evaluation of the velocity-profile constant.

Incorporating these concepts, the overall HETP equation describing mobile-phase dispersion may be written:

$$\text{HETP} = 2(\phi D_l/U + \lambda d_p) + 2hR^2/(\phi D_l/U + \lambda d_p) \quad (11)$$

Such phenomena as eddy diffusion, molecular diffusion, velocity-profile effects in the mobile phase, dead-volume effects, sorptive effects, viscosity effects, and dispersion due to diffusion into and out of the pores (the permeation process) are expected to be encountered to varying degrees in the GPC process. In this study, the permeation effect has been eliminated; viscosity effects have been minimized by using the lowest practical solute concentration; sorptive effects have been minimized by using relatively-nonpolar solutes; and dead-volume effects have been neglected.

EXPERIMENTAL

These studies were carried out utilizing a Waters Associates (Framingham, Mass.) Model 100 Gel Permeation Chromatograph with toluene as the solvent at room temperature. A microrefractometer detection cell having a volume of 10 μl was used with a $^1/_{16}$-in. null glass. The flow system of the chromatograph was slightly modified as previously described (*15*) to permit accurate dispersion measurements with single 4-ft length columns. Recorder-chart speeds up to 60 in./hr were used to allow precise measurement of peak widths at half-height and of retention times.

Standard GPC columns, 4 ft in length and having an inside diameter of 0.305 in., with Waters Associates end fittings, were packed with nonporous glass beads. The beads ("Superbrite," 3M Company) were carefully sieved into desired mesh cut ranges with U. S. Standard Sieve Screens and a Rotap Sieve Shaker. The sieving procedure was repeated at least six times to ensure that the amount of fines in the desired mesh range was minimal. Prior to column packing, the beads were washed in sequence with toluene, tetrahydrofuran, water, acetone, and anhydrous ether to remove surface impurities. They were dried and then immersed in a beaker containing pure toluene. The empty column with the bottom end fitting in place was completely filled with toluene to remove all air. The packing was slowly added at the top until the column was completely packed. As packing was added to the column, a small stream of solvent was continually withdrawn from the bottom and the column was inter-

Table II. Diffusivities of Materials Used in This Study

Substance	Supplier	Concentration, wt. %	Diffusivity in toluene,[a] cm^2/sec	Schmidt number[b]
Hexane	Fisher Scientific	0.25	1.955×10^{-5}	326
Cyclohexane	Matheson Coleman & Bell	0.25	2.177×10^{-5}	293
n-$C_{36}H_{74}$	Humphrey & Wilkinson Inc.	0.50	7.031×10^{-6}	907
2000 PS[c]	ArRo Laboratories	0.25	4.65×10^{-6}	1,370
3600 PS	ArRo Laboratories	0.25	3.33×10^{-6}	1.920
10,300 PS	Waters Associates	0.25	1.8247×10^{-6}	3,500
19,800 PS	Waters Associates	0.25	1.2438×10^{-6}	5,130
97,200 PS	Waters Associates	0.125	5.134×10^{-7}	12,400
160,000 PS	Waters Associates	0.125	3.710×10^{-7}	17,200

[a] Diffusivities of hexane, cyclohexane, and n-$C_{36}H_{74}$ were estimated from references *42* and *43;* those of the other materials were taken or extrapolated from the data of reference *18*.
[b] Schmidt number $N_{Sc} = \nu/D_L$.
[c] PS = polystyrene.

mittently vibrated. The packing material in a toluene slurry was slowly inserted into the column with a 10-ml hypodermic syringe (with no needle), in about 5-ml quantities, making sure that no air passed into the column. After the column was completely filled, the upper end fitting was put on and the packed column was purged overnight at a high flow rate to settle the packing. The end fitting was then removed to determine if the packing had settled, and more packing material was added if necessary. In most cases, none was needed. The characteristics of the packed columns employed in the study are given in Table I.

Because one of the primary objectives of this investigation was to determine the effects of diffusivity upon the resulting mobile-phase dispersion, a number of different solute molecules ranging from hexane to a low-polydispersity polystyrene (PS) of 160,000 molecular weight were employed. These solutes with pertinent supplier, concentration, and diffusivity data are listed in Table II.

THEORETICAL RESULTS

The variation (according to Equation 11) of HETP with molecular diffusivity and Reynolds number ($N_{RE} = d_p U/\nu$ where ν is the kinematic viscosity) is shown in Figure 2 for a system typical of those encountered in GPC. The calculations were carried out for toluene solvent, a column i.d. of 0.305 in., and a uniform packing material of 40-microns diameter. The dispersion parameter $h\delta^2$ was taken as 0.48 from Figure 1. Typical Reynolds numbers encountered in GPC range from about 0.01 to 1.0. In this region, the lower the molecular diffusivity, the higher the HETP. At high Reynolds numbers, the dispersion appears to become independent of the molecular diffusivity. On the other hand, at very low flow rates, molecular diffusion becomes controlling and the HETP increases very rapidly. In the intermediate regions, the predicted HETP curves bend concave downward with decreasing flow rate, reaching a minimum below which molecular diffusion dominates. These curves are very similar to those predicted by Giddings' coupling theory (*13, 41*). The minimum is determined by the magnitude of the molecular diffusivity, and as this is lowered by a factor of 10, the minimum occurs at a Reynolds number a decade lower. Therefore, if one were to replot Figure 2 as HETP *vs.* (Reynolds number times Schmidt number) = Ud_p/D_L, a single curve would result. This product is analogous to the "reduced velocity" which is often employed in chromatographic studies.

The predicted effect of particle size on HETP as a function of Reynolds number is shown in Figure 3. These calculations were also carried out for a toluene system, with a solute species having a molecular diffusivity of 10^{-5}cm²/sec, a column i.d. of 0.305 in. and uniform particle-size packings. In each case, the dispersion parameter $h\delta^2$ was estimated using Figure 1. At a given Reynolds number, the higher the particle diameter of the packing (the lower the aspect ratio) the greater the predicted dispersion. The curves show the same overall shape as in Figure 2. However, it is interesting to note that in the Reynolds number region between 0.01 and 1.0, the slope of the curve becomes much greater with increasing particle diameter.

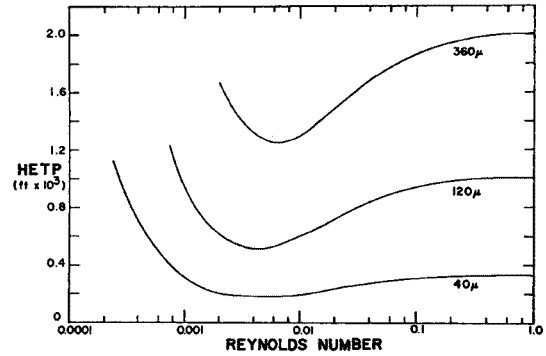

Figure 3. Theoretical variation of HETP with Reynolds number as a function of uniform particle diameter

Calculated using Equation 11, toluene data, 40-micron uniform particle diameter, 0.305 in. i.d. column, molecular diffusivity of 10^{-5} cm²/sec, and $h\delta^2$ taken from Figure 1

EXPERIMENTAL RESULTS AND DISCUSSION

Diffusivity and Flow Rate Effects. A series of solute molecules representing a Schmidt-number range from 293 to 17,200 was used to determine the effect of molecular diffusivity on dispersion in the mobile phase as a function of Reynolds number for a column packed with nonporous glass beads. The HETP data presented in Figure 4, obtained with a column packed with 120–140 mesh nonporous glass

(41) J. C. Giddings, "Dynamics of Chromatography," Part I, Marcel Dekker, New York, 1965.

(42) C. R. Wilke and P. Chang, *Amer. Inst. Chem. Eng. J.*, **1,** 264 (1955).
(43) R. C. Reid and T. K. Sherwood, "The Properties of Gases and Liquids," McGraw-Hill, New York, 1958, p 51.

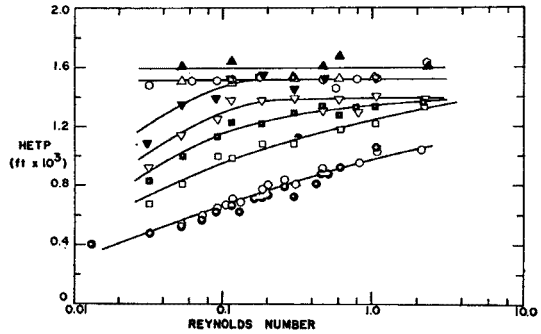

Figure 4. HETP *vs.* Reynolds number for 120–140 mesh nonporous glass bead column

○ Hexane	▽ 10,300 PS
○ Cyclohexane	○ 19,800 PS
□ n-$C_{36}H_{74}$	△ 97,200 PS
◻ 2,000 PS	▲ 160,000 PS
▽ 3,600 PS	

Toluene solvent at room temperature; solute concentrations and diffusivity data are given in Table II

beads, show that the molecular diffusivity of the solute species and the Reynolds number are important parameters determining dispersion. The dispersion of high-Schmidt-number (low-diffusivity) solutes such as 160,000 PS in flow through the packed bed is independent of flow rate over the entire range of Reynolds numbers studied. On the other hand, HETP drops with decreasing Reynolds number for low-Schmidt-number solutes such as hexane, cyclohexane, and n-$C_{36}H_{74}$. At a low Reynolds number, as the molecular diffusivity is decreased, the HETP increases from 0.4×10^{-3} ft for hexane to 1.6×10^{-3} ft for 160,000 PS. The HETP of low-Schmidt-number systems more closely approaches that of solutes with high Schmidt numbers as the Reynolds number is increased.

These experimental data closely follow the predicted curves shown in Figure 2, except that the overall dispersion is greater. The broadening should be greater for the experimental case since the particle diameter is larger and there is a distribution of particle sizes which leads to a larger velocity-profile constant. It is significant, however, that the theoretically-predicted trends are closely followed experimentally.

A series of runs was carried out at varying flow rates with a column packed with 40–45 mesh (~385 microns) nonporous glass beads. Cyclohexane, n-$C_{36}H_{74}$, 3600 PS, 19,800 PS, and 97,200 PS were the solutes, giving a relatively

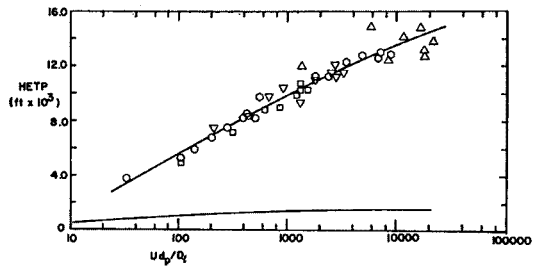

Figure 6. HETP *vs.* UD_p/D_l for 40–45 mesh nonporous glass bead column

Legend and conditions same as in Figure 4. Data obtained with the 120–140 mesh column are represented as a line near the bottom of the figure

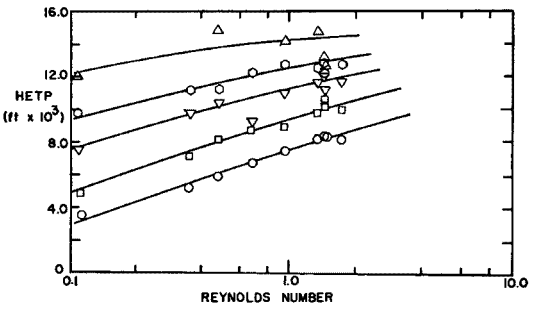

Figure 5. HETP *vs.* Reynolds number for 40–45 mesh nonporous glass bead column

Legend and conditions same as in Figure 4

wide spread (293–12,400) in Schmidt number. Because of the very low aspect ratio of 20, the dispersion was greatly increased as shown in Figure 5. The experimental curves show similar trends with decreasing diffusivity as obtained in Figure 4 and further substantiate the utility of the theoretical model.

The data of Figure 5 were replotted in Figure 6 as a function of Ud_p/D_l. For comparison purposes, the data obtained for the 120–140 mesh column are represented as a single line near the bottom of Figure 6. Almost all experimental points for the 40–45 mesh column system fall on a single line, within experimental error, as theoretically predicted.

Figure 7 presents dispersion data obtained with a column packed with 200–230 mesh (~68 microns) nonporous glass beads. The HETP curves again follow the predicted trends as a function of solute diffusivity and Reynolds number, except that the expected increase in efficiency over the 120–140 mesh column was not obtained. Microscopic examination revealed the beads to have many small surface depressions in contrast to the smooth surface of the 120–140 mesh packing material. Such depressions could account for the lower efficiency observed.

Particle Size Effects. Figure 3 shows that the mathematical model predicts a much higher dispersion level with decreasing aspect ratio. Therefore, higher efficiencies should

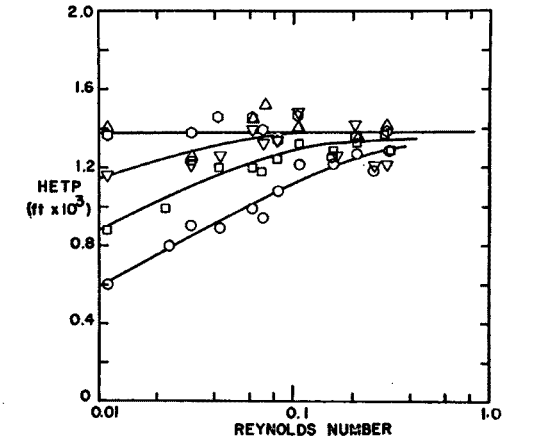

Figure 7. HETP *vs.* Reynolds number for 200–230 mesh nonporous glass bead column

Legend and conditions same as in Figure 4

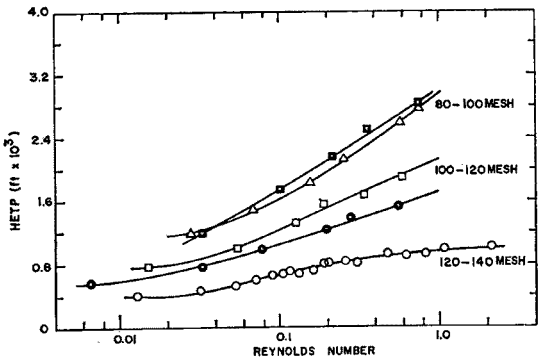

Figure 8. Effects of particle size and segregation on dispersion of cyclohexane

Conditions same as in Figure 4

- □ **1/1 by Volume 80–100 mesh/100–120 Mesh**
- ○ **1/1/1 by Volume 80–100 mesh/100–120 mesh/120–140 mesh**

be attained as the particle size of the packing is lowered with a given diameter column. Achieving such benefits with small-diameter particles is, however, often difficult because of problems involved in obtaining a uniform particle diameter. In addition, Figure 3 shows that the slope of the HETP curve over the Reynolds-number region of interest is greatly increased with increasing particle size.

Data in Figure 6 show that as the aspect ratio of the system for a fixed column diameter is lowered, the HETP is increased and the slope of the HETP curve as a function of flow rate is increased.

To further illustrate particle size effects, a series of runs was made using three successive mesh cuts; 80–100, 100–120, and 120–140 mesh. The results in Figure 8 and 9 again show that the higher the particle size, the greater the dispersion in the same diameter column.

The effect of aspect ratio could also be explored using columns of different diameters and a single packing material. This would eliminate problems associated with preparation of uniform packing materials at different size levels, but would introduce other problems such as end effects (*15*).

Segregation Effects. Segregation has been shown to be a major factor contributing to dispersion in gaseous systems by greatly increasing the magnitude of the velocity-profile constant (*24*). Three consecutive mesh ranges were mixed to give column packings with a wide distribution of particle sizes. Figures 8 and 9 show that greatly increasing the range of the particle size distribution does not significantly increase the resulting broadening.

Figure 10 compares the theoretically-predicted HETP curves for uniform particles and segregated particles with experimental data obtained with the 120–140 mesh column. The dispersion parameter $h\delta^2$ was evaluated for both cases from work on gaseous systems by Johnson (*24*). From these data, it is also evident that segregation effects are relatively unimportant in these liquid systems; this supports the conclusions of Horne, Knox, and McLaren (*44*).

In summary, our experimental data generally follow the theoretically-predicted trends, indicating that this model should have great utility in predicting mobile-phase dispersion in liquid as well as gaseous systems. If one assumes that

(44) D. S. Horne, J. H. Knox, and L. McLaren, *Separation Sci.*, **1** (5), 531 (1966).

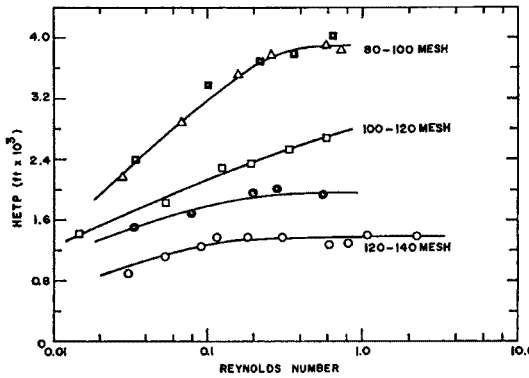

Figure 9. Effects of particle size and segregation on dispersion of 3,600 polystyrene

Legend and conditions same as in Figure 8

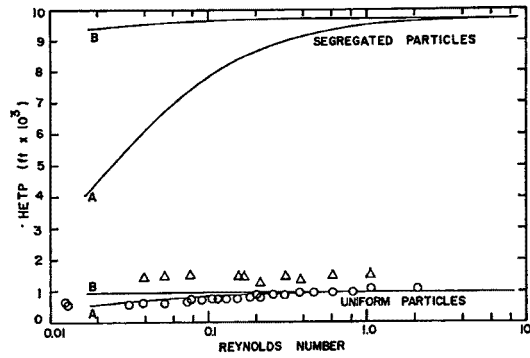

Figure 10. Experimental data for 120–140 mesh compared to theoretically predicted dispersion of segregated and uniform particles

Conditions same as in Figure 4, dispersion parameter $h\delta^2$ taken from Ref. 24

- ○ **Cyclohexane**
- △ **97,200 Polystyrene**
- *A* **Theoretical curves for cyclohexane**
- *B* **Theoretical curves for 97,200 polystyrene**

mobile-phase dispersion and broadening due to permeation into and out of the gel are statistically independent processes, it should ultimately be possible to determine the functional form of the relationship governing broadening arising from the permeation process itself. Such information would be extremely useful in developing a comprehensive model describing gel permeation chromatography.

ACKNOWLEDGMENT

We are grateful to John C. Moore and Glenn W. Johnson for encouragement and many helpful discussions.

RECEIVED for review December 10, 1968. Accepted March 17, 1969. Work supported jointly by the Texas Division of the Dow Chemical Company and Waters Associates, Inc. In addition, one of us (R.N.K.) wishes to thank Hercules, Inc., for fellowship support. The research was carried out at Rensselaer's Materials Research Center Laboratory, a facility supported by the National Aeronautics and Space Administration.

Versatile Reciprocal Time Computer for Reaction Rate Methods

S. R. Crouch

Department of Chemistry, Michigan State University, East Lansing, Mich. 48823

A new method is described for computing the reciprocal of time for use in reaction rate methods. The instrument is all-electronic and can be used to measure the rates of both fast and slow reactions. The computer can be directly calibrated in reciprocal time or concentration units. Results are presented for synthetic signals which vary in rate from 5 mV/sec to 20 V/sec. Standard deviations and relative errors are less than 1% in most cases. Data for the determination of phosphate by a spectrophotometric rate method are presented to demonstrate the application of the reciprocal time computer to routine analysis.

SEVERAL RECENT PUBLICATIONS have dealt with automated measurement systems for reaction rate methods (*1*, *2*). Two general approaches have proved most reliable (*3*): the fixed time method in which the concentration change occurring in a preselected time interval is measured; and the variable time method in which the time required for the reaction to proceed by a fixed amount is measured. As Pardue has observed (*4*), this latter approach has several advantages for many reactions. The major disadvantage of the variable time method is the inverse relationship between the measured time interval and concentration. To overcome this disadvantage, Pardue and coworkers (*1*, *5*, *6*) have developed systems for computing the reciprocal of the time interval and have obtained a direct proportionality between readout and concentration. In the most elegant of these systems (*1*), a voltage is generated proportional to the time interval required for the reaction to proceed by a preset amount. The logarithm of the voltage is computed and summed with a reference voltage. The final step computes the antilogarithm of the inverted sum, giving a voltage readout proportional to the reciprocal of the time interval.

The system described here computes the reciprocal of time by measuring the period of a pulse train whose frequency is directly proportional to the desired time interval. This approach eliminates the critical logarithmic elements which are necessary in other all electronic systems (*1*) and is extremely versatile. The instrument is easily calibrated in reciprocal time or concentration units and can be used for reaction time intervals from 5 msec to several minutes. The instrument requires a voltage input and can measure the rates of both positive- and negative-going signals. In addition, a simple modification allows rates to be monitored continuously during a single reaction. Although the system described here does not possess the noise-averaging characteristics of the fixed-time integration method (*2*), the fixed concentration interval can be easily adjusted to minimize the effects of noisy input signals and experimental results on synthetic signals are comparable in precision and accuracy. The circuit is readily constructed from a few commercially available circuit cards and digital modules, and a digital instrument.

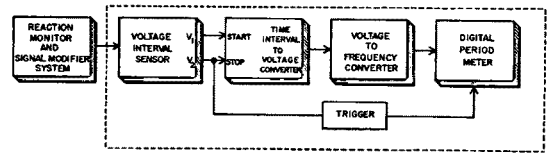

Figure 1. Block diagram of reaction-rate measurement system

Reciprocal time computer shown in dotted lines

INSTRUMENT DESCRIPTION

A block diagram of a rate measuring system using the reciprocal time computer is shown in Figure 1. The chemical reaction is monitored in a reaction cell by a suitable transducer whose signal is modified to obtain a voltage input for the reciprocal time system. The reciprocal time computer is shown in dotted lines in Figure 1.

The voltage interval sensor has two set comparison voltages V_1 and V_2, corresponding to two concentrations of the monitored reactant or product. When the input voltage reaches V_1, a trigger signal begins a linear sweep generator which serves as a time interval to voltage converter. When the input voltage reaches V_2, the linear sweep generator is stopped. Its output voltage is then proportional to the time required for the input signal to change by $\Delta V = (V_2 - V_1)$. The voltage output of the time interval to voltage converter is the input to a voltage to frequency converter whose output frequency is thus proportional to the time interval. A digital period meter, triggered when level V_2 is reached, measures the reciprocal of the frequency and hence the reciprocal of the time interval.

Voltage Interval Sensor. The voltage interval sensor is shown in Figure 2. Switch S_1 and relay R_1 comprise an on–off switch for the reciprocal time computer. During periods of sample and reagent introduction, this switch is placed in the off position to prevent false triggering by noise. The voltage interval sensor consists of two high speed voltage comparators and two stable reference voltages, which provide the comparison voltages V_1 and V_2. Comparison voltage V_1 is obtained directly from reference voltage source V_1. Comparison voltage V_2 is obtained from the sum of a second voltage source ΔV and V_1. Thus V_2 always differs from V_1 by ΔV. This configuration allows the first comparator trigger level V_1 to be varied without varying ΔV. In addition, this configuration allows multiple measurements to be made on the same reaction. If a stair case generator is substituted for V_1, the absolute magnitudes of V_1 and V_2 can be advanced in steps while ΔV remains constant. Hence the comparators can be programmed to move along the reaction curve, allowing the reciprocal of time to be computed at various concentration intervals throughout the reaction. For high versatility, voltage reference sources V_1 and ΔV are continuously variable and reversible in polarity.

Logic driver outputs of $\simeq$0 V and +5 V from the comparators are used to trigger the time interval to voltage con-

(1) G. E. James and H. L. Pardue, ANAL. CHEM., **40**, 797 (1968).
(2) E. M. Cordos, S. R. Crouch, and H. V. Malmstadt, *ibid.*, p 1812.
(3) W. J. Blaedel and G. P. Hicks, "Advances in Analytical Chemistry and Instrumentation," Vol. 3, Wiley, New York, 1964, pp 105–42.
(4) H. L. Pardue, *Rec. Chem. Progress*, **27**, 151 (1966).
(5) H. L. Pardue, C. S. Frings, and C. J. Delaney, ANAL. CHEM., **37**, 1426 (1965).
(6) H. L. Pardue and R. L. Habig, *Anal. Chim. Acta.*, **35**, 383 (1966).

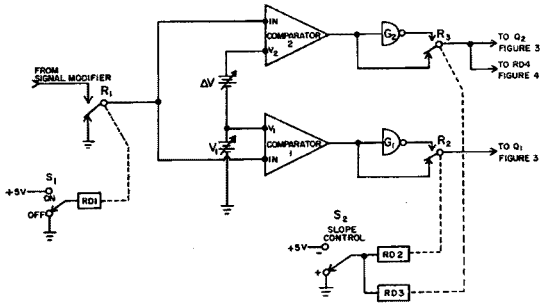

Figure 2. Voltage interval sensor

Comparators—Heath EU-800-HB comparator cards
***G_1, G_2*—*NAND* gates, Heath EU-800-JC *NAND* gate card**
***RD*1, 2, 3 and R_1, R_2, R_3—Relay drivers and relays, Heath EU-800-JD Relay Card**
V_1, ΔV—Voltage reference sources, Heath EUW-16

verter and the digital period readout. For positive-going input signals, the comparator logic driver outputs are used directly to trigger these subsequent circuits. For negative input slopes, however, the slope control switch S_2 activates relays R_2 and R_3 which introduce *NAND* gates G_1 and G_2. This inverts the logic levels so that the same switching circuits can be used to start and stop the time interval to voltage converter. The actual polarities of reference voltages V_1 and ΔV will depend on the polarity of the input signal from the signal modifier and the polarity of its slope. For an input signal which begins at zero V or some positive voltage with respect to ground and continues to move positive, the polarities of V_1 and ΔV will be as shown in Figure 2. Other cases can be accommodated by reversing V_1 and/or ΔV and adjusting switch S_2.

Time Interval to Voltage Converter. The linear sweep generator, used to produce a voltage proportional to the time interval, is an operational amplifier integrator whose integration time is controlled by the outputs of comparators 1 and 2. Figure 3 shows the integrator and associated solid-state switches. Transistors Q_1 and *FET* 1 make up a fast analog gate which is closed, shorting integrating capacitor C_f until the input signal reaches comparator level V_1. When V_1 is reached, a +5-V signal from the output of comparator 1 is applied to the base of Q_1, which turns Q_1 and *FET* 1 OFF, allowing C_f to charge. Likewise, Q_2 and *FET* 2 switch off the integrator input voltage E_{in} when level V_2 is reached. Thus the output voltage of OA_1 increases linearly for a time interval (Δt) when the input signal is between V_1 and V_2. The integrator output voltage is thus given by Equation 1

$$E_0 = -\frac{E_{in}\Delta t C_f}{R_{in}} \qquad (1)$$

Solid-state switches are used to control the time interval to voltage converter because of their rapid switching times when compared to mechanical switches. The switches shown in Figure 3 are capable of switching in about 20 μsec.

The input voltage of OA_1, E_{in}, is variable from 0–10 V so that a wide variety of input rates can be handled with high accuracy. For rapid reactions, Δt is short, and E_{in} should be large enough to make E_0 in Equation 1 several mV for accurate voltage to frequency conversion. Conversely, when Δt is large, E_{in} should be small enough to avoid limiting OA_1 before the end of the time interval. Usually, the sweep rate of the integrator was 1 V/sec for rapidly changing input signals and 100 mV/sec for slow signals. Potentiometer P_2 at the output of OA_1 allows a selected fraction of E_0 to be fed to the voltage to frequency converter. This adjustment can

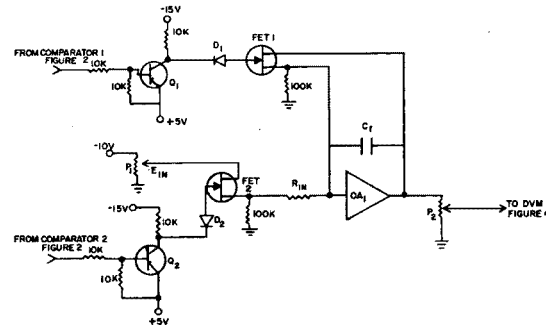

Figure 3. Time interval to voltage converter

Q_1, Q_2—2N1274
D_1, D_2—1N4149
FET 1, FET 2—MPF 105
OA_1—Philbrick PP25AU
P_1, P_2—100K on Heath EU-801A Analog Digital Designer
R_{in}, C_f—typically 1 meg, 1μf

be used for direct concentration or rate readout as explained in a later section.

Voltage to Frequency Converter and Period Meter. The voltage to frequency converter operates on the output voltage of the integrator E_0, and produces pulses at a frequency f, which is proportional to E_0 as shown by Equation 2

$$f = kE_0 \qquad (2)$$

where k is the conversion rate in Hz/V. If a period meter is used to read the reciprocal of the frequency, the resulting period T is directly proportional to the reciprocal of the time interval Δt, as shown by combining Equations 1 and 2

$$T = \frac{1}{F} = \frac{1}{kE_0} = \frac{R_{in}C_f}{kE_{in}\Delta t} \qquad (3)$$

where the minus sign in Equation 1 has been dropped because E_{in} is always a negative voltage.

Any accurate and stable voltage to frequency (V-F) converter can be used to provide input pulses to the period meter. In this work, however, it was convenient to use the internal V-F converter in the Heath Universal Digital Instrument (UDI, Heath EU-805A). This V-F converter is normally used only when the instrument is in the digital voltmeter (DVM) mode. However, the output of the V-F converter is available at the rear panel even when the instrument is used in another mode, such as the period mode. Hence, the same instrument can provide V-F conversion and period measurement. For high accuracy, the instrument was usually operated in the multiple period averaging mode as explained in the next paragraph.

The V-F converter in the Heath UDI has a conversion rate of 100 KHz/V. Because of this high conversion rate, it is not practical to obtain high accuracy by measuring single periods. For example, a 1-V signal at the output of OA_1 would result in a V-F output period of only 10 μsec. Thus, to obtain higher resolution, multiple periods were taken. In this mode, the internal 1-MHz oscillator of the UDI is counted for a scaled number of input periods (1, 10, 100, etc.), permitting 1 μsec resolution. To accomplish this, the V-F converter output at the rear panel was connected to UDI input *B* and the rear panel clock output was connected to input *A*. The frequency meter push button was pushed (7). The front panel scaling factor switch selects the number

(7) *Heath Instruction Manual EU-805A*, Universal Digital Instrument (1968).

of periods to be averaged. The necessary connections for multiple period averaging of the V-F output are shown in Figure 4. Relay R_4 is used to keep the readout off until comparator 2 (Figure 2) has switched. This switch can operate leisurely and hence an electromechanical relay was used.

In the multiple period averaging mode, Equation 3 is altered somewhat. If F periods are averaged by selecting a scaling factor of F, the UDI counts the number of μsec in F periods and Equation 3 becomes

$$\text{Readout } (\mu\text{sec}) = \frac{10^6 F R_{in} C_f}{k E_{in} \Delta t} \quad (4)$$

Substituting for the fixed constants in Equation 4 (k = 100 KHz/V, $R_{in}C_f$ = 1 sec), gives

$$\text{Readout } (\mu\text{sec}) = \frac{10F}{E_{in}} \left(\frac{1}{\Delta t}\right) \quad (5)$$

Thus the scaling factor F and the integrator input voltage E_{in} can be adjusted to accommodate a wide variety of input slopes with high accuracy. If E_{in} is a multiple of 10 (100 mV, 1 V, etc.), the readout will indicate the reciprocal time directly with only a decimal conversion factor.

PROCEDURES

Circuit Layout and Construction. The circuit cards listed in Figures 2 and 3 were inserted into a Heath "Analog-Digital Designer," EU-801A, which supplied the necessary power to operate the system. A special printed circuit card containing the two analog gates shown in Figure 3 was prepared. The Philbrick operational amplifier was mounted on a Heath circuit board (Heath part no. 85-247-1). Connections within and between cards were made with No. 22 patch wires. Once the initial instrument testing had been completed, a motherboard containing all necessary card connections was prepared by mounting several 32 pin connector strips (Heath part No. 432-79) on 2 Heath EU-50-MD multiple connector/blank pc cards. The necessary connections were then made by etching the circuit board.

Table I. Automatic Reciprocal Time Measurements

Input rate, mV/sec	Digital readout,[a] μsec	Rel std dev, %	Rel error,[b] %
+5	497	0.15	−0.6
10	1,004	0.25	+0.4
30	2,998	0.22	−0.1
50	5,007	0.21	...
70	7,004	0.13	+0.1
100	9,979	0.06	−0.2
300	29,780	0.34	−0.7
500	49,740	0.27	−0.6
1,000	1,001	0.38	+0.1
5,000	5,020	0.59	+0.4
7,000	7,041	0.87	+0.6
10,000	10,100	1.32	+1.0
20,000	19,840	1.82	−0.8

[a] Averages of 10 results; comparators ΔV = 100 mV; for rates to 500 mV/sec, $F = 10^2$, E_{in} = 100 mV; for rates $\geq$1 V/sec, F = 10, E_{in} = 1 V.
[b] Based on calibration with 50 mV/sec input rate.

Table II. Automatic Phosphate Determinations

Digital concentration readout[a]	Phosphorus concentration, ppm		
	Taken	Rel error,[b] %	Rel std dev, %
2.98	3.0	−0.7	2.8
5.02	5.0	...	3.7
8.03	8.0	+0.4	2.3
9.96	10.0	−0.4	1.2

[a] Averages of 5 results; V_1 = 0.975 V, ΔV = 25 mV, E_{in} = 50 mV, F = 10.
[b] Based on calibration with 5.0 ppm standard.

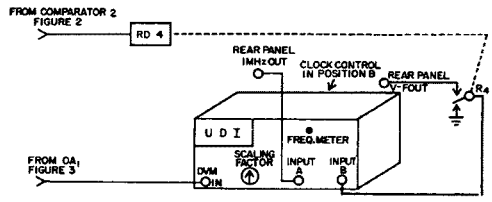

Figure 4. Connections for V-F conversion and multiple period averaging

UDI—Heath EU-805A Universal Digital Instrument
***RD4*, R_4—Relay driver and relay, Heath EU-800-JD relay card**

Preparation of Instrument. To prepare the reciprocal time computer for measurements, it is necessary to choose comparison voltages V_1 and V_2. This is most easily done by recording the signal modifier output voltage on a strip chart recorder and picking the appropriate levels from the chart paper. Exact trigger levels are then set as described in the comparator card instruction manual (*8*).

For direct concentration or rate readout, potentiometer P_2 (Figure 3) provides a convenient adjustment. Because OA_1 has a low bias current, the output of OA_1 stays constant for some time, allowing P_2 to be adjusted to give the desired readout. Alternate adjustments such as ΔV or E_{in} can be made only once for any given reaction.

Spectrophotometric Measurements. A Heath single beam spectrophotometer EU-701 was used for all spectrophotometric measurements. The photomultiplier current was converted to a voltage using a standard operational amplifier circuit. The spectrophotometer slit width and photomultiplier power supply voltage were adjusted to give a 1.000-V output of the operational amplifier for 100% transmittance. The voltage output of the operational amplifier was the input to the reciprocal time computer (input to relay R_1, Figure 2). The reaction cell was a standard 1.00-cm spectrophotometric cell surrounded by a brass jacket through which water at 25.0 °C was circulated. A magnetic stirrer was positioned below the cell to allow rapid mixing.

Phosphate Determinations. For the determination of phosphate, all reagents except the acid-molybdate solution were prepared as previously described (*9*). The acid–molybdate reagent was prepared by dissolving 1.089 grams of $Na_2MoO_4 \cdot 2H_2O$ in water in a 250-ml volumetric flask. A total of 9.4 ml of concentrated H_2SO_4 was then added and the solution was diluted to volume.

The reaction was followed at 650 mμ. Two milliliters of the acid–molybdate reagent and one milliliter of the phosphate sample were added to the cell. The reaction was begun by injecting 0.25 ml of 0.10*M* ascorbic acid with a hypodermic syringe. At the end of the measurement time, the result appears automatically on the Universal Digital Instrument.

(8) *Heath Instruction Manual EU-800-HB*, V to F/Comparator Card, (1968).
(9) S. R. Crouch and H. V. Malmstadt, ANAL. CHEM. **39**, 1090 (1967).

RESULTS

The reciprocal time computer was tested by applying voltage signals of known input slopes to the voltage interval sensor (Figure 1) to simulate outputs of typical reaction monitor-signal modifier systems. Table I shows the results of measurements of input rates from 5 mV/sec to 20 V/sec. The instrument was calibrated with a 50 mV/sec input rate by adjusting P_2 (Figure 3) to give the desired readout. This adjustment is necessary because of component tolerances in the linear sweep generator. The entire range of input rates shown in Table I was measured with only one instrument change. For rates $\geq$ 1V/sec, the scaling factor F and integrator input voltage E_{in} were changed by factors of ten. At the highest rate measured, the actual time interval (Δt) was 5 msec. With this short Δt, the time interval to voltage converter output was only 5 mV. Faster rates could be measured by increasing E_{in}. However, the analog gates used to switch E_{in} (Figure 3) are only capable of switching up to 5 V.

Table II shows results for the determination of phosphate. For this procedure, the input voltage to the reciprocal time computer had a negative slope, and the *NAND* gates shown in Figure 2 were used. With the 100% transmittance set at 1.000 V, recorded curves enabled the selection of V_1 and ΔV. V_1 was set at 0.975 volt and ΔV was adjusted to be 25 mV. Because of the slowness of the reaction, E_{in} was reduced to 50 mV to avoid limiting OA_1. Potentiometer P_2 (Figure 3) was adjusted to give a direct concentration readout using a phosphate standard of 5 ppm P. At the lowest concentration used, the measurement time Δt was about 120 sec.

The results shown in Tables I and II are typical of many which have been obtained. The reciprocal time computer was constructed using the same digital modules as used in the fixed time readout system described earlier (*2*). By a simple change of circuit cards and intercard connections, the same basic modules can be used for both variable time and fixed time methods. This allows the user of reaction rate methods to have both automated readout systems readily available for use with different reactions.

RECEIVED for review March 14, 1969. Accepted April 11, 1969.

Computer-Assisted Gas–Liquid Chromatography

H. M. Gladney, B. F. Dowden, and J. D. Swalen

International Business Machine Corp., Research Division, San Jose, Calif. 95114

The use of computers for data acquisition and analysis in gas–liquid chromatography is becoming increasingly widespread. We describe an implementation of computer-assisted chromatography within a general-purpose time-shared laboratory automation system. Particular attention is paid to a method of avoiding timing conflicts at the computer, to an inexpensive method of providing a computer-to-instrument interface, and to an economical method of curve-fitting to resolve overlapping skewed peaks. It is anticipated that many of the methods and some of the computer programs will be directly applicable to various spectroscopic experiments.

THE RECENT IMPLEMENTATION in this laboratory of a time-shared laboratory automation system for spectroscopic-type instruments (*1*) has made possible on-line data collection and computation for a high-sensitivity gas chromatograph. We wish to describe our system which includes two novel features: a simple and inexpensive interface for time-shared communications between an instrument and a remote computer, and a method for the resolution of overlapping skewed peaks, involving a least-squares curve fitting procedure. In Figure 1 is shown a simple calculated curve compared with the observed chromatogram.

In general, the methods used to schedule the communications between a process-control computer and several instruments are largely selected by considerations of economy and of the relative requirements of the instruments being connected. The choice of method becomes particularly difficult if the full requirements of the laboratory cannot be anticipated—which is usually the case. It is also conceded that an extremely desirable, if not absolutely necessary, feature be that each experiment can be programmed and run independently. From the point of view of the experiment and experimenter, it is perhaps conceptually simpler if the computer is enslaved to the laboratory instrument. However, at the computer, this arrangement implies not one master, but several, usually with conflicting requirements. There are at least three possible resolutions of the problem: To dedicate a computer or a sub-computer (commonly called a data channel) either permanently or temporarily to each experiment (*2*). To employ a computer which is so fast relative to the time-sensitive experiments that the unavoidable inter-

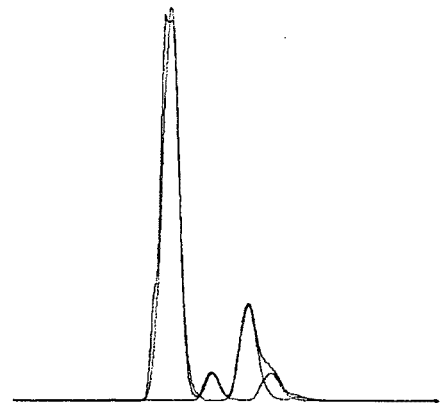

Figure 1. A poorly resolved chromatogram of 30–60 °C petroleum ether showing computer fitted peaks

(1) H. M. Gladney, *J. Comp. Physics*, **2**, 255 (1968).

(2) T. R. Lusebrink and C. H. Sederholm, *IBM J. Res. Develop.*, **13**, 65 (1969).

ferences become negligibly small (*3*). To avoid guaranteeing the user precisely controlled timing. The last possibility becomes viable when it is recognized that it is generally not necessary to sample at equal time intervals, but only to know, *a posteriori*, when you have sampled. It is not the purpose of this paper to argue the relative merits of the three approaches, but only to show that the last one, which has not been heretofore exploited, works very well even for our time-dependent experiments, in which the sampling interval varies between 0.5 and 2.0 seconds with allowable but infrequent delays resulting in the loss of up to four data points.

Data reduction for gas chromatography can be considered in two consecutive operations: estimation of integrated detector response for a number of peaks and comparison of those peaks with standards for qualitative and quantitative analysis of the sample's components. The arithmetic of the second stage is trivial, although the interpretation of areas as concentrations is still only imperfectly understood (*4*). In any case, in this laboratory the anticipated variety of samples is large and the expected duration of interest in any particular sample is short, so that the planning for cataloging multiple samples has not yet seemed worthwhile. Accordingly, discussion will be restricted to a method of resolving overlapping peaks.

Until now, changes in the sign of the first derivatives of the absorption have been used to detect multiple peaks, followed by *ad hoc* methods for estimating the area of each peak of the group. This procedure seemed to us to be inadequate and unsatisfactory. Differentiation is notoriously sensitive to high frequency noise, even if analog and digital filtering have already been applied to the signal. Another way to look at the problem of using derivatives is that their determination depends only on a few points in the neighborhood of the extremal points. The bulk of the data, which one has presumably taken some pains to collect, is, for the most part, simply ignored. Of more import, however, is that, if two peaks overlap, the estimate of the area of one, particularly if it is the smaller of the two, is sensitive to the amplitude of the other. Now, least squares methods of resolving overlapping peaks are well known (*5*, *6*) and are relatively free of the problems cited. It seemed to us worthwhile, therefore, to investigate whether they could be made reliable, completely automatic, and fast enough to be feasible on a relatively small process control computer working in real time. In addition we propose a new line shape function, a convoluted Gaussian distribution, which has the desired shape, is valid over the complete range of variables, and requires only four parameters (amplitude, retention time, line width, and asymmetry) for acceptable fitting.

Data Collection and Control. Direct connection of a gas–liquid chromatograph to a digital computer is no longer novel. However, a brief description of our hardware and software interface is perhaps of interest.

The output signal of the Varian Aerograph 1200, prior to attenuation is applied to an automatic ranging device (*7*) capable of switching over three decades. The output signal from this, together with the ranging information are transmitted to unfiltered, low-level analog inputs of the 1800 ADC. The instrument is removed from the computer by some 500 feet; to minimize noise pick up, shielded twisted pairs are used to carry these low level (0–50 mV) signals. Run conditions may be specified by means of toggle switches connected to a digital input group and action by the computer is initiated by means of a momentary closure switch connected across the terminals of a contact interrupt input. A typewriter at the location of the chromatograph completes the hardware interface.

Closure of the interrupt switch causes a program to be loaded and executed which either reads the data switches or initiates data collection, depending upon the position of one of the data switches. Data acquisition is carried out by the submonitor system (*1*), commanded by a single FORTRAN subroutine call. At the conclusion of the run a second program is queued which upon execution reads the data switches, which are now used to specify the type of data reduction required—*i.e.*, initial peak and area determination, Calcomp plots, and least squares fitting of overlapped peaks. The data reduction is then performed and a report is presented at the typewriter.

Resolution and Integration of Overlapping Distributions. As has already been mentioned, we felt it worthwhile to investigate the possibility of using least squares methods for the final data reduction. However, first-order iterative least squares calculations are known to be subject to divergence on occasion; even when they do converge, the process may require an inordinate number of iterations and may not result in the desired solution. It appeared that these potential difficulties might be resolved if fairly accurate starting estimates of the peak descriptors could be provided by the conventional peak searching methods, and if a suitable order for variation of the adjustable parameters could be discovered and implemented by program decisions. Before such a procedure could be considered a suitable distribution function for the shape of a single skewed peak had to be discovered; it was desirable that the function include a minimum number of variable parameters. We chose four numbers, A, w, t_0, τ, which could be identified as measures of amplitude, width, retention time, and asymmetry, respectively.

Criteria for an acceptable calculation method for GLC suggest themselves naturally. The final estimate for the concentration of any component should be independent of the concentrations of interfering components. This requires, *inter alia*, that the width and skewing of peaks, which are known to vary with retention time, should not be constrained to be uniform, even for overlapping peaks. If this objective is achieved, the criteria for acceptable separations on a column are significantly relaxed. The calculations must be relatively insensitive to noise in the signal. Curve fitting is much superior to extremum sensing in this respect. In any case, as much analog and digital filtering as is economically possible without sacrificing resolution is indicated. Spurious solutions should be infrequent, and fairly obvious when they occur. The computation must be entirely automatic, with no need for human decisions or intervention to help an iterative method to a reasonable solution. Hand adjustment of interacting parameters, such as employed with some recent analog curve comparison devices, or their digital counterpart, is impossibly time-consuming if large numbers of samples are to be processed. Finally, the method must be economical; on a time-shared process-control computer as powerful as the IBM 1800, which is expected to support a large number of instruments, one or two minutes computation for a record with about 10 overlapping peaks seems an acceptable time.

(3) IBM 1800 Gas Chromatograph Monitoring Program 1800-23.5.001.
(4) W. O. Caster, P. Ahm, and R. Pogue, *Chem. Phys. Lipids*, **1**, 393 (1967).
(5) W. O. Keller, T. R. Lusebrink, and C. H. Sederholm, *J. Chem. Phys.* **44**, **782** (**1966**).
(6) H. Stone, *J. Op. Soc. Amer.*, **52**, 998 (1962).
(7) D. Horne, private communication, IBM Research Laboratory, San Jose, Calif., 1968.

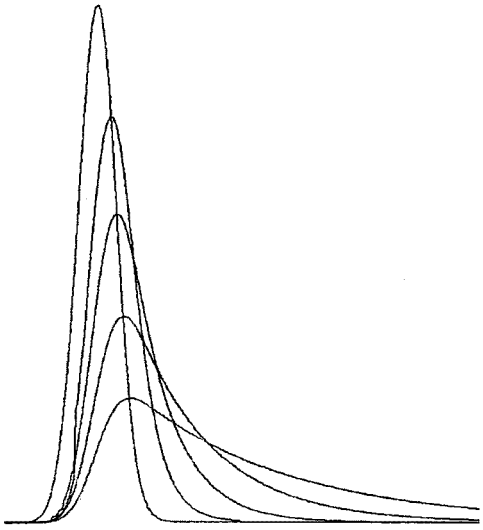

Figure 2. Skewed-Gaussian distributions for varying relative asymmetries

Our search for an analytic form to approximate skewed GLC lines started from the well-known fact that for symmetric peaks the Gaussian distribution $\exp\{-(t - t_o)^2/2w^2\}$ is usually acceptable (*8*). Functions with *ad hoc* skewing factors, such as $\{1 + a(t - t_o) + b(t - t_o)^3\}\{\exp\}-(t - t_o)^2/2w^2\}$ and $\exp[-(t - t_o)^2/\{2w^2 + d(t - t_o)\}]$ were considered. However, the former has negative regions, and the latter a singularity, so they are not very appealing and, in fact, have been shown by us not to fit experimental curves very well. However, a Gaussian probability distribution convoluted by an exponential decay does not possess such difficulties. Let:

$$v(t, t_o, w, \tau) = \frac{1}{\tau}\int_{-\infty}^{t} dt' \exp\{-(t' - t_o)^2/2w^2\} \times \exp\{-(t - t' + t_o)/\tau\}, \quad (1)$$

where t_o is the retention time, w the line width, and τ the asymmetry. Its functional shapes, plotted for a series of values of τ/w in Figure 2, are certainly evocative of variously skewed GLC absorptions. A least-squares fit, illustrated in Figure 3, to a line from methanol on a 20% SE-30 column at 110 °C was convincing enough to justify the adoption of this line shape function. It may be well to point out however, that most of the calculation methods used can easily be adapted to other line shape functions which might be considered appropriate (*9, 10*).

The useful properties of $v(t, t_o, w, \tau)$ follow directly from its definition and an examination of Figure 3. For small τ, v is approximated closely by a Gaussian distribution function:

$$\lim_{\tau \to o} v(t, t_o, w, \tau) = \exp\{-(t - t_o)^2/2w^2\} \quad (2)$$

and for our purposes can be so estimated when $\tau/w < 0.4$. For larger values of τ, the integral must be evaluated using the simple expression:

(8) J. C. Bartlett and D. M. Smith, *Can. J. Chem.*, **38**, 2057 (1960).
(9) E. J. Levy and A. J. Martin, Pittsburgh Conference on Analytical Chemistry and Applied Spectroscopy, Cleveland, Ohio, March 3-8, 1968.
(10) R. D. B. Frazer and Eikichi Suzuki, ANAL. CHEM., **41**, 37 (1969).

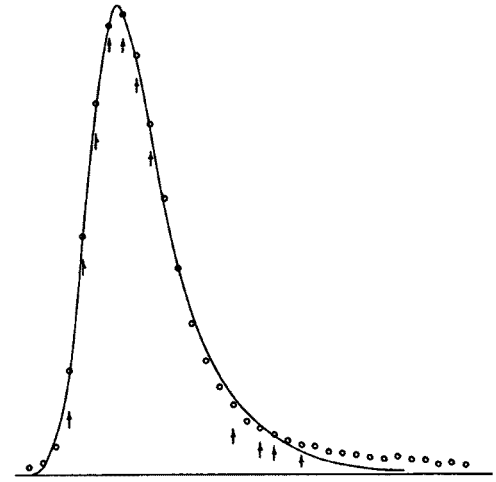

Figure 3. This least squares fit to an experimental skewed chromatographic peak indicates that the functional form adopted to represent peaks is reasonable

$$v(t, t_o, w, \tau) = 2z\sqrt{\pi}\exp(z^2 - 2yz)\,\mathrm{erf}(y - z) \quad (3)$$

with $y = (t - t_o)/w\sqrt{2}$ and $z = w/\tau\sqrt{2}$,

and where $\mathrm{erf}(x) = \frac{1}{\sqrt{\pi}}\int_{-\infty}^{x} \exp(-x^2)dx$ and

is the error integral or probability integral normalized on the full range of the abscissa (*11*). If erf(x) is calculated by linear interpolation into a table of about 20 unequally spaced values, v can be sufficiently accurately calculated by Equation 3 for $\tau/w > 1.0$. In the intervening region of τ/w, for convenience, our algorithm combines a delayed Gaussian curve on the leading edge with values calculated by Equation 3 on the trailing edge.

Further, the area of $f(t) = Av$, where A is the amplitude of the peak, can be determined by integration in closed form

$$\int_{-\infty}^{\infty} dt\, f(t) = \sqrt{2\pi}\, Aw = 2.506\, Aw \quad (4)$$

with a result which is independent of the asymmetry.

For least squares calculations, derivatives of the distributions with respect to the parameters are required. Trivially,

$$\frac{\partial f}{\partial A} = v. \quad (5)$$

For small τ, or on the leading edge of the curve, the derivative with respect to t_o may be approximated as the derivative of the limiting Gaussian

$$\frac{\partial f}{\partial t_o} \simeq A\left[\frac{t - t_o}{w^2}\right]\exp\left\{-\frac{(t - t_o)^2}{2w^2}\right\}, \quad (6)$$

but this approximation is considerably improved upon by replacing the Gaussian on the right by the distribution function itself. (This is also very convenient as a calculation algorithm.)

$$\frac{\partial f}{\partial t_o} \simeq \left[\frac{t - t_o}{w^2}\right] f \quad (7)$$

(11) B. O. Pierce, "A Short Table of Integrals," Ginn & Company, Boston, Mass., 1929.

Table I. Peak Maximum *vs.* Relative Asymmetry

τ/w	y_{max}
0.0	1.000
0.2	1.000
0.4	0.998
0.6	0.971
0.8	0.832
1.0	0.782
1.2	0.738
2.0	0.599
4.0	0.397
10.0	0.202
20.0	0.111
40.0	0.059

similarly

$$\frac{\partial f}{\partial w} \simeq \frac{(t - t_o)^2}{w^3} f. \quad (8)$$

The derivatives with respect to τ we estimate numerically.

To perform least squares fit of individual lines, it is important to know how many experimental points are necessary for a noise-insensitive fit, how they are best distributed within the line, whether a Newton-Raphson local linearization procedure can be employed, which parameters should be simultaneously varied, and how sensitive the convergence is to bad initial estimates of the parameters. A series of test calculations with a general nonlinear least-squares program (*12*) on an IBM 360/50 indicated that Newton-Raphson least squares converged fairly quickly, particularly if the calculated corrections were somewhat damped at each iteration. The parameters A, w, and t_o were simultaneously adjusted by fitting about six points on the leading edge and about half way down the trailing edge of the peak (Figure 3). A separate adjustment of τ was made by using four points in the tail. The whole procedure, repeated once, was found to give an acceptable fit to the entire line. It was also determined that the A, w, and t_o convergence was much faster if the estimate of τ was too small rather than if it was too large.

A strategy to fit multiple overlapping peaks is suggested by the work of Keller, Lusebrink, and Sederholm (*5*) in connection with the similar problem for nuclear magnetic resonance. The necessary matrix inversions become cumbersome if all peaks in a group are simultaneously fit. However, at any stage in the calculation, estimates of the parameters of all peaks are available, so that one can correct the intensity for a single peak of interest by the expected overlaps of all other peaks before undertaking a fit of that peak alone. The accuracy of this procedure is enhanced if one weights the corrected observations by their own values. By ordering the calculation with the largest peaks first, three iterations of the entire procedure can give excellent results.

Good initial estimates of A and t_o are available for each peak from the coordinates correspondence to a local minimum of the second derivative of the observations. Because these coordinates are, however, a function of the asymmetry, τ, (large τ values results in a delayed peak and reduced amplitude as shown in Figure 2), corrections are necessary. The delay of the peak may be approximated by

$$t_{max} = t_o + \text{Max}\,(0.5\,\tau, 2w) \quad (9)$$

where Max(x_1, x_2) is a function which selects the larger of x_1 or x_2. The peak amplitudes, y_{max}, are listed in Table I for various asymmetries for the normalized function v.

The width of one peak moderately well separated from its neighbors can be estimated by locating the point of half amplitude on the leading edge. For the other peaks, the approximation that the observed width is nearly proportional to the retention time has been exploited. This is particularly effective if the width estimate for the Nth peak fit is taken from the least squares value for the $(N-1)$th peak. No such self-evident procedure exists for initial estimates of τ, so we adopted an analogous procedure.

Data Reduction Programs. In the preliminary data reduction program, following recovery (from disk file) of the intensities and the time intervals between successive readings and the correction for analog-to-digital converter d.c. offset, the data are interpolated to equal time intervals and the range factors for automatic gain control are included. If a digital plot of the input data has been requested, it is presented at this time. Smoothing with the 9-point 3rd degree polynomial fit (*12*).

$$y_i' = 59y_i + 54(y_{i-1} + y_{i+1}) + 39(y_{i-2} + y_{i+2}) + 14(y_{i-3} + y_{i+3}) - 21(y_{i-4} + y_{i+4}) \quad (10)$$

is performed at every even numbered point. The intervening odd numbered points are no longer used but note their large contribution in Equation 10. The background reduction program compensates for a linearly varying instrument drift by locating line-free regions near the beginning and end of the record, estimating a baseline and subtracting it from each datum. At the same time this program estimates the root-mean-square noise. "Interesting regions" containing a line or a group of overlapping peaks are identified as sets of contiguous points whose amplitude exceeds twice the noise plus about 20% of the mean background correction. Fortunately, noise spikes are quite effectively differentiated against. Over each "interesting region" the smoothed second derivative correct to third differences is calculated at alternate points. Peaks and valleys are identified as minima and maxima in this quantity—changes in sign of the derivative are acknowledged only relative to a threshold about 40 times the noise. Peaks too close together ($<0.7w$) are identified as a single peak. In this program we found it convenient to type for each group of overlapping peaks the area, the mean position, the number of peaks, and their retention times. In addition, we print a crude estimate of the area of each peak for comparison with the least-squares estimate later obtained. The data which are passed to the least squares program are the corrected and abbreviated intensity file and the peak and valley table.

The least squares calculation begins by finding estimates of the peak width and the asymmetry parameter. Initially the program locates a peak which either is the only peak in its group or is separated from its neighbors by local minima less than half the peak height on the leading edge and less than $^2/_3$ the peak height on the trailing edge. From the half-amplitude point of the leading edge, the variation of the width with retention time

$$\frac{\partial w}{\partial t_o} \simeq \frac{w_t}{t_{ot}} \quad (11)$$

is estimated. Subsequently as each group of peaks is fit, this estimate is updated, so that the starting width estimate for any group of lines is extrapolated from the least squares estimate of the width of the final line in the preceding group. The starting estimates of τ for fitting each group of lines are

(12) E. T. Whittaker and G. Robinson, "The Calculus of Observations," Blackie & Son, Ltd., London, 1924.

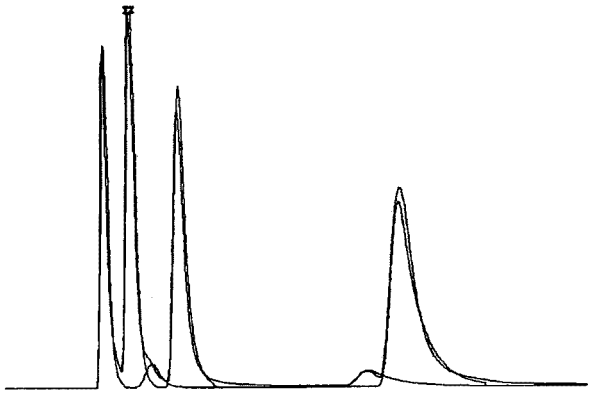

Figure 4. Experimental chromatogram and fitted peaks for a mixture of four alcohols

(ethanol, *n*-propanol, *n*-butanol, and *n*-hexanol)

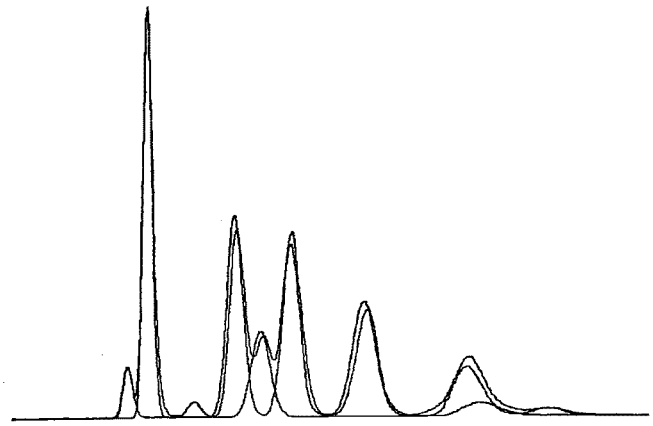

Figure 5. Experimental chromatogram and fitted peaks for a mixture of petroleum ethers

GAS CHROMATOGRAPHY RUN

DATE 6/20/68 TIME 14.49 HRS
SAMPLE IDENT. 30-60°C/60-90°C. Pet Ether
SCAN TIME = 20 MIN COLUMN 5 F. 30.20%
ISOTHERMAL RUN TEMPERATURE = 75°C
LIQUID SAMPLE

INSTRUMENT ZERO = 0.04 MV.

START A.G.L.C. RUN
LIQUID SAMPLE ... INJECT NOW

RET. TIME (SEC.)	AREA
278.7	1410.7
475.4	2855.6
758.5	689.4
896.8	2.4

3 PEAKS AT	258. SEC.	AREA	259.
	279. SEC.	AREA	1003.
	310. SEC.	AREA	147.
4 PEAKS AT	402. SEC.	AREA	853.
	448. SEC.	AREA	654.
	493. SEC.	AREA	742.
	586. SEC.	AREA	605.
4 PEAKS AT	712. SEC.	AREA	427.
	761. SEC.	AREA	201.
	834. SEC.	AREA	50.
	872. SEC.	AREA	9.

TIME IN VPC 39.6 SEC.

GROUP	PEAK	TIME	AREA	AMPL.	WIDTH	SKEW
1	1	249.3	153.	8.87	6.60	0.00
1	2	277.8	1189.	71.54	6.06	0.00
1	3	340.4	62.	2.72	8.87	0.00
2	4	401.5	830.	32.40	10.14	0.00
2	5	437.1	406.	13.85	11.58	0.00
2	6	476.3	904.	29.99	12.28	0.00
2	7	582.5	673.	18.68	14.99	0.00
3	8	711.7	459.	8.46	19.80	8.80
3	9	728.2	174.	3.30	17.93	11.65
3	10	823.6	95.	1.44	19.40	9.99
3	11	872.9	34.	0.22	32.80	16.85

ELAPSED TIME FOR GLC FIT PLOT AT IBM 1800 68.4 SECONDS

Figure 6. Laboratory typewriter output for the run shown in Figure 5

N.B. Peak 11 is only slightly discernible in Figure 5 at the extreme right as a broadening of the base line. All others are clearly identifiable

made in a similar fashion, except that it is not assumed that τ vanishes for zero retention time. For each line in an overlapping group, initial estimates of the retention time t_{ot} and amplitude A_t are made with the aid of Equation 9 and Table I.

Apart from the initial estimation procedures, each overlapping group of peaks is treated separately. In order of decreasing peak height, improved estimates of A_t, t_{ot}, and w_t are made for each peak. First of all, from 7 to 14 calculation points are selected between a point about $1.4w$ ahead of and $0.7w$ following the maximum. At each point the expected mathematical functional contribution of the other peaks of the group evaluated using Equation 3 is deducted, with the limitation that each corrected point is non-negative. Then A_t, t_{ot}, and w_t are adjusted by the well-known Newton-Raphson least squares procedure until A_t and w_t have converged to within about 10% or until four iterations have been executed. When all lines have been fit, τ is fit to four selected points chosen between $1.0w$ and $0.6w$ past the last line in the group. In the present version of the programs, it is assumed that, within any group of overlapping lines, τ is proportional to w, but this restriction could be removed.

This entire procedure is repeated several times, with tighter tolerances for A_t and w_t until on the final iteration, convergence to better than one-half per cent is required. The convergence criteria for τ are not so stringent. At all stages of the calculation, checks are performed that the parameters remain reasonable. We find these checks necessary to recover from frequent divergences of the least squares procedure.

DISCUSSION

The primary objective of this project has been to provide an arithmetic capability suitable for gas–liquid chromatography as practiced in a research laboratory. In a research laboratory, as opposed to a quality-control analytical laboratory, interest in a particular sample or class of samples is of short duration, so that much of the use of a chromatograph is devoted to finding suitable columns and run conditions. If the resolution required for accurate separation of components is diminished, many chromatographic records previously considered unacceptable may be used, and the search for suitable conditions is much reduced. However, crude methods of area analysis of overlapping peaks, with ill-understood errors, are not acceptable. The greater part of this paper has been devoted to the exploration of a method for resolution of overlapping peaks by least-squares calculations. As secondary objectives, a number of the conventional goals of computer-

assisted gas–liquid chromatography have been met—*i.e.*, automatic ranging, base line reduction, data-filtering, and report generation.

Data-gathering is commanded by a single subroutine call to a time-sharing monitor for laboratory automation. The major unusual feature of the method employed is that it is not predicated on guaranteed uniform time intervals. Instead, from a table of the intervals realized in a run, recorded from a clock internal to the computer, the output is converted by interpolation to a table at equal intervals as the first calculation step. Linear interpolation was chosen for reasons of economy and found to be acceptable for a number of experimental records. By this mechanism we avoid possible timing conflicts between experiments, even if some experiments require complete dedication of the computer for 1 or 2 seconds (as we are using for a fast-scan mass-spectrometer). It should be pointed out, however, that the time interval file doubles the memory requirements for a particular chromatographic record.

To determine the validity of the data reduction software, a number of test samples have been run on our 1800 laboratory system. All the examples given in this paper were run using a $5' \times 1/8''$ 20% SE-30 Chromosorb-W column. The chromatogram in Figure 1 shows a plot of the original data obtained from a sample of 30–60 °C petroleum ether run at a column temperature of 125 °C so as to give poor separation. Also given are over-plots of individual fitted peaks. It should be noted that the extraneous noise spike on the major peak is effectively discriminated against by the peak location routine. An example of peaks with considerable tailing was obtained with a sample containing ethanol, *n*-propanol, *n*-butanol, and *n*-hexanol. The original data, with overplots of the fitted peaks, are given, in Figure 4. The last example shown in Figure 5 is from a 1:1 mixture of 30–70 °C/60–90 °C petroleum ether and exhibits both skewing and tailing. The printout from the run is shown in Figure 6. The data presented is divided into three parts, the first of which refers to approximate centers of significant regions or groups of peaks of the record and the areas of these regions. In this instance, three groups of peaks were detected. The second portion relates to the number of peaks found in each group by the preliminary data reduction program. Approximate retention times and areas, calculated by integrating between perpendiculars dropped from the valley points separating overlapped peaks are presented. This was done merely to allow the user to check that the final fitted areas are at least reasonable. The last section gives the retention times and areas of fitted peaks together with the final estimates of A, w, and τ.

As has already been mentioned, least squares calculations of the type we have adopted are not always successful. Although the programs give satisfactory results for most cases of overlap, occasionally irrecoverable divergences occur. Our approach has been to provide in the tabulated output enough information so that the experimenter can clearly recognize a divergence. For instance, the areas and retention times estimated after the least squares data-reduction should agree semi-quantitatively with those printed by the preliminary data-reduction program. Also, peak widths vary roughly linearly with retention times, so that an unusually small or large width reported in the final table may indicate a poor fit. We anticipate that as we accumulate experience with the system, that minor modifications in the order of operation in the least squares fit and in the checks and corrections for divergences will decrease the number of poor fits. In particular, the assumption that the relative asymmetry is uniform within a group of overlapping lines is not entirely adequate. The final areas reported are insensitive to small errors in the curve fitting, because, rather than employing Equation 4 directly, we have adopted the less economical stratagem of numerical integration from the original data points, which are first corrected for contributions of overlapping peaks.

It is pleasant to be able to report that calculation times are quite short even though the IBM 1800 has no floating-point hardware. The preliminary data reduction, which is similar to methods used in many laboratories, takes about 45 seconds. (We do not compute until the run is complete, but save all the data. This permits us to use much of the memory of the machine for data reduction). The peak-fitting takes about 6 to 8 seconds per peak, depending on the amount of overlap. No attempt, such as assembly language coding, has been made to make the programs as efficient as possible, so that a factor of 2 to 3 improvement in computation time might be possible. In addition, digital output plots of the ameliorated data and the fits are relatively time consuming with the plotter programs presently available, but are available on an optional basis.

An important feature of our programs is that most of the data reduction package has been constructed in modular form with general purpose subroutines. Many of the modules are expected to be useful in data reduction for a variety of spectroscopic and analytical instruments. A library of programs for laboratory automation is being assembled in this laboratory, and these programs will be included. We anticipate using many of them in connection with nuclear magnetic resonance and gel permeation chromatography in the near future.

ACKNOWLEDGMENT

It is a pleasure to thank T. Kuga and T. Horikawa for technical assistance, D. Horne for the design and construction of the automatic ranging device, and R. Gritter for critical commentary.

RECEIVED for review November 12, 1968. Accepted March 26, 1969.

Computer Characterization of Chromatographic Peaks by Plate Height and Higher Central Moments

Eli Grushka, Marcus N. Myers, Paul D. Schettler,[1] and J. Calvin Giddings

Department of Chemistry, University of Utah, Salt Lake City, Utah 84112

Computer methods make possible the detailed analysis of chromatographic peak shape, and can be used to obtain the various moments of experimental peaks. The importance of the statistical moments and related properties is discussed here. The moments characterize a peak completely and are related to parameters such as theoretical plate height and forms of asymmetry such as peak tailing. They may also reflect peak contamination. A rapid and accurate method for measuring moments is described. This involves a digitizer coupled with a gas chromatograph. The data obtained are analyzed by a Univac 1108 computer.

THE DETAILED FORM of chromatographic peaks has been the subject of considerable theoretical inquiry, but not of experimental investigation. The latter often ends with a specification of peak location and area, sometimes width, and infrequently with a statement about asymmetry. Too often the Gaussian approximation by itself is assumed to contain all relevant characteristics of the peak. The advent of computerized data reduction systems has so far done little to alter this outlook.

Indeed resolution is ordinarily measured to a very good approximation in terms only of peak location and width. However, the more subtle characteristics of a peak may contain valuable information of a diagnostic type. First of all, the non-Gaussian terms may contain information about strongly overlapping peaks and forms of contamination generally. Second, they may reflect the condition of the column and, if understood, could possess sufficient information to specify improved, perhaps even optimized, conditions. Third, they may be solute-selective and thus offer an adjunct tool for identification. A necessary step toward implementing these approaches is, of course, the development of a methodology for detailing peak characteristics. This is the subject of the present paper.

Several options exist for the mathematical expression of the peak profile. We choose here to characterize a peak by its statistical moments (and related parameters). The importance and theoretical evaluation of these moments in chromatography has been discussed in a number of papers (*1–6*). The choice of moments for experimental characterization hinges on the fact that they completely specify any peak (*7*), and that each one is easily interpreted.

[1] Present address: Department of Chemistry, Juniata College, Huntingdon, Pa. 16652.

(1) J. C. Giddings and H. Eyring, *J. Phys. Chem.*, **59**, 416 (1955).
(2) E. Kucera, *J. Chromatogr.*, **19**, 273 (1965).
(3) H. Vink, *ibid.*, **20**, 305 (1965).
(4) H. Yamazaki, *ibid.*, **27**, 14 (1967).
(5) J. C. Sternberg, "Advances in Chromatography," J. C. Giddings and R. A. Keller, Eds., Marcel Dekker, New York, Vol. 2, 1966, pp 205–270.
(6) O. Gruber, "Advances in Chromatography," J. C. Giddings and R. A. Keller, Eds., Marcel Dekker, New York, Vol. 6, 1968, pp. 173–246.
(7) G. A. Korn and T. M. Korn, "Mathematical Handbook for Scientists and Engineers," McGraw-Hill Book Company, New York, 1968, p 599.

The individual moments characterize a peak in the following fashion. The zeroeth moment of the peak (if the peak is not normalized) is its area. The first moment is the coordinate of the center of gravity of the peak and thus equals the retention time (or migration distance). The second moment, when taken around the center of gravity, is a measure of the peak's width. The third moment (also taken around the first) shows the magnitude as well as the direction of the peak's asymmetry. The fourth moment (again around the first) is a measure of peak flattening as well as peak width. All other odd moments are related to asymmetry while the higher even moments measure characteristics similar to the fourth moment.

The *skew* and *excess* are two moment-related quantities which are useful because they measure directly the deviations from a Gaussian profile. The skew is a measure of peak asymmetry and the excess reflects the flattening of a peak relative to the Gaussian norm.

While many chromatographic peaks approach Gaussian shape to a fair approximation, the precise mathematical form of the peak profiles for a general retention mechanism has never been deduced. Giddings has pointed out that the simplest conceivable retention mechanism (single step sorption-desorption) does not lead to a Gaussian profile, but to a considerably more complicated form containing a Bessel function and an exponential term (*8*, *9*). The plate model itself leads to binomial and Poisson distributions. Only in the limit of infinitely long times do all these mathematical expressions approach a Gaussian form (*8*). The departure from this limit within a single peak reflects the finite rate of various column processes. These rates are a function of column conditions and of the solute itself. In contaminated peaks the non-Gaussian terms reflect, in addition, a distortion due to the contamination.

THEORY

Mathematical Characterization of the Peak. The normalized nth moment of a peak is defined by

$$m_n = \int_{\text{all } t} t^n f(t)dt \Big/ \int_{\text{all } t} f(t)dt \qquad (1)$$

where $f(t)$ is the peak profile and t is the time (or distance) coordinate. For convenience it is better to take all moments higher than the first around the center of gravity of the peak—*i.e.*, around the t coordinate of the first moment

$$m_n = \int_{\text{all } t} (t - m_1)^n f(t)dt \Big/ \int_{\text{all } t} f(t)dt; \quad n > 1 \qquad (2)$$

It was mentioned before that the moments completely define a peak. Consistent with this, the function $f(t)$ can

(8) J. C. Giddings, "Dynamics of Chromatography, Part I: Principles and Theory," Marcel Dekker, Inc., New York, 1965, pp 20–26.
(9) J. C. Giddings in "Gas Chromatography, 1964," A. Goldup, Ed., Elsevier Publishing Company, Amsterdam, 1964.

be expanded in terms of its moments. One such expression is (*10*)

$$f(t) = \frac{1}{\sigma\sqrt{2\pi}} e^{-\frac{t^2}{2\sigma^2}}\left[1 + \sum_{i=3}^{\infty} \frac{c_i}{i!} H_i\left(\frac{t}{\sigma}\right)\right] \quad (3)$$

where t is now the time relative to the first moment, H_i is the ith Hermite Polynomial (*11*), σ^2 is the variance of the peak ($= m_2$) and the c_i's are the expansion coefficients which, as Equation 3 shows, measure directly the departure from Gaussian. These coefficients are:

$$c_3 = \frac{m_3}{m_2^{3/2}}, \quad c_4 = \frac{m_4}{m_2^2} - 3, \quad c_5 = \frac{m_5}{m_2^{5/2}} - 10\frac{m_3}{m_2^{3/2}}$$

etc. (4)

The skew and the excess are defined as c_3 and c_4, respectively; these quantities are thus seen to express the simplest departures from Gaussian. All the odd c's in Equation 4 will vanish for a symmetrical peak and all c's will vanish if the peak is Gaussian.

In theory all the moments of a peak can be measured, but we have found that in practice one is limited to roughly the first 5 moments, m_0 through m_4. By the nature of their definition in Equation 2 the higher moments magnify the importance of those points which are far from the center of gravity of the peak. Thus base line noise and drift will be amplified and will contribute increasingly to the magnitude of the higher moments. In fact the importance of the base line is even evident in some of the first five moments, as will be shown in the results section.

Measurements of the Moments, Skew, and Excess. If the detector output is divided into finite intervals and digitized, the moments become

$$m_n = \frac{\sum_{\text{all } i} t_i^n y_i}{\sum_{\text{all } i} y_i} \quad (5)$$

where y_i is the peak height "count" in the ith interval. Here, again, t_i is relative to m_1 for $n > 1$.

EXPERIMENTAL

Apparatus. Figure 1 shows the experimental system. The gas chromatograph consisted of a constant temperature oven and a Beckman flame ionization detector and electrometer (Model GC-4). The electrometer was connected to an Infotronic CRS-30D Digitizer which in turn operated a high-speed tape perforator (Teletype BRPE 11) and an Esterline Angus SpeedServo Recorder. The latter allowed the visual monitoring of peak shape and elution times. The paper-tape data were converted to card form with an IBM 46 tape-to-card punch for input to a Univac 1108 Computer. Additional information such as perforator start time, peak identification, etc., were added after the conversion of the data to card form.

Peak Generation. Two peak generators were made. The first was a *square wave* (SW) generator which consisted of an Eveready No. 735 NEDA 900 1.5-V battery, a voltage divider, and a microswitch. The circuitry was such that when the switch was in the open position the digitizer input was shorted. A signal of about 10 mV was introduced to the digitizer by closing the microswitch for a certain predetermined time interval.

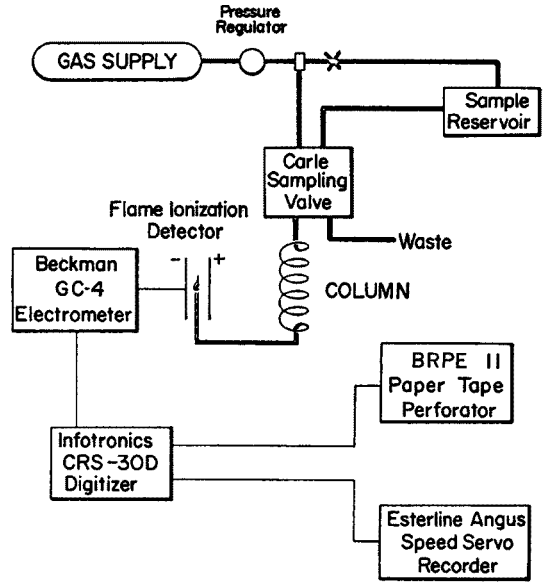

Figure 1. Block diagram of apparatus

The second signal generator employed a *cam system*. The cam was connected to a 1-rpm Hurst motor. An arm, which was attached at its pivot to a Bourns 35105-1-102 1 Kohm variable resistor, followed the cam periphery. This produced a change of about 40 ohms in the resistor. A Hewlett-Packard Model 6215A Power Supply was used as a voltage source. Its output was varied until a signal of desirable magnitude was obtained. The signal shape resembled a chromatographic peak.

Materials Used. The two columns employed were an open stainless steel tube 1520-cm long with inner radius of 0.263 cm, and a 200-cm long copper tube with an inside radius of 0.241 cm, packed with Chromosorb W coated with 5% by weight Apiezon L. Methane and pentane were used as the chromatographic solutes, while helium was employed as the carrier gas.

Procedure. Sample injection was accomplished with a Carle valve (No. 2014) which switched a small amount of sample vapor into the carrier stream. Two timers were automatically started as the injection was made. One was stopped when the tape perforator was started, immediately before the emergence of the peak from the column. The second timer was used to obtain either the retention time (the peak maximum) or perforator stop time. The perforator was stopped manually when the trace on the recorder indicated the signal had reached the base line. Spacing punches were used to separate data from different peaks.

Studies of the effect of the base line setting of the digitizer were carried out by first adjusting the base line to zero according to the manufacter's instructions, then moving the base about 900 counts above and below that true base line.

Computer Program. A computer program was written to calculate and print the peak's area, retention time, skew, excess, and plate height. The latter was calculated by three methods: a) from the second moment, b) from the width at half-height, assuming a Gaussian peak shape, and c) by non-linear least-squares fitting a Gaussian peak (*12*) to the observed peak and using the resultant σ value.

(10) F. Zernike, "Handbuch Der Physik," Vol. III, J. Springer, Berlin, 1928, p 448.

(11) H. Margenau and G. M. Murphy, "The Mathematics of Physics and Chemistry," D. Van Nostrand Company, Princeton, N. J., 2nd ed., 1964, p 121.

(12) D. W. Marquardt, "Least Squares Estimation of Non-Linear Parameters," IBM Share General Program Library, No. 3094, March 1964.

Table I. Generated Peaks Study

	Peak shape	Dig. time (sec)	m_1 (sec)[a]	m_2 (sec)[b]	Area[c] $\times 10^{-4}$	Width (sec) ½ height	Skew	Excess
Averages	Square wave	0.1	...	8.31 ± 0.042	9.103 ± 0.036	9.9	Negligible	1.1993 ± 0.0001
% Error	...	...	...	0.50	0.40	...	...	0.0050
Averages	Square wave	0.1	...	8.44 ±0.052	9.180 ±0.031	10	Negligible	1.1993 ±0.0001
% Error	...	...	...	0.6	0.3	...	...	0.005
Averages	Square wave	0.1	...	8.65 ±0.058	9.299 ±0.030	10.1	Negligible	1.1991 ±0.0001
% Error		...	...	0.7	0.3	...	...	0.005
Averages	Cam generated	1.0	22.05 ± 0.012	64.16 ± 0.015	12.588 ± 0.0006	20.36 ± 0.003	−0.0779 ± 0.0003	−0.537 ± 0.0003
% Error	...	...	0.05	0.023	0.047	0.017	0.39	0.044
Averages	Cam generated	0.1	21.16 ± 0.049	64.199 ± 0.021	12.577 ± 0.0014	21.599 ± 0.027	−0.07820 ± 0.00017	−0.5895 ± 0.0009
% Error	...	...	0.23	0.03	0.11	0.13	0.21	0.15

[a] First moment.
[b] Second moment.
[c] Area in arbitrary units.

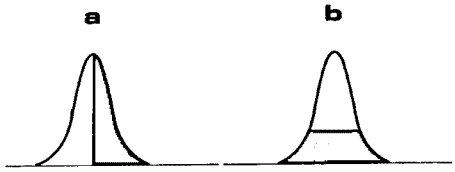

Figure 2. Skew and excess for normal Gaussian peaks and bisected Gaussian peaks

RESULTS AND DISCUSSION

Magnitude of Skew and Excess. Because skew and excess are unfamiliar quantities to many, it is useful for interpreting the following chromatographic data to "bracket" our numerical values through easily visualized cases. We have mentioned that the Gaussian, at one end of the spectrum, has zero skew and excess. If we bisect the Gaussian (Figure 2a), the highly asymmetrical half has a skew of 0.995. By comparison a right angle triangle has the value 0.566.

If we divide the Gaussian into two equal areas by a "horizontal" cut (Figure 2b) the "flattened" lower half is another good reference. Its excess is 1.377. We may also compare with a square profile, which has the negative value of excess, −1.200.

Accuracy and Precision Based on Artificial Peaks. The accuracy of the digitizer system was checked by feeding square wave and cam generated peaks directly to the digitizer. Table I shows the accuracy of the system. Ball, Harris, and Habgood (*13*) discussed the accuracy and sources of error for manual peak-area measurements. They found that the relative error in such measurements varies from about 0.5% up.

(13) D. L. Ball, W. E. Harris, and H. W. Habgood, ANAL. CHEM., **40**, 129 (1968).

Table II. Effect of Base Line Variation for 10 Methane Peaks

Data Accumulated Roughly 3σ on Either Side of the Peak

	Case[e] *A*	Case[e] *B*	Case[e] *C*
Skew	0.0858 ±0.0088	0.2039 ±0.0488	0.3378 +0.0408
Excess	−0.2184 ±0.0419	0.5576 ±0.0958	2.0372 ±0.0416
Plate ht (cm)[a]	0.1923 ±0.0174	0.2182 ±0.0083	0.2987 ±0.0080
Plate ht (cm)[b]	0.1939 ±0.0036	0.2091 ±0.0019	0.2261 ±0.0022
Plate ht (cm)[c]	0.2041 ±0.0082	0.2110 ±0.0099	0.2159 ±0.0064
Plate ht (cm)[d]	0.2122 ±0.0058	0.2117 ±0.0045	0.2131 ±0.0044

[a] Computer—second moment.
[b] Computer—width at half-height.
[c] Computer—least-squares Gaussian.
[d] Manual—using width-at-half-height method.
[e] Cases *A*, *B*, and *C* are described in Figure 3.

Table I shows that the relative errors in peak areas, as determined by the digitizer, are 0.3–0.4% in the square wave case and about 0.1% for the cam generated peaks. It should be noted that the square wave analysis is a rather challenging test for the digitizer due to the sharp rise and drop of the signal. Moreover for peaks of that shape much of the error undoubtedly comes from the lack of exact coincidence between the peaks and the digitizer intervals. It is estimated that the latter effect itself would yield about 0.25% error, leaving perhaps 0.20% error in the operation of the system.

Effect of Digitizer Base Line Position. This and the remaining parts of the paper will deal with the properties of "real" chromatographic peaks. First we examine base line effects.

The digitizer base line, with respect to the true electrometer base line, has been variously positioned as shown in Figure 3. The base line position will affect the measured values of plate height, skew, and excess as follows:

Table III. Comparison of Different Methods for Computing Plate Heights

Retention time (min)	H (cm)[a]	H (cm)[b]	H (cm)[c]	H (cm)[d]	H (cm)[e]
33.69	0.2923	*0.2332	0.2605		
33.99	0.2925	0.2602	0.2601	0.2270	0.2688
33.18	0.3293	0.2679	0.2681	0.2190	0.3034
33.35	0.3250	0.2691	0.2677	0.2170	0.2793
32.73	*0.3702	0.2698	*0.2970	0.2252	0.2482
32.77	0.3266	0.2597	0.2663	0.2245	0.3110
		Average of the six runs ± standard deviation			
33.29	0.3131	0.2653	0.2645	0.2225	0.2822
±0.5	±0.019	±0.0050	±0.0039	±0.0043	±0.0254

* These values were eliminated when averages and standard deviations were computed.

[a] Computer—second moment.
[b] Computer—width at half-height.
[c] Computer—least-squares Gaussian.
[d] Manual—using width-at-half-height method.
[e] Manual—base line intercept method.

Table IV. Computer Results on Plate Height, Skew, and Excess, for Successive Runs of Pentane

t_R (min)	H (cm)[a]	H (cm)[b]	H (cm)[c]	Skew	Excess
48.71	0.3910	0.2535	0.2647	1.3350	4.2771
47.71	0.4218	0.2435	0.2782	1.4649	4.4867
48.70	0.3750	0.2106	0.2456	1.3341	4.2068
48.79	0.3697	0.2321	0.2566	1.4786	4.9769
48.43	0.4013		0.2725	1.5356	4.8853

[a] Computer—second moment.
[b] Computer—width at half-height.
[c] Computer—least-squares Gaussian.

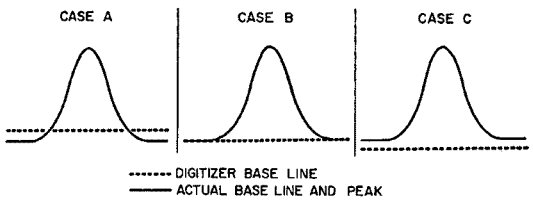

Figure 3. Illustration of base line shift

Plate Height: Case A < Case B < Case C

Skew: No general relationship

Excess: Case A < Case B < Case C

Table II shows experimental results for these cases obtained from running ten methane peaks through the open column. The relative height change was estimated to be 1.5%. In Case C the detector base line, as seen by the digitizer, is a constant background signal which manifests itself as a large value of the excess. In Case A, on the other hand, the digitizer sees only parts of the peak and thus the excess is less than its true value. The relative magnitude of the error caused by these base line shifts is larger in Case C than in Case A because in the former the background signal contributes indefinitely to the error. Thus the base line output of the digitizer must be calibrated to coincide with, or be "placed" very slightly above the true detector base line. This is of major importance since any base line fluctuation or "noises" will contribute greatly to the moments as well as to the skew and excess.

Normal Chromatographic Peaks. Table III shows additional plate height values from runs of methane on the 2-m packed column without the base line shift. In Tables II and III it is seen that the plate height values obtained from the second moment (Method *a*) are larger than all other values. The reason probably relates to the fact that this method receives a more substantial contribution from peak tailing than the other methods. Table III also shows that the plate height values measured manually from the base line intercept method have the least precision, but that generally the manual methods yield a comparable precision. This conclusion probably reflects variations in the peaks themselves. The better precision of the earlier "artificial" peaks confirms this. The lack of peak reproducibility may stem from nonreproducible injection and similar factors which could be improved in a high precision system. Thus we believe that, ultimately, machine methods will yield much better precision and accuracy.

Table IV illustrates the calculation of skew, excess, and plate height values for successive pentane peaks. In this particular experiment the perforator mispunched some of the points in several peaks, thus simulating noise. Nonetheless, all the values, except those for the plate height via the moments, are consistent in their agreement, and illustrate that meaningful values can be achieved by this method.

RECEIVED for review January 31, 1969. Accepted March 17, 1969. This investigation was supported by Public Health Service Research Grant GM 10851-12 from the National Institutes of Health.

Quantitative Interpretation of Semilogarithmic Gas Chromatographic Data

R. L. Wade and S. P. Cram

Department of Chemistry, University of Florida, Gainesville, Fla. 32601

Semilogarithmic chromatograms are shown to be useful in eliminating peak attenuation and for enhancing the display of small peak areas and shoulders. Furthermore, the detector output current is known at all times and is of analytical significance. The logarithmic ordinate is deceptive because the amount of effluent tailing appears to be greater than that displayed on a linear ordinate and the resolution and column efficiency appears to be less. Methods of calculating the resolution, column efficiency, and tailing factors are given by treating a Gaussian elution profile as a parabola in the semilog mode. Peak areas may be calculated from the area of a parabola by use of a floating-base line method or by choosing a fixed, arbitrary base line. The calculations are shown to give improved accuracy and precision over conventional methods. The errors associated with the instrumentation and interpretation of semilogarithmic chromatograms are discussed. Application of the relationships presented allows the analyst to use the semilogarithmic display mode exclusively. The techniques are applicable to all chromatographic methods which approach conditions of linear elution.

LOGARITHMIC AMPLIFIERS offer numerous advantages for the display of gas chromatographic data. They have not been widely used for this purpose because the quantitative interpretation of semilogarithmic chromatograms has not been previously described. A semilogarithmic chromatogram has a much greater dynamic range on a recorder display than a linear presentation and, therefore, does not require range switching or attenuation. This type of display results in a negligible loss of pertinent information when small peaks lie close to large peaks or when peaks elute too rapidly to permit manual attenuation. Furthermore, the detector current is shown at all times, and thus, the true column output before and after the elution of a peak may be measured accurately.

The semilogarithmic chromatogram eliminates the necessity of making successive runs in order to keep all peaks on scale. Sampling errors and the time required for manipulation and interpretation of the gas chromatographic data are significantly reduced. Peaks of low concentration may be better observed by using the semilog display because the most sensitive part of the ordinate display is in the small current region. The sensitivity of the display decreases exponentially up to a full scale display, and in this manner, large concentration peaks are also kept on scale. The minimum detectable signal height with a linear electrometer is nominally 2% of full scale, whereas the minimum detectable signal height with a four-decade logarithmic electrometer, for example, is 0.01% of full scale. Thus, peaks up to ten thousand times smaller in height than the main peaks can be observed.

The design of logarithmic electrometers has been described previously (*1–3*). Problems of excessive drift, calibration, and limited dynamic range have now been eliminated. Instrumentation is commercially available (*4*) which includes a calibrated full-scale display, an internal current standard for calibration of the electrometer, and a drift of less than 0.5% per hour. The analytical significance of displaying chromatographic data in the semilogarithmic mode has been pointed out, and the measurement errors have been discussed (*5*).

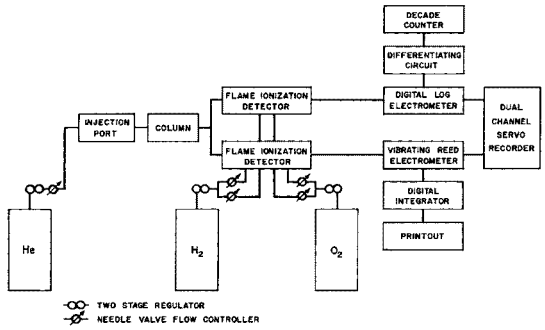

Figure 1. Schematic diagram of the chromatographic system with semilog and linear readout

Several instrument companies include a "log" attenuator display option on their digital integrators. Presently, however, these instruments do not give a true semilogarithmic chromatogram, as the recorder output from the integrator is a hybrid combination of a linear and a log display. Consequently, the "log" display is not calibrated, and quantitative interpretation of the analog display is not possible. This type of display is useful for indicating the relative peak heights and the retention times.

The number of decades to be displayed on the ordinate must represent a compromise between the dynamic range required and the amount of data interpretation desired. If the analyst is interested in measuring the column efficiency, resolution, etc., as well as the peak area, then the display of four decades has been found to be the most applicable solution. If only the retention times are of interest and all samples are to include concentration ranges of the order of 10^6:1, then a larger number of decades may be desirable.

EXPERIMENTAL

The chromatographic system shown in Figure 1 was used to compare the outputs of a vibrating reed electrometer (Model 4010-1, Victoreen Instrument Co.) and a digital log electrometer (Model 4010-2, Victoreen Instrument Co.).

A 20-ft, 1/8-in. column packed with 5% SE-30 (Varian Aerograph) on 80/100 mesh Chromosorb P (AW/DMCS) (Johns-Manville) was used for the separations reported. A 1:1 sample splitter was constructed to give equal flow and

(1) R. A. Dewar and V. E. Maier, *J. Chromatog.*, **15**, 461 (1964).
(2) H. W. Moll, Pittsburgh Conf. on Anal. Chem. and Appl. Spectry., Pittsburgh, Pa., March 1-5, 1965.
(3) R. D. Moeller and A. W. Hartz, Pittsburgh Conf. on Anal. Chem. and Appl. Spectry., Pittsburgh, Pa., Feb. 21-25, 1966.
(4) Victoreen Instrument Co., Cleveland, Ohio, Bulletin GC4000, 1965, p 8.
(5) S. P. Cram, Pittsburgh Conf. on Anal. Chem. and Appl. Spectry., Cleveland, Ohio, March 3-8, 1968.

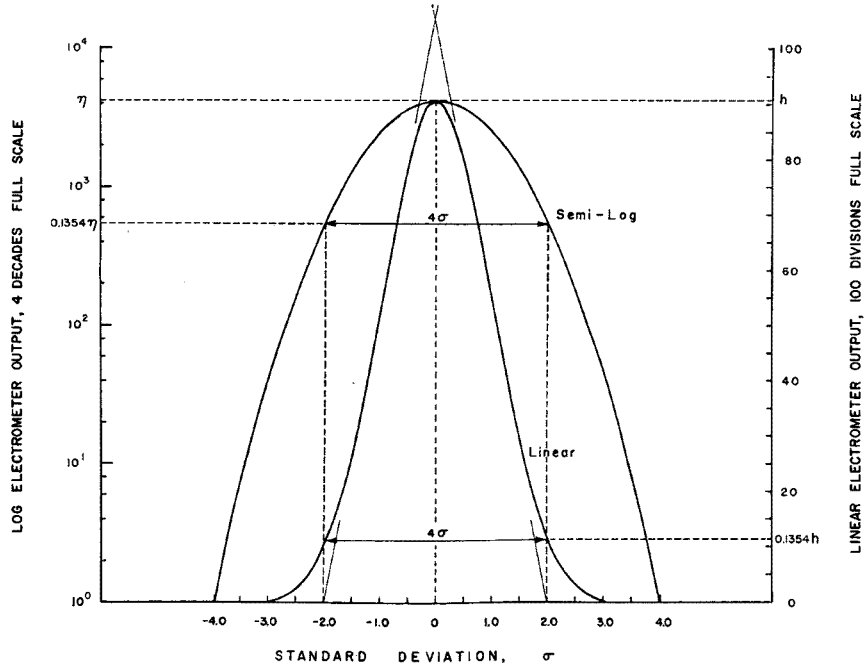

Figure 2. Comparison of linear and semilog Gaussian peaks normalized to the same peak height

equal dead volume to each flame detector. The hydrogen and oxygen flow rates were 70 ml/min and 200 ml/min, respectively, and these flow rates were matched as closely as possible for each flame of the dual-flame detector. The carrier gas flow rate was nominally 50 ml/min.

A +340 V polarizing voltage was applied to the flame detector (Model 4016-1, Victoreen Instrument Co.) from the digital log electrometer power supply. A positive input is required for the digital log electrometer, and thus the polarizing voltage on the second flame was −340 V. The digital log electrometer output was integrated by a six decade preset count scaler (Model 27104, Nuclear Chicago Corp.), and a digital integrator (Model 480 Varian Aerograph) was used to integrate the linear display. A dual-channel recorder (Model 7100B, Hewlett-Packard) was run in series with the electrometers for the analog display.

RESULTS AND DISCUSSION

The model generally accepted for ideal chromatographic behavior is that of a Gaussian distribution of eluent with respect to time. The solution to Fick's second law for longitudinal diffusion may be given by Equation 1

$$\frac{n}{m} = \frac{1}{2(\pi Dt)^{1/2}} \exp \frac{-l^2}{4Dt} \qquad (1)$$

where n is the number of molecules/cm³, m is the total quantity of diffusing material, D is the diffusion coefficient, and l is the diffusion distance down the column at time t. This equation is a form of the normal error curve. However, when a logarithmic electrometer is employed, the electrometer output of this function will be described by the logarithm of Equation 1

$$\log \frac{n}{m} = \log \frac{1}{2(\pi Dt)^{1/2}} - \frac{l^2}{9.2Dt} \qquad (2)$$

where Equation 2 is of the form $y = a + bx^2$ which is a quadratic equation whose trace is parabolic. Thus, chromatographic peaks will appear as parabolas rather than as the nominal Gaussian distribution. Because there is no zero line with a semilog display, the problem of where to measure the peak widths arises for the calculation of the number of theoretical plates, the resolution, and the tailing factor. Furthermore, methods of integration such as planimetry, cutting and weighing, and triangulation are no longer valid.

Peak Width Measurement. A Gaussian distribution is shown on both a linear and logarithmic ordinate in Figure 2. The peaks have been normalized to the same peak height for purposes of illustration. The method of extrapolating tangents through the inflection point corresponds to a 4σ peak width at the base line where σ represents the standard deviation from the mean or the peak quarter-width. This 4σ peak width also can be determined by measuring the width of a Gaussian peak at 13.54% of the peak height, h. The same peak width, ω, on the semilog trace will be found at 13.54% of the peak height, η, under conditions of ideal, linear-elution chromatography. Peak widths measured in this manner, therefore, should be identical with those measured with base line tangents on a linear display. A comparison of the results obtained for a mixture of n-pentane, 2-methylpentane, and n-hexane is given in Table I. The peaks were compared from chromatograms run simultaneously in the linear and semilog modes and at a chart recorder speed of 0.2 inch per second.

The differences in the measured values of the peak widths are less than the experimental error of measuring peak widths by extrapolating tangents to the base line. Therefore, the semilog chromatogram may be interpreted with at least the same precision and accuracy in the peak width as by conventional method, and fewer steps are required in the measurement.

Table I. Comparison of Measured Peak Widths

Sample No.	Peak width, mm *n*-Pentane log	*n*-Pentane Linear	*n*-Pentane Relative error	2-Methyl-pentane Log	2-Methyl-pentane Linear	2-Methyl-pentane Relative error	*n*-Hexane Log	*n*-Hexane Linear	*n*-Hexane Relative error
1	61.0	60.0	1.7%	71.0	71.0	0.0%	75.5	78.0	3.2%
2	62.2	61.8	0.6%	73.0	73.0	0.0%	76.0	75.5	0.7%

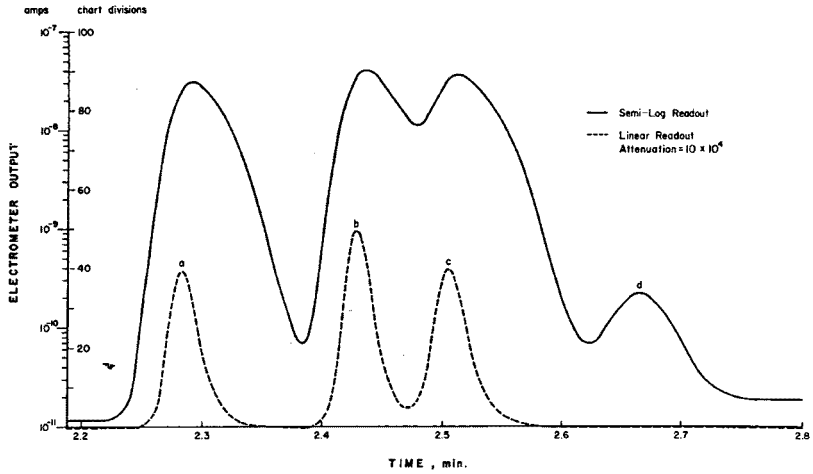

Figure 3. Comparison of resolution from linear and semilog electrometers

Sample size 0.24 μl, Column temp, 150 °C
Sample (*a*) *n*-pentane, (*b*) 2-methylpentane, (*c*) *n*-hexane, (*d*) hexane isomer
Chart speed 0.5 in./min

If the 0.1354η base line for the peak falls near or below a valley between peaks, the measured peak width will be too large because of the increased sensitivity of the semilogarithmic display in the region of peak overlap. This situation may arise for peaks which are shoulders on larger peaks, peaks eluting on the tail of a solvent peak, or incompletely resolved peaks. This is illustrated by the second peak in Figure 3. Inaccurate or infrequent calibration of the full-scale display will give incorrect peak heights, and, subsequently, the base line width will likewise be in error.

The column efficiency and resolution of the separation for a semilogarithmic chromatogram may be characterized by Equations 4 and 5,

$$N = 16\left(\frac{t_R}{\omega}\right)^2 \tag{4}$$

$$R = \frac{2\Delta t_R}{\omega_1 + \omega_2} \tag{5}$$

and the results should agree with the values of N and R measured from chromatograms displayed on linear ordinates.

Peak asymmetry will be more readily apparent with the semilog display because of the change in sensitivity along the y-axis. At the same time, the resolution and column efficiency will appear to be markedly less on the semilog plot. This is shown in Figure 3 where a three-component mixture was run with the linear display. The hexane isomer, peak *d*, appears only on the log display. The two chromatograms were obtained simultaneously, and because R and N are functions of the column rather than the mode of display, these functions must be identical. It should be noted that base line resolution is obtained between peaks *a* and *b* as noted on the linear display, whereas the semilog display indicates the true current at all times between the peaks. Furthermore, the resolution between peaks *b* and *c* is 1.7 even though this is not readily apparent from the semilog chromatogram. The asymmetry of peak *a* results from the slight tailing of the peak and is clearly shown on the semilog display.

The tailing factor (6) for the C_7 peak in Figure 4 is 70%, although it is not readily apparent from the linear trace. The benzaldehyde peak, however, would be expected to tail on a nonpolar column. The tailing factor of 15% for this peak may be calculated by using either mode of display. Although the tailing appears to be greater on a semilog display, it is not; the semilogarithmic chromatogram, however, is advantageous for characterizing small peaks in the tailing region.

Peak Area Measurement. The most accurate and desirable method of measuring peak areas of semilogarithmic chromatograms is by digital integration. However, if voltage-to-frequency converters and data storage systems are not available, the peak area may be readily calculated from the formula for the area of a parabola

$$A = \frac{2}{3}\eta\omega \tag{6}$$

by either of two methods.

(6) H. M. McNair and E. J. Bonelli, "Basic Gas Chromatography," 1st Ed., Varian Aerograph, Walnut Creek, Calif., 1967, p 52.

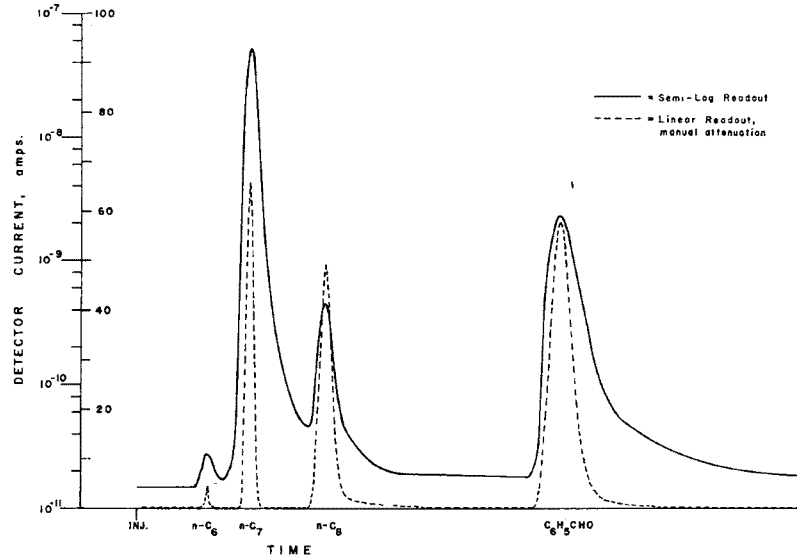

Figure 4. Apparent increased tailing for polar compounds displayed in semilog readout mode
Column: 5-ft, 1/8-in. stainless steel with 5% SE-30 on 60/80 mesh (AW/DMCS) Chromosorb W

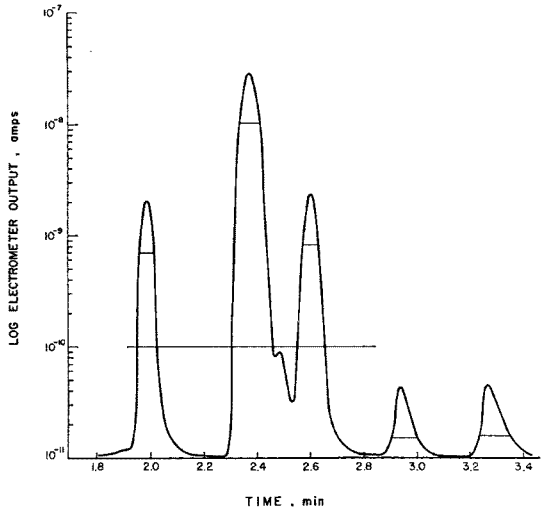

Figure 5. Arbitrary and floating base line methods of calculating peak areas for semilogarithmic chromatograms

Sample: C_5 and C_6 saturated hydrocarbons

Table II. Comparison of Relative Area Measurements for Semilogarithmic Gas Chromatographic Peaks

Peak No.	Digital output	Base line at 35% of peak max	Base line at 10^{-10} A
1	2.89%	4.2%	3.5%
2	92.46	90.2	91.4
3	0.15	...	...
4	4.14	5.2	5.2
5	0.16	0.17	...
6	0.20	0.22	...
Total	100.00%	99.99%	100.0%

If the relative peak areas of each component are to be measured for a sample which has a wide range of concentrations, then the peak width must be measured at the same per cent of maximum peak height for all peaks. The base width lines for peaks 1, 2, 4, 5, and 6 in Figure 5 were drawn at 35% of the peak maximum in each case. This is an arbitrary number dictated by the height of the smallest peak in the mixture and by the resolution between peaks. The base width line must not be below a point on the curve where the peaks no longer follow the form of a parabola—*i.e.*, in the tailing and overlapping regions of the curve. This base width line then may be used to calculate the area of each peak from Equation 6. In no case should the linear distance from the base width line to the peak maximum be used as the parabola height.

If the sample follows a pure Gaussian distribution on the column, exhibits no tailing, and has good resolution, the relative accuracy of measuring the peak area increases as the width is taken at smaller fractions of the peak height. If peak profiles such as those in Figure 5 are obtained, one arbitrary base line can be drawn for all peaks as long as it is significantly below the maximum of the smallest peak of interest. This method will give an accuracy of 1–2% which is as good as the height and width measurements themselves. Table II compares the results obtained by using a base width at 35% of each peak height and by using an arbitrary base line set at 10^{-10} A with the integrated digital data obtained. By setting the base line at 10^{-10} A, all peaks below this line are disregarded, and this is seen to represent an insignificant error in the analysis of the major components. If the base line had been set arbitrarily at 10^{-9} A, the peak area measurements likewise would have concerned only the 3 major components. In practice, small peaks such as peaks 3, 5, and 6 are often attenuated off-scale and consequently missed in manual calculation methods. Another justification for disregarding all peaks below 10^{-10} A is the elimination of the problems of drawing parabolic tangents to the leading edge of peak 3 in

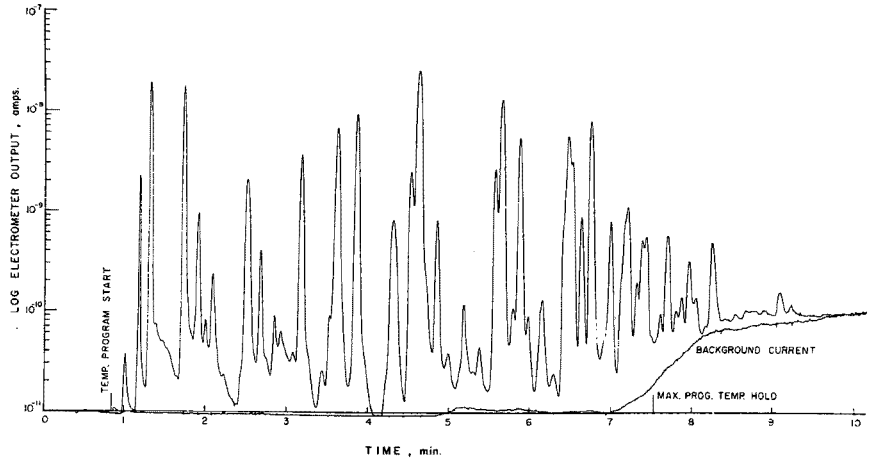

Figure 6. Application of semilogarithmic gas chromatography to rapid, multicomponent analyses

Sample: 0.50 μl. American Oil Co., ethyl grade gasoline
Column temperature programmed from 50° to 250° at 20 °C/min

order to be able to estimate its area. The largest error in the peak area calculations for the semilog display in Table II arises from the nonlogarithmic response of the 10^{-8}–10^{-7} A decade. This introduces an appreciable error in the major component peaks by compressing the last decade and directly affects the accuracy of the relative peak areas. This electrometer error was found only in the last decade in the log diode pump and, therefore, does not affect the digital output.

Fewer steps and less "eyeball accuracy" are required for the parabola measurements than in triangulation. The number of significant figures in the measurement of the peak height is determined by the location of the peak maxima in the decade. In the lower part of a decade, three significant figures may be reported, and for the chromatographer doing routine analyses with an accuracy of ±1–2%, this method of quantitation should suffice.

Several integration methods are compared in Table III for mixtures similar in concentration to the chromatogram shown in Figure 3. The parabola area measurements show good agreement with the digital data and are consistently accurate.

The peak area measurements using the 10^{-10} A base line will generally reflect any non-Gaussian behavior on the column and therefore give broader peaks, depending on the amplitude of a given peak. However, the peak widths measured at the same fraction—*e.g.*, 35%—of the peak maximum for all peaks will reflect the same amount of non-Gaussian behavior for all of the peaks measured.

The triangulation and peak height ratio data clearly indicate larger errors than those obtained from the semilog display. The difference between the values obtained with the decade scaler and the linear integrator is due to the fact that the flame detectors used could not be perfectly matched and therefore had different sensitivities. A small amount of fractionation in the splitter, and the estimation of the count rate minimum on the decade scaler between peaks also contributes to the difference obtained. Current calibration experiments show that the 10^{-8}–10^{-7} decade was compressed, and because peak 2 falls in this region, an additional error was incorporated in the height, width, and the area measurement of this peak. The necessity of accurate calibration of all decades is emphasized for quantitative work.

The application of the digital log electrometer is illustrated by a single run taken on a gasoline sample in Figure 6. This chromatogram is shown to illustrate the fact that all peaks are kept on scale without manual attenuation, the small peak areas are increased in size and allow area calculation, the total number of peaks in complex samples may be determined, the flame detector ion current is known at all times during the separation, and that the resolution is excellent although not immediately obvious. The latter point is a distinct advantage in locating shoulders on larger peaks.

Work is presently in progress to explore the analytical potential of using a log–log display of chromatographic data. Log–log chromatograms offer the advantages of convenient storage of chromatograms on standard 16 ½ × 11 in. paper by using an *X–Y* plotter for the readout. Peaks which normally elute very rapidly in the early part of the chromatogram are more spread out on the abscissa than on a linear

Table III. Comparison of Integration Methods

Method	*n*-Pentane		2-Methyl-pentane		*n*-Hexane	
	Av %	Rel σ	Av %	Rel σ	Av %	Rel σ
Decade counter	27.9	0.13	36.3	0.10	35.8	0.10
Parabola area, 10^{-9} A base	27.9	0.26	36.2	0.50	36.0	0.33
Parabola area, 10^{-10} A base	28.1	0.04	25.7	0.0	36.2	0.00
Integrator	28.9	0.56	36.9	0.29	34.2	0.31
Triangulation	27.9	1.04	37.8	2.19	34.3	2.19
Peak-height ratio	34.3	0.44	35.3	0.22	30.3	0.26
Peak-height × retention time	32.7	0.38	35.7	0.19	31.6	0.24

display, very broad peaks with long retention times are compressed in width, and the distance between late peaks is decreased markedly. Any number of decades may be used on the abscissa and the retention time per decade may be calibrated in any units of time so that very long or very short chromatograms all have the same standard format of display.

RECEIVED for review January 23, 1969. Accepted April 7, 1969. Research supported by the Petroleum Research Fund of the American Chemical Society Grant 1200-G3, The U. S. Department of the Interior as authorized under the Water Resources Research Act of 1964, Public Law 88-379, and the Graduate School of the University of Florida.

Cyanolysis and Spectrophotometric Estimation of Trithionate in Mixture with Thiosulfate and Tetrathionate

D. P. Kelly, L. A. Chambers, and P. A. Trudinger

Baas Becking Geobiological Lab., Bureau of Mineral Resources, P.O. Box 378, Canberra City, A.C.T. 2601, Australia

A sensitive method for estimating trithionate is described, which gives a quantitative assay of trithionate in the presence of thiosulfate and tetrathionate. The conditions affecting cyanolysis of the three sulfur compounds were examined, including a brief examination of the catalysis of thiosulfate cyanolysis by cupric ions. The method could be extended to estimate trithionate in mixture with higher polythionates.

IN RECENT YEARS there has been a growing interest in the chemistry and biology of thiosulfate and the polythionic acids (*1–3*), and sensitive methods for the estimation of these compounds in mixtures have become increasingly desirable. Methods have been described for the titrimetric analysis of mixtures of thiosulfate, trithionate, and higher polythionates (*4–6*). We have found these methods to be relatively insensitive for the analysis of the small amounts of these materials frequently encountered in experiments on bacterial sulfur compound oxidation (*7–9*), and that values obtained for trithionate in mixtures were not always reliable. Sensitive colorimetric methods for estimating thiosulfate and tetra-, penta- and hexathionates have been described (*10–16*), but no similar consideration appears to have been given to the colorimetric determination of trithionate. We have devised a sensitive method for estimating trithionate in mixtures, based on the procedures of Koh *et al.* (*10–13*) and Sörbo (*16*). The method depends on the alkaline cyanolysis of thionates to yield thiocyanate which can be estimated colorimetrically. Tetrathionate, thiosulfate, and trithionate react with cyanide according to Equations 1, 2, and 3.

$$S_4O_6^{2-} + 3CN^- + H_2O = S_2O_3^{2-} + SO_4^{2-} + 2HCN + SCN^- \quad (1)$$

$$S_2O_3^{2-} + CN^- \xrightarrow[\text{catalyst}]{Cu^{2+}} SO_3^{2-} + SCN^- \quad (2)$$

$$S_3O_6^{2-} + 3CN^- + H_2O = SO_3^{2-} + SO_4^{2-} + 2HCN + SCN^- \quad (3)$$

The present method depends on the fact that Reaction 1 occurs spontaneously at low temperatures, Reaction 2 occurs at low temperature in the presence of cupric ions, while Reaction 3 takes place only at high temperatures. The factors affecting the reaction of thiosulfate, trithionate, and tetrathionate under our assay conditions are described.

EXPERIMENTAL

Assay procedure for a mixture of thiosulfate, trithionate, and tetrathionate. Three replicate reaction mixtures were prepared in 25-ml volumetric flasks. The sample to be analyzed (containing up to 8 μmoles total thionate) was added to 4 ml of NaH_2PO_4–NaOH buffer (*10*), pH 7.4, and water added to give a total volume of 10 ml. The replicates were separately treated as follows.

I. The mixture was cooled to 5 °C; 5 ml of 0.1*M* KCN was added and mixed rapidly, thereby giving 0.033*M* cyanide and raising the pH to pH 9.65. The mixture was maintained at 5 °C for 20 min.

II. A replicate mixture was cooled to 5 °C and 5 ml of 0.1*M* KCN added. After maintaining at 5 °C for 10 min 1.5 ml of 0.1*M* $CuSO_4$ was added with rapid mixing, thereby lowering the pH to pH 7.35 and giving a concentration of 0.0091*M* Cu^{2+}. The mixture was maintained at 5 °C for 10–15 min.

III. A third replicate was mixed with 5 ml of 0.1*M* KCN and heated in a boiling water bath for 45 min, then cooled to 5 °C and 1.5 ml of 0.1*M* $CuSO_4$ rapidly mixed. The mixture was maintained at 5 °C for 10–15 min.

Finally, 3 ml of 1.5*M* ferric nitrate in 4*N* $HClO_4$ was added to each replicate with continuous agitation; the flask contents were warmed to room temperature with constant shaking to redissolve any precipitate, then made up to 25 ml with distilled water. The ferric thiocyanate color which developed was read at once at 460 mμ in 10-mm round cuvettes in a Coleman Junior spectrophotometer. Samples and thiocyanate standards were read against a sulfur-free reagent blank prepared as in treatment I. Thiocyanate standards were prepared in the same mixture and gave optical density readings deviating only

(1) M. Goehring, *Fortschr. Chem. Forsch.*, **Bd2,** 444 (1952).
(2) N. Kharasch, Ed., "Organic Sulphur Compounds," Vol. 1, Pergamon Press, 1961, Chapters 2 and 9.
(3) P. A. Trudinger, *Rev. Pure Appl. Chem.*, **17,** 1 (1967).
(4) R. R. Jay, ANAL. CHEM., **25,** 288 (1953).
(5) A. Kurtenacker, in "Handbuch der Anorganischen Chemie," R. Abegg, F. Auerbach, and I. Koppel, Eds., Vol. 4, part 1, 1st half, S. Hirzel, Leipzig, 1927.
(6) R. L. Starkey, *J. Gen. Physiol.*, **18,** 325 (1935).
(7) D. P. Kelly and P. J. Syrett, *Biochem. J.*, **98,** 537 (1966).
(8) D. P. Kelly, *Aust. J. Sci.*, **31,** 165 (1968).
(9) P. A. Trudinger, *Aust. J. Biol. Sci.*, **17,** 459, 738 (1964).
(10) T. Koh, *Bull. Chem. Soc. Japan*, **38,** 1510 (1965).
(11) T. Koh and I. Iwasaki, *ibid.*, **38,** 2135 (1965).
(12) T. Koh and I. Iwasaki, *ibid.*, **39,** 352 (1966).
(13) T. Koh and I. Iwasaki, *ibid.*, p 703.
(14) O. A. Nietzel and M. A. De Sesa, ANAL. CHEM., **27,** 1839 (1955).
(15) N. H. Schöön, *Acta. Chem. Scand.*, **13,** 525 (1959).
(16) B. Sörbo, *Biochim. Biophys. Acta*, **23,** 412 (1957).

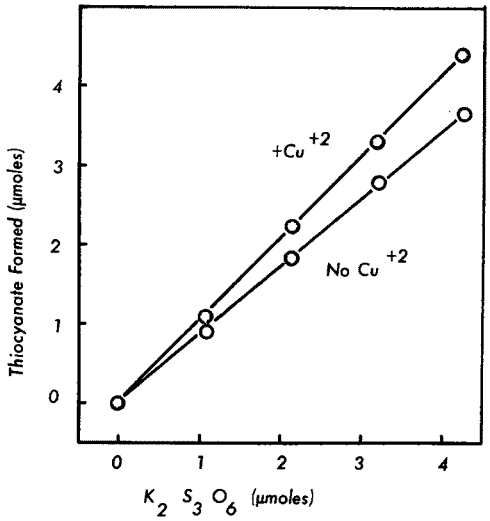

Figure 1. Effect of adding Cu^{2+} to trithionate mixtures after treatment III

○—○, no Cu^{2+} added; ●—● Cu^{2+} added as in treatment III

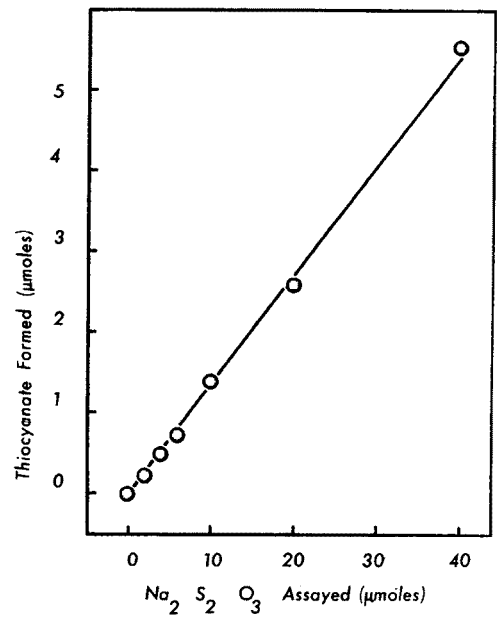

Figure 2. Hot cyanolysis of thiosulfate

The indicated amounts of thiosulfate were heated for 45 min at 100 °C as in treatment III, but thiocyanate formation *without* Cu^{2+} was estimated

slightly from Beer's law; 3.2 and 6.8 μmoles of thiocyanate gave absorbance values of 0.5 and 1.0, respectively. The same optical density readings were obtained if blanks or standards were treated as in treatment II or III. The color developed with the ferric nitrate–$HClO_4$ reagent was stable for at least 45 min, so no stabilizing agents were required. The intensity of the color developed was unaffected by the phosphate or by the cupric ions. Temperatures between 2°–10 °C were suitable for treatments I and II.

The three sulfur compounds thus gave the following equivalents of thiocyanate in the three procedures (see Equations 1–3):

I $S_4O_6^{2-} \equiv 1\ SCN^-$

II $S_4O_6^{2-} \equiv 2\ SCN^-$; $S_2O_3^{2-} \equiv 1\ SCN^-$

III $S_4O_6^{2-} \equiv 2\ SCN^-$; $S_2O_3^{2-} \equiv 1\ SCN^-$; $S_3O_6^{2-} \equiv 1\ SCN^-$

Two equivalents of thiocyanate were formed from tetrathionate in treatments II and III by copper-catalyzed cyanolysis of thiosulfate formed by its initial cyanolysis.

The trithionate content (μmoles) of a mixture was given directly as the difference in thiocyanate (μmoles) formed by procedures III and II. Tetrathionate was given directly by procedure I, and thiosulfate by subtracting twice the value for I from the value for II.

Titrimetric analysis of thionates. Classical procedures were used to estimate the purity of standard sulfur compounds. (i) Thiosulfate was estimated by titration in 5% acetic acid with standard iodine and by iodometric titration with standard iodate; (ii) thiosulfate and polythionates were estimated separately and in mixture by titration in 6*N* HCl with iodate (*17*); (iii) tetrathionate was determined by cyanide and sulfite degradation as described by Foss (*18*).

In addition to method (ii), the following methods were also used to estimate the purity of standard trithionate: (iv) acid production after treatment with mercuric chloride (*6*) was determined by titrating to a standard pH 5.0 with 0.1*N* KOH; (v) approximately 0.01*M* $K_2S_3O_6$ was heated with 0.2*M* $CuSO_4$ at 70 °C for 15 hr and the CuS formed was weighed as described by Riesenfeld, Josephy, and Grünthal (*5*); and (vi) approximately 0.005*M* trithionate was hydrolyzed with 1.25*N* KOH in a boiling water bath for 30 min before cooling and titrating thiosulfate with standard iodine after adding formaldehyde and excess acetic acid (*5*, *6*). Using these methods, the composition of mixtures could be determined, for example, as described by Kurtenacker (*5*) and Starkey (*6*).

Reagents. AnalaR $Na_2S_2O_3 \cdot 5H_2O$ was used without further purification; $K_2S_4O_6$ was prepared as described by Trudinger (*19*); and $K_2S_3O_6$ by the method of Stamm and Goehring (*20*). NaH_2PO_4–NaOH buffer, pH 7.4, was a mixture of 0.2*N* NaOH and 0.2*M* NaH_2PO_4 (*10*).

RESULTS AND DISCUSSION

Standard assay procedure. Table I shows the results of analyzing known mixtures, and demonstrates good recoveries of small amounts of added trithionate.

The method was extremely reproducible. Variation among replicates was generally insignificant and the deviation around the mean recovery for the three compounds separately or in mixtures never exceeded ±0.3%.

Reactivity of trithionate with cyanide. Under the standard assay conditions, trithionate produced no detectable thiocyanate at 5 °C, either in the presence or absence of cupric ions. Its presence does not, therefore, interfere with the estimation of thiosulfate or tetrathionate. At 40 °C, however, about 23% of added trithionate was converted to thiocyanate in 30 min. Using the conditions employed by Koh and Iwasaki (*13*), some 5.1% of the added trithionate underwent cyanolysis

(17) A. I. Vogel, "Quantitative Inorganic Analysis," 2nd ed., Longmans, London, 1951, p 358.
(18) O. Foss, *Det Kgl. Norske Vidensk. Selskabs Skr.*, **1945**, Nr. 2, Bruns, Trondheim, 1947.
(19) P. A. Trudinger, *Biochem. J.*, **78**, 680 (1961).
(20) H. Stamm and M. Goehring, *Z. Anorg. Allg. Chem.*, **250**, 226 (1942).

Table I. Colorimetric Analysis of Mixtures of Tetrathionate, Thiosulfate, and Trithionate

The mixtures used contained the following amounts of tetrathionate, thiosulfate, and trithionate (μmoles), respectively: *Expt. 1 and 4*, 1, 1, and 1; *Expt. 2*, 0.4, 1.6, and 0.4; *Expt. 3*, 0.8, 3.2, and 0.8.

		Thiocyanate formed (μmoles)			Recoveries (μmoles)		
		Treatment I	Treatment II	Treatment III	I $S_4O_6^{-2}$	II $S_2O_3^{-2}$	III $S_3O_6^{-2}$
Expt. 1	Found	1.08	2.96	4.00	1.08	0.80	1.04
	Expected	1.00	3.00	4.00	1.00	1.00	1.00
Expt. 2	Found	0.48	2.43	2.82	0.48	1.47	0.39
	Expected	0.40	2.40	2.80	0.40	1.60	0.40
Expt. 3	Found	0.98	4.80	5.66	0.98	2.84	0.86
	Expected	0.80	4.80	5.60	0.80	3.20	0.80
Expt. 4	Found	1.14	3.10	4.09	1.14	0.82	0.99
	Expected	1.00	3.00	4.00	1.00	1.00	1.00

(Table II). Trithionate would thus cause positive interference in the assay of thiosulfate or higher polythionates by Koh's procedure or in assays employing elevated temperatures.

Trithionate underwent cyanolysis at a decreasing rate on heating at 100 °C as in treatment III (Table III) and less than 100% of the expected thiocyanate was obtained in 45 min. The low recovery was attributed to possible hydrolysis of some of the trithionate to thiosulfate. This possibility was tested by heating trithionite with cyanide, cooling, and assaying thiocyanate with and without the prior addition of cupric ions (Table IV). Cu^{2+} catalyzed the cyanolysis of any thiosulfate formed from the trithionate and the results show that thiocyanate formation was complete provided that copper ions were added. In the *absence* of cyanide, trithionate heated at 100 °C for 45 min in KOH at the assay pH 9.6 was hydrolyzed by about 55% to thiosulfate (Table IV).

Heating at 100 °C at pH 9.6 with cyanide thus produced both thiocyanate and thiosulfate from trithionate, but the ratio of products was independent of the trithionate concentration (Figure 1) and some 87% of the trithionate was converted to thiocyanate.

Cyanolysis of tetrathionate and thiosulfate in the standard assay. Tetrathionate reacted completely and essentially instantaneously at 5 °C to give two or one moles of thiocyanate per mole of tetrathionate in the presence and absence of cupric ions, respectively. Thiocyanate recovery was unaffected by heating at 100 °C for 45 min.

Thiosulfate (1–6 μmoles) gave no detectable thiocyanate with cyanide at 5 °C unless cupric ions were added [Sörbo (*16*)]. On heating at 100 °C, thiosulfate was slowly cyanolyzed (Table V). The proportion of thiosulfate converted to thiocyanate in 45 min was only slightly increased by increasing the thiosulfate concentration, and about 12–13% of the added thiosulfate was cyanolyzed (Figure 2).

Effect of cupric ions on the cyanolysis of thiosulfate. As previously shown (*13*, *16*), complete cyanolysis of thiosulfate depended on the ratio of cyanide to cupric ions used. This relationship for our assay conditions is shown in Figure 3. As the cyanolysis of trithionate required a relatively high cyanide concentration, routinely KCN and $CuSO_4$ to give final concentrations (in 15 ml and 16.5 ml, respectively) of 0.033*M* and 0.0091*M*, respectively, were used. It is noteworthy that the proportion of thiosulfate cyanolyzed by a limiting amount of copper was independent of the amount of thiosulfate used when the cyanide concentration was constant (Table VIa). The reaction with cupric ions to produce thiocyanate was virtually instantaneous and no progressive thiocyanate formation occurred in the presence of a limiting amount of copper (Table VIb). Presumably the cyanolytic process is complex and depends on reaction of the copper with a preformed thiosulfate–cyanide complex. The recovery of thiocyanate was unaffected by heating thiosulfate with cyanide at 100 °C for 45 min prior to cooling to 5 °C and adding cupric ions as in treatment III.

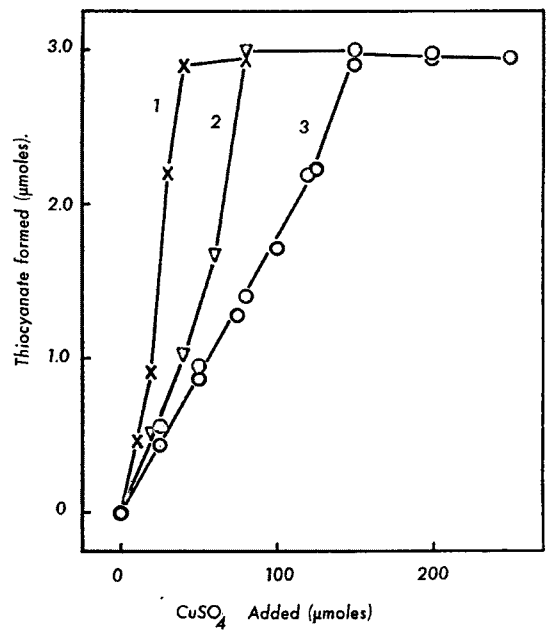

Figure 3. Effect of cupric ions on the cyanolysis of thiosulfate (3 μmoles) at three concentrations of cyanide, basically by treatment II

Curve 1. 0.00667*M* KCN before Cu^{2+} added
Curve 2. 0.01667*M* KCN before Cu^{2+} added
Curve 3. 0.033*M* KCN (standard assay concentration) before Cu^{2+}, O and ○ denote results of two experiments

Application of the method to the analysis of complex mixtures. Clearly this procedure gives accurate estimates of trithionate in mixtures also containing thiosulfate and tetrathionate. It has also been routinely used to estimate trithionate in bacterial culture media during the growth of *Thiobacillus*. The method was unaffected by any compounds present in the small quantities of media (0.1–0.4 ml) used for the analysis. It should be possible to use this procedure to estimate trithionate in mixture with polythionates higher than tetra-

Table II. Partial Cyanolysis of Trithionate at 40 °C

Procedure A of Koh and Iwasaki (*13*) was used, using 2.5 ml of 0.1*M* KCN instead of the 5 ml used in our procedure

$K_2S_3O_6$ added (μmoles)	KSCN formed (μmoles)	Amount of $K_2S_3O_6$ converted (%)
2	0.10	5.0
3	0.14	4.7
4	0.20	5.0
5	0.26	5.2
6	0.34	5.7
	Average	5.1

Table III. Time Course of Trithionate Cyanolysis at 100 °C

$K_2S_3O_6$ (3.1 μmoles) was heated as in Treatment III for the indicated time before estimating thiocyanate without adding copper ions

Period of heating (min)	KSCN formed (μmoles)	% of theoretical 3.1 μmoles KSCN
0	0.05	1.6
5	1.28	41.3
15	2.32	74.8
30	2.63	84.8
45	2.75	88.7

Table IV. Thiosulfate Formation during Trithionate Cyanolysis[a]

Treatment	KSCN formed (μmoles)	% of initial $K_2S_3O_6$ recovered as KSCN
KCN only	2.77	86.6
KCN, then Cu^{2+}	3.30	103.1
KOH, then KCN and Cu^{2+}	1.75	54.7

[a] Replicate samples of $K_2S_3O_6$ (3.2 μmoles) were heated with KCN as for treatment III and parallel triplicate samples assayed for thiocyanate with and without prior treatment with Cu^{2+} at 5 °C. Further samples were heated at 100 °C for 45 min with 0.0064*N* KOH, pH 9.6, without cyanide, cooled to 5 °, then KCN and $CuSO_4$ added as in treatment II. Mean values for triplicates agreeing within ±0.015 μmoles KSCN are given.

thionate as the higher polythionates would also be completely cyanolyzed by treatments I and II in the Experimental Section. The method could find application in the analysis of polythionate-containing mixtures, such as biological fluids in medicine; in the evaluation of inorganic sulfur compounds in soils; and possibly in the analysis of sewage and gas works effluent liquors. It has the advantages over existing methods of great simplicity, a much greater sensitivity than volumetric methods, and an unequivocal discrimination between trithionate and other polythionates or thiosulfate. Our procedure can also be used to estimate the amounts of thiosulfate and tetrathionate in unknown mixtures (Table I), but it was noted that recoveries of tetrathionate in known mixtures tended to be high and recoveries of thiosulfate to be correspondingly low. This discrepancy was found only when mixtures were analyzed, the recoveries using individual compounds were always close to the theoretical values. An erroneous high recovery for tetrathionate could occur if thiosulfate and tetrathionate reacted to yield trithionate and significant amounts of pentathionate (*5*) as shown in Equation 4:—

$$2\,S_2O_3^{2-} + S_4O_6^{2-} \rightleftharpoons S_5O_6^{2-} + S_3O_6^{2-} \qquad (4)$$

Table V. Time Course of Hot Cyanolysis of Thiosulfate

$Na_2S_2O_3$ (20 μmoles) was heated as in treatment III for the indicated time, cooled, and thiocyanate determined, without adding copper ions

Heating period (min)	NaSCN formed (μmoles)	% of initial $Na_2S_2O_3$ transformed
0	0.39	1.95
15	0.87	4.35
30	1.93	9.65
45	2.60	13.00

Table VI. Partial Cyanolysis of Thiosulfate in the Presence of Limiting Amounts of Cu^{2+} Ions

(a) $Na_2S_2O_3$ was treated by procedure II, except that only 0.8 ml of 0.1*M* $CuSO_4$ was added, to give a concentration of 0.00506*M* in 16.5 ml

$Na_2S_2O_3$ added (μmoles)	NaSCN formed (μmoles)	% of theoretical maximum NaSCN
1	0.42	42.0
2	0.87	43.5
3	1.34	44.7
4	1.82	45.5

(b) $Na_2S_2O_3$ (3 μmoles) was treated as in (a), but the ferric nitrate–$HClO_4$ reagent was added at the indicated times after the addition of the $CuSO_4$

Length of incubation with Cu^{2+} at 5 °C (min)	Thiocyanate formed
1	1.44
5	1.32
10	1.38
20	1.37

Pentathionate would react spontaneously with cyanide to yield two thiocyanate ions, thus raising the apparent tetrathionate content of the sample. However, the recovery of thiosulfate plus tetrathionate (treatment II) would be lowered, and the recovery of trithionate raised above the expected values. As this was not the case, pentathionate formation by the reaction shown in Equation 4 was presumably negligible, and unlikely to be the cause of the discrepancy. The discrepancy persisted when lower concentrations of cyanide and copper were used and may presumably be due to some interaction of cyanide with a thiosulfate–tetrathionate association complex of the kind possibly involved in isotope exchange reactions between thiosulfate and tetrathionate. If this is the case, other cyanolytic methods for determining thiosulfate in mixture with polythionates would be subject to similar errors —*e.g.* Ref. *16*. It should be noted that these discrepancies are no greater than those reported by Koh and Iwasaki (*13*) for the recovery of higher polythionates in mixtures with each other, using copper ion catalyzed cyanolysis.

ACKNOWLEDGMENT

We thank J. M. Swan, Professor of Organic Chemistry, Monash University, for commenting on the manuscript of this paper.

RECEIVED for review October 21, 1968. Accepted January 9, 1969. The Baas Becking Geobiological Laboratory is supported by the Bureau of Mineral Resources, Canberra, the Commonwealth Scientific and Industrial Research Organization, and the Australian Mineral Industries Research Association.

Determination of Piperazine Rings in Ethyleneamines, Poly(Ethyleneamine) and Polyethylenimine by Infrared Spectrometry

Harry L. Spell

The Dow Chemical Co., Texas Division, Freeport, Texas 77541

Infrared spectrometry has been proved to be successful in identifying and determining the concentration of piperazine rings in these amine products. The success of the infrared analysis stems from the fact that the piperazine ring produces a set of characteristic vibrations which are readily distinguishable from the absorptions arising from the attached alkyl amine structures. To develop the analytical method, spectra-structure correlations were established for the piperazine ring from the study of 38 *N*- and *N,N'*-substituted piperazine compounds. The ring was found to be associated with sharp, well-defined absorptions in the 1300–1345 cm^{-1}, 1125–1170 cm^{-1}, 1010–1025 cm^{-1}, and 915–940 cm^{-1} regions of the infrared spectrum. The infrared analysis of a typical commercial product of tetraethylenepentaamine indicated approximately 10% piperazine rings. This result compared favorably with the gas–liquid chromatographic analysis which showed four piperazine compounds with a total concentration of 9.4% calculated as piperazine ring. The results of the analysis of several experimental polyethylenimine products ranged from <0.2% to 5% piperazine rings. A concentration range of 20% to 30% piperazine rings was determined for a number of experimental poly(ethyleneamine) products.

THE REACTION of ethylene dichloride with ammonia or ethyleneamines may lead to the formation of compounds containing the piperazine ring in addition to higher molecular weight ethyleneamines. Similarly, the mechanism by which polyethylenimine is formed from initiation with ethylene dichloride also can result in the formation of piperazine rings. This ring can be readily detected and in some instances can be quantitatively measured by infrared spectrometry. To our knowledge there have been no reports of other instrumental analyses or reliable methods of chemical analyses of polymers for piperazine rings.

The success of the infrared analysis stems from the fact that the piperazine ring produces a set of characteristic vibrations—*i.e.*, vibrations that are relatively insensitive to changes in the rest of the molecule. These absorptions differ appreciably from those arising from the attached alkyl amine structures. There is no record in the literature of infrared spectral-structural correlations for piperazine compounds; therefore, a survey was made of the spectra of about thirty-eight of these type compounds and empirical correlations of absorptions with this ring system were established. This set of bands is not useful for the unequivocal detection of the piperazine ring attached to any type group because the bands are displaced, for example, by carbonyl and other double and triple bonded groups. They are, however, highly characteristic of the ring in alkyl amines.

EXPERIMENTAL

Materials and Standards. Crude tetraethylenepentaamine (TEPA) was separated by preparative scale gas-liquid chromatography into its various components. One of these fractions which had an estimated purity of 98% linear TEPA was used as the infrared standard. The polyethylenimines were prepared by polymerizing ethylenimine with ethylene dichloride as the initiator, and the poly(ethyleneamine) products were produced from the reaction of ethylene dichloride and the ethylene amines in the presence of NaOH. The various substituted piperazine compounds used in this study were synthesized in the Organic Research Laboratory of the Texas Division of The Dow Chemical Co. The usual precautions and techniques to ensure their purity were employed.

Infrared Spectra. The infrared spectra were recorded on a Beckman IR-9 spectrometer. The liquid ethylene amines were examined in a cell of 0.025 mm thickness and the polymeric amines were studied as anhydrous films supported by KBr plates. The polymers were received in aqueous solutions and dried under vacuum at 55 °C. All of the amines were handled in a dry box with a CO_2-free atmosphere because they are extremely hygroscopic and readily react with CO_2.

Calibrations for Quantitative Analysis. Absorbances were measured at the analytical wavelength, approximately 1010 cm^{-1}, for several of the model piperazine compounds similar to those expected in the amine products. The absorptivities of the 1010 cm^{-1} band for the various compounds were calculated by the following formula:

a = Absorbance

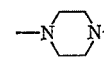

—N N—conc gram/liter × b(cm)

The results from ten of the model compounds were averaged to give an absorptivity of 0.901. The 1010 cm^{-1} band was chosen because the absorptivities of this band for the individual piperazine compounds were fairly constant throughout the series and this particular band occurs in a clear region of the spectra of the ethylene amines and polyamines.

The concentration of piperazine rings in the liquid ethylene amines was determined by scanning the sample in the 0.025-mm cell through the 900 to 1100 cm^{-1} region of the spectrum and measuring the absorbance of the piperazine ring band at *ca.* 1010 cm^{-1}. A base line for this measurement was established from the scan of the corresponding linear ethylene amine. The average absorptivity given above was used to calculate the ring concentration. In the case of the polymeric amine products, determinations of the sample thickness were impractical, thus in order to relate the intensity changes of the 1010 cm^{-1} to changes in piperazine ring concentration, relative intensities were computed using the 1605 cm^{-1} —NH_2 band as a reference. A knowledge of the primary amine content of the sample was necessary in order to use this absorption as a reference. The 1605 cm^{-1} is a reliable reference because the absorptivity of this brand remained invariant at a value of 2.26 in this series of polyamines and ethylene amines.

RESULTS AND DISCUSSION

***N*-Substituted Piperazine Compounds.** A comparison of the spectra of the *N*-substituted piperazine compounds on the basis of the single structural unit, the piperazine ring, re-

Table I. Characteristic Infrared Absorptions of *N*- mono- and *N,N'*-disubstituted Piperazines (in cm^{-1})

Compound	CH_2 Tw.	C—N Str. (ring)	CH_2 Rock	Skeletal (ring)
1. 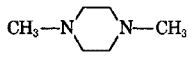	1300	1170, 1125	1018	918
2. 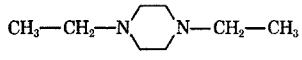	1310	1170, 1110	1025	950
3. 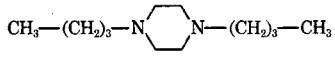	1315	1165, 1110	1015	935
4. 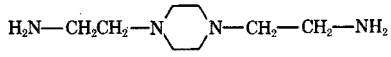	1340	1150, 1125	1010	928
5. 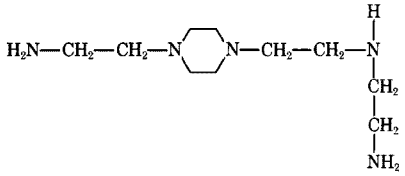	1310	1155	1020	940
6. 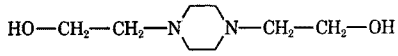	1320	1160, 1126	1020	927
7. 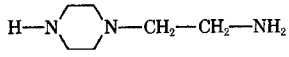	1320	1175, 1126	1012	912
8. 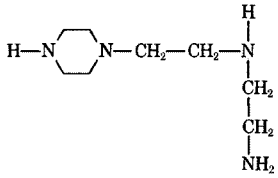	1335	1150	1022	920
9. 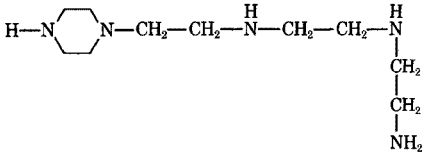	1335	1148	1018	...
10. 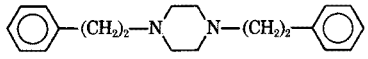	1315	1162, 1135	1010	908
Relative intensity	Very sharp Med.	Strong	Very sharp Med.	Weak

vealed that there are absorption bands highly characteristic of this ring and that these bands are readily distinguishable from the vibrations arising from >NH, —NH_2, alkyl groups, and other groups occurring in these compounds. All 38 piperazines studied exhibited the set of characteristic bands shown by the selected group in Table I. Hendra and Powell (*1*) have presented a detailed vibrational analysis of piperazine and the following assignments are based on their work.

1300–1340 Cm^{-1} Bands. All of the piperazine compounds investigated exhibited at least one strong sharp band in this region. The well-defined sharpness of these bands made them readily distinguishable from the ill-defined, broad absorptions arising from the polyamine structures. These bands are probably associated with the CH_2 twisting modes.

1125–1170 Cm^{-1} Bands. Two strong absorptions, one at approximately 1125 cm^{-1} and the other at approximately 1170 cm^{-1}, which appear to be characteristic of piperazine rings occur in this region. These bands probably can be assigned to C—N stretching modes. They are more intense and sharper than the corresponding bands of open chain amines.

1010–1025 Cm^{-1} Bands. The ring CH_2 rocking motions would be expected to account for this vibration. This is the most useful of the five bands for detecting the presence of *N,N'*-di-substituted piperazines. It is strong in intensity and very sharp.

915–940 Cm Bands. All of the compounds in Table I produced a band of medium intensity in this region. It has been assigned as an A_u skeletal mode by Hendra and Powell. In addition to the above set of absorptions, most of the piperazine compounds produced a major absorption in

(1) P. J. Hendra and D. B. Powell, *Spectrochim. Acta*, **18**, 305 (1962).

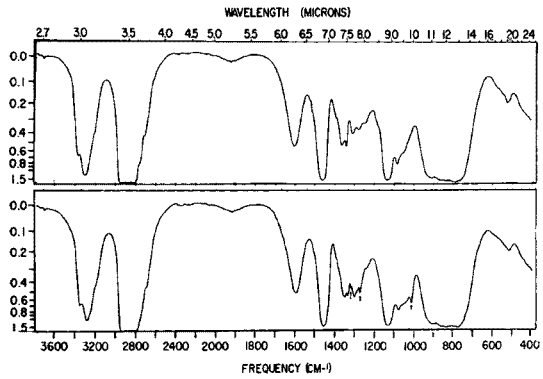

Figure 1. Infrared spectra of tetraethylenepentaamine recorded in 0.025-mm cells

Top spectrum—linear TEPA; bottom spectrum—crude TEPA

the 800 cm^{-1} region of the spectrum which probably can be assigned to a ring skeletal vibration; however, this band displayed considerable variation in intensity and frequency and thus cannot be classified as a good group frequency.

Ethylene Amines. Tetraethylenepentaamine (Figure 1) was selected as an example of the ethylene amines because the crude product contained a high concentration of piperazine rings and its spectrum most nearly resembled the spectra of the amine polymers. Practically all of the absorptions of linear TEPA can be ascribed to well-known group frequencies. According to Colthup, Daly, and Wiberly (*2*), the NH_2 group of amines in dilute solution gives a band due to the antisymmetric mode at 3500 cm^{-1} and a band due to the symmetric vibration at *ca.* 3400 cm^{-1}. Secondary amines in solution exhibit the N—H stretching mode at *ca.* 3400 cm^{-1}. In the liquid phase, hydrogen bonding causes a small shift to lower frequencies. The bands due to two of these modes in TEPA occur at 3290 cm^{-1} where the symmetric stretch of the NH_2 group and NH group stretch coincide. The shoulder on the high frequency side at 3360 cm^{-1} is due to the antisymmetric stretching mode of the NH_2 group. The NH_2 bending vibration gives rise to the band at 1605 cm^{-1}. In liquid amines, the shoulder near 3200 cm^{-1} is an overtone of the 1605 cm^{-1} NH_2 deformation intensified by Fermi resonance due to its proximity to the stretching fundamentals.

The NH_2 wagging and twisting vibrations give rise to the broad multiple absorption bands in the 850 to 950 cm^{-1} region. The strong broad absorption at 780 cm^{-1} is due to the N—H wagging of secondary amine groups. The absorption at 1055 cm^{-1} can be assigned to the C—N stretch of the $—CH_2—NH_2$ group. The broad medium strong band at 1130 cm^{-1} arises from the antisymmetric stretching of the C—C—N and C—N—C groups. The C—N stretching of tertiary amino groups is more difficult to characterize and occurs in the 1050 to 1150 cm^{-1} region of the spectrum.

The strong absorptions at 2941 and 2820 cm^{-1} are clearly the antisymmetric and symmetric C—H stretching modes of the CH_2 group. The increased intensity of the symmetrical stretching as well as its lowered frequency is characteristic of the CH_2 groups attached to amino nitrogens. The CH_2 bending vibrations are located at 1460 cm^{-1} (antisymmetric) and 1360 cm^{-1} (symmetric). The CH_2 wagging motion gives rise to the broad band at 1300 cm^{-1}.

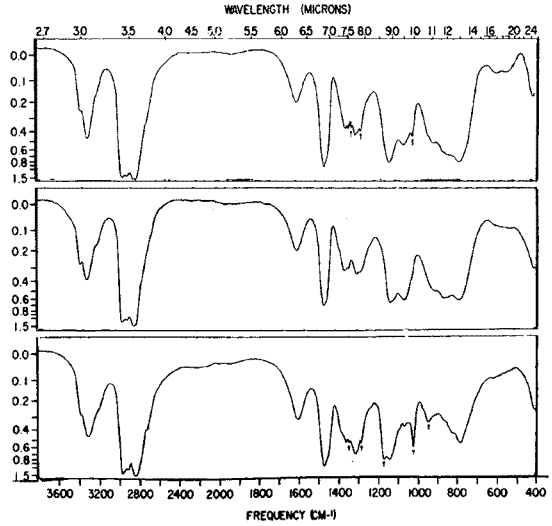

Figure 2. Infrared spectra of polyethylenimine and poly(ethyleneamine) recorded as films on KBr plates

Top spectrum—polyethylenimine containing 5% piperazine rings; middle spectrum—polyethylenimine with approximately 0.2% piperazine rings; bottom spectrum—poly(ethyleneamine) containing 27% piperazine rings

The lower spectrum shown in Figure 1 is that of a crude TEPA which contained approximately 10% piperazine rings. The ring group is readily identifiable by the characteristic absorption at 1340 cm^{-1}, 1325 cm^{-1}, and 1010 cm^{-1}. Linear TEPA is shown in the top spectrum of Figure 1. The branched chain TEPA has been isolated and its infrared absorptions do not interfere with the unique piperazine bands.

The other common ethylene amines commercially available, DETA, TETA, and PEHA have been analyzed for piperazine rings by the same techniques as the example discussed in this report. In each case, the results of GLC and infrared spectrometry analyses were in good agreement.

Polyethylenimine. A comparison of the spectrum of PEI (Figure 2) with that of TEPA reveals expected similarities. However, a characteristic feature of polymeric spectra is the ill-defined broadening of specific bands as a result of a molecular weight spread and variations in chain configurations. The sharp absorptions in the 1320 cm^{-1} and 1010 cm^{-1} regions of the spectrum offer strong support for the presence of approximately 5% piperazine rings. The middle spectrum in Figure 2 is practically devoid of the piperazine bands. An estimated concentration range of 0.2% to 5% piperazine rings was found in a series of eight of these experimental products. The isolated 1605 cm^{-1} $—NH_2$ band was employed as a thickness calibration in making these determinations.

Poly(Ethyleneamine). A comparison of the spectrum of poly(ethyleneamine) (bottom spectrum, Figure 2) with the PEI shows many features which result from the same structural group. The $—NH_2$ group, with a concentration somewhat weaker in this polymer than in PEI is revealed in absorptions at 1605 cm^{-1}, 1055 cm^{-1}, and 900 cm^{-1}. The presence of open chain secondary amine groups is supported by the broad C—N stretching vibration at 1130 cm^{-1}.

(2) N. B. Colthup, L. H. Daly, and S. E. Wiberly, "Introduction to Infrared and Raman Spectroscopy," Academic Press, New York, N. Y. 1964.

The major differences between the spectra of these two polymers are due to the greatly increased concentration of piperazine rings in the poly(ethyleneamines). The piperazine rings are supported by absorptions at 935 cm^{-1}, 1010 cm^{-1}, 1160 cm^{-1}, and 1340 cm^{-1}. An estimation of their concentration is made possible by ratioing the absorption of the 1010 cm^{-1} ring mode band to the $-NH_2$ absorption at 1605 cm^{-1}. As previously stated, the absorptivities of these two bands and a knowledge of the primary amine content of the polymer are requisites for quantitative analysis. The infrared analysis indicated a piperazine ring concentration of 27% in the poly(ethyleneamine) product shown in Figure 2.

ACKNOWLEDGMENT

The author is grateful to G. E. Ham for helpful discussions during the course of this work.

RECEIVED for review November 14, 1968. Accepted April 10, 1969.

Spectrophotometric Studies of Iron(II) Complexes of Pyridyl Benzodiazepin-2-ones

J. D. Sabatino, O. W. Weber, G. R. Padmanabhan, and B. Z. Senkowski

Analytical Research Laboratories, Hoffmann-La Roche Inc., Nutley, N. J. 07110

Ferrous ions form purple complexes with 7-bromo-1,3-dihydro-5-(2-pyridyl)-2H-1,4-benzodiazepin-2-one (A) and 7-bromo-1,3-dihydro-1-(3-dimethylaminopropyl)-5-(2-pyridyl)-2H-1,4-benzodiazepin-2-one dihydrochloride (B). Compounds A and B have the basic dipyridyl type bond structure which has excellent metal complexing properties. Iron(II) complexes with A and B are pH dependent, and the optimum pH range for the formation of these complexes is between 5 and 7. The mole ratio of ligand to metal for these complexes is 3 to 1. The formation constants of the A and B complexes are 8.9×10^{13} and 3.2×10^{11}, respectively. The effect of various anions and cations on the formation of these complexes is discussed. These complexes are adapted to the determination of iron. Some advantages of compounds A and B over the dipyridyl type are presented.

COMPOUNDS A (*1*) and B (*2*) have the following structures:

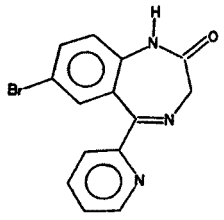

A

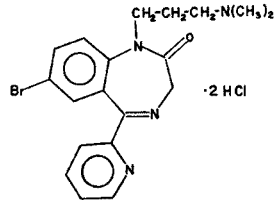

B

These compounds are similar to α,α'-dipyridyl in having the following basic structure:

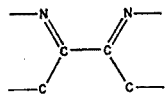

Because of this structural similarity, it was of interest to investigate the nature of the iron(II) complexes of A and B, compare these complexes with those obtained with the dipyridyl type compounds (*3–10*), and evaluate their relative merits for the determination of iron.

Table I. Preparation of Stock Buffer Solutions

pH	Components	Final volume, ml
1	20 ml of 0.5*M* oxalic acid + 3.6 ml of 1.0*M* potassium hydroxide	100
2	20 ml of 0.5*M* oxalic acid +8.5 ml of 1.0*M* potassium hydroxide	100
3	50 ml of 0.1*M* potassium acid phthalate + 22.3 ml of 0.1*M* hydrochloric acid	100
4	50 ml of 0.1*M* potassium acid phthalate + 0.1 ml of 0.1*M* hydrochloric acid	100
5	50 ml of 0.1*M* potassium acid phthalate + 22.6 ml of 0.1*M* sodium hydroxide	100
6	136 grams of sodium acetate + 6 ml of glacial acetic acid	100
7	10 ml of 0.5*M* THAM[a] + 46.6 ml of 0.1*M* hydrochloric acid	100
8	10 ml of 0.5*M* THAM + 29.2 ml of 0.1*M* hydrochloric acid	100
9	10 ml of 0.5*M* THAM + 5.7 ml of 0.1*M* hydrochloric acid	100

[a] Tris (hydroxymethyl) aminomethane.

EXPERIMENTAL

Apparatus. Optical absorption measurements were made with Beckman Model DU and Model DK spectrophotometers. A Corning Model 12 pH meter was employed for pH determinations.

Solutions. Stock buffer solutions were made as described in Table I.

(1) R. Ian Fryer, R. A. Schmidt, and L. H. Sternbach, *J. Pharm. Sci.*, **53**, 264 (1964).
(2) L. H. Sternbach, G. A. Archer, J. V. Earley, R. Ian Fryer, E. Reeder, N. Wasyliw, R. O. Randall, and R. Banziger, *J. Med. Chem.*, **8**, 815 (1965).
(3) W. W. Brandt, F. P. Dwyer, and E. C. Gyarfas, *Chem. Rev.*, **54**, 959 (1954).
(4) H. Diehl and G. F. Smith, "The Iron Reagents: Bathophenanthroline, 2,4,6-Tripyridyl-s-Triazine, Phenyl-2-Pyridyl Ketoxime" G. Frederick Smith Chemical Co., Columbus, Ohio, 1960.
(5) D. D. Bly and M. G. Mellon, ANAL. CHEM., **36**, 1276 (1964).
(6) T. S. Lee, I. M. Kolthoff, and D. L. Leussing, *J. Amer. Chem. Soc.*, **70**, 3596 (1948).
(7) G. Anderegg, *Helv. Chim. Acta*, **46**, 2397 (1963).
(8) J. H. Baxendale and G. George, *Nature*, **162**, 777 (1948).
(9) A. A. Schilt and G. F. Smith, *J. Phys. Chem.*, **60**, 1546 (1956).
(10) M. A. McKenzie, *Aust. J. Chem.*, **8**, 569 (1955).

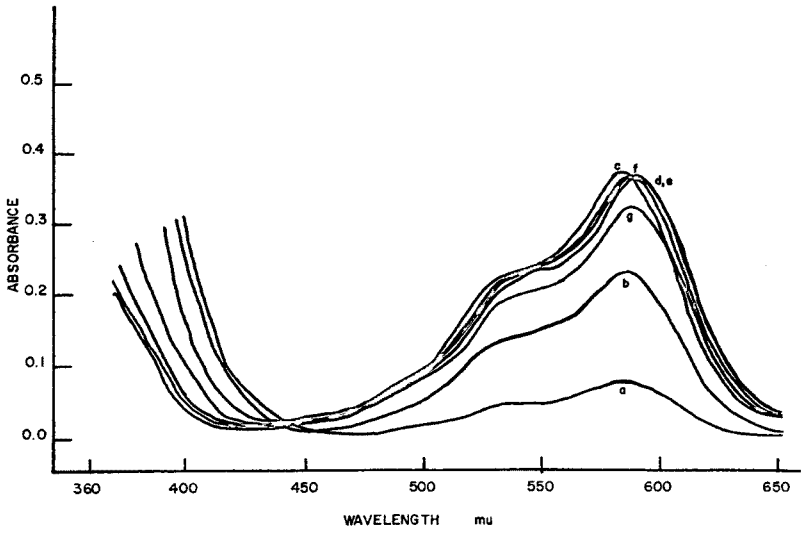

Figure 1. The effect of pH on the absorption spectra of iron(II) A complex

$C_{Fe} = 2 \times 10^{-4}M$ and $C_A = 1 \times 10^{-3}M$ in *a* and *b*
$C_{Fe} = 2 \times 10^{-5}M$ and $C_A = 1 \times 10^{-3}M$ in *c* through *g*
pH of $a = 1.5$, $b = 2.0$, $c = 3.0$, $d = 4.0$, $e = 5.0$, $f = 6.9$, and $g = 8.1$

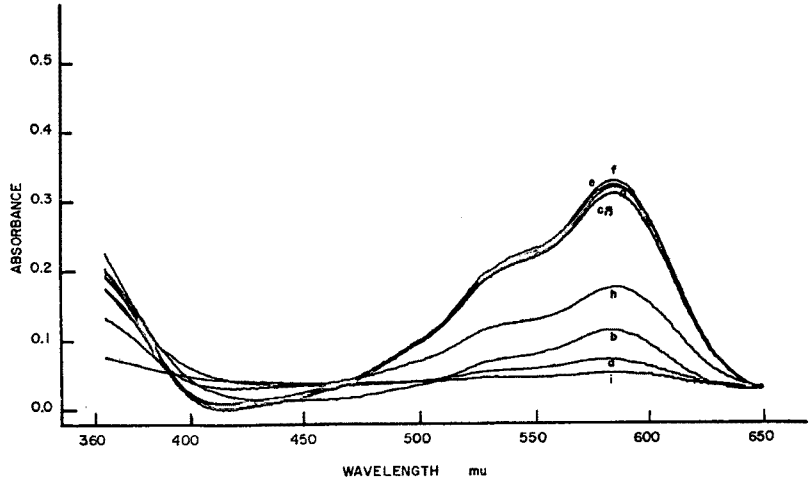

Figure 2. The effect of pH on the absorption spectra of iron(II) B complex

$C_{Fe} = 2 \times 10^{-4}M$ and $C_B = 1 \times 10^{-3}M$ in *a* and *b*
$C_{Fe} = 2 \times 10^{-5}M$ and $C_B = 1 \times 10^{-3}M$ in *c*–*g*
pH of $a = 1.5$, $b = 2.2$, $c = 3.0$, $d = 4.1$, $e = 5.0$, $f = 6.9$, and $g = 8.1$

A 10m*M* stock solution of compound A (*1*) was prepared in a 100-ml volumetric flask by dissolving 316.0 mg of the solid sample in 50 ml of methanol and diluting to volume with water. A 10m*M* solution of compound B (*2*) was prepared by dissolving 474.3 mg of the solid sample in 100 ml of water.

A 10m*M* stock solution of ferrous sulfate was freshly prepared by weighing accurately 278 mg of ferrous sulfate (Mallinckrodt analytical reagent) and dissolving in 100 ml of water. Further dilutions were made to obtain the required concentrations and the resulting solutions were immediately used.

Solutions were prepared by taking 1 ml of ferrous sulfate, 1 ml of ligand solution, and 8 ml of the appropriate stock buffer solution. Reference blank solutions were also prepared substituting 1 ml of water for 1 ml ferrous sulfate. The solutions were mixed well and their absorbances measured after 10 minutes against the respective blank solutions.

Effect of pH on the Complexes. In a series of solutions, the pH was changed from 1 to 8 maintaining an iron concentration of $1 \times 10^{-5}M$ and ligand concentrations of $1 \times 10^{-3}M$, respectively. Because the absorption of solutions at pH 1 and 2 were low, ferrous ion concentration was increased to $2 \times 10^{-4}M$. The spectrum was recorded from 650 mμ to 360 mμ. The results are shown in Figures 1 and 2.

Determination of Ligand to Metal Ratio. JOB'S METHOD (*11*). In a series of solutions, the total concentration of metal and ligand was kept constant at $1 \times 10^{-4}M$ and the individual

(11) P. Job, *Ann. Chim.* (Paris), **9**, 113 (1928).

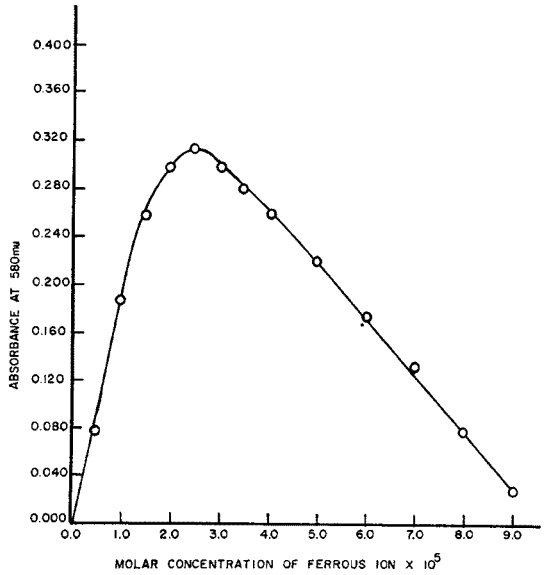

Figure 3. Job's curve. Effect of metal–ligand mole ratio on iron(II) A complex

The ratio $C_A:C_{Fe(II)}$ was varied from 19:1 to 1:0; ($C_{Fe(II)}$ + C_A) was maintained constant at $1.0 \times 10^{-4}M$. The solutions were buffered at pH 5. The curve showed the maximum absorbance to be at ligand to metal ratio of 3.1

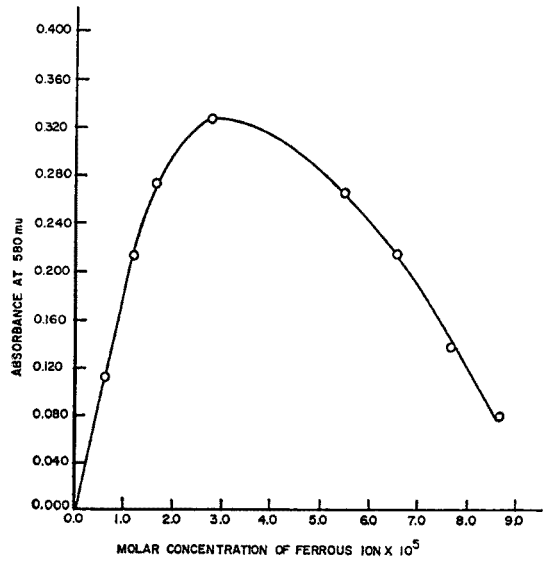

Figure 4. Job's curve. Effect of metal–ligand mole ratio on iron(II) B complex

The ratio $C_B:C_{Fe(II)}$ was varied from 19:1 to 1:19; ($C_{Fe(II)}$+ C_B) was maintained constant at $2.0 \times 10^{-4}M$. The solutions were buffered at pH 6. The curve showed the maximum absorbance to be at a ligand to metal ratio of 2.8

concentrations were varied. The absorbances measured were plotted against the molar concentration of ferrous ion. The mole ratio at the maximum absorbance gave the mole ratio of the complex formed (Figures 3 and 4).

Modified Yoe and Jones' Method (*12*). The metal ion concentration was maintained constant in a series of solutions and the concentration of ligand was varied. Readings were taken at three different concentrations of metal ion ($3.6 \times 10^{-5}M$, $7.2 \times 10^{-5}M$, and $10.8 \times 10^{-5}M$). A pH of 5 was maintained for all solutions. The absorbances *vs.* the ligand concentrations were plotted (Figure 5). The absorption varied linearly at low ligand concentrations and remained constant at high ligand concentrations. The ratio of ligand to metal at the point where the two linear sections intersected gave the ratio of ligand to metal in the complex.

Determination of Stability Constant. A series of solutions was prepared varying the metal concentration from $2 \times 10^{-5}M$ to $7 \times 10^{-5}M$ and the ligand concentration from $6 \times 10^{-5}M$ to $21 \times 10^{-5}M$. These solutions were all buffered at pH 5 and the absorbances were measured ten minutes after preparation of the solutions. The concentrations of iron and ligand were chosen so that the amount of complex formed was in the order of $1 \times 10^{-5}M$ to $5 \times 10^{-5}M$. The absorbances of these solutions ranged from 0.2 to 0.8. The concentrations of the complexes were calculated assuming that the absorbance at 580 mμ was due to only the 1:3 complex. The free metal and free ligand concentrations were calculated by difference. The conditional formation constant K was calculated using the formula: $K = [C_c]/[C_{Fe}][C_{Le}]^3$. The calculated values are given in Table II.

Analysis of Iron Using Compound A and B. A standard calibration curve was prepared from the measurements of a series of solutions varying in ferrous ion concentration from $2 \times 10^{-5}M$ to $1 \times 10^{-4}M$. A ligand concentration of $10^{-3}M$ and a pH of 5 were maintained for all solutions. The absorbances of the solutions were measured at 580 mμ against appropriate blanks. Sample solutions containing unknown quantities of iron(II) were treated similarly with buffer and

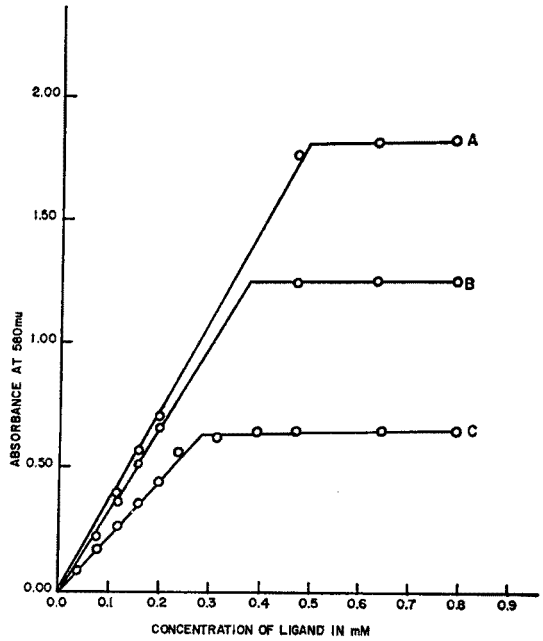

Figure 5. Modified Yoe and Jones Method. Effect of ligand A concentration on the complex. All solutions were buffered at pH 5

A. $C_{Fe} = 10.8 \times 10^{-5}M$; $C_A:C_{Fe} = 4.6$
B. $C_{Fe} = 7.2 \times 10^{-5}M$; $C_A:C_{Fe} = 5.4$
C. $C_{Fe} = 3.6 \times 10^{-5}M$; $C_A:C_{Fe} = 8.1$

(12) J. H. Yoe and A. L. Jones, Ind. Eng. Chem., Anal. Ed., **16**, 111 (1944).

Table II. Calculations for K

Fe (II) A Complex

Sample	$10^5 \times C_{Fe}$[a]	$10^5 \times C_{Lg}$[b]	A[c]	$10^5 \times [C_c]$[d]	$10^5 \times [C_{Fe}]$[e]	$10^5 \times [C_{Lg}]$[f]	$10^{-13} \times K$[g]
1	2.06	6.00	0.211	1.15	0.913	2.56	7.49
2	3.09	9.00	0.384	2.09	1.003	2.74	10.1
3	4.12	12.00	0.555	2.99	1.131	3.03	9.50
4	5.15	15.00	0.720	3.91	1.237	3.26	9.13
5	6.18	18.00	0.889	4.83	1.348	3.50	8.36
							8.87

Fe (II) B Complex

Sample	$10^5 \times C_{Fe}$	$10^5 \times C_{Lg}$	A	$10^5 \times [C_c]$	$10^5 \times [C_{Fe}]$	$10^5 \times [C_{Lg}]$	$10^{-11} \times K$
1	4.28	12.00	0.148	0.85	3.43	9.45	2.94
2	5.35	15.00	0.252	1.45	3.90	10.65	3.08
3	6.47	18.00	0.365	2.10	4.32	11.7	3.04
4	7.49	21.00	0.520	2.99	4.50	12.03	3.82
							3.20

[a] C_{Fe} = total molar concentration of iron.
[b] C_{Lg} = total molar concentration of ligand.
[c] A = absorbance at 580 mμ.
[d] $[C_c]$ = calculated molar concentration of the complex formed.
[e] $[C_{Fe}]$ = calculated molar concentration of free iron.
[f] $[C_{Lg}]$ = calculated molar concentration of free ligand.
[g] K = formation constant.

ligand reagents. From the absorbance measurements at 580 mμ, the concentrations of ferrous ion present were determined from the standard calibration curve.

RESULTS AND DISCUSSION

Effect of pH on the Iron(II) Complexes of A and B. The effects of pH on the spectra of the iron complexes are shown in Figures 1 and 2. The absorbance at 580 mμ showed minimum change in the pH range of 4 to 7. Hence pH 5 was chosen for further studies. The molar absorptivities at pH's below 4 and at pH's above 7 were found to be lower than in the pH range 4 to 7. The effect of low pH on the complexes was similar to the effects observed by Nielands (*13*) in the case of the ferric hydroxamate complex and by Krumholz (*14*) in the case of the iron(II) dipyridyl complex. Nielands pointed out that at low pH's, the hydroxamic acids tended to form a 1:1 complex with iron due to the protonation of ligands, and the complexes dissociated to free metal and ligand at high acid concentration. Lee, Kolthoff, and Leussing (*6*) presented the following mechanism for the pH effects on the iron(II) *o*-phenanthroline complexes:

$$Fe^{2+} + (phen) \rightleftharpoons Fe(phen)^{2+}$$

$$Fe(phen)^{2+} + (phen) \rightleftharpoons Fe(phen)_2^{2+}$$

$$Fe(phen)_2^{2+} + (phen) \overset{k_1}{\rightleftharpoons} Fe(phen)_3^{2+}$$

$$(phen) + H^+ \rightleftharpoons H\,phen^+$$

At low pH's free *o*-phenanthroline is protonated thus decreasing the rate of formation and concentration of the complex. At high pH's complexation is inhibited due to depletion of ferrous ion by the formation of the ferrous hydroxide precipitate.

Krumholz (*14*) and Burgess and Prince (*15*) proposed a mechanism for the dissociation of iron(II) dipyridyl complexes in acid medium which involved the decomposition of the protonated species $[Fe\,Dipy_3H^{3+}]$. The effect of adding acid to the iron(II) complexes of compound A, α,α′-dipyridyl and *o*-phenanthroline is presented in Figure 6. This figure showed that once formed, the compound A complexes were exceptionally stable in acid medium.

Table III. Molar Absorptivities and Conditional Formation Constants of Iron(II) Complexes

Ligand	Molar absorptivity	log K
α,α′-Dipyridyl (*7*)	8,820	17.1
2,2′-Dipyrimidines (*5*)	4,540	7.5
o-Phenanthroline (*9*)	11,100	21.3
A	18,400	13.9
B	17,400	11.5

Determination of Molar Absorptivity of the Complexes. Table III gives the values obtained for the molar absorptivities for the iron(II) complexes of A and B. Because the molar absorptivities of the A and B complexes with iron are almost twice that of the dipyridyl type complexes, the sensitivity of photometric ferrous ion determinations with ligands A and B is nearly doubled.

Determination of Molar Ratio of Ligand to Metal. JOB'S METHOD (*11*). Figures 3 and 4 show that the ligand to metal mole ratio for the iron(II) complex of both A and B is 3. It should be pointed out that Job's method of calculating the mole ratio is reliable only for a 1:1 type complex.

YOE AND JONES' METHOD (*12*). The results obtained by this method are presented in Figure 5. The ratio of ligand to metal for the iron (II) A complex varied from 8 to 4.8 when the iron concentration was changed from $3.6 \times 10^{-5}M$ to $10.8 \times 10^{-5}M$. When the apparent ligand to metal ratio was plotted against the reciprocal of metal concentration and the plot extrapolated to $1/C_{Fe^{2+}} = 0$, the ratio of ligand to metal was found to be 2.8 for the A complex.

(13) J. B. Nielands, *Science*, **156**, 1443 (1967).
(14) P. Krumholz, *Nature*, **163**, 724 (1949).
(15) J. Burgess and R. H. Prince, *J. Chem. Soc.*, **1965**, 6061.

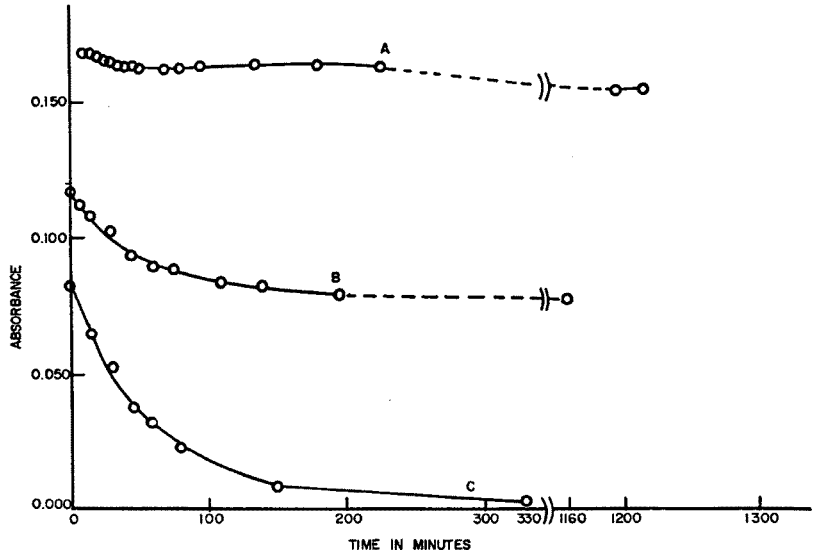

Figure 6. The effect of adding acid to iron(II) complexes of compound A, *o*-phenanthroline, and α,α'-dipyridyl

Two and one-half milliliters of $10^{-4}M$ Fe(II) was added to 2.5 ml of $10^{-4}M$ ligands. The solutions were allowed to stand for 10 minutes. Two and one-half milliliters of $1N$ HCl was added to each and the solutions diluted to 25-ml volume with water. The absorbance of each solution was read at the appropriate maximum, at various time intervals. Curve *A* represents absorbance readings of compound A complex at 580 mμ, Curve *B*, *o*-phenanthroline complex at 515 mμ, and Curve *C*, α-α'-dipyridyl complex at 525 mμ

The following structure was ascribed to the 1:3 iron(II) complexes of pyridyl benzodiazepinones.

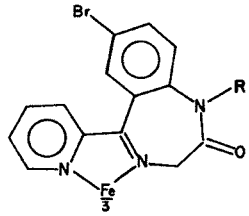

where *R* is aliphatic

Formation Constants of Iron(II) Complexes of A and B. Table II shows the obtained data and the calculated value of *K* for the iron(II) complexes with ligands A and B. Even though the molar absorptivities of the A and B complexes are much higher than those of α,α'-dipyridyl and *o*-phenanthroline, the formation constants are lower. The lower *K* values for A and B are probably due to the size of the ligand molecules. However, the accuracy of the ferrous ion determination is not affected by this lower *K* value; because the ligand concentration is always in excess, complete complexation is obtained.

Determination of Iron Using Compounds A and B. As mentioned earlier, compounds A and B offered higher sensitivity for the determination of iron. These complexes followed Beer's law from 2.5 to 30 μg of iron per 100 ml of final solution. An ammoniacal solution of these complexes was extracted with dichloromethane. The dichloromethane extractions obeyed Beer's law from 5 to 30 μg of iron per 25 ml of final solution.

The water solubility of the dihydrochloride compound B eliminated the introduction of organic solvents to effect solution. Thus B offered an additional advantage over compound A, α,α'-dipyridyl, and *o*-phenanthroline.

The bathochromic shift found with the iron complexes of compounds A and B, reduces potential interferences due to extraneous color common at lower wavelengths.

The effect of the anions (phosphate, tartrate, citrate, and borate) on the complexes of iron with A and B were investigated. No interferences were observed with these anions. As might be expected, in the presence of EDTA, no complexing of iron with compounds A or B was observed.

The cations Zn^{2+} (996 μg/ml), Pb^{2+} (1,282 μg/ml), Al^{3+} (266 μg/ml), Mn^{2+} (566 μg/ml), and Ni^{2+} (476 μg/ml) did not form colored species absorbing at 580 mμ. Cobalt (2+) and copper (+1 and +2) formed colored complexes with compound A. However, if the concentrations of Co^{2+}, Cu^{2+}, and Cu^{1+} were less than 50 μg/ml, 77 μg/ml, and 135 μg/ml, respectively, no interference was observed.

ACKNOWLEDGMENT

The authors acknowledge the helpful discussions held with Mr. H. L. Newmark and Dr. R. I. Fryer.

RECEIVED for review January 15, 1969. Accepted March 18, 1969.

Coulometric Titration of Microgram Amounts of Americium at the Conducting Glass Electrode

R. C. Propst

Savannah River Laboratory, E. I. du Pont de Nemours and Co., Aiken, S. C. 29801

Coulograms of Am(III) in 0.1*M* $LiClO_4$–0.05*M* Na_2CO_3 electrolyte exhibit a well-defined wave for the Am(III)–Am(V) oxidation step at the conducting glass electrode. This wave provides the basis of a method for the quantitative titration of this element at the 30-microgram level with a precision of 1.5%. The method is restricted to pure solutions. Most cations interfere: Pu, Np, V, and Ru are reduced near the Am(III)–Am(V) wave. Fe precipitates and scavenges Am. Radiolysis products from radioelements also interfere. SO_4^{2-} produces an anodic shift, and F^- damages glass surfaces. Cl^- or NO_3^- do not interfere at 0.01*M*. Corrections are required for the partial oxidation of Am(V) to Am(VI) and the reduction of Am(VI) by water. The useful pH range is 10.0 to 11.5. The Am(III)–Am(V) couple is indicated to be irreversible.

AMERICIUM, a byproduct of nuclear fuel processing, is an important intermediate in the production of the transamericium elements *via* reactor irradiation. Therefore, analytical methods for accountability and control must be precise. Although coulometric methods would be ideal for this application, the high oxidation potential of the Am(III)–Am(V) couple has prevented the development of a successful coulometric method involving the electrochemical oxidation of Am(III). As a consequence, most assay methods have been based on alpha counting methods which are limited by uncertainties in the nuclear data (*1*).

Previous work on the coulometric titration of Am is due to Koehly (*2*) and Stokely (*3*). Koehly oxidized Am(III) to Am(VI) by exhaustive electrolysis at the platinum electrode and then determined the americium by coulometrically reducing Am(VI) to Am(V). This method requires excessively long electrolysis times (several hours) to oxidize the americium quantitatively.

Stokely (*3*) shortened the procedure by replacing the electrolysis with a chemical oxidation. However, the excess oxidant must be destroyed, and electrolysis is still required to ensure complete conversion to the Am(VI) state before coulometric reduction to Am(V). Neither of these authors attempted to determine Am(V) by coulometric oxidation, presumably because the required oxidation potential was beyond the useful working range of the platinum electrode.

Kuwana (*4*) has reported, and we have confirmed, a wide working range for the tin oxide semiconducting electrode as compared to conventional electrode materials. We have developed a successful coulometric method for Am based on the use of this electrode and on the stability of Am(III) and Am(V) in carbonate electrolyte. The direct electrochemical oxidation of americium from (III) to (V) is achieved at essentially 100% current efficiency. This method combined with precise alpha counting has been used to determine the half-life of ^{243}Am (*1*).

EXPERIMENTAL

Reagents. The ^{243}Am stock solution was purified by ion exchange, solvent extraction, and finally by the method of Moore (*5*). Alpha pulse height analysis of the product showed it to be 98.8 alpha per cent ^{243}Am with less than 0.05 alpha per cent ^{244}Cm. The ^{243}Am solution was standardized at 1.49 mg Am/ml by alpha pulse analysis and precision alpha counting in combination with mass spectrometry (*1*).

The isotopic purity of the ^{241}Am solution was confirmed by mass spectrometry.

All other solutions were prepared from reagent grade chemicals and demineralized laboratory distilled water.

During titration, the solutions were purged continuously with helium that had been bubbled through distilled water.

Apparatus. The scanning coulometer with automatic scan rate control has been described (*6*); both the controlled-potential and scanning modes were used. All titrations were initiated at the equilibrium potential of the working electrode with respect to the solution. For electrolysis at controlled-potential, the potential was advanced manually from the equilibrium potential to the desired electrolysis potential. This precaution prevented amplifier overload.

The titration cell assembly (Figure 1), was similar to those previously described (*7*) except for the conducting glass electrode (CGE) (*4*) which consisted of a layer of antimony-doped, tin oxide on the inner surface of the titration cell. A platinum wire sealed through the side of the cell made ohmic contact with the conducting coating. All potentials were measured with respect to the mercury:mercurous sulfate (1*M* H_2SO_4) reference electrode (MSE). The MSE had a potential of 0.420 V (includes junction potentials) *vs.* the saturated calomel electrode in 0.1*M* $LiClO_4$–0.05*M* Na_2CO_3.

The CGE's were fabricated from borosilicate glass. To assure positive contact between the platinum wire and the tin oxide coating, the inner platinum connection was spotted with Liquid Bright Platinum (Engelhard Industries, East Newark, N. J.). This coating was air dried and fired at 650 °C. The tin oxide coating was next applied by heating the cell to 600 °C and spraying the inside surface with a solution that was 2.8*M* in stannic chloride, 0.04*M* in antimony trichloride, and 1.2*M* in hydrochloric acid (*8*). A DeVilbiss #40 Nebulizer (DeVilbiss Co., Somerset, Pa.) was used for spraying. The air pressure was 5 psig, and the spraying time was two minutes. This technique produced essentially uniform and haze-free coatings. The uniformity was indicated by resistance measurements. Finally the completed CGE's were leached in concentrated H_2SO_4 for 24 hours and then rinsed thoroughly with demineralized water. During the electrolysis, any resistance inherent in the design of the cell

(1) L. C. Brown and R. C. Propst, *J. Inorg. Nucl. Chem.*, **30**, 2591 (1968).
(2) G. Koehly, *Anal. Chim. Acta.*, **33**, 418 (1965).
(3) J. R. Stokely and W. D. Shults, Paper presented at the Eleventh Conference on Analytical Chemistry in Nuclear Technology, Gatlinburg, Tenn. October 10–12, 1967.
(4) T. Kuwana, R. K. Darlington, and D. W. Leedy, ANAL. CHEM., **36**, 2023 (1964).
(5) F. L. Moore, ANAL. CHEM., **35**, 715 (1963).
(6) R. C. Propst, *ibid.*, p 958.
(7) *Ibid.*, **40**, 244 (1968).
(8) J. M. Mochel, U. S. Patent 2,546,707 (1951).

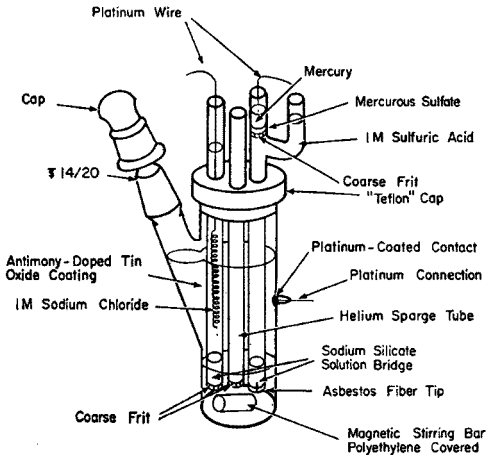

Figure 1. Titration cell assembly

effectively appears in series with the electrochemical impedance of the interface. Therefore the resistance of each cell was determined by substituting an equivalent volume of mercury (10 ml) for the sample solution, and recording current–voltage curves between the mercury pool and the platinum contact. The scan rate was 5 V per minute.

Because the platinum contact was well above the level of the mercury, Figure 1, the measured resistance represented the sum of the resistances of the platinum–tin oxide contact, the tin oxide layer above the mercury pool and the tin oxide–mercury interface all in series. The resulting current–voltage curves were linear, indicating no potential dependence for this measured resistance; the series resistance was typically 14 to 40 ohms.

The CGE's were evaluated by recording cyclic voltammetric and chronopotentiometric curves for the ferrocyanide–ferricyanide couple in 0.1*N* potassium chloride as was done by Kuwana (*4*). The results for the cyclic voltammetric studies gave values for E_p and ($E_{pa} - E_{pc}$) of +0.21 V *vs.* SCE and 0.07 V, respectively. Thus the E_p value is in good agreement with that reported by Kuwana (*7*), and the ($E_{pa} - E_{pc}$) value is in resaonable agreement with the theoretical value of 0.056 V for a one electron process.

The chronopotentiometric studies also produced consistent results although the observed values for $E_{\tau/4}$ and $i\,\tau^{1/2}/C$ probably reflect the influence of the nonuniform distribution of the current over the surface of the electrode (geometry effect). The observed value for $E_{\tau/4}$ was +0.24 V *vs.* SCE and values for $i\,\tau^{1/2}/C$ were reproducible to within ±4%. Because of the geometry effect, these values could not be compared with calculated theroetical values.

Procedure. The general titration procedure has been described (*6*), double-layer compensation was used, but residual current compensation was not required. The capacitance of the electrical double-layer at the CGE as estimated from the slope of the background coulogram was 130 μF/cm².

In this study, the electrolyte was preoxidized and reduced and background scans were recorded to assure that no americium remained in the cell from previous titrations. Carryover of electroactive contaminants from previous titrations was minimized by oxidizing the americium before discarding the solution. The cell was filled with 1*M* nitric acid when not in use.

Because cell resistance was low (<40 ohms) and the electrolysis currents were small (<30 μA), the coulograms were not corrected for the voltage drop introduced by the resistance of the cell.

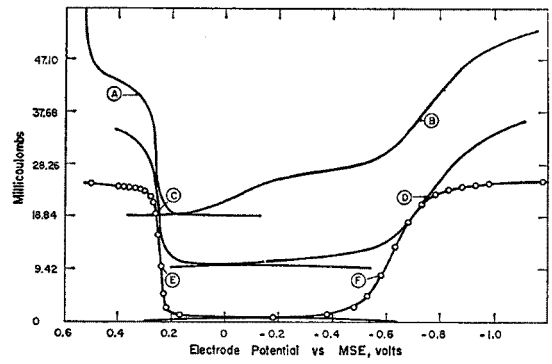

Figure 2. Coulograms of 29.8 μg ^{243}Am in 0.1*M* $LiClO_4$–0.05*M* Na_2CO_3

A. **Am(III)–Am(V) wave and anodic limit of electrolyte**
B. **Am(VI)–Am(V) and Am(V)–Am(III) waves**
C. **Am(III)–Am(V) wave**
D. **Am(V)–Am(III) wave**
E. **Calculated Am(III)–Am(V) wave**
F. **Calculated Am(V)–Am(III) wave**

$\alpha = 0.126$ $\quad a = 10^{-9}$ V A sec^{-1}
$\beta = 5 \times 10^{-3}$ sec^{-1} $\quad E_c^\circ = 0.118$ V
$\sigma_r = 4 \times 10^{-3}$ cm $\quad k_{s,h} = 3.44 \times 10^{-7}$
$D_r = 10^{-5}$ cm² sec^{-1}

RESULTS AND DISCUSSION

Titration Behavior. Typical coulograms depicting the titration behavior of americium in carbonate electrolyte at the CGE are shown in Figure 2. The useful pH range for the titration was 10.0 to 11.5. Below pH 10.0, the wave at +0.26 V shifted in the anodic direction and merged with the wave corresponding to the anodic limit for the solvent-electrolyte system. Above pH 12.0, no oxidation of Am(III) was observed. The wave near −0.04 V always appeared on the reduction scan when the previous oxidation scan extended into the region more positive than +0.45 V. Because high carbonate concentrations (>0.05*M*) appeared to favor the production of the species responsible for the wave at −0.04 V, an electrolyte of 0.1*M* $LiClO_4$–0.05*M* Na_2CO_3 was selected to minimize this effect.

Am(III)–Am(V) Couple. The wave at +0.26 V was assigned to the oxidation of Am(III) to Am(V); the wave at −0.77 V was assigned to the reduction of Am(V) to Am(III). These assignments were based on Am^{3+} as the stable species in aqueous solution, a two-electron change for the oxidation and reduction steps and the irreversible behavior of the system.

Because the higher valence states of americium are known to be unstable in aqueous solution, the americium stock solution was assumed to contain only the Am^{3+} species. This assumption was supported by coulograms for the reduction of aliquots of the stock solution which essentially duplicated background scans.

The number of electrons involved in the oxidation–reduction steps at +0.26 V and −0.77 V was determined by titrating aliquots of the isotopically pure solution of ^{241}Am. The ^{241}Am solution was utilized here for the half-life has been determined accurately by calorimetry (*9*), and the solution could thus be standardized precisely by alpha counting. Although the results were consistent with a two-electron transfer for

(9) F. L. Oetting and S. R. Gunn, *J. Inorg. Nucl. Chem.*, 29, 2659 (1967).

both the oxidation and reduction steps, the number of electrons calculated from the height of the oxidation wave was always slightly more than two. This behavior was later attributed to a partial oxidation of Am(V) to Am(VI) as will be explained.

The irreversibility of the Am(III)–Am(V) (*10*) couple was indicated by the widely separated oxidation and reduction waves. This response from a scanning coulometer is typical of an irreversible system, and can be predicted for coulometric processes in stirred solution (*11*) as follows. (The terms are as defined in Reference *11*.)

The coulometer records well defined waves for an irreversible process due to a unique method of scan rate control in which the instrument maintains the product of the electrolysis current (i) and the scan rate (dE/dt) at a constant value. Thus the slope of the recorded coulogram is given by,

$$\frac{dQ}{dE} = -\frac{i^2}{a} \tag{1}$$

where a = scan rate constant, 10^{-9} V A sec^{-1}. The electrolysis current (reduction) in stirred solution is given by,

$$i = \frac{nFA\ D_o}{\delta_o}[C_o - C_o(0)] \tag{2}$$

and the equation for the current in the case of an irreversible process in which the rate for the backward reaction can be neglected ($k_{s,h} \lesssim 10^{-5}$ cm sec^{-1}) is

$$i_c = nFA\ k_{s,h}C_o(0) \exp -\frac{\alpha nF}{RT}(E - E^\circ_c) \tag{3}$$

From Faraday's law and a material balance on the system, the bulk concentrations can be expressed in terms of integrated current. The following equation for the reduction wave is obtained by making the necessary substitutions in Equations 2 and 3, and then combining Equations 1, 2, and 3 and integrating.

$$\frac{Q_c}{Q_t(Q_t - Q_c)} = \frac{\beta^2 RT}{a\alpha nF} \times \left[\frac{D_o}{D_o + k_{s,h}\delta_o \exp -\frac{\alpha nF}{RT}(E - E^\circ_c)} - \frac{D_o}{D_o + k_{s,h}\delta_o} + ln\left(\frac{D_o + k_{s,h}\delta_o \exp -\frac{\alpha nF}{RT}(E - E^\circ_c)}{D_o + k_{s,h}\delta_o}\right)\right] \tag{4}$$

where Q_c is the integrated current at potential E, Q_t is the total integrated current corresponding to the complete conversion of the species, and β is the coulometric rate constant—*i.e.*, $\beta = AD_o/\delta_o V$. The corresponding equation for the oxidation process is identical except that $-\alpha$ is replaced by $(1 - \alpha)$, D_o by D_r, δ_o by δ_r and Q_c by Q_a.

Before the theoretical coulograms could be calculated, β had to be determined by controlled-potential coulometry, and $k_{s,h}$, E°_c, and α had to be estimated from the coulograms. Thus current–time curves were recorded at controlled potential in the limiting current region for both the oxidation and reduction steps. In each case, graphs of log i *vs.* t were convex upward, indicating that the electrode reactions were more complex than could be explained in terms of simple irreversible theory. Similar phenomena have been reported for vanadium solutions by Israel and Meites (*12*).

Because of this complex behavior, the values for β, $k_{s,h}$, E°_c, and α as estimated from the data are admittedly suspect; nevertheless, coulograms were calculated from these estimated values to illustrate the type of response to be expected with an irreversible system. The results (Figure 2) show that the theoretical coulograms indeed agree qualitatively with the observed response.

Further evidence to support the above findings concerning the irreversible nature of the Am(III)–(Am(V) couple was obtained in experiments in which the Am(III) solution was electrolyzed to produce calculated amounts of Am(V). Following the electrolysis, attempts were made to record the equilibrium potentials for the various Am(III):Am(V) ratios under zero current conditions. In every instance, the potentials were so unstable that no steady state values could be obtained.

Because of the better definition of the oxidation step, this wave would be less subject to interferences and was therefore preferred for the quantitative determination of americium. Thus the factors responsible for the increased height of this wave were investigated.

Am(V) Oxidation. Two explanations for the increased height of the Am(III)–Am(V) wave were considered. The first, the formation of Am(III) *via* disproportionation of Am(V) proved to be negligible. The second, a one-electron oxidation of Am(V) by a colulometric process, proved to be responsible for the increased height of the Am(III)–Am(V) wave.

The disproportionation of Am(V) was studied by coulometrically oxidizing Am(III) to Am(V), allowing the Am(V) solution to stand for periods of one hour, and then scanning the region from 0.0 to +0.45 V to determine the amount of Am(III) formed by disproportionation. In no case was the presence of Am(III) detected in the Am(V) solutions.

The coulometric oxidation of Am(V) was established by controlled-potential coulometry. Reduction coulograms of americium solutions that had been exhaustively electrolyzed at 0.55 V indicated that the height of the unidentified wave at −0.04 V approached one half that of the waves assigned to the Am(III)–Am(V) couple. Thus the wave at −0.04 V was tentatively assigned to the one electron reduction of Am(VI). To identify the mechanism responsible for the formation of Am(VI), the electrolyte solution containing 29.8 μg of ^{243}Am was exhaustively electrolyzed at controlled-potential (+0.4 V) to oxidize Am(III) to Am(V) and Am(VI). Immediately following the oxidation, the solution was reduced at −0.36 V to reduce the Am(VI) to Am(V). The oxidation procedure was repeated in 30 -mV increments from +0.4 to +0.55 V. The amount of Am(VI) produced at each potential was calculated from the integrated current at −0.36 V and corrected for background processes (*13*) and for the reduction of Am(VI) by water. The corrected results gave a Nernst plot with a value of 0.065 for RT/F and a half-wave potential of +0.44 V. Although these results indicate that the oxidation of Am(V) to Am(VI) was a coulometrically reversible process, the irreversible nature of the reduction process as evidenced by the potential for the Am(VI)–Am(V) wave cannot be explained at this time.

(10) G. T. Seaborg and J. J. Katz, "The Chemistry of the Actinide Elements," Methuen, London, 1957, p 358.
(11) P. Delahay, "New Instrumental Methods in Electrochemistry," Interscience, New York, N. Y., 1954, Chapter 9.
(12) Y. Israel and L. Meites, *J. Electroanal. Chem.*, **8**, 99 (1964).
(13) L. Meites and S. A. Moros, ANAL. CHEM. **31**, 23 (1959).

Reduction of Am(VI) by Water. During studies of the Am(V) oxidation process, Am(VI) solutions were observed to decompose slowly on standing; with a rate of decomposition that was greater than could be explained on the basis of self-reduction *via* radiolysis. Stokely and Shults (*3*) attribute the loss to the reduction of Am(VI) by water by a process that is first order with respect to the Am(VI) concentration. This reaction was investigated because results for the amount of Am(VI) in solution determined by controlled-potential reduction must be corrected for the reduction of Am(VI) by water.

If the loss of Am(VI) *via* reduction by water is first order in terms of the Am(VI) concentration, then the following equation for the coulometric reduction of Am(VI) can readily be derived (*13*).

$$\mathrm{Am(V)}_e = \frac{\beta}{\beta + k}\,\mathrm{Am}_t[1 - \exp - (\beta + k)t] \qquad (5)$$

In this equation, $\mathrm{Am(V)}_e$ is the amount of Am(V) produced by coulometric reduction of Am(VI), β is the rate constant for the electrochemical reduction, k is the rate constant for the reduction of Am(VI) by water, and Am_t is the total concentration of Am(VI) at the start of the electrolysis. For long electrolysis times, this equation reduces to,

$$\mathrm{Am(V)}_e = \frac{\beta}{\beta + k}\,\mathrm{Am}_t \qquad (6)$$

The ratio $\beta/(\beta + k)$ was obtained by exhaustively electrolyzing known amounts of americium at +0.56 V to produce Am(VI). The solutions were then reduced immediately at −0.36 V and the amounts of $\mathrm{Am(V)}_e$ calculated from the integrated current. The oxidation step was assumed to give essentially complete conversion of the americium to Am(VI). This assumption was justified on the basis of a small value for k as will be seen. Values for β and k were obtained in a like manner except that the Am(VI) solutions were allowed to stand for periods of up to one hour before the reduction titration was begun. The Am(VI) remaining in the solutions after known periods were calculated by Equation 5, and k was determined from the following equation for the reduction of Am(VI) by water.

$$\mathrm{Am(VI)} = \mathrm{Am}_t \exp - kt \qquad (7)$$

where Am(VI) = amount of Am(VI) remaining after standing for time = t.

Average values for β, k, and $\beta/(\beta + k)$ were 5.0×10^{-3} sec^{-1}, 2.2×10^{-4} sec^{-1}, and 0.98, respectively.

Am(VI) Correction. The amount of Am(VI) produced in recording a coulogram of the Am(III)–Am(V) wave is a function of the amount of americium in solution and the anodic potential limit for the scan. To correct the Am(III)–Am(V) wave for the amount of Am(VI) produced, a correction curve was prepared as follows:

The potential at which the wave height corresponded to 99.5% conversion of Am(III) to Am(V) was estimated from the equation for the coulometric wave by assuming that $n = 2$, $(1 - \alpha) = 0.9$, $Q_t = 0.1$ coulomb and that the apparent half-wave potential occurred where $Q_a = Q_t/2$. The remaining parameters are given on Figure 2. The result of +0.40 V was consistent with that obtained for a Nernst plot of the data from a coulogram of the Am(III)–Am(V) wave. Thus solutions containing from 7.4 to 59.6 μg of americium were scanned to +0.4 V and the amounts of Am(VI) thus produced determined by reduction at controlled-potential at −0.36 V. When corrected for a blank titration and for the reduction of Am(VI) by water, the results were conveniently expressed by the following equation.

Table I. Coulometric Determination of Americium

Sample, 1/10 dilution of ^{243}Am solution

Sample size μl	No. of titrations	Am taken, μg	Am found μg(av)	Am found μg/ml(av)
50	4	7.5	7.4	148
100	4	14.9	14.9	149
150	3	22.4	22.6	150
200	5	29.8	30.0	149
250	2	37.3	37.1	148
300	1	44.7	44.0	147
400	1	59.6	59.2	148
			σ = 0.46 μg	148

$$\text{Correction, } mQ = 0.3 + 10^{(0.023H - 1.15)}$$

where H = observed wave height at +0.4 V, millicoulombs.

This equation was used to correct the analytical data for the amounts of Am(VI) produced in recording the coulogram for the Am(III)-Am(V) oxidation.

Analytical Results. The results for the coulometric titration of ^{243}Am are given in Table I. The amount of ^{243}Am taken was calculated from the half life for ^{243}Am(*1*); the results are included for comparison purposes. The amount of ^{243}Am found was calculated from the height of the wave at +0.40 as corrected for the amount of Am(VI) produced. The standard deviation for the method was calculated by the method of least squares. The intercept of the least-squares curve was not statistically significant at the P = 0.02 level. The slope of the least-squares curve indicated an average value of 1.48 mg ^{243}Am/ml for the stock solution. This compares favorably with the value of 1.49 mg ^{243}Am/ml determined by radiochemical methods. The precision of the method at the 30-μg level was 1.5%.

Interferences. A limited study of the effect of diverse ions indicated that purification will be necessary if this technique is to be used with other than pure solutions.

Neither chloride nor nitrate interferes at 0.01*M* concentrations. However, sulfate and fluoride must be avoided. Sulfate produces an anodic shift of the Am(III)–Am(V) wave, and fluoride damages glass surfaces.

Most cations interfere; plutonium, neptunium, uranium, and ruthenium undergo redox reactions near the Am(III)–Am(V) wave. Iron precipitates and scavenges some of the americium. Curium and other radioelements interfere because radiolysis products contribute to the background processes.

ADDENDUM

Since the completion of this study, pertinent papers by Laitinen, Vincent, and Bednarski (*14*) and Strojek and Kuwana (*15*) have been published concerning the response of the tin oxide electrodes. Laitinen (*14*) and workers report peaks in the current-potential curves at the tin oxide electrode

(14) H. A. Laitinen, C. A. Vincent, and T. M. Bednarski, *J. Electrochem. Soc.*, **115**, 1024 (1968).
(15) J. W. Strojek and T. Kuwana, *J. Electroanal. Chem.*, **16**, 471 (1968).

(CGE) which they attribute to the charging and discharging of surface states (oxidation and reduction of surface tin atoms containing protonated oxide ions). In this study, such a charge-discharge process is estimated to have produced waves on the background scans equivalent to 3 to 20 millicoulombs. However, no such waves were observed, indicating either that the process was insignificant in this instance ($<2 \times 10^{-5}$ coul/cm^2), or that the peaks were outside the selected working range.

Strojek and Kuwana (*15*) report an interesting "pH effect" for the ferrocyanide–ferricyanide system at the tin oxide electrode (CGS) which they attribute to the properties of the semiconductor surface. Although the pH range of this study was too narrow (pH 10 to pH 12) to show this effect, we have observed that the Np(V)–Np(VI) couple is coulometrically reversible at the CGE in 0.1*M* NaOH.

ACKNOWLEDGMENTS

The author is indebted to Dr. L. C. Brown and Dr. H. P. Holcomb who provided the ^{241}Am and ^{243}Am solutions, respectively, and to D. A. Brown for counting data. The cooperation of R. H. Searle in preparing the CGE is acknowledged.

RECEIVED for review November 25, 1968. Accepted March 17, 1969. The information contained in this article was developed during the course of work under Contract AT(07-2)-1 with the U. S. Atomic Energy Commission.

Adsorption of Organic Molecules at a Carbon Paste Electrode

Eugene P. Meier and James Q. Chambers

Chemistry Department, University of Colorado, Boulder, Colo. 80302

The specific adsorption of the diphosphate ester of 2-methylnaphthohydroquinone at a carbon paste electrode has been determined using the techniques of linear potential sweep voltammetry and chronocoulometry. This adsorption process was studied as a function of concentration, electrode potential, solution pH, and buffer composition. The adsorption is maximum in acidic solutions, attaining a limiting value of 1.9×10^{-10} mole/cm^2 in 1*M* H_2SO_4 at potentials between 0.0 and +0.6 V *vs.* SCE. The adsorbed species is postulated to be the neutral molecule associated with the organic phase of the carbon paste electrode at the carbon paste/electrode interface. Mechanistic implications of these results are discussed briefly.

IN THE COURSE of an extensive study of the electrochemical oxidation of organic phosphate esters, we have been led into an investigation of adsorption effects at carbon paste electrodes. The results of this study are complete without reference to the detailed mechanism and kinetics of the electrode processes and are of interest to those who study anodic electrode reactions at various solid electrodes. Specific adsorption of an electroactive species causes electrochemical parameters such as the peak current function (*1*, *2*) and the chronopotentiometric constant (*3*, *4*) to exhibit marked positive deviations from constancy as the time scale of the experiment decreases. Hence adsorption effects must be sorted out before conclusions regarding electrode mechanisms can be made.

The system studied in this work is the oxidation of the diphosphate ester of 2-methylnaphthohydroquinone (PQP) in

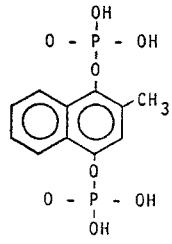

aqueous buffer solutions. Chemical oxidation of this and related compounds has been shown to produce phosphorylated species, presumably via a metaphosphate, HPO_3, intermediate which is released upon oxidation (*5*, *6*). Phosphate esters of hydroquinones have been suggested as components of model oxidative phosphorylation systems (*5*, *7*) and consequently their detailed oxidation mechanisms are of current interest. A carbon paste working electrode (*8*, *9*) was employed in this study because well-defined, reproducible current–potential curves were obtained with this electrode material. The oxidation wave of PQP occurs in the region of platinum oxidation and the current–potential curves on platinum are poorly defined. It appears that the oxidation of PQP occurs very slowly, if at all, on an oxide-covered platinum electrode.

Most examples of specific adsorption at electrode surfaces concern mercury or mercury amalgam electrodes for which the techniques of the dropping mercury electrode and the Lippman capillary electrometer are available. A review of the experimental evidence for adsorption at solid electrodes is given in the monograph by Delahay (*10*). Surface and adsorption effects at carbon paste electrodes have been indicated in the literature (*11*, *12*), but there are no clear examples of specific adsorption. Chambers and Lee (*13*) have shown that electroactive species can be extracted into the

(1) R. A. Osteryoung, G. Lauer, and F. C. Anson, *J. Electrochem. Soc.*, **110**, 926 (1963).
(2) R. H. Wopschall and I. Shain, ANAL. CHEM., **39**, 1514 (1967).
(3) W. Lorenz, *Z. Elektrochem.*, **59**, 730 (1955).
(4) W. H. Reinmuth, ANAL. CHEM., **33**, 322 (1961).
(5) V. M. Clark, G. W. Kirby, and A. R. Todd, *Nature*, **181**, 1650 (1958).
(6) V. M. Clark, D. W. Hutchinson, G. W. Kirby, and A. Todd, *J. Chem. Soc.*, 715 (1961)
(7) V. M. Clark and D. W. Hutchinson, *Progr. Org. Chem.*, **7**, 75 (1968).
(8) R. N. Adams, ANAL. CHEM., **30**, 1576 (1958).
(9) C. Olson and R. N. Adams, *Anal. Chim. Acta*, **22**, 582 (1960).
(10) P. Delahay, "Double Layer and Electrode Kinetics," Interscience, New York, 1965, Chapters 6 and 10.
(11) T. A. Miller, B. Lamb, K. Prater, J. K. Lee, and R. N. Adams, ANAL. CHEM., **36**, 418 (1964).
(12) C. A. Chambers and J. Q. Chambers, *J. Amer. Chem. Soc.*, **88**, 2922 (1966).
(13) C. A. H. Chambers and J. K. Lee, *J. Electroanal. Chem.*, **14**, 309 (1967).

organic phase of a carbon paste electrode and can then be electrolyzed at the electrode/solution interface.

In this paper the specific adsorption of PQP at a carbon paste electrode has been determined quantitatively using the techniques of linear potential sweep voltammetry and chronocoulometry (*14*). The PQP adsorption has been studied as a function of concentration, electrode potential, solution pH, and buffer composition. The adsorption is maximum in acid solutions, attaining a limiting value of 1.9×10^{-10} mole/cm^2 in 1*M* H_2SO_4 at potentials less than +0.6 V *vs.* SCE. The adsorbed species is postulated to be the neutral PQP molecule associated with the organic phase of the carbon paste electrode at the carbon paste/solution interface.

EXPERIMENTAL

Apparatus. The instrumentation for the potential sweep voltammetry has been described (*15*). The potentiostat which was used in this study is based on a design of Brown *et al.* (*16*) and provides for compensation of the *iR* drop between the tip of the reference electrode and the working electrode input. The chronocoulometry plug-in board for integration of the current–time signal was similar to the design of Christie *et al.* (*17*).

The preparation of the carbon paste electrode surfaces has been described (*12*). White bond No. 40 powder paper which gave good reproducible surfaces was used to finish the electrode surfaces. A Bausch and Lomb measuring magnifier was used to determine electrode diameters. The electrodes used in this study had areas of 0.763, 0.349, and 0.113 cm^2. The large platinum gauze counter electrode was immersed directly in the test solution. All potentials were measured *vs.* a saturated calomel reference electrode.

Materials. The diphosphate ester derivative of naphthohydroquinone, PQP, was a gift from Hoffman LaRoche, Inc., and was used without further purification. It was supplied as the tetrasodium salt and contained a nonstoichiometric amount of water. By drying under vacuum to constant weight, the water content could be reduced to that of the dihydrate (*18*). All PQP samples were standardized by an acid–base titration. Analysis of the titration curves indicated that $pK_{a1} \simeq pK_{a2} \simeq 2.88$ and $pK_{a3} \simeq pK_{a4} \simeq 6.65$.

Buffer solutions were prepared from triply-distilled water and reagent grade chemicals. The solutions were composed of various combinations of acetic, chloroacetic, phosphoric, and boric acids, each at a concentration of 0.02*M*. The supporting electrolyte was $NaClO_4$ which was twice recrystallized from water. A standardized, concentrated $NaClO_4$ solution was used to prepare the stock buffer solutions.

Procedures. All procedures were standard. Prepurified nitrogen, saturated with water vapor, was bubbled through the buffer solutions prior to dissolution of a weighed amount of PQP. The acidic PQP solutions were found to be stable up to 24 hours. A fresh electrode surface was prepared for each experiment and each experiment was performed in duplicate or triplicate. The temperature was 24 ± 2 °C.

The coulomb–time oscilloscope traces were measured by hand and analyzed according to the integrated Cottrell equation (*14*).

$$Q = Q_{d.l.} + Q_{ads.} + \frac{2\,nFACD^{1/2}}{\pi^{1/2}}\,t^{1/2} \qquad (1)$$

In this equation $Q_{d.l.}$ represents the coulombs required to charge the double layer, $Q_{ads.}$ is the coulombs required to electrolyze adsorbed materials, Q is the total coulombs passed, and the other terms have their usual significance. Because the overall electrode process was irreversible, care was taken to make sure that the potential step was in the diffusion limiting-current region of the PQP oxidation wave (*17*).

The basic assumption in using single step chronocoulometry to measure adsorption quantitatively is that the difference in specific charge on the electrode, $Q_{d.l.}$, is invariant in the presence and absence of the electroactive species. For the high concentrations of supporting electrolyte employed in this study, $Q_{d.l.}$ is expected to be independent of the amount of specifically adsorbed PQP to a first approximation. Support for this assumption is afforded by chronocoulometric studies which show that the charge on a mercury electrode is changed relatively little by adsorption of an anthroquinone monosulfate (*19*) or uncharged cadmium halide complexes (*20*). Several experiments were performed in which $Q_{d.l.}$ was measured at pH 1.90 in the presence and absence of PQP for potential steps below the oxidation wave of PQP. The change in $Q_{d.l.}$ was ca. + 2 μC/cm^2 at these potentials. This amounts to less than 5% of the measured $Q(t = 0)$ at this pH. The analysis is complicated further by the possible adsorption of the electrode product, the uncharged naphthoquinone molecule, which might change $Q_{d.l.}$ slightly. However, in view of the difficulties—*i.e.*, the proximity of the PQP oxidation wave to solvent decomposition processes and the use of carbon rather than mercury electrodes—and the significance of adsorption studies to an understanding of electrode processes at solid electrodes, an uncertainty of 5 to 10% in the surface concentrations is tolerable.

The values of $\Gamma_{ads.}$ were not a strong function of ionic strength. All measurements reported in this work were obtained in 0.500*M* $NaClO_4$. The surface concentrations were also independent of the electrode immersion time in solution (1 to 200 sec). This implies that the adsorption equilibrium is established rapidly. All measurements were made after the electrodes had been in solution for ca. 2 minutes.

The precision of these measurements is $\pm 0.08 \times 10^{-10}$ mole/cm^2 at the 95% confidence level. This interval was obtained by analysis of a large sample of the experimental data.

RESULTS

The oxidation of PQP proceeds in an overall irreversible two-electron step to produce 2-methyl-1,4-naphthoquinone, Q. The phosphate which is released probably appears either as inorganic ortho- or pyrophosphate (*5, 6, 21*)

$$\text{PQP} \xrightarrow{-H_2O} \text{Q} + \text{P-O-P} + 2\,e^- \qquad (2)$$

The production of Q was established by cyclic voltammetry and is analogous to the behavior of the monophosphate derivative (*12*). A detailed kinetic analysis is not required to obtain Γ_{ads} from the chronocoulometry experiment; only the overall number of electrons, *n*, transferred per PQP molecule is needed.

(14) F. C. Anson, ANAL. CHEM., **38**, 54 (1966).
(15) J. Q. Chambers, A. D. Norman, M. R. Bickell, and S. H. Cadle, *J. Amer. Chem. Soc.*, **90**, 6056 (1968).
(16) E. R. Brown, T. G. McCord, D. E. Smith, and D. D. DeFord, ANAL. CHEM., **38**, 1119 (1966).
(17) J. H. Christie, G. Lauer, and R. A. Osteryoung, *J. Electroanal. Chem.*, **7**, 60 (1964).
(18) T. F. Fieser and E. M. Fry, *J. Amer. Chem. Soc.*, **62**, 228 (1940).
(19) F. C. Anson and B. Epstein, *J. Electrochem. Soc.*, **115**, 1155 (1968).
(20) F. C. Anson and D. J. Barclay, ANAL. CHEM., **40**, 1791 (1968).
(21) R. D. Dallam and L. H. Chen, *Arch. Biochem. Biophys.*, **123**, 565 (1968).

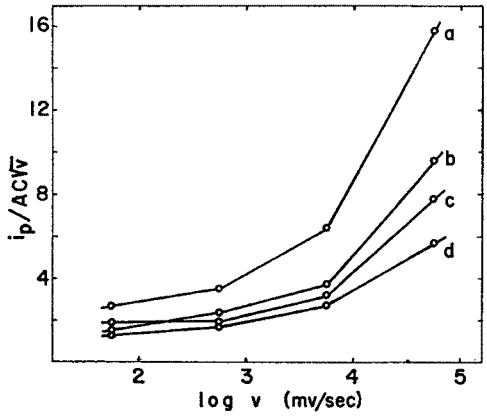

Figure 1. Linear potential scan chronoamperometric current function data for PQP in 1*M* H_2SO_4

(a) **0.23 × 10^{-3}*M*, *(b)* 0.46 × 10^{-3}*M*, *(c)* 1.01 × 10^{-3}*M*, and *(d)* 1.57 × 10^{-3}*M* PQP. The units of $i_p/AC\sqrt{v}$ are amp, cm^{-2}, M^{-1}, $(V/sec)^{-1/2}$**

Cyclic Voltammetry. In acidic solutions and at slow sweep rates (<1 V/sec) cyclic voltammograms of PQP solutions are very similar to those of the monophosphate derivative (*12*) except that the main oxidation wave occurs at *ca.* 550 mV more positive potentials. As the sweep rate increases or the concentration of PQP decreases, the value of the experimental equivalent of the current function, $i_p/A\ C\sqrt{v}$, increases markedly. This behavior is shown in Figure 1. Both effects are indicative of adsorption of PQP (*2*). At fast sweep rates the PQP oxidation wave consists of two overlapping peaks separated by approximately 50 mV. At low concentrations of PQP—*e.g.*, 0.2 × 10^{-3} *M*—the oxidation wave contains a relatively large contribution from the more positive peak current. As the concentration is increased, the relative height of the initial peak increases. A quantitative analysis is difficult because of the overlap of the two peaks; however, this behavior is consistent with an adsorption effect. For reversible electron transfer, adsorption of the electroactive species will give rise to a postwave provided the adsorbed species does not inhibit electron transfer from the nonadsorbed species to the electrode (*2*). If the *initial* electron-transfer step in the PQP oxidation is reversible, the two peaks can be explained by invoking an adsorption postwave for the oxidation of (PQP) ads.

Chronocoulometry. The advantages of this technique for the detection of adsorbed species in electrode processes are well known (*14*, *22*). Figure 2 shows a typical experiment demonstrating the presence of adsorbed PQP. Because the electrode process is irreversible, only the initial anodic potential step gives useful information. The value of Q_{rev} (see Figure 2) was found to be time independent and in general was less than the value of $Q_{d.l.}$ determined in the absence of PQP. Evidently, adsorption of the oxidation product (see below) has changed the double layer capacity.

The faradaic charge evident in the background process (curve *b*) cannot be eliminated in practice because the potential must be stepped close to the solvent decomposition potential in order to be in the diffusion-controlled region of the PQP oxidation process.

(22) R. Koopman, *Ber. Bunsenges. Phys. Chem.*, **72**, 32 (1968).

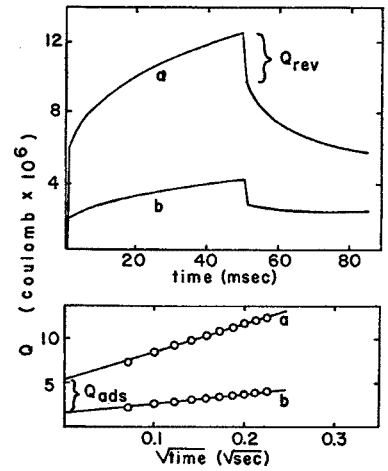

Figure 2. Charge-time curves for a potential step from 0.000 to 1.258 V *vs.* SCE

(a) **0.24 × 10^{-3}*M* PQP in 1*M* H_2SO_4, *(b)* 1*M* H_2SO_4. In this example the potential is stepped back into the region of Q reduction**

It was found that PQP is adsorbed to a significant amount only in acidic solutions. The Γ_{ads}–pH curve is shown in Figure 3. These data were obtained with several different compositions of the buffer solutions. Neither the substitution of chloroacetic acid for acetic acid nor the use of sulfuric acid markedly changed the value of Γ_{ads}. Thus the solution pH is the principal parameter which governs the adsorption of PQP from solution and as PQP is protonated it becomes more-strongly specifically adsorbed at the electrode surface.

Adsorption isotherms at two representative pH values, 1*M* H_2SO_4 and pH 1.90, are shown in Figure 4. The limiting value of Γ_{ads} in 1*M* H_2SO_4 corresponds to 90 A^2 per adsorbed PQP molecule at potentials more negative than 0.6 V *vs.* SCE. A rough calculation of the molecular area of the fully pro-

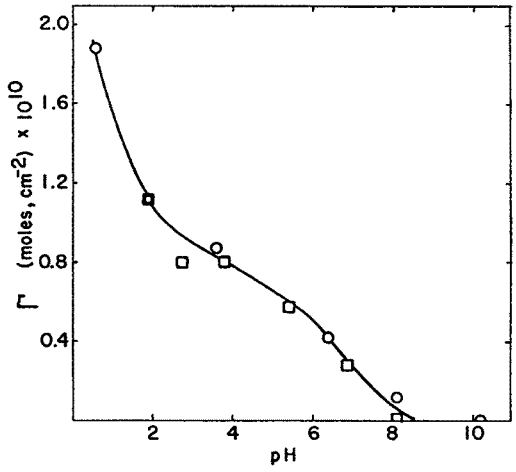

Figure 3. Variation of Γ with solution pH for *E* less than 0.6 V *vs.* SCE

Circles (○) and squares (□) are data for buffer solutions prepared with acetic and chloroacetic acid, respectively

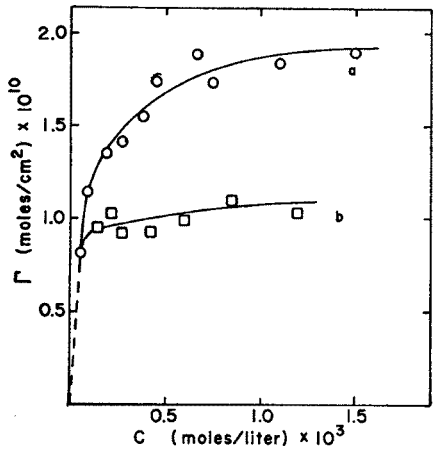

Figure 4. Adsorption isotherms of PQP in (*a*) 1*M* H_2SO_4 and (*b*) pH 1.90

The potential was stepped from 0.000 to 1.330 V *vs.* SCE for (*a*) and from 0.700 to 1.294 V *vs.* SCE for (*b*)

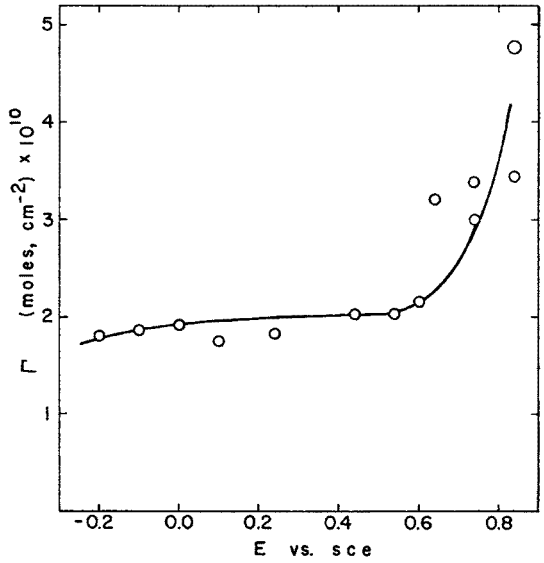

Figure 5. Variation of Γ_{ads} with electrode potential in 1*M* H_2SO_4

tonated PQP molecule indicates that this is a reasonable value for complete monolayer coverage of the electrode surface by adsorbed PQP, assuming that the naphthalene ring is parallel to the electrode surface and that the surface roughness factor factor is unity. In pH 1.90 solutions the amount adsorbed is constant over the concentration range from 0.1 to 1.6 $\times 10^{-3}M$. A plot of Γ_{ads} *vs.* E for 1*M* H_2SO_4 is shown in Figure 5. The surface concentration is constant up to *ca.* 0.6 V *vs.* SCE and then increases rapidly at potentials before the foot of the oxidation wave. This increase probably reflects the inherent surface roughness of a carbon paste electrode. An exhaustive study of the adsorption isotherms at different potentials was not carried out.

There is also evidence that the product of the oxidation process, 2-methyl-1,4-naphthoquinone, is adsorbed at the electrode surface. The experimental current functions for the quinone, Q, reduction wave and the hydroquinone, QH_2, oxidation wave observed in the cyclic voltammograms of PQP in 1*M* H_2SO_4 exhibit marked increases at fast sweep rates. These increases parallel the increase of the current function of the main oxidation wave. Double potential step chronocoulometry data either on solutions of Q or on carbon paste electrodes doped with Q (*13*, *23*) and immersed in background solution indicate that Q and QH_2 are not adsorbed in a significant amount from the bulk of the solution.

DISCUSSION

Carbon paste electrodes have the novel property of extracting some substances from aqueous solution into the organic phase of the electrode itself (*13*, *23*, *24*). Electroactive species in the organic phase—*i.e.*, Nujol in this study—can then be electrolyzed at the carbon paste/solution interface by discharge of cations or anions into the aqueous solution concurrent with uptake or discharge of electrons from the graphite particles. Therefore, if a species is specifically adsorbed at a carbon paste electrode, it can reside either on the electrode or the solution side of the electrode/solution interface. The results of this study suggest that the adsorbed PQP species is associated with the Nujol layer at the electrode surface.

The pH dependence of Γ_{ads} is consistent with the adsorption of the uncharged PQP molecule. Interaction of the π cloud of aromatic molecules with positive charge on the electrode surfaces accounts for specific adsorption of aromatic compounds at metallic electrodes (*10*, p 25). An interaction of this type is possible for the naphthalene ring of PQP regardless of the protonation state of the phosphate substituents. Because PQP is specifically adsorbed only in acidic regions, an additional factor must be involved in the adsorption process. The shape of the Γ_{ads} *vs.* pH curve (Figure 3) can be understood if one assumes that the phosphate ester is extracted into the organic phase. Thus the adsorbed species is suggested to be the neutral PQP molecule, associated with the Nujol layer at the electrode/solution interface, and positioned so that the naphthalene ring is parallel to the electrode surface. Adsorption effects of this type are likely to be observed when uncharged aromatic compounds are oxidized at carbon paste electrodes.

The behavior of the current functions for the quinone and hydroquinone waves indicates that the oxidation product is slowly desorbed from the electrode surface. In support of this conclusion is the cyclic voltammetric behavior of a carbon paste electrode prepared with Nujol doped with 2-methylnaphthoquinone at an approximately 1-*mM* level. When this electrode is immersed in a background buffer solution, the peak heights for the reversible Q/QH_2 couple decrease steadily with time.

The equilibria which are coupled to the electrode process proper are summarized in the following scheme.

$$(PQP^{2-})_{soln} \xrightarrow{\text{diffusion}} (PQP^{2-})_{x=0} \quad (3a)$$

$$(PQP^{2-})_{x=0} + 2H^+ \rightleftharpoons (PQP^{\circ})_{x=0} \quad (3b)$$

$$(PQP^{\circ})_{x=0} \rightleftharpoons (PQP^{\circ})_{ads} \quad (3c)$$

$$(PQP^{\circ})_{ads} \xrightarrow{-2e^-} (Q)_{ads} \quad (3d)$$

(23) T. Kuwana and W. G. French, ANAL. CHEM., **36**, 241 (1964).
(24) D. G. Davis and M. E. Everhart, *ibid.*, **36**, 38 (1964).

$$(Q)_{ads} \rightleftharpoons (Q)_{x=0} \quad (3e)$$

$$(Q)_{x=0} \xrightarrow{\text{diffusion}} (Q)_{soln} \quad (3f)$$

Equation 3a represents the mass transport step, Equations 3b and 3c are equilibria involved in the adsorption of the uncharged PQP molecule, Equation 3d represents the overall electron transfer step (not balanced), and Equations 3e and 3f indicate that the adsorbed quinone is desorbed and diffuses into the bulk of the solution.

The peak voltammetry experiments most conclusively indicate that adsorbed PQP participates in the charge transfer step. For an adsorption postwave to occur, PQP must not desorb from the electrode surface in the time required to sweep the potential through the oxidation wave. Because the postwave is first observed at ca. 1 V/sec, this time is in the range of 5×10^{-2} to 5×10^{-4} sec. This scheme is not meant to imply that the oxidation pathway must proceed via an adsorbed species. Indeed, in the potential region of diffusion control, the concentration of PQP at $x = 0$ will be zero, Equation 3c will be driven to the left, and PQP which reaches the electrode by diffusion will be oxidized at $x = 0$. Thus the oxidation process is distributed between two pathways. A subsequent paper will discuss the effect of the adsorption equilibria on the electrochemical oxidation of PQP at carbon paste electrodes.

RECEIVED for review October 11, 1968. Accepted March 26, 1969. Work supported by U. S. Public Health Service Grant No. 5 R01 GM14815-02.

Optimizing Concentration Determinations in the Presence of Maxima and Catalytic and Kinetic Waves Using the Vibrating Dropping Mercury Electrode

Richard E. Cover and James G. Connery

Department of Chemistry, St. John's University, Jamaica, New York 11432

Studies with the vibrating dropping mercury electrode (VDME) at different vibrational frequencies demonstrate that the VDME is significantly superior to the DME for most analytical purposes. At a frequency of 210 Hz (drop times about 5 msec), maxima of the first and second kinds are suppressed at the VDME without the addition of surfactants. Catalytic and kinetic currents can also be minimized or eliminated at the VDME at this frequency. In addition, the VDME permits the analysis of agitated solutions.

THE VIBRATING DROPPING MERCURY electrode (VDME) consists essentially of a dropping mercury electrode (DME) in which the drop rate is controlled by periodic mechanical shock or vibration of the electrode. Such premature drop detachment has been used over the last twenty years for a variety of purposes—e.g., to permit the analysis of agitated solutions (*1–3*), to synchronize the dropping of multiple capillaries (*4–5*), to permit higher voltage scan rates (*6–8*), and in oscillographic polarography (*9*).

The work reported here demonstrates that for most analytical purposes, the VDME is significantly superior to the DME. Plateau irregularities such as maxima of the first and second kinds are frequently observed with the DME, complicating or preventing the collection of useful data. The use of surfactants for the control of these irregularities is highly empirical and can result in the total suppression of polarographic waves (*10*). Furthermore, the search for a useful maximum suppressor for a given system can be very time-consuming and, often, unsuccessful. At the VDME, under proper conditions, these plateau irregularities are not observed. Useful data can thus be obtained without recourse to surfactants.

Waves are frequently observed at the DME which are related to bulk concentrations in a complex, nonlinear manner. These waves, common especially in organic polarography, reflect the occurrence of catalytic, kinetic, or adsorption phenomena. They are generally not reliable for analytical purposes and, indeed, can obscure useful analytical data. No general technique is available that permits elimination of such nonlinear data from DME output. Proper use of the VDME can minimize the occurrence of such nonlinear response and frequently eliminate it entirely.

Finally, the adsorption of species from solution on the DME surface can inhibit electrode reaction, obscuring useful data. Under the proper conditions at the VDME, such inhibition can often be eliminated and analytical data obtained. Various adsorption complications will be discussed in a subsequent paper.

The prime experimental variable which permits the control of these phenomena with any given capillary is the frequency of vibration of the electrode. The relationships between currents observed for the various phenomena and the more fundamental parameters such as drop time and rate of mercury flow are currently under investigation and will be reported in a separate paper. These relationships are quite complex—*e.g.*, the number of drops per cycle varies from about to 0.25 at 42 Hz to 1.0 at 210 Hz. In the experiments reported here, then, the drop time reached a lower limit of about 5 msec at a vibrational frequency of 210 Hz.

(1) D. A. Berman, P. R. Saunders, and R. J. Winzler, ANAL. CHEM., **23**, 1040 (1951).
(2) P. W. Carr and L. Meites, *J. Electroanal. Chem.*, **12**, 373 (1966).
(3) J. G. Connery and R. E. Cover, ANAL. CHEM., **40**, 87 (1968).
(4) S. Stankoviansky, *Chem. Zvesti*, **2**, 133 (1948); *Chem. Abstr.*, **43**, 8946f (1949).
(5) V. A. Tsimmergakl, *Zavod. Lab.*, **15**, 1370 (1949); *Chem. Abstr.*, **44**, 3817b (1950).
(6) V. G. Mairanovskii, *Zavod. Lab.*, **31**, 1187 (1965); *Chem. Abstr.*, **64**, 3049b (1966).
(7) S. Wolf, *Angew. Chem.*, **72**, 449 (1960).
(8) D. Wolf, *J. Electroanal. Chem.*, **5**, 186 (1963).
(9) J. Horyna and V. Jehlicka, *Collect. Czech. Chem. Commun.*, **27**, 1326 (1962).
(10) L. Meites and T. Meites, *J. Amer. Chem. Soc.*, **73**, 177 (1951).

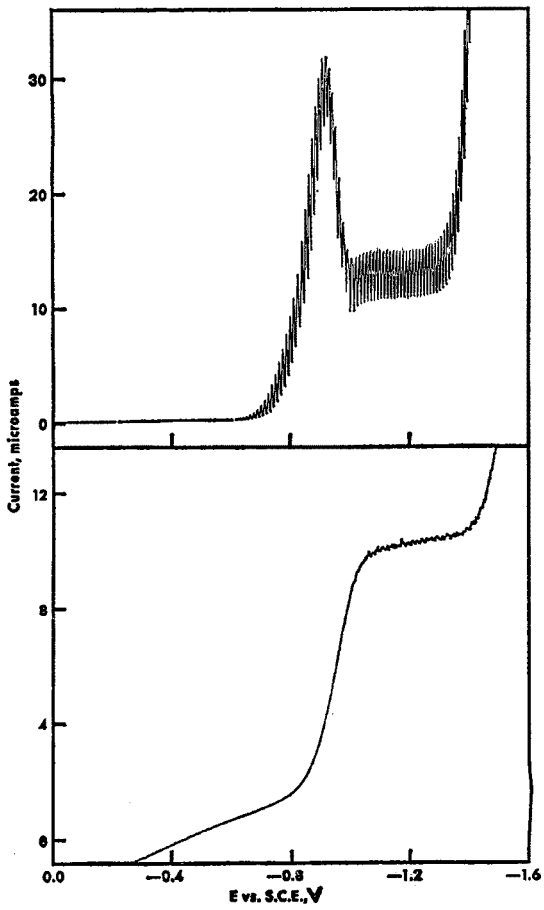

Figure 1. Elimination of a maximum of the first kind at the VDME

4.00m*M* Cr(III), 0.100*M* $NaClO_4$, pH 3.10
Top: DME, mercury pressure 60 cm. Bottom: VDME, 210 Hz, mercury pressure 160 cm

EXPERIMENTAL

Apparatus. Our electrode vibrator differed essentially from previously used equipment in two respects: (a) the motion of the electrode was constrained to linear movement in the plane of the cut end of the capillary and (b) the frequency of vibration was continuously variable and precisely controllable over a wide range.

A variable-speed motor with tachometer feedback was used to power a gear train with an output/input ratio of 4/1. The output shaft of the gear train had a radius of eccentricity of 0.18 mm. The eccentric was linked to a reciprocating shaft which transmitted the motion to the electrode.

All polarograms and voltammograms were recorded with a Sargent Model (XV) Polarograph. No damping was used in obtaining any of these data beyond that inherent in the recorder. The cell used was of the Meites type (Sargent No. S-29396).

Prepurified nitrogen scrubbed with chromous chloride solution and subsequently with water was used for deaeration and for blanketing the solution after deaeration. All potentials in this work were referred to the saturated calomel electrode. All measurements were made at 25.00 ± 0.05 °C.

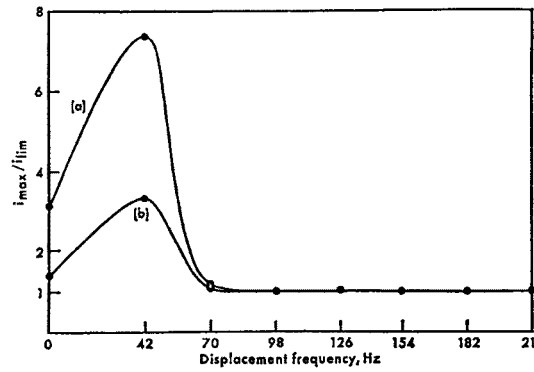

Figure 2. Relative heights of maximum of the first kind to limiting current at the VDME

4.00m*M* Cr(III), 0.100*M* $NaClO_4$, pH 3.10, mercury pressure (a) 60 cm, (b) 160cm. Also see Figure 8

Table I. Analyses Possible with the VDME[a]

Determinable	Concentration range	Medium	Relative standard deviation
Os(VI)[b,c]	0–9.0m*M*	10.0*M* NaOH	±0.75%
U(VI)[b,d]	0.04–0.7m*M*	0.1*M* $HClO_4$ 0.3*M* $NaClO_4$	±5.%
Cr(III)	0.1–10.0m*M*	0.1*M* $NaClO_4$ pH = 3.1	±0.2%
Cd(II)	0.1–10.0m*M*	Saturated KCl	±0.2%
Quinine	0.02–1.0m*M*	5.0m*M* HCl 1.00*M* NaCl	±0.7%

[a] All data were obtained amperometrically.
[b] Data were obtained in agitated solutions.
[c] Reference (*3*).
[d] Reference (*2*).

Reagents. All reagents used were Mallinckrodt, Baker, or Alfa Inorganics reagent grade.

RESULTS AND DISCUSSION

Plateau Irregularities. Maxima of the first and second kinds are phenomena of very frequent occurrence which, like experimental error, are appreciated only when absent. The causes of these phenomena seem to have been identified (*11*) and their control with maximum suppressors is, at times, effective.

Maxima of both kinds can be controlled at the VDME at sufficiently high vibrational frequencies. Figures 1 through 4 demonstrate these effects on maxima of the first kind. The maximum on the Cr(III) wave in $NaClO_4$ is clearly eliminated when the electrode is vibrated at 210 Hz (Figure 1). The effect of varying the frequency on the maximum is shown in Figure 2, where, i_{max} is the peak current of the maximum and i_{lim} is the limiting current due to the normal reduction of Cr(III). The ratio of these two current terms quickly approaches unity above 70 Hz showing control of this maximum over a fairly wide range of frequencies. This is substantiated by the analytical data for this system in Table I.

(11) L. Meites, "Polarographic Techniques," Second ed., Interscience Publishers, New York, N. Y., 1965, pp 303–332.

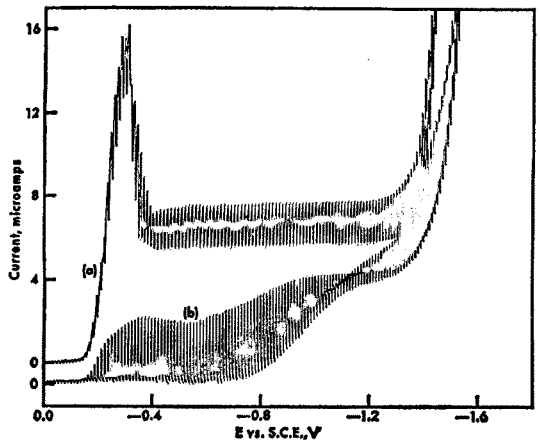

Figure 3. Effect of Triton X-100 on the polarography of Cu–EDTA

1.0m*M* Cu(II)–EDTA, 9.0m*M* EDTA, 0.1*M* Tartrate buffer, pH 3.5. Mercury pressure 60 cm. Triton X-100 (a) 0% (b) 0.009%

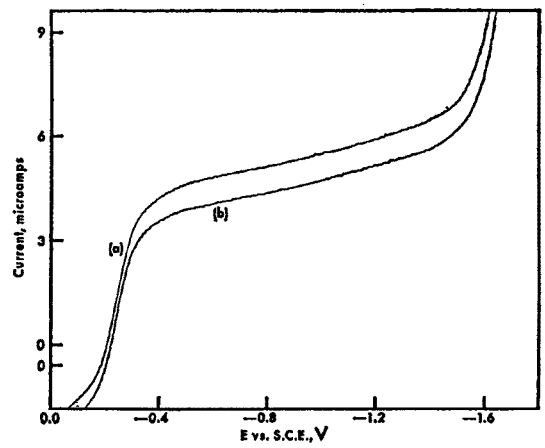

Figure 4. Voltammetry of Cu–EDTA at the VDME

1.0m*M* Cu(II)–EDTA, 9.0m*M* EDTA, 0.1*M* tartrate buffer, pH 3.5, VDME, mercury pressure 160 cm, 210 Hz, Triton X-100 (a) 0% (b) 0.009%

At frequencies below 70 Hz, the ratios of these current terms go through maxima. This cause of this phenomenon is not clear but our facts are consistent with the observation of Meites (*11*) that maxima of the first kind are accentuated by decreasing drop time, a condition approximated at the VDME as the frequency increases from zero.

The decrease in the ratio of the current terms with increasing mercury pressure reflects the occurrence of "the inversion of the maximum" (*12*). As the mercury pressure is increased in this system, the acute maximum of the first kind decreases because of formation of a maximum of the second kind. The resulting polarograms are qualitatively very similar to those given by Heyrovsky and Kuta for oxygen in 0.01*M* KCl.

Similar control of another maximum of the first kind is shown by the data in Figures 3 and 4 for the Cu(II)–EDTA complex in a tartrate buffer, a system investigated by Schmid and Reilley (*13*). In contrast to their observations, we obtain a sharp maximum at the DME in the absence of maximum suppressor. The addition of rather large amounts (0.009%) of Triton X-100 results in gross distortion of the polarogram. Large currents are still observed although the data are analytically useless. The current–time curves of the individual drops show the spiked behavior characteristic of electrode reactions inhibited by the adsorption of surface-active substances (*13, 14*).

The voltammetric VDME data obtained for this system at 210 Hz (Figure 4) show (a) that the maximum can be completely eliminated at the VDME and (b) that the VDME data are not affected in any detectable way by the presence of the Triton X-100. This last effect will be discussed in a subsequent paper.

Control of maxima of the first kind has been demonstrated as well for both lead and nickel in KCl solutions. It must be made clear that this control of maxima is achieved only with the loss of some sensitivity. As can be seen from curve (a) in Figure 8, at a constant mercury column height, the limiting current for a purely mass-transfer controlled wave decreases to about 1/3 of the polarographic value at 210 Hz.

Figure 5 contains data obtained for Cd(II) in saturated KCl solution. This system was studied since it exhibits a pronounced maximum of the second kind at the DME. As can be seen, vibration of the electrode at 210 Hz results in a complete suppression of this maximum and permits the collection of reliable analytical data (see Table I).

It has been demonstrated for maxima of both kinds that when they are observed, streaming of the solution past the drop surface occurs (*15*). The maximum of the first kind is said to be caused by asymmetry of the electrical field around the drop while the maximum of the second kind is attributed to turbulence within the drop arising from the flow of mercury into it.

Because maxima of both kinds are associated with vertical convection of the solution, one might theorize that the high degree of horizontal convection prevents observation of these phenomena at the VDME. This explanation seems unlikely in the light of the data obtained by Kolthoff and coworkers (*16, 17*) for the rotating dropping mercury electrode (RDME).

At the RDME, the velocity of the capillary tip was in the range of 11 to 31 cm/sec while the mean velocity of the VDME at 210 Hz is 7.46 cm/sec. Maxima of the second type were frequently observed at the RDME but neither kind of maxima was detected by the VDME. The relatively large mercury flow rates at the RDME no doubt contributed to the occurrence of maxima of second type. Maxima of the first kind were not reported to occur at the RDME, probably because the tips of the capillaries used were tapered, thus minimizing asymmetry in the electrical field around the drop.

(12) J. Heyrovsky and J. Kuta, "Principles of Polarography," Academic Press, New York, N. Y., 1966, p 457.
(13) R. W. Schmid and C. N. Reilley, *J. Amer. Chem. Soc.*, **80**, 2087 (1958).
(14) J. Kuta and I. Smoler in "Progress in Polarography," P. Zuman and I. M. Kolthoff, Eds., Interscience Publishers, New York, N. Y., 1962, pp 60–61.
(15) V. G. Levich, "Physicochemical Hydrodynamics," Prentice-Hall, Inc., Englewood Cliffs, N. J., 1962, pp 561–589.
(16) W. Stricks and I. M. Kolthoff, *J. Amer. Chem. Soc.*, **78**, 2085 (1956).
(17) Y. Okinaka and I. M. Kolthoff, *ibid.*, **79**, 3326 (1957).

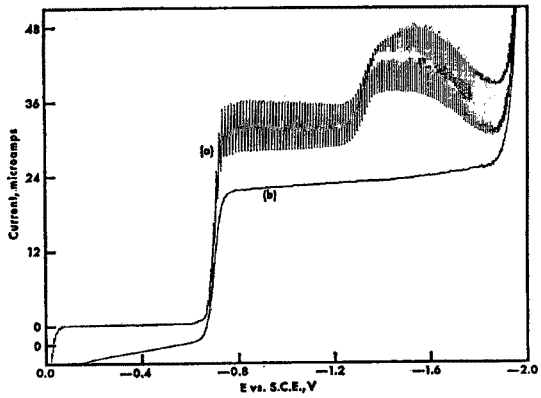

Figure 5. Elimination of maximum of the second kind at the VDME

4.00m*M* Cd(II), saturated KCl
(a) DME, mercury pressure 60 cm
(b) VDME, mercury pressure 160 cm, 210 Hz

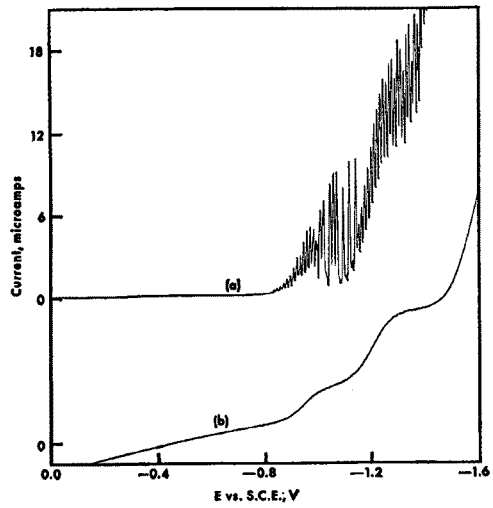

Figure 6. Elimination of plateau irregularities at the VDME

0.20mm each of Cr(III) and EDTA in 50 ml 0.100*M* $NaClO_4$, pH 3.60
(a) DME, mercury pressure 60 cm (b) VDME, mercury pressure 160cm, 210 Hz

It seems likely, then, that the fundamental property of the detector which prevents the observation of maxima at the VDME is its extremely short drop life. At 210 Hz, where all maxima are suppressed, the drop life is about 5 msec. At the RDME, drop life was in the 1 to 10 sec range. Apparently, at the VDME, the drop life is so short that no detectable vertical convection can occur during this small time interval. This conclusion is similar to that reached by Rao, Suryanarayana, and Doss (*18*) in their work on the effect of ultrasonic irradiation on polarographic maxima. Wolf (*7*) reported that for oxygen in KCl solutions, maxima of the second type were not observed at the VDME but maxima of the first kind were still found. These data probably reflect the fact that his drop life was 0.6 sec, lower than normal drop times but not sufficiently short to suppress maxima of the first kind.

All too frequently other types of plateau irregularities are observed which are highly erratic and serve merely to obscure useful data. A typical case is shown in curve (a) of Figure 6. Traditionally, people have sought to eliminate such undesirable response by adding a maximum suppressor to the system, a gambit which was unsuccessful in this case. At the VDME, however, two well-defined waves are resolved. The first wave at about −0.9 V is due to the reduction of the aquo–chromium ion (see Figure 1) while the second wave at about −1.2 V is due to the reduction of a Cr–EDTA intermediate. The data in Figure 6 were obtained within 20 minutes of the addition of EDTA to the chromium solution.

Several conclusions can be obtained from amperometric data of the system. Contrary to the implications of Reilley, Scribner, and Temple (*19*), the reaction is quite rapid and it attains the equilibrium indicated by the VDME data within 10 sec of mixing. Furthermore, the visible spectrum of this solution shows no evidence of the presence in solution of the possible Cr–EDTA products reported by Hamm (*20*). This evidence indicates that the second voltammetric wave is due to the reduction of a reaction intermediate, namely that of a partially coordinated complex.

Wolf (*7*) reported the suppression of similar plateau irregularities on the potassium ion wave at the VDME with a drop life of 0.17 sec.

Catalytic Waves. Catalytic currents are frequently observed at the DME, particularly in organic polarography. From the analytical point of view, these waves are useless except in certain special cases since the currents are related to bulk concentrations in a complex, nonlinear manner. Furthermore, the currents are frequently quite large and can obscure other more meaningful data.

Mairanovskii (*21*) has presented the best summary of present knowledge of this subject. In all such processes, a cyclic mechanism is involved in which the electrochemical step is accompanied by subsequent chemical reactions. At least one of the products of these chemical reactions is electroactive and further electrode reaction can thus occur.

For the two catalytic systems investigated and reported here, the VDME responses differ significantly from those obtained with the DME. In both cases, the VDME drop life is so short that the subsequent chemical reaction cannot occur to a detectable extent and the catalytic natures of the processes are not observed.

The uranium-catalyzed reduction of nitrate ion demonstrates this behavior most clearly. This process, first reported by Kolthoff, Harris, and Matsuyama (*22*), was investigated in detail by Koryta (*23*). Koryta suggested this mechanism. At the potential where the catalytic wave is observed, U(VI) is electroreduced to U(III). The U(III) chemically reduces NO_3^- to give U(IV) which is then also

(18) K. N. Rao, C. V. Suryanarayana, and K. S. G. Doss, *Naturwissenschaften*, **52**, 588 (1965).
(19) C. N. Reilley, W. G. Scribner, and C. Temple, ANAL. CHEM., **28**, 450 (1956).
(20) R. E. Hamm, *J. Amer. Chem. Soc.*, **75**, 5670 (1953).
(21) S. G. Mairanovskii, "Catalytic and Kinetic Waves in Polarography," Plenum Press, New York, N. Y., 1968.
(22) I. M. Kolthoff, W. E. Harris, and G. Matsuyama, *J. Amer. Chem. Soc.*, **66**, 1782 (1944).
(23) J. Koryta, *Collect. Czech. Chem. Commun.*, **20**, 667 (1955).

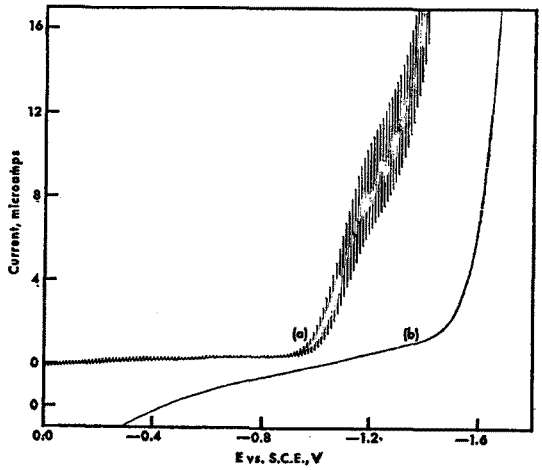

Figure 7. Elimination of a catalytic wave at the VDME

0.02m*M* U(VI), 0.100*M* KCl, 0.01*M* HCl, 1.00m*M* KNO_3
(a) DME, mercury pressure 60 cm
(b) VDME, mercury pressure 160 cm, 210 Hz

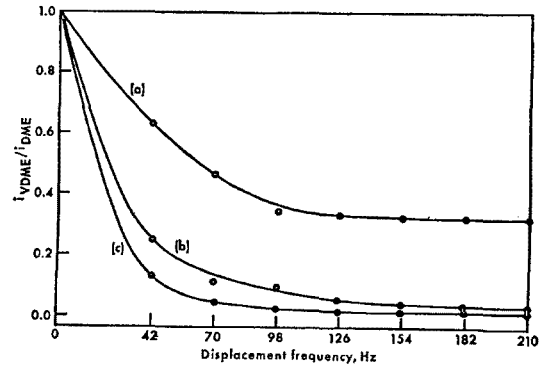

Figure 8. Effects of vibrational frequency on VDME currents

(a) 4.0m*M* Cd(II), 0.1*M* KNO_3,
(b) 4.0m*M* formaldehyde, 0.102*M* NaOH
(c) 0.02m*M* U(VI), 0.100*M* KCl, 0.01*M* HCl, 1.00m*M* KNO_3,

electroreduced to U(III). This regeneration of U(IV) results in a polarographic wave which is considerably larger than that which would be caused by the uranium alone. Figure 7 contains both the DME and VDME data for this system.

As can be seen, at the VDME, effectively no wave is observed at the potential where the catalytic wave is seen at the DME. Actually, the net current at the VDME at this potential is about 1% of the DME wave height. This net signal is no doubt due to the reduction to U(III) of the small amount of U(VI) in the system (*24*). This conclusion is substantiated by computations based on Koryta's value for the rate constant of the catalytic process (*23*), Koutecky's asymptotic solution for this system at the DME (*25*) and our observation that VDME currents for purely mass-transfer controlled processes at 210 Hz are about 1/3 the values obtained at the DME (Figure 8). These calculations predict that the uncatalyzed reduction of U(VI) at the VDME at 210 Hz should result in net currents that are 0.7% of the catalytic current at the DME.

Curve (c) in Figure 8 summarizes the effect of VDME frequency on the height of this catalytic wave. Comparison with curve (a) for the reduction of Cd(II) in 0.1*M* KNO_3, a purely mass-transfer controlled process, succinctly illustrates the nature of VDME response.

As mentioned before, the suppression of the detectability of the catalytic regeneration reaction is in large part due to the short drop life at the VDME. The vibration of the electrode must surely contribute to this suppression as well because the U(III) and the chemically-produced U(IV) are thereby removed from the vicinity of the electrode. In this case, the VDME can actually prevent the detection of processes which, in the analysis of complex mixtures, might obscure useful data.

The catalytic evolution of hydrogen is a commonly occurring process in organic polarography. Like other catalytic processes, it is rarely useful for analytical purposes. Mairanovskii (*21*) has thoroughly investigated this phenomenon and has developed a theory which seems to explain all the known facts. The appearance of this catalytic behavior seems to be related to the presence of unshared electron pairs at nitrogen, sulfur, phosphorus, or other atoms in an organic molecule to which a proton can be added.

The general mechanism postulated by Mairanovskii for this process is

$$B + DH^+ \rightleftharpoons BH^+ + D \quad (1)$$

$$BH^+ + e \rightarrow BH \quad (2)$$

$$2BH \rightarrow 2B + H_2 \quad (3)$$

that is, the organic catalyst, *B*, is in protolytic equilibrium with some proton donor, DH^+—*e.g.*, hydronium ion. The protonated organic compound undergoes electron transfer at the electrode to produce the species, *B*H, which is relatively unstable. Finally, the *B*H species reacts chemically to give hydrogen and two molecules of the catalyst. This catalyst can again be protonated and recycle through the entire process.

The catalytic hydrogen wave observed in the presence of quinine is a well-investigated example of a surface catalytic wave. In this case, the catalyst, *B*, in the above equations represents the basic form of quinine which is strongly adsorbed on mercury. The protolysis reaction then occurs between adsorbed quinine and hydronium ion in acid solutions.

Figure 9 contains both the DME and the VDME data for this system. The limiting current on the polarographic wave [curve (a)] is much too large to be explainable on the basis of the simple reduction of the 1.0m*M* quinine present and it is not proportional to the quinine concentration.

The VDME response to this system is considerably more complex. Three waves are observed, the first of which occurs at −1.0 V at the same potential as the catalytic wave found at the DME. In contrast to the DME wave, however, no catalytic behavior is found at this potential at the VDME. The currents are not unusually large nor are they sensitive to acid concentration. The limiting current of this wave is a linear function of quinine concentration permitting the quantitative determination of quinine with good precision up to the 1.0m*M* level (see Table I). At this upper concentration level, the current-concentration response drops off

(24) L. Meites, "Polarographic Techniques," Second ed., Interscience Publishers, New York, N. Y., 1965, p 184.
(25) J. Koutecky, *Collect. Czech. Chem. Commun.*, **18**, 311 (1953).

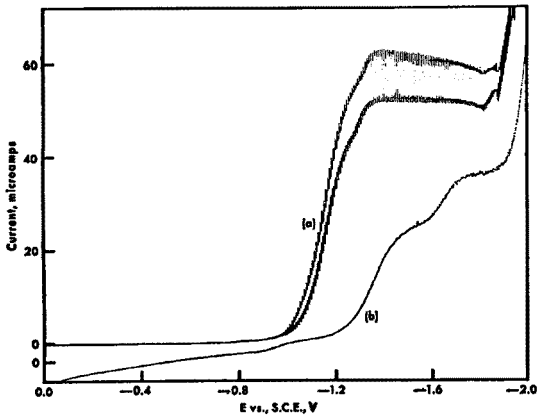

Figure 9. Voltammetry of quinine

1.0m*M* quinine, 5.0m*M* HCl, 1.00*M* NaCl
(a) DME, mercury pressure 60 cm,
(b) VDME, mercury pressure 160 cm, 210 Hz

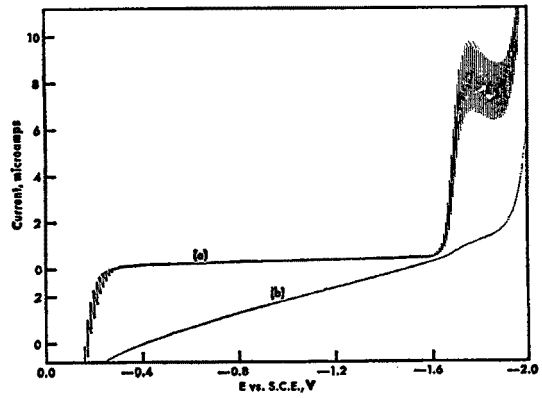

Figure 10. Elimination of kinetic wave at the VDME

4.0m*M* formaldehyde, 0.102*M* NaOH
(a) DME, mercury pressure 60 cm
(b) VDME, mercury pressure 160 cm, 210 Hz

to a limiting value in a manner similar to adsorption-limited waves such as are observed with methylene blue (*26*).

The process causing the first wave at the VDME is apparently an abbreviated version of the catalysis mechanism observed at the DME. At the VDME, the protolysis of adsorbed quinine and the same electron transfer process still occur. The recycle step regenerating quinine is apparently not detected, however. This difference between VDME and DME abilities to detect catalyst regeneration again doubtless reflects both the short detector life of the VDME and the convection which carries reaction products away from the electrode.

The first wave is certainly not due to a change in double layer capacity caused by quinine adsorption. The limiting currents of this wave are far too large to be so explained; also, no charging current suppression is detectable in the presence of quinine at the VDME. Furthermore, this first wave is not an adsorption pre-wave in the classical sense. The heights of both the first and second waves increase with quinine concentration over the entire range from 0.01 to 1.0m*M*.

The second wave found at the VDME at −1.3 V is catalytic in character. Similar to the results reported by Mairanovskii (*27*), the currents are nonlinearly related to bulk quinine concentration and exhibit great sensitivity to acid concentration. Apparently, catalytic hydrogen evolution is occurring but the mechanism clearly must differ from that which obtains at the DME. The final wave at −1.7 V is due to the direct reduction of hydronium ion.

In the quinine system, then, while VDME response is considerably more complex than the DME data, it is also more useful. Analytical determinations can be made with the VDME and the detection of other voltammetric waves becomes feasible.

Kinetic Waves. Kinetic waves, like catalytic waves, have frequently been observed in organic polarography. Similarly, electrode responses to such processes are of questionable analytical utility because (a) the effects on such responses of adventitious impurities in complex mixtures can be severe and (b) these waves can actually obscure useful data. When confronted with these difficulties, behavior could generally best be optimized analytically by eliminating all electrode response to kinetic waves. In the case of the formaldehyde kinetic wave, this ideal is approximately satisfied by the VDME.

Kinetic waves are due to mechanisms in which the electron-transfer step is preceded by a chemical reaction, the rate of which limits the overall process. The topic has been well reviewed by Mairanovskii (*21*) and Heyrovsky and Kuta (*28*).

Formaldehyde exists in aqueous solution both as the anhydrous aldehyde and as its hydrate, methylene glycol, which are in equilibrium. The equilibrium concentration of the anhydrous form is very small but this is the only formaldehyde species which can be electroreduced. Thus, the overall rate of the electrode process is limited by the rate of dehydration of the methylene glycol.

The VDME and DME data for formaldehyde in 0.102*M* NaOH are given in Figure 10. This medium was selected because maximum wave heights had been observed for the formaldehyde wave in this electrolyte by previous workers (*28*).

As can be seen, a small wave is detected by the VDME at the same potential at which the kinetic wave is seen at the DME; actually, the VDME response is about 4% of the DME wave. A wave of this magnitude cannot be attributed to the reduction of the equilibrium bulk concentration of the anhydrous species. According to Schou's estimate of the equilibrium constant for the dehydration reaction (*29*), the bulk concentration of the anhydrous aldehyde should be about $10^{-6}M$ which is much too small to account for these currents.

Within the limits of our experiments, apparently the drop life at the VDME becomes sufficiently short to suppress almost completely the detectability of the kinetic process. When the drop life is in the millisecond range, the dehydration process can still be observed to a small extent.

(26) J. Heyrovsky and J. Kuta, "Principles of Polarography," Academic Press, New York, N. Y., 1966, pp 291–295.
(27) S. G. Mairanovskii, *J. Electroanal. Chem.*, **6**, 77 (1963).
(28) J. Heyrovsky and J. Kuta, "Principles of Polarogrraphy," Academic Press, New York, N. Y., 1966, pp 340–380.
(29) S. A. Schou, *J. Chim. Phys.*, **26**, 69 (1929).

This conclusion is supported by calculations based on Valenta's experimental data (*30*) and Koutecky's rigorous solution for this system at the DME (*31*). These computations predict that at the VDME at 210 Hz, a kinetic current should be observed which is 1.4% of that detected at the DME. Curve (b) in Figure 8 summarizes the effect of VDME frequency on the height of this kinetic wave.

(30) P. Valenta, *Collect. Czech. Chem. Commun.*, **25**, 855 (1960).
(31) J. Koutecky, *ibid.*, **18**, 597 (1953).

Wolf (*8*) found a similar decrease in response for the kinetic wave of pyruvic acid at the VDME.

RECEIVED for review January 16, 1969. Accepted March 17, 1969. Presented in part before the Division of Analytical Chemistry, 156th National Meeting, ACS, Atlantic City, N. J., September 13, 1968. This work supported by a summer research stipend from St. John's University for R. E. Cover, and a 1968 Summer Fellowship Award from the ACS Division of Analytical Chemistry for J. G. Connery.

Kinetic Waves in Systems Containing Cobalt(II) and Cysteine-Like Compounds

Polarographic Catalytic Hydrogen Waves in Acid Solutions of Mercaptoanilines in Presence of Cobalt(II) or -(III)

I. M. Kolthoff and P. Mader

School of Chemistry, University of Minnesota, Minneapolis, Minn. 55455

2-Mercaptoaniline [pK(SH) = 5.9; pK(NH_3^+) = 2.9] in alkaline medium gives rise to a cobalt(II) prewave. In the pH range between about 8 and 3, in the presence of cobalt(II) or -(III), two catalytic hydrogen currents, *A* and *B*, are observed with flat maxima followed by minima. The characteristics of these waves are quite different from those of Brdička waves. Currents *A* and *B* are observed at considerably less negative potentials than those of Brdička currents, and cobalt (III) has the same effect as cobalt(II), the dependence of current *B* on pH and concentration of buffer constituents being quite different from that of Brdička currents. Also, currents *A* and *B* are greatly repressed with increasing ionic strength and by increase of the valence of the cation. The cobalt complex of the thiol is strongly capillary active at the potentials of maximum *A*, while the uncombined thiol is still capillary active at maximum *B*. Characteristics of currents *A* and *B* differ in many respects. The mechanism of current *A* is postulated to be due to protonation of adsorbed Co(0)RS complex and reduction of the proton. Current *B* is attributed to hydrogen reduction of adsorbed RSH, the adsorbed component stabilizing the metallic cobalt on the electrode, and the metallic cobalt greatly decreasing hydrogen overvoltage as compared to that on mercury. 4-Mercaptoaniline qualitatively behaves like the 2-compound.

IN AN extensive study of the so-called Brdička catalytic hydrogen currents which exhibit maxima and which occur at the dropping mercury electrode (DME) in alkaline solutions containing aliphatic sulfhydryl compounds and cobalt (II), we observed with all compounds studied a cobalt(II) prewave (*1*). Several of these compounds exhibited a maximum on the prewave and another wave with a maximum at more negative potentials at pH values, where complex formation between cobalt(II) and the sulfhydryl compound is very small. These maxima, which were not due to stirring and also did not have the characteristics of the Brdička maxima, occurred at potentials less negative than those where Brdička maxima were observed. We will use for the non-Brdička currents the notations *A* and *B* with maxima *A* and *B*, respectively.

In spite of the fact that some thousand papers have been written about the Brdička waves, their mechanism is still not well understood. Good reviews have been given by Brdička *et al.* (*2*), Müller (*3*), Mairanovskii (*4*), and Calusaru (*5*). The Brdička waves will be the subject of a subsequent paper. One of the many difficulties in an interpretation of Brdička waves, especially of the pH effect, is that the experiments are always carried out in the pH range of about 9 ± 1, where the cobalt(II) is kept in solution in the form of a complex CoL_x, where L is ammonia or tris or borate or another ligand which is also the alkaline form of the buffer constituent. The effect of pH on the Brdička maxima at a constant ionic strength is to change the ratio of acid to base constituent. With the change in concentration of L the value of x in CoL_x often changes. This makes it impossible to get conclusive information on the effect of pH alone on the Brdička maxima.

In acid medium in the absence of complex formers other than sulfhydryl compounds, the cobalt(II) is present as aquo cobalt ion, and the concentration of buffer constituents can be changed without materially affecting the aquo cobalt(II) concentration. To gain insight in the characteristics of the non-Brdička currents with maxima, we have worked in acid media using mainly aromatic sulfhydryl compounds, the K_{SH} of which are many orders of magnitude greater than those of cysteine and related compounds. Of the many compounds investigated, 2-mercaptoaniline was most suitable. Some experiments have also been carried out with 4-mercapto-

(1) I. M. Kolthoff, P. Mader, and S. E. Khalafalla, *J. Electroanal. Chem.*, **18**, 315 (1968).

(2) R. Brdička, M. Březina, and V. Kalous, *Talanta*, **12**, 1149 (1965).
(3) O. H. Müller, "Methods of Biochemical Analysis," D. Glick, Ed., Interscience Publishers, New York, 1963, Vol. 11, p 329.
(4) S. G. Mairanovskii, *J. Electroanal. Chem.*, **6**, 77 (1963).
(5) A. Calusaru, *ibid.*, **15**, 269 (1967).

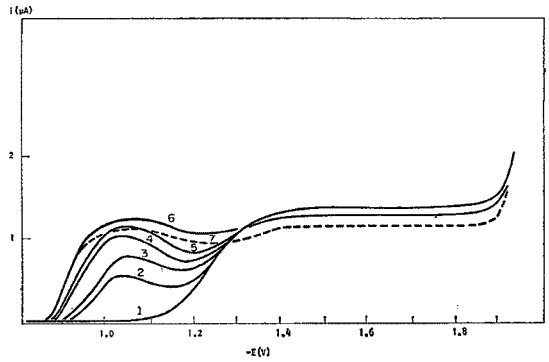

Figure 1. Polarograms of MAN in 0.06*M* borax, pH 9.2

Concn of $CoCl_2$ 0.4 m*M*; concn of MAN: (1) 0, (2) 0.5, (3) 1, (4) 2.5, (5) 5, (6) 18, (7) 30 × 10^{-5}*M*

aniline. Most other aromatic sulfhydryl compounds have a very small solubility in water, and their cobalt salts are extremely insoluble. With the aromatic compounds studied, only *A* and *B* currents were observed but not catalytic currents with characteristics of the Brdička currents.

EXPERIMENTAL

2- and 4-Mercaptoaniline were Aldrich Chemical Co. reagents; 0.02*M* solutions of each chemical were freshly prepared in previously deaerated absolute ethanol containing 0.02*M* HCl. A few experiments have been run also with thiophenol and pentachlorothiophenol. Tetrabutylammonium perchlorate was prepared from Eastman Kodak tetrabutylammonium iodide by reaction with sodium perchlorate. Polyvinylpyrrolidone, type NP-K30, was a product of Antara Chemicals. Polyvinyl alcohol was a Du Pont, and Triton X-114 a Rohm and Haas reagent. Sodium dodecyl sulfate was a product of K and K Laboratories. All other chemicals have been used previously (*1*).

Recordings of the current–voltage and current–time curves have also been described previously (*1*).

Unless otherwise stated, polarograms were run with an ordinary vertical type of capillary, 1, with the characteristics at 76 cm mercury pressure and zero applied voltage of m = 1.14 mg/sec, t = 5.64 sec. For the recording of current–time curves and some polarograms, capillary 2 was used, tilted at an angle (*6*) of 45°, to overcome depletion at the mercury surface of electroactive species at the beginning of formation of a new drop. At 49 cm mercury pressure and zero applied voltage, the characteristics of capillary 2 were m = 0.41 mg/sec, t = 7.60 sec. Drop time curves were recorded by measuring the drop time of a minimum of 10 drops at a given potential. For these measurements, a vertical capillary 3 was used, with the characteristics at 50 cm Hg and zero applied voltage m = 1.08 mg/sec, t = 6.68 sec.

Stationary electrode polarograms have been recorded with a hanging mercury drop electrode of the commercial type (Metrohm, Switzerland); the radius of the drop, calculated from its weight, was 0.42 mm. A Leeds and Northrup electrochemograph type E with no damping was used, with a rate of scanning 3.33 mV/sec.

All potential values are referred to the saturated calomel electrode (SCE) which was used as a reference electrode. Values of pH were measured with a Beckman pH meter, model G. Unless otherwise stated, the experiments were run at 25°.

(6) I. Smoler, *Collect. Czech. Chem. Commun.*, **19**, 238 (1954).

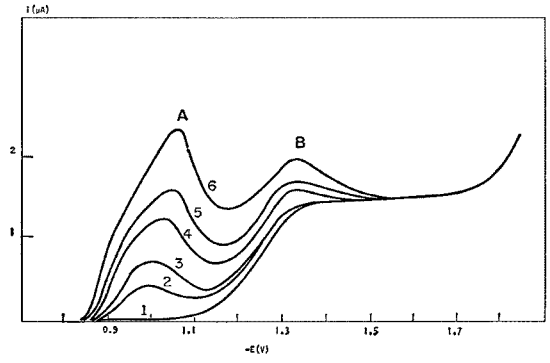

Figure 2. Polarograms in 0.06*M* borax plus 0.6*M* in H_3BO_3, pH 7.3

Concn of $CoCl_2$ 0.4 m*M*; concn of MAN: (1) 0, (2) 0.5, (3) 1, (4) 2.5, (5) 5 (6) 17.5 × 10^{-6}*M*

RESULTS

Polarograms with 2-Mercaptoaniline at Various pH. Like all other sulfhydryl compounds investigated (*1*), 2-mercaptoaniline (MAN) decreases appreciably the cobalt(II) reduction overvoltage. Polarograms run in a 0.06*M* borax solution (pH 9.2) at MAN concentrations varying between 5 × 10^{-6} and 3 × 10^{-4}*M* at a cobalt(II) concentration of 0.4 m*M* exhibited a cobalt(II) to cobalt(0) prewave, $E_{1/2}$ being about 0.3 V less negative than that in absence of MAN. The prewaves exhibited a flat maximum followed by a flat minimum as illustrated in Figure 1. At lower MAN concentrations (curves 1–5), the prewave currents exceeded many times the diffusion current of the 1:1 cobalt(II):MAN complex [the diffusion coefficients of the cobalt(II) borate and cobalt(II) complex of MAN were assumed to be the same]. Thus, *e.g.*, at 5 × 10^{-6}*M* MAN, the prewave current was about 25 times as great as the diffusion current of the cobalt(II)-MAN complex at the same concentration. When the prewave current was less than 20% of the diffusion current of the cobalt, it was independent of the height of mercury in reservoir, indicating kinetic character of the prewave. At an MAN concentration of 1.8 × 10^{-4}*M* or higher, a gray-blue precipitate of a cobalt salt was formed in the solution. Precipitate formation resulted in a decrease of currents at all potentials (see curves 6 and 7 in Figure 1).

In borax medium, the prewave currents never exceeded the diffusion current of cobalt(II). No other currents were observed until at about −1.9 V, when reduction of the supporting electrolyte started. Neither Brdička currents nor so-called "presodium currents" [hydrogen reduction in SH group (*5*)] were observed. This was to be expected as no free R(SH) is present at pH 9.2. Values of acid dissociation constants of MAN in water–ethanol mixture are reported (*7*) to be p$K(NH_3^+)$ = 3.00, pK(SH) = 6.59; those in 50% water–dioxane mixture are (*8*) p$K(NH_3^+)$ < 2, pK(SH) = 7.90, respectively. We have determined pK values potentiometrically in water solutions containing 0.35% ethanol and found p$K(NH_3^+)$ = 2.9 and pK(SH) = 5.9, respectively.

Figure 2 presents polarograms at a pH of 7.3 by making the 0.06*M* borax solution 0.6*M* in boric acid. Again, the

(7) J. D. Danehy and C. J. Noel, *J. Amer. Chem. Soc.*, **80**, 2511 (1960).
(8) H. Freiser, R. G. Charles, and W. D. Johnston, *ibid.*, **74**, 1383 (1952).

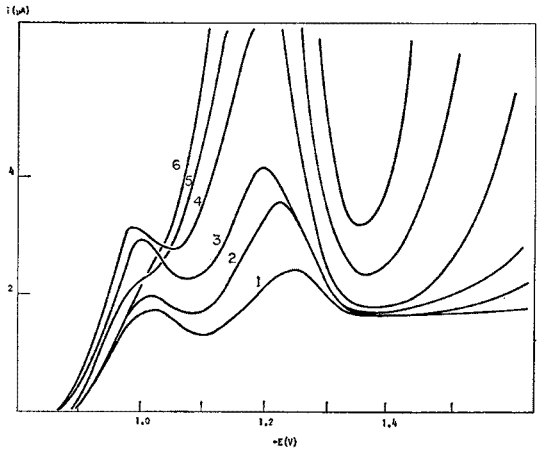

Figure 3. Effect of pH on maxima *A* and *B* in veronal acetate buffer

0.4 m*M* $CoCl_2$, 1 × 10^{-5}*M* MAN, 0.1*M* NaAc, μ = 0.1. Value of pH: (1) 6.43, (2) 5.85, (3) 5.64, (4) 5.11, (5) 4.55, (6) 4.29

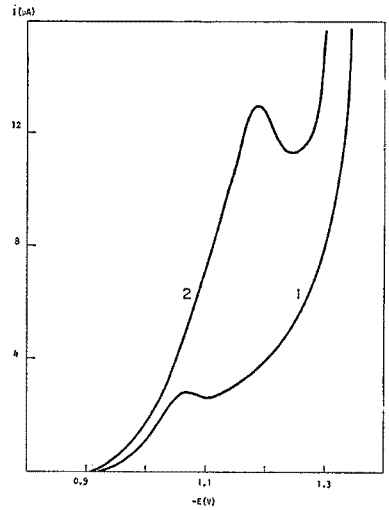

Figure 4. Polarograms at pH 2.0

Solution 0.4 m*M* in $CoCl_2$, 0.01*M* in $HClO_4$, 0.04 *M* in $NaClO_4$. Concn of MAN: (1) 0, (2) 2.5 × 10^{-6}*M*

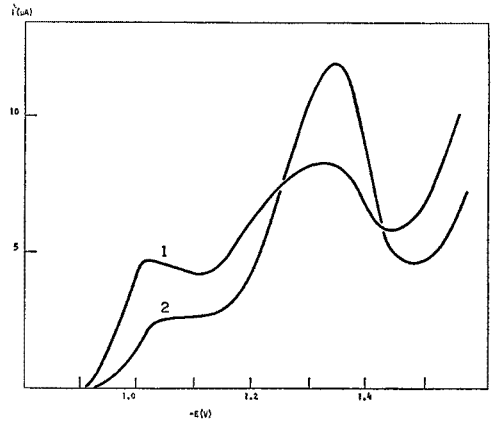

Figure 5. Effect of temperature

0.1*M* NaAc, 0.1*M* HAc, 0.4 m*M* $CoCl_2$, 1 × 10^{-4}*M* MAN, pH 4.55. (1) 30 °C; (2) 0 °C. Capillary 2

cobalt prewave is observed which is characterized by a maximum at about −1.02 V. At higher concentrations of MAN (curve 6, Figure 2), the current at the maximum is considerably greater than the diffusion current of cobalt. The total current is called current *A* with maximum *A*, the value of the cobalt prewave current being unknown. At all MAN concentrations the current passes through a minimum of about −1.15 V to yield a second maximum *B* at −1.33 V, which also exceeds the diffusion current of cobalt. Polarograms were also run in 0.06*M* borax saturated with boric acid at a pH of 6.0. The currents at both maxima *A* and *B* were considerably greater than in Figure 2. It may be stated here that neither maximum *A* nor *B* at any pH is of the first kind—*i.e.*, a result of stirring (see below).

With further decrease of pH, maxima *A* and *B* become much more pronounced. The effect in veronal acetate buffers of pH 6.43 to 4.29 at an ionic strength of 0.1, the solutions being only 1 × 10^{-5}*M* in MAN, is shown in Figure 3. The potentials at maxima *A* and *B* shifted to somewhat less negative values with decreasing pH. At pH 4.5 or less, the current–potential line of *A* in the presence of small amounts of MAN started to coincide with that of *B*, and currents *A* were no longer observed at pH smaller than 4. However, at higher concentrations of MAN, maximum *A* is still observed at pH 4.5 (see, e.g., Figure 5). Figure 4 illustrates that at pH 2.0 (0.01*M* perchloric acid plus 0.04*M* sodium perchlorate), a trace of MAN (2.5 × 10^{-6}*M*) produces a large catalytic current *B* which exhibits a pronounced maximum. Higher concentrations of MAN cannot be used at this low pH of 2.0, as the maximum *B* soon overlaps with the "presodium currents" of hydrogen evolution observed also in the absence of cobalt.

The general shape of patterns of currents *A* and *B* at varying pH hardly varies with the concentration of cobalt(II). Both maxima *A* and *B* increase with increasing cobalt(II) concentration.

Cobalt(III) in the form of cobalt(III)hexammine chloride, after its first electron reduction, gives practically identical patterns of those observed with the same concentration of cobalt(II). In alkaline medium, cobalt(III) does not give rise to Brdička currents in the presence of small amounts of low molecular weight aliphatic sulfhydryl compounds, such as cysteine and thioglycolic acid, whereas such currents are very much pronounced with cobalt(II).

The effect of the height of mercury, h_{Hg}, in the reservoir was studied in acetate buffers of pH 4.3 and 4.55 at different MAN concentrations. Both currents *A* and *B* decreased somewhat with increasing height of the reservoir. Current–time curves run at the potential of −1.02 V (maximum *A*) had a monotonous parabolic appearance, while plots of log *i* *vs.* log *t* were straight lines which had the same slope of 0.86 at heights of mercury between 49 and 96 cm. Current–time curves run at potentials of the second maximum *B* exhibited a more complex shape (see below).

The effect of temperature was normal for kinetic currents as far as maximum *A* is concerned, but abnormal with regard to the maximum *B*. At 0 °C, the current at maximum *B*

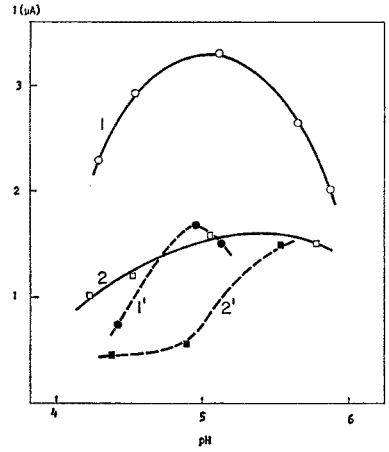

Figure 6. Plot of currents at maximum *A vs.* pH

0.4 m*M* $CoCl_2$, 1 × 10^{-5} *M* MAN, acetate buffer. Solid lines: Concn of NaAc 0.1*M*, concn of HAc was changed. Dashed lines: Concn of HAc 0.01*M*, concn of NaAc was changed. Ionic strength was kept constant with $NaClO_4$: (1,1′) μ = 0.1; (2,2′) μ = 0.3

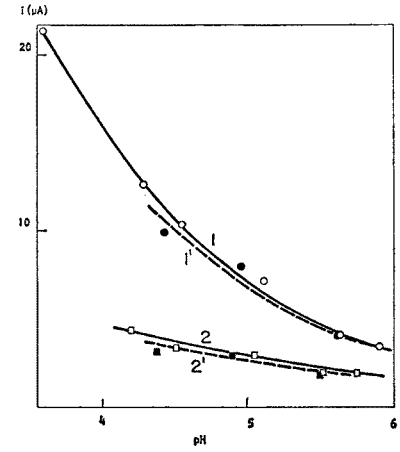

Figure 7. Plot of currents at maximum *B vs.* pH. 0.4 m*M* $CoCl_2$, 1 × 10^{-5} *M* MAN, acetate buffer

Solid lines: Concn of NaAc 0.1*M*, concn of HAc was changed. Dashed lines: Concn of HAc 0.01*M*, concn of NaAc was changed. Ionic strength was kept constant with $NaClO_4$: (1,1′) μ = 0.1; (2,2′) μ = 0.3

was considerably greater than at 30 °C, as is clearly seen in Figure 5. The slope of the log *i vs.* log *t* curves at −1.02 V (maximum *A*) was found to increase with decreasing temperature, being 0.84 at 30 °C and 1.01 at 0 °C.

Effect of Concentration of Buffer Constituents in Acetate Buffer at Constant Ionic Strength. The measurements in Figure 6 were made in the pH range between 4.2 and 5.8. Curve 1 in Figure 6 gives the current at the maximum *A* at an ionic strength of 0.1 and at a constant concentration of 0.1*M* sodium acetate. The dotted curve 1′ presents the data at constant acetic acid concentration, the ionic strength being kept 0.1 with sodium perchlorate. Maximum *A* exhibits a well defined maximum at pH of about 4.9, the *A* currents being about twice as large in curve 1 as in curve 1′. In curve 1 at pH 4.55, the acetic acid concentration is some 10 times greater than in curve 1′. At the ionic strength of 0.3, the maxima are less pronounced (curves 2 and 2′), a larger current being observed again at the higher acetic acid concentration. The pH pattern for maximum *B* at a constant ionic strength (Figure 7) is strikingly different. Current *B* increases continuously with increasing hydrogen ion concentration, while a change in the acetic acid concentration has no effect on the magnitude of the *B* current (compare curves 1 and 1′ in Figure 7).

Effect of Ionic Strength and Charge of Cation. From Figures 6 and 7, it is evident that both currents *A* and *B* greatly decrease with increasing ionic strength. The effect was studied more systematically using cations of various charge. Figure 8 illustrates the fact that at the same ionic strength the trivalent cation lanthanum has a greater suppressing effect on maximum *B* than the divalent cation calcium and the latter a much greater effect than the monovalent sodium cation. Similar effects were observed for maximum *A*. Both the ionic strength and the charge of the cation greatly affect currents *A* and *B*.

Electrocapillary Curves. From drop time *vs. E* curves in Figure 9, it appears that the cobalt salt of MAN in ammoniacal medium (curve *c*) is much more capillary active than its anion, RS^-. As a matter of fact, curve *c* coincides with the electrocapillary curve in the buffer alone (curve *a*) close to potentials where the prewave of cobalt starts, and where in more acid medium current *A* is observed. Figure 10 shows that the SH form of MAN in acetate buffer of pH 4.5 is capillary active at least until a potential of −1.2 V, at which potential, hydrogen evolution became appreciable while the mercury drops became covered with bubbles of hydrogen at more negative potentials. The large decrease of the

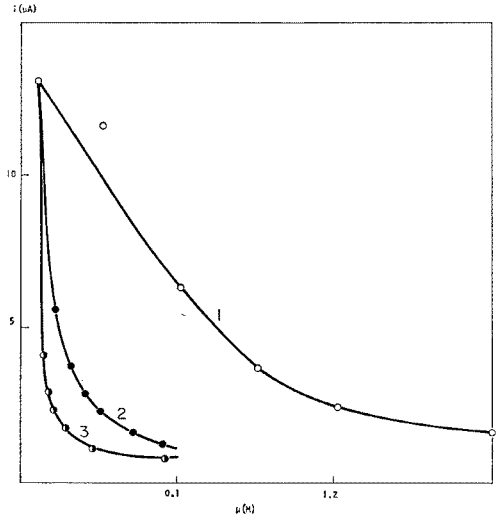

Figure 8. Plot of currents at maximum *B vs.* ionic strength

Solution 0.01*M* NaAc, 0.01*M* in HAc, 0.4 m*M* in $CoCl_2$, 1 × 10^{-5} *M* in MAN. (1) $NaClO_4$, (2) $CaCl_2$, (3) $LaCl_3$

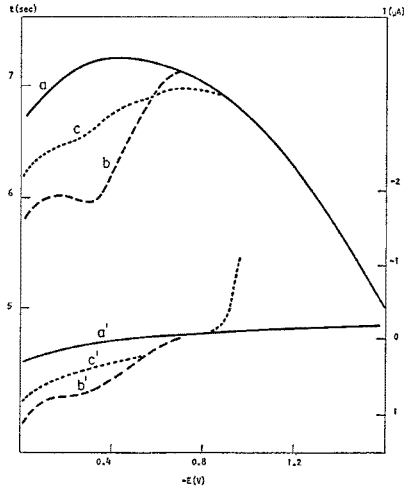

Figure 9. Drop time *vs.* *E* curves in ammonia buffer, pH 9.3

(a) **0.1*M* NH_3, 0.1*M* NH_4Cl; *(b)* plus 0.1 m*M* MAN; *(c)* as *b* plus 0.4 m*M* $CoCl_2$. *(a')*, *(b')*, *(c')* polarograms corresponding to the curves *(a)*, *(b)*, *(c)*. Capillary 3**

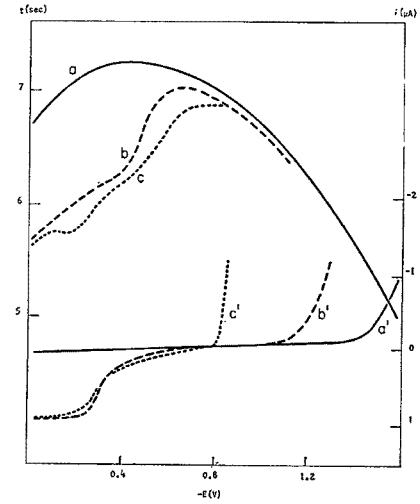

Figure 10. Drop time *vs.* *E* curves in acetate buffer, pH 4.55

(a) **0.1*M* NaAc, 0.1*M* HAc; *(b)* plus 0.4 m*M* MAN; *(c)* as *b* plus 0.4 m*M* $CoCl_2$. *(a')*, *(b')*, *(c')* polarograms corresponding to the curves *(a)*, *(b)*, *(c)*. Capillary 3**

surface tension at potentials where the anodic wave is observed is caused by the anodic formation of the mercury salt of MAN.

Effect of Surfactants. The cobalt(II) to cobalt(0) reduction is uninhibited in the presence of small concentrations of the surfactants polyvinyl alcohol (PVA) and polyvinylpyrrolidone (PVP). As a matter of fact, the cobalt(II) reduction wave at pH 7.8 and 4.5 is shifted to somewhat less negative potentials in the presence of low concentrations of these surfactants. An example of this effect is shown in Figure 11 with PVP in acetate buffer of pH 4.5. Note the considerable increase of the small maximum at −1.3 V on the cobalt(II) reduction wave in Figure 11 in the presence of small concentrations of PVP. This type of maximum on the cobalt(II) reduction wave is often observed in the absence of MAN and surface active substances in acetate buffers of pH lower than 5. The height of the maximum in Figure 11 increases with decreasing pH and decreasing ionic strength of the solution.

At higher PVA or PVP concentrations, the cobalt(II) waves are shifted to more negative potentials. Under these conditions no maximum is observed at pH 7.8, while at pH 4.5 the inhibited cobalt reduction wave coalesces with the hydrogen evolution wave (curves 5 and 6). It is apparent from Figure 11 that PVP (and also PVA) considerably decreases the hydrogen overvoltage in the presence of cobalt(II). In the absence of cobalt, these surfactants also decrease the overvoltage, but the effect is much smaller than in the presence of cobalt (see curves 7 and 8 in Figure 11).

In the presence of MAN and at the highest pH of 9.2, PVA in concentrations between 1 and 5 × 10^{-3}% decreases the cobalt(II) prewave but does not affect the cobalt(II) reduction current at more negative potentials. At lower pH of 8.2 (0.06*M* borax plus 0.3*M* H_3BO_3) the effect of PVA on the prewave is similar to that observed at pH 9.2. The cobalt (II) reduction current at −1.2 to −1.4 V, however, increases considerably in the presence of PVA and 1.5 × 10^{-4}*M* MAN

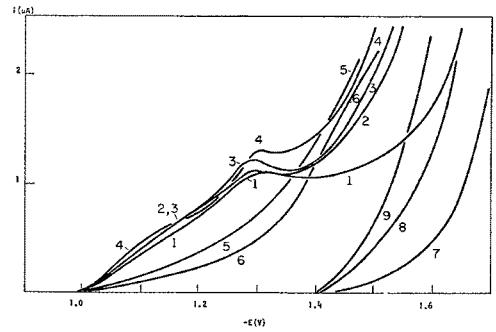

Figure 11. Effect of polyvinylpyrrolidone on reduction of cobalt(II)

0.1*M* NaAc, 0.1*M* HAc, 0.4 m*M* $CoCl_2$, pH 4.55. Concn of PVP: (1) 0, (2) 0.5, (3) 1, (4) 5, (5) 8, (6) 11 × 10^{-3}%. Capillary 2. Curves 7, 8, and 9 in the absence of Co(II): (7) 0, (8) 1, (9) 11 × 10^{-3}% PVP. Capillary 2

and a maximum similar to maximum *B* is observed whereas this maximum is absent in the absence of PVA.

In borate buffers with pH 7.3 to 6.0, PVA in the presence of MAN and cobalt(II) brings about a reduction of maximum *A*, whereas maximum *B* is greatly increased with increasing concentration of PVA until at a concentration of about 10 × 10^{-3}% PVA a slight reduction occurs.

In acetate buffers of pH 4.3 to 5.7, the effect of PVA on maximum *A* is similar to that at pH 6.0 to 7.3. However, maximum *B* is increased only when the concentration of PVA is less than about 5 × 10^{-3}%; further increase of the PVA concentration causes a large decrease of currents at maximum *B*. Polyvinylpyrrolidone has qualitatively the same but quantitatively a much greater effect than PVA (Figure 12). The greatest increase of maximum *B* was observed at the

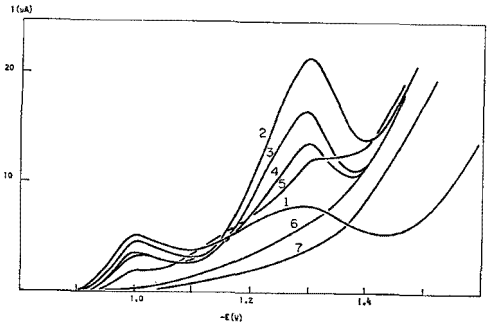

Figure 12. Polarograms in presence of polyvinylpyrrolidone in solution 0.1 M in NaAc, 0.1 M in HAc, 0.4 mM in $CoCl_2$, and 1×10^{-4} M in MAN. pH 4.55. Concn of PVP: (1) 0, (2) 0.5, (3) 1, (4) 2, (5) 5, (6) 8, (7) 11×10^{-3}%. Capillary 2

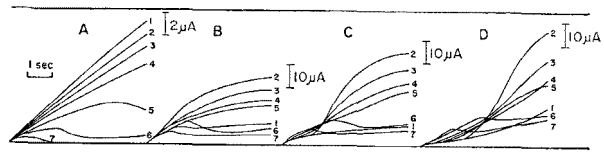

Figure 13. Current-time curves in presence of PVP in solution 0.1 M NaAc, 0.1 M in HAc, 0.4 mM in $CoCl_2$, and 1×10^{-4} M in MAN

pH 4.55. Concn of PVP: (1) 0, (2) 0.5, (3) 1, (4) 2, (5) 5, (6) 8, (7) 11×10^{-3}%. Applied potential: (A) −1.0, (B) −1.25, (C) −1.30, (D) −1.35 V. Capillary 2

smallest concentration of PVP (5×10^{-4}%, curve 2). With increasing PVP concentration the exaltations became increasingly less and with the largest concentrations used, maximum B became suppressed. Current–time curves were measured with the tilted capillary 2 under the same conditions as in Figure 12 (Figure 13). From these measurements it is clear that the instantaneous currents at maximum A are significantly suppressed already by the smallest concentration of surfactant used (see Figure 13A). At potentials of maximum B, the greatest increase of the instantaneous current is observed at the smallest concentration of PVP (Figure 13, B, C, D). The exaltation decreases continuously with increasing concentration of PVP and finally at the highest concentration of PVP used (1.1×10^{-2}%) the instantaneous current is suppressed.

Triton X-114 has an effect analogous to that of PVA. On the other hand, tetrabutylammonium perchlorate (TBAP) brings about a gradual decrease of both currents A and B at all concentrations tested. This capillary active cation greatly suppresses the double layer around the electrode, and in this respect resembles a higher valent cation. The anionic surfactant sodium dodecyl sulfate (SDS) in an acetate buffer of pH 4.5 decreases current A, and at higher concentrations also current B.

Stationary Electrode Polarograms. In agreement with statements in the literature (*9*, *10*), cyclic polarograms recorded with a stationary hanging mercury drop electrode in acetate buffers of pH 4.7 to 5.7 in the presence of 0.4 mM $CoCl_2$, exhibited a cathodic peak at approximately −1.25 V corresponding to the cobalt(II) to cobalt(0) reduction and an anodic peak of the cobalt(0) dissolution at −0.17 V. In the additional presence of 1×10^{-4} M MAN, two new cathodic peaks at approximately −0.92 and −1.05 V were observed, while the anodic peak at −0.17 V increased considerably in height. When the electrode was polarized for a few minutes at a potential of −0.92 V or at more negative potentials, it became covered with bubbles of hydrogen.

The hydrogen overvoltage at a stationary cobalt wire electrode is much less than that at mercury, and is further decreased in the presence of MAN. Thus, in an acetate buffer of pH 4.5, the potential at which the reduction of hydrogen at a cobalt electrode starts was decreased by 80 mV in a cobalt free solution which was 1×10^{-4} M in MAN.

"Presodium Currents" of MAN in Absence of Cobalt(II). Like many other thiol and/or amino-containing substances (*11–14*) MAN decreases the hydrogen overvoltage at mercury at a pH where the thiol group is not completely dissociated. This occurs both in presence and in absence of cobalt(II), the hydronium ion reduction potential being shifted to less negative values. Such currents are denoted in the literature (*5*) as "presodium currents." The decrease in the hydrogen reduction potential is especially large at lower pH. Thus, in an acetate buffer of pH 4.7, the difference between the potential at which the evolution of hydrogen starts in the presence and in the absence of 1.5×10^{-4} M MAN is 270 mV; at the higher pH of 5.17 and at the same concentration of MAN, the difference is only 180 mV. No "presodium currents" have been observed at pH greater than 6.2.

Other Aromatic Thiol Compounds. 4-Mercaptoaniline qualitatively behaves like its 2-isomer. Two maxima A and B and "presodium currents" of hydrogen evolution are observed in cobalt(II) solutions in acetate buffer containing this thiol. The solubilities of 4-mercaptoaniline and its cobalt salt are considerably greater than those of MAN. Because of the similarity of all polarograms with those obtained with MAN, no further details are reported.

Thiophenol and pentachlorothiophenol are only slightly soluble in water and ethanol, and their cobalt salts are extremely insoluble. Experiments with these compounds are limited to very small concentrations. Therefore, no detailed study has been made with these compounds. At lower pH (4–5) two maxima similar to maxima A and B of MAN are observed. All aromatic thiol compounds tested in this work bring about a cobalt(II) prewave in borax medium, similar to that observed with cysteine and other aliphatic sulfhydryl compounds (*1*).

DISCUSSION

MAN, like other thiol compounds, forms complexes with cobalt(II) from which the cobalt is reduced with a much smaller overvoltage than from the aquo cobalt ion. Traces of MAN bring about the cobalt(II) prewave, which is kinetic in nature, and the thiol liberated upon reduction recombines with the cobalt(II) diffusing to the electrode (*1*). The surface concentration of the electroactive species is increased as a

(9) W. Kemula and Z. Galus, *Bull. Acad. Polon. Sci., Ser. Sci. Chim. Geol. Geograph.*, **7**, 729 (1959).
(10) B. K. Hovsepian and I. Shain, *J. Electroanal. Chem.*, **12**, 397 (1966).
(11) R. Brdička, *Collect. Czech. Chem. Commun.*, **8**, 366 (1936).
(12) G. Sartori and A. Liberti, *J. Electrochem. Soc.*, **97**, 20 (1950).
(13) M. v. Stackelberg, W. Hans, and W. Jensch, *Z. Elektrochem.*, **62**, 839 (1958).
(14) V. F. Toropova and L. A. Anisimova, *Zh. Anal. Khim.*, **22**, 1264 (1967).

result of the absorption of the Co(II)RS complex on the surface of mercury electrode (Figure 9). Decreasing adsorption of this complex with increasing negative potential explains the decrease of the prewave to a flat minimum after the flat maxima of the prewave (Figure 1).

The maxima *A* and *B*, which appear at lower pH and often considerably exceed the cobalt(II) diffusion current, are of a nonstirring character and are caused by the reduction of hydrogen, all of which is facilitated in the simultaneous presence of cobalt(II) and MAN. This conclusion is substantiated by the observation of hydrogen bubbles at the hanging mercury drop at potentials of the two peaks and also by the characteristic dependence of both maxima on pH. The characteristics of the currents at both maxima *A* and *B* differ drastically from those of Brdička currents (*2–5*). The former currents occur at considerably less negative potentials then those at which Brdička currents are observed. This is clearly illustrated in Figure 14. The maximum of the Brdička current of thioglycolic acid in borax occurs at −1.7 V (curve 3), whereas at pH 7.7 in borate buffer, maxima *A* and *B* are at −1.15 and −1.35 V, respectively (curve 4). Similar observations have been made in unpublished studies with thiosalicylic acid and 2-mercaptoethanol. Quite generally, maximum *A* is found at potentials of the cobalt(II) prewave, while maximum *B* occurs at potentials where the cobalt(II) reduction wave in the absence of MAN approximately attains its limiting value (Figure 2).

Another striking difference between the characteristics of maxima *A* and *B* and those of Brdička maxima is the effect of trivalent cobalt. While both currents *A* and *B* are unaffected by replacing cobalt(II) with -(III), practically no Brdička currents of low molecular aliphatic thiol compounds are observed with cobalt(III). Also, the effects of pH and of the concentration of the acid buffer constituents, particularly on *B* currents, are quite different from those on Brdička maxima. In many respects, characteristics of maxima *A* and *B* differ considerably from each other (*e.g.*, effect of pH, temperature, and surface active substances), and two different mechanisms are postulated to be responsible for the occurrence of catalytic current *A* and *B*. Below, the characteristics of maxima *A* and *B* are discussed separately.

Maximum A. Current *A* attains a maximum value at the pH at which the complex between Co(II) and MAN, denoted by Co(II)RS, has maximum stability. It decreases with decreasing and increasing pH. At potentials of currents *A*, Co(II)RS is adsorbed on the electrode (Figure 9). Mechanism I accounts for the kinetic hydrogen currents associated with currents *A*:

$$\text{I:}\quad \text{Co(II)RS}_{ads} + 2\,e \rightarrow \text{Co(0)RS}_{ads} \qquad \text{(a)}$$

$$\text{Co(0) RS}_{ads} \rightarrow \text{Co(0)} + \text{RS}^- \qquad \text{(b)}$$

$$\text{Co(II)} + \text{RS}^- \rightarrow \text{Co(II)RS}_{ads} \qquad \text{(c)}$$

$$\text{Co(0)RS}_{ads} + \text{H}^+ \rightarrow \text{Co(0)RSH}^+_{ads} \qquad \text{(d)}$$

$$\text{Co(0)RSH}^+_{ads} + e \rightarrow \text{Co(0)RS}_{ads} + {}^1/_2\,\text{H}_2 \qquad \text{(e)}$$

Reactions (a), (b), and (c) account for the kinetic cobalt(II) prewave current (*1*). With regard to the strong chemical affinity of both nitrogen and sulfur toward cobalt, it is reasonable to assume that the Co(0)RS formed upon reduction of Co(II)RS has some stability (*15*). In the proper pH range this unstable complex is protonated and then reduced to

(15) A. A. Vlček, *Z. Elektrochem.*, **61**, 1014 (1957).

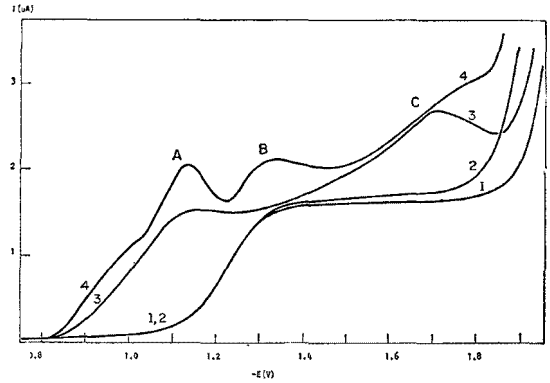

Figure 14. Polarograms of thioglycolic acid

Concn of $CoCl_2$, 0.4 m*M*: (1) 0.06*M* borax, pH 9.2; (2) 0.06*M* borax plus 0.48*M* H_3BO_3, pH 7.7; (3) as 1 plus 1 × 10^{-6}*M* TGA; (4) as 2 plus 1 × 10^{-4}*M* TGA

yield hydrogen. Reactions (d) and (e), as well as reactions (a), (b), and (c) constitute a chain reaction.

From *i–t* curves it can be concluded that currents *A* have a mixed adsorption-kinetic character. The value of x in the expression $i_{\max A} = kt^x$ at 30° C was found to be 0.84, intermediate between that for a purely kinetic current ($x = 0.66$) and that for a current accelerated by absorption ($x = 1.17$) (*16*). Decrease in temperature promotes adsorption, but decreases the rates of chemical and electrochemical reactions. Maximum *A* is much smaller at 0 °C than at 30 °C (Figure 5). It has more the characteristics of an adsorption current at 0 °C, the value of x being found equal to 1.01 at 0 °C as compared to 0.84 at 30 °C. The decrease of current *A* after the maximum is attributed to decreasing adsorption of Co(II)RS with increasing negative potential (Figure 9). Surfactants decrease the adsorption of Co(II)RS and also the rate of chemical and electrochemical reactions, resulting in a decrease of maximum *A*. At a high pH (pH $\cong$ 7), there is little protonation and current *A* is very small, unless large concentrations of MAN are used. On the other hand, at small pH (pH $\lesssim$ 3) Co(II)S is unstable and reaction (c) does not occur. From Figure 6 it is apparent that not only hydronium ions but also the acid form of the buffer (acetic acid) plays a role in the protonation reaction.

Maximum B. Current *B* increases continuously with increasing hydrogen ion concentration and is not affected by the concentration of acetic acid in the buffer (Figure 7). Therefore Co(II)RS is not involved in the mechanism which accounts for current *B*, and protonation is determined only by hydronium ions. Current *B* is observed at potentials at which the reduction of the aquo cobalt ion starts. The primary product of this reduction is metallic cobalt, which is unstable and quickly amalgamates and reacts further with mercury (*9*, *10*);

$$\text{Co(II)} + 2\,e \rightarrow \underset{\text{unstable}}{\text{Co(0)metal}} \xrightarrow[k_1]{+\text{Hg}}$$

$$\underset{\text{unstable}}{\text{Co(O)amal}} \xrightarrow[k_2]{+\text{Hg}} \underset{\text{stable}}{\text{Co}_x\text{Hg}_y} \qquad \text{(f)}$$

Under certain conditions the amalgamation of the deposited metallic cobalt is inhibited. This has been observed, for

(16) J. Weber, J. Koutecký, and J. Koryta, *Z. Elektrochem.*, **63**, 583 (1959).

example, in the reduction of divalent cobalt from solutions containing potassium thiocyanate (*17*, *18*), alkaline earth metal salts (*19*), surface active substances (*20*), and under certain conditions of electrolysis (*21–23*). When the amalgamation is inhibited, a layer of cobalt microcrystals has been observed on the surface of the mercury electrode. The hydrogen overvoltage on cobalt is much less than that on mercury. In very acidic solutions, the liberation of hydrogen accompanies the cobalt(II) reduction even in cases when the metallic deposit is not stabilized (*13*, *24*, *25*). In acetate buffers with a pH as high as 4.6, we have observed that the cobalt(II) reduction wave exhibits a small maximum because of hydrogen evolution and not to streaming, as it increases in presence of small amounts of polyvinylpyrrolidone (Figure 11), the latter increasing the life period of the cobalt metal.

The above observations are important for the interpretation of current and maximum *B* of MAN. The RSH form of MAN is still appreciably adsorbed at potentials of maximum *B*. This adsorbed RSH aids in stabilizing the metallic cobalt deposited on the electrode, thus considerably reducing the hydrogen overvoltage. This proton reduction may be further enhanced by the formation of a semistable complex between metallic cobalt and adsorbed RSH (reaction g) as proposed in mechanism II:

$$\text{II:}\quad \text{Co(0)metal} + \text{RSH}_{ads} \rightarrow \text{Co-}\text{-RSH}_{ads} \qquad \text{(g)}$$

$$H_3O^+ + e \rightarrow H_2O + {}^1/_2\,H_2 \text{ (at stabilized Co)} \qquad \text{(h)}$$

$$\text{RSH}_{ads} + e \rightarrow RS^- + {}^1/_2\,H_2 \text{ (at stabilized Co)} \qquad \text{(i)}$$

$$RS^- + H_3O^+ \rightarrow \text{RSH} + H_2O \qquad \text{(j)}$$

The symbol -- denotes the chemisorption bond between cobalt and MAN. At potentials more negative than that at maximum *B*, the current decreases as a result of decreasing adsorption of RSH and hence of decreasing stability of deposited metallic cobalt. The current increases again at potentials of the "presodium wave." At a high pH (*e.g.*, 8.2), the thiol group of MAN is completely in the anionic form and reaction (h) accounts for the observed small *B* currents. At still higher pH (9.2, Figure 1), no current *B* is observed, indicating that it is the reduction of H_3O^+ [reaction (h)] and not of H_2O which determines current *B*. At low pH, both reactions (h) and (i) become increasingly more important.

Scheme II suggests typical surface-kinetic character of current *B* and this is substantiated by the shape of current–time curves and also by the large effect of ionic strength and of valence of cations. With decreasing temperature the adsorption of RSH increases, and also the stability of the freshly deposited cobalt. Even though the rates of reactions (h) and (i) decrease, the overall result is that maximum *B* increases with decreasing temperature (Figure 5). The increase of maximum *B* in the presence of small amounts of surfactants like polyvinylpyrrolidone is accounted for by the stabilizing effect of the adsorbed surfactant on the deposited metallic cobalt and by decreasing the free area of the electrode. With larger concentrations of surfactant, the cobalt(II) reduction becomes greatly inhibited. Moreover, the surfactant replaces RSH from the surface with the overall result that maximum *B* becomes very small (Figure 11).

In conclusion it may be added that the appearance of large catalytic hydrogen maxima observed in solutions containing cobalt(II) and potassium thiocyanate in the presence of several surfactants (*26*) can be explained in the light of mechanism II. It has been shown in the literature (*17*, *18*) that the reduction of divalent cobalt from its thiocyanate solutions is often accompanied by a separation of cobalt microcrystals on the mercury surface. Presence of surfactants can further increase the stability of the cobalt deposit and thus promote the catalytic discharge of hydrogen at metallic cobalt.

ACKNOWLEDGMENT

We are greatly indebted to Prof. C. Y. Myers from the Southern Illinois University, Carbondale, Ill., for kindly having made available to us liberal amounts of thiophenol and pentachlorothiophenol.

RECEIVED for review December 6, 1968. Accepted March 18, 1969. This investigation was supported by Public Health Service Grant No. CA-08723-02 from the National Cancer Institute.

(17) G. N. Babkin, *Izv. Vyssh. Ucheb. Zaved. Khim. Khim. Tekhnol.*, **7**, 90 (1964).
(18) H. Shirai, *Nippon Kagaku Zasshi*, **85**, 322 (1964).
(19) G. N. Babkin and Sh. S. Sambetov, *Izv. Vyssh. Ucheb. Zaved. Khim. Khim. Tekhnol.*, **7**, 95 (1964).
(20) V. F. Ivanov and Z. A. Ioffa, *J. Phys. Chem. (USSR)*, **38**, 563 (1961).
(21) V. F. Ivanov and Z. A. Ioffa, *Dokl. Akad. Nauk SSSR*, **140**, 1368 (1961).
(22) J. Mindowitz, *Elektrochim. Acta*, **5**, 202 (1961).
(23) G. N. Babkin, M. S. Kazakishcheva, and M. Zh. Graisina, *J. Phys. Chem. (USSR)*, **39**, 73 (1965).
(24) I. M. Reibel, *Tr. Kishinevsk. Sel'skokhoz. Inst.*, **1962**, p 35; *Chem. Abstr.*, **59**, 9594c.
(25) I. M. Reibel, *Teoriya i Prakt. Polarograph. Analiza, Akad. Nauk Moldavsk., SSR, Materialy Pervogo Vses. Soveshch.*, **1962**, p 323; *Chem. Abstr.*, **59**, 6032d.
(26) M. Shinagawa, H. Nezu, H. Sunahara, F. Nakashima, H. Okashita, and T. Yamada, "Advances in Polarography," Pergamon Press, Oxford, 1960, Vol. 3, p 1142.

Kinetic Waves in Systems Containing Cobalt(II) and Cysteine-Like Compounds

Adsorption Phenomena in the Cystamine–Cobalt(II) System in Borax Medium

P. Mader and I. M. Kolthoff
School of Chemistry, University, of Minnesota, Minneapolis, Minn. 55455

The reduction wave of cystamine in 0.06*M* borax starts at −0.5 V (*vs.* SCE), the current rising to an acute maximum, which is completely suppressed by traces of cobalt(II). The cystamine wave is shifted by cobalt(II) to considerably more negative potentials. The main cystamine wave in the presence of cobalt(II) is preceded by a small prewave, which attains a constant value at a cobalt concentration of $1.2 \times 10^{-4}M$ and which has the characteristics of an adsorption wave. The prewave is attributed to the reduction of cobalt(II) cystamine complex to cobalt(II) cysteamine complex. The capillary activities of cystamine and of cysteamine are greatly enhanced by cobalt(II). The cobalt(II) cysteamine complex is strongly adsorbed at potentials of the prewave and it greatly inhibits the electroreduction of cystamine. When the surface of the mercury is completely covered, the area of an adsorbed molecule of cobalt(II) cysteaminate is calculated to be of the order of 60 Å².

In connection with polarographic studies of a cobalt(II) prewave observed by us in borate medium in the presence of traces of cystine, cysteine, and similar compounds (*1*), a brief study was made of the effect of divalent cobalt on the polarographic reduction of cystamine in this medium. At pH 2 to 10, cystamine (RSSR) at a dropping mercury electrode gives a two-electron reduction wave with formation of two molecules of cysteamine (RSH)

$$RSSR + 2H^+ + 2e^- \rightarrow 2RSH$$

The reduction is quasireversible (*2*), the half-wave potential depending on pH. In 0.06*M* borax, pH 9.2, the reduction of cystamine starts at about −0.5 V and the current rises to a large maximum of the first kind. Traces of cobalt(II) bring about a complete suppression of this maximum and a shift of the wave to more negative potentials. At larger cobalt(II) concentrations, a well-developed small prewave preceding the inhibited cystamine wave is observed. In the present paper a more detailed study has been made of the inhibiting effect of cobalt(II) on the cystamine reduction in borax medium.

EXPERIMENTAL

Cystamine was a product of Nutritional Biochem. Corp., Cleveland. Before a set of experiments, a $10^{-2}M$ stock solution was freshly prepared in doubly-distilled water. All other chemicals used were of c.p. quality. In order to avoid depletion of reducible material when a new drop of mercury forms, a capillary tilted at an angle (*3*) of 45° with characteristics $m = 0.64$ mg/sec, $t = 4.9$ sec at 76 cm Hg, and zero applied voltage was used. The cell and apparatus were the same as described previously (*1*). The experiments were run at 25 °C and in absence of air.

RESULTS

Reduction of Cystamine in Presence of Cobalt(II). The reduction wave of $1 \times 10^{-3}M$ cystamine in 0.06*M* borax, pH 9.2, is shown in Figure 1, curve 1. The large maximum accompanying the wave is of the first kind (stirring). This was substantiated by the shape of current–time curves at potentials of the maximum, which show irregularities (Figure 2) typical of stirring. Surfactants like gelatin or methyl cellulose in low concentrations suppress the maximum without otherwise affecting materially the characteristics of the wave. Addition of cobalt(II) to the cystamine solution in borax has a striking effect (Figure 1). In the presence of $4 \times 10^{-5}M$ $CoCl_2$, the maximum on the cystamine wave is almost completely suppressed, while the reduction is shifted to more negative potentials. At a cobalt(II) concentration of the order of $1.2 \times 10^{-4}M$ and higher, the half wave potential of the inhibited cystamine wave is about 0.25 V more negative than $E_{1/2}$ in the absence of cobalt. In the presence of cobalt (II), a distinct but very small prewave with $E_{1/2}$ of −0.51 V is observed, which attains a constant height at concentrations of cobalt equal to or greater than $1.2 \times 10^{-4}M$ (Figure 1). The limiting currents at potentials more negative than about −1.0 V increase with increasing cobalt(II) concentration and are equal to the sum of the diffusion currents of cystamine and cobalt(II) (see inset in Figure 1). At cobalt concentrations exceeding $4 \times 10^{-4}M$, this linearity does not hold any longer, and at a concentration of $8 \times 10^{-4}M$ Co(II), the limiting current attains a constant value which is independent of further increase of the cobalt concentration. At cobalt concentrations greater than $8 \times 10^{-4}M$, a colloidal precipitate of cobalt (II) borate (*4*) becomes visible in the solution. The large currents at potentials more negative than −1.3 V have the characteristics of currents due to hydrogen evolution observed with aliphatic sulfhydryl compounds in the presence of cobalt (II) [Brdička currents (*5*)].

Prewave. Current–time curves recorded at potentials of the prewave are shown in Figure 3*A*, *B*. At small cobalt(II) concentrations and potentials between −0.55 and −0.70V *i–t* curves exhibit irregularities which appear as a break or sudden increase of current at some time after the drop has started—*e.g.*, curves 2 and 3 in Figure 3*A*, *B*. These irregularities are due to stirring, the marked stirring observed in the absence of cobalt (Figure 1) not being completely suppressed in the presence of small concentrations of cobalt(II). When the cobalt concentration is $2 \times 10^{-4}M$ or greater, the

(1) I. M. Kolthoff, P. Mader, and S. E. Khalafalla, *J. Electroanal. Chem.*, **18**, 315 (1968).
(2) M. Asthana, R. C. Kapoor, and M. L. Nigam, *Electrochim. Acta*, **11**, 1587 (1966).
(3) I. Smoler, *Collect. Czech. Chem. Commun.*, **19**, 238 (1954).
(4) P. Mader and I. M. Kolthoff, *J. Polarographic Soc.*, **14**, 42 (1968).
(5) A. Calusaru, *J. Electroanal. Chem.*, **15**, 269 (1967).

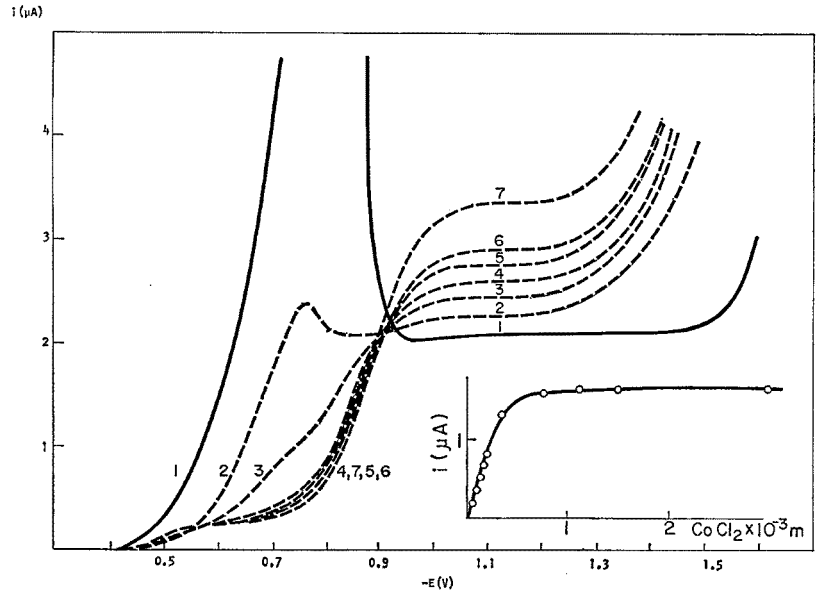

Figure 1. Reduction of cystamine in presence of cobalt(II)

0.06M borax, $1 \times 10^{-3}M$ cystamine, pH 9.2. Concn of $CoCl_2$: (*1*) 0; (*2*) 4; (*3*) 8; (*4*) 12; (*5*) 16; (*6*) 20; (*7*) $30 \times 10^{-6}M$. Inset: i_1-$(i_d)_{cystamine}$ *vs.* $C_{Co(II)}$ at −1.1 V

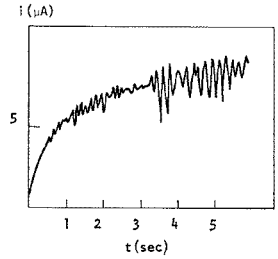

Figure 2. Current–time curve recorded at the potential of the maximum on the cystamine wave, 0.06M borax, $1 \times 10^{-3}M$ cystamine

$E = -0.80$ V

current attains a maximum value very rapidly and then decreases continuously with time (curve 6, Figure 3*B*). Under these conditions the log i *vs.* log t plots at times longer than 0.5 sec yield straight lines (Figure 4) with a slope of −0.37 which is close to the value of −0.33, characteristic of adsorption curves (*6*). The adsorption character of the prewave is substantiated also by the effect of the height of mercury in the reservoir. At $8 \times 10^{-4}M$ cobalt(II), when the electrode becomes fully occupied by the adsorbed species almost immediately after formation of the drop, the limiting prewave current is found to increase linearly with the first power of the height of mercury (Figure 5), a relation which is typical of adsorption currents (*6*).

Inhibited Wave of Cystamine. From Figure 1 it is apparent that the shift of the cystamine reduction wave to more negative potentials increases with increasing cobalt concentration until the latter is $1.2 \times 10^{-4}M$. Further increase of the cobalt concentration has only a small effect on the location of

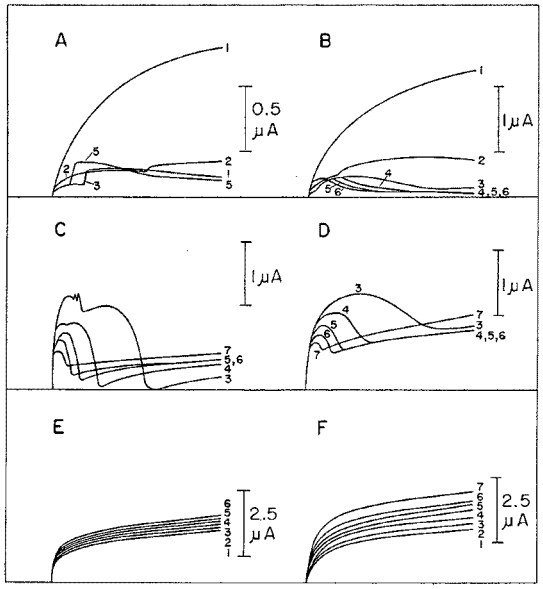

Figure 3. Current–time curves at different concentrations of $CoCl_2$ in 0.06M borax, $1 \times 10^{-3}M$ cystamine

Concn of $CoCl_2$: (*1*) 0; (*2*) 4; (*3*) 8; (*4*) 12; (*5*) 16; (*6*) 20; (*7*) $30 \times 10^{-6}M$. Applied potential: (*A*) −0.55; (*B*) −0.60; (*C*) −0.75; (*D*) −0.81; (*E*) −0.95; (*F*) −1.05 V. Height of mercury 53 cm

(6) R. Brdička, *Z. Elektrochem.*, **48**, 278 (1942).

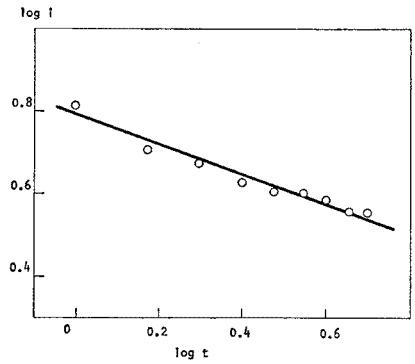

Figure 4. Log i *vs.* log t analysis of the i–t curve 6 of Figure 3*B*, for $t > 0.5$ sec

Slope $x = -0.37$

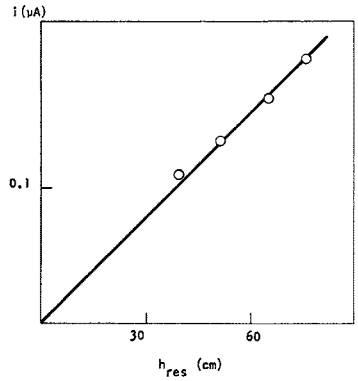

Figure 5. Plot of prewave current, i_p, *vs.* height of mercury in reservoir, h_{res}

Solution 0.06*M* in borax, 8 × 10^{-4}*M* $CoCl_2$, 1 × 10^{-3}*M* cystamine. Vertical capillary; m = 1.14 mg/sec, t = 5.64 sec at zero applied voltage and h_{Hg} = 76 cm

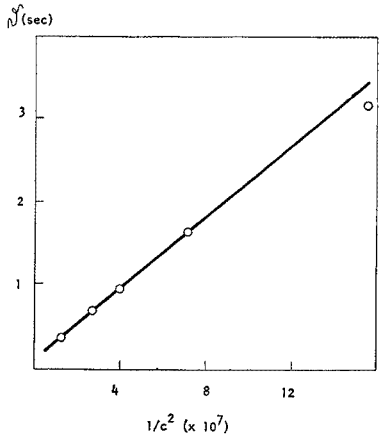

Figure 6. Plot of time of coverage, ϑ, *vs.* reciprocal of second power of cobalt(II) concentration, $1/c^2$

Solution 0.06*M* in borax, 1 × 10^{-3}*M* in cystamine. E = −0.75 V

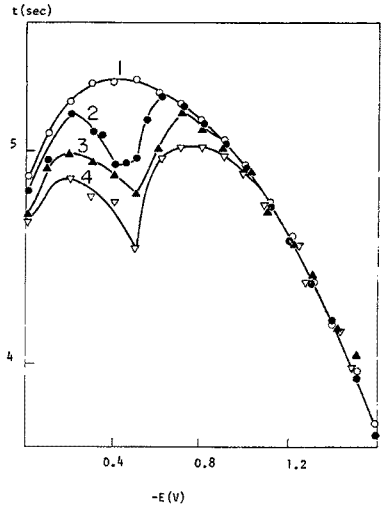

Figure 7. Drop time *vs.* E curves in 0.06*M* borax

Concn of cystamine: (*1*) 0; (*2–4*) 1 × 10^{-3}*M*. Concn of $CoCl_2$: (*1–2*) 0; (*3*) 4; (*4*) 8× 10^{-5}*M*. Height of mercury 60 cm

the wave. Current–time curves recorded at potentials between −0.70 and −0.85 V (Figure 3*C* and *D*) show a strong inhibition of the rate of cystamine reduction by cobalt(II) after the surface has become covered with the adsorbed species. The values of the time, ϑ, necessary for a complete coverage of the electrode surface, plotted *vs.* the reciprocal of the second power of the cobalt concentration, $1/c^2$, give straight lines (Figure 6) indicating the fast establishment of adsorption equilibrium which is diffusion-controlled (*7, 8*).

At −0.75 to −0.78 V and at the lowest cobalt(II) concentrations, the *i–t* curves exhibit irregularities especially at the beginning of formation of the drop—*e.g.*, curve 3 in Figure 3*C*. These irregularities again are caused by marked stirring in the presence of small concentrations of cobalt(II), when the surface coverage by the adsorbed species is very small. With increasing time and also at higher cobalt(II) concentrations the degree of coverage of the surface by the adsorbed species increases and the stirring ceases.

Current–time curves recorded at −0.95 and −1.05 V have the appearance of monotonous parabolas (Figure 3*E, F*). The limiting currents at −1.05 V are diffusion controlled, as follows from the value of the exponent x in the expression $i = kt^x$, x = 0.20, as compared to the theoretical value of 0.17.

Electrocapillary Curves. Electrocapillary measurements have been made in the presence of cystamine and in the presence and absence of cobalt(II). From drop time *vs.* E curves in 0.06*M* borax (Figure 7) it is clear that cystamine is strongly adsorbed at the mercury electrode at potentials in the vicinity of the electrocapillary maximum. Curve 2 in Figure 7 coincides with the electrocapillary curve in the buffer in the absence of cystamine (curve 1) at slightly more negative potential than that at which the reduction of cystamine starts, indicating that the reduction product cysteamine is not appreciably adsorbed at this potential. Addition of cobalt(II) to the cystamine solution results in a large decrease of the surface tension which extends to potentials more distant from the electrocapillary maximum than in the absence of cobalt (compare curves 3 and 4 in Figure 7 with curve 2). No decrease of the surface tension has been observed at potentials more negative than −0.95 V.

Analogous measurements run with cysteamine revealed that the cobalt(II) cysteamine complex is also strongly adsorbed at the electrode surface. In the absence of cobalt, cysteamine decreases the surface tension only at the potentials at which it reacts anodically with mercury, giving mercury cysteaminate which is strongly adsorbed. Both cysteamine alone and cysteamine in the presence of cobalt(II) are extremely sensitive toward oxidation by atmospheric oxygen at a pH of 9.2, and extreme precautions had to be taken to protect solutions against oxidation.

DISCUSSION

In the absence of cobalt(II), cystamine in borax solution is reduced in the adsorbed state at the DME (compare Figures 1 and 7). The adsorbed cystamine causes a large maximum of the first kind (*9*). In alkaline medium, cystamine forms with divalent cobalt a fairly stable complex in which the sulfur atoms participate in the coordination (*10*). The stability constants of this complex could not be determined because the complex is only sparingly soluble in water and precipitates during the titration (*10*). The slightly soluble cobalt(II) cystamine complex is strongly capillary-active at the solution–mercury interface (Figure 7). The prewave of cystamine observed in the presence of cobalt(II) starts at about the same potential as the cystamine reduction wave in the absence of cobalt (Figure 1). The reduction product in the prewave is a cobalt(II) complex of cysteamine, which is strongly capillary

(7) J. Koryta, *Collect. Czech. Chem. Commun.*, **18**, 206 (1953).
(8) R. W. Schmid and C. N. Reilley, *J. Amer. Chem. Soc.*, **80**, 2087 (1958).
(9) G. C. Barker and J. A. Bolzan, *Z. Anal. Chem.*, **216**, 215 (1966).
(10) E. Gonick, W. C. Fernelius, and B. E. Douglas, *J. Amer. Chem. Soc.*, **76**, 4671 (1954).

active. In the presence of two molecules of cysteamine per one cobalt ion, Gonick (*11*) found a composition corresponding to Co(II)(RS)$_2$, which has stability constants of $pK_1 = 7.68$, $pK_2 = 7.03$. The limiting current of the prewave has typical characteristics of an adsorption current, as has been shown in the experimental section. At potentials between about -0.7 and -0.82 V, the rate of electroreduction of the free (noncomplexed) cystamine in the presence of the adsorbed complex is no longer negligible, as is evident from *i–t* curves *C* and *D* in Figure 3. The current decreases abruptly at the time when the surface becomes covered with the complex and from then on the current increases parabolically with time, the rate becoming greater with increasing negative potential (compare *C* and *D* in Figure 3). At potentials more negative than -0.95 V, no adsorption of a cobalt complex occurs (Figure 7) and the current–time curves have the characteristics of a diffusion-controlled current (*E* and *F* in Figure 3). In unreported experiments with mixtures of cysteamine and cobalt(II), the reduction of the latter started at about -0.85 V, the reduction waves having a similar appearance as the main cystamine waves in the presence of sufficient cobalt(II) (curves 4, 5, 6, and 7 in Figure 1).

In solutions 0.06*M* in borax and $1 \times 10^{-3}M$ in cystamine, the surface at -0.75 V becomes completely covered with the cobalt(II) complex after 3.2, 1.6, 0.9, 0.7, and 0.4 seconds in the presence of 0.8, 1.2, 1.6, 2.0, and $3.0 \times 10^{-4}M$ cobalt(II), respectively (Figure 3, *C*). By extrapolation it is found that the surface is covered with the adsorbed species virtually immediately at the time of formation of a drop at a cobalt concentration of $8 \times 10^{-4}M$. It is under this condition that the limiting current of the prewave is found proportional to the height of mercury in the reservoir (Figure 5).

The validity of the expression

$$\vartheta c^2 = \text{const.}$$

(ϑ denoting the time of coverage of the surface) has been found to hold (Figure 6). This relation indicates that adsorption equilibrium is established rapidly and that it is diffusion-controlled (*7*, *8*). Under this condition the maximum number, Γ_m, of moles of adsorbed species per cm^2 can be calculated (*7*, *8*)

$$\Gamma_m = 7.36 \times 10^{-4}\, c\, D_a^{1/2} \vartheta^{1/2}$$

D_a denoting the diffusion coefficient of the adsorbed species. From the values of the cystamine diffusion currents in 0.06*M* borax at 25 °C, its diffusion coefficient, D_{RSSR}, was calculated to be 3.5×10^{-6} cm^2 sec^{-1}. Assuming the diffusion coefficient of the cobalt(II) cystaminate to be the same, the value of Γ_m at a cobalt concentration greater than $1.2 \times 10^{-4}M$ was found to be 2.4×10^{10} mole cm^{-2}, which corresponds to an area of 69 Å^2 per adsorbed molecule of cobalt(II) cysteaminate.

The maximum number of moles adsorbed per unit electrode surface can also be calculated from the value of the mean adsorption current, provided the adsorption equilibrium is so favorable that the drop surface is fully covered as soon as the drop is formed, and that the reduction proceeds reversibly (*6*). From the height of the limiting prewave current, $i_p = 0.13$ μA (corrected for the residual current) in the presence of $1 \times 10^{-3}M$ cystamine and $1.6 \times 10^{-4}M$ cobalt(II), a value of Γ_m of 2.6×10^{-10} mole cm^{-2} is calculated, corresponding to an area covered by one molecule of 61 Å^2. The size of the cobalt(II) cysteamine molecule, Co(II)(RS)$_2$, calculated from a stereo model, is of the order of 55 Å^2. If the molecule is spread flatly on the surface, this value is in satisfactory agreement with the above values.

(11) E. Gonick, Thesis, University of Pennsylvania, 1951.

RECEIVED for review December 31, 1968. Accepted March 18, 1969. This investigation was supported by Public Health Service Grant No. Ca-08723-02 from the National Cancer Institute.

Corrections

Resolution of Overlapping Bands: Functions for Simulating Band Shapes

In this article by R. D. B. Fraser and Eikichi Suzuki [ANAL. CHEM., **41**, 37 (1969)] an error appears on page 38, column 2, Equation 16. The first equation should be:

$$Y_0 = \Delta X_m \cdot Y_m \exp(1/2)$$

Rapid Separation by Carbon Number and Determination of Naphthene and Paraffin Content of Saturate Petroleum Distillates up to 185 °C

In this article by J. V. Brunnock and L. A. Luke [ANAL. CHEM., **40**, 2158 (1968)] there is an error in the last sentence on page 2158. The sentence should read "It is essential to eliminate all traces of oxygen from the helium gas stream; otherwise, partial oxidation of the sample on the sieve will commence at temperatures in excess of 300 °C.

An Analyzer for the Dynamic Microdetermination of Carbon, Hydrogen, Nitrogen, Sulfur, and Oxygen

In this article by George Dugan and V. A. Aluise [ANAL. CHEM., **41**, 495 (1969)] there is an error in the third sentence of the Abstract. It should read as follows: "Retention and separation of the combustion gases, N_2, CO_2, SO_2, and H_2O are accomplished by using chromatographic columns in liquid nitrogen."

A Unified Treatment of Electrolysis at an Expanding Mercury Electrode

Keith B. Oldham

Science Center, North American Rockwell Corporation, Thousand Oaks, Calif. 91360

This article describes a general treatment of voltammetry at an electrode expanding in accord with any power law: the stationary electrode and the dropping mercury electrode are special cases. Reversible, irreversible, and quasireversible electrode processes are embraced by the treatment. An equation of very wide generality is derived, the solution of which under appropriate conditions gives the equations associated with the names of Ilkovic, Cottrell, Heyrovsky–Ilkovic, Matsuda–Ayabe, Delahay–Strassner, Koutecky, Smutek Karaoglanoff, Sand, Delahay–Berzins, and Reinmuth. Many new voltammetric relationships are derived, several of which have attractive possibilities in electroanalysis.

THOUGH the dropping mercury electrode is the prime example of an electrode whose area increases with time, other types of electrode which share this property are conceivable. Thus, mercury could be allowed to flow into the base of a funnel (a conical funnel will yield a $t^{2/3}$ area dependence; a paraboloidal funnel will give an electrode area proportional to $t^{1/2}$) or a vessel holding a mercury pool electrode could be progressively inclined. These devices do not necessarily share the dropping electrode's $t^{2/3}$ area law. Moreover, recent work (*1*) in which a piston driven by a synchronous motor was used to replace the usual gravity feed, opens up the possibility of introducing other than $t^{2/3}$ dependence of area, even for the capillary mercury electrode. Here, therefore, the electrode area is considered to obey the general law

$$A(t) = at^p \tag{1}$$

where a and p are positive constants. [For a conventional dropping electrode $p = {}^2/_3$ and $a = (36\pi)^{1/3}\, \dot{m}^{2/3}\, \rho^{-2/3}$ where $\dot{m}$ and ρ are, respectively, the mass rate of flow of mercury and its density.] The constant area case is also covered by including the $p = 0$ possibility.

Consider the n-electron electroreduction

$$\text{Ox(soln)} + ne^-\text{(Hg)} = \text{Rd(soln)} \tag{2}$$

occurring at an expanding electrode, where Ox is present in solution at an initially uniform concentration C; Rd is soluble either in the solution or by amalgamation in the electrode phase, but is initially absent. It will be assumed that the expanding electrode is either planar, or can be approximated by an expanding plane. [Several investigations (*2, 3*) suggest that, for a dropping mercury electrode, the effect of sphericity is minor]. Moreover, linear semi-infinite diffusion is regarded as the sole mode of transport of Ox and Rd relative to their solvents. Yet another assumption is that the expansion of the electrode is uniform in the sense that in a given time interval all subregions of the electrode surface increase in area by the same factor. Unlike stretched flat membranes, planar or spherical liquid–liquid interfaces may expand uniformly, though nonuniform expansion is also possible.

Inasmuch as uniform expansion has been prescribed, the concentration of Ox at any point in the solution depends only on the distance r separating that point from the electrode and the time t since the birth of the electrode: $C(r,t)$ will be the symbol used to denote this concentration. In this terminology $C(0,t)$ and $\partial C(0,t)/\partial r$ then denote the surface concentration and the surface concentration gradient. The latter is related to the cathodic faradaic current (which may be time-dependent) by

$$D\left(\frac{\partial C}{\partial r}\right)(0,t) = \frac{I(t)}{nFA(t)} \tag{3}$$

which follows from the requirements of Fick's and Faraday's laws. All symbols are fully defined in Appendix A.

To derive the partial differential equation appropriate to the concentration of Ox in the vicinity of a uniformly expanding plane, let us first consider the situation in the absence of diffusion. Since the concentration is a function solely of distance and time we can write

$$dC(r,t) = \left(\frac{\partial C}{\partial r}\right)_t dr + \left(\frac{\partial C}{\partial t}\right)_r dt \tag{4}$$

Now, if no diffusion occurs, the concentration of Ox will remain constant in a moving plane defined such that a constant volume is enclosed between that plane and the electrode surface. We therefore insert the conditions $dC = 0$ and $d[rA(t)] = 0$ into equation (4), whence, by use of relation (1), $(\partial C/\partial t)_r = (pr/t)(\partial C/\partial r)_t$ is derived. In the presence of diffusion but without expansion, the usual Fick's second law relationship $(\partial C/\partial t)_r = D(\partial^2 C/\partial r^2)_t$ applies. In the present situation the effects of expansion and diffusion are additive and hence

$$\left(\frac{\partial C}{\partial t}\right)(r,t) = \frac{pr}{t}\left(\frac{\partial C}{\partial r}\right)(r,t) + D\left(\frac{\partial^2 C}{\partial r^2}\right)(r,t) \tag{5}$$

We seek to solve this equation subject to the initial condition

$$C(r,0) = C \tag{6}$$

and to a variety of boundary conditions. There are two boundaries to consider. One is a plane at an infinite distance from the electrode: within a finite time the Ox concentration here will not be perturbed by the electrode reaction and hence

$$C(\infty,t) = C \tag{7}$$

The other boundary is the electrode itself and the appropriate condition here is determined by the electrolysis regime (potentiostatic, galvanostatic, etc.). We choose not to specify this second boundary condition yet.

In Appendix B it is demonstrated that the surface Ox concentration is related to the electrode potential and to the

(1) S. Roffia and E. Vianello, *J. Electroanal. Chem. & Interfacial Electrochem.*, **17**, 13 (1968).
(2) I. M. Kolthoff and J. J. Lingane, "Polarography," Interscience, New York, 1952, p 44.
(3) J. Koutecky and J. Cizek, *Coll. Czech. Chem. Commun.*, **21**, 836 (1956).

cathodic faradaic current (either or both of which may be time-dependent) by the equation

$$C(0,t) = \frac{I(t)}{nFk_hA(t)} \exp\left\{\alpha \frac{nF}{RT}[E(t) - E_h]\right\} + [C - C(0,t)] \exp\left\{\frac{nF}{RT}[E(t) - E_h]\right\} \quad (8)$$

where all new symbols are fully defined in Appendix A. Certain assumptions concerning the kinetics of reaction (2) are implicit in equation (8), but this equation is general in the sense that it applies equally to reversible, irreversible and quasireversible (*4*) electrode reactions. However, should the reaction be reversible the first right-hand term in equation (8) may be ignored, whereas if the reaction is totally irreversible the first term is dominant and the second may be omitted.

To aid in the solution of equation (5), it is convenient to define new independent variables

$$X \equiv \frac{rt^p k_h^{2p+1}}{(2p+1)^p D^{p+1}} \quad (9)$$

and

$$Y \equiv \frac{t^{2p+1} k_h^{4p+2}}{(2p+1)^{2p+1} D^{2p+1}} \quad (10)$$

to replace r and t, respectively. The choice of these definitions is motivated by the simplification to equation (6) which thereby results, and by a wish to undimensionalize the variables. This is also a convenient juncture at which to replace the current and potential variables by the following dimensionless analogues

$$\iota(Y) \equiv \frac{I(t)k_h^{2p-1}}{naFCD^p(2p+1)^p} \quad (11)$$

and

$$\epsilon(Y) \equiv \exp\left\{\frac{nF}{RT}[E(t) - E_h]\right\} \quad (12)$$

Yet a further convenience is the introduction of a parameter ω,

$$\omega \equiv \frac{1}{4p+2} \quad (13)$$

to play the role hitherto assumed by p. Note that ω values in the range $0 < \omega \leq 1/2$ only are permitted. Particularly interesting values of ω are $3/14$ (corresponding to a conventional dropping mercury electrode), $1/4$, and $1/2$ (corresponding to a stationary electrode).

In terms of the new independent variables, equations (5) through (7) become

$$\frac{\partial C}{\partial Y}(X,Y) - \frac{\partial^2 C}{\partial X^2}(X,Y) = 0 \quad (14)$$

and

$$C(X,0) = C = C(\infty,Y) \quad (15, 16)$$

When equations (14) and (16) are Laplace transformed with respect to Y,

$$S\bar{C}(X,S) - \frac{\partial^2 \bar{C}}{\partial X^2}(X,S) = C(X,0) = C \quad (17)$$

(the latter equality following from (15)) and

$$\bar{C}(\infty,S) = \frac{C}{S} \quad (18)$$

result, where S^{-1} and $\bar{C}(X,S)$ are the transforms of Y and $C(X,Y)$. Subject to the requirement of equation (18), the general solution to differential equation (17) is

$$\bar{C}(X,S) = Q(S) \exp\{-X\sqrt{S}\} + \frac{C}{S} \quad (19)$$

where $Q(S)$ is a function of the dummy variable determined by the as-yet-unspecified boundary condition. This unknown function may be eliminated by combining equation (19) with the result of its own X-differentiation; this yields

$$\bar{C}(X,S) = \frac{C}{S} = \frac{1}{\sqrt{S}} \frac{\partial \bar{C}}{\partial X}(X,S) \quad (20)$$

Inserting the $X = 0$ condition, and adopting the symbol $L\{\ \}$ to indicate the operation of Laplace transformation with respect to Y, equation (20) becomes

$$L\{C(0,Y)\} = \frac{C}{S} - \frac{1}{\sqrt{S}} L\left\{\frac{\partial C}{\partial X}(0,Y)\right\} \quad (21)$$

Equation (21) is a very general result interrelating the surface Ox concentration and its surface concentration gradient, as functions of time, at an expanding electrode under any electrolysis regime. Usually, however, these two variables are not accessible to measurement or to direct control. Accordingly, a more useful relationship is obtained by solving equation (8) for $C(0,t)$ and inserting this expression together with equation (3) into (21), thereby producing an equation interrelating potential and current. In terms of the dimensionless quantities defined in identities (10) through (13) the interrelationship is found to be

$$L\left\{\frac{Y^{\omega-\frac{1}{2}}\iota(Y)\epsilon^{\alpha}(Y) + \epsilon(Y)}{1 + \epsilon(Y)}\right\} = \frac{1}{S} - \frac{1}{\sqrt{S}} L\{Y^{2\omega-1}\iota(Y)\} \quad (22)$$

The generality of this equation is extremely wide and the remainder of this article is devoted to its solution under specific electrolysis regimes. Though all degrees of reversibility are embraced by equation (22) as it stands, the left-hand side may be simplified to $L\{\epsilon(Y)/[1 + \epsilon(Y)]\}$ or to $L\{Y^{\omega-\frac{1}{2}}\iota(Y)\epsilon^{\alpha}(Y)\}$, respectively, under conditions of total reversibility or irreversibility.

We shall consider four electrolysis regimes: very negative potential, constant potential, constant current, and linearly increasing current. These regimes correspond to electrolysis orders (*5*) of 0, 2, 3, and 5.

Very Negative Potentials. As E approaches $-\infty$, ϵ becomes vanishingly small and the left hand side of equation (22) becomes zero, leading to the simple transform equation

$$L\{Y^{2\omega-1}\iota(Y)\} = \frac{1}{\sqrt{S}} = L\left\{\frac{1}{\sqrt{\pi Y}}\right\} \quad (23)$$

Hence $\iota(Y) = Y^{\frac{1}{2}-2\omega}/\sqrt{\pi}$, which on insertion of the original variables becomes

$$I(t) = naFCt^{p-1/2}\sqrt{\frac{(2p+1)D}{\pi}} \quad (24)$$

(4) P. Delahay, *J. Amer. Chem. Soc.*, **75**, 1430 (1953).

(5) K. B. Oldham, ANAL. CHEM., **40**, 1912 (1968).

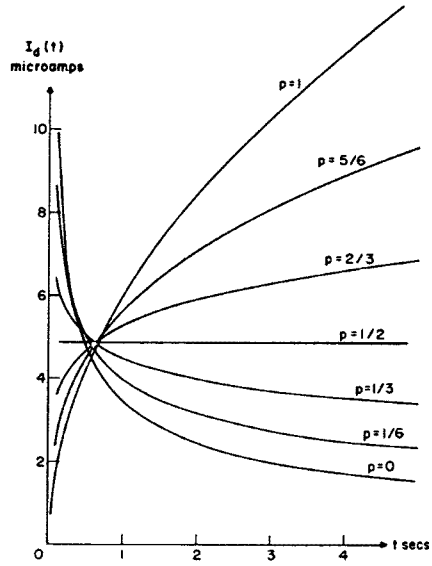

Figure 1. Current–time relationships for very negative potentials and various p values

The following constant values were assumed: $n = 2$ equiv mole^{-1}, $C = 10^{-6}$ mole cm^{-3}, $a = 10^{-2}$ cm^2 sec^{-p}, and $D = 10^{-5}$ cm^2 sec^{-1}

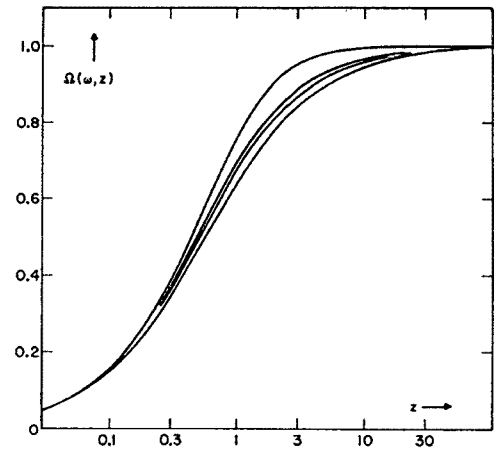

Figure 2. $\Omega(\omega,z)$ plotted semilogarithmically as a function of z for four values of ω: reading downward ω = $^1/_2$, $^1/_4$, $^1/_6$, and 0

These graphs also depict the irreversible behavior of $I(t)/I_d(t)$ for p values of 0, $^1/_2$, 1 and ∞; the abscissa in this case is linear in potential. The plot for the dropping mercury electrode case (ω = $^2/_{14}$, p = $^2/_3$) is not included but it lies between the second and third curves

For the case $p = {}^2/_3$, this is the equation derived 34 years ago by Ilkovic (*6*). For the $p = 0$ case, equation (24) correctly reduces to the Cottrell expression (*7*). For the intriguing $p = {}^1/_2$ case, equation (24) predicts a time-independent current of magnitude $naFC\sqrt{2D/\pi}$.

Expression (24) is independent both of potential and of the kinetics of reaction (2). Diffusion alone limits the extent of reaction and such a current is termed a "diffusion limited current," $I_d(t)$. Figure 1 shows graphically how $I_d(t)$ depends on p, for p values of 0, $^1/_6$, $^1/_3$, $^1/_2$, $^2/_3$, $^5/_6$, and 1.

Reversible Potentiostatic Regime. At constant potential, ϵ does not depend on Y, which leads to a marked simplification of equation (22). If, additionally, the reversibility simplification is introduced, there remains

$$\frac{1}{S} - \frac{1}{\sqrt{S}} L\{Y^{2\omega-1}\iota(Y)\} = L\left\{\frac{\epsilon}{1+\epsilon}\right\} = \frac{\epsilon}{(1+\epsilon)S} \tag{25}$$

Thereby $L\{Y^{2\omega-1}\iota(Y)\} = 1/\sqrt{S}(1+\epsilon)$, which gives $\iota(Y) = Y^{\frac{1}{2}-2\omega}/(1+\epsilon)\sqrt{\pi}$ on inversion. Returning to the original variables:

$$I(t) = \frac{naFCt^{p-\frac{1}{2}}\sqrt{(2p+1)D/\pi}}{1+\exp\left\{\frac{nF}{RT}[E-E_h]\right\}} \tag{26}$$

The numerator of this equation is identical with the expression given in equation (24) for the diffusion-limited current $I_d(t)$. Rearrangement therefore gives $E = E_h + [RT/nF]\ln\{[I_d(t) - I(t)]/I(t)\}$, which is the well-known Heyrovsky–Ilkovic equation (*8*) of polarography, with $E_{1/2}$, the half-wave potential, equal to E_h.

A time-independent current

$$I(t) = naFC\sqrt{\frac{2D}{\pi}}\left(1+\exp\left\{\frac{nF}{RT}[E-E_h]\right\}\right)^{-1} \tag{27}$$

is again the case if $p = {}^1/_2$. It should be appreciated that this time-independence does not result from a steady state having been established. Rather, the concentration profile is time-dependent in such a way that the fall-off in current density is exactly compensated by the area increase.

Irreversible Potentiostatic Regime. The situation here is less simple. The prescription of constant ϵ reduces the irreversible version of equation (22) to

$$\epsilon^{\alpha} L\{Y^{\omega-\frac{1}{2}}\iota(Y)\} = \frac{1}{S} - \frac{1}{\sqrt{S}} L\{Y^{2\omega-1}\iota(Y)\} \tag{28}$$

Clearly no simple power expression $\iota(Y) = Y^{\beta}$ will satisfy this equation. However, it is easy to show that either of the two power series $\iota(Y) = \sum_0^{\infty} B_j Y^{b\pm j\omega}$ do satisfy equation (28) provided that, in each case, the index b and the coefficients B_j are suitably chosen. The procedure for finding b and each B_j is given in Appendix C, wherein is also defined a function $\Omega(\omega,z)$ in terms of which the solution to equation (28) is $\iota(Y) = \pi^{-1/2}Y^{1/2-2\omega}\Omega(\omega, Y^{\omega}\epsilon^{-\alpha})$. In terms of the original variables the solution is

$$I(t) = naFCt^{p-\frac{1}{2}}\sqrt{\frac{(2p+1)D}{\pi}}\,\Omega\left(\frac{1}{4p+2}, k_h\sqrt{\frac{t}{(2p+1)D}}\exp\left\{\frac{-\alpha nF}{RT}[E-E_h]\right\}\right) \tag{29}$$

(6) D. Ilkovic, *Coll. Czech. Chem. Commun.*, **6**, 498 (1934).
(7) F. G. Cottrell, *Z. Physik. Chem.*, **42**, 385 (1902).
(8) J. Heyrovsky and D. Ilkovic, *Coll. Czech. Chem. Commun.*, **7**, 198 (1935).

The pre-Ω term on the right-hand side of this equation is $I_d(t)$.

For $p = 2/3$, equation (29) proves to be identical with that derived by Matsuda and Ayaba (9) for a totally irreversible reduction at a dropping mercury electrode [see Appendix C, also see Smith, *et al.* (10).]

There is some simplification to the Ω function when $p = 1/2$, but no pseudo-steady-state is developed as in the reversible case. As demonstrated in Appendix C, equation (29) reduces drastically when $p = 0$, yielding

$$I(t) = naFC\sqrt{\frac{D}{t}}\,\xi \exp(\xi^2)erfc(\xi) \qquad (30a)$$

where

$$\xi = k_h\sqrt{\frac{D}{t}} \exp\left\{\frac{-\alpha nF}{RT}[E - E_h]\right\} \qquad (30b)$$

This result is identical with that first derived by Delahay and Strassner (11) for an irreversible reduction at a stationary electrode.

Figure 2 shows the shapes predicted by equation (29) for irreversible current–voltage curves. Notice that the asymmetry of the curve is marked when p is small, but that symmetry improves as p increases, becoming perfect in the $p \to \infty$ limit (as is apparent in equation (C12) of the appendix). Already for $p = 2/3$ little asymmetry exists, a fact that has been made use of in an empirical method (12, 10) for the analysis of irreversible polarographic waves.

The term p appears in both arguments of the Ω function [equation (29)] and this leads to a complex dependence of the half wave potential [the potential, $E_{1/2}$, at which $I(t) = I_d(t)/2$] on p. As p increases, $E_{1/2}$ becomes more negative, in accordance with the equation

$$E_{1/2} = E_h + \frac{RT}{\alpha nF}\ln\left\{k_h\sqrt{\frac{t}{D}}\right\} - \frac{RT}{\alpha nF}\ln\left\{.564\sqrt{2p+1} - \frac{.201}{\sqrt{2p+1}} + \frac{.070}{(2p+1)^{3/2}}\right\} \qquad (31)$$

which is obtained by combining equations (29), (C13) and the definition of $E_{1/2}$. Equation (31) suggests the possibility of determining kinetic parameters from a study of the variation of $E_{1/2}$ with t and p: this suggestion was made previously (13).

Because t occurs in equation (29) both as an argument of the Ω function and as a pre-Ω term, the dependence of current on time is complex. The behavior is most striking when $0 < p < 1/2$, for then the pre-Ω term decreases with time while Ω increases. Figure 3 shows examples of chronoamperometric relationships for a constant potential somewhat more negative than $E_{1/2}$.

General Potentiostatic Regime. For a reduction under quasireversible conditions, neither of the foregoing simplifications apply and it is necessary to solve the complete equation (22) subject to constancy of $\epsilon(Y)$. The relationship

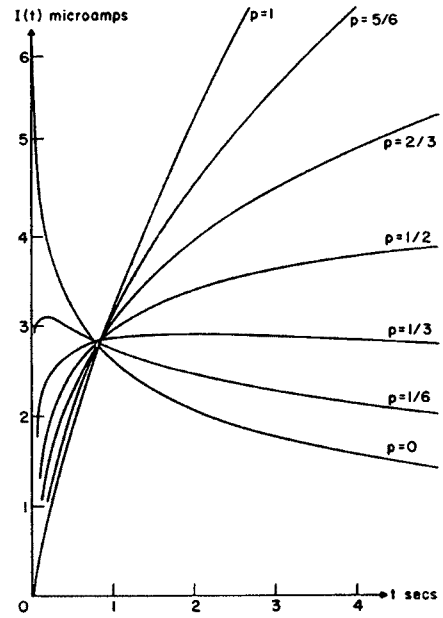

Figure 3. Current–time relationships for an irreversible reduction, at various values of p

In annotating the axes the same parameter values were used as in Figure 1, together with $k_hD^{-1/2}\exp\{-\alpha nF[E-E_h]/RT\} = 1.0$ sec.$^{-1/2}$ The constant potential, E, used in this example, lies somewhat negative of $E_{1/2}$

$$\epsilon^{\alpha}L\{Y^{\omega-\frac{1}{2}}\iota(Y)\} = \frac{1}{S} - \frac{1+\epsilon}{\sqrt{S}}\,L\{Y^{2\omega-1}\iota(Y)\} \qquad (32)$$

is easily derived and will be seen to differ from equation (28) only by the presence of the constant factor $(1 + \epsilon)$. The solutions of equation (32) therefore parallel closely those given in Appendix C and lead to $\iota(Y) = [Y^{\frac{1}{2}-2\omega}/(1+\epsilon)\sqrt{\pi}]\Omega(\omega,[1+\epsilon]Y^{\omega}\epsilon^{-\alpha})$ in dimensionless variables, or

$$I(t) = \frac{naFCt^{p-\frac{1}{2}}}{\left(1 + \exp\left\{\frac{nF}{RT}[E - E_h]\right\}\right)}\sqrt{(2p+1)D}\,\Omega\left(\frac{1}{4p+2}, k_h\sqrt{\frac{t}{(2p+1)D}}\,\frac{1+\exp\{nF[E-E_h]/RT\}}{\exp\{\alpha nF[E-E_h]/RT\}}\right) \qquad (33)$$

in experimental variables.

When $p = 2/3$, equation (33) becomes identical to the expression derived by Koutecky (14) for the general case of reduction at a dropping mercury electrode. (See Appendix C for the relation between Ω and the Koutecky function F).

When $p = 0$, equation (33) reduces to

$$I(t) = \frac{naFCk_h}{\exp\left\{\alpha\frac{nF}{RT}[E - E_h]\right\}}\exp(\xi^2)erfc\,\xi \qquad (34a)$$

where

$$\xi = k_h\sqrt{\frac{t}{D}}\left[\frac{1+\exp\{nF[E-E_h]/RT\}}{\exp\{\alpha nF[E-E_h]/RT\}}\right] \qquad (34b)$$

(9) H. Matsuda and Y. Ayabe, *Bull. Chem. Soc. Japan*, **28**, 422 (1955).
(10) D. E. Smith, T. G. McCord, and H. L. Hung, ANAL. CHEM., **39**, 1149 (1967).
(11) P. Delahay and J. E. Strassner, *J. Amer. Chem. Soc.*, **75**, 5219 (1951).
(12) L. Meites and Y. Israel, *ibid.*, **83**, 4903 (1961).
(13) K. B. Oldham and E. P. Parry, ANAL. CHEM., **40**, 65 (1968).
(14) J. Koutecky, *Coll. Czech. Chem. Commun.*, **18**, 597 (1953).

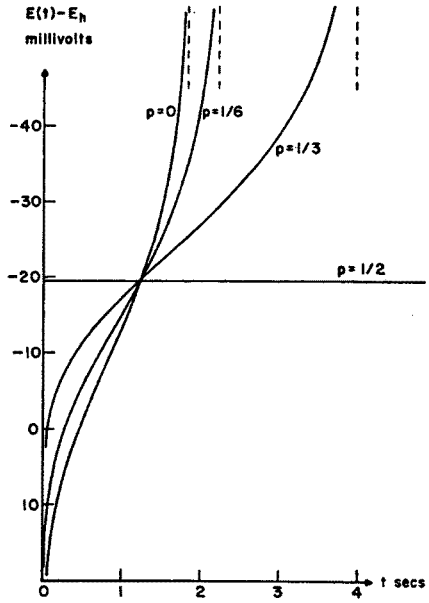

Figure 4. Chronopotentiograms for reversible reductions at a constant current I of 4.00 microamperes

A temperature of 25 °C has been assumed and other parameters take the values given in the legend of Figure 1. The dashed lines show the transition time asymptotes for the $p = 0$, $1/5$ and $1/3$ cases. No transition time exists for $p = 1/2$ and for $p > 1/2$ constant current chronopotentiometry is impossible

This equation is equivalent to that originally derived by Smutek (*15*) and others (*16*).

Reversible Galvanostatic Regime. A constant current implies a constant ι and if this condition is inserted into the reversible version of equation (22), there results

$$L\left\{\frac{\epsilon(Y)}{1+\epsilon(Y)}\right\} = \frac{1}{S} - \frac{\iota}{\sqrt{S}} L\{Y^{2\omega-1}\} = L\left\{1 - \frac{\iota\Gamma(2\omega)}{\Gamma(2\omega+1/2)} Y^{2\omega-\frac{1}{2}}\right\} \quad (35)$$

whence $\epsilon(Y) = [Y^{\frac{1}{2}-2\omega}\Gamma(2\omega + 1/2)/\iota\Gamma(2\omega)] - 1$. Written in terms of experimental variables, this becomes

$$E(t) = E_h + \frac{RT}{nF} \ln\left\{-1 + \frac{\Gamma\left(\frac{2p+3}{4p+2}\right) naFC\sqrt{(2p+1)D}}{\Gamma\left(\frac{1}{2p+1}\right) It^{\frac{1}{2}-p}}\right\} \quad (36)$$

This is the equation which expresses the potential-time relation at an expanding electrode at which a reversible reaction is occurring at a constant current I. Examples of the E *vs.* t relationships are shown as Figure 4.

Let us first consider $0 \leqslant p < 1/2$. In this case, the final term in equation (36) is initially infinite, so that $E(0) = +\infty$. As time passes, however, this term will diminish in magnitude, leading to a negatively-shifting potential. At the time $t = \tau$, where τ is termed the transition time (*17*) and is given by

$$\tau = \left[\frac{\Gamma\left(\frac{2p+3}{4p+2}\right) naFC\sqrt{(2p+1)D}}{\Gamma\left(\frac{1}{2p+1}\right) I}\right]^{\frac{2}{1-2p}} \quad (37)$$

the logarithmic argument in equation (36) becomes equal to zero and hence $E(\tau) = -\infty$. For $t > \tau$, equation (36) cannot be satisfied—*i.e.*, it is impossible for reaction (2) to continue to deliver a faradaic current of magnitude I. Combination of equation (36) with definition (37) gives,

$$E(t) = E_h + \frac{RT}{nF} \ln\left\{\left(\frac{\tau}{t}\right)^{\frac{1}{2}-p} - 1\right\} \quad (38)$$

For $p = 0$, equation (38) is identical with the chronopotentiometric equation for a stationary electrode, first derived by Karaoglanoff (*18*), and for this case equation (37) gives $\tau = \pi n^2a^2F^2C^2D/4I^2$, the well-known result due to Sand (*19*).

With $p = 1/2$, equation (36) gives

$$E(t) = E_h + \frac{RT}{nF} \ln\left\{\frac{naFC}{I}\sqrt{\frac{2D}{\pi}} - 1\right\} \quad (39)$$

and shows that (provided $I < naFC\sqrt{2D/\pi}$) the potential should remain constant indefinitely. This condition corresponds to the pseudo-steady-state discussed earlier in this article. Equations (39) and (27) are, in fact, equivalent.

For $p > 1/2$, equation (36) has no short-time solution, corresponding to the inability of a rapidly expanding electrode to provide a constant faradaic current. This is the state of affairs which pertains for a dropping mercury electrode ($p = 2/3$) and "constant current" electrolysis at such an electrode is feasible only if precautions are taken to avoid high polarization early in the drop-life (*20*).

Irreversible Galvanostatic Regime. When ι is a constant, the irreversible version of equation (22) becomes

$$L\{Y^{\omega-\frac{1}{2}}\epsilon^{\alpha}(Y)\} = \frac{1}{\iota S} - \frac{1}{\sqrt{S}} L\{Y^{2\omega-1}\} = L\left\{\frac{1}{\iota} - \frac{\Gamma(2\omega)Y^{2\omega-\frac{1}{2}}}{\Gamma(2\omega+1/2)}\right\} \quad (40)$$

whence $\epsilon^{\alpha}(Y) = [Y^{\frac{1}{2}-\omega}/\iota] - [Y^{\omega}\Gamma(2\omega)/\Gamma(2\omega + 1/2)]$. Reverting to the original variables, we find

$$E(t) = E_h + \frac{RT}{\alpha nF} \ln\left\{\frac{naFCk_ht^p}{I} - \frac{\Gamma\left(\frac{1}{2p+1}\right)k_h}{\Gamma\left(\frac{2p+3}{4p+2}\right)}\sqrt{\frac{t}{(2p+1)D}}\right\} \quad (41)$$

As in the previous section, it is convenient to examine equation (41) separately for different p values: here we shall consider successively $p = 0$, $0 < p < 1/2$, $p = 1/2$, and $p > 1/2$.

(15) M. Smutek, *Chem. Listy*, **45**, 241 (1951); *Coll. Czech. Chem. Commun.*, **18**, 171 (1953).
(16) P. Delahay, "New Instrumental Methods in Electrochemistry," Interscience, New York, 1954, Chap 4.
(17) J. A. V. Butler and G. Armstrong, *Proc. Roy. Soc. A*, **139**, 406 (1933).
(18) Z. Karaoglanoff, *Z. Elektrochem.*, **12**, 5 (1906).
(19) H. J. S. Sand, *Phil. Mag*, **1**, 45 (1901).
(20) H. B. Mark, E. M. Smith, and C. N. Reilley, *J. Electroanal. Chem.*, **3**, 98 (1962).

When p is zero, the argument of the logarithmic term in equation (41) is initially positive, but becomes progressively less positive until it vanishes at a transition time τ given by the Sand expression $\pi n^2a^2F^2C^2D/4I^2$. Accordingly, equation (41) may be rewritten as

$$E(t) = E(0) + \frac{RT}{\alpha nF} \ln \left\{1 - \sqrt{\frac{t}{\tau}}\right\} \tag{42a}$$

where

$$E(0) = E_h + \frac{RT}{\alpha nF} \ln \left\{\frac{naFCk_h}{I}\right\} \tag{42b}$$

a result originally due to Delahay and Berzins (*21*).

For p lying between 0 and $^1/_2$, the initial potential $E(0)$ is $-\infty$, but E rapidly becomes more positive, passes through a maximum and then drifts negative again, reattaining $-\infty$ at a transition time τ given by equation (37). The chronopotentiometric relation is

$$E(t) = E_h + \frac{RT}{\alpha nF} \ln \left\{\frac{naFCk_h\tau^p}{I}\right\} + \frac{RT}{\alpha nF} \ln \left\{\left(\frac{t}{\tau}\right)^p - \sqrt{\frac{t}{\tau}}\right\} \tag{43}$$

an equation of which (42) is seen to be a special case. Figure 5 shows plots of this chronopotentiometric relationship for p values of 0, $^1/_6$, and $^1/_3$, as well as the unique $p = {}^1/_2$ case.

With $p = {}^1/_2$ and provided that $I < naFC\sqrt{2D/\pi}$ the initial potential, $E(0) = -\infty$, but no transition time is developed. Instead the potential drifts to ever more positive values in accord with the relationship

$$E(t) = E_h + \frac{RT}{\alpha nF} \ln\left\{k_h\sqrt{t}\left(\frac{naFC}{I} - \sqrt{\frac{\pi}{2D}}\right)\right\} \tag{44}$$

As for the reversible case, $p > {}^1/_2$ leads to no meaningful solution of equation (41).

General Galvanostatic Regime. A solution of the unsimplified equation (22) subject to the constancy of ι is

$$Y^{\omega-\frac{1}{2}}\,\epsilon^{\alpha}(Y) + \frac{\Gamma(2\omega)Y^{2\omega-\frac{1}{2}}}{\Gamma(2\omega + {}^1/_2)}[1 + \epsilon(Y)] = \frac{1}{\iota} \tag{45}$$

and this may be converted to experimental variables by employing equations (10) through (13). The result, representing a situation intermediate between those of the two preceding sections, cannot be written to give the potential as an explicit function of time. Moreover, the expressing of time as an explicit function of potential is possible only for the special cases $p = 0$ or $^1/_2$. These special expressions are, respectively

$$t = \frac{\pi D}{k_h^2} \frac{\left[\frac{naFCk_h}{I} - \exp\left\{\frac{\alpha nF}{RT}[E(t) - E_h]\right\}\right]^2}{\left[1 + \exp\left\{\frac{nF}{RT}[E(t) - E_h]\right\}\right]^2} \tag{46}$$

and

$$t = \frac{\frac{2D}{\pi k_h^2} \exp\left\{\frac{2\alpha nF}{RT}[E(t) - E_h]\right\}}{\left[\frac{naFC}{I}\sqrt{\frac{2D}{\pi}} - 1 - \exp\left\{\frac{nF}{RT}[E(t) - E_h]\right\}\right]^2} \tag{47}$$

(21) P. Delahay and T. Berzins, *J. Amer. Chem. Soc.*, **75**, 2486 (1953).

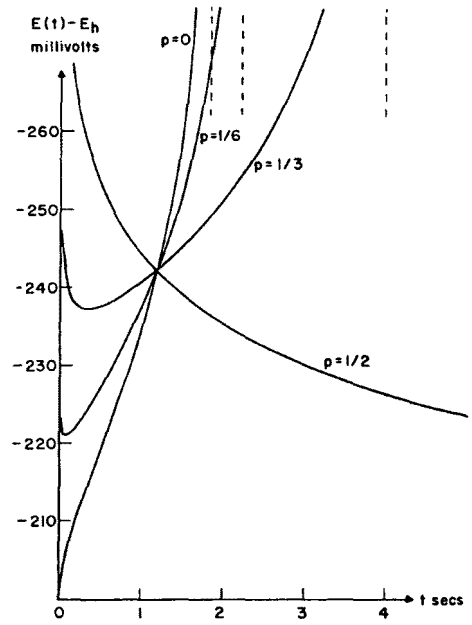

Figure 5. Chronopotentiograms for totally irreversible electroreductions at constant current

In addition to the parameter values used in constructing Figure 4, the values $\alpha = 0.5$ and $k_h = 8.63 \times 10^{-7}$ cm sec^{-1} were assumed. Notice that the transition times are identical with those in Figure 4, but that there is a more leisurely approach to the asymptotes. Note also that all $E(0) = -\infty$, except for the $p = 0$ case wherein $E(0)$ is finite (and equal to $E_h + 200$ mV for the values used here)

the first of which has been reported earlier (*22*).

However, it is evident from equation (45) that a transition time is developed generally for $0 \leqslant p < {}^1/_2$ and that its magnitude is given by equation (37).

Reversible Linear Current-Scan Regime. In this section and the next two, the situation is treated in which the current through the expanding electrode increases linearly with time—*i.e.*,

$$I(t) = \dot{I}t \tag{48}$$

where $\dot{I}$ is constant. It is convenient to introduce a dimensionless analogue of $\dot{I}$, namely

$$\iota \equiv \frac{(2p + 1)^{1-p}D^{1-p}\dot{I}}{naFCk_h^{3-2p}} \tag{49}$$

Combining the above two equations with definitions (10), (11), and (13) yields

$$\iota = iY^{2\omega} \tag{50}$$

When equation (50) is introduced into the reversible version of equation (22),

$$L\left\{\frac{\epsilon(Y)}{1 + \epsilon(Y)}\right\} = \frac{1}{S} - \frac{i}{\sqrt{S}} L\{Y^{4\omega-1}\} = L\left\{1 - \frac{i\Gamma(4\omega)Y^{4\omega-\frac{1}{2}}}{\Gamma(4\omega + {}^1/_2)}\right\} \tag{51}$$

(22) K. B. Oldham, *Electrochim. Acta*, **11**, 1481 (1966).

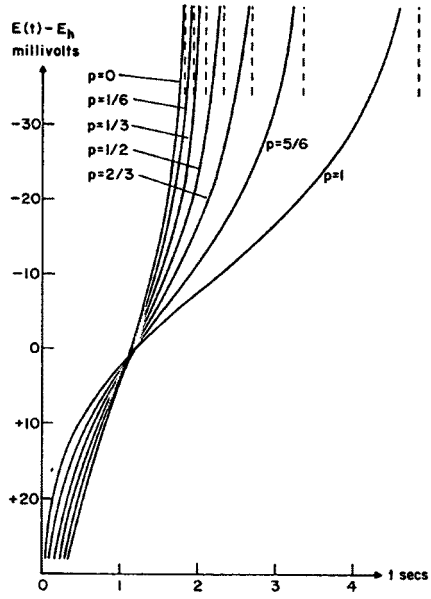

Figure 6. Linear current-scan chronopotentiograms for reversible electroreductions with p = 0, $^1/_6$, $^1/_3$, $^1/_2$, $^2/_3$, $^5/_6$, and 1

A current scan rate $\dot{I}$, equal to 3.3 μA per second has been assumed; other parameters are as for Figure 4. Note that all curves approach $E(0) = +\infty$ and $E(\tau) = -\infty$ asymptotically, the dashed lines indicating the value of the transition time τ

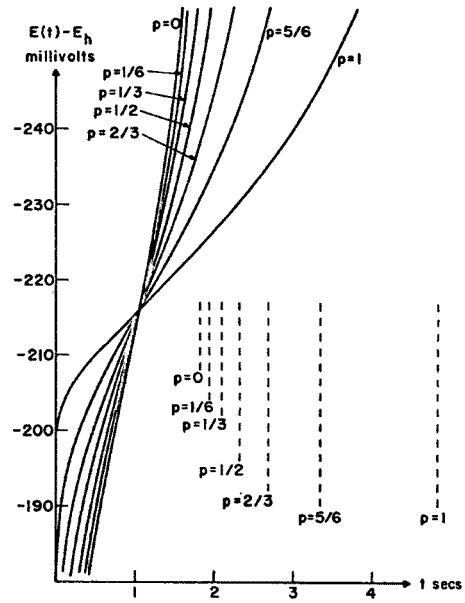

Figure 7. Similar to Figure 6 but for irreversible electroreductions

Assumed values of k_h and α as in Figure 5. The dashed lines indicate the values of the transition times, τ: the full curves approach these values asymptotically as $[E(t) - E_h] \to -\infty$

results. Therefore $\epsilon(Y) = [Y^{\frac{1}{2}-4\omega}\Gamma(4\omega + {}^1/_2)/i\Gamma(4\omega)] - 1$, or in experimental terms

$$E(t) = E_h + \frac{RT}{nF}\ln\left\{-1 + \frac{\Gamma\left(\frac{2p+5}{4p+2}\right) naFC\sqrt{(2p+1)D}}{\Gamma\left(\frac{2}{2p+1}\right)\dot{I}t^{\frac{1}{2}-p}}\right\} \tag{52}$$

This equation will be seen to resemble (36) closely.

If we exclude p values $\geq {}^3/_2$, equation (52) predicts a chronopotentiometric relation in which $E(0)$ is $+\infty$ and $E(\tau) = -\infty$, where

$$\tau = \left[\frac{\Gamma\left(\frac{2p+5}{4p+2}\right) naFC\sqrt{(2p+1)D}}{\Gamma\left(\frac{2}{2p+1}\right)\dot{I}}\right]^{\frac{2}{3-2p}} \tag{53}$$

It is again appropriate to term τ a "transition time": the existence of transition times during voltammetry with inconstant currents was explored by Kambara and Tachi (*23*). During $0 < t < \tau$, the potential variation is given by

$$E(t) = E_h + \frac{RT}{nF}\ln\left\{\left(\frac{\tau}{t}\right)^{\frac{1}{2}-p} - 1\right\} \tag{54}$$

which is a close analogue of equation (38). Figure 6 includes graphs exemplifying these expressions.

When $p = 0$, equations (54) and (53) reduce to

$$E(t) = E_h + \frac{RT}{nF}\ln\left\{\frac{\tau^{1/2} - t^{1/2}}{t^{1/2}}\right\} \tag{55a}$$

and

$$\tau^{1/2} = \frac{3naFC\sqrt{\pi D}}{4\dot{I}} \tag{55b}$$

These equations were originally derived by Reinmuth (*24*), in his treatment of reversible linear current scan chronopotentiometry at a stationary electrode.

For the important case $p = {}^1/_2$, equations (54) and (53) become

$$E(t) = E_h + \frac{RT}{nF}\ln\left\{\frac{\tau - t}{t}\right\} \tag{56a}$$

where

$$\tau = \frac{naFC}{\dot{I}}\sqrt{\frac{\pi D}{2}} \tag{56b}$$

so that the chronopotentiogram is symmetrical about $E(\tau/2) = E_h$. For the experimentally convenient $p = {}^2/_3$ case

$$E(t) = E_h + \frac{RT}{nF}\ln\left\{\frac{\tau^{5/6} - t^{5/6}}{t^{5/6}}\right\} \tag{57a}$$

where

$$\tau^{5/6} = \frac{\Gamma\left(\frac{19}{14}\right) naFC}{\Gamma\left(\frac{6}{7}\right)\dot{I}}\sqrt{\frac{7D}{3}} = \frac{1.2301naFC\sqrt{D}}{\dot{I}} \tag{57b}$$

(23) T. Kambara and I. Tachi, *J. Phys. Chem.*, **61**, 1405 (1957).

(24) W. H. Reinmuth, ANAL. CHEM., **32**, 1509 (1960).

These two cases are among those graphed in Figure 6.

Irreversible Linear Current-Scan Regime. Introduction of relation (50) into the irreversible version of equation (22) leads to

$$L\{Y^{3\omega-\frac{1}{2}}\epsilon^{\alpha}(Y)\} = \frac{1}{\imath S} - \frac{1}{\sqrt{S}} L\{Y^{4\omega-1}\} = L\left\{\frac{1}{\imath} - \frac{\Gamma(4\omega)Y^{4\omega-\frac{1}{2}}}{\Gamma(4\omega+\frac{1}{2})}\right\} \quad (58)$$

whence $\epsilon^{\alpha}(Y) = [Y^{\frac{1}{2}-3\omega}/\imath] - [Y^{\omega}\Gamma(4\omega)/\Gamma(4\omega+\frac{1}{2})]$. In terms of experimental variables, we have

$$E(t) = E_h + \frac{RT}{\alpha nF}\ln\left\{\frac{naFCk_h}{\dot{I}t^{1-p}} - \frac{\Gamma\left(\frac{2}{2p+1}\right)k_h}{\Gamma\left(\frac{2p+5}{4p+2}\right)}\sqrt{\frac{t}{(2p+1)D}}\right\} \quad (59)$$

If p is less than unity, equation (59) predicts that the potential will initially be infinitely positive, but will drift negatively to a transition time given by (53) according to the chronopotentiometric relation

$$E(t) = E_h + \frac{RT}{\alpha nF}\ln\left\{\frac{naFCk_h}{\dot{I}\tau^{1-p}}\right\} + \frac{RT}{\alpha nF}\ln\left\{\left(\frac{\tau}{t}\right)^{1-p} - \sqrt{\frac{t}{\tau}}\right\} \quad (60)$$

A finite $E(0)$ is predicted when $p = 1$. Figure 7 depicts examples of the relationships. It is noteworthy that the potential approaches its final value, $E(\tau) = -\infty$ much more slowly in the irreversible case than in the reversible.

General Linear Current-Scan Regime. A solution to the unsimplified equation (22) with (50) inserted is

$$Y^{3\omega-\frac{1}{2}}\epsilon^{\alpha}(Y) + \frac{\Gamma(4\omega)Y^{4\omega-\frac{1}{2}}}{\Gamma(4\omega+\frac{1}{2})}[1+\epsilon(Y)] = \frac{1}{\imath} \quad (61)$$

As for equation (45), an explicit relation between t and $E(t)$ can be derived only for special p values: in this case for $p = 1$ or $\frac{3}{2}$.

From equation (61) it is evident that $\epsilon(Y) = 0$ when $Y^{4\omega-\frac{1}{2}} = \Gamma(4\omega+\frac{1}{2})/\imath\Gamma(4\omega)$, from which expression (53) for the transition time may be derived. As expected, since it arises from complete concentration polarization of the electrode, the transition time in no way depends on the degree of reversibility.

Other Regimes. It is possible to solve equation (22) for other relations between $\imath(Y)$ and/or $\epsilon(Y)$ and Y. Some of these [such as $\imath(Y) \propto Y^{\frac{1}{2}-2\omega}$—*i.e.*, $I(t) \propto t^{p-\frac{1}{2}}$] lead to particularly simple solutions. Others correspond to easily attained experimental conditions. However, sufficient examples have already been treated to illustrate more than adequately the principles involved.

Summary. Much of this article has been devoted to the rederivation of already well-established results. These rederivations have pedagogical interest in that they provide a bridge between the body of theory associated with stationary electrodes and that associated with the dropping mercury electrode.

Several new results are also included, and these have potential applications in electroanalytical or electrode kinetic studies. These applications will not be developed here, but it is obvious that any result which includes C may be used analytically and any result which involves k_h and/or α can be used to determine these kinetic parameters.

One new result which is particularly attractive is embodied in equation (27) or (39): for a reversible reaction at an electrode whose area increases as the square-root of time, a time-independent current-potential relationship exists. If such an electrode can be satisfactorily engineered, a rapid and elegant analytical method will be created.

Another result which has interesting analytical applications is equation (57b). This relationship may be exploited for both reversible and irreversible reductions by combining the reproducibility of the dropping mercury electrode with the experimental utility of chronopotentiometry. To utilize linear scan chronopotentiometry at a dropping mercury electrode all that will be necessary is to synchronize a current ramp generator with a drop detachment device.

APPENDIX A—NOTATION

$A(t)$ = electrode area at time t [cm^2]
$B_0, B_1 \ldots B_j$ = coefficients in the power expansions of $\imath(Y)$
C = bulk concentration of Ox [mole cm^{-3}]
$C(r,t)$ = concentration of Ox at a distance r from the electrode surface at time t [mole cm^{-3}]
$C'(\pm r,t)$ = concentration of Rd at a distance r from the electrode (measured into or away from the solution phase) at time t [mole cm^{-3}]
$\bar{C}(\bar{r},t)$ = concentration defined by equation (B5) [mole cm^{-3}]
$C(X,Y)$ = the concentration $C(r,t)$ in terms of the dimensionless variables X and Y [mole cm^{-3}]
$\bar{C}(X,S)$ = Laplace transform of $C(X,Y)$ with respect to Y—*i.e.*, $\int_0^{\infty}\exp\{-SY\}C(X,Y)dY$ [mole cm^{-3}]
D; D' = diffusion coefficients of Ox and Rd [cm^2 sec^{-1}]
$E(t)$ = potential of the electrode at time t, with respect to any convenient reference [volt]
E = constant applied electrode potential [volt]
E_s = the standard potential of the Ox/Rd couple with respect to the chosen reference [volt]
E_h = a convenient reference potential defined as $E_s + (RT/2nF)\ln(D'/D)$ [volt]
$E_{1/2}$ = half-wave potential, the potential at which $2I(t) = I_d(t)$ [volt]
F = Faraday's constant [9.65 × 10^4 coulomb equiv^{-1}]
$F(z)$ = the Koutecky function (*12*, *10*) of z
$I(t)$ = faradaic current at time t [ampere]
$I_d(t)$ = diffusion limited current at time t [ampere]
I = constant applied faradaic current [ampere]
$\dot{I}$ = constant applied rate of faradaic current increase [ampere sec^{-1}]
$L\{\ \}$ = operator of Laplace transformation with respect to Y, $L\{f(Y)\} \equiv \int_0^{\infty}\exp\{-SY\}f(Y)dY$
Ox = an electroreducible solute
$Q(S)$ = an arbitrary function of S [mole cm^{-3}]
R = the gas constant, [8.31 joule deg^{-1} mole^{-1}]
Rd = the soluble reduction product of Ox
S = dummy variable of Laplace transformation with respect to Y
T = absolute temperature [deg]

X; Y = dimensionless variables defined in expressions (9) and (10)

a = constant of proportionality of electrode area, defined by equation (1) [cm^2 sec^{-p}]

b = index in power expansion of $\iota(Y)$

e^- = an electron

$f(z)$ = an arbitrary function of z

j; J = running indices

k_s = standard heterogeneous rate constant [cm sec^{-1}]

k_h = a convenient rate constant reference, defined as $k_s(D/D')^{\alpha/2}$ and equal to the rate constant for reduction at potential E_h[cm sec^{-1}]

$\dot{m}$ = mercury mass flow rate [gram sec^{-1}]

n = number of faradays to reduce one mole of Ox [equiv mole^{-1}]

p = the power of time by which electrode area increases, see equation (1)

r = distance measured normally from the electrode surface [cm], being positive for a point in the solution phase

$\bar{r}$ = distance variable defined in equation (B4) [cm]

t = time since birth of electrode or (if $p = 0$) onset of experiment [sec]

z = arbitrary variable

$z_{1/2}$ = value of z for which $\Omega(\omega,z) = 0.5$

$\Gamma(z)$ = gamma function (*25*) of z

$\Omega(\omega,z)$ = bivariate function defined and discussed in Appendix C.

α = dimensionless cathodic transfer coefficient

β = arbitrary index

$\epsilon(Y)$ = dimensionless analogue of $E(t)$, defined by equation (11)

ϵ = constant dimensionless analogue of E

$\iota(Y)$ = dimensionless analogue of $I(t)$, defined by equation (12)

ι = constant dimensionless analogue of I

$\dot{\iota}$ = constant dimensionless analogue of $\dot{I}$, defined by equation (49)

ξ = abbreviation used in equations (30) and (34)

ρ = density of mercury [13.5 g cm^{-3}]

τ = transition time, time at which electrode potential equals $-\infty$ [sec]

$\psi(z)$ = Matsuda–Ayabe (*9*, *10*) function of z

ω = dimensionless variable defined by equation (13)

APPENDIX B

The dependence that the bivariate function $C(r,t)$ has on r and t will depend upon the electrolysis condition, but relationships (3), (5), and (6) must be satisfied. Likewise there are three relationships:

$$\mp D' \frac{\partial C'}{\partial r}(0,t) = \frac{I(t)}{nFA(t)} \tag{B1}$$

$$\frac{\partial C'}{\partial t}(\pm r,t) = \pm \frac{pr}{t}\frac{\partial C'}{\partial r}(\pm r,t) + D'\frac{\partial^2 C'}{\partial r^2}(\pm r,t) \tag{B2}$$

and

$$C'(\pm r,0) = 0 \tag{B3}$$

which must be satisfied by any acceptable expression for $C'(\pm r,t)$, the Rd concentration. The alternative signs occurring in equations (B1) through (B3) embrace the possibilities that Rd is soluble in the solution (upper signs) or by amalgamation (lower signs). Now, if we define

$$\bar{r} \equiv \pm r\sqrt{D/D'} \tag{B4}$$

and

$$\tilde{C}(\bar{r},t) \equiv C - \sqrt{D'/D}\, C'(\pm r,t) \tag{B5}$$

equations (B1) through (B3) may be recast as

$$D\frac{\partial C}{\partial \bar{r}}(0,t) = \frac{I(t)}{nFA(t)} \tag{B6}$$

$$\frac{\partial \tilde{C}}{\partial t}(\bar{r},t) = \frac{p\bar{r}}{t}\frac{\partial \tilde{C}}{\partial \bar{r}}(\bar{r},t) + D\frac{\partial^2 \tilde{C}}{\partial \bar{r}^2}(\bar{r},t) \tag{B7}$$

and

$$\tilde{C}(\bar{r},0) = C \tag{B8}$$

These last three equations will be recognized as identical, apart from the presence of tildes, with equations (3), (5), and (6). It follows, therefore, that if C is a certain function of r and t, then $\tilde{C}$ must be the same function of $\bar{r}$ and t. In particular, it follows that

$$C(0,t) \equiv \tilde{C}(0,t) \equiv C - \sqrt{D'/D}\, C'(0,t) \tag{B9}$$

An argument similar to the foregoing has been used previously (*26*).

If reaction (2) obeys the simplest kinetics, and if there are no complications resulting from the presence of a double-layer at the electrode surface, the net rate of cathodic reaction may be related both to the current and to the difference between the forward and reverse electron transfer reaction rates thus:

$$\text{Specific reaction rate (mole cm}^{-2}\text{ sec}^{-1}) = \frac{I(t)}{nFA(t)} =$$

$$k_s\, C(0,t)\exp\left\{\frac{-\alpha nF}{RT}[E(t) - E_s]\right\} - k_s\, C'(0,t)\exp\left\{\frac{(1-\alpha)nF}{RT}[E(t) - E_s]\right\} \tag{B10}$$

where k_s and E_s are defined in Appendix A. After $C'(0,t)$ is eliminated between (B9) and (B10), and the definitions of E_h and k_h are introduced (see Appendix A), it requires only rearrangements to derive equation (8).

APPENDIX C

When the series $\iota(Y) = \sum_0^\infty B_j Y^{b-j\omega}$ is inserted, equation (28) becomes

$$\frac{1}{S} - \sum_{j=0}^{\infty} B_j \frac{\Gamma(b - j\omega + 2\omega)}{S^{b-j\omega+2\omega+\frac{1}{2}}} = \epsilon^\alpha \sum_{j=0}^{\infty} B_j \frac{\Gamma(b - j\omega + \omega + \frac{1}{2})}{S^{b-j\omega+\omega+\frac{1}{2}}} \tag{C1}$$

Selection of the values $b = \frac{1}{2} - 2\omega$ and $B_0 = 1/\sqrt{\pi}$ enables

(25) M. Abramowitz and I. A. Stegun, Eds., "Handbook of Mathematical Functions," National Bureau of Standards, Washington, D. C., 1964, Chap 6.

(26) K. B. Oldham, ANAL. CHEM., **40**, 1024 (1968).

the first two left-hand terms to be eliminated, leaving

$$-\sum_{j=1}^{\infty} B_j \frac{\Gamma(1/2 - j\omega)}{S^{1-j\omega}} = \epsilon^{\alpha} \sum_{j=0}^{\infty} B_j \frac{\Gamma(1 - j\omega - \omega)}{S^{1-j\omega-\omega}} = \epsilon^{\alpha} \sum_{j=1}^{\infty} B_{j-1} \frac{\Gamma(1 - j\omega)}{S^{1-j\omega}} \quad \text{(C2)}$$

Choice of the recurrence identity $B_j = -\epsilon^{\alpha} B_{j-1} \Gamma(1 - j\omega)/\Gamma(1/2 - j\omega)$ evidently satisfies equation (C2) and thus provides expressions for all the remaining unknown coefficients. The series is thus

$$\iota(Y) = \frac{Y^{1/2-2\omega}}{\sqrt{\pi}} \left[1 + \sum_{J=1}^{\infty} \left(\frac{-\epsilon^{\alpha}}{Y^{\omega}}\right)^J \prod_{j=1}^{J} \frac{\Gamma(1 - j\omega)}{\Gamma(1/2 - j\omega)}\right] \quad \text{(C3)}$$

Using the alternative series $\iota(Y) = \sum_{0}^{\infty} B_j Y^{b+j\omega}$ in equation (28), leads to

$$\epsilon^{\alpha} \sum_{j=0}^{\infty} B_j \frac{\Gamma(b + j\omega + \omega + 1/2)}{S^{b+j\omega+\omega+1/2}} = \frac{1}{S} - \sum_{j=0}^{\infty} B_j \frac{\Gamma(b + j\omega + 2\omega)}{S^{b+j\omega+2\omega+1/2}} \quad \text{(C4)}$$

Selection of $b = 1/2 - \omega$ and $B_0 = \epsilon^{-\alpha}$ permits the elimination of the first term on either side of the equation and leaves

$$\epsilon^{\alpha} \sum_{j=1}^{\infty} B_j \frac{\Gamma(1 + j\omega)}{S^{1+j\omega}} = -\sum_{j=0}^{\infty} B_j \frac{\Gamma(1/2 + j\omega + \omega)}{S^{1+j\omega+\omega}} = -\sum_{j=1}^{\infty} B_{j-1} \frac{\Gamma(1/2 + j\omega)}{S^{1+j\omega}} \quad \text{(C5)}$$

The recurrence relation this time is $B_j = -\epsilon^{-\alpha} B_{j-1} \Gamma(1/2 + j\omega)/\Gamma(1 + j\omega)$, so that

$$\iota(Y) = \frac{Y^{1/2-\omega}}{\epsilon^{\alpha}} \left[1 + \sum_{J=1}^{\infty} \left(\frac{-Y^{\omega}}{\epsilon^{\alpha}}\right)^J \prod_{j=1}^{J} \frac{\Gamma(1/2 + j\omega)}{\Gamma(1 + j\omega)}\right] \quad \text{(C6)}$$

It is convenient to define a bivariate transcendental function Ω by the alternative equivalent expressions

$$\Omega(\omega,z) = \begin{cases} 1 + \sum_{J=1}^{\infty} (-z)^{-J} \prod_{j=1}^{J} \frac{\Gamma(1 - j\omega)}{\Gamma(1/2 - j\omega)} & \text{(C7a)} \\ z\sqrt{\pi}\left[1 + \sum_{J=1}^{\infty} (-z)^{J} \prod_{j=1}^{J} \frac{\Gamma(1/2 + j\omega)}{\Gamma(1 + j\omega)}\right] & \text{(C7b)} \end{cases}$$

so that equations (C3) and (C6) both reduce to $\iota(Y) = \pi^{-1/2} Y^{1/2-2\omega} \Omega(\omega, Y^{\omega}\epsilon^{-\alpha})$. This result is equivalent to (29).

Whereas the full (C7) expressions are needed to define $\Omega(\omega,z)$ when ω is an irrational number, certain simplifications result if ω is expressible as the quotient of two whole numbers. Thus when $\omega = 3/14$, the terms in (C7a) corresponding to $J = 7$ through 13 are zero [for a discussion of the evaluation of terms for $J \geq 14$ see Cizek and Koutecky (27)]. For $\omega = 1/4$ we have

$$\Omega(1/4,z) = 1 - \frac{\Gamma(3/4)}{z\Gamma(1/4)} + \Gamma(3/4)\sqrt{\pi} \sum_{k=1}^{\infty} \frac{z^{-4k}}{\Gamma(1/2 - k)} \left[\frac{1}{\Gamma(3/4 - k)} - \frac{1}{z\Gamma(1/4 - k)}\right] \quad \text{(C8a)}$$

$$\Omega(1/4,z) = z\sqrt{\pi}\left[1 + \Gamma(3/4) \sum_{J=1}^{\infty} \frac{(-z)^J}{\Gamma\left(\frac{3}{4} + \frac{J}{4}\right)\Gamma\left(1 + \frac{J}{4}\right)}\right] \quad \text{(C8b)}$$

For $\omega = 1/2$, there is drastic simplification

$$\Omega(1/2,z) = z\sqrt{\pi}\left[1 + \sum_{J=1}^{\infty} \frac{(-z)^J}{\Gamma\left(1 + \frac{J}{2}\right)}\right] = z\sqrt{\pi}\,\exp(z^2)\,\mathrm{erfc}\,(z) \quad \text{(C9)}$$

It is easy to show that $\Omega(3/14,z)$ is related to the functions F and ψ introduced, respectively, by Koutecky (*14*) and by Matsuda and Ayabe (*9*) by the simple equivalences

$$\Omega(3/14,z) \equiv F(2z) \equiv z\sqrt{\pi}\,\psi(z\sqrt{7/3}) \quad \text{(C10)}$$

One distinction should be noted between the present derivation and that of the previous dropping mercury electrode solutions: whereas the two forms of the solution [equations (C3) and (C6)] appear here on an equal footing, the original workers (*14*, *9*) derived one form asymptotically from the other.

For ease of computation, it is convenient to replace the gamma functions of negative argument in formula (C7a) by application of the Gauss reflection formula (*28*). After some algebra, this leads to

$$\Omega(\omega,z) = 1 + \sum_{J=1}^{\infty} J! \left(\frac{-\omega}{z}\right)^J \prod_{j=1}^{J} \cot(\pi j\omega) \prod_{J=1}^{J} \frac{\Gamma(1/2 + j\omega)}{\Gamma(1 + j\omega)} \quad \text{(C11)}$$

wherein the final product term is identical with that in (C7b).

Using equation (C7b) for small z, and (C11) for large z, values of $\Omega(\omega,z)$ were computed for a variety of ω values in the range $0 \leqslant \omega \leqslant 1/2$: some of the results are displayed in Figure 2. Computed values were checked (in the cases $\omega = 3/14$ and $\omega = 1/2$) *vs.* established algorithms (*28*, *29*). Though $\omega = 0$ does not correspond to an experimentally realizable situation, it represents the limit $p \to \infty$, and for this limit the Ω function degenerates to

$$\Omega(0,z) = \frac{z\sqrt{\pi}}{1 + z\sqrt{\pi}} \quad \text{(C12)}$$

As Figure 2 shows, $z_{1/2}$ (the value of z for which $\Omega(\omega,z) = 1/2$) decreases somewhat as ω increases. This small drift has been found to fit the empirical equation

$$z_{1/2} = .564 - .402\,\omega + .28\,\omega^2 \quad \text{(C13)}$$

Received for review December 30, 1968. Accepted March 12, 1969.

(27) J. Cizek and J. Koutecky, *Coll. Czech. Chem. Commun.*, **28**, 2803 (1963).

(28) K. B. Oldham and D. E. Smith, Anal. Chem., **40**, 1360 (1968).

(29) K. B. Oldham, *Mathematics of Computation*, **22**, 454 (1968).

Temperature Profiles of Turbulent Hydrogen Diffusion Flames Used in Atomic Fluorescence Spectrometry

R. Smith, C. M. Stafford, and J. D. Winefordner

Department of Chemistry, University of Florida, Gainesville, Fla. 32601

The temperatures of H_2/Air, H_2/Ar/entrained Air, H_2/N_2O, and H_2/entrained Air flames supported on total-consumption burners have been measured with the aid of an iridium/60% iridium–40% rhodium thermocouple. The flames have been used in atomic fluorescence and atomic emission studies, and results are quoted for flame temperatures measured with and without the aspiration of water. A full discussion of the use of thermocouples in measuring flame temperatures is given together with complete temperature contours and also vertical height profiles for a variety of flames. The principal source of oxidant in all the flames examined was entrained air, the main purpose of the aspirant gas being to create sufficient turbulence. As a result, the enhancement of atomic fluorescence quantum efficiency, obtained by aspiration using argon, is small (ca. 10–20%). Generally, easily volatilized and atomized elements can be determined above the visible portion of the flame, whereas other elements must be determined within the flame. For the latter elements, the height at which maximum fluorescence occurs does not necessarily correspond to the most favorable signal-to-noise ratio.

THE STRUCTURE AND physical characteristics of turbulent, hydrogen flames used in flame spectrometry, has received little study in the past, partly because of the complexity and small dimensions of the flames involved. Turbulent flames have been used to a considerable extent in many of the recent studies on atomic fluorescence spectrometry, and it would also appear that low-background, turbulent flames such as the H_2/Ar/entrained-air and H_2/entrained-air flames may have some applications in atomic emission spectrometry. Recent studies in this laboratory (*1*), between premix and total-consumption burners, indicate the considerable value of the latter in atomic fluorescence analysis as a result of higher uptake rate and simplicity.

The characteristics of high-temperature turbulent flames have been investigated by Winefordner *et al.* (*2*), and Gilbert (*3*) who studied the H_2/O_2 and C_2H_2/O_2 flames supported on Beckman total-consumption burners. Other work on H_2/air, H_2/Ar/entrained-air, H_2/O_2 and C_2H_2/O_2 turbulent flames by de Galan and Winefordner (*4*) confirmed the earlier results obtained (*2*) for the high-temperature flames but indicated considerable lack of thermal equilibrium in the cooler H_2/air and H_2/Ar/entrained-air flames. Additional results by Kirkbright *et al.* (*5*) for the H_2/O_2 flame have been in good agreement with the values reported previously. All of the workers referred to have used spectrometric methods for measuring the flame temperature. In the higher temperature flames, the Ornstein iron two-line method has been used (*2, 4, 5*), although this gave results which are very much in error with the lower temperature flames (*4*). The sodium, line-reversal method has been used with turbulent flames (*4, 6*), but the work of de Galan and Winefordner (*4*) indicates that even sodium may give slightly high results when used with the lower temperature, turbulent flames. In addition, to the problems of thermal equilibrium, spectrometric methods have the disadvantage that they measure an average temperature across the flame and not the temperature at a specific point in the flame. This could be overcome to some extent by the use of narrow light beams and subsequent mathematical treatment (Abel Inversion) of the results, however, in this instance it appears that the use of an alternative method of temperature measurement might prove advantageous.

The results given here, describe the use of a thermocouple probe for temperature measurement in flames. The method is susceptible to many errors and is not simple to use although results may be obtained rapidly and easily once the thermocouple has been calibrated. All the flames used were supported on Hetco or Zeiss burners as these burners give better sensitivities in atomic fluorescence (*7*) than do Beckman burners; this is the first report on temperature measurements carried out in conjunction with these burners.

Finally, the recent use of the premixed flame produced with a Hetco burner, reported by Mossotti and Duggan (*8*), has led to an investigation of such flames for atomic fluorescence (*9*). For the sake of completeness the temperature profiles of premixed H_2/air and premixed H_2/N_2O flames supported on a total-consumption burner (*9*) have been included in the results of this publication, even though these flames have, as yet, no uses in atomic spectrometry.

EXPERIMENTAL

Apparatus. BURNERS. The total-consumption burners used were Jarrell-Ash 82-341 HETCO (Jarrell-Ash, Co., Waltham, Mass.) and the Zeiss (Carl Zeiss, Inc., New York, N. Y.) burners. The two burners were almost identical, and many parts were interchangeable. There appears to be no difference in comparable flames burned on each of these burners, although differences in solution uptake rate occurred. For premixed flames, on total-consumption burners, the Tescom hand-welder (Tescom 11-1101, Tescom Corp. Minneapolis, Minn.) premixing chambers were used as recommended (*8*). Gas flow rates were measured on rotameters, calibrated with the respective gases used by means of a wet test meter.

THERMOCOUPLE. Thermocouples were made from 0.005-inch diameter iridium and iridium–rhodium (60%–40%) wire (Sigmund Cohn, Co., Mount Vernon, N. Y.) which

(1) M. P. Bratzel, R. M. Dagnall, and J. D. Winefordner, ANAL. CHEM., **41**, 713 (1969).
(2) J. D. Winefordner, C. T. Mansfield, and J. T. Vickers, *ibid.*, **35**, 1611 (1963).
(3) P. T. Gilbert, *A.S.T.M. Spec. Tech. Publ.*, **269**, 73 (1959).
(4) L. de Galan and J. D. Winefordner, *J. Quant. Spect. Radiat. Transfer*, **7**, 703 (1967).
(5) G. F. Kirkbright, M. K. Peters, M. Sargent, and T. S. West, *Talanta*, **15**, 663 (1968).
(6) J. H. Gibson, W. E. L. Grossman, and W. D. Cooke, ANAL. CHEM., **35**, 266 (1963).
(7) M. P. Bratzel and J. D. Winefordner, *Anal. Letters*, **1**, 43 (1967).
(8) V. G. Mossotti and M. Duggan, *Appl. Optics.*, **7**, 1325 (1968).
(9) M. P. Bratzel, R. M. Dagnall, and J. D. Winefordner, unpublished work, University of Florida, Gainesville, Florida, 1969.

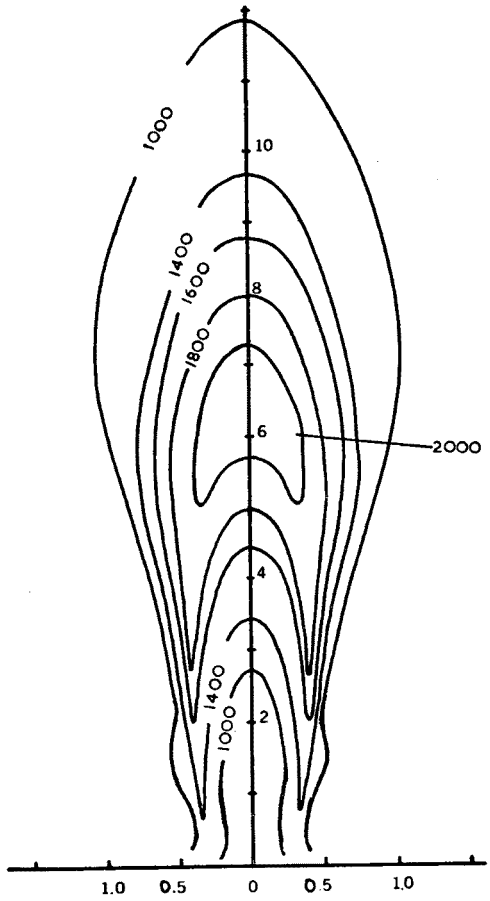

Figure 1. Full temperature profile of H_2/Ar/entrained-air flame (*B*), all dimensions in cm, expanded abscissa

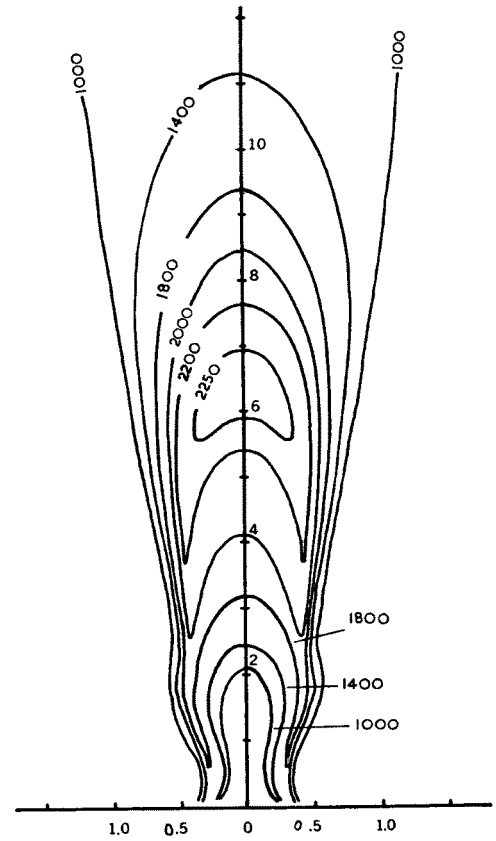

Figure 2. Full temperature profile of H_2/Air flame (*E*), all dimensions in cm, expanded abscissa

was welded in a natural-gas/O_2 flame to give a bead junction of *ca.* 0.01-inch diameter. The joined wires were mounted in two-bore, ceramic insulators of high-purity recrystallized alumina, having an outer diameter of 0.03 in. (Omegatite 350, TRA 005132, Omega Engineering, Inc., Stamford, Conn.), and the insulators were protected along two thirds of their length by inconel metal sheaths (INC 1165-6, Omega Engineering). The welded junctions and exposed leads were thinly coated with zirconia cement (ESP1-MR32, Electronic Space Products Inc., Los Angeles, Calif.), to prevent catalytic effects and the assembly was mounted in a two-pin connector having copper terminals (MP-UNCO-MF, Omega Engineering).

Thermocouples were mounted on a manually-operated horizontal/vertical traverse mechanism having the horizontal traverse capable of positional precision of ±0.04 mm and the vertical traverse capable of ±0.2 mm. Measurements of thermoelectric e.m.f. were by means of a digital millivoltmeter (Digitec, United Systems Corp., Dayton, Ohio) which was calibrated in units of 0.02 mV and which operated on a null-balance principle, having effectively infinite impedance at balance.

Line Reversal. A premix H_2/air burner with facility for a flowing nitrogen sheath and designed by Zeegers (*10*) was used for line-reversal calibrations of the thermocouple. This burner was capable of supporting a range of $H_2/O_2/N_2$ flames having uniform temperature over the flame cross-section and height. A tungsten strip lamp (Eppley Laboratory, Inc., Newport, R. I.), was calibrated in terms of absolute energy output by the makers between 2500 Å and 7500 Å at 35 A using National Bureau of Standards reference sources (EU-238 and EU-275E) and was used as a background light source. The schematic arrangement of the line-reversal apparatus was similar to that described by Gibson, *et al.* (*6*) and Snelleman (*11*); a 0.5-m Ebert grating monochromator (Model 8200, Jarrell-Ash Co.) having a 20-μ by 2-mm slit, was used with an RCA 1P-28 photomultiplier operated at 850V. A solid state nanoammeter (*11*) and galvanometric recorder were used for amplification and readout.

Procedure. Thermocouple Calibration. Blackburn and Caldwell (*13*) have provided calibration tables for the variation of the thermal emf of iridium/iridium–rhodium thermocouples. At temperatures above 1200 °K, radiational heat losses from the thermocouple become appreciable, and a correction must be applied to compensate for the apparent reduction in the measured temperature. The radiational correction was obtained by measuring the temperature of well-defined, uniform, laminar flames by the sodium line-reversal method and with the uncalibrated thermocouple.

(10) P. J. T. Zeegers, *Ph.D. Thesis*, Utrecht, Netherlands (1966).

(11) W. Snelleman, *Comb. and Flame*, **11**, 453 (1967).
(12) T. C. O'Haver and J. D. Winefordner, *J. Chem. Educ.*, in press.
(13) G. F. Blackburn and F. R. Caldwell, *J. Res. NBS.*, **68C**, 41 (1964).

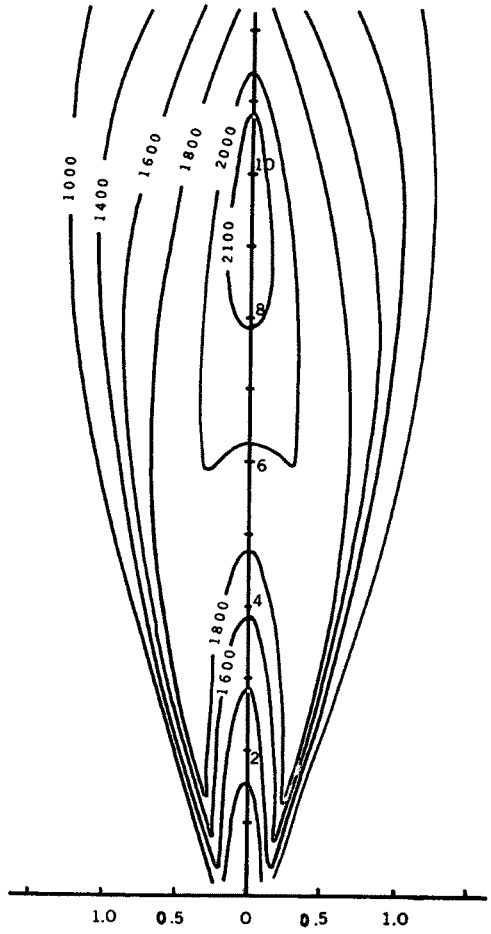

Figure 3. Full temperature profile of reversed H_2/entrained-air flame (*G*)

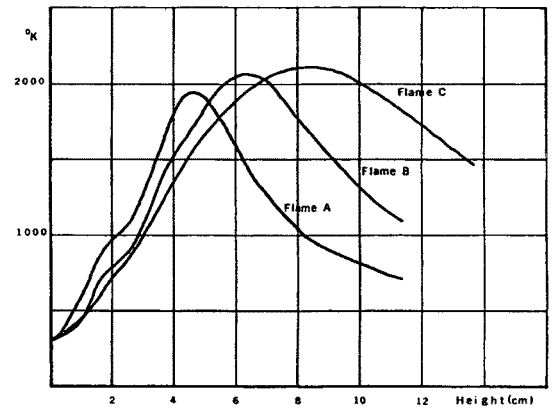

Figure 4. Temperature variation along central, vertical axis of H_2/Ar/entrained-air flames *A, B, C*

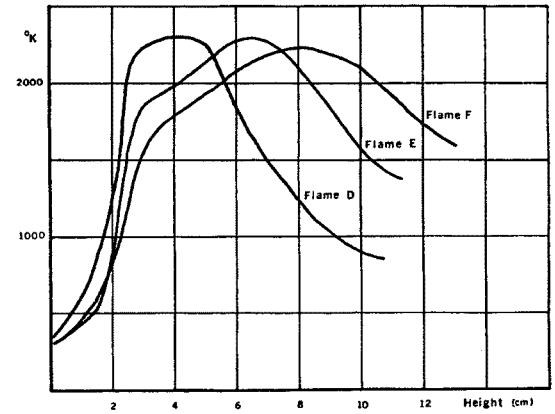

Figure 5. Temperature variation along central, vertical axis of H_2/Air flames *D, E, F*

The difference between the thermocouple and reversal temperatures, ΔT, was found to fit Equation 1 to ±25 °K for the range 1760 °K–2350 °K:

$$\Delta T = kT_c^4 \quad (1)$$

where:

ΔT = temperature reduction due to radiational heat loss—*i.e.*, difference between uncorrected thermal couple temperature and line-reversal temperature.
k = constant depending on thermocouple.
T_c = thermocouple temperature, uncorrected for radiation losses.

The general procedure for the sodium line-reversal method has been discussed in detail (*4, 6, 10, 11*) and will not be repeated here. Reversal measurements were carried out using 1000 ppm, 500 ppm, 100 ppm, 50 ppm, and where possible 10 ppm concentrations of sodium solution introduced into the flame *via* an aspiration chamber. The reversal temperature was found by extrapolation of these results to low sodium concentrations—*i.e.*, 10–100 ppm. The brightness temperature of the tungsten light source at 5890 Å was found from the makers absolute energy calibration and radiation tables after correcting for an intensity reduction of 8% (*11*) for the quartz lens used to focus the radiation on the flame. $H_2/O_2/N_2$ premixed flames were used together with the nitrogen sheath; nitrogen was used as the aspirant gas. Reversal temperatures for hydrogen flames using the premix burner could be reproduced to within 20 °K of the values published by Zeegers (*10*) for the same gas flow rates and burner.

Temperature Profiles. Complete profiles of selected flames (Figures 1–3) were obtained by scanning the whole width of the flame at height intervals of 0.5 cm or less. The variation in temperature with height, for the flame center only, was measured for more flames (Figures 4–6) with and without the aspiration of water. For all the flames used, the vertical temperature profiles could be reproduced to ±10 °K at any point on the central axis of the flame, and the maximum measured temperature of any flame could also be reproduced to ±10 °K. The experimental gas flow rates, maximum measured temperatures, and other details are given in Table I.

Thermocouple temperatures were corrected for radiational heat losses and for small errors involved in the use of uncompensated iridium/copper and copper/iridium–rhodium connections as the reference junction (*13*).

Table I. Flame Types and Characteristics

Flame	Type	Fuel (l./min)	Aspirant (l./min)	H_2O uptake (ml/min)	T max (°K)	T max with H_2O (°K)	Entrained-air required[a] (l./min)
A	H_2/Ar/Ent.-air	9.3	5.9	2.07	1894	1560	23.3
B	"	14.0	5.9	2.07	2040	1812	35.0
C	"	17.0	5.9	2.07	2122	2110	42.5
D	H_2/Air	9.3	5.9	1.08	2287	2110	17.4
E	"	14.0	5.9	1.08	2256	2135	29.1
F	"	17.0	5.9	1.08	2208	2133	36.6
G	H_2/Ent.-air	...	16.0	0.92	2182	2104	40.0
H	H_2/N_2O	15.0	4.75	2.93	2525	2405	25.7
I	premix H_2/N_2O	16 psi[b]	20 psi[b]	2.36	2630	2530	
J	premix H_2/Air	16 psi[b]	20 psi[b]	2.46	2250	2058	

[a] Calculated as the minimum amount required for complete combustion of hydrogen.
[b] See text for explanation.

RESULTS AND DISCUSSION

Thermocouple Errors. Operating characteristics of iridium/iridium–rhodium (60%–40%) thermocouples have been given by Blackburn and Caldwell (*13*), and sections of the volume edited by Herzfeld (*14*) deal exhaustively with these thermocouples and associated equipment. The thermocouple materials used were chosen because of their ability to withstand typical flame conditions without failure or appreciable change in thermoelectric characteristics. Alumina insulators were used despite their high conductivity at temperatures above 2000 °K (*14*); the insulator used had a resistance in excess of 5 K ohms when immersed in a flame at 2100 °K for a depth of about one inch. This test was carried out using a thermocouple with an unwelded junction.

Catalytic effects were noted with uncoated thermocouple junctions, and therefore a coating of zirconia ceramic was applied to prevent this. The use of silica coatings as recommended by Fristrom and Westenberg (*15*) was not suitable in this instance as the silica rapidly vaporized and at high temperatures may react with iridium or rhodium (*14*). Temperature differences of *ca.* 300 °K were noted in some *turbulent* hydrogen flames between coated and uncoated thermocouples, whereas differences of less than 10 °K were observed when the same thermocouples were inserted in *premixed* natural gas/air flames. In one instance, an apparent maximum temperature of over 2650 °K was noted for a hydrogen/air turbulent flame when measured with an uncoated thermocouple; when a zirconia coated thermocouple was used the maximum temperature noted was 2287 °K.

The radiation heat loss was determined by measuring the temperature of uniform flame gases using the thermocouples and line-reversal method. This represents the largest correction applied and also the greatest source of error. A variation in the gas velocity of the turbulent and calibration flames will affect the heat transfer to the thermocouple and result in an error in the radiation correction. However, Kaskan (*16*) has shown that the heat transfer depends on the fourth root of the reciprocal of gas velocity and as a result the expected error, arising from differences in velocity between

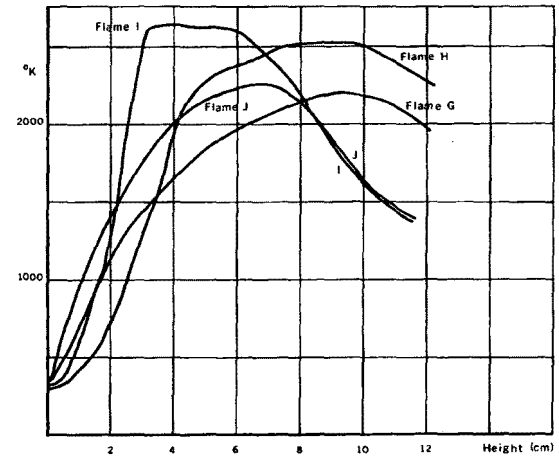

Figure 6. Temperature variation along central, vertical axis of reversed H_2/entrained air flame G, H_2/N_2O flame *H*, premixed H_2/N_2O flame *I* and premixed H_2/Air flame *J*

turbulent flame and calibration flame, will be less than 32 °K for a turbulent flame temperature of *ca.* 2400 °K. This estimate is based on maximum gas rise velocities measured by the authors for turbulent flames and also on published (*10*) rise velocities for the type of flames used in calibration. Smaller uncertainties will arise from the differences in thermal conductivity, viscosity, and isothermal gas densities between the two types of flame. These considerations will also apply to different regions of the same turbulent flame. A total error for the radiation correction of about 8%—*i.e.*, 32 °K for a flame at 2400 °K with a thermocouple having a radiation correction of 400 °K is to be expected.

The error involved in using uncompensated iridium/copper and copper/iridium–rhodium connections as the reference junction was eliminated by the application of the tabulated (*13*) emf values for these couples at room temperature. This compensation is of the order of 10–20 °K.

Conduction errors were minimized by the thermocouple design which ensured the junction leads were in contact with flame gases over a distance of about 1 cm. Errors due to the effect of the thermocouple acting as a heat sink on the flame will be negligible because of the small dimensions of the thermocouple and the high mass burning rates of the flame gases.

(14) C. M. Herzfeld, "Temperature," 3 (Part 2), Reinhold, New York, 1962.
(15) R. M. Fristrom and A. A. Westenberg, "Flame Structure," McGraw-Hill, New York, 1965.
(16) W. E. Kaskan, "Sixth Symp. (Int.) Comb.", Reinhold, New York, 1957, p 134.

Heating effects due to the dissipation of kinetic energy of the flame gases on striking the thermocouple are of minor importance in the turbulent flames investigated here and have been included to some extent in the compensation for the radiation error. For a gas rise velocity of *ca.* 80 m sec^{-1}, this error would be less than 2 °K (*17*).

The millivoltmeter used for measuring thermoelectric emf had a large impedance at balance, and no corrections were necessary for the thermoelectric current required to drive the meter.

The thermoelectric emf tables (*13*) have an expected maximum error of *ca.* 10 °K at the upper temperature limits of the thermocouples resulting from variations between lots of wire. The wire used in this study was obtained from the same source as that of Blackburn and Caldwell (*13*), and a temperature error of ±0.4% has been assumed for possible differences between tabulated and experimental thermal emf.

Systematic errors due to the effect of the thermocouple on the flame have been minimized as far as possible by thermocouple design but will not have been completely eliminated. Such errors arise from the mixing action of the thermocouple on the unburned gases issuing from the burner, the effect of the turbulent wake above the thermocouple, and the averaging effect due to the size of the thermojunction. Most of these errors are of unknown magnitude and are inherent in all thermocouple measurements in flames; the mixing effect is mainly important at low height above the burner in regions of steep temperature gradient and of little analytical importance.

Random errors resulting from positioning precision could be reduced to less than 10 °K even for flame regions where the temperature gradients were large but the temperature steady.

The above discussion of the main possible sources of error leads to a maximum uncertainty of about ±50 °K for flame temperatures of 2400 °K and about ±40 °K at 2000 °K. Although the estimated error is larger than might be expected using the line-reversal method, better resolution of temperature contours is possible using thermocouples. Simon (*18*) has measured the sodium reversal temperatures of a turbulent H_2/O_2 diffusion flame and found a maximum difference of 150 °K between the average temperature and the tem perature in the center of the flame, resulting from radial inhomogeneity of the flame temperature.

Flames Examined (see Table I). H_2/Ar flames *B* and *C* and H_2/air flames *E* and *F* were representative of the flames used by previous workers (*7*, *19*) in atomic fluorescence. Flames *A* and *D* were examined to extend the range of flow rates so that virtually all the flames likely to be used for analysis would be covered. To facilitate comparison, the argon or air flow rates were maintained at 5.9 l. min^{-1} for flames *A* through *F*.

H_2/entrained-air flames have been used by Ellis and Demers (*20*) for atomic fluorescence and appear to have some applicability in atomic emission spectrometry. Hydrogen was supplied to the flame through the burner port usually used for the aspirant gas, and the flow rates were limited by the hydrogen flow required for aspiration and lift-off of the flame from the burner. It is quite possible, however, that lifted H_2/-entrained-air flames could be used for analysis.

(17) E. F. Fiock, L. O. Olsen, and P. D. Freeze, "Third Symp. on Comb. Flame and Explosion Phenomena," Williams & Wilkins, Baltimore, 1949, p 655.
(18) L. Simon, *Optik*, **19**, 621 (1962).
(19) K. E. Zacha, M. P. Bratzel, J. D. Winefordner, and J. M. Mansfield, ANAL. CHEM., **40**, 1733 (1968).
(20) D. W. Ellis and D. R. Demers, *ibid.*, **38**, 1945 (1966).

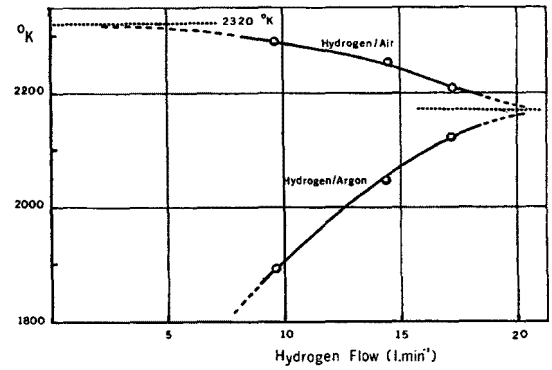

Figure 7. Maximum temperatures of H_2/Ar flames *A*, *B*, *C*, and H_2/Air flames *D*, *E*, *F*, having the same flow of aspirant gas (5.9 l. min^{-1}) but different fuel flow rates

The 2320 °K asymptote represents the calculated adiabatic temperature of the H_2/Air flame

The premixed H_2/air, premixed H_2/N_2O, and unmixed H_2/N_2O flames have recently been examined in this laboratory (*9*) and show considerable advantages over the flames, commonly used in atomic fluorescence spectrometry. Because of the complex mixing arrangements used for the premixed flames, the gas characteristics given in Table I, are gas pressures. However, a detailed description of how to reproduce the premixed flames will be given in another report currently being prepared for publication. Flames *H*, *I*, and *J* have the same gas flow rates and compositions as those examined in the fluorescence studies (*9*). An unmixed H_2/N_2O flame, having gas flow rates corresponding to flames *B* and *E*—*i.e.*, H_2 = 14.0 l. min^{-1} and N_2O = 5.9 l. min^{-1} caused failure of the thermocouple and unfortunately could not be included in the results. Similarly, H_2/O_2 turbulent flames could not be included in this study because of their high temperature; however, measurements of the temperatures of these flames have been made by several authors (2–6), and there is general agreement of the published values. Premixed H_2/Ar turbulent flames were found (*9*) to give no advantages in analysis over the unmixed H_2/Ar flames, as the aspirant did not act as an oxidant and the degree of turbulence was not reduced appreciably by premixing. Consequently, these flames were not included in this study.

Temperatures of Flames. Temperature profiles of H_2/Ar flame *B*, H_2/air flame *E* and H_2/entrained-air flame *G* are given in Figures 1, 2, and 3, respectively. The variations of temperature along the vertical axes of the flames listed in Table I are given in Figures 4, 5, and 6. The maximum temperatures found along the vertical axes of these flames are listed in Table I.

The maximum adiabatic temperature for a H_2/air flame has been calculated by Lewis and von Elbe (*21*) as 2320 °K, and it appears that this temperature is approached as the flow of hydrogen relative to air is decreased to the *stoichiometric ratio* (Figure 7). However, such a flame would be far too small for analytical purposes, and most useful flames are apparently very fuel rich. As the ratio of hydrogen-to-air is increased, the flame becomes larger, and the maximum temperature decreases until a limiting value of about 2180 °K is reached.

(21) B. Lewis and G. von Elbe, "Combustion, Flames and Explosions of Gases," 2nd Ed., Academic Press, New York, 1961.

It was thought, at first, that incomplete combustion of hydrogen occurred especially as the amount of entrained-air required for complete combustion appeared excessively large. However, analysis of the flame gases, by gas chromatogaphy after extracting a sample using a stainless steel probe, indicated that hydrogen combustion was complete at least to $\frac{1}{2}\%$ (the limit of measurement). In these experiments, helium was used as a reference tracer and was mixed with hydrogen before combustion. It appears, therefore, that the decrease in temperature is dependent on the amount of entrained-air (and hence turbulence) required for complete combustion. The higher the degree of air-entrainment, the greater the exchange of heat with the surroundings and the greater the possibility of entrainment of *excess* air from the atmosphere.

These generalizations appear to be borne out in the case of the H_2/Ar/entrained-air flames *A*, *B*, and *C* (see Figure 7). When the ratio of hydrogen-to-argon is small, a cooling effect due to the presence of argon will be expected, as well as a possible increase in the degree of turbulence. At higher flow rates of hydrogen, the cooling effect of argon should be reduced, and eventually the H_2/Ar flame should exhibit a temperature approaching that of a H_2/air flame for which the ratio of hydrogen to aspirant-air is also large. The results in Figure 7 indicate that this expectation is fulfilled at least within the range of gas compositions examined in this study.

The premixed H_2/air flame used in this study had a temperature which was representative of the unmixed flames. However, the flame was not stoichiometric, and some degree of air entrainment was necessary to ensure combustion. Similarly, the two H_2/N_2O flames could not be directly compared, as their compositions were based on their analytical utility. However, the reduction in turbulence obtained by premixing has been demonstrated photographically by schlieren (*8*) and shadow (*9*) techniques, and it is expected that premixing would give higher flame temperatures because of this.

Flame Structure. The unmixed H_2/Ar, H_2/air, and H_2/N_2O flames are characterized by the same shape (see Figures 1 and 2). Immediately above the burner, the flame widens in a similar manner to a hydrogen diffusion flame. In this region (0–8 mm above the burner), mixing of the aspirant and fuel gases is incomplete, and turbulence is not developed. About 2 cm above the burner, the flame shows a pronounced pinching effect, and it is likely that air entrainment becomes important in this region, above which the flame widens to give a transparent, almost invisible and poorly defined flame which is typical of the extended or fragmented reaction zones of turbulent flames at high Reynolds numbers.

The inner flame structure of the unmixed flames is difficult to observe because of their transparency. An unburned gas zone, in the center of the flame, extending 2 cm or so above the the burner, is usually obvious, but little structure can be observed visually. In the H_2/N_2O flame, however, a yellow reaction zone is easily observed and appears as a cone extending from a little above the "pinched" region at the edges of the flame (*ca.* 2 cm above the burner) to between 3.5 and 4.5 cm in the center. This yellow cone is about 1 cm wide in the unmixed flame and about 3 mm wide in the premixed flame.

The temperature profiles for the central, vertical axes of the unmixed flames (Figures 4, 5, and 6) show quite pronounced inflexions, between the burner tip and the region of maximum temperature. The inflexions appear as decreases in temperature above an otherwise gradually increasing profile. In the H_2/air and H_2/N_2O flames, they occur just above the regions where the aspirant gases react with hydrogen (this can be observed visually with the H_2/N_2O flame), and with the H_2/Ar flame, the inflexions occurs at a height where the "pinching" effect is greatest. In the unmixed flames, the inflexions of the temperature profiles are most apparent as the flow of aspirant relative to fuel is increased. The same inflexions were noticed with premixed flames *I* and *J* (Figure 6) but are less obvious.

Aspiration of Water. The flames considered, hitherto, have been 'dry' flames and have not had water aspirated through them, as is the usual practice in analysis. The measurement of flame temperature is even more complicated by the fact that the evaporation of water droplets in the flame is only partially complete and at *heights lower than 3 cm* above the burner, water droplets will actually cool the thermocouple considerably but will reduce the temperature of the flame to a much lesser extent. However, this represents a region of the flame which has no analytical utility. Analytical measurements are usually made at, or above, the hottest part of the flame. Over this region, the cooling effect of water on all the flames examined represented a temperature decrease of 5–15%, depending on the flame type and solution uptake rate (see Table I) but independent of flame height.

Turbulent Flames in Atomic Fluorescence. Although several reports have appeared from this laboratory (*7*, *19*) concerning the use of turbulent hydrogen flames in atomic fluorescence, it is not generally appreciated that many elements are determined most satisfactorily *above* the visible portion of the flame. This is particularly true for volatile elements which are easily atomized such as Cd, Cu, Hg, Ag, Zn, etc., while the more difficultly atomized elements such as Fe, Mg, Ni, etc., are best determined *within* the visible portion of the flame itself. The low background of the region above the flame is mainly responsible for some of the extremely low limits of detection which have been obtained using turbulent flames. The authors have re-examined the atomic fluorescence of several metals in solutions containing no matrix elements, and found the fluorescence above the flame to be quite genuine. For example, when a continuum excitation source is used, the atomic fluorescence spectral line can be observed when the monochromator is scanned over a narrow wavelength region.

Elements such as magnesium and iron, which are normally determined within the flame, appear to give their maximum signals at the region of maximum flame temperature. These observations have since been confirmed as part of this study. In this study, the atomic fluorescence from flame segments about 5 mm high was observed at different heights above the burner.

Although the fluorescence emission from metals such as magnesium and iron was greatest in the high-temperature region of the flame, this was not necessarily the best region to use for analytical purposes. With magnesium, the background, due to the OH emission around 2852 Å, is high at the region of maximum temperature. Consequently, it is necessary to *optimize the height of measurement on the basis of signal-to-noise considerations, rather than on the basis of only flourescence intensity*. In the case of iron, however, the atomic resonance line (2483 Å) occurs at a wavelength where flame background is fairly low, and as a result the atomic fluorescence determination of iron can be carried out at the region of maximum temperature, whereas the determination of magnesium is carried out at the tip of the visible portion of the flame where the background noise is lower. The results of Bratzel and Winefordner (*7*) have been optimized with regard to signal-to-noise, and it is instructive to compare their

heights of measurement for various elements, with the temperature profiles of Figures 4 and 5.

The relationships between heights of observation and fluorescence emission for the premixed and unmixed H_2/air and H_2/N_2O flames will be the subject of a series of comparative papers (*9*) and will not be discussed here.

With laminar flames, the use of Ar/O_2 mixtures in place of air generally results in increased fluorescence quantum efficiencies of the order of two-to-five-fold. Because of the high degree of air-entrainment in the turbulent flame, this enhancement was found to be small and of the order of about 10% in the most favorable cases after allowance for different solution uptake rates had been made.

Received for review February 10, 1969. Accepted March 21, 1969. This work was supported by AFOSR (SRC)-OAR, U.S.A.F. Grant No. AF-AFOSR-69-1685.

Determination of Arsenic by Atomic Absorption Spectrometry with an Electrodeless Discharge Lamp as a Source of Radiation

Oscar Menis and T. C. Rains

Analytical Chemistry Division, National Bureau of Standards, Washington, D.C. 20234

The determination of arsenic in cast iron and high-purity selenium metal by atomic absorption spectrometry was facilitated by the extraction of the arsenic with diethylammonium diethyldithiocarbamate (DDDC) followed by a stripping process from the organic phase by displacement reaction. In addition, the high background absorption of arsenic radiation encountered in various oxidant-fuel systems was overcome with an argon (entrained air)-hydrogen flame. The electrodeless discharge lamp was found to be an excellent high intensity source of radiation for use in atomic absorption in the far ultraviolet region. The detection limits for arsenic in an aqueous medium free of interfering cations was 0.1 μg/ml.

In recent years atomic absorption spectrometry (AAS) has provided an excellent means for the determination of a large number of elements. However, very little work has been reported for those elements, such as arsenic, which have ground-state resonance lines in the far ultraviolet region of the spectrum. Allan (*1*) in an unpublished paper in 1963 presented working curves for arsenic. The major difficulties in the determination of this element include the high absorption losses due to air and flame gases and the correction for the scattering of light due to solid particles. Slavin, Sebens, and Sprague (*2*) reported the determination of arsenic in glass by AAS but obtained a higher value than the one reported by chemical analysis. The authors attributed the high value to an improper correction for the light scattering which was made at 199 nm. To overcome the absorption of air and flame gases, Massmann (*3*) used an electrically-heated graphite cell and double beam spectrometer in an argon atmosphere which did not completely eliminate the difficulties encountered. Since the oral presentation of this paper, Dagnall and West (*4*) described the sensitivities of the arsenic electrodeless discharge lamp and Dagnall, Thompson, and West the fluorescence and analytical characteristics of arsenic (*5*).

To make the method applicable to the determination of trace quantities of arsenic in a large variety of materials required the application of high-intensity electrodeless discharge lamps, the use of a total consumption burner with an argon (entrained air)–hydrogen flame, and appropriate chemical separations. All contributed in overcoming the difficulties due to absorption and light scattering in the far ultraviolet region.

In our investigation of the determination of arsenic in National Bureau of Standards, Standard Reference Material (NBS-SRM) high purity selenium and cast iron, parameters such as the source of radiation, the resonance lines of arsenic, interfering ions, separations, nebulizers, and oxidant fuel systems were investigated.

EXPERIMENTAL

Reagents. Arsenic, Standard Solution was prepared in HNO_3 from NBS-SRM 83c.

Diethylammonium diethyldithiocarbamate (DDDC), 0.1% solution in chloroform. Prepare this reagent fresh daily.

2-Thenoyltrifluoroacetone (TTA), 1*M*, was dissolved in carbon tetrachloride. Store in a dark bottle.

Ammonium Acetate Buffer Solution, 5*M* ammonium acetate was adjusted to pH 4.5 with 5*M* acetic acid.

Other solutions are prepared from ACS reagent-grade chemicals.

Apparatus. The instrument is a 0.5m Ebert mount monochromator with a grating blazed for 3000 Å. The hollow-cathode power supply and tube holder are used unmodified, as received from the manufacturer. The electronic circuitry consists of three units and a chart recorder. The three units are the 0 to 2100 V multiplier phototube power supply, the selective amplifier and synchronous detector, and the DCR-2 digital readout.

The electrodeless discharge lamp is powered by an RF generator from a medical-type diathermy unit which supplies 100 W at 2450 MHz. The resonant frequency of $^1/_4$ wave cavity described by Fehsenfield, Evenson, and Broida (*6*) is adjusted for the minimum reflected power by a tuning stub and a coupling slider on the cavity. To observe minimum reflected power, an RF power meter is placed between the cavity and power generator. The lamps were prepared as described by Dagnall and West (*4*).

Slit Width. Because the 0.5m monochromator was equipped with adjustable bilateral slits, the slits were adjusted to give the maximum absorption of arsenic radiation with the

(1) J. E. Allan, Fourth Australian Spectroscopy Conference, Canberra, Australia, August 1963.
(2) Walter Slavin, Carl Sebens, and Sabina Sprague, *At. Absorption Newsletter* **4**, 341 (1965).
(3) H. Massmann, *Z. Anal. Chem.*, **225**, 203 (1967).
(4) R. M. Dagnall and T. S. West. *Appl. Opt.*, **7**, 1287 (1968).
(5) R. M. Dagnall, K. C. Thompson, and T. S. West, *Talanta*, **15**, 677 (1968).
(6) F. C. Fehsenfield, K. M. Evenson, and H. O. Broida, *Rev. Sci. Instrum.*, **36**, 294 (1965).

minimum voltage on the multiplier phototube. This was obtained when the entrance and exit slits were at 100 μm.

Calibration and Procedures. Transfer 1-, 2-, 3-, 4-, and 5-ml aliquots of the standard solution of arsenic (which contains 20 μg of arsenic per ml) to 60-ml separatory funnels. Add 4 ml of HCl and dilute to 15 ml with water. Add 5 ml of freshly prepared 20% KI and 5 ml of 5% $Na_2S_2O_5$. Place the separatory funnel in a hot water bath (approximately 50 °C) for 15 minutes. Cool to room temperature by placing the funnel under the cold water tap. Add 20 ml of 0.1% DDDC in $CHCl_3$ and equilibrate for 5 minutes. Drain the organic phase into a 60-ml separatory funnel. Repeat the extraction with 5 ml of 0.1% DDDC in $CHCl_3$. Combine the two organic phases. Add 10 ml of a copper solution which contains 1 mg of copper as the chloride per ml in 2*N* HCl. Equilibrate the sample for 5 minutes. Transfer the aqueous phase to a 10-ml volumetric flask, and measure the absorbance of the standard solution according to conditions given in Table I.

HIGH PURITY SELENIUM. Transfer a 2- to 4-gram sample to a 400-ml beaker and dissolve in 10 ml of HNO_3 and follow in general the procedure described by Reed (*7*). The precipitation was made, however, in 2*N* HCl instead of the recommended 6*N* HCl. While the precipitate is more dense in 6*N* HCl, the recovery, when tested with ^{77}As tracer, is the same. This led to the elimination of the acid adjustment prior to the extraction with the DDDC reagent. Proceed as directed in the section on preparation of the calibration curve.

CAST IRON. Transfer a one-gram sample to a 125-ml Erlenmeyer flask. Add 10 ml of H_2O and 20 ml of HNO_3. Cover the flask with a cover glass until the sample dissolves. Centrifuge to remove carbon and silica. Decant and wash the residue with two 5-ml portions of 1*N* HNO_3. Return the sample to the Erlenmeyer flask and evaporate to approximately 3 ml. Transfer the solution to a 50-ml volumetric flask and dilute to volume.

Transfer an aliquot containing 20 to 100 μg of arsenic to the extraction cell (*8*). Add 40 ml of the TTA solution. Place the electrodes of a properly standardized pH meter in the aqueous phase and agitate the solution mechanically; then add the ammonium acetate buffer solution to adjust the aqueous phase to pH 1.5. Continue the agitation for 10 minutes. Stop the agitation and allow the phases to separate. Drain the organic (lower) phase. (Note. Because the iron–TTA complex is highly colored, place a light source behind the extraction cell to observe the separation of the two phases.) Repeat the extraction, but adjust the pH to 2.5 with the acetate buffer solution. Generally, two extractions will remove up to one gram of iron. Remove the organic layer and wash the aqueous phase with 40 ml of chloroform. Again remove the organic phase. Transfer the aqueous solution to a separatory funnel and adjust the acidity with HCl to 3*N*. Proceed as directed under preparation of the calibration curve.

RESULTS AND DISCUSSION

Absorption Due to Flame Gases. Because the resonance lines of arsenic are in the far ultraviolet region of the spectrum, the absorption of the flame gases is of major concern. The absorption of arsenic was investigated for different burners with premixed and turbulent flames. The argon (entrained air)–hydrogen flame provided the least absorbance from the flame background, as shown in Table II. Veillon *et al.* (*9*) applied the argon (entrained air)–hydrogen flame in atomic fluorescence work, while Zacha and Winefordner (*10*) used it for flame emission. The argon–hydrogen flame with a premix burner was unstable. The study with the premixed gases was discontinued in favor of the stable total-consumption burner, which provided a colorless, low audio-noise flame.

Table I. Operating Conditions

Wavelength, Å	1937
Slit width, μm	100
Light source, electrodeless discharge lamp in (1/4 wave) Evenson cavity	AsI_3
RF power supply, W	50
Burner, Zeiss, multiple pass	3
Oxidant–fuel, Argon (entrained air)	Hydrogen
Scale expansion—DCR-2	5
Time constant	3
Multiplier phototube, R-106, V	450

Table II. Absorbance of Various Flame Gases at 1937 Å

Flame	Oxidant–fuel	Absorbance
Premix[a]	Air–C_2H_2	1.350
	Air–H_2	0.960
	Air–H_2	0.270
Turbulent[c]	O_2–H_2	0.700
	Air–H_2	0.290
	Ar[b]–H_2	0.210

[a] Single pass.
[b] Argon-entrained air.
[c] Three passes.

Detection Limits of Arsenic. The detection limits of the three resonance lines of arsenic at 1890, 1937, and 1972 Å were 0.1, 0.1, and 0.2 μg/ml of arsenic, respectively. Detection limit is defined as 2 σ above the mean obtained from a background or a matrix blank. These limits were obtained using the electrodeless discharge lamp in an argon–hydrogen flame with the total consumption burner. The lines at 1890 and 1937 Å give the same sensitivity; however, the line at 1890 Å is greatly affected by light scattered by solid particles or water vapor.

Comparison of Sources. Of the sources explored, the electrodeless discharge lamp in a 1/4-wave cavity offered the highest intensity. This lamp is of the type developed by Meggers and Westfall (*11*) which has been used only briefly as a source in AAS. Rann and Hambly (*12*) used an electrodeless discharge lamp which operated at 15 MHz in the determination of selenium. Recently, West and coworkers (*5*, *13–16*) used electrodeless discharge lamps powered by 2450 MHz as a source in atomic absorption determinations for As, Bi, Fe, Hg, Se, and Te.

(7) J. F. Reed, ANAL. CHEM., **30**, 1122 (1958).
(8) T. C. Rains, Marion Ferguson, and H. P. House, *ibid.*, **33**, 1645 (1961).
(9) C. Veillon, J. M. Mansfield, M. L. Parson, and J. D. Winefordner, ANAL. CHEM., *ibid.*, **38**, 204 (1966).
(10) K. Zacha and J. D. Winefordner, *ibid.*, **38**, 1537 (1966).
(11) W. F. Meggers and F. O. Westfall, *J. Res. Nat. Bur. of Stand.*, **44**, 447 (1950).
(12) C. S. Rann and A. W. Hambly, *Anal. Chim. Acta*, **32**, 346 (1965).
(13) G. B. Marshall and T. S. West, *Talanta*, **14**, 823 (1967).
(14) R. M. Dagnall, K. C. Thompson, and T. S. West, *ibid.*, **14**, 551 (1967).
(15) R. M. Dagnall, K. C. Thompson, and T. S. West, *ibid.*, **14**, 1467 (1967).
(16) D. N. Hingle, G. F. Kirkbright, and T. S. West, *Analyst* (London), **92**, 759 (1967).

Table III. Results of AAS Determination of Arsenic in Selenium and Cast Iron

NBS SRM number	Number of determinations[a]	As found, μg/gram	Rel std dev, %
4i (cast iron)	4	224 (202)[b]	4
4j (cast iron)	4	260 (277)[b]	6
726 (Selenium)	6	<1	

[a] Each determination represents a separate test portion.
[b] Determined independently by the molybdenum-blue spectrophotometric method.

The usefulness of the electrodeless discharge lamp depended upon the selection of cavity, lamp size, and filler gas pressure. The hemispheric antenna which was used by some of the early workers to transfer the power from the microwave generator to the gas contained in the lamps was very inefficient and the RF produced has an adverse effect on the electronics of the instrument. Fehsenfield, Evenson, and Broida (*6*) designed a cavity with an adjustable tuning screw and probe which eliminated scattered RF radiation within the laboratory and produced a discharge which was readily maintained. Because the resonance lines for arsenic are below 2000 Å (1890, 1937, and 1972 Å), the source of radiation must be of high intensity to overcome the absorption due to the air. The intensity of the arsenic electrodeless discharge lamp was found to be two orders of magnitude greater than that produced by the arsenic hollow cathode lamp; however, the electrodeless lamp was slightly less stable (a drift of approximately 5%, per hour) than the hollow cathode lamp.

Separation. Arsenic is generally separated from ferrous and nonferrous alloys by distillation as $AsCl_3$, and then determined by one of several methods. The recovery is better than 95%. Tests with ^{77}As added to solutions of cast iron indicated a recovery of 80–90% of the ^{77}As. This incomplete recovery led to an investigation of a number of separation procedures. NBS cast iron standards 4i and 4j could be dissolved in HNO_3 with no loss of arsenic, and traces of arsenic occurring in the insoluble silica and carbide residues could be removed with two washings of 1*N* HNO_3. The iron was then removed by an extraction with 1*M* TTA in carbon tetrachloride.

The procedure for the separation of arsenic from selenium was essentially the same as described by Reed (*7*).

Extraction of Arsenic. Two requirements are essential for the separation of the arsenic. The method should be selective and it should provide conditions which would allow reversible back extraction into an aqueous phase. The interference of CH and C_2 radicals in flame gases in the far ultraviolet region at 1937 Å is serious and precludes the direct burning of the organic solutions. Any prior wet oxidation of the organic material would lead to volatilization of pentavalent arsenic. A series of solvent extraction systems were investigated and of these, diethylammonium diethyldithiocarbamate (DDDC) served to meet these requirements. Starý (*17*) has listed this reagent as an extractant for arsenic from 10*N* H_2SO_4 and from 6*N* HCl. It was established with ^{77}As tracer that the extraction of arsenic was quantitative at 2*N* HCl under the conditions similar to those for the precipitation of selenium. Šedivec and Vašak (*18–20*) have also reported that copper displaces Ni, Bi, and Pb from the complex. The reported order for the metal dithiocarbamates is $Hg^{2+} > Pd^{2+} > Ag^{+} > Cu^{2+} > Te^{3+} > Ni^{2+} > Bi^{3+} > Pb^{2+} > Cd^{2+} > Zn^{2+} > In^{3+} > Sb^{3+} > Fe^{3+} > Te^{4+}$ (*17*). Because no data are reported for As, the exchange reaction was investigated with Cu^{2+}, Te^{3+}, and Ni^{2+}. Copper exchanged quantitatively with $^{77}As^{3+}$; Te^{3+} produced a partial exchange only, and Ni^{2+} produced no effect. Thus the order $Cu^{2+} > Te^{3+} > As^{3+} > Ni^{2+}$ can be postulated.

Interferences. The major interference in the AAS determination of arsenic results from light scattering. It was observed that all elements in concentrations greater than one mg/ml produced an absorption at the arsenic wavelengths of 1890, 1937, and 1972 Å. Corrections can be made for light scattering by using the Ne 1916 or 1930 Å line or the nonabsorbing arsenic line at 1990 Å, although the proper correction is often difficult to obtain. No interference of HCl or HNO_3 with arsenic was observed up to 1*N* acidity. Higher acid concentrations produced a slight loss of absorption due to the change in the rate of aspiration.

Application. The method was tested on two ferrous alloys, NBS Standard Reference Materials 4i and 4j as well as on selenium metal, NBS 726. The results are shown in Table III. In a determination of the recovery of the arsenic in selenium metal, 20 μg of arsenic was added to a 2-gram test portion of the sample and 19.8 μg was recovered.

In summary, this study reveals that AAS is applicable to the determination of arsenic in a wide variety of samples after the removal of the matrix material.

RECEIVED for review November 7, 1968. Accepted March 13, 1969. Presented in part before the Division of Analytical Chemistry, 154th National Meeting, ACS, Chicago, Ill., September 12, 1967. The mention of a commercial product does not constitute an endorsement by the National Bureau of Standards.

(17) Jiří Starý, "The Solvent Extraction of Metal Chelates," Pergamon Press, Oxford, 1964.
(18) V. Šedivec and V. Vašak, *Chem. Listy*, **44**, 103 (1950).
(19) V. Šedivec and V. Vasak, *ibid.*, **45**, 435 (1951).
(20) V. Šedivec and V. Vašak, *ibid.*, **46**, 607 (1952).

Simultaneous Determination of Trace Elements in Platinum by Isotope Dilution and Spark Source Mass Spectrometry

Robert Alvarez, Paul J. Paulsen, and Daniel E. Kelleher

Spectrochemical Analysis Section, National Bureau of Standards, Washington, D. C. 20234

An isotope dilution technique using the spark source mass spectrograph was investigated for applicability to simultaneous multi-element trace determinations. Isotopically altered Ag, Cu, Ni, Pb, and Pd were separated from a 250-mg sample of platinum by cation exchange, and electrodeposited onto gold electrodes for sparking in the spectrograph. Electrodeposition provided the spiked analytes in an adherent form, relatively free of anions and organic residue from the ion exchange resins, both of which could complicate the spectrum. Contamination, the principal limitation of the method, was minimized by isothermally distilling the reagent acids and by isolating the operations from the laboratory environment. After determining the isotope ratios, the concentrations were computed, ranging from 0.5 ppm (μg/gram) for Ni to 14 ppm for Pb. Improved precision and accuracy was obtained compared to conventional spark source analysis. The results were compared with those of other methods and the platinum material was issued by NBS as Standard Reference Material 681.

STABLE ISOTOPE DILUTION ANALYSES are usually performed using mass spectrometers with thermal ionization sources. These methods depend on the chemical form of the element for optimum results and are generally not suitable for simultaneous multi-element trace determinations. This is particularly true if elements having high ionization potentials are to be included in the analysis. Webster (*1*) presents an excellent description of the general method including applications. The spark source mass spectrograph has been employed by Leipziger (*2*) to determine copper in Nickel Oxide NBS Standard Reference Material (SRM) 673 and antimony in Tin SRM 835 using isotope dilution techniques. The average values obtained, 21 and 121 ppm, respectively, agreed with the NBS certificate values.

Because the high voltage spark source ionizes all elements with approximately the same efficiency, isotope dilution spark source mass spectrometry (ID-SSMS) should enable the simultaneous determination of many trace elements in a sample. The object of this investigation was to apply this method to determine five trace elements in a sample of platinum. Isotopically altered Ag, Cu, Ni, Pb, and Pd were separated from the platinum matrix by cation exchange and eluted with HCl into an electrolysis cell. After neutralizing the acid, the spiked analytes were electrodeposited onto gold wires and sparked in the spectrograph. The mass spectra were photographically recorded, isotopic ratios determined, and the results calculated. After comparing these results with those of other analytical methods, this platinum material, previously examined for homogeneity, was subsequently issued by the National Bureau of Standards as SRM 681.

The authors have also developed an ID-SSMS method for determining trace elements in each of two NBS zinc standard reference materials (*3*). Compared to this zinc method, the platinum procedure required a greater number of analytical operations using special techniques and apparatus to reduce contamination to an acceptable level.

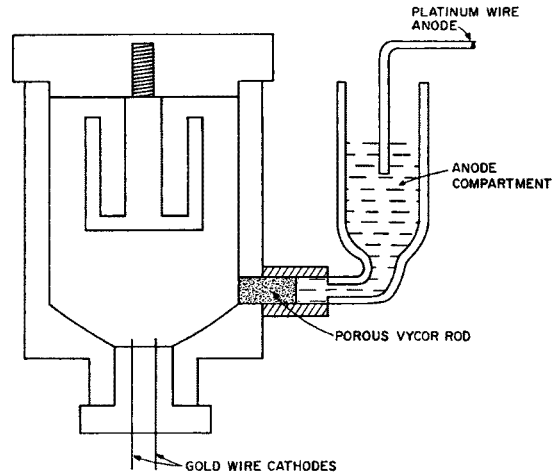

Figure 1. Cell for acid neutralization and electrodeposition

EXPERIMENTAL

Reagents. Deionized water is made immediately before use by passing distilled water from the laboratory distribution system through a mixed bed resin column. HCl and HNO_3 are prepared by isothermal distillation. Aqueous ammonia is prepared by bubbling NH_3 into deionized H_2O, after passing the gas into a gas washing bottle.

Evaporator for Sample Solutions. A borosilicate glass chamber, similar to the one described by Thiers (*4*), provides a clean environment for evaporating solutions. The apparatus is fabricated from a crystallizing dish 150 mm in diameter by 75 mm high, and a culture dish of the same diameter. A lateral displacement of the coincident edges of the two units is prevented by three lengths of glass rod that are fused to the outside of the culture dish (lower unit) and project upward. Filtered nitrogen is introduced through a tube sealed at the center of the crystallizing dish, and escapes from between the edges of the modified dishes to prevent entry of particulate contaminants. The gas is filtered by a cellulose filter which has a mean pore size of 0.1 μm and is supported by porous polypropylene disks in a Nylon filter holder.

Glove Box. A fiber glass glove box is employed to reduce airborne contamination during ion exchange and miscellaneous operations.

Ion Exchange Column. The column consists of an 8-mm i.d. borosilicate glass tubing drawn to a fine tip, containing a resin bed 4 cm in height. The resin has a 100 to 200 mesh size and is of an analytical-grade, sulfonic acid type with an 8% divinylbenzene crosslinkage. Before use, the column is

(1) R. K. Webster in "Advances in Mass Spectrometry," J. D. Waldron, Ed., Pergamon Press, New York, N. Y., 1959, pp 103–119.
(2) F. D. Leipziger, ANAL. CHEM., 37, 171 (1965).
(3) P. J. Paulsen, R. Alvarez, and D. E. Kelleher, *Spectrochim. Acta*, in press.
(4) R. E. Thiers in "Trace Analysis," John H. Yoe and H. J. Koch, Eds., John Wiley and Sons, Inc., New York, N. Y., 1957, p 637.

Table I. Natural and Spike Isotopic Abundance of Isotopes

Isotope	Natural abundance, atomic per cent	Isotopic abundance in spike, atomic per cent
^{107}Ag	51.83	0.9
^{109}Ag	48.17	99.1
^{63}Cu	69.17	0.30
^{65}Cu	30.83	99.7
^{58}Ni	67.88	0.38
^{62}Ni	3.66	99.02
^{108}Pd	26.71	10.6
^{110}Pd	11.81	87.5
^{206}Pb[a]	—	92.15
^{208}Pb[a]	—	1.255

[a] Lead exhibits isotopic variability in nature and is therefore not listed.

Table II. Trace Element Concentrations in Platinum Standard Reference Material 681 Determined by Isotope Dilution Analysis

Element	Concentration in ppm (μg/gram)	No. of samples	95% Confidence limits in ppm for the concentration[a]
Ag	2.09	7	±0.15
Cu	5.04	6	±0.54
Pd	5.92	4	±0.32
Pb	13.6	6	±0.9
Ni	0.46	4	±0.06

[a] These confidence limits are based upon $tS_{\bar{x}}$ where $S_{\bar{x}}$ is an estimate of the uncertainty in the average concentration and is based upon the observed variation between the k samples. The t is Student's t factor for 95% confidence and $k - 1$ degrees of freedom.

pretreated with 50 ml of 6*M* HCl and washed with 5 ml of water.

Neutralization and Electrolysis Cell. The cell shown in Figure 1 was designed for neutralization of the acid eluate and subsequent electrodeposition of the isotopically-altered trace elements. The components are fabricated of polytetrafluoroethylene (PTFE) except as otherwise indicated. The cell body has a 25-mm i.d. and a volume of 13 ml. For the neutralization step, the cylindrical compartment, shown suspended by a reentrant centerpost threaded into the lid, is filled with 1 ml of aqueous NH_3. This assembly is removed prior to electrodeposition. Two high-purity gold wires, inserted into a removable PTFE plug, serve as the cathode during electrodeposition. When this plug is fitted tightly into the body of the cell, the 0.7-mm diameter cathode wires project 2 mm into the cell body. An isolated anode compartment is formed by inserting a 3.5-mm diameter by 6-mm long porous Vycor (5) rod into an undersize hole at the side of the cell and connecting this rod to a glass reservoir with plastic tubing. A platinum wire makes an electrical contact with diluted HNO_3 added to this compartment as an electrolyte. During electrodeposition, the cells are housed in a plastic enclosure under a slight positive pressure of nitrogen to minimize airborne contamination.

Enriched Isotope ("Spike") Solutions. With the exception of ^{206}Pb, the enriched isotope materials in amounts equivalent to 10 mg of the element were obtained from the Oak Ridge National Laboratory. Solutions containing one mg per ml of ^{109}Ag, ^{65}Cu, ^{62}Ni, and ^{110}Pd were prepared by weighing each material to ±0.02 mg, dissolving it in the appropriate acid, and diluting the solution to volume in a 10-ml volumetric flask. The possible presence of impurities in these materials and the small sample weights used made it advisable to verify the solution concentrations. However, because these solutions were diluted to add the required submicrogram additions of the spikes to the sample solution, the concentrations of the diluted spike solutions were determined by isotope dilution as follows: Measured volumes containing 5 μg of each spike were mixed with solutions containing known amounts of the normal elements. The pure element additions were computed from Equation 1 to yield isotope ratios approximating one for all elements except Ag (see Calculations and Results). The solution was electrolyzed for one hour at a current of 2 mA in the previously described cell. The gold wire electrodes were then sparked, the isotope ratios were determined, and the spike weights were computed from Equation 1. A reliable ^{206}Pb solution could be prepared by weighing 100.0 mg of the NBS radiogenic lead isotopic standard, SRM 983 (6), dissolving it in HNO_3, and diluting to volume with water in a 100-ml volumetric flask.

Mass Spectrograph. A double-focusing Mattauch-Herzog design, spark source instrument (Consolidated Electrodynamics Model 21-110) that had been modified to give 22 exposures per plate is operated at an ion accelerator voltage of 24 kV.

Microphotometer–Analog Computer. A microphotometer having a precision screw (Jarrell-Ash Model 23-500) and equipped with an analog computer to measure peak areas (7) is used. A function generator, which is the basic component of the analog computer, provides an output proportional to relative ion intensities when the input is a voltage proportional to per cent absorption. An integrator follows the function generator to give signals proportional to peak intensity areas as the line is scanned.

Procedure. A 250-mg sample of platinum was treated with warm aqua regia for several minutes and rinsed in water to remove possible surface contamination. The sample was weighed into a 25-ml quartz erlenmeyer flask and heated with 3 ml of HCl and 1 ml of HNO_3 until dissolved. After adding measured volumes of the spike solutions, the platinum solution was transferred to a 20-ml low form, quartz crucible and evaporated almost to dryness in the chamber described. The resulting salts were dissolved in 5 ml of H_2O and the solution was passed through the cation exchange column using the full flow rate of the column. During this step, the isotopically altered trace elements were adsorbed on the resin and the chloroplatinate solution was the effluent. The column was washed with 4 ml of H_2O, and eluted with 5 ml of 3*M* HCl into the electrolysis cell after the washings had been discarded. To neutralize the acid eluate with a minimum of contamination, aqueous ammonia was pipetted into the cylindrical compartment and the cell was closed with its tightly fitted lid. This distillation step yielded a small solution volume that was favorable for the electrodeposition of the analytes. After removal of the cylindrical compartment, the acidity of the solution was adjusted to read approximately 6 with indicating pH paper. The acidity is not critical. The solution was then electrolyzed for 5 hours at a current of 2 mA, while stirring at approximately 200 rpm. After withdrawing the solution, the gold electrodes were rinsed in water and transferred to the mass spectrograph.

A graded series of exposures was made with the pair of electrodes at integrated beam currents of 0.3×10^{-10} to 1×10^{-7} coulomb to obtain optimum intensities for the isotope lines of the various amounts of electrodeposited elements. By moving one electrode so as to expose a fresh surface, the electrodeposit was consumed more effectively and a greater signal was obtained. The ion-sensitive photographic plates (Ilford Q-2), were developed in a high contrast

(5) R. A. Durst, *J. Chem. Educ.*, **43**, 437 (1966).

(6) E. J. Catanzaro, T. J. Murphy, W. R. Shields, and E. L. Garner, *J. Res. Natl. Bur. Stand.*, **72A**, 261 (1968).

(7) P. J. Paulsen and P. E. Branch, NBS Technical Note 401, Washington, D. C., Sept. 1966.

Table III. Comparison of Results by Isotope Dilution with Other Analytical Methods for Platinum Standard Reference Material 681

Concentration in ppm (μg/gram)

Element	Isotope dilution	Activation analysis[a]	Polarography[b]	Optical emission spectrochemical[c]			
				Lab A	Lab B	Lab C	Lab D
Ag	2.1	1.8		1.4	2.0	2	...
Cu	5.0	5.0	5.2	6.3	3.0	2	...
Pd	5.9	5.6		5.0	6.1	4.0	...
Pb	13.6		10.3	8.5	15.0	10	12.3
Ni	0.46			<1	N.D.[d]	0.8	0.44

[a] Activation analyses by Michel Crambes and Gilbert W. Smith, NBS Analytical Chemistry Division.
[b] Polarographic analyses by E. June Maienthal, NBS Analytical Chemistry Division.
[c] Spectrochemical analyses by outside laboratories cooperating with NBS.
[d] N.D. Not Detected.

developer (Kodak D-19) for 2½ min, placed in a short stop solution for 10 sec, fixed for 1 min, washed 15 min in tap water, and rinsed in distilled water. The intensity areas of the lines for the isotopes listed in Table I were measured and their ratios were calculated. From 6 to 20 ratio measurements were made for each element depending on the availability of lines having suitable intensity.

To correct the determination for contamination, the entire analytical procedure was performed using the same sample size of high-purity platinum, SRM 680. A direct mass spectrographic comparison of SRM 680 with SRM 681 had indicated that the elements of interest except for Ni were substantially lower in SRM 680 than in the material being analyzed. Consequently, to obtain favorable intensity ratios, the SRM 680 solution was spiked with one tenth of the amount added to SRM 681 and both materials were analyzed concurrently. Use of the higher-purity matrix to evaluate contamination, which did not exceed 10% of the reported values, yielded more reproducible results than were obtained by spiking the reagents alone. For Ni however, this latter procedure had to be used.

CALCULATIONS AND RESULTS

The concentrations were computed from Equation 1.

$$C = \frac{WK(A_{sp} - B_{sp}R)}{M(BR - A)} \quad (1)$$

where C is the concentration in ppm (μg/gram), W is the weight of isotopically enriched material ("spike") added in μg, M is the weight of sample in grams, A and B are the natural abundances of the analyte isotopes a and b, A_{sp} and B_{sp} are the abundances of isotopes a and b in the spike, R is the measured altered ratio of isotope a to isotope b, and K is the ratio of the natural atomic weight to the atomic weight of the spike.

In the method, it is desirable to alter the isotopic compositions of the analytes to obtain isotope ratios, R, approximating one whenever possible. This minimizes the effect of photographic emulsion calibration errors, and could be done for all analytes except Ag. For that element, ^{109}Ag spike was added to change the $^{109}Ag/^{107}Ag$ ratio from its natural value of 0.93 to 2. To obtain the desired R values, the spike additions were computed from Equation 1 using the elemental concentrations estimated from a direct sparking of the platinum sample. This photographically recorded spectrum was also used to determine the ^{206}Pb and ^{208}Pb natural abundances in the platinum material. These determinations were necessary because of the isotopic variability of Pb in nature (*6*). For the other analytes, an experimental determination of the natural abundances of the isotopes was not required; and the values listed in Table I, supplied by the NBS Analytical Mass Spectrometry Section, were used. The isotopic analyses provided by the Oak Ridge National Laboratory for its isotopically enriched materials and by Catanzaro *et al.*, (*6*) for the radiogenic lead isotopic standard, SRM 983, are also listed in this table. These isotope analyses are of sufficient accuracy that errors from this source do not significantly affect our results.

In all, seven samples were run, the first three using experimental conditions that did not satisfactorily preconcentrate all of the elements. However, using the experimental conditions described under Procedure, the last four samples yielded all of the analytes for simultaneous determination. The elemental concentrations obtained for the first three samples are also included in the results. The determination of Ag was satisfactory for all of the samples. Table II lists the average concentrations obtained, the number of samples, and the 95% confidence limits. A comparison of the isotope dilution results with the results obtained by other analytical methods is given in Table III. Except for Pb, the agreement among methods having high precision was satisfactory.

DISCUSSION AND CONCLUSIONS

Unlike most trace analytical methods, isotope dilution analysis does not require analyzed or synthesized standards of the same matrix material for reliable determinations. As applied to spark source mass spectrometry, the simplest procedure consists of evaporating a portion of an isotopically spiked solution of the sample on a suitable substrate for sparking in the spectrometer. Compared to direct sparking of the sample, poorer limits of detection will be obtained. Moreover, a trace element may be undeterminable if the only isotope lines suitable for measurement are interfered with by isotope lines of the matrix elements or complex ionized species of the matrix and anion fragments. For example, copper could not be determined in platinum by this direct-evaporation technique because one of its two stable isotopes, $^{65}Cu^+$, is interfered by $^{195}Pt^{3+}$.

To obtain improved limits of detection and remove these interferences, the isotopically spiked analytes can be separated from the matrix before sparking. A preconcentration procedure should be selected that minimizes contamination which is the principal limitation of these methods. These procedures can be relatively simple or incompletely characterized because determinations by isotope dilution methods are unaffected by analyte losses once equilibrium has been established with the added spikes. However, to obtain isotope lines of sufficient intensity for precise ratio measurement, a high recovery of the spiked analytes is desirable.

Concentration limits of detection comparable and even superior to those obtained by the direct sparking technique are possible if contamination can be reduced to an acceptable value. Although the experimental procedure should be designed to achieve a low method blank, its variability is an important factor affecting the precision of the results. Therefore, the least number of manipulations is desirable and should be performed in a clean environment to reduce spurious contamination. In the platinum method, contamination can occur during sample dissolution, evaporation, ion exchange, and transfer of the spiked analytes to the substrate for sparking. Gold is a suitable substrate for it does not react with the solution being electrolyzed; it is mononuclidic thus producing a simple spectrum; and it is obtainable in high purity. The gold wire that was used has the composition of NBS Standard Reference Material 685-W listed in the Certificate of Analysis.

For the dissolution step, minimal quantities of isothermally distilled acids are used. The contribution to the total blank from the reagents is relatively constant and can be corrected for. The spiked platinum sample solution is evaporated in a quartz vessel surrounded by filtered nitrogen. The ion exchange step is performed in a glove box using methylmethacrylate rods and holders to support the ion exchange columns. The last stage, during which the submicrogram amounts of the analytes are being transferred to the wire substrate for sparking, is particularly sensitive to spurious contamination. Although the eluate solution can be evaporated to a small volume and pipetted onto the gold wires, it is preferable to electrodeposit the analytes. This procedure yielded an adherent form for sparking, relatively free of anions and organic residue from the resin, both of which would complicate the spectrum. Moreover, electrodeposition required less handling and, therefore, was less subject to contamination. The electrolysis cell design incorporated a replaceable porous Vycor plug to prevent cross-contamination from the eluate solutions.

To determine elements that are not ordinarily electrodeposited, evaporation of the eluate would have been required. In this case, the electrodeposition step could be followed by evaporation and possible ignition of the residue on fresh electrodes. Ignition would remove the organic residue, one of the disadvantages of this evaporation procedure.

In conclusion, isotope dilution techniques provide spark source mass spectrometry with methods for independently analyzing homogeneous materials that can serve as standards for the direct sparking comparison procedures. In general, these standards of the matrix either are not available or often have values that are not as precise as required. Although ID-SSMS is not a rapid method (for the procedure developed, four samples required approximately 8 days to run), its capability of simultaneous multi-element determinations and applicability to most of the elements having two or more stable isotopes, makes it very attractive for reliable trace element determinations.

RECEIVED for review March 3, 1969. Accepted April 4, 1969. Presented in part before the Division of Analytical Chemistry, 155th National Meeting, ACS, San Francisco, Calif., April 1, 1968. Certain commercial materials and equipment are identified in this paper in order to adequately specify the experimental procedure. In no case does such identification imply recommendation or endorsement by the National Bureau of Standards, nor does it imply that the material or equipment identified is necessarily the best available for the purpose.

Ultra-Trace Determination of Oxygen and Carbon by Charged Particle Activation Analysis

Harry L. Rook and Emile A. Schweikert

Activation Analysis Research Laboratory, Texas A&M University, College Station, Texas 77843

When considering ultra-trace analysis by charged particle activation using the equivalent thickness method of quantization, three factors are of prime importance to ensure valid results. First, accurate and well defined activation curves of the nuclear reactions being employed must be obtained. Second, all interfering reactions must be experimentally categorized to ensure the integrity of the radioisotope used for analysis. Third, all usable reactions for the analysis of a given element should be investigated to allow the best possible choice of reactions for analysis in a given matrix and impurity level. This paper presents a study of the ultra-trace determination of oxygen and carbon by charged particle activation analysis following the above outlined procedure. Analytical results are given for the nondestructive determination of oxygen in silicon in the part-per-million to the part-per-billion range. Results of some selected samples are compared to results independently obtained by infrared spectrometry.

IN QUANTITATIVE analyses using charged particle activation, carried out with protons, deuterons, tritons, helium-3 and helium-4 ions, the analytical method must account for the nonuniform activation of the sample under investigation, inasmuch as the activation cross section varies continuously with the energy degradation of the bombarding particles in matter. Different methods of quantization have been devised for the specific case in charged particle activation (*1–5*). The "equivalent thickness" method proposed first by Engelmann (*5*) was used in this work for obtaining quantitative results. The principle and the features of this method have been described in detail elsewhere (*5–8*); it need only be recalled here that this method is based on an experimentally established activation

(1) Ph. Albert, P. Sue, and G. Chaudron, *Bull. Soc. Chim. France*, **2016**, 97 (1953).
(2) S. S. Markowitz and J. D. Mahony, ANAL. CHEM., **34**, 329 (1962).
(3) E. Ricci, R. L. Hahn, J. E. Strain, and F. F. Dyer, *Proc. 2nd Int. Conf. on Modern Trends in Activation Analysis*, ed. by Texas A&M University, 200 (1965).
(4) E. Ricci and R. L. Hahn, ANAL. CHEM., **40**, 54 (1968).
(5) Ch. Engelmann, *C. R. Acad. Sci. Paris*, **258**, C, 4279, (1964).
(6) N. Chevarier, J. Giroux, M. D. Tran, and J. Trousset, Lycen Report 6714, University of Lyon, France, (Feb. 1967).
(7) Ch. Engelmann, "Radiochemical Methods of Analysis," Vol. 1, International Atomic Energy Agency, Vienna, 1964, p 405.
(8) Ph. Albert, *Chimia (Aarau)*, **21**, 32 (1967).

curve for a given nuclear reaction in a given matrix material. However, when considering the application of charged particle activation for the determination of trace elements in a large variety of matrices using different nuclear reactions, the establishment of the corresponding activation curve for each analytical case becomes a tedious task.

In the present study, a solution to this problem is presented by showing that a complete, well-defined activation curve, determined experimentally in any matrix, can be transformed into the corresponding activation curve of any other matrix by using a differential range–energy relationship. The energy calculation is carried out using a computer program written for this purpose. An obvious advantage of this method is that inasmuch as an activation curve for a given reaction need only be established once, more efforts can be devoted to the curve to ensure its quality.

Other analytical applications can be derived from this technique, such as the ability to determine the quantitative importance of interfering reactions. Also, more accurate "equivalent thickness" values, which are calculated from the activation curves, can be obtained for quantitative determinations. Equivalent thickness values used for analysis were obtained using a subroutine calculation on the range–energy transformation program. These features will be illustrated by experimental data on various charged particle reactions. Finally, the described method and data have been applied to a case study on the determination of oxygen in silicon.

EXPERIMENTAL

Polyethylene, Mylar, mica, and aluminum foils, in stacks thick enough to absorb the entire beam, were irradiated using the external beam of the 88-inch variable energy sector focused cyclotron at Texas A&M University. The thickness of the Mylar, aluminum, and polyethylene foils were 13.1, 25.9, and 78.0 microns, respectively. The thicknesses of the mica foils were determined individually by weighing on a microanalytical balance with an assumption of a uniform surface (average thickness for a mica foil was ~10 microns).

Because all product radioisotopes of interest decayed by positron emission, the annihilation photons were counted with a gamma–gamma coincidence counting system coupled to an automatic sample charger. This method of counting was used to eliminate interference from noncoincidence photons as well as to reduce background levels to as low as 0.2 cpm.

The foils of a given stack were counted in a repetitive sequence until a minimum of five counts per half-life component present was obtained for each foil. The counting data, coupled with the proper timing and sample sequence, were resolved into half-life components and decay-corrected to the time at the end of irradiation (t_0) using the least squares computer routine (CLSQ) developed by Cumming (*9*) and modified by Yule (*10*) with an input for sample sorting and midpoint time calculation.

To obtain an activation curve, the specific activity at t_0 for each foil was divided by that of the foil at the initial energy minus 0.5 MeV, yielding the activity ratio ρ. The foils of the initial 0.5 MeV were discarded because of uncompensated recoil effects. Thus, the activation curve obtained was the relative cross section as a function of particle energy or matrix thickness.

Because a charged particle's range in matter is dependent on the matrix composition, an activation curve is not directly valid for matrices other than that in which it was determined. To overcome this, a computer program has been written which calculates the range and corresponding energy of a given particle in a given matrix and transforms it to a range and penetration thickness in any other desired matrix, simple or compound.

The program uses as input data the range–energy values of pure elements tabulated by Williamson *et al.* (*11*). A differential range–energy table is constructed for the compound matrices by summing the weighted fractions of elemental ranges where the weighting functions correspond to the weight per cent of the pure element in the compound matrix. Because the range of charged particles is the integral of the reciprocal stopping power, this procedure is only valid if differential range tables are used. Accordingly, 1-MeV increments of energy were used with linear interpolation within energy intervals. This has proved satisfactory above 1-MeV particle energy when compared to experimental results. Smaller energy intervals may easily be used if needed for low energy work. The limitation mentioned above can be considered as negligible because almost all analytically-useful charged particle reactions have a negligibly-small cross section below 1 MeV when the incident particle energy is 10 MeV or above.

Considering the range transformation from a matrix "A" to a matrix "B," the program calculates the two differential ranges, corresponding energies, and midpoint penetrations of each step for both matrices where the step function is the thickness of individual foils in matrix "A." This type of procedure lends itself well to computer calculation when large numbers of foils are used in the determination of activation curves, because each foil must be range-corrected to be applied to other matrices. In addition to this, equivalent thickness calculations are then carried out simultaneously by numerical integration of the ρ values for the desired irradiation energy.

For the determination of oxygen and carbon, activation curves were determined independently using mica and Mylar for oxygen and Mylar and polyethylene for carbon. The individual curves were transformed to a common matrix and combined to give a single activation curve which was then used in conjunction with the equivalent thickness method for analytical calculations.

As an application, oxygen analyses on high-purity silicon were carried out. The silicon samples were positioned in a water-cooled sample holder with six mica foils (each approximately 10 microns thick) placed in front as beam monitors. The samples were irradiated with a collimated 1-cm^2 beam of the appropriate particle energy at beam currents from 2 to 12 μA for 30 minutes. After irradiation, the samples were etched by a procedure previously described (*12*) to remove surface oxygen contamination, and then decay-counted for a minimum of three half-lives. After discarding the first and last foils because of recoil considerations, the mica monitor foils were counted on the same system after an adequate decay period to eliminate dead time losses. The activity of the isotope used for analysis was separated from the gross decay activity and decay-corrected to the time at the end of irradiation by the CLSQ half-life resolution computer routine. From the activity of the mica monitor foils and the sample, the oxygen concentration was calculated by the equivalent thickness method.

RESULTS AND DISCUSSION

Different methods of quantization have been devised for charged particle activation analysis. The "equivalent thickness" method was used in this work and the discussions here

(9) J. B. Cumming, BNL-6470; NAS-NS 3107, ed. by G. D. O'Kelley, *Proc. Symp.*, Gatlinburg, Tenn. (Oct. 1962).
(10) H. P. Yule, *Nucl. Phys.*, **A94**, 442 (1967).
(11) C. F. Williamson, J. P. Boujot, and J. Picard, Commissariat a l'Energie Atomique Report, CEA-R 3042, Saclay, France, (July 1966).
(12) H. L. Rook, E. A. Schweikert, and R. E. Wainerdi, ANAL. CHEM., **40**, 1194 (1968).

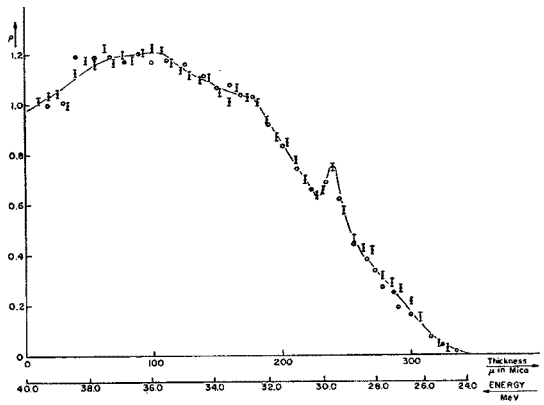

Figure 1. Activation curve for $^{16}O(\alpha,pn)^{18}F$ comparison of mica and Mylar

⊙ Experimentally determined with mica foils
Φ Experimentally determined with Mylar foils

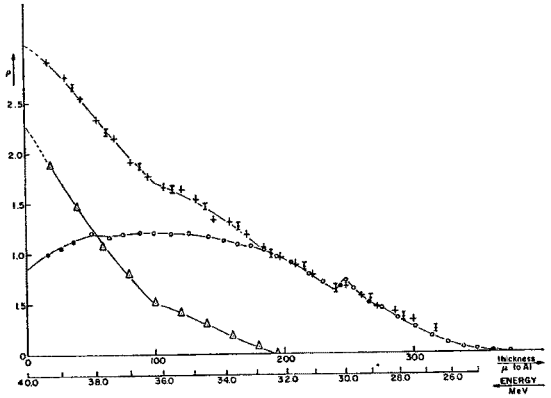

Figure 2. Fluorine-18 production from aluminum via $^{16}O(\alpha,pn)^{18}F$ plus $^{27}Al(\alpha,x)^{18}F$ compared to that due to $^{16}O(\alpha,pn)^{18}F$ in mica

\+ ^{18}F from 12.7-μ-thick Al foils
Φ ^{18}F from 25.4-μ-thick Al foils
⊙ $^{16}O(\alpha,pn)^{18}F$ curve from mica
△ $^{27}Al(\alpha,x)^{18}F$

will be mainly limited to our results as they relate to the equivalent thickness method although they can find application in other methods of quantization.

Initial experiments were conducted to determine activation curves for the $^{16}O(\alpha, pn)^{18}F$ reaction using matrices of different chemical composition. The experimental curves were transformed to a common thickness and energy base to validate the computer calculation of compound range–energy transformations.

Mylar and mica were chosen as experimental matrices because of their wide difference in chemical character while both contained oxygen as a major constituent, thereby minimizing the relative effect of any possible interfering reactions. The difference in the chemical character of the matrix was an important consideration because the assumption was made in the range–energy calculation that a compound range function could be constructed from a weighted sum of elemental range functions when differential ranges were used. Mylar and mica foils were irradiated with 40-MeV alpha particles to obtain the experimental activation curves for the $^{16}O(\alpha, pn)^{18}F$ reaction. The individual data points from the Mylar curve were then transformed to a corresponding particle penetration in mica for comparison (Figure 1). As can be seen from the threshold energy and the magnitude of ρ, the transformed Mylar curve agreed with that of mica within the limits of experimental errors.

The use of computer-calculated range transformation of activation curves has several advantages over present experimental methods. Using this technique, an activation curve for a given reaction need only be determined once in a convenient matrix for use in any other matrix of analytical interest. The present technique allows more effort to be devoted to obtain a single detailed curve. Also, curves can be constructed by the superposition of two curves determined independently in dissimilar matrices, giving a greater assurance of accuracy.

Three improvements are obtained in quantization when using the well defined curves. First, with the greater detail of the activation curve, there is a greater reliability in the ρ value used for the monitor foil. Second, with the larger number of points in the action curve, the numerical integration of the curve is obtained with greatly improved statistics, thus reducing the overall error. Third, because it is virtually impossible to get absolutely pure foils of a given element, interfering reactions can be elucidated by the superposition of curves obtained from matrices containing minor and major amounts of the element thought to give an interfering reaction.

This method of quantitatively determining an interfering reaction can be well illustrated in the case of the $^{16}O(\alpha, pn)^{18}F$ reaction when used for the determination of oxygen in aluminum. Previously, Albert *et al.* (*8*) have reported that when alpha particles above 35 MeV were used in aluminum, an erroneously-high apparent oxygen content was always found. These authors have indicated that this was caused by a reaction on the aluminum matrix which also gives fluorine-18.

To determine quantitatively the importance of this interfering reaction, a study was made on two sets of aluminum foils; one 12.7 and the other 25.4 microns thick. The purity of the 25-micron aluminum foils was 99.995% with oxygen being the major impurity. These foils were irradiated with 40-MeV α particles, decay-counted and the activity due to fluorine-18 in each foil was determined by half-life resolution using the CLSQ decay curve analysis program. The fluorine-18 activity was normalized to that obtained from mica foils below 30 MeV and the resultant activation curves were superimposed with that obtained in mica by range transformation (Figure 2). As can be seen, the curves coincide below 32.8 MeV, indicating that all of the fluorine-18 produced in the aluminum below this energy is caused by a reaction with oxygen. Above 33 MeV a marked divergence from the $^{16}O(\alpha, pn)^{18}F$ curve can be noted. Because of the purity of the 25-micron aluminum foils and the agreement between the two sets of foils, it can reasonably be concluded that the increased fluorine-18 activity above 33 MeV is caused by a reaction of the type $^{27}Al(\alpha, x)^{18}F$ on the aluminum matrix. Fragmentation reactions of a similar type on aluminum producing beryllium-7 and sodium-24 have been reported by Lindsay and others at similar energies (*13*). The exact reaction producing the fluorine-18 is difficult to ascertain and is outside the scope of this paper, the importance being that this reaction does

(13) R. H. Lindsay and R. J. Carr, *Phys. Rev.*, **120**, 2168 (1960).

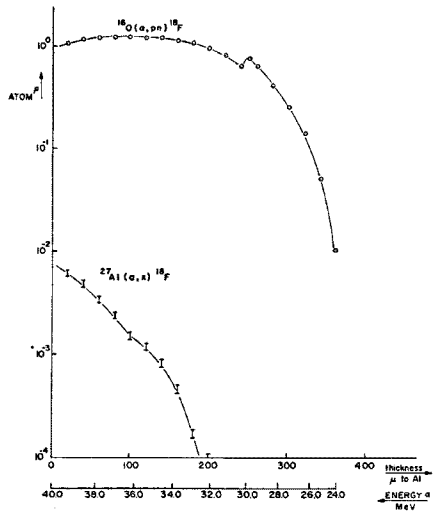

Figure 3. Aluminum interference on the $^{16}O(\alpha,pn)^{18}F$ reaction corrected for atom ratio of oxygen to aluminum

occur in aluminum, giving significant interference in the determination of oxygen in aluminum using α particles above 32.8 MeV.

The $^{27}Al(\alpha, x)^{18}F$ activation curve was obtained by subtraction of the aluminum matrix curve from the mica matrix curve. The activation curve was weighed for the atom per cent to give a relative magnitude of the $^{27}Al(\alpha, x)^{18}F$ reaction compared to the $^{16}O(\alpha, pn)^{18}F$ reaction (Figure 3).

This type of interference has been noted in silicon with alpha particles above 34 MeV and with helium-3 particles above 11.8 MeV (*6, 14*). It is thus reasonable to assume that such fragmentation reactions, although small in terms of absolute cross section, may cause significant errors when analyzing matrices of the light elements unless incident particle energies are held below the threshold of such fragmentation reactions.

The usual type of interference due to isotopes belonging to neighboring elements and yielding the same radioisotope must also be considered. Quantitative interferences of such reactions have been previously studied, as for example, $^{19}F(\alpha, \alpha n)^{18}F$ with respect to $^{16}O(\alpha, pn)^{18}F$ (*15*). In the course of this work, the reaction pair $^{13}C(p, n)^{13}N$ and $^{16}O(p, \alpha)^{13}N$ was studied to determine the usefulness of the latter reaction. The $^{12}C(p, \gamma)^{13}N$ reaction may also add to the interference at low energy, but its contribution may be neglected because high proton energies were used in this work.

Stacks of mica and Mylar foils were irradiated with 20-MeV protons. The mica stack, with carbon only present at the trace impurity level, gave an activation curve where the $^{16}O(p, \alpha)^{13}N$ reaction could be considered to be the exclusive means of nitrogen-13 production. The activation curve obtained from Mylar was determined as a confirmation of the mica results on oxygen, as well as an attempt to see if sig-

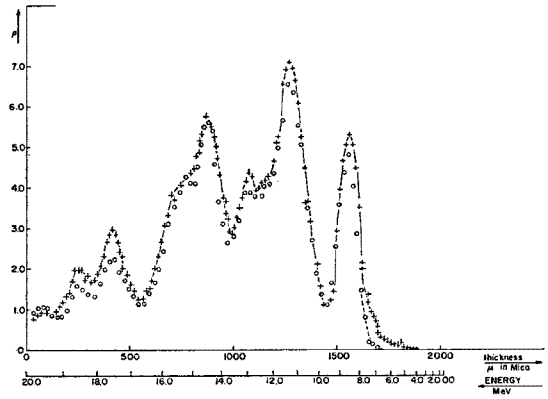

Figure 4. Activation curve for the $^{16}O(p,\alpha)^{13}N$ reaction using mica and Mylar foils activated with 20-MeV protons

+ Mylar foils
⊙ Mica foils

nificant interference would occur from the $^{13}C(n, p)^{18}N$ reaction. The results of these irradiations are shown in Figure 4 where the Mylar curve was range-transformed to a mica thickness for comparison. As can be seen, excellent agreement was obtained between the two curves with the only significant interference from the $^{13}C(p, n)^{13}N$ reaction occurring below the threshold of the $^{16}O(p, \alpha)^{13}N$ reaction. To establish the relative magnitude of the interference of the $^{13}C(p, n)^{13}N$ reaction, an activation curve of this reaction was determined using polyethylene foils of low oxygen content. The two activation curves shown in Figure 5 were corrected for the relative weights of naturally occurring carbon and oxygen in the respective foils. From these results, it can be seen that if carbon and oxygen are at the same impurity level, carbon will offer less than 0.5% error. Thus, provided the carbon content of the sample is known and the proton energy is below 13 MeV avoiding an interfering contribution due to the $^{14}N(p, pn)^{13}N$ reaction, the $^{16}O(p, \alpha)^{13}N$ reaction offers

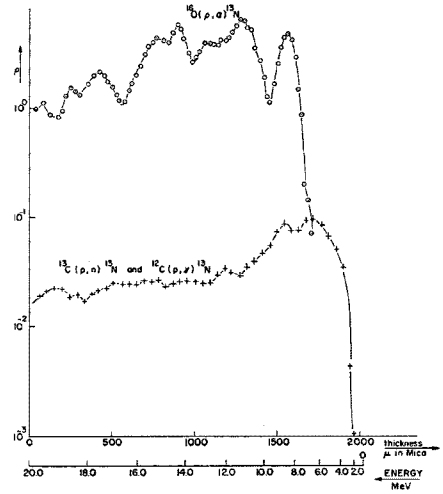

Figure 5. Relative interference of the $^{13}C(p,n)^{13}N$ reaction on the $^{16}O(p,\alpha)^{13}N$ reaction per gram of natural element

(14) T. Nozaki, Y. Yatsurgi, N. Akiyama, and I. Imai, Proc. 3rd Int. Conf. on Modern Trends in Activation Analysis, ed. by National Bureau of Standards, Gaithersburg, Md., Paper No. 8 (October 1968), in press.

(15) J. N. Barrandon, J. L. Debrun, and Ph. Albert, Proc. of 2nd Conf. on Practical Aspects of Activation Analysis with Charged Particles, Euratom Report, Eur 3896 d-f-e, (1967), 277.

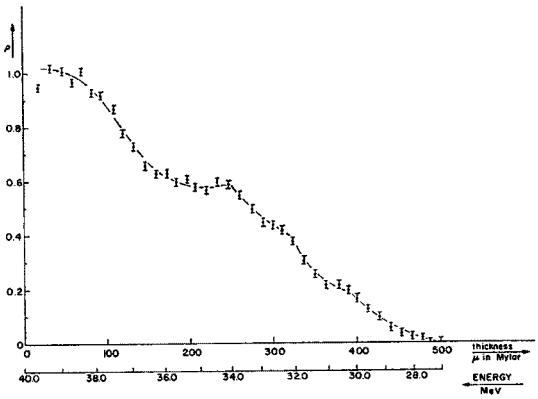

Figure 6. Activation curve for the $^{12}C(\alpha,\alpha n)^{11}C$ reaction

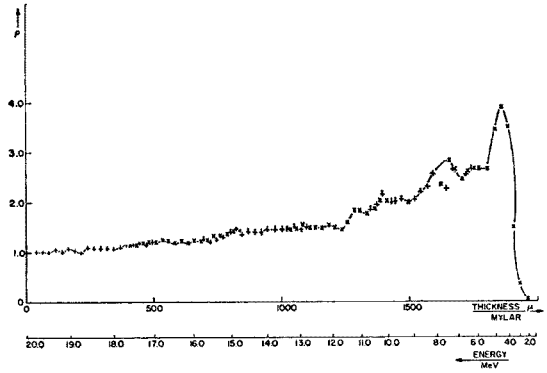

Figure 7. Activation curve for $^{12}C(d,n)^{13}N$

an interesting possibility for the determination of oxygen with similar or better inherent sensitivity than that using alpha or helium-3 particles.

Besides the above mentioned reactions, other charged particle reactions useful for the determination of oxygen are: $^{16}O(^3He, p)^{18}F$ and $^{16}O(^3He, n)^{18}Ne \xrightarrow{\beta^+} {}^{18}F$ as well as $^{18}O(p, n)^{18}F$. These reactions, as well as the possible interfering reactions $^{19}F(^3He, \alpha)^{18}F$, $^{19}F(p, pn)^{18}F$, have been previously studied and activation curves necessary for analysis have been reported (*2, 7, 16*).

For the determination of carbon, two useful reactions have been investigated. The $^{12}C(\alpha, \alpha n)^{11}C$ reaction was studied simultaneously with the $^{16}O(\alpha, pn)^{18}F$ reaction using Mylar foils with the carbon-11 activity being resolved from the fluorine-18 activity by the CLSQ computer program. The resulting activation curve is shown in Figure 6. In order to attain high sensitivity, it will be necessary to use alpha particles in the region of 40 MeV or above. However, interferences from fragmentation reactions of the type discussed with aluminum are then possible and investigations on these must be carried out.

The $^{12}C(d, n)^{13}N$ reaction was studied using stacked Mylar foils irradiated with 20-MeV deuterons. The reaction was determined in detail to allow proper placement of monitor foils in analysis and better integration of the activation curve for the calculation of the equivalent thickness. The results are shown in Figure 7; the × and + symbols are used to differentiate between overlapping stacks of Mylar foils used to determine the curve. This reaction offers approximately the same inherent sensitivity for the determination of carbon as ^{12}C $(^3He, ^4He)^{11}C$ which has been previously reported (*2, 16, 17*).

The analytical method and data described in this article were applied to the nondestructive determination of oxygen in silicon using the experimental procedure previously described.

Results were obtained on two sets of samples and are given in Tables I and II. The impurity content for all samples is given in weight ppm. The first set was analyzed using 34-MeV alpha particles with results compared to those independently obtained by Baker using infrared spectrometry (*18, 19*). The second set was analyzed using, for each sample, two of three possible charged particle reactions, $^{16}O(\alpha, pn)^{18}F$, $^{18}O(p, n)^{18}F$, or $^{16}O(^3He, p)^{18}F$, which gives a confidence level, normally associated with two independent analytical methods, to the results.

The errors associated with the analyses were estimated by differences between results in similar levels of oxygen concentration because the statistics due to counting severely underestimate the analytical error. The most probable contributors to this uncertainty are the assumption of uniform impurity distribution within the sample and the assumption of the normal isotopic ratio of oxygen-16 to oxygen-18 in zone refined material.

In the type of trace analysis reported here, high accuracy in the absolute values of concentration is of prime concern. The results given in Tables I and II are of particular interest because for each sample duplicate results have been obtained by two different methods, either infrared spectrometry and one activating charged particle or two kinds of

(16) R. L. Hahn, and E. Ricci, *Phys. Rev.*, **146**, 650 (1964).

Table I. Comparison of Oxygen Content Found in Silicon as Determined by Charged Particle Activation Analysis and Infrared Spectrometry

	Oxygen, ppm	
Sample	Using 34 MeV α particles	By infrared spectrometry[a]
622368	10.9 ± 1.1	9.4
623364	8.3 ± 0.8	7.4
623363	5.6 ± 0.6	5.7
623352	4.7 ± 0.5	4.8

[a] Results obtained by Baker (*18*) based on an absolute calibration curve by Kaiser and Keck (*19*).

Table II. Comparison of Oxygen Content Found in Silicon as Determined by Charged Particle Activation Analysis Using Different Activating Particles

	Oxygen, ppm		
Sample	Using 34 MeV ^4He	Using 12 MeV ^1H	Using 10 MeV ^3He
Pulled #1	12.0 ± 1.2	11.9 ± 1.2	...
Pulled #2	...	15.4 ± 1.5	14 ± 2
ZR #1	0.072 ± 0.020	≤0.060 ± 0.030	...

(17) D. R. F. Cochran and J. D. Knight, *Phys. Rev.*, **128**, 1281 (1962).
(18) J. A. Baker, Dow Corning Corp., Hemlock, Michigan, Personal Communication, 1969.
(19) W. Kaiser and P. H. Keck, *J. Appl. Phys.*, **28**, 882 (1957).

activating charged particles. Furthermore, as far as charged particle activation analysis is concerned, our experimental data indicate that the detection limit for oxygen in silicon using the $^{16}O(\alpha, pn)^{18}F$ reaction can be increased by a factor of 10. This would result in the possibility of nondestructive analyses with a practical detection limit of 5–10 ppb by weight.

ACKNOWLEDGMENT

Thanks are due to R. E. Wainerdi for valuable suggestions and for making available the facilities of the Activation Analysis Research Laboratory. We are especially indebted to H. P. Yule for helping in the adaptation and use of the decay curve analysis program.

RECEIVED for review January 27, 1969. Accepted March 25, 1969. One of us (HLR) acknowledges the National Aeronautics and Space Administration for a graduate research assistantship. Financial support for this work by the National Science Foundation (Grant GP-8200) and the Research Council, Texas A&M University, is gratefully acknowledged.

NOTES

Separation and X-Ray Spectrographic Determination of Microgram Quantities of Arsenic in Copper-, Iron-, and Nickel-Base Alloys

Keith E. Burke and Michael M. Yanak

The International Nickel Company, Inc., Paul D. Merica Research Laboratory Sterling Forest, Suffern, N.Y. 10901

A CHEMICAL SEPARATION is required for the determination of trace amounts of arsenic in various metallurgical systems because spectrophotometric techniques are not selective and spectrographic methods lack sensitivity below the 100 ppm level. Relatively low levels of arsenic can be determined directly by X-ray spectrometry when standards are available and providing an interference, such as lead, is not present. Campbell and Thatcher (*1*) show the theoretical limit of detection for arsenic to be 3.8 ppm for an iron matrix or 1.8 ppm in water. Our experience shows direct measurements are accurate at the 0.1% arsenic level but serious errors result when the direct determination is attempted at less than 0.01%.

Luke (*2*) discussed the determination of trace levels of various metals by X-ray spectrometry and suggests the use of a carbamate or ammonium hydroxide as precipitants for arsenic. Ammonium hydroxide has been used as the precipitant for iron(III) in the determination of 0–300 μg of arsenic (*3*) in copper (*4*). Iron(III) hydroxide together with precipitated arsenic was collected on a sintered glass disk, covered with collodion, and the intensity of the arsenic Kα radiation measured. The use of iron(III) hydroxide as a carrier could not be applicable to the determination of arsenic in iron-base systems, without a preliminary separation.

It has been shown that traces of tellurium(*5*) and selenium (*6*) can be selectively separated and subsequently determined by X-ray spectrometry. McKaveney, Baldwin, and Vassilaros (*7*) applied these methods to selenium and tellurium in steels using 300 μg of arsenic as a carrier. Similarly, elemental arsenic may be precipitated from hot 6*N* hydrochloric acid with sodium hypophosphite. An existing spectrophotometric method (*8*) for the determination of 0.01–0.5% arsenic is based on this separation with sodium hypophosphite. This method has been modified so that the separation is applicable below the 100 μg level. The final determination is by X-ray spectrometry.

EXPERIMENTAL

Apparatus. An X-ray spectrograph capable of measuring the arsenic Kα doublet, a platinum target X-ray tube, lithium fluoride crystal, 0.01 × 4-inch collimator, gas-flow proportional and scintillation counters with power at 50 kV and 50mA.

Reagents. STANDARD ARSENIC SOLUTION, 500 and 5 μg per ml. Dissolve 0.5000 gram of 99.999% arsenic (Spex Industries, Metuchen, N.J.) in 10 ml of nitric acid, and dilute to one liter with water. This solution contains 500 μg of arsenic per ml. Also prepare the 5 μg per ml solution.

STANDARD TELLURIUM SOLUTION, 50 μg per ml. Dissolve 0.5000 gram of high purity tellurium (Spex Industries) in 10 ml of aqua regia and dilute to 1 liter with water. Dilute 10 ml of this solution to 100 ml.

TIN(II) CHLORIDE, 1 gram per ml. Weigh 250 grams of stannous chloride, $SnCl_2 \cdot 2H_2O$, into a 400-ml beaker, add 100 ml of concentrated hydrochloric acid, and place on a warm hot plate until the solution becomes clear. Stir occasionally. Transfer the solution to a 250-ml bottle and dilute to 250 ml with concentrated hydrochloric acid.

COPPER, 4 grams per 100 ml. Dissolve 4 grams of high purity copper in nitric acid and fume with 20 ml of perchloric acid, dilute to 100 ml with water.

(1) W. J. Campbell and J. W. Thatcher, "Fluorescent X-Ray Spectrography Determination of Trace Elements", U. S. Dept. of the Interior, Bureau of Mines TN23.U7 (1962).
(2) C. L. Luke, *Anal. Chim. Acta*, **41**, 237 (1968).
(3) V. I. Plotnikov and L. P. Msatova, *Zh. Anal. Khim.*, **19**,1183 (1964).
(4) S. Hirano and Y. Ujihira, *Bunseki Kagaku*, **12**, 747 (1963); *Chem. Abstr.*, **59**, 12166b (1963).
(5) K. E. Burke, M. M. Yanak, and C. H. Albright, ANAL. CHEM., **39**, 14 (1967).
(6) C. H. Albright, K. E. Burke, and M. M. Yanak, *Talanta*, **16**, 309 (1969).
(7) J. P. McKaveney, H. E. Baldwin, and G. L. Vassilaros, *J. Metals*, **1968**, 54.
(8) O. P. Case, ANAL. CHEM., **20**, 902 (1948).

Use reagent grade chemicals and Class A volumetric glassware for the preparation of all solutions.

Procedure. CALIBRATION CURVE. Place aliquots containing 0, 5, 10, 20, 50, and 100 μg of arsenic into 100-ml beakers, add 2 ml of copper solution, 2 grams of sodium hypophosphite, and make the hydrochloric acid concentration 6 *N*. Heat the solution to near boiling, add 100 μg of tellurium and 5 ml of tin(II) chloride solution. Boil the solutions for 5 minutes. Filter the precipitates on 0.22-μ filters, (apparatus XX-1002500, Millipore Filter Corporation; Bedford, Mass.), wash, dry, and mount. Measure the intensity of the arsenic radiation and plot counts per second versus micrograms of arsenic. Copper is added to all systems analyzed for arsenic because it is present with any arsenic or arsenic–tellurium precipitated in the presence of copper, A calibration curve prepared in the absence of copper will produce high results for the analysis of a copper-base alloy.

DISSOLUTION. Select a sample weight so that 5 to 100 μg of arsenic will be present. Accurately weigh the sample into a 150-ml beaker and add 2 ml of copper solution. Dissolve the sample with nitric acid, add hydrochloric acid if necessary, after dissolution add 5 ml of perchloric acid (10 ml for a 2-g sample) and fume. Cool and add 30 ml of water and 20 ml of hydrochloric acid.

PREFILTRATION. Add 10 ml of tin(II) solution and filter off any selenium or tellurium along with any residue such as silicon, graphite, etc. Use an 8-μ micropore filter for the separation. Rinse the precipitate with 6*N* hydrochloric acid. The addition of tin(II) may be eliminated if less than 20 μg of selenium and tellurium are present in the sample.

ARSENIC PRECIPITATION. Add 2 grams of sodium hypophosphite, $NaH_2PO_2 \cdot H_2O$, heat to near the boiling point, add 100 μg of tellurium and 10 ml of tin(II) solution. Boil the sample for about 5 minutes so that the precipitate coagulates. Filter the solution through an 0.22-μ micropore filter. Wash with 6*N* hydrochloric acid, water, and finally a 50% ethyl alcohol solution to wash off any precipitate which might cling to the funnel. Dry, mount, and measure the intensity of the arsenic Kα radiation using an X-ray spectrometer. Calculate the arsenic content after using the calibration curve.

Table I. Recovery of Arsenic Precipitated from 6*N* Hydrochloric Acid with Sodium Hypophosphite by X-Ray Spectrometry

[As], μg		
	Found	
Added	No carrier	100 μg Tellurium
0	0	0
5	<5	6
11	<5	10
22	<5	22
54	<5	50
80	<5	84
216	215	...

Table II. Effect of Selenium or Tellurium on the Recovery of Arsenic

		[As], μg	
Element	Added, μg	Added	Found
Te	100	50	51
	110	50	54
	120	50	53
	150	50	57
	200	50	66
	500	50	69
Se	0	50	51
	10	50	49
	20	50	47
	50	50	56
	100	50	65

Table III. Verification of Arsenic Recovery

	Arsenic, μg		
Added	10	50	100
Found on micropore filter	10 ± 0.5	50 ± 1	100 ± 2
Found in filtrate	<1	<1	<1

Table IV. Precision of the Chemical Separation–X-Ray Method

A. Reproducibility of the X-ray Measurement (sigma based on 60 measurements).

Arsenic, μg		
Present	Found ± σ	% σ
10	10.2 ± 0.1	2
50	50.5 ± 0.4	1

B. Reproducibility of the Method (sigma values based on 20 measurements).

Matrix	Arsenic found, ppm ± σ
Nickel	12 ± 2
Nickel	47 ± 3
Nickel	103 ± 7
Iron	15 ± 5
Copper	21 ± 6
Copper	54 ± 3
Copper	113 ± 7

RESULTS AND DISCUSSION

The proposed technique is based on the separation described by Case (*8*). He separated elemental arsenic after digesting the sample with sodium hypophosphite at 80–90 °C in 50% hydrochloric acid. After separation of the arsenic it was dissolved and determined spectrophotometrically. The method was designed for arsenic levels greater than 0.02%—*i.e.*, 200 μg for a gram sample. Details have also been worked out for the precipitation of arsenic with sodium hypophosphite and its subsequent titration with iodine (*9*). The latter has a reproducibility of ±0.003% arsenic for a 5-gram sample—*i.e.*, ±150 μg of arsenic. Evans (*10*) has noted a 150-μg limit of detection for arsenic. Similarly another titrimetric method is applicable when the arsenic level is greater than 0.005% (*11*). They used a 30-minute digestion in concentrated hydrochloric acid at 45 °C to perform the separation of arsenic with tin(II). Luke (*12*) also indicated the separation of arsenic with hypophosphorus acid gave low results.

Substituting an 0.22-μ micropore filter for the fritted glass disk, used by Case, we found low recovery of arsenic when the arsenic level was less than 200 μg (see Table I). Good recovery of arsenic was obtained when 100 μg of tellurium was added as a carrier. Tellurium probably does not act simply as a carrier of arsenic but as a nucleating agent in the precipitation process. When the precipitation was carried out in the

(9) B.I.S.R.A., *J. Iron Steel Institute*, **1958**, 331.
(10) B. S. Evans, *Analyst (London)*, **54**, 523 (1929); *Chem. Abstr.* **23**, 5432 (1929).
(11) S. Maekawa and K. Kato, *Japan Analyst*, **16**, 354 (1967); *Anal. Abstr.* **15**, 6665 (1968).
(12) C. L. Luke, ANAL. CHEM., **15**, 626 (1943).

Table V. Determination of Arsenic in Various Standards

Sample No.	Matrix	Arsenic, % Certified	Arsenic, % Found ± σ
NBS 101f	Steel	(0.003)	0.0025 ± 0.0005
BCS 321	Mild steel	0.003	0.0026 ± 0.0005
NBS C1102	Cartridge brass C	0.004	0.0050 ± 0.0003
BCS 180/1	Copper-nickel	0.006	0.006
NBS 55e	Ingot iron	0.007	0.007
NBS 1118	Aluminum brass A	0.007	0.007
NBS C1101	Cartridge brass B	0.009	0.0090 ± 0.0007
BCS 322	Mild steel	0.012	0.0125 ± 0.0005
NBS 7g	Cast iron	0.014	0.015
NBS C1100	Cartridge brass A	0.019	0.017
BCS 179	Manganese brass "B"	0.03	0.028
BCS 320	Mild steel	0.031	0.033
NBS 50a	Steel, Ni8, Cr4, V 1	0.042	0.047
NBS 1119	Aluminum brass B	0.044	0.043
BCS 323	Mild steel	0.058	0.060 ± 0.001
NBS 1120	Aluminum brass C	0.090	0.090
BCS 183/1	Bronze	0.14	0.14

absence of tellurium, at the 5- to 50-μg arsenic levels, no evidence of arsenic was found on a filter having a very fine pore size, 0.05 μ. This indicates that precipitation probably was not induced in the absence of a nucleating agent.

Either tellurium or selenium could have been selected as carriers for arsenic because they are easily reduced to their elemental states by tin(II) and readily separated by filtration through a micropore filter (*5*, *6*). Neither element is an ideal spectrographic choice because selenium enhances the arsenic radiation while tellurium has a third order line near the arsenic Kα analytical wavelength.

Sodium hypophosphite is a powerful but slow reducing agent. It will reduce tellurium, selenium, gold, mercury, and silver as well as arsenic to their elemental states. Tin(II) chloride is used for the preliminary separation of tellurium and selenium; of course gold, mercury, and silver would also be separated from the 6*N* hydrochloric acid solution. Arsenic may be precipitated by tin(II) but only from a hot solution of concentrated hydrochloric acid. Sodium hypophosphite will also reduce nitric acid, therefore it is necessary to remove this acid by fuming with perchloric acid. Perchloric acid concentrations greater than 0.5*N* interfere when tin(II) is used as the reductant but no such effect was observed with the sodium hypophosphite reductant. Iron(III), chromium (VI), and manganese (VII) are reduced to their bivalent states by sodium hypophosphite as well as by tin(II). Thus tin(II) acts in the preliminary separation to prevent selenium and tellurium contamination of the arsenic. It also reduces ions which would consume the reductant and precipitates the tellurium carrier so it may serve as a nucleus to initiate the arsenic precipitation.

Of the elements which are precipitated by the reductants used for the determination, only selenium and tellurium are likely to be present. Table II gives the data which show the effect of various levels of selenium and tellurium on the recovery of arsenic. A preliminary separation of selenium and tellurium is included in the procedure. However for a 1-gram sample which is known to contain less than 0.002% selenium and tellurium the preliminary separation can be eliminated.

In order to verify the recovery of lower levels of arsenic several samples were prepared and analyzed for arsenic, by X-ray spectrometry and then by a second method. First attempts to determine the arsenic by the molybdenum blue procedure (*8*) failed, apparently because of the presence of tellurium. Data in Table III were obtained with the proposed method. The filtrate which remains after the removal of the arsenic–tellurium precipitate was treated with 100 μg of tellurium and the separation procedure repeated. Less than one microgram of arsenic was found in the solution so the separation procedure is greater than 99% complete.

Only a few standards for arsenic are available below the 0.01% level. In order to evaluate the precision of the method in the range between 10 and 100 ppm, chemically prepared standards were used. First the reproducibility of the X-ray counting was measured. Part A of Table IV shows the standard deviation for two different samples. The excellent precision, illustrates that if any inhomogeneous distribution of arsenic occurs, it does not produce a serious error because the counting method includes the entire surface. After each 15 measurements the disk was rotated a quarter of a turn. Part B of Table IV shows the precision of the complete chemical separation and the subsequent X-ray measurement as a function of 3 matrices. The coefficient of variation at the 100 ppm level is 6%.

The data in Table V give an indication of the method's accuracy with standards at higher arsenic levels. Small sample weights were taken so that the arsenic level in the sample would correspond to the calibration curve. The standard BCS 180/1 contains 0.006% selenium, the preliminary separation was performed without any loss of arsenic due to separation with tin(II). The presence of 500 μg of selenium but not tellurium will produce low results due to coprecipitation.

ACKNOWLEDGMENT

The authors wish to thank Ute Moehring and Emil Stumpp for obtaining many of the analytical data.

RECEIVED for review February 5, 1969. Accepted March 14, 1969. Paper presented at Twentieth Pittsburgh Conference on Analytical Chemistry and Applied Spectroscopy, Cleveland, Ohio, March 3, 1969.

An Improved Flux-Fusion Technique for X-Ray Emission Analysis

D. A. Stephenson

Research and Development Laboratories, Corning Glass Works, Corning, N. Y. 14830

THE FLUX-FUSION technique used in the preparation of X-ray emission analysis samples was introduced by Claisse (*1*) more than a decade ago and has proved to be extremely useful in eliminating particle size effects on X-ray intensity measurements and in reducing interelement effects. Variations upon the technique have been reported by Townsend (*2*), Rose, Adler, and Flanagan (*3*), Rinaldi and Aguzzi (*4*), Andermann (*5*), Larson, Winkler, and Guffy (*6*), Luke (*7*), Tingle and Matocha (*8*), and Strasheim and Brandt (*9*). The principal disadvantages of some of the reported flux fusion techniques are: the resulting glass is highly stressed and must either be annealed to remove stresses, or crushed and briquetted; each sample must be treated on an individual rather than a mass production basis; the use of ordinary graphite crucibles frequently leads to reduction of some elements to the metallic state. The procedures described here overcome these difficulties.

EXPERIMENTAL

Development of Flux Compositions. Just as there is no "universal acid," there is no one flux composition suitable for all sample materials. The aforementioned authors have developed many fluxes adequate for the particular sample compositions encountered in their studies. In the present investigation, prime consideration was given to simple fluxes containing no elements ordinarily determined by X-ray emission analysis, yet capable of dissolving a sufficient amount of nonmetallic samples to provide good yields of characteristic X-rays of the lighter elements ($Z = 11$ to 17) at the 1 wt % concentration level.

Three lithium-borate-base fluxes have been developed which will dissolve a wide variety of sample materials and yield mechanically stable glass disks. Table I summarizes the composition of the fluxes, crucibles used to contain the melt, and typical sample materials suited to the particular flux. The flux components may be homogenized in large quantities in a roller mill for subsequent use. The fluxes should not be premelted, because the decomposition of lithium carbonate upon heating greatly aids in mixing the melt and sample during the fusion process. In fact, it is rarely necessary to swirl or stir the melt to achieve excellent homogeneity, even for fusion times as short as 5 minutes. Highly refractory samples such as ZrO_2 and HfO_2 may, however, require that the melt be swirled, particularly if the particle size of the sample is large.

Flux A is used whenever the sample contains no reducible components or when reducible components are present in small concentrations and are unaffected by fusion in graphite. Flux B is employed when reduction problems are encountered.

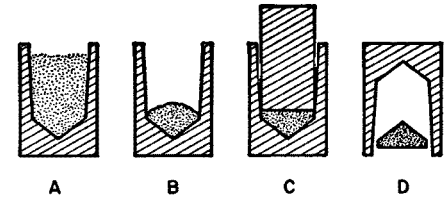

Figure 1. Step in the flux-fusion process

(*a*) **Sample and flux at beginning of fusion**
(*b*) **Melted after 5 minutes at 1100 °C**
(*c*) **Carbon flattening rod introduced and heating continued for 5 minutes**
(*d*) **After cooling and removal of the flattening rod, the glass disk is freed from the crucible**

Besides being an excellent high-temperature oxidizing agent, the ceric oxide component is a strong X-ray absorber as favored by Rose *et al.* (*3*). Flux C works well for samples consisting mainly of alkaline-earth oxides that tend to produce glasses that crack easily. The SiO_2, Al_2O_3, or GeO_2 component may be selected to avoid interferences in analysis of the sample. For particularly difficult sample compositions, the basic fluxes can usually be tailored by the addition of minor components. The review article by Hutchins and Harrington (*10*) describes the role of many common oxides in glass-forming systems and can be used as an elementary guide to tailoring flux compositions.

Carbon crucibles have been used throughout, because they are seldom wet by the melt and can be used repeatedly without fear of contamination. Platinum–gold alloy crucibles and palau crucibles, although not ordinarily wet by flux-fusion

(1) F. Claisse, *Norelco Reptr.*, **4**, 3 (1957).
(2) J. E. Townsend, *Appl. Spectrosc.*, **17**, 37 (1963).
(3) H. J. Rose, Jr., I. Adler, and J. F. Flanagan, *ibid.*, **17**, 81 (1963).
(4) F. F. Rinaldi and P. E. Aguzzi, *Spectrochim. Acta*, **23B**, 14 (1967).
(5) G. Andermann, ANAL. CHEM., **33**, 1689 (1961).
(6) J. O. Larson, R. A. Winkler, and J. C. Guffy, "Advances in X-Ray Analysis," Vol. **10**, Plenum Press, New York, N. Y., 1967.
(7) C. L. Luke, ANAL. CHEM., **35**, 56 (1963).
(8) W. H. Tingle and C. K. Matocha, *ibid.*, **30**, 494 (1958).
(9) A. Strasheim and M. P. Brandt, *Spectrochim. Acta*, **23B**, 183 (1967).
(10) J. R. Hutchins and R. V. Harrington, *Encyc. Chem. Tech.*, Vol. **10**, 2 ed., 533 (1966), John Wiley & Sons, N. Y.

Table I. Fluxes for Fusion of Materials for X-Ray Emission Analysis

Flux	Crucible	Typical samples
Flux A 90 wt % $Li_2B_4O_7$ 10 wt % Li_2CO_3	Graphite	Silicate glasses, silica- or alumina-bearing refractories, geological samples, cements.
	Vitreous carbon	Samples containing components that wet graphite such as oxides of Pb, Bi, Sb, As, Ni, Cu, and others.
Flux B 90 wt % $Li_2B_4O_7$ 8 wt % Li_2Co_4 2 wt % CeO_2	Graphite	Samples containing components that are reduced in graphite crucibles using Flux A.
	Vitreous carbon	Oxides of Pb, Bi, Sb, As, Ni, Cu, Zn, and others that are still reduced in graphite crucibles.
Flux C 90 wt % $Li_2B_4O_7$ 8 wt % Li, Co_3 2 wt % SiO_2, Al_2O_3, or GeO_2	Graphite	Oxides or carbonates of the alkaline earths, samples containing no glass-forming components.

melts, are susceptible to attack by metals such as lead and arsenic that can drastically reduce the life of the crucible. Either graphite crucibles (#A2260 Fusion Crucible, Ultra Carbon Corp., Bay City, Mich.) or vitreous carbon crucibles (#170 Crucible, Beckwith Carbon Corp., 16140 Raymer St., Van Nuys, Calif.) are well suited for this flux-fusion technique. Vitreous carbon crucibles are employed when reduction of sample components is a problem or when melts tend to wet graphite crucibles. Although vitreous carbon crucibles are rather expensive, 20 to 25 melts can be made in one crucible before it is destroyed by oxidation.

Mixtures consisting of 90 wt % flux and 10 wt % sample give good characteristic X-ray yields for the lighter elements. The flux/sample ratio can be changed within reasonable limits to suit particular needs. All samples should be ground to pass at least −100 mesh.

Preparation of Flux-Fusion Glasses. After mixing the flux and sample, the mixture is transferred to the proper crucible and fused according to the schedule depicted in Figure 1. An initial 5-minute fusion at 1100 °C will completely dissolve all but the most refractory samples, in which case the initial fusion time may be increased or the melt swirled in the crucible to promote solution of the sample. A medium-sized muffle furnace is satisfactory for either single or multiple fusions. After the initial fusion, a short carbon rod is placed on top of the melt to flatten the surface and an additional 5-minute heating period is begun (no carbon rod is used with vitreous carbon crucibles.) The crucible, melt, and flattening rod are then removed from the furnace intact and are cooled for 10 or 15 minutes to room temperature. The glass disks can be removed easily by lifting off the flattening rod and tapping the inverted crucible against a flat surface. Machining about a 2° taper on graphite crucibles which originally have vertical walls greatly facilitates removal of the disks. Identification marks may be scribed on the bottom of the disks with a hand-held grinder or similar tool without fear of breakage.

Although the carbon flattening rod produces a fairly good sample surface, it is normally not adequate for accurate quantitative analysis. The quality of the surface finish required depends upon the longest characteristic X-ray wavelength used for analysis, longer wavelengths requiring a superior finish. The disks can be finished to 100, 200, 400, or 600 grit by wet grinding on silicon carbide paper or diamond-embedded grinding disks. The total grinding time for a 600-grit finish for one sample is around 3 minutes, depending upon the quality of the original surface.

RESULTS AND DISCUSSION

The glass disks produced by this method may be presented directly to an X-ray spectrometer for analysis. They are stable indefinitely when stored in a desiccator to prevent the polished surface from picking up water. An electron microprobe study of a variety of flux-fusion glasses prepared from highly refractory samples (ZrO_2, HfO_2), easily reducible samples (PbO, CuO, NiO), and samples containing no glass-forming components (limestone, dolomite) demonstrated no significant compositional variation across the glass disks. A similar study by Parker (*11*) reached the same conclusion, so grinding and briquetting the glass seems to be an unnecessary step. Because of the simplicity of this method and the fact that sample preparation times are much shorter than for the previously reported methods, batch processing of numerous samples is possible. Quantitative X-ray emission analysis of a variety of samples prepared by this technique showed excellent agreement with wet-chemical results.

RECEIVED for review January 21, 1969. Accepted March 21, 1969.

(11) A. Parker, *Anal. Chim. Acta.*, **40**, 513 (1968).

Potentiometric Titrations of Sulfate Using an Ion-Selective Lead Electrode

James W. Ross, Jr., and Martin S. Frant

Orion Research, Inc., 11 Blackstone Street, Cambridge, Mass. 02139

IN SPITE of the large number of sulfate determinations being performed at the present time, there is still no simple, direct titration procedure available to the analytical chemist. Direct titrations using indicators have been reported (*1*, *2*), but these suffer from numerous interferences and are difficult to automate. Sulfate has been titrated potentiometrically with barium chloride as a reagent, and using a heterogeneous membrane electrode as an indicator (*3*). The extreme sensitivity of the electrode to chloride (and probably other anions) almost totally obscures the end point break, and renders the titration almost useless except in some special circumstances. Kolthoff and Pan (*4*) studied the titration of sulfate with lead nitrate, using an amperometric end point, and found the titration to be accurate and relatively free of interferences from most common ions. The necessity for purging the sample with nitrogen, however, limits the usefulness of the method in routine applications.

We have found that the recent commercial introduction of a lead-selective electrode (*5*) allows the potentiometric determination of end points in the direct titration of sulfate with standard lead solutions.

EXPERIMENTAL

Standard lead solutions were prepared from $Pb(ClO_4)_2$ and distilled water, and were standardized against EDTA. Standard Na_2SO_4 solutions were prepared by weighing the dried reagent grade salt and dissolving in distilled water. Other chemicals and solvents used were reagent grade.

(1) N. H. Furman, Ed., "Standard Methods of Chemical Analysis," Vol. I, 6th ed., Van Nostrand, New York, 1962, p 1011.
(2) "1967 Book of ASTM Standards," A.S.T.M., Philadelphia, Pa., 1967, p 57.
(3) G. A. Rechnitz, Z. F. Lin, and S. B. Zamochnik, *Anal. Letters*, **1**, 29 (1967).
(4) I. M. Kolthoff and Y. D. Pan, *J. Amer. Chem. Soc.*, **62**, 3332 (1940).
(5) J. W. Ross, Jr., Symposium on Ion-Selective Electrodes, National Bureau of Standards, Gaithersburg, Md., Jan. 30, 1969; J. W. Ross, Jr., and M. S. Frant, Pittsburgh Symposium on Analytical Chemistry and Spectroscopy, Cleveland, Ohio, March 7, 1969.

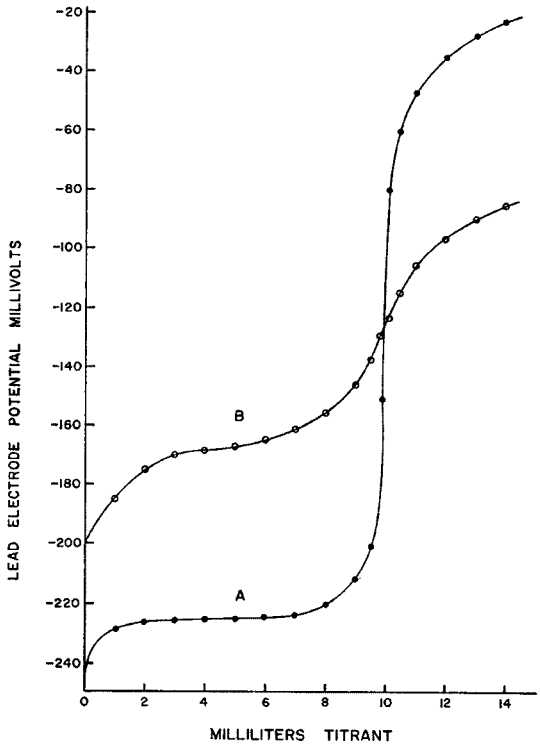

Figure 1. Sulfate titration curves in pure solutions

A. **Titration of 100 ml 10^{-3} *M* Na_2SO_4 with 10^{-2} *M* $Pb(ClO_4)_2$ 50% dioxane solution**

B. **Titration of 100 ml 5×10^{-6} *M* Na_2SO_4 with 5×10^{-4} *M* $Pb(ClO_4)_2$ 50% dioxane solution**

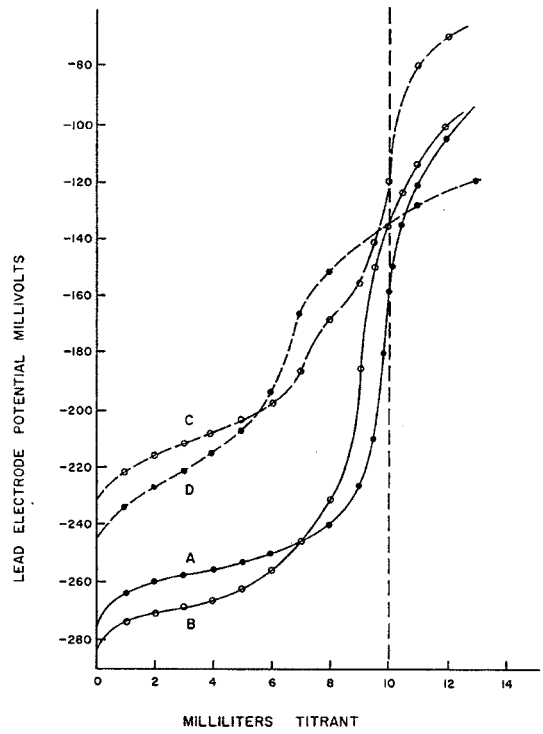

Figure 2. Effect of interferences on sulfate titration curves

All solutions 50% dioxane, and titrated with 10^{-2}*M* $Pb(ClO_4)_2$

A. **100 ml 10^{-3}*M* Na_2SO_4 + 10^{-2}*M* NaNO,**

B. **100 ml 10^{-3}*M* Na_2SO_4 + 10^{-1}*M* NaNO,**

C. **100 ml 10^{-3}*M* Na_2SO_4 + 10^{-2}*M* NaCl**

D. **100 ml 10^{-2}*M* Na_2SO_4 + 10^{-1}*M* NaCl**

Curves *A* and *B* are displaced slightly in the negative direction for clarity in reproduction

Measurements were made using an Orion Research Model 94-82 lead electrode in conjunction with an Orion double junction reference electrode, Model 90-02. The salt bridge compartment of the reference electrode was filled with 1*M* $NaNO_3$ to prevent precipitation of $KClO_4$. Potential readings were taken on an Orion Model 801 digital pH/mV meter.

RESULTS

Solvent System. The relatively high solubility of $PbSO_4$ in aqueous media ($K_{sp} = 1.6 \times 10^{-8}$) limits the magnitude of the potential change at the end point and makes it impractical to titrate dilute solutions. Kolthoff (*4*) recommended adding ethanol to the solution to be amperometrically titrated in order to decrease the solubility of the precipitate. We found that the addition of dioxane gave an even greater decrease in $PbSO_4$ solubility than similar amounts of ethanol. The optimum dioxane concentration in the solution to be titrated is about 50% by volume. Below 25% dioxane, end point breaks are considerably smaller. Above 70% dioxane, precipitation of alkali metal sulfates occurs, resulting in a sluggish establishment of equilibria as the precipitates redissolve on the addition of titrant. Typical titration curves are shown in Figure 1 for two levels of sulfate in a 50% dioxane background.

Lower Limit of Sample Concentration. The lower limit of sulfate concentration for useful titrations is determined by the solubility of $PbSO_4$. The difference in electrode potentials between the end point and the 50% titration point on the titration curves of Figure 1 allows an estimation of the solubility product of $PbSO_4$. We obtain a value of 10^{-14} in 50% dioxane. If an arbitrarily chosen value of 60 mV is considered the minimum change in potential at the end point for an analytically useful titration, equilibrium calculations indicate that the minimum titrable sulfate concentration would be about 10^{-6} *M*. In practice, we find that at very low initial sulfate levels, the formation of $PbSO_4$ is very slow, requiring 5 to 10 minutes for equilibrium to be obtained after each addition of titrant. Above 5×10^{-5}, however, equilibrium time is essentially that of the mixing of the solutions, and the titration is practical.

Interferences. The lead electrode suffers interferences from Cu^{2+}, Hg^{2+}, Ag^+, and these ions should be absent from the sample (Orion Instruction Manual for Lead Electrode, Model 94-82). Anions which form more insoluble lead salts than $PbSO_4$ should be absent. Phosphate, for example, interferes and must be removed prior to titration.

Chloride, nitrate, and bicarbonate at high concentrations interfere by forming mixed precipitates, such as $Pb_2(NO_3)_2SO_4$, and in addition, tend to decrease the end point potential break because of complex formulation with Pb^{2+}. Up to ten-fold excesses of Cl^- and NO_3^- produce no detectable error

in end point volume determination. Serious interference occurs when Cl^- and NO_3^- are present in 100-fold excess over SO_4^- (See Figure 2). The adverse effect of bicarbonate can be eliminated by adjusting the sample pH to 4. Titration curves in the absence of carbonate are independent of pH in the range pH 3.0 to pH 6.5. At low pH, the solubility of the electrode membrane increases the electrode potential, thereby decreasing the end point potential break.

Precision. In the absence of the interferences described in the preceding section, end point volumes are stoichiometric and reproducible to ±0.2% at concentrations above $5 \times 10^{-4}M$ sulfate. Precision decreases with sample dilutions, approaching ±1.0% at $10^{-5}M$ initial sulfate concentrations.

RECEIVED for review February 7, 1969. Accepted March 19, 1969.

Nuclear Magnetic Resonance Analysis of Rubber Vulcanizates

David W. Carlson and Alan G. Altenau

The Firestone Tire & Rubber Co. Central Laboratories, Akron, Ohio 44317

THE QUANTITATIVE DETERMINATION of the polymer composition of vulcanized stocks has always been a very difficult problem. Present methods consist of dissolving the vulcanizates in boiling *o*-dichlorobenzene, removal of the carbon black by filtration, and then infrared determination of the polymer (*1*). This procedure is time consuming and may suffer from selective adsorption of different elastomer types on the filtration medium. Pyrolysis of the stock followed by infrared analysis of the products has also been used (*2*). This technique had the disadvantages of requiring calibration of the infrared instrument and of having some uncertainty about changes in the microstructure of the polymer due to pyrolysis procedure. Other infrared spectrophotometric studies have been made but no quantitative measurements were reported (*3–6*).

The use of NMR rather than infrared was investigated as a means of solving this problem. Various vulcanizates containing two or three of the following, natural rubber, polybutadiene, and butadiene styrene copolymer (SBR), were analyzed.

EXPERIMENTAL

Apparatus. A Varian HA-60-IL nuclear magnetic resonance spectrometer was used to record the spectra while a Varian V3521A integrator/decoupler was used to integrate the area of the peaks. All integrals were run in internal lock field sweep mode using 30 db-rf attenuation and a setting of 0.5 on the manual oscillator.

Procedure. Samples of the vulcanized rubber were cut into small pieces and extracted with acetone overnight in a Soxhlet apparatus to remove the oil, antioxidant, and any other extractable compounds. Four milliliters of hexachlorobutadiene were then added to 0.25 gram of the extracted sample in a 15-ml beaker. The uncovered beaker and contents were placed on a hot plate having a surface temperature of about 160 °C. After one to two hours the polymer was in solution. In several cases complete dissolution of the polymer was not obtained in this time. If several more hours of heating still resulted in no change, a higher temperature was used and usually helped. It was noticed, however, that too long a heating period could precipitate the polymer from solution.

The black solution was cooled and filtered by pushing the solution through Reeve Angel 802 filter paper which was supported in a millipore Sweeney pressure filter and attached to the end of a 2-ml syringe. This filtration only removed pieces of undissolved stock and a small amount of carbon black. The filtrate and a trace of TMS were added to the NMR sample tube and the spectrum was obtained at room temperature.

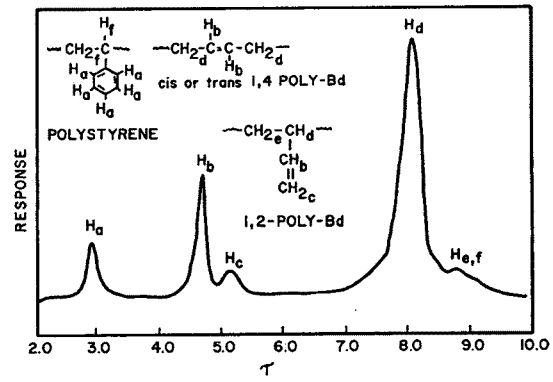

Figure 1. NMR spectrum of vulcanizate containing a mixture of polybutadiene and butadiene–styrene copolymer

RESULTS AND DISCUSSION

Equations used to calculate polymer compositions by NMR have been published by Mochel (*7*). These same equations were used in this work. The quality of the spectra was comparable to that of uncompounded polymers.

Good agreement was obtained between the calculated amounts of butadiene, natural rubber, and styrene and the found values; however, the method will not distinguish between butadiene from polybutadiene and butadiene styrene copolymer (Table I). The relative amounts of 1,2-butadiene and 1,4-butadiene were found in the cases of polybutadiene and SBR blends. The individual amounts of *cis* and *trans* 1,4-butadiene could not be calculated because of complete

(1) H. L. Dinsmore and D. C. Smith, *Rubber Chem. Technol.*, **22**, 572 (1949).
(2) D. A. MacKillop, ANAL. CHEM., **40**, 607 (1968).
(3) D. L. Harms, *ibid.*, **25**, 1140 (1953).
(4) D. Hummel, *Rubber Chem. Technol.*, **32**, 854 (1959).
(5) M. Lerner and R. C. Gilbert, ANAL. CHEM., **36**, 1382 (1964).
(6) M. Tryon, E. Horowitz, and J. J. Mandel, *J. Res. Nat. Bur. Std.*, **55**, 219 (1955).
(7) V. D. Mochel, *Rubber Chem. Technol.*, **40**, 1200 (1967).

Table I. Determination of Polymer Composition

Calculated compounded formula					Found compounded formula				
	Natural	Butadiene				Natural	Butadiene		
Styrene	Rubber	Total	1,4-	1,2-	Styrene	Rubber	Total	1,4-	1,2-
15.5			75.2	9.3	13.7			76.5	9.8
12.0			50.5	37.5	11.3			47.3	41.4
	25.0	75.0				27.1	72.9		
	40.0	60.0				42.0	58.0		
20.0	20.0	60.0			20.0	24.3	55.7		
17.0	30.0	53.0			15.5	31.0	53.5		
16.7	35.0	51.7			16.0	36.0	48.0		
15.6	40.0	44.4			16.6	41.7	41.7		
13.2	40.0	46.8			11.8	44.0	42.9		
11.0	50.0	39.0			9.7	50.0	40.3		
8.8	60.0	31.2			5.0	64.0	31.0		

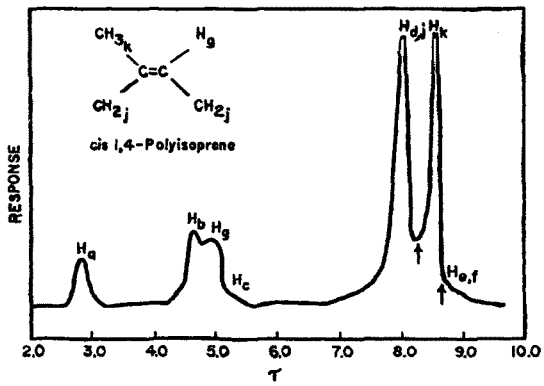

Figure 2. NMR spectrum of vulcanizate containing a mixture of natural rubber and butadiene–styrene copolymer

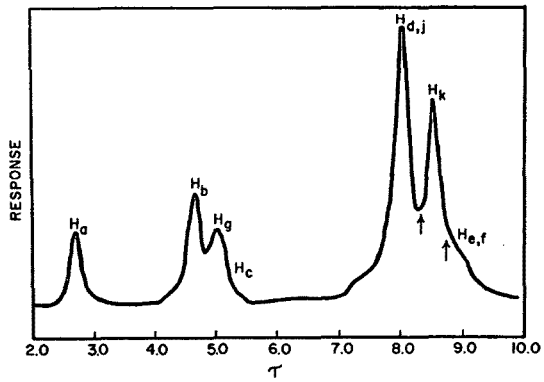

Figure 3. NMR spectrum of vulcanizate containing a mixture of natural rubber, polybutadiene, and butadiene–styrene copolymer

overlapping of the two signals as is also the case in uncompounded polymers (Figure 1).

Determination of the different microstructures in a blend of polybutadiene and/or SBR with natural rubber is very difficult because the signals from the olefinic protons severely overlap one another. No attempt was made to calculate the percentages of the different microstructures in these blends of rubber. Natural rubber is essentially 100% *cis* 1,4-polyisoprene.

The signal of the methylene hydrogens from the butadiene and natural rubber overlap the methyl group signal of natural rubber. The degree of overlap will vary with the effectiveness of sample dissolution. Therefore, the area of the methyl group signal was measured exactly from the initial rise to the end of the signal in order to reduce any contribution from the overlapping signals (as shown by the arrows in Figures 2 and 3). If the measurement was not done that way, the results were usually high.

o- and *p*-Dichlorobenzene, 1,2,4-trichlorobenzene, 1,1,2,2-tetrachloroethane, and naphthalene also dissolved the vulcanizates at temperatures around 160 °C. Tetrachloroethylene at its reflux temperature did not dissolve the polymers. The reason in the latter case was probably due to its lower reflux temperature.

The disadvantage of using an aromatic solvent is the interference of the aromatic proton signals of styrene with those of the solvent. If styrene were absent, aromatic solvents could be used.

Although we say the rubber is dissolving in hexachlorobutadiene, there is first a breakdown, possibly at the sulfur bonds which result from the vulcanization process. Some breakdown or reduction in the molecular weight of the polymer during the dissolution period probably also occurs.

The carbon black had minimal detrimental effects in the NMR spectrum as evidenced by the sharpness of the signals (Figures 1, 2, and 3) and the excellent quantitative results.

ACKNOWLEDGMENT

The authors thank The Firestone Tire & Rubber Company for permission to publish this work.

RECEIVED for review January 31, 1969. Accepted March 27, 1969.

Determination of Total Paraffins, Monochloroparaffins, and Polychloroparaffins by the Fluorescent Indicator Adsorption Method

Thomas A. Washall

ARCO Chemical Co., Research Division, Philadelphia, Pa.

THE TOTAL MONOCHLOROPARAFFIN CONTENT of products from paraffin chlorination can be determined readily by chloride analysis when di- and polychloroparaffins are absent. However, because the latter are almost always present to some extent, other techniques which differentiate monochlorinated products from polychlorinated products must be employed. For example, products from chlorination of multicarbon number range *n*-paraffins have been analyzed by gas chromatography. In this case, total *n*-paraffins, most of the individual monochloroparaffin isomers, and total polychloroparaffins were determined. However, the analysis was not simple in spite of the tremendous resolving power of this analytical tool. In many cases, there was significant overlap between higher molecular weight monochloroparaffins and lower molecular weight dichloroparaffins.

The work reported in this paper describes the results obtained from application of the Fluorescent Indicator Adsorption (FIA) Method (*1*) to the determination of total paraffins, monochloroparaffins, and polychloroparaffins in products from paraffin chlorination and in fractions from further separation of chlorination products. Previously, the FIA technique outlined in ASTM Method D1319-66-T (*1*) had been employed almost exclusively for the determination of hydrocarbon types in petroleum fractions. Essentially, this technique employs silica gel adsorption to differentiate saturates, olefins, and aromatics. It has been found recently that olefins and monochloroparaffins of about the same molecular weight have similar adsorbabilities on silica gel. Consequently, the yellow fluorescent dye employed in the FIA method to mark the boundary between the separated paraffin and olefin zones of a hydrocarbon mixture can also serve to mark the paraffin–monochloroparaffin boundary in paraffin chlorination products. In addition, it has been observed that di- and polychloroparaffins have adsorbabilities similar to aromatics on silica gel. As a result, separated di- and polychloroparaffins can be visualized by the same blue fluorescent dye normally employed to mark the aromatic zone of a separated hydrocarbon mixture.

EXPERIMENTAL

Apparatus. The apparatus employed was essentially the same as that detailed in ASTM Method D1319-66-T (*1*).

Reagents. Except for the specially prepared dyed gel enriched in the blue component, the reagents employed in the analysis of paraffin–chloroparaffin mixtures were the same as those described in ASTM Method D1319-66-T (*1*). Dyed gel enriched in blue component was prepared by fractionation of the Standard Dyed Gel employed in the FIA method. Approximately 60 grams of Davison Code 923 silica gel were packed into a 24 inch- × 3/4 inch-diameter adsorption column followed by eight grams of Standard Dyed Gel. After a preliminary elution with cyclohexane, the yellow component was separated by elution with hexene-1 and the blue component was recovered by elution with benzene. The benzene effluent was evaporated to near dryness under a stream of nitrogen at 40–50 °C. The residue was diluted with diethyl ether and the resulting mixture was slurried with four grams of Davison's Code 923 silica gel under a stream of nitrogen. After the gel became partially dry, the mixture was transferred to a round bottom flask attached to a rotary evaporator. Final traces of ether were removed under vacuum at 40–50 °C. The resulting dyed gel enriched in blue component was placed in a small bottle and stored in the refrigerator. The Standard Dyed Gel mixture was employed for all samples except those in which the ratio dichloroparaffins/monochloroparaffins was high. In the latter cases, a mixture containing 90 wt % dyed gel enriched in blue component and 10 wt % Standard Dyed Gel was employed.

Procedure. The procedure employed in the analysis of paraffin–chloroparaffin mixtures was essentially the same as that described in ASTM Method D1319-66-T (*1*). The following minor changes in procedure were made in the application of the FIA method for the analysis of paraffin–chloroparaffin mixtures: 1. The plug of dyed gel was placed at the bottom of the charger section and in the capillary connecting the charger and separator sections rather than in the center of the separator section. 2. The hypodermic syringe used to charge the sample to the silica gel column was not chilled below room temperature. 3. A 50 vol % mixture of isopropyl and isoamyl alcohols was used as the desorbent in all cases. 4. Two pounds air pressure were applied to the top of the silica gel column after introduction of the desorbent and maintained until the red, alcohol-sample boundary passed through the capillary connecting the charger and separator sections. At that time, the air pressure was increased to 5–7 lbs. and maintained at that level to the end of the determination.

Calculations on a weight per cent basis can be obtained using the densities of the three component types. Densities for normal paraffins and some chloroparaffins are available in the literature (*2*, *3*). If appropriate values for monochloroparaffins and polychloroparaffins are not available, they can be separated readily by silica gel adsorption on a larger scale and the densities of the recovered fractions can be determined experimentally. In the present investigation, density values of 0.742, 0.867, and 0.972 were determined experimentally on paraffin, monochloroparaffin, and polychloroparaffin concentrates separated from a C_{10}–C_{13} mixture having an average carbon number of about 11.2.

Scope. The procedure outlined above is applicable to the determination of total paraffins, monochloroparaffins, and polychloroparaffins in the C_6–C_{16} range.

RESULTS AND DISCUSSION

Analysis of Synthetic Mixtures Containing Paraffins, Monochloroparaffins, and Polychloroparaffins. Initially, the FIA technique outlined above was applied to a series of synthetic mixtures containing *n*-hexane, 1-chlorohexane, and

(1) ASTM Method D1319-66-T, ASTM Standards, Petroleum Products, Part 17, Jan. 1968, Philadelphia, Pa.

(2) "Selected Values of Physical and Thermodynamic Properties of Hydrocarbons and Related Compounds," API Project 44, Carnegie Press, Carnegie Institute of Technology, Pittsburgh, Pa. 1953.

(3) E. H. Huntress, "Organic Chlorine Compounds," John H., Wiley and Sons, Inc., New York, N. Y., 1948.

Table I. Analysis of Synthetic Mixtures of C_{10}–C_{13} Paraffin, Monochloroparaffin, and Polychloroparaffin by the FIA Method

	Component	Wt % component Known	Determined		Mean error
Mixture #1	P[a]	85.0	85.2, 85.6	85.4	+0.4
	MCP[b]	10.9	10.7, 10.3	10.5	−0.4
	DPCP[c]	4.1	4.1, 4.1	4.1	0
Mixture #2	P	84.3	84.2, 84.3	84.2	−0.1
	MCP	13.3	12.6, 12.9	12.8	−0.5
	DPCP	2.4	3.2, 2.8	3.0	+0.6
Mixture #3	P	84.8	84.8, 84.7	84.7	−0.1
	MCP	14.1	13.4, 13.8	13.6	−0.5
	DPCP	1.1	1.8, 1.6	1.7	+0.6
Mixture #4	P	50.2	50.6, 50.7	50.6	+0.4
	MCP	38.2	37.8, 37.3	37.6	−0.6
	DPCP	11.6	11.6, 12.0	11.8	+0.2
Mixture #5	P	9.8	9.8, 9.6	9.7	−0.1
	MCP	58.3	56.7, 57.7	57.2	−1.1
	DPCP	31.9	33.5, 32.7	33.1	+1.2
Mixture #6	MCP	27.6	28.3, 29.3	28.8	+1.2
	DPCP	72.4	71.7, 70.7	71.2	−1.2

[a] P = paraffins.
[b] MCP = monochloroparaffins.
[c] DCPC = di- and polychloroparaffins.

Table II. Analysis of Synthetic Mixtures of Mono- and Polychloroparaffins Using the Total FIA Dye and the Modified FIA Dye Mixture

	Component	Wt % component Known	Total dye		Modified dye[a]	
Mixture #1	MCP[b]	27.8	28.3, 29.3	28.8	28.6, 29.0	28.8
	DPCP[c]	72.2	71.7, 70.5	71.2	71.4, 71.0	71.2
Mixture #2	MCP	19.7	17.2, 17.0	17.1	17.7, 17.9	17.8
	DPCP	80.3	82.8, 83.0	82.9	82.3, 82.1	82.2
Mixture #3	MCP	10.6	cannot be analyzed		8.0, 8.2	8.1
	DPCP	89.4	cannot be analyzed		92.0, 91.8	91.9
Mixture #4	MCP	5.0	cannot be analyzed		4.9, 5.0	5.0
	DPCP	95.0	cannot be analyzed		95.1, 95.0	95.0

[a] 90 wt % prepared blue component dye, 10 wt % conventional FIA dyed gel.
[b] MCP = C_{10}–C_{13} monochloroparaffins.
[c] DPCP = C_{10}–C_{13} di- and polychloroparaffins.

1,6-dichlorohexane. Results from the initial evaluation indicated excellent agreement between known and determined values for all three component types. However, the ultimate objective of this investigation was to develop a technique for the analysis of products from chlorination of heavier paraffins having a 4–5 carbon atom spread. In addition, it was desirable to apply the same technique to the analysis of fractions from subsequent separation of the chlorinated products. Consequently, a series of synthetic mixtures containing various concentrations of C_{10}–C_{13} paraffins, monochloroparaffins, and di-plus polychloroparaffins were analyzed by the FIA technique. Pure paraffins, monochloroparaffins, and di-plus polychloroparaffins were separated from a C_{10}–C_{13} chlorination product by silica gel adsorption. Purity of the fractions was checked by gas chromatography and chloride analysis. Results from chloride analysis of the polychloroparaffin fraction indicated that it contained almost exclusively dichloroparaffin. The data shown in Table I indicate that there was excellent agreement between known and determined values for all three component types over wide concentration ranges. It was found subsequently that zone boundary differentiation was extremely difficult or impossible in the analysis of paraffin free mixtures containing more than about 85% dichloroparaffins. Because of the high intensity of the yellow dye fluorescence and the relatively low intensity of the blue dye fluorescence, the monochloroparaffin–dichloroparaffin zone could not be differentiated. In order to overcome this difficulty, the blue component was recovered from the dyed gel mixture by elution chromatography and re-adsorbed on Davison Grade 923, 100–200 mesh silica gel. In order to increase the intensity of the blue fluorescence, the isolated blue component was re-adsorbed from ether solution on only one half the weight of silica gel that was used in the isolation procedure. A mixture containing 90% of the blue component gel and 10% standard FIA dyed gel was prepared and compared with the standard FIA dye mixture for the analysis of samples that contained 70–95% dichloroparaffin. The data shown in Table II indicate that almost identical results were obtained with the standard FIA dye and the prepared dye mixture in the analysis of mixtures containing 70–80% dichloroparaffin. However, at the 90–95% dichloroparaffin levels, the samples could not be analyzed with the conventional FIA dye while samples of this type were analyzed successfully with the modified dye mixture.

Application of the FIA Method to the Analysis of Products from Paraffin Chlorination. Subsequently, the FIA technique was employed for the analysis of a variety of laboratory chlorinated products and fractions from subsequent separation of chlorinated products. A comparison of FIA and gas chromatographic results from the analysis of four samples is shown in Table III. Examination of the data indicates that there was excellent agreement between the FIA and gas chromatographic analyses.

In general, the data from this investigation indicate that the FIA method, previously employed exclusively for hydrocarbon analysis, can be applied to the analysis of mixtures containing paraffins, monochloroparaffins, and polychloroparaffins. In addition, mixtures having broad carbon number ranges and wide variations in the distribution of paraffins, monochloroparaffins, and polychloroparaffins can be analyzed successfully by the FIA technique. The apparatus is inexpensive and the manipulation and interpretation is uncomplicated. Because olefins exhibit an adsorbability on silica gel similar to monochloroparaffins and polychloroparaffins are similar to aromatics, it is obvious that the presence of these two hydrocarbon types will interfere. However, because chloroparaffins are relatively inert, it should be possible to remove these unsaturated hydrocarbons by acid treating or other chemical treatments prior to FIA analysis. In addition, it has been found that the FIA technique as applied to paraffin–chloroparaffin mixtures is also applicable to other paraffin–haloparaffin mixtures. For example, paraffin–bromoparaffin and paraffin–iodoparaffin mixtures have been analyzed successfully by the FIA technique.

Table III. Analysis of Chloroparaffin Products by the FIA Method and Gas Chromatography

		Wt % component		
	Component	FIA		GC
Sample 1[a]	P[b]	88.3 88.3	88.3	88.1
	MCP[c]	10.2 10.1	10.2	10.6
	DPCP[d]	1.5 1.6	1.5	1.3
Sample 2[a]	P	...		...
	MCP	96.4 96.5	96.5	96.2
	DPCP	3.6 3.5	3.5	3.8
Sample 3[e]	P	...		...
	MCP	98.9 98.6	98.8	97.6
	DPCP	1.1 1.4	1.2	0.7
Sample 4[e]	P	71.2 70.9	71.1	70.6
	MCP	27.9 28.3	28.1	29.0
	DPCP	0.9 0.8	0.8	0.4

[a] C_{12} product.
[b] P = paraffin.
[c] MCP = monochloroparaffin.
[d] DPCP = di- and polychloroparaffin.
[e] C_{10}–C_{13} product.

ACKNOWLEDGMENT

The author thanks D. J. Skahan and N. P. Kilargis for the gas chromatographic analyses of the paraffin chlorination products.

RECEIVED for review February 18, 1969. Accepted April 1, 1969.

Principles and Methods of External Photochemical Titrant Generation

H. D. Drew[1] and J. M. Fitzgerald[2]

Department of Chemistry, Seton Hall University, South Orange, N. J. 07079

BRICKER AND SCHONBERG (*1*) first demonstrated that the rate of photochemical reaction could be made to proceed reproducibly from day to day and developed a method, called photochemical titration, wherein a titrant is generated by photons much as electrons are used in coulometric titrations. Photochemical titrations reported to date all use an *in situ* method; that is, the sample and the titrant generator are photolyzed together using an ultraviolet source of constant intensity. A bibliography of *in situ* methods is available (*2*).

The analogy between photochemical and coulometric titrant generation can be extended to external photochemical generation, which has characteristics similar to external coulometric generation developed by DeFord and coworkers (*3*). It is reasonable to assume that problems similar to those of *in situ* coulometry will be encountered with the photochemical technique. For example, using high-energy photons to irradiate a sample might cause photolysis of the sample as well as titrant generation. Internal filter effects (*4*) and solvents which are strong UV absorbers would prevent use of *in situ* photolysis. Unlike most electrochemical processes, primary photochemical reactions are often followed by "dark" reactions involving free radicals formed in the primary process. Such is the case in the system employed in the present study. The overall quantum efficiency for titrant production requires a constant efficiency of the secondary, "dark," reaction to produce iron(II) (*5*). External generation allows the photochemical conversion to proceed to completion without interference.

The important parameters for external photochemical titrant generation were studied with the iron(III)–oxalate system, which has been well characterized (*5, 6*) and has been used for *in situ* photochemical generation (*1*). In the latter case, small irregularities were reported in stoichiometry for titration of vanadium(V) (*1*). The cause is a slow, thermal oxidation of oxalate by vanadium(V) (*7*). By the use of external generation, iron(II) can be photogenerated in oxalate medium and then added to vanadium(V), thus minimizing the time for the vanadium–oxalate side reaction.

It is also important to consider the application of the general rate equation for photochemical titrant generation to the case of external generation. The rate of formation of titrant, *B*, from the generator, *A*, by the absorption of energy, $h\nu$, is given by:

$$\frac{dC_B}{dt} = \Phi I_0 [1 - \exp - (abC_A/0.434)] \qquad (1)$$

where C_B and C_A are the analytical concentrations of photoproduct and titrant generator, Φ is the overall quantum yield, I_0 is the incident intensity of photochemically effective photons, and the exponential term simply represents the absorbance of the solution at the wavelength used (*8*).

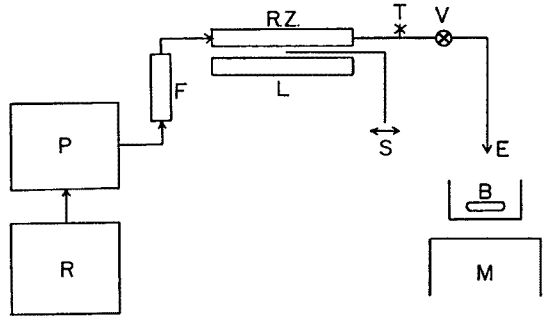

Figure 1. Apparatus for external photochemical titrant generation

R—Solution reservoir; *P*—Pump; *F*—Flow meter; *R.Z.*—Quartz tubing (reaction zone); *L*—Germicidal lamp; *S*—Sliding shutter; *T*—Bubble trap; *V*—Teflon (DuPont) leak valve; *E*—Titrant exit; *B*—Titration vessel; *M*—Magnetic stirrer.

EXPERIMENTAL

Apparatus. The flow chart for the apparatus is shown in Figure 1. The photogenerator was pumped at a constant rate past the photolysis source by a bellows pump (Manostat #72–894–2). The flow rate was measured with an in-stream meter (Manostat #36–541–05) and varied by a Teflon (DuPont) leak valve (Manostat #78–425–01). The emerging photolyzed solution was delivered to the titration vessel. A 57-cm low-pressure mercury discharge vycor lamp (Hanovia Model 94A–1, Engelhard Inc., Newark, N. J.) was used for photolysis. A 60-cm length of 6-mm i.d. quartz tubing was mounted parallel to the lamp and about 5 cm away. A sliding shutter, placed between the lamp and the quartz tubing, could be positioned so that only a portion of the tube was exposed to the source. The fraction of tube length used for photolysis is referred to hereafter as the reaction zone. The lamp and tubing were covered with an aluminum reflector to increase the radiation flux and also to protect the operator.

The special distribution of the lamp was determined with a Beckman DK-2A spectrophotometer in the emission mode. The main wavelength from the germicidal lamp was at 2537Å (Table I). The input voltage to the lamp transformer was controlled at 120 V (*1, 2*).

[1] Present address, Chemistry Faculty, Southern Illinois University, Edwardsville, Ill. 62025

[2] Present address, Department of Chemistry, University of Houston, Houston, Texas 77004

(1) C. E. Bricker and S. S. Schonberg, ANAL. CHEM., **30**, 922 (1958).
(2) R. J. Lukasiewicz and J. M. Fitzgerald, *Anal. Letters*, **1**, 455 (1968).
(3) D. D. DeFord, J. N. Pitts, Jr., and C. Johns, ANAL. CHEM., **23**, 938 (1951).
(4) W. A. Noyes, Jr., and P. A. Leighton, "The Photochemistry of Gases," Dover Publications, Inc., New York, N. Y., 1966, p 152.
(5) C. A. Parker and C. G. Hatchard, *J. Phys. Chem.*, **63**, 22 (1959).
(6) W. M. Riggs and C. E. Bricker, ANAL. CHEM., **38**, 897 (1966).
(7) H. A. Taylor, Ph.D. Thesis, Princeton University, Princeton, N. J., 1963.
(8) J. M. Fitzgerald, R. J. Lukasiewicz, and H. D. Drew, *Anal. Letters*, **1**, 173 (1967).

The flow meter was calibrated and the stability of the system evaluated by the weight of water delivered per min. The flow rate could be varied by adjusting the leak valve and/or pump current; an inverted "T" trap was required to trap bubbles of CO_2 formed in iron(III)–oxalate photolysis. At flow rates around two ml/min, the mean values differed less than 0.02 ml/min from day to day. On a given day the flow rate has an rsd of less than 1%. Titration data, discussed confirm that the flow rate can be reproduced to better than below, 1%.

End points of the vanadium (V)–iron(II) titrations were determined potentiometrically (Pt/SCE) and recorded; the time of titrant delivery to the inflection point was read directly from the chart paper.

Reagents. Stock solutions of iron(III)–oxalate were prepared in 1*M* H_2SO_4 from either $K_3Fe(C_2O_4)_3 \cdot 3H_2O$ (Alpha Inorganic) or by combining standardized ferric sulfate with a 3 mole ratio of potassium oxalate (*5*, *7*). The total amount of photoreducible iron(III) was determined by the method of Riggs and Bricker (*6*). Standard solutions of reagent grade NH_4VO_3 in 1*M* H_2SO_4 were prepared by weight and used as the reference to evaluate the parameters of external generation.

Procedure. With a stock solution of about 4m*M* iron(III)–oxalate, start the pump and adjust the needle valve to give a flow rate between 1 and 2 ml/min. Allow 15 min for conditions to stabilize; discard the delivered titrant. A sample containing between 15 and 100 micromoles of vanadium is diluted with 1*M* sulfuric acid. The titrant stream is then diverted so that it flows into the sample, and the recorder chart drive is started at the same time. After the end point is reached, the titrant is again diverted to a drain until a new sample is ready for titration. The time, in minutes, to reach the inflection point is read directly from the chart paper. A calibration plot of time to the end point *vs.* micromoles of vanadium can be prepared, or the data can be treated by least-squares.

The slope of the calibration curve, in micromoles/min, is equal to the micromoles of iron(II) delivered per minute. If the flow rate is known, then the concentration of iron(II) in micromoles/ml may be calculated. Furthermore, if the original concentration of stock iron(III)–oxalate is known, the percent photoconversion from iron(III) to iron(II) can be calculated. This method of data treatment was used to study some of the fundamental parameters of external photochemical titrant generation. It should be emphasized that satisfactory working curves for routine determinations can be prepared without knowing the exact iron(III)–oxalate concentration or flow rate. So long as these two factors are held constant, a calibration curve can be prepared by use of a standard vanadium solution.

The flow rate, concentration of iron(III)–oxalate, and fraction of quartz tubing exposed to the lamp were varied and know amounts of standard vanadium were titrated in order to establish slopes of calibration curves, which were used to assess the effect of each variable. The time any one portion of solution was photolyzed (residence time in the reaction zone) can be calculated from the volume of the quartz tube (17.6 cm^3), fraction of tube length exposed, and the flow rate in ml/min. Effects of turbulence were not considered in these calculations.

Table I. Spectral Characteristics of the Photolysis Source Molar Absorptivities and Quantum Efficiencies of Iron(III) Oxalate

Wavelength (nm)	Relative lamp intensity[a], %	Molar absorptivity Fe(III) oxalate[b]	Quantum yield, Fe(II) production[c]
576	0.6	...	0.013
578	0.3	...	0.013
545	7.8	...	0.15
435	6.2	38.4	1.01
404	1.4	120	1.13
366	0.5	400	1.21
313	1.4	2.06×10^3	1.24
312	0.8	2.06×10^3	1.24
254	100.0	2.89×10^3	1.28

[a] Relative intensities are referred to 254 nm and are not corrected for spectral response of the 1P28 photomultiplier.
[b] Determined from the slopes of Beer's Law Plots.
[c] Data of Parker and Hatchard (*5*).

RESULTS AND DISCUSSION

The criteria of first importance for evaluating the utility of external photochemical generation include the precision, sensitivity, dynamic range, and convenience of the method. The results of several different sets of titrations, designed to test one or more of the criteria, are presented in Table II. It can be seen that the technique works at the micromolar level, and can yield precision of better than one per cent. The major inconvenience of the method is the necessity of disposing of unwanted titrant. In order to maintain stability of flow and photochemical reaction conditions, it is necessary to keep the system in operation continuously. A short term shutdown can be obtained by closing the needle valve; the exhaustively photolyzed solution in the reaction zone should be expelled before resuming titrations. The major convenience of the method seems to be the possibility of varying the titrant delivery rate by changing either the concentration of photogenerator, or the flow rate, or length of reaction zone as required for a particular sample concentration range.

Table II. Titration of Vanadium(V) with Externally Photogenerated Iron(II)

Range of V taken, μmoles	Titrn time, min	Slope calib. plot,[a] μmoles/min	Flow rate, ml/min	Photolysis time,[b] min (calc)	Photo-conversion, %	rsd, %[c]
50–200	5–20	10.80	1.28	13.60	101[d]	1.15
15–100	4–20	5.126	1.28	13.60	97.5[e]	0.71
50–150	5–14	11.09	2.79	6.22	96.2[e]	...
50–150	4–13	12.35	3.20	5.42	93.5[e]	...
50–150	4–12	14.53	3.95	4.39	89.2[e]	...
10–30	5–13	2.595	1.43	2.10[f]	43.0[e]	0.58

[a] Calculated by least-squares fit of time to end point *vs.* micromoles vanadium taken. This figure is also the delivery rate of iron(II).
[b] Calculated time for a given increment to be pumped through the reaction zone. (Turbulence neglected.)
[c] Coefficient of variation calculated for the median concentration of range titrated.
[d] 8.26 m*M* iron(III) oxalate used as photogenerator. Per cent photoconversion calculated from slope and flow rate.
[e] 4.13 m*M* iron(III) oxalate used as photogenerator. Per cent photoconversion calculated from slope and flow rate.
[f] 17.0% of length of quartz tube exposed to lamp (Reaction Zone).

Table III. Iron(II) Production as a Function of Reaction Zone Exposure

Reaction zone,[a] %	Generation rate (μmoles/min)[b]	Photolysis time[c]	Photoconversion, %[d]
100.0	5.714	12.36	97.1
50.0	5.649	6.18	96.0
33.9	4.508	4.19	76.6
25.0	3.731	3.09	63.4
22.0	3.123	2.72	52.5
18.7	2.786	2.31	47.3
17.0	2.532	2.10	43.0
12.5	1.902	1.54	32.3

[a] Per cent of maximum length available for photolysis.
[b] Calculated slope of least-squares fit of titration data.
[c] Calculated using flow rate of 1.43 ml/min.
[d] Calculated from slope of calibration curve and flow rate, 4.13 m*M* iron(III) oxalate used.

For example, titrations summarized in the first two lines of Table II were carried out under identical conditions except for the concentration of photogenerator solution used. Since the flow rate and reaction zone parameters were such that photoconversion was complete, doubling of the photogenerator concentration doubled the rate of delivery of iron(II). An upper concentration limit of about 10m*M* is set by the release of bubbles of CO_2. For generators which do not evolve gas as a photolysis product, the upper limit is set by the concentration where the photoreaction takes place in a shallow layer (*8*).

A second variable of interest is the flow rate; lines 2 to 5 of Table II provide the results of such a variation. The situation is complex because an increase in flow rate decreases the residence time of a given portion of solution in the reaction zone, and consequently the per cent photoconversion is decreased. Nevertheless, the rate of titrant delivery, in terms of micromoles/minute, is increased; this increase in delivery rate overpowers the decrease in photoconversion. The result, as seen in Table II, is that the slope of a calibration curve increases as the flow rate is increased. Because the solution is not photolyzed exhaustively, it now becomes important that the intensity of the lamp be constant. When photoconversion is complete, the precision of the titrations depends solely on the stability of the flow rate.

The precision possible under conditions where lamp stability is a factor was also examined. The last line of Table II shows that it is possible to carry out titrations under such conditions with good precision. Riggs and Bricker have reported that the iron(III)–oxalate photoreduction suffers from a slight reversal when exhaustive photolysis is carried out with short wavelength UV (*6*). Therefore, it may actually be advantageous to operate under conditions of less than 100% photoconversion. The titrations summarized in the last line of Table II were carried out with the sliding shutter between the mercury lamp and quartz tube positioned so that the reaction zone used was 17% of the maximum.

External generation may prove useful as a method of quickly and reproducibly changing the concentration of titrant without the necessity of dilution. It is possible to select the desired titrant molarity by merely changing the length of reaction zone. The manner in which the titrant concentration can be varied with length of reaction zone was studied and the results are given in Table III. The relation between titrant

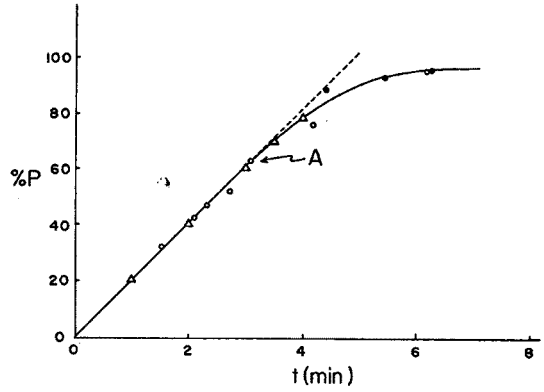

Figure 2. Correlation of Fe(II) concentration with photolysis time

%P—Per cent photolysis of 4.130 m*M* iron(III) oxalate photogenerator
t —Calculated time photogenerator is exposed to lamp illumination, in minutes
○ —Experimental—Reaction zone data
● —Experimental—Flow rate data
△ —Theoretical calculation from Equation 3
A —Point at which absorbance becomes less than 2.00 and exponential term of Equation 2 must be considered (See text).

normality and reaction zone length is nonlinear, which is to be expected from consideration of Equation 1. If there were a linear relation between length of the zone and the concentration of phototitrant, selection of appropriate titrant concentration would be quite simple. It can be seen from Equation 1 that the rate of formation of phototitrant *B* will be constant so long as the exponential term of the equation is small which is true if the absorbance is greater than 2.00. The value of the exponent depends on the concentration of photogenerator, C_A. The integration of the rate equation is simple if the exponential term can be neglected and the concentration of iron (II) at any time, $C_{Fe(II)}$, t is thus:

$$C_{Fe(II)}\, t = \Phi I_0 t \qquad (2)$$

where t is the time of photolysis.

However, the concentration of iron(III) is decreased by photolysis until a point where the exponential term of Equation 1 becomes significant. The integration of the rate expression for time-dependent values of the exponent is somewhat more difficult. This problem has been treated by Kessler (*9*). A detailed consideration of the equation obtained is beyond the scope of the present study. However, some simplifications of the equation are useful for rough estimations of the required conditions for generation of a given titrant concentration. First, an estimate of the incident intensity of the generating lamp, I_0, is easily calculated from the slope of a plot of iron(II) concentration versus time. From Equation 2 it follows that the initial slope of the plot is equal to ΦI_0. Data obtained from variation of flow rate and reaction zone length are plotted in Figure 2. The initial slope of the plot is 0.86 millimole/l-min; with the value of the quantum yield at 254 nm one calculates I_0 as 4.18×10^{20} photons/l-min.

(9) H. C. Kessler, Jr., *J. Phys. Chem.*, **71**, 2736 (1967).

For the volume of reaction zone in this study the incident flux is therefore 7.36×10^{18} photons/min. This is a reasonably large value for a low-pressure lamp and demonstrates the benefits of the long length and close proximity of the reaction zone and source; the aluminum reflector also increases the intensity.

Figure 2 also demonstrates the good agreement between theory and experiment. By taking the value of I_0 calculated from the initial slope of Figure 2, using the molar absorptivity at 254 nm (Table I), and assuming that the i.d. of the tubing, 0.6 cm, is b, one calculates that the exponential term becomes significant at an iron(III)–oxalate concentration of 2.65 mM. For the concentration of generator used here, 4.18 mM, deviation from linearity should occur at about 65% photoconversion. This is the case as can be seen in Figure 2. It would be possible to construct a sliding shutter with calibration marks so that a variety of titrant concentrations could be selected with a single flow rate, thus eliminating the need for a variable pump.

Some conclusions can be drawn regarding the practical value of external photochemical generation. First, it is clear that reproducible flow rates and lamp intensity can be obtained with reasonable care. Second, it is possible to obtain a sufficient intensity from a low-power lamp to generate useful titrant concentrations, and the intensity is constant over many months of continuous operation. It should be noted that *in situ* titrations employ medium-pressure lamps which must be turned off when not in use (*1*, *2*). Finally, the titrant concentration can be easily changed by changing the length of the photolytic reaction zone.

RECEIVED for review December 9, 1968. Accepted March 21, 1969. Taken in part from Ph.D. Thesis of H. D. Drew; presented at the 156th National ACS Meeting, September 1968, Atlantic City, N. J.

Determination of Amphetamine and Related Amines in Blood by Gas Chromatography

Robert B. Bruce and William R. Maynard, Jr.

A. H. Robins Co. Inc., 1211 Sherwood Avenue, Richmond, Va. 23220

A NUMBER OF METHODS have been presented during recent years for the determination and identification of amphetamine and its derivatives in urine. These methods are based primarily on GLC (*1–3*) and TLC (*4–7*) or specific color reactions (*8*, *9*). However, none of these procedures are applicable to the determination of these drugs in blood because of their lower limits of detection. Axelrod (*10*) adapted a nonspecific colorimetric procedure to the determination of amphetamine in plasma and tissues of animals that received relatively large doses.

The method described below is based on the formation of the heptafluorobutryl derivatives of four of these amines and their subsequent determination by GLC using an electron-capture detector. Halogenated amide and ester derivatives prepared from amines and alcohols usually give high sensitivity with the electron-capture detector. A number of these were prepared and from the results obtained it appeared that the heptafluorobutyramides gave the best results.

(1) A. H. Beckett and M. Rowland, *J. Pharm. Pharmacol.*, **17**, 59 (1965).
(2) H. Brandenberger and E. Hellback, *Helv. Chim. Acta*, **50**, 958 (1967).
(3) C. R. Hall, V. Cordova, and F. Rieders, *Pharmacologist*, **7**, 148 (1965).
(4) B. Davidow, *Psychopharmacol. Bull.*, **3**, 30 (1966).
(5) H. Eberhardt and M. Debackere, *Arzneim.-Forsch.*, **15**, 929 (1965).
(6) M. Debackere and A. M. Massart Leen, *Arch. Intern. Pharmacodyn.*, **15**, 459 (1965).
(7) M. L. Weischer and K. Opitz, *Arzneim.-Forsch.*, **17**, 625 (1967).
(8) M. S. Karawya, M. A. El-Kiey, S. K. Wahba, and A. R. Kozman, *J. Pharm. Sci.*, **56**, 1005 (1967).
(9) R. D. Eastman and P. A. G. Cox, *Brit. Med. J.*, **1965**, (5439) 924.
(10) J. Axelrod, *J. Pharmacol. Exp. Therap.*, **110**, 315 (1954).

EXPERIMENTAL

Reagent. Heptafluorobutyric anhydride—Pierce Chemical Co., Rockford, Ill. Keep refrigerated.

Method. An internal standard is used in each determination. Any of the other three amines may be used as the standard for the amine being determined. The internal standard is added to the blood sample before the initial extraction. Chlorphentermine (0.5–2 γ) was used as the internal standard for amphetamine, methamphetamine, and fenfluramine. Amphetamine was the internal standard when chlorphentermine was being determined.

The procedure for the analysis of a blood sample is as follows: Add the internal standard to 5.0 ml of blood, mix and add 1.0 ml of 2N NaOH and 5.0 ml of water. Extract the sample with 10.0 ml, then 5.0 ml of redistilled, chromatoquality pentane. Centrifuge the sample after each extraction and pass the pentane through a layer of anhydrous Na_2SO_4. After passing both extracts through the Na_2SO_4, wash the Na_2SO_4 with an additional two ml of pentane. Evaporate the pentane to dryness under a gentle stream of nitrogen and add 100 μl of heptafluorobutyric anhydride. Allow the reaction to proceed for 30 minutes with occasional mixing. Evaporate the excess heptafluorobutyric anhydride with a gentle stream of nitrogen and cool the tube in an ice bath. Add 0.5 ml of 2N NaOH, keeping the mixture cold, mix and extract with 4, 3, and 3 ml portions of pentane, filtering each portion through anhydrous Na_2SO_4 after each extraction. Wash the sodium sulfate with an additional 2 ml of pentane. Allow the sample to stand overnight at this point. Evaporate the pentane under a gentle stream of nitrogen. Dissolve the residue in 0.20 ml of pentane and inject 2 to 4 μl into the gas chromatograph.

A Barber-Colman gas chromatograph with a ^{63}Ni detector was used in this study. The column was stainless steel, 6 feet long by $^1/_8$" in o.d., with 5% OV-1 on Gas-Chrom Q as the stationary phase. The temperature of the oven was 110 °C, injection port 250 °C, detector 250 °C, and the nitrogen flow rate 30 ml/minute. The retention times found under

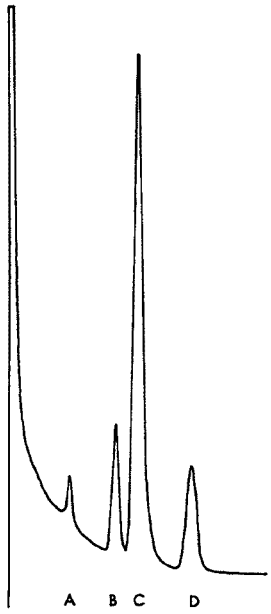

Figure 1. The electron-capture response from the injection of 400 picograms, each of the heptafluorobutyramide derivatives of (*A*) amphetamine, (*B*) methamphetamine, (*C*) fenfluramine, and (*D*) chlorphentermine

these conditions were: amphetamine—3 minutes, methamphetamine—5 minutes, fenfluramine—6 minutes, and chlorphentermine—8.8 minutes.

It was found that pre-conditioning of the column with a pentane solution of heptafluorobutyric anhydride was necessary in order for the column to respond. A 1 to 4 mixture of heptafluorobutyric anhydride in pentane was used in this preconditioning. Five μl of this mixture was injected at 110 °C. The injection was repeated four times, and after 30 minutes the temperature was raised to 200 °C and left for 2 hours. The column exit, of course, was not connected to the detector during the preconditioning. One such conditioning for each column appeared to be sufficient.

After connecting the column exit to the detector, column saturation with the derivative desired (3 injections of 20 γ) aids in the overall response.

It has been found to be necessary to heat the column to about 270 °C, after each four determinations to drive off accumulated extraneous material. The ^{63}Ni detector should be cleaned at intervals in order to maintain the necessary sensitivity.

RESULTS AND DISCUSSION

Preconditioning of the column with heptafluorobutyric anhydride appears to be essential. Two columns prepared in the usual manner failed to give a response to the heptafluorobutyramides, even after repeated injections of large amounts. The columns were then preconditioned as described above under Method. Following this, the response was satisfactory. Silanizing alone is not sufficient. The anhydride appears to react with some sites on the packing material so that these sites can no longer tie up the amides as they pass through.

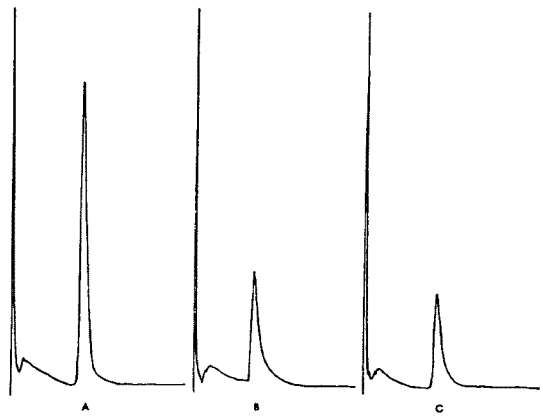

Figure 2. Comparative responses given by equal amounts (2 mg) of the heptafluorobutyramide derivatives of (*A*) fenfluramine, (*B*) methamphetamine, and (*C*) ethamphetamine

The relative responses of the four heptafluorobutyramides are shown in Figure 1. This curve represents 1 μl injection of a mixture of 400 picograms of each of the amines. The response to the fenfluramine amide is seen to be much greater than that of the other three. Fenfluramine does not give a significant response to the electron-capture detector unless a derivative is made. It has formerly been determined in blood (*11*) by flame ionization.

The greater response of the fenfluramine derivative to electron capture could be due to either the trifluoromethyl substitutions on the aromatic ring or to the replacement of the *N*-methyl by the *N*-ethyl group in methamphetamine. That it is due to the former is seen from the response to the ethamphetamine amide (Figure 2) whose response is in the same order of magnitude as that of the amphetamine or metham-

(11) R. B. Bruce and W. R. Maynard, Jr., *J. Pharm. Sci.*, **57** 1173 (1968).

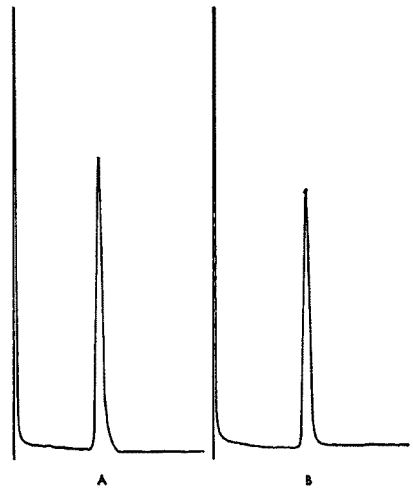

Figure 3. Comparative responses given by 400 picograms of fenfluramine (*A*) and *p*-fenfluramine (*B*) heptafluorobutyramide

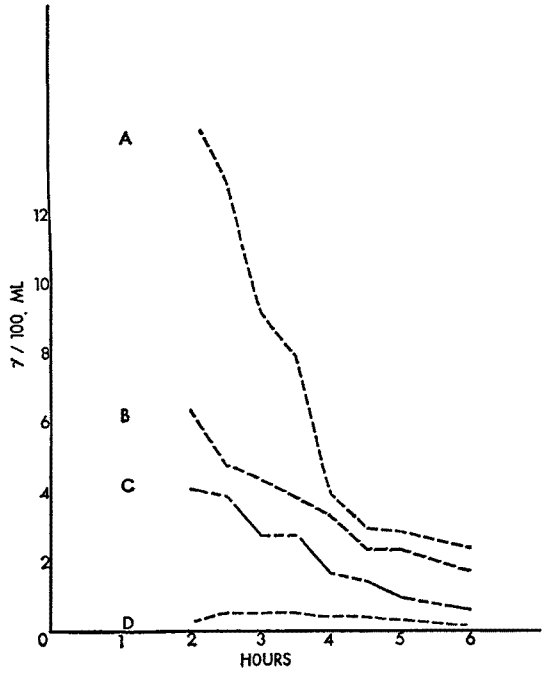

Figure 4. Average blood levels of four subjects following the oral administration of a solution of 5 mg of each of the following drugs: *A*—methamphetamine, *B*—amphetamine, *C*—chlorphentermine, and *D*—fenfluramine

phetamine amides. Chlorphentermine is substituted in the *para* position with a chlorine atom but this does not appear to contribute significantly to the molecule's response. It seemed possible that the *meta* substitution in fenfluramine might be affecting the response in some way. The amide was prepared of the corresponding compound that has the trifluoromethyl group in the *para* position. This amide gave a response (Figure 3) comparable to that of the fenfluramine amide. The substitution of the benzene ring of amphetamine with a trifluoromethyl group contributes significantly to the electron-capture response of the heptafluoroamide even though the trifluoromethyl and heptafluorobutyryl groups are not close to each other.

In earlier studies ether was used for the extraction of the amines from blood but interferences were experienced from the control samples. Pentane was found to give satisfactory recovery with little interference.

In order to confirm that the peaks obtained in gas chromatography were actually due to the heptafluorobutyramides, larger (500 mg) amounts were carried through the procedure as described above using ether instead of pentane as the solvent. The resulting compounds were taken up in chloroform and their structures confirmed by their NMR and IR spectra. Injection of these compounds into the gas chromatograph gave retention times and responses corresponding to those found by carrying submicroquantities through the procedure.

Table I. Recovery from Blood

Compound	Added, ng/ml	Found, ng/ml	Recovery, %
Fenfluramine	12	12	100
	20	20	100
Methamphetamine	100	103	103
	60	62	103
Chlorphentermine	20	21	105
	30	29	97
	40	40	100
	50	51	102
Amphetamine	60	62	103
	80	78	98
	100	99	99

The rationale for the steps in the procedure are apparent except for that of allowing the pentane solution to stand overnight. It has been found from experience that the chromatograms thus obtained show greater response than when this is not done. The reaction tube is cooled after evaporation of the excess heptafluorobutyric anhydride to prevent possible losses due to volatilization from the heat of neutralization with alkali.

The recovery of the amines after adding known amounts to blood are shown in Table I. These results indicate that the procedure is satisfactory. Analysis of control samples of blood did not show interference.

Blood levels of the four drugs were determined in four normal male subjects in a cross-over designed study. Each subject received 5 mg of each of the drugs. This quantity is considerably below the recommended dose for fenfluramine and chlorphentermine. However, it appeared to be of interest to determine blood levels at the same dosage in this preliminary study. Samples were taken at 2.0, 2.5, 3.0, 3.5, 4.0, 4.5, 5.0, and 6.0 hours. The average results are shown in Figure 4. These results show that the method is satisfactory for the determination of these drugs even when administered below the recommended doses.

RECEIVED for review February 13, 1969. Accepted March 13, 1969.

Determination of $E_2°-E_1°$ for Overlapping Waves in Stationary Electrode Polarography

R. Lee Myers and Irving Shain
Chemistry Department, University of Wisconsin, Madison, Wis. 53706

A NUMBER of organic materials are known to undergo a reversible two-electron reduction (*1*). In a few cases, these reactions have been shown to be two one-electron charge transfers, sometimes with an interposed reversible protonation reaction. For example, in studying the reduction of methylene blue (*2*), two one-electron waves are observed in nonaqueous solvent, and on addition of acid, the second wave moves anodically until, when an excess of proton donor is present, the two-electron wave is obtained.

In the methylene blue case, the two-electron reduction apparently is reversible by most of the criteria of stationary electrode polarography. That is, the current function $i_p/\sqrt{v}$ (where i_p is the peak current and v is the rate of voltage scan) is independent of the rate of voltage scan over a wide range, and the ratio of the cathodic to anodic peak currents is unity over the same range. However, a careful analysis of the shape of the wave indicates that it is slightly broader than expected for a simple two-electron reversible charge transfer: the difference between the peak potential, E_p, and the half-peak potential, $E_{p/2}$, was about 34 mV, rather than 28.25 mV as expected. This was attributed to a small difference between the $E°$ values for the two individual one-electron transfers. A theory derived earlier in this laboratory (*3*) was used to calculate $\Delta E°$, and the value obtained was +51 mV, with the second charge transfer taking place at more anodic potentials than the first charge transfer.

Since this mechanism may be fairly common as new systems are investigated, it appeared useful to extend the previous work, so that values of $\Delta E°$ could be more conveniently evaluated from experimental values of $E_p - E_{p/2}$. Calculations were carried out using the numerical method and programs described by Polcyn (*3*, *4*). For the reactions

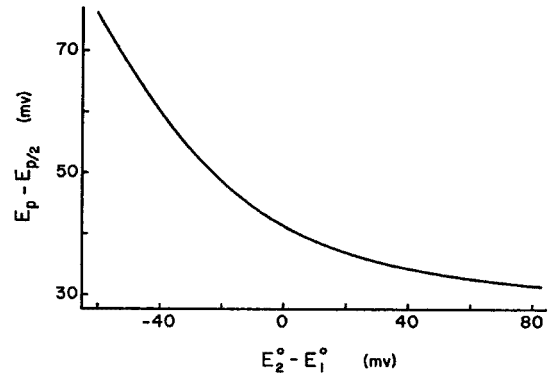

Figure 1. Peak width ($E_p - E_{p/2}$) as a function of $E_2° - E_1°$ for overlapping multistep waves in stationary electrode polarography

$$A \overset{e}{\rightleftarrows} B \overset{e}{\rightleftarrows} C \qquad (1)$$

or

$$A \overset{e}{\rightleftarrows} B \underset{k_{-1}}{\overset{k_1}{\rightleftarrows}} B' \overset{e}{\rightleftarrows} C \qquad (2)$$

involving two one-electron steps, and where k_1 and k_{-1} are very large, the results are shown in Figure 1. When $E_2°$ is very anodic of $E_1°$, the value of $E_p - E_{p/2}$ approaches 28.25 mV, and the wave appears as a concerted two-electron reaction. As $E_2°$ shifts toward less anodic values, the wave broadens. Calculations were not carried out for cases in which $E_2°$ is cathodic of $E_1°$ by more than about 60 mV, because the wave becomes distinctly misshapen and the two one-electron waves begin to separate (*5*). For accurate work, a large scale plot similar to Figure 1 would be required. Data for construction of such a plot are listed in Table I.

The location of the peak with respect to $E_1°$ can also be determined from the data in Table I. When $E_2°$ is so anodic of $E_1°$ that a normal two-electron wave is obtained, the peak appears at a potential centered between $E_1°$ and $E_2°$, as discussed previously (*3*). As $E_2°$ is shifted to less anodic potentials, the entire wave moves toward $E_1°$; and when $E_2°$ is cathodic of $E_1°$, the peak shifts to potentials cathodic of $E_2°$.

It must be emphasized that these results cannot be used to calculate $\Delta E°$ or to locate $E_1°$ unless all other criteria, over a wide range of scan rates, indicate that the reaction is reversible and not complicated by chemical reaction.

RECEIVED for review February 6, 1969. Accepted March 20, 1969. Work supported in part by the U. S. Atomic Energy Commission under Contract No. AT(11-1)-1083. Other support received from the National Science Foundation under Grant No. GP-3907.

(1) D. J. Pietrzyk, ANAL. CHEM., **40**, 194 R (1968).
(2) R. H. Wopschall and I. Shain, *ibid.*, **39**, 1527 (1967).
(3) D. S. Polcyn and I. Shain, *ibid.*, **38**, 370 (1966).
(4) D. S. Polcyn, Ph.D. Thesis, University of Wisconsin, Madison, Wis., 1965.

Table I. Peak Width ($E_p - E_{p/2}$) and Location of Peak Potential ($E_p - E_1°$) as a Function of $E_2° - E_1°$

$E_2° - E_1°$, mV	$E_p - E_{p/2}$, mV	$E_p - E_1°$, mV
179.8	29	74.5
89.9	31	28.8
77.1	32	22.1
64.3	33	15.4
41.1	34	3.6
30.8	35	−2.6
20.6	37	−8.7
10.3	39	−14.7
0.0	41.5	−21.1
−10.3	44	−27.2
−20.6	48	−34.4
−30.8	54	−42.6
−41.1	61	−51.9
−51.4	69	−62.2

(5) See Figure 2 in Ref. 3.

Spectrophotometric Determination of Iron with 2-Pyridyl-2′-Hydroxymethane Sulfonic Acid

E. E. H. Pitt and V. M. Stanway[1]

Department of Chemistry and Metallurgy, Lanchester College of Technology, Coventry, England

Complexes of copper, zinc, nickel, and cobalt with 2-pyridyl-2′-hydroxymethane sulfonic acid have been reported (*1*). The ligand exhibits properties of 8-hydroxyquinoline in that the acid dissociation constants, of the pyridinium proton and the hydroxyl group, have similar values (*1*). Relative positions of the nitrogen atom and the hydroxyl group are also similar. On the basis of this evidence, it was thought possible that 2-pyridyl-2′-hydroxymethane sulfonic acid would form metal complexes, analogous to those of 8-hydroxyquinoline, which might be colored. A qualitative survey showed that colored complexes were formed with cobalt, nickel, copper, zinc, vanadium, and iron(II), the latter reacting quantitatively at the 0.1 to 4 ppm level to give a wine red color. Aspects of the chemistry of the reaction with iron have been investigated and a procedure for the spectrophotometric determination of this element is proposed.

EXPERIMENTAL

Apparatus. Absorbance measurements were made with a Unicam SP 600 spectrophotometer. A Cambridge pH meter was used to determine pH.

Reagents. Reducing Solution. A solution was prepared by dissolving 50 grams of hydroxylamine hydrochloride in one liter of distilled water.

Ligand Solution. A solution was prepared by dissolving 0.2 gram of 2-pyridyl-2′-hydroxymethane sulfonic acid in a small amount, about 20 drops, of 4*N* ammonia and diluting to 100 ml with distilled water. This solution was stable for several days but was discarded when it attained a pale yellow color.

Buffer Solution. A buffer solution of pH 10 was prepared by dissolving 70 grams of ammonium chloride in a minimum of distilled water and adding 570 ml of 0.880 ammonia. This solution was diluted to one liter with distilled water.

Standard Iron Solution. A stock solution containing 200 ppm iron was prepared by dissolving 0.7025 gram of ferrous ammonium sulfate in about 50 ml of 1*N* sulfuric acid and diluting to 500 ml with distilled water. A 20 ppm iron solution was prepared by dilution with distilled water.

Procedure. Pipet an aliquot of the sample containing 2.5–100 μg of iron into a 25-ml graduated flask. Add approximately 5 ml each of the reducing solution, the ligand solution, and the pH 10 buffer solution. Make up to volume with distilled water and mix well. Prepare a blank and standard in a similar manner using distilled water and 5 ml of the standard iron solution in place of the sample. After one hour, measure the absorbance of the sample and standard, at 525 mμ, against the reagent blank using 1-cm glass cells. The concentration of iron in the sample is then calculated from the ratio of absorbances of sample and standard and the concentration of iron in the standard. The calibration graph is linear in the range 0–4 ppm of iron.

[1] Present address, Chemical Analysis Section, Nelson Research Laboratories, Beaconhill, Stafford, England.

(1) L. Banford and W. J. Geary, *J. Chem. Soc.*, **1964**, 378.

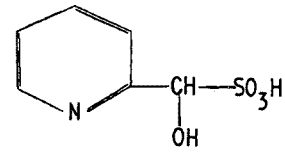

Figure 1. 2-Pyridyl-2′-hydroxymethane sulfonic acid

RESULTS AND DISCUSSION

Preliminary qualitative tests showed that under specific conditions the ligand (Figure 1) gave a wine-red color with micro amounts of iron. Under alkaline reducing conditions the absorption spectra of the complex in both ammonia and sodium hydroxide, measured over the 400–600 mμ wavelength range, were found to be identical with the color more intense and of greater stability when the solvent was ammonia. A single rather broad peak was observed which had a maximum at about 520 mμ, the exact position of the maximum being dependent on the final pH of the system.

The chemistry of the reaction was investigated by a systematic study of the effects of time, pH, reducing conditions, and

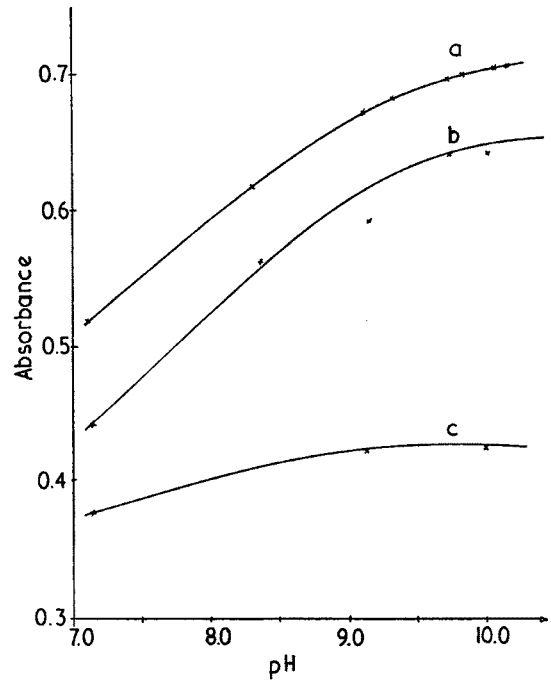

Figure 2. Variation of absorbance with pH of the iron complex after a development time (*a*) 60 minutes, (*b*) 30 minutes, and (*c*) 10 minutes

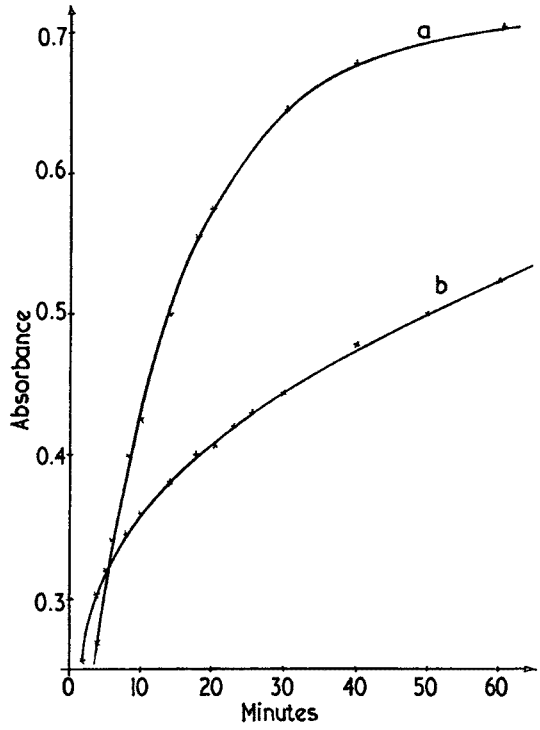

Figure 3. Kinetics of color formation at (*a*) pH 10.0 and (*b*) pH 7.2

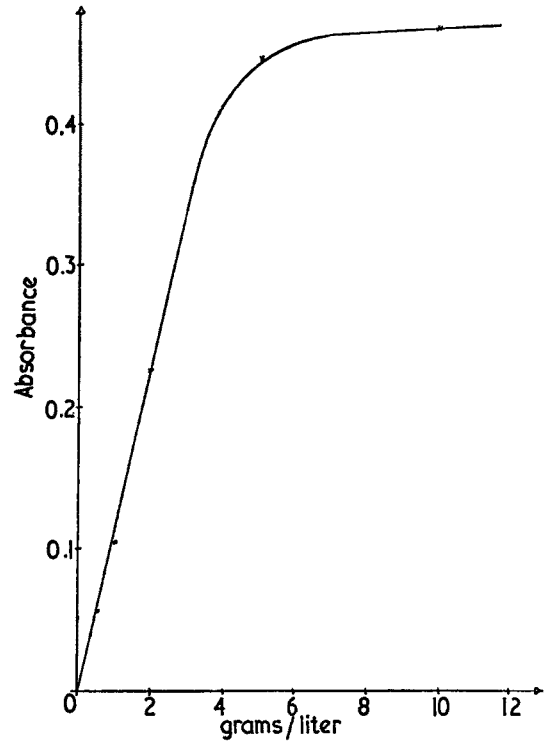

Figure 4. Effect of hydroxylamine hydrochloride concentration on complex formation

ligand concentration. The pH and time parameters were investigated simultaneously using an excess of reductant and ligand. Measurement of the absorbance of the color, given by a constant amount of iron reacting under these conditions, over a range of pH values and time intervals showed that the rate of formation and maximum color intensity were both affected by the pH of the system (Figures 2 and 3). It was found that both intensity and rate of color formation increased with pH. However, if the pH was increased much above 10, the color intensity was found to be variable. At pH 10, the rate of color formation was initially high but decreased rapidly with time and after one hour the rate of change became negligible. The color formed at this pH value was found to have maximum absorption at 525 mμ and remained stable for several hours. In order to obtain consistant results in replicate determinations, it was found that the pH of the system had to be controlled to within 0.5 pH unit of the value selected for the determination. An ammonium hydroxide/ammonium chloride buffer solution of pH 10 was found to be satisfactory.

It was initially considered that the only function of the hydroxylamine was to maintain the iron in the +2 oxidation state but when a more powerful reductant, hydrazine sulfate, was used no colored complex was produced. Hydroquinone and sulfur dioxide also failed to yield a colored complex. With an excess of ligand at pH 10, it was observed that the absorbance of solution containing a fixed amount of iron varied initially with reductant concentration (Figure 4). For iron concentrations up to 4 ppm, a hydroxylamine concentration of 1% (w/w) was required in order to obtain constant absorbance for replicate determinations. With an iron concentration of 4 ppm, the ratio of Fe(II):hydroxylamine was approximately 1:2500. By using the Method of Continuous Variations (*2*), with 1% (w/w) reductant at pH 10, it was found that the maximum corresponded to a complex of the type $Fe(Ligand)_2$. A deviation from linearity was also observed at a point corresponding to the complex $Fe(Ligand)_4$ (Figure 5). It was found impracticable to determine the mole ratio of hydroxylamine present in the complex as a large excess of it was always found to be required in order to obtain a measurable amount of complex. From these observations it was concluded that the hydroxylamine took part in the reaction as a ligand as well as a reductant (*3*). The relatively high concentration of hydroxylamine suggests that this reagent may be replacing some of the water molecules in the hexaquoiron(II) ion, $[Fe(H_2O)_6]^{2+}$, and/or competing with 2-pyridyl-2′-hydroxymethane sulfonic acid for the central metal ion. It is possible that both these reactions take place simultaneously and on this basis structures for $Fe(Ligand)_2 \cdot (NH_2OH)_2$ and $Fe(Ligand)_4 \cdot (NH_2OH)_2$ have been postulated and are shown in Figures 6 and 7.

With conditions specified it was established that Beer's law held over the range 0–4 ppm. The relative standard deviation of five determinations at the 0.4 ppm level was ±2.93% with a mean of 0.41 ppm and at the 1.6 ppm level was ±0.72% with a mean of 1.67 ppm. The relative standard deviation at the 0.4 ppm level would probably have been reduced if longer light path cells had been used, the measure-

(2) W. C. Vosburgh and G. R. Cooper, *J. Amer. Chem. Soc.*, **63**, 437 (1941).
(3) V. M. Stanway, BSc. Thesis, Lanchester College of Technology, Coventry, England, 1967.

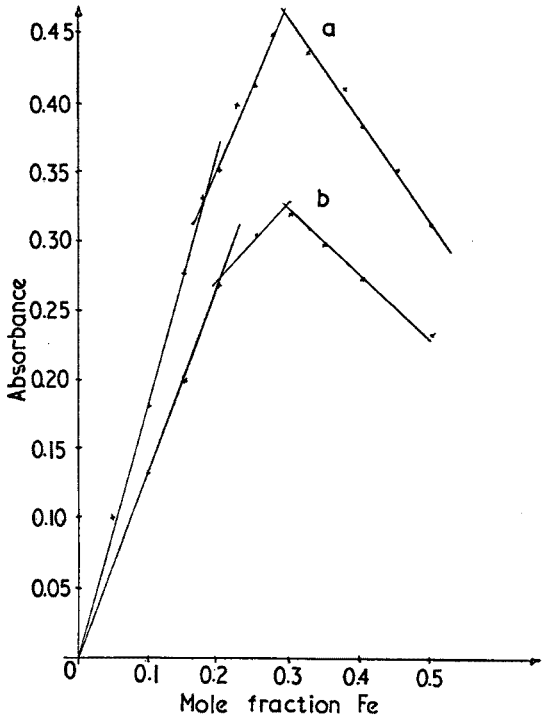

Figure 5. Mole ratio of the complex by the Method of Continuous Variations using (*a*) 6.7 × 10^{-4} *M* and (*b*) 5.0 × 10^{-4} *M* iron and ligand solutions

ment of small absorbances being the limiting factor at this level. Interferences by copper and cobalt appear to be due to their reaction with the pH 10 buffer solution to give colored compounds. The blue copper-amine color gave an apparent increase in the measured iron content which should be minimized by increasing the hydroxylamine concentration to 5% (w/w). For a cobalt to iron ratio of 10:1, measured iron content was approximately 10% lower than the true result. Zinc at a concentration of approximately 300 ppm, gave a pink complex of low absorptivity, with an absorbance maximum at 500 mμ, which did not affect the measurement of iron. Similarly, nickel gave a pale orange coloration at a concentration of 300 ppm with an absorbance maximum in the ultraviolet region of the spectrum. At a concentration of 500 ppm, vanadium gave a yellow colored complex with an absorbance maximum at 400 mμ and consequently had little effect on the measurement of iron. Qualitative tests indicated that no colored complex was produced when the ligand reacted with manganese, chromium, silver, tin(II), lead, molybdenum, and titanium, although some of these metals may interfere by virtue of their reaction with ammoniacal buffer solution.

The proposed method has some advantages over existing methods. Control over reaction conditions is more easily

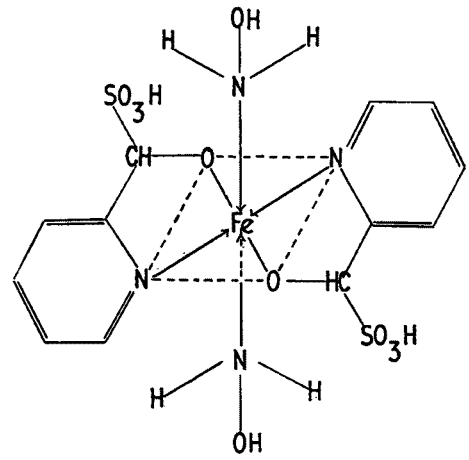

Figure 6. Postulated structure for the complex Fe(Ligand)$_2$·(NH$_2$OH)$_2$

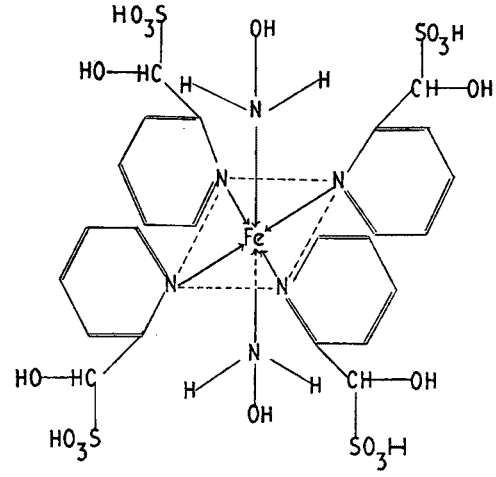

Figure 7. Postulated structure for the complex Fe(Ligand)$_4$·(NH$_2$OH)$_2$

attained than for the thiocyanate and 1:10 phenanthroline methods. The sensitivity is similar to that with 1:10 phenanthroline while the determination of 0.1 ppm iron by the thiocyanate method requires the use of solvent extraction. Concentrations in excess of 2 ppm nickel, 10 ppm zinc, 20 ppm copper and chromium seriously interfere in the formation of the 1:10 phenanthroline–iron complex while the proposed reaction is relatively free from these interferences.

RECEIVED for review October 10, 1968. Accepted February 26, 1969. Mr. V. M. Stanway thanks the Staffordshire County Council Education Committee for financial support during the period of research.

Methods for the Isolation and Characterization of Constituents of Natural Products

A Periodic Acid Column Procedure for the Oxidation of Vic-Glycols, Epoxides, and α-Hydroxy Acids at the Micromole Level

D. P. Schwartz, J. L. Weihrauch, and L. H. Burgwald[1]

Dairy Products Laboratory, Eastern Utilization Research and Development Division,[2] *Washington, D. C. 20250*

THE UTILIZATION of periodic acid and its salts in organic structural studies, in certain syntheses, and in organic analyses has been thoroughly documented in a number of reviews (*1–3*). In an attempt to expand the scope of the periodic acid reaction and make it more suitable for the oxidation of susceptible structures in lipids, a two-phase oxidation procedure has been evolved in which the polar phase (aqueous periodic acid) is impregnated onto a support (calcium sulfate) and a water-immiscible solvent containing the substrate is passed over the support. The product(s) of the reaction then emerge at the exit end of the column.

EXPERIMENTAL

Reagents and Apparatus. Calcium sulfate, anhydrous powder, was obtained from the J. T. Baker Co., Phillipsburg, N. J.; paraperiodic acid (H_5IO_6) was a product of the G. Frederick Smith Co., Columbus, Ohio; methylene chloride (Baker) was used as received; benzene, ACS grade (thiophene-free) (Baker) was rendered carbonyl-free as described by Schwartz and Parks (*4*) then distilled from glass; *n*-hexane, High purity grade (Phillips Petroleum Co., Bartlesville, Okla.) was purified by the method of Hornstein and Crowe (*5*) but using a greatly reduced flow rate—*i.e.*, approximately one liter/24 hours than was recommended in that paper. The purified hexane was then distilled from glass; aluminum oxide, Brockman activity grade I, acidic, for chromatography (Baker) was partially deactivated by the addition of 8% distilled water. The substrates employed in the study are listed in Table I along with their source and estimated purity.

Procedure. PREPARATION OF PERIODIC ACID COLUMNS. One milliliter of a saturated solution of periodic acid in distilled water is pipetted into a 4-inch mortar and ground with 5 grams of $CaSO_4$ until the powder appears homogeneous. This entails grinding, scraping the mortar with a flat spatula, and regrinding. This operation is repeated several times. The powder is then stored in a suitable receptacle with a secure lid. The powder has been stored for up to 6 months at room temperature with no apparent ill-effects.

Columns are prepared by transferring 0.5 gram of the powder to a chromatography tube approximately 0.8 × 15 cm. The powder is tamped lightly with a tamping rod so that after the column is wetted with hexane, 1 ml of this solvent will flow completely into the column in 9 to 11 minutes. If the flow rate exceeds that, the column should be tamped tighter at this point until the desired flow rate is attained. With a little experience, columns can be prepared with very little variation in flow rate. The column is then washed with a column volume of benzene and is ready for the sample. The periodic acid columns prepared as described contain over 300 μmoles of periodic acid and can be used repeatedly. The entire study was done with two such columns.

PREPARATION OF 2,4-DINITROPHENYLHYDRAZINE COLUMN. The extent of the periodic acid reaction was followed by permitting the effluent from the $CaSO_4$ column to drip directly onto a column of Celite impregnated with a phosphoric acid solution of 2,4-dinitrophenylhydrazine (*4*). The carbonyl fragments are immediately derivatized and subsequently analyzed. Columns are prepared by transferring 2.5 grams of the impregnated Celite to a column (1.7 cm i.d. × 17 cm) and tamping fairly tightly so that the flow rate of hexane through the column will be between 40–50 ml/hr. The column is washed with 2 column volumes of benzene and then with hexane until the effluent emerges colorless. Celite impregnated with the 2,4-dinitrophenylhydrazine solution can be stored at −18 °C and used as needed.

PREPARATION OF SUBSTRATE SOLUTIONS. Solutions of the glycols, epoxides, and α-hydroxy acids listed in Table I were made in benzene except for lactic and mandelic acids and 1,2-propanediol which were made in methylene chloride which is pure as far as carbonyl-contaminants are concerned (*4*). Solutions of the substrates were prepared to contain between 0.8 to 4.0 μmoles/ml. The concentrations of the substrate employed are listed in Table I.

OXIDATION AND DERIVATIZATION PROCEDURE. The periodic acid column is positioned in the 2,4-dinitrophenylhydrazine column so that the tip of the former is just above the top of the bed. An aliquot of the substrate solution (0.25 to 1.0 ml) is pipetted onto the periodic acid column and when drained the sides of the column are washed with 1 ml of benzene. When this has drained the periodic acid column is washed with 1 ml more of benzene which completes the removal of the products of oxidation. All washings are permitted to drain into the bed of dinitrophenylhydrazine and 5 ml of benzene is added. When this has percolated into the column, hexane is added until the effluent emerges colorless.

ISOLATION, ESTIMATION, AND IDENTIFICATION OF DERIVATIVES. The effluent is mixed and transferred to a 5-gram column of alumina contained in a chromatographic tube approximately 0.8 cm × 15 cm. The simple aliphatic carbonyls are eluted with (1:1) hexane:benzene; aromatic and polyfunctional carbonyls are removed with benzene. In any case, when dealing with unknowns, elution should be first attempted with benzene:hexane (1:1) for this also gives some clue regarding the nature of the derivative.

The solvent is evaporated and the optical density of the residue dissolved in $CHCl_3$ is determined at the wavelength of maximum absorption (Table I). Concentrations were calculated using the molar absorptivities listed in Table I.

The derivatives were spotted on thin-layer partition plates

[1] Deceased August 16, 1968.

[2] Agricultural Research Service, U. S. Department of Agriculture.

(1) E. L. Jackson, "Organic Reactions," Vol. 2, John Wiley and Sons, Inc., New York, N. Y., 1966, pp 341–375.
(2) J. M. Bobbitt, "Advances in Carbohydrate Chemistry," Vol. 1, Academic Press, New York, N. Y. 1956, pp 1–40.
(3) B. Sklarz, *Quart. Rev. (London)*, **21**, 3 (1967).
(4) D. P. Schwartz and O. W. Parks, ANAL. CHEM., **33**, 1386 (1961).
(5) I. Hornstein and P. F. Crowe, *ibid.*, **34**, 1037 (1962).

Table I. Periodic Acid Column Oxidation of Glycols, Epoxides, and α-Hydroxy Acids

Substrate	Source	Estimated purity, %	Amount of substrate employed, μmoles	Average yield, %	Identity of 2,4-dinitrophenylhydrazones	γ Max $CHCl_3$ used	$E \times 10^{-3}$ used
Benzoin	Aldrich[a]	...	0.5–2.0	100	Benzaldehyde	378	28
Benzopinacol	Aldrich	...	0.25–1.0	0	...	...	...
Threo-9,10-dihydroxymethyl stearate	EURDD[b]	95	0.2–0.8	99	Nonanal, methyl azelaldehydate	355 355	22.5 22.5
DL-1,2-Diphenyl-1,2-ethanediol	Schuchardt[c]	...	0.25–1.0	102	Benzaldehyde	378	28
Meso-1,2-diphenyl-1,2-ethanediol	Schuchardt	...	0.35–1.4	103	Benzaldehyde	378	28
9,10-Epiminooctadecane	EURDD	98.5	0.25–1.0	0	...	...	...
1,2-Epoxy butane	Aldrich	99[h]	1.0–4.0	79	Propanal	355	22.5
1,2-Epoxy octane	EURDD	95[h]	0.6–2.4	90	Heptanal	355	22.5
9,10-Epoxy methyl stearate	EURDD	95	0.45–1.8	63	Nonanal, methyl azelaldehydate	355 355	22.5
Glyceryl-1-hexadecyl ether	Fluka[d]	puriss	0.8–3.2	93	Hexadecoxy acetaldehyde	355	22.5
Glyceryl-1-octadecyl ether	Fluka	puriss	0.75–3.0	95	Octadecoxy acetaldehyde	355	22.5
α-Hydroxy lauric acid	Aldrich	...	0.5–2.0	72	Undecanal	355	22.5
2-Hydroxy-2-methyl 3-butanone	Aldrich	87[h]	0.75–3.0	100	Acetone	362	22.5
2-Hydroxy-2-methyl butyric acid	Aldrich	...	0.5–2.0	73	2-Butanone	362	22.5
α-Hydroxy-methyl eicosanoate	Applied Science[e]	99	0.4–1.6	0	...		
α-Hydroxy-myristic acid	Aldrich	...	0.5–2.0	74	Tridecanal	355	22.5
DL-Lactic acid	Lachat[f]	...	0.75–3.0	38	Acetaldehyde	362	22.5
DL-Mandelic acid	Aldrich	...	0.5–2.0	102	Benzaldehyde	378	28
Methyl mandelate	Aldrich	...	1.0–4.0	0	...		
1-Monopalmitin	Supelco[g]	99	0.5–2.0	95	Glycolaldehyde palmitate	350	20
1-Monostearin	Supelco	99	0.5–2.0	91	Glycolaldehyde stearate	350	20
1-Phenyl-1,2-ethanediol	Aldrich	...	1.0–4.0	105	Benzaldehyde	378	28
Pinacol	Aldrich	98	0.2–0.8	87	Acetone	362	22.5
1,2-Propanediol	Aldrich	...	1.0–4.0	56	Acetaldehyde	355	22.5
trans-Stilbene oxide	Aldrich	...	0.7–2.8	83	Benzaldehyde	378	28
Styrene oxide	Aldrich	...	0.75–3.0	97	Benzaldehyde	378	28

[a] Aldrich Chemical Co., Milwaukee, Wis.
[b] Eastern Utilization Research and Development Division, ARS, USDA, Philadelphia, Pa.
[c] Schuchardt Chemische Fabrik, Munich, Germany.
[d] Fluka Ag., Chemische Fabrik, Buchs, Switzerland.
[e] Applied Science Laboratories, Inc., State College, Pa.
[f] Lachat Chemicals, Inc., Chicago, Ill.
[g] Supelco, Inc., Bellefonte, Pa.
[h] By vapor phase chromatography 50′ × 3/8″ SE-30 column 240–280 °C.

along with the expected authentic derivatives. The neutral and alkaline partition systems described by Schwartz *et al.*, (*6*) were utilized.

RESULTS AND DISCUSSION

Pertinent data are presented in Table I. Yields are the average of four levels of substrate (2, 3, and 4 times the lowest concentration) analyzed and are based on the estimated purity of the substrate when known, or on 100% purity if unknown.

Yields were, for the most part, very good for vic-glycols with the exception of 1,2-propanediol and for pinacol. Benzopinacol, a highly hindered vic-glycol, did not oxidize at all.

Epoxy compounds with the exception of styrene oxide failed to oxidize quantitatively. Maerker and Haeberer (*7*) could get quantitative yields on only one epoxide out of four which they subjected to periodic acid oxidation in dioxane–water mixtures.

The α-hydroxy acids investigated unexpectedly were oxidized and in fair yields. This structure is not readily attacked by periodic acid in solution even at elevated temperatures (*1*, *8*, *9*), although both lead tetraacetate and sodium bismuthate attack that structure (*10*). Mandelic acid yielded the theoretical amount of benzaldehyde. The aliphatic α-hydroxy acids, however, gave lower yields. The methyl esters of α-hydroxy acids as expected, did not undergo oxidation.

In connection with yields, it should be pointed out that one set of conditions only, chosen arbitrarily at the outset, was used. No attempt was made to improve yields in those instances where quantitative yields were not obtained. Consequently, it is possible that improved yields could be obtained

(6) D. P. Schwartz, Jennie Shamey, C. R. Brewington, and O. W. Parks, *Microchem. J.*, **13**, 407 (1968).
(7) G. Maerker and E. J. Haeberer, *J. Amer. Oil Chem. Soc.*, **43**, 97 (1966).
(8) P. Fleury and R. Boisson, *J. Pharm. Chim.*, **30**, 145 (1939).
(9) D. B. Sprinson and E. Chargaff, *J. Biol. Chem.*, **164**, 433 (1946).
(10) W. Rigby, *J. Pharm. Soc.*, **1960**, 1907.

by the appropriate variation of parameters, for example, by changing flow rates, solvent, raising the temperature, adjusting the pH, manipulating the periodic acid concentration, or by incorporating salt into the aqueous phase.

An interesting observation made during this study was the complete absence of formaldehyde in the products of oxidized substrates in which formaldehyde is predicted. No trace of the 2,4-dinitrophenylhydrazone of formaldehyde was evident on the thin layer plates. Even when 100 mg of 1-monopalmitin or glycerin-1-octadecylether were oxidized formaldehyde was not detected by odor or by analysis of the 2,4-dinitrophenylhydrazones. The fate of the formaldehyde was not determined.

Periodic acid-impregnated Celite and fine glass beads were unsatisfactory supports for the oxidation.

The most obvious advantage of employing the periodic acid column for the oxidation of susceptible structures in lipids is that the need for finding a suitable mutual solvent is circumvented. Maerker and Haeberer (*7*) point out that the ratio of water to dioxane which they used as a solvent in their studies was fairly critical as far as yields and solubility of the substrate were concerned.

The periodic acid column procedure would seem to be more amenable than a one-phase system for structural studies on microgram quantities of an organic compound. The columns can be reduced in size which accordingly will decrease the volumes involved. Thus analysis of the effluent by gas–liquid chromatography–mass spectrometry, for example, should be possible without further manipulations such as extraction or evaporation.

ACKNOWLEDGMENT

We thank G. Maerker and his colleagues, EURDD, Philadelphia, Pennsylvania, for generous samples of many epoxides used in this study.

RECEIVED for review November 26, 1968. Accepted March 25, 1969. Mention of brand or firm names does not constitute an endorsement by the Department of Agriculture over others of a similar nature not mentioned.

AIDS FOR ANALYTICAL CHEMISTS

High-Stability Low-Noise Precision Spectrometer Using Optical Feedback

Harry L. Pardue and Stanley N. Deming

Department of Chemistry, Purdue University, Lafayette Ind. 47907

IN recent years there has been a rapid growth of interest in analyses based upon measured initial rates of chemical reactions (*1–3*). The resultant need to detect very small concentration changes in reactants or products places stringent requirements on the stability of the detection system used. For highest precision and accuracy in these measurements, it is important that any observed change of signal not be caused by the measuring instrument itself. This is of special consideration if the kinetic run is made over a long period of time, if the observed change in signal is a small part of the total signal, or especially if both situations exist. Furthermore, the ultimate sensitivity, precision, and accuracy of equilibrium methods based upon photometric techniques are dependent upon the stability of the photometer used.

Recent reports have demonstrated that the use of optical feedback to stabilize photometric sources can lead to improved stability (*4, 5*). The instrument reported by Loach and Loyd (*4*) utilized a high quality monochromator and yielded excellent short term stability. However, no information on the long term stability was given. The instrument reported by Pardue and Rodriguez (*5*) yielded high long term stability but utilized interference filters to isolate desired wavelength regions. To date, no optical feedback system employing a grating or prism monochromator and having the ultra-high stability required for the indicated kinetic studies has been reported. This report describes a high-stability, low-noise precision spectrometer utilizing optical feedback and including a monochromator for continuous wavelength variation between 400 and 625 nm.

The working stability of the spectrometer system was evaluated on NiEDTA solutions at 590 nm. Results demonstrate that over the absorbance region studied (0–0.007 absorbance unit), the standard error of estimate is 0.000056 absorbance unit. These data are compared with results obtained using the 0–0.1 absorbance unit scale of a Cary Model 14 recording spectrophotometer. Consecutive 1-hour observations over periods greater than 10 hours demonstrated minimal drifts in the modified instrument of $\pm 0.007\%$ T per hour with average drifts of about $\pm 0.02\%$ T per hour.

INSTRUMENT DESIGN

A Bausch and Lomb Spectronic 20 spectrometer was modified for optical feedback stabilization. The existing electronics in the spectrometer are disconnected. Modifications in the optics and control and measurement circuitry are described below.

Spectrometer Modifications. A rigid bulb mount is constructed from a block of bakelite plastic. The bulb occupies the same position it does in the unmodified instrument but is rotated 60° about its symmetrical axis from its normal orientation to increase the light intensity and to minimize effects caused by filament motion. Leads from the programmable power supply are soldered to the bulb for external control of intensity.

A 0.25- × 0.50-inch^2 rectangular hole is cut in the base of the instrument directly under the light path between the

(1) E. M. Cordos, S. R. Crouch, and H. V. Malmstadt, ANAL. CHEM., **40**, 1812 (1968).
(2) G. E. James and H. L. Pardue, *ibid.*, **40**, 796 (1968).
(3) H. L. Pardue, *Rec. Chem. Progr.*, **27**, 151 (1966).
(4) P. A. Loach and R. J. Loyd, ANAL. CHEM., **38**, 1709 (1966).
(5) H. L. Pardue and P. A. Rodriguez, *ibid.*, **39**, 901 (1967).

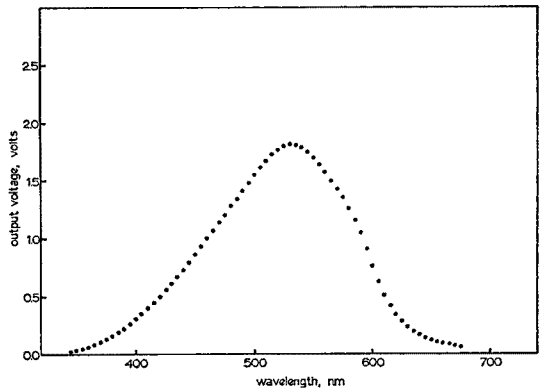

Figure 1. Spectral response of spectrometer

Bulb voltage: 6.2 V
Sample amplifier feedback: 20M, 0.005 mF
Phototubes: 1P39

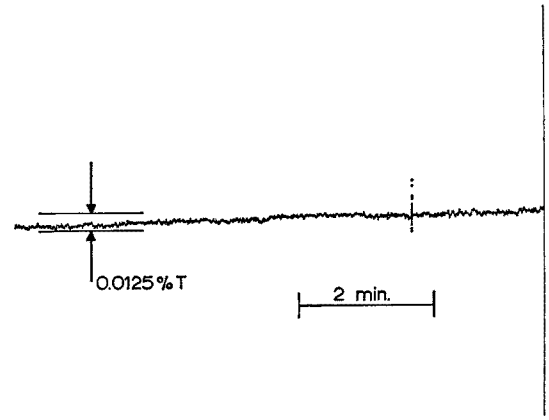

Figure 2. Short-term stability and noise

Time increases to the left
Wavelength: 522 nm
Reference amplifier feedback: 0.001 mF
Sample amplifier feedback: 20M, 0.005 mF
Reference current: 0.05 μA

attenuating slit and the wavelength-defining slit. The hole is centered approximately 0.375 inch away from the pedestal supporting the attenuating slit mechanism; the longer dimension of the hole is parallel to the light path. A beam splitter is supported above the hole to direct a portion of the light beam downward while allowing the remainder of the beam to pass through the sample cell.

A phototube housing (McKee Pedersen Instruments, Danville, Calif.) is attached to the spectrometer directly beneath the rectangular hole by means of light-tight Cannon connectors. The reference phototube is rigidly held in a plexiglas mount which is fastened directly to the phototube housing. A slit of the same dimensions as that in front of the cell in the spectrometer is placed within the Cannon connectors to define the light beam and to allow approximately the same portion of the spectrum to fall on the reference and sample phototubes. (No attempt was made to optimize the phototubes in this respect.) Care is taken to assure that the reference beam does not strike the anode of the reference phototube and cause shadowing.

The cell is a fully-thermostated 1- × 1-cm² cell similar in design to that described by Pardue and Rodriguez (*5*) but the jacket is cylindrical and made of copper. The opening in the jacket through which the light beam passes is approximately 0.375 inch in diameter.

The sample phototube is disconnected from the existing electronics and external leads are provided. Sample and reference beams are detected by 1P39 phototubes (S-4 response).

All internal surfaces of the modified spectrometer are sprayed with ultra-flat black paint to minimize stray light.

To minimize thermally-generated mechanical stresses and movement, the base of the spectrometer was placed in a box and surrounded with insulating material to increase the thermal time constant of the spectrometer. Instrument warm-up is approximately 4 hours for maximum stability; thus the instrument is turned off only for bulb replacement or other minor repairs.

Control Circuit. The control circuit is essentially that shown in Figure 1 of Pardue and Rodriguez (*5*) with the following changes. The stabilized operational amplifiers are powered from a Philbrick/Nexus 2101 voltage regulator. The −1.35 V in the reference current circuit is dropped through a 20K resistor to a 5K potentiometer and then to ground. The 1M resistor at the input of OA1 in their Figure 1 is replaced with a switch which can be used to select any one of 12 resistance values from 250K to 20M. The feedback of OA1 is capacitive only (0.001 μF). The feedback loop of OA2 contains switches to select resistance values from 1M to 55M and capacitance values from 0.4 μF to 0.002 μF. A 100K potentiometer is in series with the selected resistor and both resistances are in parallel with the selected capacitor. These modifications allow greater versatility in obtaining the desired output voltage and time constant over the useful spectral region of the spectrometer.

EXPERIMENTAL

The spectrometer was evaluated by making transmittance measurements on NiEDTA solutions.

Preparation of NiEDTA Solutions. All glassware was cleaned with hot dichromate cleaning solution, rinsed three times with 3 g/liter EDTA solution, and finally rinsed with distilled water. All solutions were prepared using reagent grade chemicals and distilled water which was passed through a mixed anion–cation resin (Amberlite MB-3).

Four test solutions were prepared. Borosilicate-glass-stoppered bottles, 125-ml capacity, were cleaned and dried thoroughly. Into each bottle was pipetted 100 ml of 0.020*M*, pH 7.0, EDTA solution and 0.0, 1.03, 5.15, or 10.0 ml of a solution 0.00919*M* in NiEDTA and approximately 0.011*M* in free EDTA to give solutions 0.0*M*, 0.937 × 10^{-4}*M*, 4.50 × 10^{-4}*M*, and 8.36 × 10^{-4}*M* in NiEDTA. Each test solution contained at least a 20-fold excess of EDTA which served to keep Ni in the complexed form and to buffer the system at pH 7.0.

Procedure. All absorbance readings were taken at 590 nm. Transfer of solutions was accomplished using a glass syringe with polyethylene "needle." Before filling, cells were rinsed twice with the solution to be observed.

Modified Spectrometer. Dark current was zeroed by placing opaque material in the cell and adjusting the balance control of the sample amplifier until its output was near zero. Distilled water was used for the reference blank as 0.020*M* EDTA had an insignificant absorbance at 590 nm (+0.000007 ± 0.000014 absorbance unit). Transmittance readings were taken from a Hewlett-Packard 3460-A digital voltmeter, corrected for dark current, divided by the interpolated 100% T readings (reference blank) to yield % T, and then converted to absorbance.

Cary 14. All measurements were made against 0.020*M* EDTA in the reference cell. The absorbance of each solution was recorded for 2 minutes on 11-inch-wide chart paper rep-

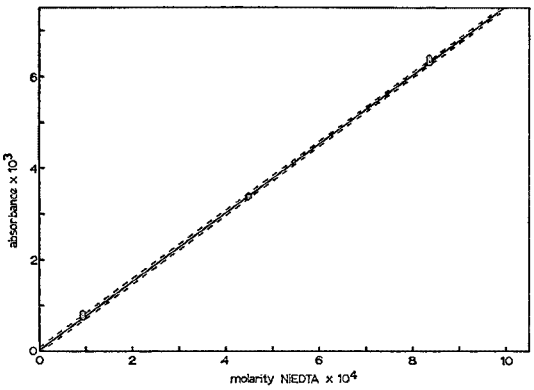

Figure 3. Absorbance *vs.* concentration of NiEDTA

Modified spectrometer
Slope: +7.531 liter mole^{-1} cm^{-1}
Intercept: +0.000035 A.U.
Standard error of estimate: 0.000056 A.U.
Dashed lines represent ± one standard error of estimate

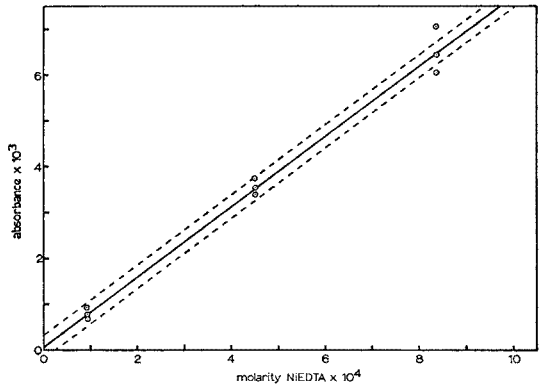

Figure 4. Absorbance *vs.* concentration of NiEDTA

Cary 14
Slope: +7.711 liter mole^{-1} cm^{-1}
Intercept: +0.000077 A.U.
Standard error of estimate: 0.000259 A.U.
Dashed lines represent ± one standard error of estimate

resenting 0.1 absorbance unit full scale. Noise was averaged visually to obtain an absorbance value. Interpolative corrections for changes in blank readings were made to obtain a final, corrected value of absorbance.

RESULTS AND DISCUSSION

Spectrometer Characteristics. The spectral response of the spectrometer described under Instrument Design is shown in Figure 1. For these measurements, the control amplifier (OA1 in Ref. 5) was saturated causing the bulb voltage to be fixed at 6.2 V by the Zener diode. The feedback resistance of the sample beam amplifier was 20 M ohms. If the bulb is operated near its maximum intensity and the maximum feedback resistor in the sample amplifier is 55 M ohms, then an output signal of 1 V representing 100% T is obtainable over the wavelength range from 400 to 625 nm.

Spectrometer performance data are reported for three wavelengths (425, 522, and 600 nm), representing the optimum (522 nm) and two wavelengths on the rapidly changing portions of the spectral response curve. Figure 2 is a recording (recorded directly on tracing paper) of the spectrometer response at 522 nm, illustrating typical short term characteristics. The noise level is observed to be well within 0.0125% T. The sharp noise spike near the right hand side of the figure caused by an electric motor starting near the spectrometer is indicative of the response speed of the system. The spectrometer is observed to exhibit short term drift. If the drift shown in Figure 2 were to continue in the same direction, it would represent a drift of ±0.06% T per hour. In practice, the drift changes directions periodically and tends to oscillate, with a period of about 45 minutes, about a gradually drifting point.

Long-term drift was determined at each of three wavelengths and is summarized in Table I. Drift is defined here as plus or minus one-half the width of the envelope enclosing the signal trace (noise included) on the Sargent Model SR recorder. Results were obtained over consecutive hour-long periods. Data representing the worst, best, and typical performance characteristics are included for the three wavelengths. The response characteristics are observed to be a function of wavelength with comparable performance obtained at 425 nm and 522 nm and slightly poorer performance at 600 nm. Also, the spectrometer has a temperature coefficient. No attempt was made to evaluate an exact temperature coefficient of the spectrometer or the source(s) of the temperature sensitivity. Some improvement over the data in Table I can be achieved by controlling variations in room temperature to be below ±1 °C per hour.

Table I. Long Term Stability of Modified Spectrometer

Wavelength	Number of hours observed	Drift (% T per hour)[a] Highest	Lowest	Average
425 nm	11	±0.018	±0.008	±0.013
522 nm	14	±0.033	±0.007	±0.013
600 nm	10	±0.055	±0.025	±0.036

[a] Room temperature variations of ±1 °C per hour.

Table II. Comparative Data on Two Spectrometers

Instrument	Standard error of estimate, A.U.	Av std dev, A.U.	Drift, absorbance units per hour
Cary 14	0.000259	0.000267	0.001[a]
Modified spectrometer	0.000056	0.000038	±0.0001

[a] Bulletin 100, Cary Instruments, Monrovia, Calif.

Equilibrium Data. Plots of absorbance *vs.* concentration of NiEDTA at 590 nm are shown in Figure 3 for the modified spectrometer and in Figure 4 for a Cary Model 14 spectrophotometer for comparison. Quoted specifications for the latter instrument (Bulletin 100, Cary Instruments, Monrovia, Calif.) are: photometric reproducibility, 0.0005 absorbance unit with 0–0.1 scale; photometric accuracy, 0.0005 absorbance unit with expanded scale.

The dashed lines in Figures 3 and 4 represent plus and minus one standard error of estimate (6) based on the nine

(6) W. E. Deming, "Statistical Adjustment of Data," Wiley, New York, 1943, p 167.

points (triplicate samples at each of three concentrations) shown in each graph. Similar results are obtained by taking the average standard deviations of the three NiEDTA solutions. Comparative data for the two spectrometers are shown in Table II. The standard error of estimate for the modified spectrometer (0-000056 A.U.) indicates that species with an absorbance of 0.0002 may be detected with 99% confidence.

The modified spectrometer has been shown to possess ultra-high stability and high precision necessary for the kinetic measurements discussed at the beginning of this report. The instrument is currently being used to measure precisely the rates of enzyme catalyzed reactions.

RECEIVED for review February 3, 1969. Accepted February 17, 1969. This work was supported in part by PHS Research Grant No. G.M. 13326-03 and in part by a grant from the Indiana Elks Association to Purdue University.

Electrolytic Dissolution of Tantalum, Niobium, and Other Refractory Metals

Abraham Aladjem

Soreq Research Center, Yavne, Israel

IN the analysis of tantalum, niobium, zirconium, tungsten, and other refractory metals, the specimens are usually prepared for analysis by dissolution in a mixture of nitric and hydrofluoric acids followed by several evaporation-dissolution stages. This procedure is cumbersome and laborious, and a new electrolytic dissolution technique developed by us offers greater simplicity and dispenses with the use of hazardous reagents; it would be especially valuable in cases in which the presence of the fluoride ion is objectional. Electrolytic dissolution techniques have found a limited use in analytical chemistry, notably in the case of uranium (*1*).

EXPERIMENTAL

Reagents. A 5% solution of NH_4Cl in methanol is used as the electrolyte: analytical-grade reagents are used, without special precautions to ensure the absence of moisture, because the electrolyte tolerates a moisture content of up to 4% without adverse effects.

Procedure. The dissolution is carried out in borosilicate glass containers, without separation of anolyte from catholyte. Tantalum or platinum wire 0.4 mm in diameter is used as the cathode. The metal to be dissolved serves as the anode, either on a suitable graphite support, or directly connected to the leads.

Dissolution occurs with a current efficiency of over 50% and is accompanied with an evolution of O_2 on the anode. No metal deposition takes place on the cathode. The initial anode-to-cathode surface ratio should be about 1:1 but naturally it decreases in the course of the electrolysis. The anode current density is not critical and may range from 3 to 150 mA/sq cm, but a density of 20-30 mA/sq cm is needed to provide reasonably short dissolution times, and densities beyond 40-50 mA/sq cm are to be avoided because of excessive heating. At current densities of the order of 40 mA/sq cm the time needed to dissolve a tantalum or niobium foil 0.1 mm thick is about 10 minutes; to avoid precipitation (probably of the oxychloride) at least 50 ml of the solution must be used for every gram of metal taken. It is preferable to use a power supply with controlled-current dc output instead of constant voltage because the conductivity of the solution increases with increasing temperature, and as some heat is evolved in the dissolution the temperature of the electrolyte may rise and the current density may rapidly increase beyond the optimum range, causing boiling of the electrolyte.

The electrolyte temperature should be kept below the boiling point but it is not critical except to avoid excessive losses of solvent by evaporation. A clear solution should be obtained at the end of the dissolution, the only possible residue being very thin (30-40 Å) flakes of the natural oxide covering the metal; in most cases these flakes are also dissolved in the process.

RESULTS AND DISCUSSION

The method has been used to dissolve tantalum, niobium, tungsten, zirconium, vanadium, hafnium, titanium, and their alloys—*e.g.*, Ni-14% Ta, Ta-Nb—and no difficulty was experienced with materials from different sources (Fansteel, Heraeus, Metallwerke Plansee) and of varying degrees of purity. Although the method is especially suitable for the dissolution of massive samples or wires which may be connected directly to the leads, crushed samples or even finely divided powders may also be dissolved by supporting them on a graphite plate or preferably on a heavily-anodized (to an oxide thickness of 4000-5000 Å) tantalum dish, which is not attacked at current densities below 50 mA/sq cm provided that the applied voltage does not exceed 10-12 volts.

In some cases the analysis may be continued directly in the methanol solution (preliminary experiments show that colorimetric measurements are possible in such solutions), but in general the methanol is evaporated and the residue is dissolved in the aqueous medium needed for subsequent analytical steps—*e.g.*, HCl or H_2SO_4 solutions—and separation or determination of impurities is carried out by conventional methods.

It should be recalled that some of the refractory metal chlorides are rather volatile; hence, care should be taken not to overheat the residue from the methanol evaporation stage —*i.e.*, the evaporation should be carried out over a water bath.

ACKNOWLEDGMENT

The author thanks Yitshak Marcus of the Hebrew University, Jerusalem, for his valuable comments.

RECEIVED for review November 5, 1968. Accepted December 30, 1968.

(1) R. P. Larsen, ANAL. CHEM., **31**, 545 (1959).

Dielectric Percentage Saturation Detector

E. J. Gelb and S. N. Steen

L. S. G. Industries Corp., P.O. Box 928, Valley Station, Wayne, N.J. 07470

PERCENTAGE SATURATION is defined as the percentage ratio of the existing weight of vapor per unit weight of vapor-free gas to the weight of vapor that would exist per unit weight of vapor-free gas if the mixture were saturated at existing temperature and pressure. In reference to water vapor, the measurement of humidity may be accomplished by wet and dry bulb thermometry for static streams but for process stream analysis the expensive lithium chloride detectors and others are usually used. These devices are only for humidity determination, whereas the detector presented here has unlimited capabilities.

By using the physical property of the dielectric constant of water vapor and its proportionality to capacitance change in an air condenser, a relatively inexpensive adiabatic per cent saturation detector was constructed. This detector is capable of many common industrial saturation analyses, such as solvent recovery in extraction processes. We are limiting ourselves, at this time, to the presentation of scientific data on its use as a per cent humidity device.

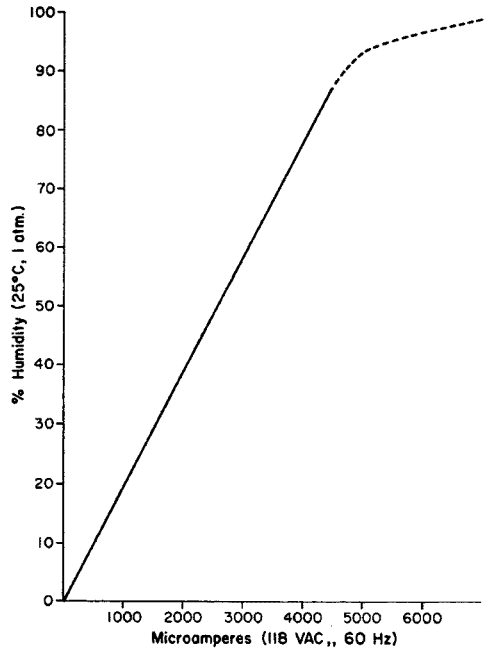

Figure 1. Typical graph illustrating linear dynamic range of detector

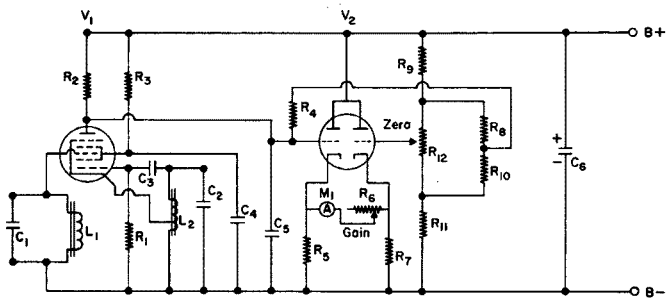

Figure 2. Wiring diagram and parts list of detector

C_1	Sensing cell		
C_2	Reference cell		
C_3	20 pf silvered mica		
$C_{4,5}$	1000 pf molded mica		
C_6	8 mfd 450 V electrolytic		
L_1	Inductor 28 turns with iron dust core		
L_2	Same as L_1 but with cathode tap 8 turns from $B-$		
M_1	1 mA meter movement		
R_1	51K ohm	5%	1/2W
R_2	510K ohm	5%	1/2W
R_3	33K ohm	5%	1/2W
R_4	51 megohms	5%	1/2W
R_5	10K ohm	5%	1 W
R_6	100K ohm	variable gain pot	
R_7	10K ohm	5%	1 W
R_8	4.7K ohm	5%	1/2W
R_9	100K ohm	5%	1/2W
R_{10}	4.7K ohm	5%	1/2W
R_{11}	51K ohm	5%	1/2W
R_{12}	1 megohm	variable zero pot	
V_1	6BE6		
V_2	6SN7		
B+ to B− = 300 V dc			

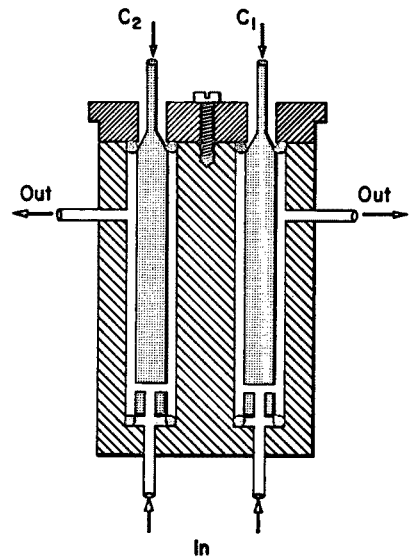

Figure 3. Dielectric percentage saturation detector

This method involving the measurement of a change in the capacitance of a condenser is not new (*1–3*). The dielectric constant of water vapor is greater than that of oxygen, nitrogen, helium, carbon dioxide, carbon monoxide, sulfur dioxide, hydrogen sulfide, methane, etc. Thus water vapor may be readily determined in the presence of the above gases.

A simple circuit was designed and the reference cell of the detector filled with the gases to be normalized at their existing temperature and pressure. Upon changing the water vapor concentration in the sensing condenser, correlation of the percentage humidity was determined.

The detector was separated from the electronic circuit and could be placed in a process stream at temperatures up to 300 °C and pressures up to 100 psi gauge.

The detector exhibited a linear dynamic range of 0.5 to 90.0% humidity (at 25 °C, 1 atm) as typified in Figure 1. A response time of less than one second was recorded for the drift-free amplifier unit shown in Figure 2. The analysis is nondestructive, and the detector shown in Figure 3 is independent of changes in temperature and flow of the stream.

(1) J. Griffith and A. Phillips, *Analyst* (London), **77**, 897 (1952).
(2) D. Turner, *Nature*, **181**, 1265 (1958).
(3) D. Winefordner, ANAL. CHEM., **33**, 515 (1961).

RECEIVED for review December 3, 1968. Accepted January 29, 1969.

An Improved Procedure for Solid Scintillation Fluorography of Tritium Labeled Compounds

Kurt Randerath

The John Collins Warren Laboratories of the Huntington Memorial Hospital of Harvard University at the Massachusetts General Hospital, Boston, Mass. 02114

AUTORADIOGRAPHY of paper and thin layer chromatograms is an important analytical tool in many chemical and biochemical studies involving compounds labeled with ^{32}P, ^{35}S, and particularly ^{14}C. The standard autoradiographic technique is, however, 500–1000-fold less sensitive for ^{3}H than for ^{14}C. Because of their short range, only a few per cent of the primary β-particles of tritium emerge from the surface of the chromatogram. Further losses occur not only in the gap between chromatogram and film, but also in the film itself because the range of the ^{3}H β-particles in the film is shorter than the average distance between the silver halide grains. Organic and inorganic scintillators have been used to convert the energy of the ^{3}H β-particles to light, which in turn produces an image in the film (liquid or solid scintillation fluorography) (*1–4*). Although most literature data are not directly comparable, the sensitivity reported for procedures of tritium autoradiography and fluorography that permit the subsequent recovery of the compounds is 0.1–0.3 $\mu c/cm^2$/day (*5*, *6*). Sensitivity is increased to 0.03 $\mu c/cm^2$/day if the chromatogram itself is treated with an X-ray emulsion, a procedure that precludes the recovery of the labeled compounds (*6*).

This note describes a novel simple procedure for solid scintillation fluorography of ^{3}H-labeled compounds. Its sensitivity is 0.006–0.008 $\mu c/cm^2$/day. The technique has been applied so far only to ^{3}H-labeled nucleotides and their derivatives separated on cellulose (Eastman 6064 sheets) and PEI-cellulose (*7*) thin layers, but there is no reason why its applicability should be restricted to this class of compounds or to cellulose-based thin layers.

(1) A. T. Wilson, *Biochim. Biophys. Acta*, **40**, 522 (1960).
(2) E. V. Parups, I. Hoffman, and H. R. Jackson, *Talanta*, **5**, 75 (1960).
(3) U. Lüthi and P. G. Waser, *Nature*, **205**, 1190 (1965).
(4) S. Prydz and K. S. Skammelsrud, *J. Chromatogr.*, **32**, 732 (1968).
(5) G. S. Richardson, I. Weliky, W. Batchelder, M. Griffith, and L. L. Engel, *ibid.*, **12**, 115 (1963).
(6) J. Chamberlain, A. Hughes, A. W. Rogers, and G. H. Thomas, *Nature*, **201**, 774 (1964).

EXPERIMENTAL

A 7% (w/v) solution of 2,5-diphenyloxazole (PPO) in diethyl ether is rapidly poured over the entire chromatographic area and is distributed evenly by tilting. This operation should take no longer than 2–5 seconds depending on the size of the layer. The chromatogram is then immediately brought into a vertical position and allowed to dry for a few minutes. The volume of the PPO solution used for this treatment is 40 $\mu l/cm^2$—*i.e.*, 16 ml for a 20 × 20-cm layer. The layer is covered with Kodak RB-54 Royal Blue Medical X-Ray film and placed between two glass plates which are held together firmly with adhesive tape. Exposure is carried out in an insulated box over dry ice (−78.5 °C) in the dark for a few hours to a few days. The film is developed with Kodak Liquid X-Ray Developer and fixed with Kodak Liquid X-Ray Fixer according to the specifications of the manufacturer.

RESULTS AND DISCUSSION

The sensitivity of this procedure was found to be 0.006–0.008 $\mu c^3H/cm^2$/day. On one-dimensional thin-layer chromatograms (spot area 0.3 cm^2) 0.002–0.003 μc^3H can be clearly visualized after exposure for 24 hours. The sensitivity depends on (a) the concentration of the scintillator, (b) the solvent in which the scintillator is applied to the chromatogram, (c) the mode of application of the scintillator, (d) the temperature during the exposure, and (e) the film material. Because a systematic study of these factors except for (d) (*3*), has not been reported in the literature, we have

(7) K. Randerath and E. Randerath in "Nucleic Acids," vol. XII A of "Methods in Enzymology," S. P. Colowick and N. O. Kaplan, Eds., Academic Press, New York, N. Y., 1968, p 323.

briefly summarized our results pertinent to the factors influencing the over-all sensitivity of the procedure.

(a) 7–10% PPO was found to be the optimum concentration range; at lower concentrations sensitivity is lower. Increasing the scintillator concentration to >10% results in irregular blackening of the photographic emulsion and in decreased sensitivity. Addition of a wavelength shifter like 2-(α-naphthyl)-5-phenyloxazole does not improve the final image. The autoradiographic sensitivity (without PPO treatment) for ^{3}H is 0.15 $\mu c/cm^2$/day on Kodak Royal Blue film and 0.4–0.5 $\mu c/cm^2$/day on Kodak No-Screen Medical X-Ray film.

(b) Application of the scintillator in diethyl ether results in homogeneous distribution of PPO over the entire chromatographic area. Substituting less volatile solvents for ether may lead to uneven distribution of the scintillator, which in turn produces uneven blackening of the film. Methanol is suitable, but aromatic hydrocarbons are not.

(c) It is difficult to apply a scintillator solution of sufficient concentration by spraying, because the jet tends to get blocked by scintillator crystals. Incorporation of the scintillator into the chromatographic support prior to carrying out the separation, as has been described for anthracene (*3*), may cause separation problems (artifacts, inadequate resolution, etc.)

(d) Exposure at low temperature [*cf.* (*3*)] is essential; at room temperature sensitivity of scintillation fluorography of ^{3}H is 15–20 times lower than at −78.5 °C. No such temperature dependence was noticed in autoradiography—*i.e.*, without PPO treatment.

(e) Kodak Royal Blue Medical X-Ray film, a blue-sensitive screen-type X-ray film, was found to be best suited for the fluorographic procedure described; its replacement by Kodak No-Screen Medical X-Ray film results in an approximately 10-fold loss in sensitivity. The sensitivity of GAF-X Medical X-Ray film (Ansco) is only slightly lower than that of Royal Blue film. Kodak Blue Brand Medical X-Ray film, another screen-type blue-sensitive film, appears to be less sensitive to the light emitted by the scintillator than either Royal Blue or GAF-X film.

The radioactive nucleotides, nucleosides, or nucleic acid bases may be recovered by extraction with aqueous solutions after removal of the scintillator by soaking the chromatograms in ether.

In the case of ^{14}C-labeled compounds the fluorographic procedure described in this note was found to be of approximately the same sensitivity as autoradiography (lower limit of detection 0.0005 $\mu c/cm^2$/day). The fact that neither a scintillator effect nor a temperature effect is observed in this case appears to indicate that the contribution of the emitted light to the over-all ^{14}C-sensitivity is negligible. Although, for the detection of ^{14}C, no-screen-type X-ray film appears to be as sensitive as blue-sensitive screen-type film, we prefer the latter because of its less dense background.

ACKNOWLEDGMENT

The author thanks G. Litt, E. Randerath, and P. C. Zamecnik for helpful discussions.

RECEIVED for review January 17, 1969. Accepted March 7, 1969. Work supported by grants-in-aid from the U. S. Atomic Energy Commission (AT(30-1)-2643) and the American Cancer Society (P-516).

Orion makes the common laboratory pH meter into the most versatile analytical instrument available.

Read 6 electrodes on one pH meter

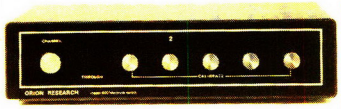

The model 605 is the 6-channel electrode switch that makes it possible to use a single pH meter with as many as six pH or specific ion electrodes – eliminates connecting and disconnecting electrodes. Individual controls for electrode calibration.

Use any pH meter as a volt-ohmmeter

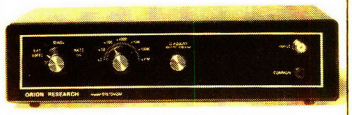

Model 615 volt-ohmmeter converter for all pH meters – or make the Orion Model 801 Digital pH/mv Meter do double duty as a **Digital Volt-Ohmmeter.** 1 volt output for 1, 10, 100, 1000 volts full scale or 1 K, 10 K, 100 K, 1 M, 10 M, 1000 M full scale.

The Model 801 digital pH/mv meter



The most sophisticated pH meter available today – binary-coded – decimal output for interfacing to printers, card punches, and computers.

ORION RESEARCH INC.
11 blackstone street
cambridge, massachusetts 02139

Circle No. 126 on Readers' Service Card

Here's Mettler's latest catalog on analytical balances

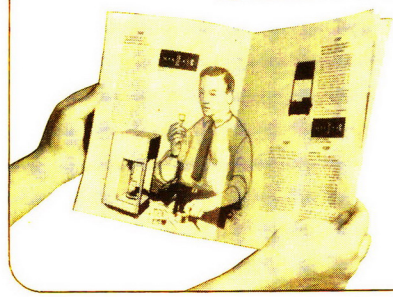

This 22-page catalog covers every feature and spec of Mettler's line of analytical balances. Described are the H balances — from the low-cost student model to automatic printout and sophisticated electronic units. Included are macros, semi-micros, micros and ultra-micros.

All are available from major laboratory supply dealers for demonstration, trial or immediate delivery.

For your copy of the new catalog, write Mettler Instrument Corp., 20 Nassau St., Princeton, N.J. 08540.

Mettler®

Circle No. 47 on Readers' Service Card

Analytical Chemistry

JUNE 1969

Valid through October 1969

NEW PRODUCTS, NEW CHEMICALS, MFG. LITERATURE:

401 402 403 404 405 406 407 408 409 410 411 412 413 414 415
416 417 418 419 420 421 422 423 424 425 426 427 428 429 430
501 502 503 504 505 506 507 508 509 510 511 512 513 514 515
601 602 603 604 605 606 607 608 609 610 611 612 613 614 615
616 617 618 619 620 621 622 623 624 625 626 627 628 629 630
631 632 633 634 635 636 637 638 639 640 641 642 643 644 645

ADVERTISED PRODUCTS:

1	26	51	76	101	126	151	176	201	226	251	276	301
2	27	52	77	102	127	152	177	202	227	252	277	302
3	28	53	78	103	128	153	178	203	228	253	278	303
4	29	54	79	104	129	154	179	204	229	254	279	304
5	30	55	80	105	130	155	180	205	230	255	280	305
6	31	56	81	106	131	156	181	206	231	256	281	306
7	32	57	82	107	132	157	182	207	232	257	282	307
8	33	58	83	108	133	158	183	208	233	258	283	308
9	34	59	84	109	134	159	184	209	234	259	284	309
10	35	60	85	110	135	160	185	210	235	260	285	310
11	36	61	86	111	136	161	186	211	236	261	286	311
12	37	62	87	112	137	162	187	212	237	262	287	312
13	38	63	88	113	138	163	188	213	238	263	288	313
14	39	64	89	114	139	164	189	214	239	264	289	314
15	40	65	90	115	140	165	190	215	240	265	290	315
16	41	66	91	116	141	166	191	216	241	266	291	316
17	42	67	92	117	142	167	192	217	242	267	292	317
18	43	68	93	118	143	168	193	218	243	268	293	318
19	44	69	94	119	144	169	194	219	244	269	294	319
20	45	70	95	120	145	170	195	220	245	270	295	320
21	46	71	96	121	146	171	196	221	246	271	296	321
22	47	72	97	122	147	172	197	222	247	272	297	322
23	48	73	98	123	148	173	198	223	248	273	298	323
24	49	74	99	124	149	174	199	224	249	274	299	324
25	50	75	100	125	150	175	200	225	250	275	300	325

RUSH: I have an immediate use for these advt. products I've circled above:

Name _____ Position _____ Company _____ Address _____ Zip _____

FIRST CLASS
Permit No. 1538
New York, N. Y.

BUSINESS REPLY CARD
NO POSTAGE STAMP NECESSARY IF MAILED IN THE UNITED STATES

POSTAGE WILL BE PAID BY

ANALYTICAL CHEMISTRY

PUBLISHER'S DATA CENTER, INC.

132 WEST 31ST STREET

NEW YORK, N. Y. 10001

The Silver Billet Electrode is Obsolete!



The Silver Billet Electrode was used to measure chloride ion. But it had to be anodized before use, and it developed redox potential errors when oxidizing agents were present — for example, ferric, cupric, chromate, or permanganate ions.

The ORION Solid State Chloride Electrode is always ready to use, and is immune to redox potential errors. It makes possible the simple, direct measurement of chloride ion in foods, ground waters, soils, plant effluents, and hundreds of other types of samples. Measurements can be made down to a few parts per million, regardless of color and turbidity. Another example of the new technology for chemical measurement — from ORION.

Orion Research Incorporated 11 Blackstone Street Cambridge, Mass. 02139

Circle No. 55 on Readers' Service Card

FROM COLEMAN...

NEW SPECTROPHOTOMETER

Now! A high resolution instrument at moderate cost

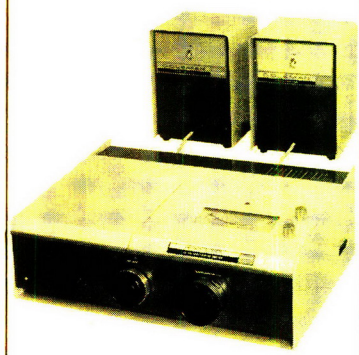

MODEL 111 UV-VIS SPECTROPHOTOMETER

Provides spectral bandpass of 2 mμ which is constant throughout the range of 200 to 900 mμ, with wavelength accuracy better than 0.5 mμ. Features exclusive dual-range phototube detector and a dual light source. Accessories extend the uses of this high performance, economical instrument. *Request Bulletin A-326.*

Write to Coleman Instruments, Division of The Perkin-Elmer Corporation, 42 Madison St., Maywood, Illinois 60153

PERKIN-ELMER

Circle No. 22 on Readers' Service Card

Name _____ Position _____ Company _____ Address _____ Zip _____

FIRST CLASS
Permit No. 1538
New York, N. Y.

BUSINESS REPLY CARD
NO POSTAGE STAMP NECESSARY IF MAILED IN THE UNITED STATES

POSTAGE WILL BE PAID BY

ANALYTICAL CHEMISTRY

PUBLISHER'S DATA CENTER, INC.

132 WEST 31ST STREET

NEW YORK, N. Y. 10001

Analytical Chemistry **JUNE 1969** Valid through October 1969

NEW PRODUCTS, NEW CHEMICALS, MFG. LITERATURE:
401 402 403 404 405 406 407 408 409 410 411 412 413 414 415
416 417 418 419 420 421 422 423 424 425 426 427 428 429 430
501 502 503 504 505 506 507 508 509 510 511 512 513 514 515
601 602 603 604 605 606 607 608 609 610 611 612 613 614 615
616 617 618 619 620 621 622 623 624 625 626 627 628 629 630
631 632 633 634 635 636 637 638 639 640 641 642 643 644 645

ADVERTISED PRODUCTS:

1	26	51	76	101	126	151	176	201	226	251	276	301
2	27	52	77	102	127	152	177	202	227	252	277	302
3	28	53	78	103	128	153	178	203	228	253	278	303
4	29	54	79	104	129	154	179	204	229	254	279	304
5	30	55	80	105	130	155	180	205	230	255	280	305
6	31	56	81	106	131	156	181	206	231	256	281	306
7	32	57	82	107	132	157	182	207	232	257	282	307
8	33	58	83	108	133	158	183	208	233	258	283	308
9	34	59	84	109	134	159	184	209	234	259	284	309
10	35	60	85	110	135	160	185	210	235	260	285	310
11	36	61	86	111	136	161	186	211	236	261	286	311
12	37	62	87	112	137	162	187	212	237	262	287	312
13	38	63	88	113	138	163	188	213	238	263	288	313
14	39	64	89	114	139	164	189	214	239	264	289	314
15	40	65	90	115	140	165	190	215	240	265	290	315
16	41	66	91	116	141	166	191	216	241	266	291	316
17	42	67	92	117	142	167	192	217	242	267	292	317
18	43	68	93	118	143	168	193	218	243	268	293	318
19	44	69	94	119	144	169	194	219	244	269	294	319
20	45	70	95	120	145	170	195	220	245	270	295	320
21	46	71	96	121	146	171	196	221	246	271	296	321
22	47	72	97	122	147	172	197	222	247	272	297	322
23	48	73	98	123	148	173	198	223	248	273	298	323
24	49	74	99	124	149	174	199	224	249	274	299	324
25	50	75	100	125	150	175	200	225	250	275	300	325

RUSH: I have an immediate use for these advt. products I've circled above: _____ _____ _____ _____ _____

Three elegant approaches to the determination of the negative logarithm of the hydrogen-ion concentration.

Our Indoor/Outdoor pH Meter:

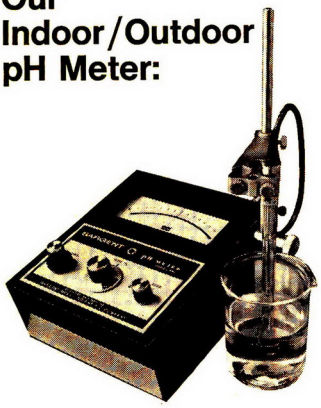

MODEL PBL. Indoors, it plugs into AC power. Outdoors, it switches over to batteries. Obviously, it's portable. 360-degree-pivot, mount-on-either-side electrode support. Reads accurately in virtually any position, because the PBL has a rugged steel case, shock-resistant taut-band meter, plus solid-state circuitry. Ranges: 0 to 14 pH (0 to ±1000 mv). Two-point calibration. Provisions for Karl Fischer titrations, automatic-temperature compensation, and recorder output. All in the Model PBL. All for $230.

Our Tells-It-Like-It-Is pH Meter:

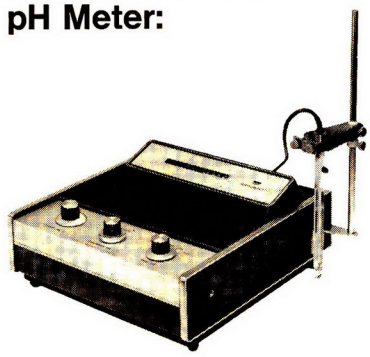

MODEL DR. Digital counter plus graduated scale for direct, continuous readout to 0.001 pH, without need to switch scales or re-calibrate. The DR's accuracy: ±0.01 pH (absolute), with a repeatability of ±0.002 pH. An accuracy immune to the effects of mechanical wear or electrical aging. High input impedance accommodates all electrodes. Proved, Sargent-Welch automatic self-balancing system for drift-free stability. Dependable solid-state circuitry. The Model DR—visible precision. Priced at $600.

Our Laboratory-Workhorse pH Meter:

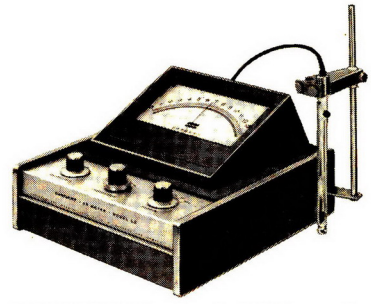

MODEL LS. Simple, straightforward design. Like a large, easy-to-read, easy-to-interpolate scale that sits up where you can see it. And an accuracy of ±0.03 pH (repeatability of ±0.01 pH). Solid-state, stable, reliable circuitry. Plus some features you might not expect: buffer-adjust control, Karl Fischer polarizing outlet, recorder output, manual or provision for automatic temperature compensation. Some of the reasons why LS stands for Laboratory Standard. A lot of pH meter for $355.

Select one (or more).

Decide with the help of your Sargent-Welch representative. Call him for a demonstration. Or write to us. 9-217

SARGENT-WELCH

Scientific instruments, apparatus, chemicals.
Sargent-Welch Scientific Company
4647 Foster Ave.; Chicago, Ill. 60630

Chicago/Anaheim/Birmingham/Cincinnati
Cleveland/Dallas/Denver/Detroit
Springfield, N.J./Toronto/Montreal/Vancouver

Circle No. 63 on Readers' Service Card

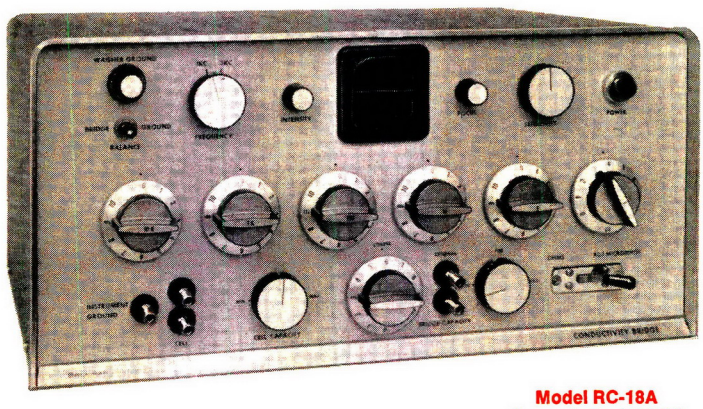

Model RC-18A
Accurate to ±0.05%

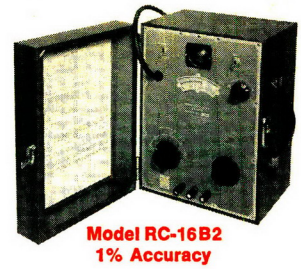

Model RC-16B2
1% Accuracy

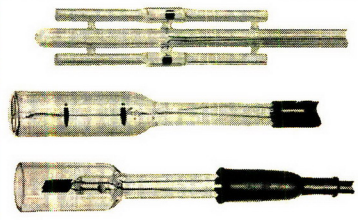

Laboratory Conductivity Cells

FOR ACCURATE MEASUREMENTS OF SOLUTION CONDUCTIVITY

RC-18A CONDUCTIVITY BRIDGE — Provides compactly and economically in one housing, an oscillator that provides both 1,000 and 3,000 Hz bridge current, decade and ratio resistors that comprise the bridge, decade and continuously variable capacitors that facilitate reactive balance, a modified Wagner ground balance, a sharply tuned high-gain amplifier, and a 2″ CRT null detector. Accuracy of the bridge is ±0.05% of the reading above 300 ohms while below this value it is limited by the resolution of the last decade dial. Sensitivity exceeds 0.005%. The overall instrument range is 0-111,111 ohms in steps of 0.1 ohms and 0-11,111 micromhos in steps of 0.01 micromho.

RC-16B2 CONDUCTIVITY BRIDGE — Line operated, compact, general purpose laboratory instrument with uniform 1% accuracy over the *whole* range of the instrument and sensitivity at least three times better. Extremely wide range: 0.2 to 2,500,000 ohms and 0.4 to 5,000,000 micromhos. True AC Wheatstone Bridge measuring circuit requires no adjustments to readout in absolute ohms. "Eye" tube null indicator for clear indication of electrode polarization. When used with conductivity cells of appropriate cell constants, the entire range of electrolytic conductivity from that of ultra-pure demineralized water to concentrated strong acids is easily covered.

LABORATORY CONDUCTIVITY CELLS — Choose from a complete range of pyrex glass dip cells with cell constants within ±1% of nominal value for use with the RC-16B2.

Jones type cells with cell holders and constant temperature bath available for use with the RC-18A.



ELECTROLYTIC CONDUCTIVITY IS OUR BUSINESS and we'd like to tell you about our other bridges, cells and accessories designed exclusively for laboratory solution conductivity measurements. A set of three highly informative pamphlets are available just for the asking. Write today to .....

Beckman INSTRUMENTS, INC.

CEDAR GROVE OPERATIONS

89 COMMERCE ROAD
CEDAR GROVE, NEW JERSEY • 07009

INTERNATIONAL SUBSIDIARIES: Geneva; Munich; Glenrothes, Scotland; Tokyo; Paris; Capetown; London; Mexico City.

Circle No. 91 on Readers' Service Card

See ACS Laboratory Guide for All Products/Sales Office

NEW PRODUCTS

Equipment
Apparatus
Instruments

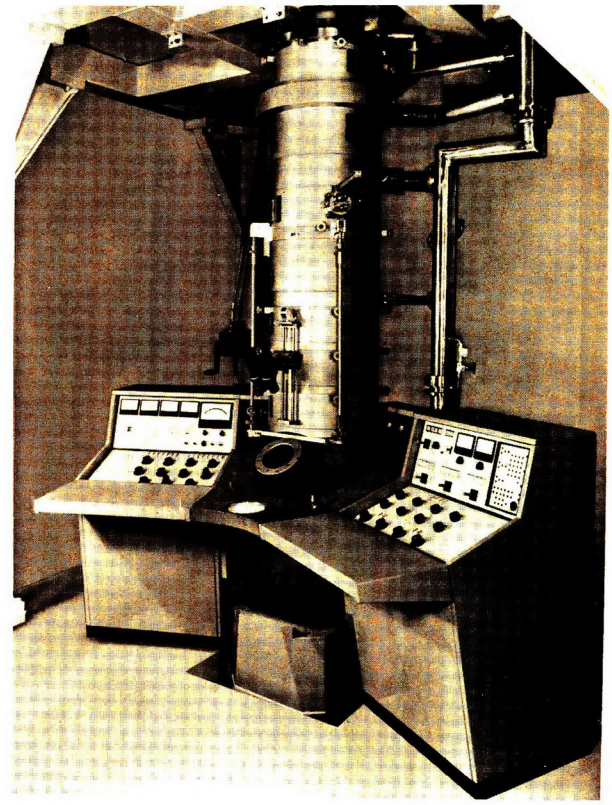

Model EM7, a one-million volt electron microscope, can be used in biological and material science research. Voltage is upgradeable to 1.5 million volts resulting in an increase in electron penetration of specimens and reduction in electron scattering within a specimen. This high-voltage beam provides the potential for achieving the theoretical resolution of 1 A. Considering that the distance between centers of two atomic nuclei is about 3 Å, visualization of subatomic particles is now theoretically possible. The availability of the EM7 is announced by Picker Nuclear in conjunction with GEC-AEI Ltd. Picker Nuclear, 1275 Mamaroneck Ave., White Plains, N.Y. 10605

401

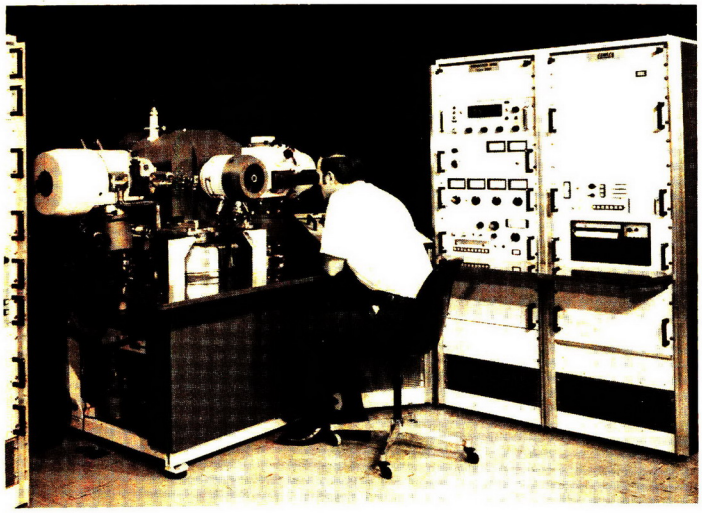

Type 27-201 ion microanalyzer combines the features of a mass spectrometer with an ion emission microscope to provide an instant photomicrograph of the chemical distribution of a specimen. The analyzer is capable of detecting all elements on the periodic chart, including isotopes of elements, with sensitivities down to the ppb level. Spatial resolution of approximately one micron is obtainable. By means of push-button controls, it is possible to program up to 10 specific elements to be analyzed. Bell & Howell, CEC/Analytical Instruments Division, 1500 S. Shamrock Ave., Monrovia, Calif. 91016

402

KRYPTON

Kr

Krypton. We have it for you pure or ultra pure or radioactive. In all kinds and sizes of containers.

For this year's catalog, write: Rare and Specialty Gases Dept., Airco Industrial Gases, 150 East 42nd Street, New York, N.Y. 10017.

AIRCO
Industrial Gases



Circle No. 7 on Readers' Service Card

New Products

Multichannel Analyzer

Model 5401A analog-to-digital converter features a clock rate of 200 MHz and makes a 10-bit A-to-D conversion in 9.5 μsec, 12 bits in 30.5 μsec. Standard memory is 1024 channels but is expandable to 4096 or 8192 channels. Model 5401A features a digital offset control which displaces the base line zero reference by any one of seven different numbers of channels, from 512 to 3584. This allows maximum resolution over a selected portion of the spectrum with fewer channels of memory. An interlaced display allows presentation of 4096 or 8192 channels without flicker. In this mode, every fourth channel is displayed during a CRT sweep, but a different set of channels is presented on each sweep. A front panel meter helps the operator make input count-rate adjustments by showing either the input count rate or the percentage dead time. Hewlett-Packard Co., 1501 Page Mill Rd., Palo Alto, Calif. 94304 **403**

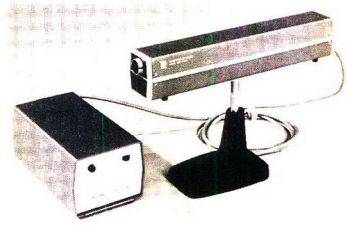

Model 133 He-Ne laser delivers one milliwatt of power (TEMoo) minimum at 632.8 nanometers. For versatility, the laser head and power supply are packaged separately. Model 133 features an internal mirror tube incorporating advances in cathode design, plasma tube sealing, and dielectric coating. Tube lifetime exceeds 5,000 hours. Intermode amplitude noise is less than 0.3% rms and amplitude ripple is less than 0.5% rms. Beam diameter is 0.8 millimeter and beam divergence is one milliradian. Spectra-Physics, Inc., 1250 W. Middlefield Rd., Mountain View, Calif. 94040 **404**

Spectrochemical Source Unit

Model 7100 high repetition rate spectrochemical source unit is a solid state electronic instrument that provides push button selection of various electrical source conditions to minimize the time required to perform optical emission spectrochemical analyses. Featuring rapid automatic switching from one set of electrical conditions to another,

CARVER LABORATORY PRESS

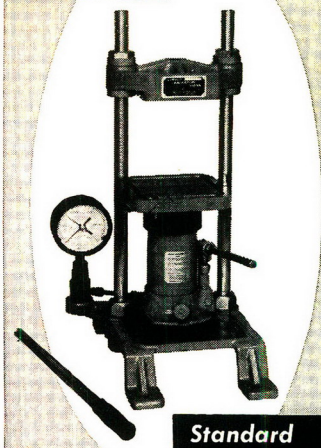

Standard For Research

. . . solves the pressing problem of forming KBr Pellets

Many insoluble materials, mixed with Potassium Bromide, can be formed in a die **under pressure** into pellets or wafers for quantitative and qualitative analysis.

The CLP supplies the pressure — up to 40,000 lbs., if needed.

This specific use is only one of the ways this versatile laboratory assistant meets the challenge of research and development.

Some of the many uses are:

- Dehydrating
- Pressing out various oils, stearines and waxes
- Pressure filtering of thick fluids
- Compression tests
- Fatty acid determinations
- Plastic molding, forming and blocking
- Embossing and forcing
- Pressing mother liquors from crystals
- Extracting Vaccines and Viruses

(The NEW Carver Laboratory Press (Model C-12 ton) complete with Gauge $430.00

20 Ton Models also available — additional Standard Accessories for other applications can be supplied.

Send for latest bulletin.

FRED S. CARVER INC.
HYDRAULIC EQUIPMENT
54 RIVER ROAD, SUMMIT, N. J.

Circle No. 19 on Readers' Service Card

LOOK AT THE

New Look

IN ARL SPECTROCHEMICAL INSTRUMENTS

MODERN in design, functional, easy to operate, these new automatic instruments are fully proven in rigorous application tests. All are available with a variety of outputs — direct reading or computer interfaced. All carry the famed ARL seal of dependability and design excellence.

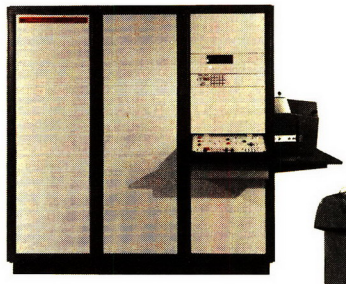

SELF-CONTAINED AUTOMATIC. Model 127 QVAC. A complete optical emission quantometer, including source unit, vacuum spectrometer, air conditioner, vacuum pump, power supplies and readout system. Measures 1700-4070A with integral argon sample stand. Up to 44 simultaneous analysis channels with 60 individual detectors.



MULTICHANNEL X-RAY. Model 128 PMXQ (Production Multichannel X-ray Quantometer) is all new for really rapid x-ray fluorescence analysis. Up to 22 simultaneous determinations in less than a minute. Fully focusing x-ray optics, fixed and/or scanning spectrometers, automatic readout.

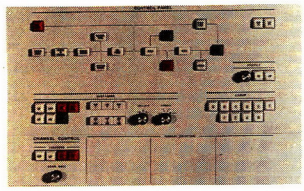

SYNOPTIC PANELS. New on all ARL instruments shown here is the "sequence schematic" operators' panel — a color coded push button panel that practically thinks for itself to speed tests and enhance operator efficiency.



HIGH REP RATE SOURCE UNIT. Model 7100. Features rapid push button selection of five spectrometer source conditions, with rep rates to 400 sparks per second. This automatic, self contained instrument slashes the time required for spectrochemical analysis.



ION MICROPROBE MASS ANALYZER. New, completely proven, the IMMA produces an ion beam two microns or less in diameter, which analyzes solid materials with a unique mass spectrometer. IMMA detects very low concentrations and all isotopes.

BROCHURES AVAILABLE on all these beautiful new instruments.

APPLICATIONS SERVICE. ARL produces more than half the spectrochemical instruments in the USA of the types shown here. There must be a reason for this leadership . . . why not take advantage of ARL knowhow; ask for applications engineering assistance, whether a small job or a complete evaluation program.

APPLIED RESEARCH LABORATORIES

Subsidiary of Bausch & Lomb

9545 Wentworth Street, Sunland, California 91040

Telephone: (213) 352-6011

ARL

Circle No. 9 on Readers' Service Card

Most precise metering pump you can buy—.02%!

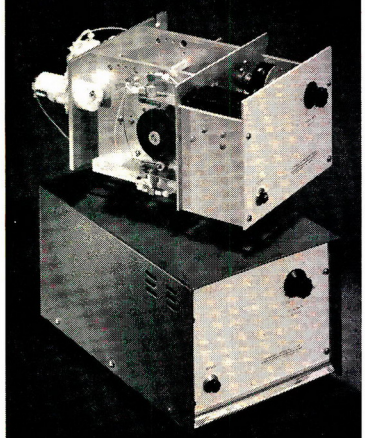

This field-proven chemically-inert pump sets pulse-free flows repeatable to .02% at pressures to 500 psi. Two cam-actuated pistons driven through a gear shift by a synchronous motor produce a smooth, constant flow, independent of liquid pressure and viscosity.

Flow rates of 2.4, 6, 12, 24, 60 and 120 ml/hour or 12, 30, 60, 120, 300 and 600 ml/hour are selected by front-panel gear shift with an absolute accuracy of 0.2%. When you set "60 ML/HOUR," you get 60 ml/hour ±0.2%. And the rate you get is repeatable from day to day to within 0.02%.

You can pump nearly any liquid—however reactive—because only Teflon, Kel-F and borosilicate glass touch the stream. No rubber "O" rings or steel parts contact the liquid.

The pulse-free high-pressure model has a unique feature, a third pre-pressuring piston that prevents flow transients when the valves switch from one drive cylinder to the other.

Cost is $980 to $1480, depending on maximum flow and pressure ratings.

CHROMATRONIX

Chromatronix, Incorporated, 2743 Eighth St., Berkeley, Calif. 94710. Phone (415) 841-7221

Circle No. 21 on Readers' Service Card

the 7100 provides variable spark discharge rates to 400 per second. Up to four pre-set source conditions, plus a 10 A dc arc, can be selected by front panel push buttons. Solid state switching circuits change the capacitance, resistance, and inductance parameters almost instantaneously. Applied Research Laboratories, 9545 Wentworth St., Sunland, Calif. **405**

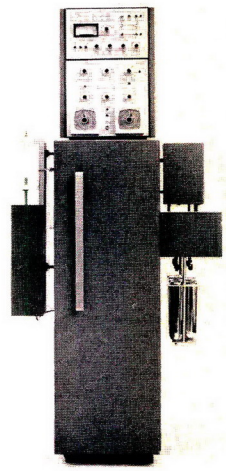

Model 750 Prepkromatic, for high resolution, preparative scale separations, features bi-wall annular columns, automatic injector, trouble-free collection system, and temperature programming. The column oven holds up to 30 sections of 2.5 feet by ¾ inch bi-wall annular column in series. Maximum oven temperature is 500 °C and gradients are kept to a minimum. The automatic injector allows reproducible operation from 200 μl to 2 ml in 200 μl increments with accuracy of ±0.5%. Six glass traps are accommodated in the collection system. All types of samples can be handled by the collection system. SCR control and temperature programming provide either automatic or manual operation. Nester/Faust Mfg. Corp., 2401 Ogletown Rd., Newark, Del. 19711 **406**

Column Monitoring System

Model DB-G monitors liquid-column chromatography effluents at one or more wavelengths over the range of 190 to 800 millimicrons. Designed around the DB-G UV spectrophotometer, the system includes a concentration converter, a wavelength programmer, and an automatic fraction collector. Data can be presented on a re-

a portable FURNACE

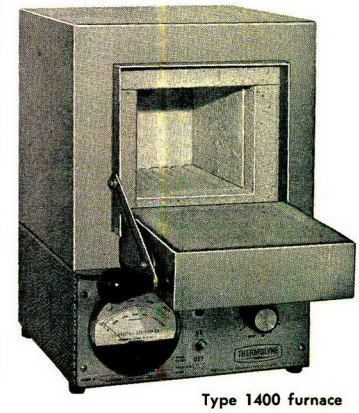

Type 1400 furnace

FAST HEAT

For schools, shops or labs to 1650°F (899°C) in 40 minutes.

PORTABLE

Weighs only 16 lbs.; plugs into ordinary outlets.

STEPLESS CONTROLS

To 1900°F (1038°C). Temperature conveniently and accurately held.

ELEMENTS EMBEDDED

Exclusive refractory plates avoid sag and damage.

QUALITY CONSTRUCTION

Welded steel case with thick insulation is strong, long-lasting. Controls kept cool for long life. Newly designed door forms work loading shelf.

Type 1300 — chamber 4" W x 3¾" H x 4½" D. Prices $97.50

Type 1400 — chamber 4⅞" W x 4 ¼" H x 6" D. Price $125.00

Write for *free* Catalog

THERMOLYNE
SYBRON CORPORATION

2555 KERPER BLVD.
DUBUQUE, IOWA 52001

Circle No. 69 on Readers' Service Card

Now!

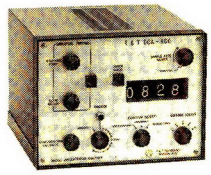

direct readout for your atomic absorption spectrophotometer.

The DCA 800 digital concentration analyzer is a new hybrid computer that permits direct accurate readouts in absorbance (optical density) or in concentration. The completely solid state instrument features an automatic Beers Law function solver, rapid analog-to-digital conversion by a dual slope integrator, single knob adjustment for concentration calibration, full range curvature correction and data averaging for 2, 4, 8, or 16 separate readings. The analyzer has four digit numerical readout and provides a simultaneous signal for pick-up by a computer/printer. In addition to computer-ready information, teletype and printer output are available.

For more information please call or write:

T&T TECHNOLOGY, INC.

813 Stewart Street
Madison, Wisconsin 53713
Area Code 608 257-4511

Circle No. 116 on Readers' Service Card

FREE!

16-PAGE CATALOG ON TEFLON LABWARE

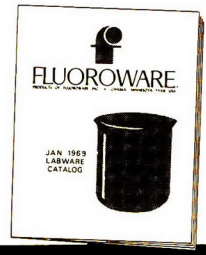

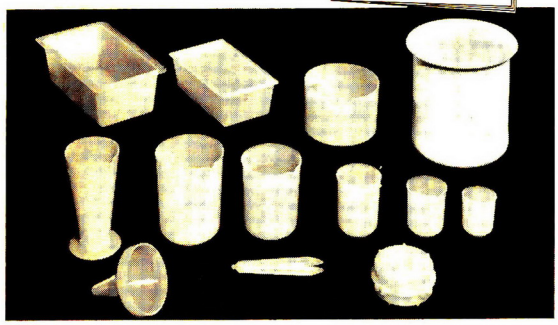

Fluoroware labware is made of FEP Teflon*, the closest thing there is to an ideal labware material—inert, useable at extreme temperatures, unwettable and unbreakable. And Fluoroware knows the secret of molding Teflon into perfect shapes with good see-through properties.

Write for a copy of Fluoroware's "Labware Catalog", including information on its physical and chemical properties.

*DuPont Trademark

FLUOROWARE.

Chaska, Minnesota 55318 • Phone 612-448-3131

Circle No. 33 on Readers' Service Card

new electronic potentiostats

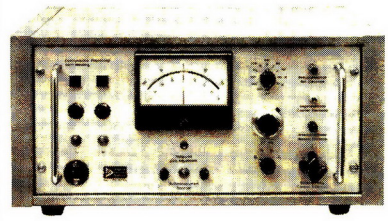

A new line of Wenking Electronic Potentiostats for various electrochemical investigations is now available. Three basic series are offered: a new laboratory model for routine requirements; a new standard series including several "high current" models (to ±10A); and a new "fast rise" series for shortest rise times and/or high output voltages.

Accessory systems, including a high precision voltmeter and motor potentiometers, are also available. For complete up-to-date information on the most widely used Electronic Potentiostats, request our Data File on the new Wenking models.

BRINKMANN INSTRUMENTS

CANTIAGUE ROAD, WESTBURY, N.Y. 11590/ED 4-7500

Circle No. 93 on Readers' Service Card

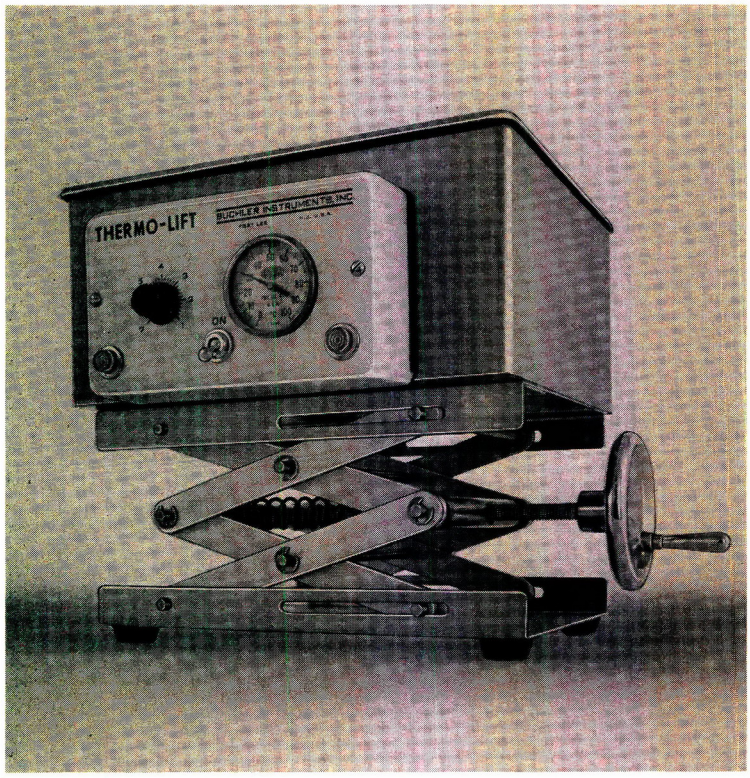

new from Buchler . . .

THERMO-LIFT™

CONTROLLED HEATING BATH

The new Thermo-Lift is a combination of a lift and a temperature controlled water bath that may be adjusted from a minimum height of 8″ to a maximum height of 16″. Made of stainless steel, the water bath is 8″x 10″ x 4″ deep. An automatic thermoregulator controls temperature to within 0.2°C accuracy. This new instrument is useful as a source of heat for rotary evaporators, for distillation procedures and for certain applications where flexibility in operational height is required. The versatile Thermo-Lift may be moved quickly and easily from one application to another.

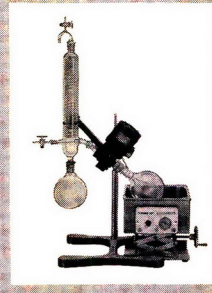

LABORATORY APPARATUS • PRECISION INSTRUMENTS

BUCHLER INSTRUMENTS, INC.

1327 16TH STREET, FORT LEE, NEW JERSEY 07024

For further information request bulletins SPF-1060A and SFE-1000B

Circle No. 130 on Readers' Service Card

corder, a teletype, or a printer. A hydrogen lamp power supply is available for applications requiring hydrogen or deuterium energy sources. Beckman Instruments, Inc., 2500 Harbor Blvd., Fullerton, Calif. 92634 **407**

Clinical Laboratory System

The GeMSAEC is a microanalytical system using a rotor containing 15 cuvettes which spin past a light beam. A signal is displayed on an oscilloscope and a peak is observed continuously for each cuvette. Standards, samples, and reagents are placed in a central loading disc, and all solutions move out into the cuvettes by centrifugal force. These solutions are mixed by a short burst of air bubbles drawn through the combined samples and reagents. Fifteen analyses are performed simultaneously in 30 seconds after the rotor is started and data is obtained photographically or fed directly into a computer for analysis. In the GeMSAEC samples are analyzed in parallel and the system offers the capacity to do 15 analyses in the time it took previously to do one sample.

Instrumentation and hardware developed at ORNL in the Molecular Anatomy (MAN) Program and the Body Fluids Analysis Program were presented in a conference held May 26 at Oak Ridge. F. C. Von der Lage, Office of Industrial Cooperation, Oak Ridge National Laboratory, P.O. Box X, Oak Ridge, Tenn.

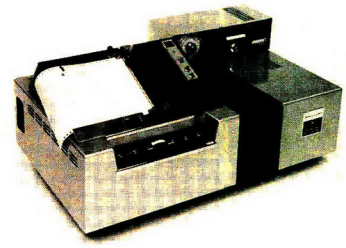

Model 402 UV. spectrophotometer, featuring the four-cell multisampler accessory, can scan four samples sequentially over a preset wavelength range. Enzyme activity or other kinetic reactions can be followed in the cells simultaneously. Additional features are the selectable wavelength limit switches and the Flowchart recording system. Scan speeds can be two, ten, and forty minutes. Wavelength limits may be set in automatic operation at any one of twelve positions between 190 and 850 millimicrons. Perkin-Elmer Corp., Norwalk, Conn. 06852 **408**



Assure Positive Identification of Unknowns with SADTLER SPECTRA...

YOUR CHEMICAL FINGERPRINTS!

Standard Reference Spectra Available:

IR—80,000 NMR—10,000
UV—28,000 DTA—2,700

Compare these compounds:

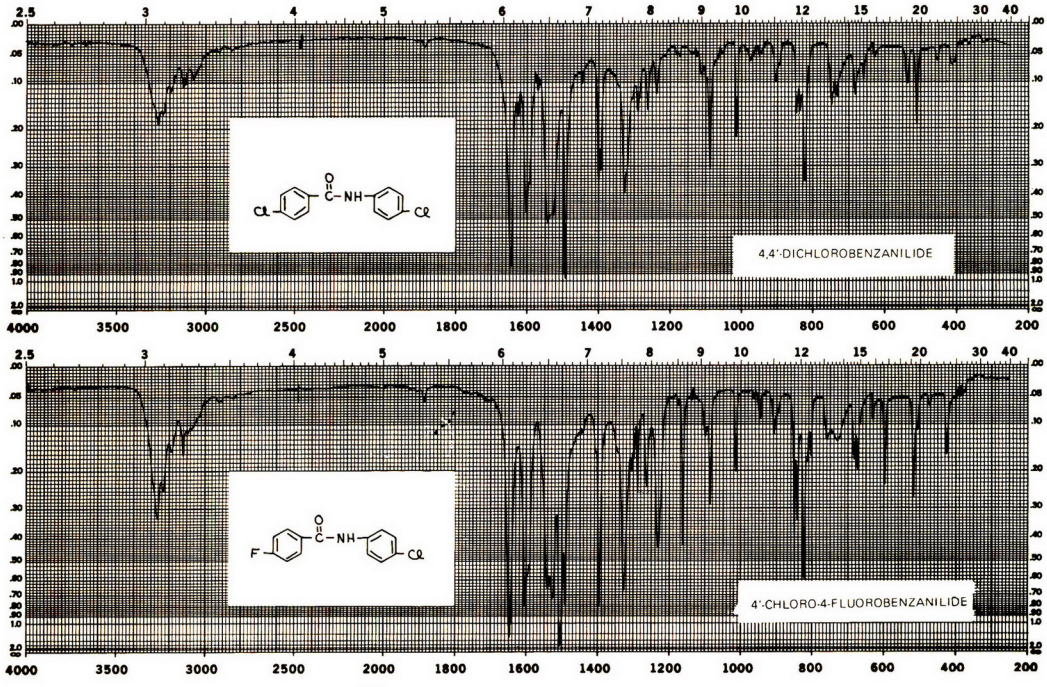

For Descriptive Brochures, Write:

SADTLER RESEARCH LABORATORIES, INC.

3316 SPRING GARDEN STREET • PHILADELPHIA • PA • 19104 AREA CODE 215 • 382 • 7800

Circle No. 98 on Readers' Service Card

ACI introduces

Epoxy coated LAB WARE

Protects from rust and corrosion

ACI epoxy coated lab ware is unaffected by organic solvents such as Toluol, Heptane, Turpentine and Xylol. Salts as well as weak acids and weak alkalies have no effect. The hard, tough film has excellent abrasion resistance, flame resistant, is self extinguishing and can be used in a wide temperature range from −370°F. to +250°F.

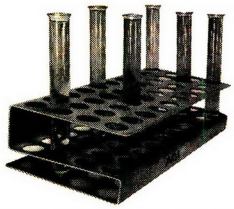

ALUMINUM TEST TUBE RACK

Coated single sheet of aluminum bent to form "S" shape. Solid stable base, two perforated shelves, smooth surfaces. Available in 24 holes for 25 mm tubes and 40 holes for 16 mm tubes.

WIRE TEST TUBE BASKET



Coated steel wire, heavy top and bottom edge ring. In rectangular and round shapes.

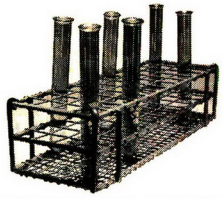

WIRE TEST TUBE RACK

Coated steel wire, square holes three deck, fine mesh on bottom deck, reinforced edges. Three sizes . . . 40 places for 22 mm tubes, 48 and 72 places for 16 mm tubes.

For coatings to specifications or stock items see your nearest laboratory supply dealer.

Send for NEW 80 page catalog 469
For your FREE copy write Dept. A-6

APPLIED COATINGS, INC.
Subsidiary of Bel-Art Products
PEQUANNOCK, N. J. 07440

Circle No. 101 on Readers' Service Card

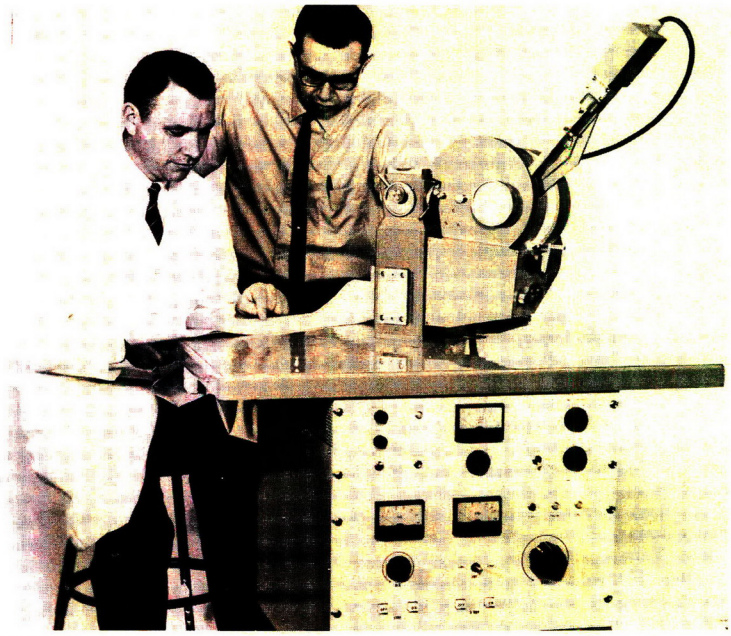

Model ADG-301 X-ray diffractometer, manufactured by Tokyo Shibaura Electric Co., Ltd., is designed for investigating the arrangement, atomic spacing, composition, and size of all crystalline structures. The ADG-301's vertically-supported X-ray tube emits rays in four directions, permitting simultaneous use of the goniometer and three X-ray cameras when studying both powdered and single crystal samples. Features include block construction, simple adjustment and operation, automatic or manual recording, and electronic circuitry. Beckman Instruments, Inc., 2500 Harbor Blvd., Fullerton, Calif. 92634 **409**

Potassium-Ion Electrode

A prototype of a liquid ion-exchange electrode has been announced. The electrode has the ability to measure potassium ion activity in the presence of sodium ions and to measure both simultaneously without making background corrections. The electrode has a Nernstian response from as low as $10^{-5}M$ and a useful pH range from 3 to 11. Response time is less than one minute. Corning Scientific Instruments, Corning Glass Works, Medfield, Mass. 02052 **410**

Sodium-Ion Electrode

This electrode is characterized by low drift and a response speed of less than one minute for 5:1 changes in concentration. Working range is from saturated to $10^{-6}M$, with a Nernstian efficiency better than 95% down to $10^{-5}M$. Temperature range is from 0 to 80 °C. The electrode responds selectively to lithium and to silver ions also. Fisher Scientific Co., 312 Fisher Bldg., Pittsburgh, Pa. 15219 **411**

Electrophoresis Computer

The Digiscreen is a computerized scanning densitometer for the quantitation of electrophoretic separations. In less than 60 seconds, the instrument scans an eight-sample strip, traces graphs of each separation, integrates them, and computes and prints relative fraction per cents. Integrated circuitry provides a zeroing device which automatically compensates for background and normalizes separation areas. The Digiscreen is available either with a computer or with a conventional servorecorder. Gelman Instrument Co., P. O. Box 1448, Ann Arbor, Mich. 48106 **412**

Atomic Absorption Spectrophotometers

Three instruments for atomic absorption have been introduced. Model 444, a double-beam instrument, features coated optics, a fine wavelength adjustment control, and digital presentation of absorbance data with an electronic

Keep ahead in Atomic Absorption. Our new Model 403 computes, types reports.

Perkin-Elmer's new Model 403 Atomic Absorption Spectrophotometer does a lot more for you than any previous AA instrument. It gives you a typewritten analytical report in any format you choose the instant you run your last sample —and produces a computer tape at the same time.

You set zero absorbance automatically. Just push a button.

You read concentration directly on four illuminated digits (part of a built-in, special-purpose, digital computer) and, on a recorder or teletypewriter.

Each sample read-out is the automatically computed average of 10 individual readings or, if you wish, of 100 individual readings.

The 403 has a working curve corrector which really corrects nonlinearity simply, accurately.

To go to flame emission, flip two switches and read your answer directly in digits. For scanning, you have four-speed wavelength drive.

We can just mention the automatic ignition, automatic gas flow regulation, new flashback-proof pre-mix burner, and pre-set lamps which are exchanged in five seconds. For full details on this new double-beam instrument contact our local sales office to see our 20-minute color movie. Or, write for our new brochure: Instrument Division, Perkin-Elmer Corporation, 702 Main Avenue, Norwalk, Conn. 06852.

PERKIN-ELMER



Circle No. 134 on Readers' Service Card

PRESSURE LOK

Gas Syringes are BETTER Gas Syringes



Markedly superior for storing, transporting, and injecting gas samples.

- LEAKTIGHT to 250 psi
- NO COLD FLOW LEAKAGE
- NO DEAD VOLUME
- FRONT VALVE for storage
- REAR PLUNGER STOP
- INTERCHANGEABLE PARTS

PS PRECISION SAMPLING CORPORATION

P. O. BOX 15119 • BATON ROUGE, LOUISIANA 70815

Yes, Send me more information on why Pressure-Lok gas syringes are better.

NAME_____

TITLE_____

COMPANY_____

ADDRESS_____

CITY_____

STATE_____ ZIP_____

ACS Lab Guide See ad, page 247

Circle No. 142 on Readers' Service Card

circuit that holds and displays photometric values at the optimum time. Single- and triple-pass optics are also offered. Model 440 is a single-beam instrument and offers the major features of Model 444. Model 448 is designed to fit limited budgets. Concentration is presented directly on a meter and the instrument is designed with single-pass coated optics. The burners featured in the spectrophotometers are Model 405, the Autolam, and the Autolam-S. Beckman Instruments, Inc., 2500 Harbor Blvd., Fullerton, Calif. 92634 **413**



A Protein Sequenator incorporates solid state program control to provide error-free sequencing in accordance with the Edman Method. The system selected can be either fully automatic using the program board or completely manual. The instrument can be set for single-cycle operation or an auto-reset cycle can be set after any stage number. An internal control system constantly monitors key functions, and 41 projected readout or indicator lights continuously display the function being performed by the Sequenator. Additional features are 40 independent stages individually adjustable from 0.05 to 50 minutes in 0.05 minute increments and 20 output functions. Illitron, 2501 N. Keeler Ave., Chicago, Ill. 60639 **414**

Specific Ion Meter

Model 407 is capable of direct readout of total concentration as well as ionic concentration and activity, pH, and millivolts. The 407 has a special scale that makes possible 2-minute total concentration measurements as precise as measurements using titration or colorimetric methods. A small known volume of a concentrated solution is added to an unknown and the initial concentration of the unknown is then read directly on the special 407 scale. No computation is required. The reagent added may be either a solution

FROM COLEMAN...

NEW LOW TEMPERATURE R-F REACTOR

Removes organic matter without loss of volatile elements



MODEL 40
LOW TEMPERATURE
R-F REACTOR

Clean, dry, low-temperature R-F ashing with Model 40 is far superior to wet and muffle furnace ashing—it's the ideal way to prepare samples for elemental analysis, air pollution tests and microscopy *without alteration of mineral or physical structure.* Other applications include radiochemistry, autoradiography, reaction chemistry, altering molecular structure of plastic surfaces, plasma chemistry, removal of photoresist. *Request Bulletin A-322.*

Write to Coleman Instruments, Division of The Perkin-Elmer Corporation, 42 Madison St., Maywood, Illinois 60153

PERKIN-ELMER

Circle No. 23 on Readers' Service Card

If you specify materials-CMC is specifically for you

All the facts you need to help speed your CPI process planning are in CHEMICAL MATERIALS CATALOG. 3-way index guides you directly to over 100 suppliers' catalogs describing more than 8,000 chemicals and raw materials with cross-reference for 1,300 brand names, trade names and trademarks. In the privacy of your office or group meeting, you can collect your facts—select your products—choose your suppliers.

And all from this one-volume library organized **by** process men specifically **for** process men.

REINHOLD PUBLISHING CORP.
SUBSIDIARY OF
LITTON PUBLICATIONS, INC.
Division of Litton Industries

CHEMICAL MATERIALS CATALOG cmc

600 SUMMER STREET, STAMFORD, CONN. 06904

Circle No. 20 on Readers' Service Card

THE HOT HEAD

This valve is the quick change artist's delight. It comes with two handles. A removable nylon outer handle for temperatures to 300°F, and metal version for temperatures to 650°F.

Stainless steel bellows is welded to the body for maximum leak-tightness. A regulating stem for small flows to a Cv of .058, or throttling stem for larger flows to a Cv of .35 is available. Connections include Gyrolok tube fittings, weldable tube extensions, and pipe ends. All models helium leak tested to .0005 MCFH. *Packless Valve Catalog has complete information.*

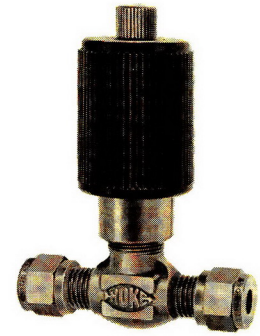

HOKE

HOKE INCORPORATED
1 TENAKILL PARK • CRESSKILL, N. J.

Circle No. 38 on Readers' Service Card

NEW in Column Chromatography

Aluminum Oxide W 200 Constant initial Activity

A fully standardized Alumina which is an asset for all chromatographic work

We guarantee
for all three types
acid, basic, and neutral

Constant initial Activity
Constant Deactivation Behavior
Constant Reproducibility

garantiert aktivitätskonstant
Woelm
constant initial activity

From now on: No difference between production lots. It pays to move over to Aluminum Oxide W 200

Never before initial activity, deactivation behavior, and inner surface were so uniform with all three types of alumina.

We kicked the guess-work out of chromatography. No guess: the price is low.

Aluminum Oxide W 200 acid
Aluminum Oxide W 200 basic
Aluminum Oxide W 200 neutral

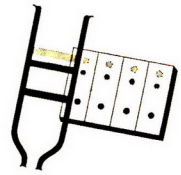

For information and price list write to:

Alupharm Chemicals
P. O. Box 30 628
New Orleans, La. 70130
Tel. JA 5-3477

Circle No. 75 on Readers' Service Card

waveform control for electrochemistry



Chemtrix's new Type 800 Waveform Source for electrochemistry provides the waveforms and waveform control necessary for successful electrochemical analyses and studies.

Offering both triangle and rectangle waveforms, the new Type 800 is completely adjustable in waveform amplitude, slope and start potential. A unique control feature (described below) permits virtually unlimited influence over waveform rise, hold-level and decay periods.

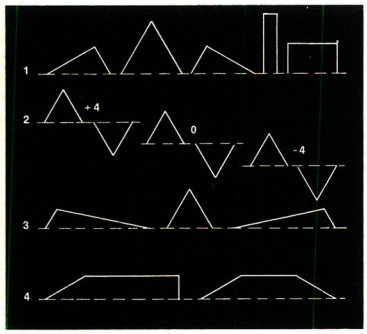

1 **Available Waveforms:** Triangle and rectangle, positive or negative polarity.
2 **Start Potential (DC Level):** Adjustable from +4 to −4 volts.
3 **Slope Control:** Adjustable over 10:1 range.
4 **Waveform Control:** Initial slope of triangle waveform can be manually stopped and held at any point. Return to starting potential may be manually effected at a fast rate or a preselected slower rate.

Other important features

Operating Modes — Single waveform triggered manually or electrically. Repetitive waveforms triggered by external source. Non-calibrated repetitive waveforms.

Velocity Range—1.0 mV/sec. to 500,000 V/sec.

Slope Period—10 microseconds to 1,000 seconds.

Amplitude—Adjustable to ±8 volts from zero DC level.

Precision Adjustments—DC Level start potential, Waveform Amplitude, Initial Slope and Return Slope all adjustable with 10-turn calibrated controls.

Priced $875, f.o.b. factory

Other Chemtrix products:

Cathode-Ray Polarographic System: single scan with stored polarogram, two- and three-electrode systems, digital readout of peak heights. Glassy carbon electrodes.

CHEMTRIX, INC.
Instrumentation for Science
P.O. Box 725 Beaverton, Oregon 97005
(503) 648-1434

Circle No. 141 on Readers' Service Card

of the ion being measured or a solution that removes the ion from solution. Total sulfide, fluoride, and cyanide can now be determined in less than two minutes regardless of the ionic composition of the sample. Orion Research Inc., 11 Blackstone St., Cambridge, Mass. 02139 **415**

ESR Spectrometer

Model 810, designed for classroom use, consists of a complete waveguide assembly, a regulated klystron power supply with internal sweep modulator, and a magnetic field modulator for the magnet. The magnet itself, magnet supply, and lock-in amplifier are supplied by the user. In its standard configuration, the spectrometer will readily detect 10^{14} spins. Micro-Now Instrument Co., Inc., 6124 N. Pulaski Rd., Chicago, Ill. 60646 **416**

Chromatographic Column

Sephadex K50/60 jacketed column is for analytical and preparative applications in gel filtration and ion exchange chromatography. The flexible design with adjustable flow adaptors and cooling jacket allows the column to be operated with aqueous systems at a constant temperature as part of an automatic or semi-automatic system. The flow adaptors permit bed volumes of 500 to 1,000 ml. The flexibility of the column allows experiments to be conducted either as descending, upward flow, or recycling chromatography systems. Pharmacia Fine Chemicals Inc., 800 Centennial Ave., Piscataway, N. J. 08854 **417**

Lead-Ion Electrode

Model 94-82 permits direct, two-minute lead ion determinations from 21,000 to 0.02 ppm (or 10^{-1} to $10^{-7}M$). The electrode and two standardizing solutions are all that are required for lead determination. Bismuth, thallium, stannous tin, sodium, or potassium ion do not interfere. The electrode is affected by ferric and cadmium ion, which may be present at levels up to the level of lead ion, and silver and mercury which must be absent from the sample. Orion Research Inc., 11 Blackstone St., Cambridge, Mass. 02139 **418**

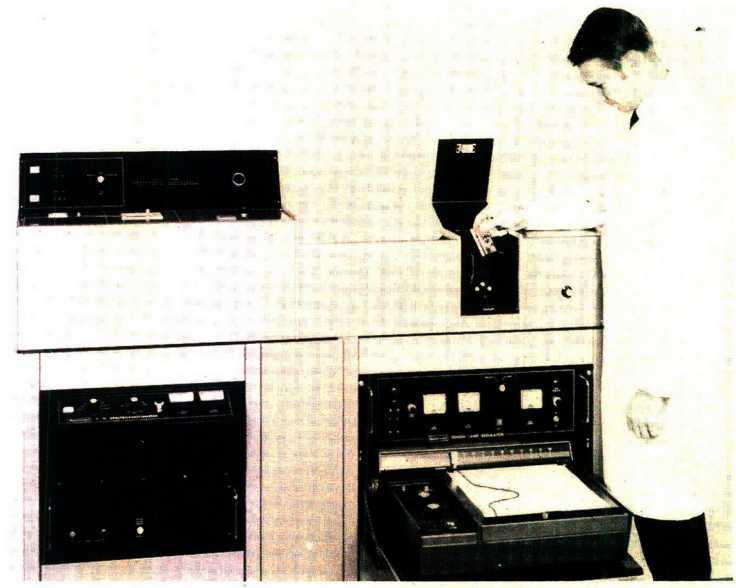

A circular dichroism spectrophotometer that performs over a wavelength range of 180 to 650 nm and attains CD sensitivities to 5×10^{-13} differential absorbance is available. The optical system of the spectrophotometer features a high-intensity point source xenon lamp, a far UV monochromator, polarizing optics, electro-optical light modulator, and a high gain photomultiplier. The optics are controlled automatically to produce right and left circularly polarized light at a frequency of approximately 200 Hz as wavelength is varied. The electronic system employs techniques for narrow band frequency discrimination and phase locking. The resultant CD signal is recorded directly in optical density units. Beckman Instruments, Inc., 2500 Harbor Blvd., Fullerton, Calif. 92634 **419**

You wouldn't beat your wife, would you?

Would you?

No?

Well, there you have it! Then why beat your Gas Chromatography supports?

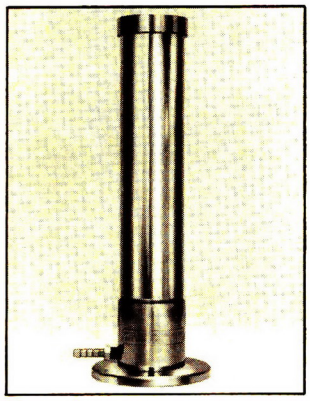

You can go easy on those supports, and yourself, by using our HI-EFF Fluidizer. With this method of drying column packing you increase column efficiencies by 20%. You reduce drying time from 45 minutes to 15. It greatly simplifies the preparation of Teflon packing and insures minimum particle attrition with a gentle, yet thorough drying of sensitive packings. The net result is not only improved results, but improved packing reproducibility. The Fluidizer is strong, non-breakable, compact, and heavily chromed to prevent packing contamination. It is easy to clean, and ideal for both high and low loaded packings. It is so straightforward in its application that inexperienced technicians can prepare top quality packings from the start. We feel that the HI-EFF Fluidizer would be invaluable to any lab. It just can't be beaten. If you will pardon the expression.

Applied Science Laboratories Inc.

P. O. Box 440 • State College, Pa. 16801 • Tel.: 814-238-2406

West Coast Office: 11135 Inglewood Avenue • Inglewood, Calif. • Tel.: 213-678-9022

Circle No. 117 on Readers' Service Card

NEW POWER AND PRECISION FOR VISCOUS MIXTURES



The HELLER 6T60 Heavy-Duty Stirrer for only $177!

The new Heller 6T60 gives precise speed control with a 1/20 HP motor having seven times the torque of the famous GT21 Lab Stirrer, of which more than 25,000 have been sold. Solid-state motor controller provides adjustable speed with automatic correction for changing viscosity and line voltage fluctuations. Two output shafts are rated 0-1800 RPM at 1.8 inch-lbs. torque and 0-180 RPM at 12 inch-lbs. torque through 10:1 gearhead. High-range control doubles maximum speeds at reduced torque. Controller operates on standard 100-130 volt 50-60 Hz AC. Price includes motor, controller, 6" stainless steel propeller, coupling, 3-jaw chuck, motor mounting bracket and base plate with rod for lab stand clamp, and regular motor base plate for shelf or wall mounting. Heller GT21 1/40 HP mixer includes chuck, propeller, paddle, pulley and mounting accessories for $117. For details, write for Bulletin 639.

Available through leading lab supply dealers

GKH — OVER 25 YEARS OF MOTOR CONTROL — SINCE 1948

G. K. HELLER CORP.
2673 S. Western Street, Las Vegas, Nev. 89114
7 Mayflower Place, Floral Park, L.I., N.Y. 11001

Circle No. 37 on Readers' Service Card

Portable • Complete • Low Cost DELMAR BASIC HIGH-VACUUM SYSTEM

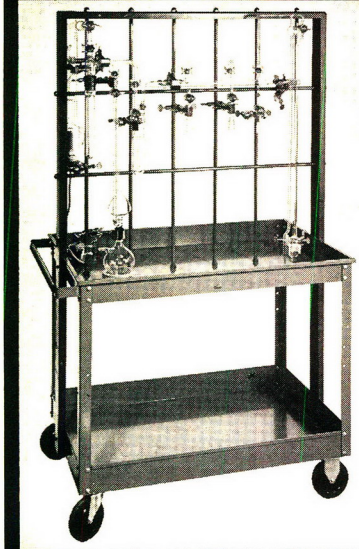

Convenient and economical for:
- student use
- demonstrations
- research

TYPICAL APPLICATIONS
- handling gaseous material
- preparing geochemical samples
- effecting molecular distributions
- preparing samples for nuclear magnetic and electron spin resonance studies

Comes complete (as illustrated) with rack and all glass components including diffusion pump, manifold, McLeod gauge, manometer, traps, adapters and hardware.

For complete details, ask for Bulletin AC-60.

Write to Coleman Instruments Division of the Perkin-Elmer Corporation, 42 Madison Street, Maywood, Illinois 60153.

PERKIN-ELMER

Circle No. 26 on Readers' Service Card

New Products

Oscillator

Model 204D has an 80 dB attenuator range in 10 dB steps with an accuracy of ±3% (+10 db through −60 dB range; ±5% on −70 dB range). A >10 dB vernier provides overlap in any range. The sine wave generated by the oscillator has less than 0.1% distortion at frequencies between 30 Hz and 100 Hz (linearly derated to <1% at the high and low ends). Hum and noise are less than 0.01% of output. A rear panel sync output supplies a sine wave in phase with the main output. A sync input on the front panel is for synchronizing the output with an external signal. Hewlett-Packard Co., 1501 Page Mill Rd., Palo Alto, Calif. 94304 **420**

ENDOR Spectrometer

The E-700 electron-nuclear double resonance spectrometer is designed for use with the E-line EPR spectrometers. The purpose of ENDOR is to improve the effective resolution of an EPR spectrum. It may be used to study low symmetry radicals in the liquid phase, the kinetics of conformational changes, and chemical equilibria of free radicals in solution. ENDOR operates by irradiating a sample with a pumping source, and by observing the effect of this irradiation on other transitions. Because this is a restrictive condition for the observation of a signal, the system is used in sorting out and analyzing complex, overlapping, and poorly resolved spectra. Varian, 611 Hansen Way, Palo Alto, Calif. 94303 **421**

Selection Electrodes

Eight ion selective electrodes, for use with any pH meter, are available. The calcium ion electrode is a solid-ion exchanger type for the direct measurement of calcium activity in aqueous solutions. The fluoride selective ion electrode is made from solid-state crystal and is designed for studies of fluoride complexes in solutions. The sulfide ion sensor is also solid-state crystal and is for use in water and waste analysis. Bromide, chloride, and iodide ion electrodes are solid silver-salt sensors for use in photography and biological and medical research. Both the sodium ion and cation sensors are glass electrodes designed for general laboratory applications. Clinical-style versions are available. Beckman Instruments, Inc., 2500 Harbor Blvd., Fullerton, Calif. 92634 **422**

Just $425* buys the Farrand "Foci-Flex" GRATING MONOCHROMATOR

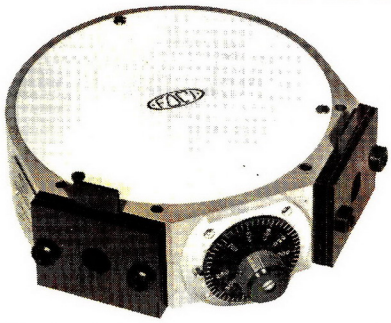

A low-cost, quality instrument ideally suited for systems operation, education and experimental uses.

*14,440 lines per inch — $425.; 28,800 lines per inch — $485.

Featuring: 200-785 mμ wavelength range
F/5.3 optical system
Interchangeable slits
1 mμ resolution capability

Accessories and attachments also available. Information on other grating monochromators on request.

FOCI®
A product of
Farrand Optical Co., Inc., New York, N. Y.

Direct inquiries to:
Farrand OPTICAL CO., INC.
Commercial Products Division
535-A So. 5th Avenue, Mt. Vernon, N. Y. 10550
(914) 668-9393/Cable Address: FOCIUS NY

Circle No. 132 on Readers' Service Card

Our Multipoint Has More Standard Features Than Others Have Options

Where else can you get manual point advance, five chart speeds, two print rates, infinite resolution conductive plastic potentiometer, plus MV, volts, T/C or RTD inputs as standard features?

And look at these exclusive options: print-on-alarm that will scan and record only off-normal inputs; programmed printing that electrically selects points to be printed and deleted; automatic dual range, which allows mixing inputs of two T/C types or DC volts and T/C on one recorder.

Learn more about this Multipoint. Write or call: Esterline Angus • Division of Esterline Corporation • Box 24000 • Indianapolis, Indiana 46224 • Phone 317/244-7611.

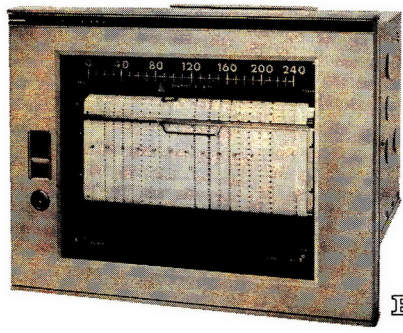

ESTERLINE ANGUS

Circle No. 31 on Readers' Service Card



What's a classy inorganic like you doing with an MCB label?

Lots of people think of MCB first when ordering organic laboratory chemicals.

But they don't think of us at all when it comes to inorganics.

It seems to be the penalty we suffer for achieving so much respect as the trustworthy producer of finest organics. Our reputation in one area has obscured our competence in the other.

We have impressive credentials when it comes to inorganics. Our new MCB Laboratory Chemicals Catalog has the story. Write for a copy and you'll quickly see that MCB is also a major source of inorganic laboratory chemicals.

The same no-compromise standards that built our reputation for organics are applied to our inorganics. Producing up-to-date laboratory chemicals matched to the most exacting analytical equipment and laboratory techniques is our sole business . . . so we can concentrate on serving you.

The label does make a difference. MCB is the label to specify.

MCB
Matheson Coleman & Bell
Manufacturing Chemists
Norwood, Ohio; Los Angeles, Calif.; East Rutherford, N. J.

All brown bottles look alike . . . until you turn them around

Circle No. 62 on Readers' Service Card

NEW CHEMICALS

Standard Reference Materials

Neutron Density Monitor Wire, SRM 953 is a cobalt-in-aluminum wire, 0.5 mm in diameter which was prepared using specially selected high-purity starting materials, for use in activation analysis in determining integrated neutron flux density and long term variations of the neutron density at given irradiation positions.

Basic Oxygen Furnace Steel, SRM 178, chip-form carbon steel is the first steel made by this basic oxygen furnace process to be certified, and is intended for the same uses for which SRM 20f, Acid Open Hearth Steel, was used.

Four radioactivity standard reference materials previously certified and issued but not announced are: Tin-113–Indium-113m (SRM 4225); Radium-226 (SRM 4953); Thorium-228–Thallium-208 (SRM 4205); and Plutonium-238 (SRM 4905). Renewal SRM's not previously announced are: Stearic Acid (SRM 372g); Natural Rubber (SRM 385b); Butyl Rubber (SRM 388e); and Sodium Cyclohexanebutyrate (SRM 1069b).

Standards may be purchased from the Office of Standard Reference Materials, Rm. B308, Chemistry Bldg., National Bureau of Standards, Washington, D. C. 20234

High Purity Metals

Twelve ultra-pure metals recently introduced are available in purities up to 99.99995% and include 99.999% cobalt and nickel powders. They are offered in rod, wire, sheet, shot, and powder forms. Apache Chemicals, P. O. Box 17, Rockford, Ill. 61105 **501**

Labeled Compounds, Deuterated Solvents, and Melamine–N^{15}

A variety of inorganic and organic compounds labeled with 90% carbon-13 are now available. Previously only 50–60% carbon-13 was available.

NMR deuterated solvents of high quality also available include acetic acid-d_4, acetone-d_6, acetonitrile-d_3, trifluoroacetic acid-d_3, and DMSO. All are supplied with NMR grade tetramethylsilane (1% v/v) at no extra cost.

Melamine–N^{15} is offered as a source of N-15 in stable solid form for use as a target in nuclear physics research. It is now available labeled with nitrogen-15 of 98+% enrichment. Isomet Corp., 433 Commercial Ave., Palisades Park, N. J. 07650 **502**

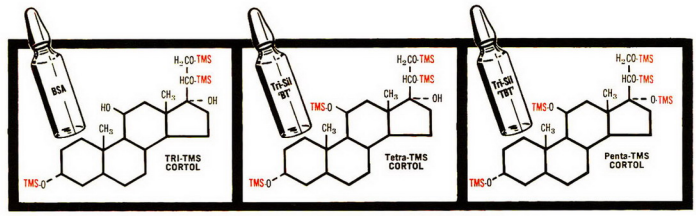

KIT FOR THE SELECTIVE SILYLATION OF STEROIDS

According to the method of Chambaz & Horning[1].

With this new set of reagents you have a reliable and reproducible method for preparing volatile and stable derivatives of steroids and related compounds for gas phase analysis; knowing in advance just which active sites you will derivatize. This method will also be valuable for studies of derivative formation in synthetic work, structural determinations and separations other than gas phase.

Recent Studies [1,2,3,4] have shown that various hydroxyl sites on steroids may be selectively converted to trimethylsilyl derivatives depending upon their relative steric hindrance. The conclusions reached in these studies were supported by GLC data and confirmed by Mass spectrometry. These sites fall into three distinct classes: unhindered, moderately hindered and highly hindered. Three reagents have been developed for the selective silylation of these sites: Tri Sil TBT will silylate all three types of sites; Tri Sil BT will silylate the moderately hindered and unhindered; BSA will silylate the unhindered groups.

An additional reagent, 'MOX', may be used to form methoxime (MO) derivatives with ketones[5], eliminating the possibility of enol-TMS ether formation in Keto-steroids.

Three useful solvents, especially prepared for silylation reactions are included in the kit; acetonitrile, dimethylformamide and pyridine.

No. 38300 Steroids Silylation Kit.....56.00 each

(We will quote attractive prices for large volume users of this kit or its components)

Circle No. 58 on Readers' Service Card

Consists of the following, available separately at prices shown:

No. 49016 TRI-SIL 'TBT', pkg of 10x1 ml ampules..20.00
No. 49015 TRI-SIL 'BT', pkg of 10x1 ml ampules...15.00
No. 38836 BSA, pkg of 10x1 ml ampules.....12.50
No. 45950 MOX, 10 ml hypovial.....12.00
No. 20062 Acetonitrile, silylation grade, 50 ml hypovial 2.50
No. 20672 Dimethylformamide, silylation grade, 50 ml hypovial..... 2.50
No. 27530 Pyridine, silylation grade, 50 ml hypovial 2.50

Ask for our technical bulletin "Steroids Silylation Brochure."

References:

1. E. M. Chambaz & E. C. Horning, Analytical Letters, 1, 201-211 (1968).
2. E. M. Chambaz & E. C. Horning, Analytical Biochemistry, in press.
3. B. Maume, W. E. Wilson and E. C. Horning, Analytical Letters, 1, 401 (1968).
4. E. M. Chambaz, G. Maume, B. Maume & E. C. Horning, Analytical Letters, 1, 749-761 (1968).
5. W. L. Gardiner and E. C. Horning, Biochim. Biophys. Acta, 115, 425 (1966).

PIERCE CHEMICAL COMPANY
P. O. Box 117 Rockford, Illinois 61105
PHONE 815/968-0747 TWX 910-631-3419

See ACS Laboratory Guide for All Products/Sales Office

Convenient, Low Cost Culligan Deionizers

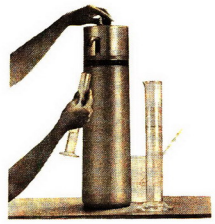

D-25 LABORATORY DEIONIZER

Designed specifically for uses requiring small quantities of high quality water. The D-25 produces water containing as little as 0.5 ppm of dissolved minerals from source water having up to 700 ppm of dissolved solids. Capacity is 2,500 grains per regeneration, flow rate 48 gallons per hour. D-25 is regenerable, eliminates costly throw away cartridges.

EXCHANGE SERVICE SYSTEM

Provides a constant supply of deionized water. Exchange Service Deionizer produces water containing as little as .04 ppm of dissolved minerals from source water having up to 850 ppm of dissolved solids. Systems can be engineered to meet a wide range of water quality and capacity requirements. We replace exhausted deionizer systems with regenerated deionizer units to provide uninterrupted flow of deionized water.



For complete information, call your local Culligan Man—or contact Culligan Inc., Northbrook, Illinois 60062, Phone (312) 272-1000.

Culligan®
THE WORLD-WIDE WATER CONDITIONING PEOPLE

Circle No. 25 on Readers' Service Card

What's a good PANELBOARD connection?

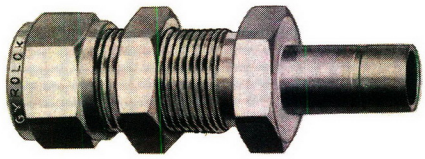

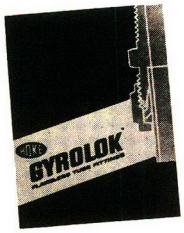

Hoke's Gyrolok tube fittings are listed in so many sizes, shapes & materials in the new catalog that even panelboard manufacturers can't outguess us.

Your Hoke distributor has catalogs, fittings & know-how on the shelf. Or you can call us.

GYROLOK
FLARELESS TUBE FITTINGS

HOKE MFG. CO • 1 TENAKILL PARK • CRESSKILL, N.J.

Circle No. 39 on Readers' Service Card

New, easier-to-use, gas-leak detector.

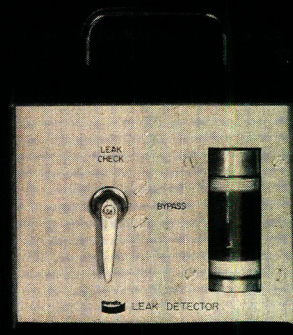

The Bendix Model 1000 leak detector discovers a gas leak less than .001 cc/min. You don't have to shut down the system to use the Model 1000. No hazards around open wiring or open flame. Compact. Weighs only 3 lbs. Permanent or portable installation. ONLY **$50**

Bendix

Circle No. 4 on Readers' Service Card

new... from pcr

CATALOG G5

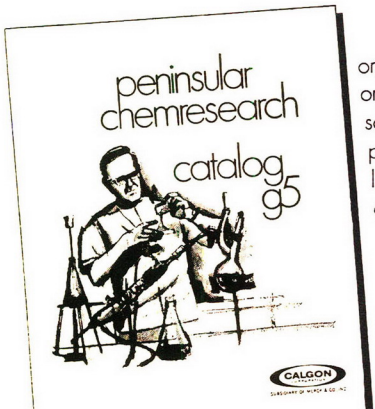

organo-fluorine
organo-silicon
scintillators
peptide reagents
liquid crystals
organic intermediates

CALGON CORPORATION
PENINSULAR CHEMRESEARCH
CALGON CORPORATION
SUBSIDIARY OF MERCK & CO., INC.
FOR YOUR COPY WRITE TO PCR, DEPT. 68-5
P.O. BOX 1466, GAINESVILLE, FLORIDA 32601

Circle No. 57 on Readers' Service Card

Use APIEZON

... Oils, Sealing Compound and Waxes



Apiezon Oils have very low vapor pressures and are very stable. They are ideally suited as vapor-diffusion pump fluids. Apiezon Sealing Compound Q is a putty-like substance, a relatively low cost, extremely versatile sealing medium. Apiezon Waxes are for vacuum joints of a more permanent nature.

Write for BULLETIN 43 AC 812

BIDDLE INSTRUMENTS
JAMES G. BIDDLE CO.
Electrical and Speed Measuring Instruments
PLYMOUTH MEETING, PENNSYLVANIA 19462
Phone 215/646-9200

Circle No. 17 on Readers' Service Card

MANUFACTURERS' LITERATURE

Stationary Phases for Gas Chromatography. The more than 1000 references contained in this 116-page booklet are indexed according to the materials separated. Brief notes about the separations are included. A new section lists most of the commercially available stationary phases, their maximum recommended operating temperatures, a suitable solvent, and specific uses. Analabs, Inc., 80 Republic Dr., North Haven, Conn. 06473 **601**

Water Purification Equipment. Water stills and accessories, specialized stills, demineralizers, storage tanks and accessories, purity meters, and sterilizers are among the items included in this 44-page comprehensive product catalog. Barnstead Co., 225 Rivermoor St., Boston, Mass. 02132 **602**

Automatic Recording Titrator. Bulletin 7148-A, eight pages, provides specifications and design information on the titrator, its modules, accessories, and supplies. Beckman Instruments, Inc., 2500 Harbor Blvd., Fullerton, Calif. 92634 **603**

Liquid Scintillation Systems. Bulletin 7128A, 14 pages, provides specifications and descriptive information for the LS-100 Series of ambient temperature systems, for the LS-200 Series of ambient or refrigerated sy tems, and for a variety of accessories. Beckman Instruments, Inc., 2500 Harbor Blvd., Fullerton, Calif. 92634 **604**

Spectroscopic Data Handling System. Bulletin 201, six pages, presents the SpectroSystem 100/Spectrophotometer data handling system that is adaptable for use with all Cary spectrophotometers and spectropolarimeters. Cary Instruments, 2724 S. Peck Rd., Monrovia, Calif. 91016 **605**

Stable Labeled Compounds. Carbon-15, deuterium, nitrogen-15, and oxygen-18 compounds are presented in this catalog. Included is a listing of NMR spectro grade deuterium solvents. Laboratory Products Division, Isotopes, A Teldyne Co., 50 Van Buren Ave., Westwood, N. J. 07675 **606**

Ultra-sensitive analysis has its price.

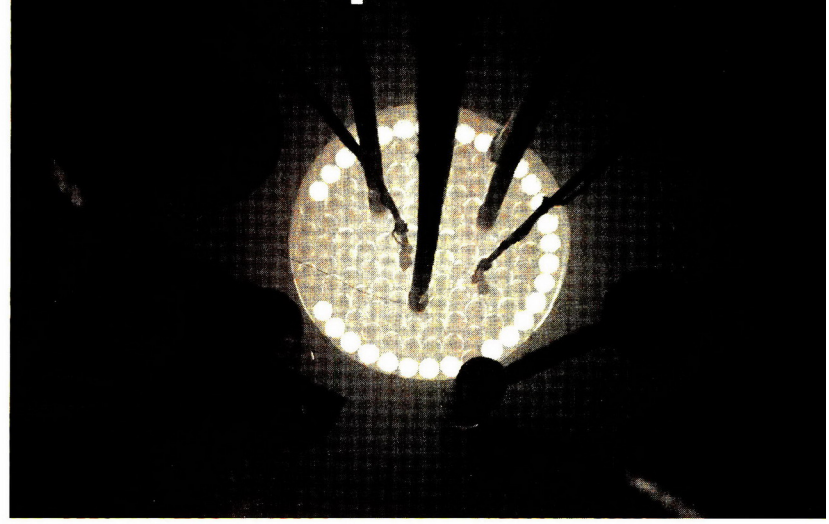

$20

Here's the fast, low-cost way to get an ultra-sensitive analysis for the elements present in a sample. It's Gulf General Atomic's **ACTIVATION ANALYSIS SERVICE.** Take a look.

COST: A typical one-element, non-destructive analysis costs $20 per sample, in quantity. Some are as little as $6 per sample.
METHOD: Samples are irradiated in one of Gulf General Atomic's TRIGA® reactors (reactor core shown above). The induced radioactivities are then identified and measured quantitatively, and the data are processed in GGA's computer center.
SENSITIVITY: Limits of detection for over 70 elements range from 10μg to 10^{-6} μg. Median sensitivity is approximately 10^{-3} μg (0.001 ppm in a one gram sample).
PRECISION & ACCURACY: Typical accuracy in a routine analysis is ±2-4% of the value, with a precision in the range of ±1-3% of the value.
SAMPLES: The technique is applicable to the analysis of virtually every conceivable solid or liquid material, including ores, semiconductors, petroleum, water, polymers, solvents, biological tissues, and agricultural products. Most analyses can be performed without destroying the sample.
CAPABILITIES: GGA's Activation Analysis Service is the largest, most comprehensive service of its type in the world. Analyses have been performed for over 600 organizations in the past eight years. Major facilities include three TRIGA reactors, several electron linear accelerators and neutron generators, and a UNIVAC 1108 computer.
GET SPECIFIC DETAILS in terms of your analytical problem. Write to Activation Analysis Service, Dept. 302, Gulf General Atomic, P.O. Box 608, San Diego, California 92112. Or phone 714/453-1000, Ext. 327.

Circle No. 99 on Readers' Service Card

Gulf General Atomic

We have a new electrometer especially for lab chromatographs.

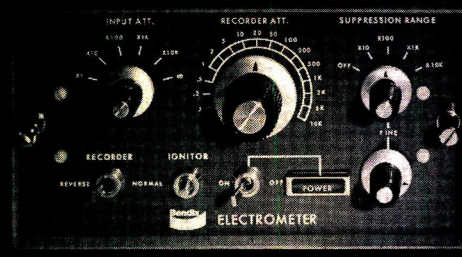

(Check the *linear* dynamic range.)

The linear dynamic range of our new electrometer is 10^7. And the total range is 10^{10} (from 1 x 10^{-14} A. to 1 x 10^{-4} A.). You'll find its junction field effect transistor circuitry highly reliable. It's completely solid state, has extremely low noise and is steady as a rock—drift less than 10^{-13} amperes a day.

The input attenuator has five positions, five decades. The recorder output attenuator has 16 positions with a total range of 10^5 (100,000 times). Can your integrator handle the linear dynamic range of this electrometer? For complete information, write: The Bendix Corporation, Process Instruments Division, Ronceverte, West Virginia 24970.

Bendix

Circle No. 15 on Readers' Service Card



how much impurity do you want?

Few people want or need really PURE water. Although IWT can engineer a mixed-bed water system which delivers pure water (.000000043 ppm impurity) it probably wouldn't be practical for you. A funny thing happens to pure water on the way—it scavenges any material it touches to satisfy its solvent hunger. It won't stay pure.

To get it pure and to keep it pure costs too much. So, it becomes a matter of which and how much impurity you can accept. When it comes to producing volumes of almost pure water economically, that's where IWT sparkles.

We can engineer a system that makes the most of your impurities.

free to you

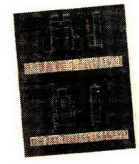

Pioneers in mixed-bed deionization, IWT can give you any degree of purity. Let us send you the full story on high quality water. Ask for Bulletin PKA-369.

ILLINOIS WATER TREATMENT COMPANY
840 CEDAR ST., ROCKFORD, ILLINOIS 61105

iwt

Circle No. 40 on Readers' Service Card

99.99995% PURE HELIUM

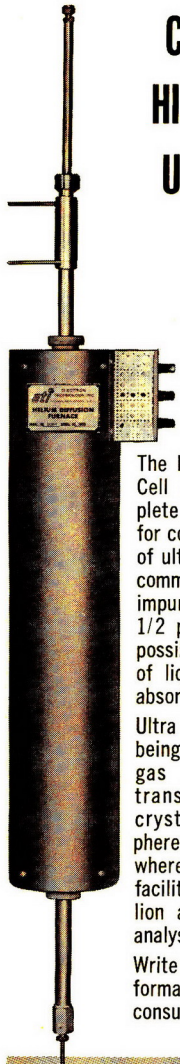

CONTINUOUS
HIGH OUTPUT
UNATTENDED
OPERATION
LOW COST
LONG LIFE

The ETI Helium Diffusion Cell Purifier is a complete equipment, ready for continuous production of ultra-pure helium from commercial grades. Total impurity levels as low as 1/2 part per million are possible without the use of liquid nitrogen-cooled absorbents.

Ultra pure helium is now being used extensively in gas chromatography, transistor processing, crystal growing atmospheres and other services where high purity helium facilitates parts per billion accuracy in critical analyses.

Write for additional information or engineering consultation.

eti

ELECTRON TECHNOLOGY, INC.
626 SCHUYLER AVE., KEARNY, N. J.

Circle No. 78 on Readers' Service Card

Manufacturers' Literature

Organic Chelating Agents. Cheelox sequestrants, available in a variety of physical forms and chemical types, are listed in Bulletin 7543-161. GAF Corp., Dyestuff & Chemical Division, 140 W. 51st St., New York, N. Y. 01120 **607**

Nuclear Detectors. Lithium drifted germanium detector systems are presented in Data Sheet 067. A discussion of the Satellite Cryostat is also included. The Harshaw Chemical Co., 1945 E. 97th St., Cleveland, Ohio 44106 **608**

Radioactive Labeled Compounds. Over 100 radionuclides required in biochemistry, biophysics, and organic research are listed in a new catalog. Laboratory Products Division, Isotopes, A Teledyne Co., 50 Van Buren Ave., Westwood, N. J. 07675 **609**

Laboratory Equipment. Plastic laboratory products and accessories are presented in Catalog 469, 80 pages. Bel-Art Products, Pequannock, N. J. 07440 **610**

Recorders. Catalog SSC 369, 16 pages, offers complete specifications for the Speed Servo recorder line. Esterline Angus, P. O. Box 24000, Indianapolis, Ind. 46224 **611**

Resistance Temperature Detectors. Bulletin I-461 describes the characteristics of resistance temperature detectors, including the functions of the components, and compares the temperature range and other features of bulbs *vs.* thermocouples. The Lewis Engineering Co., Naugatuck, Conn. 06770 **612**

Products for Instrumentation. Films, papers, chemicals, and processing equipment for instrumentation recording are listed in a new, 36-page catalog. Eastman Kodak Co., Instrumentation Products, Rochester, N. Y. 14650 **613**

Laboratory Furniture. Catalog 201-F, 24 pages, introduces the new classic line of Spanish oak formica laboratory furniture. Catalog 202-F, 32 pages, presents the company's line of steel laboratory furniture. Accessory items are included in both catalogs. Matheson Scientific, 1850 Greenleaf Ave., Elk Grove Village, Ill. 60007 **614**

NON DISPERSIVE

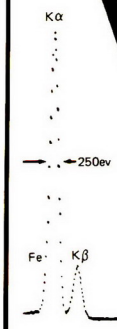

X-RAY

FLUORESCENCE SPECTROMETERS

- INSTANT ELEMENTAL ANALYSIS FROM Na THRU U
- MICROPROBES
- SCANNING ELECTRON MICROSCOPES
- RADIOISOTOPE EXCITED ANALYSIS
- BIOLOGY
- GEOLOGY
- QUALITY CONTROL

WRITE FOR DETAILS

nuclear diodes inc

box 135, prairie view, illinois 60069
Phone: 312-634-3870

Circle No. 138 on Readers' Service Card

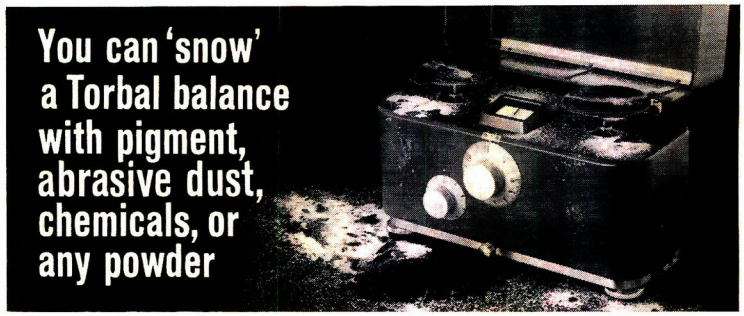

but it will never 'snow' you back.

Sometimes you can't help it. In certain weighing situations no matter how hard you try, a balance gets dirty from spilled or overflowing powders. Or from dust in the air.

When this happens on a conventional knife-edge balance, the knife-edge fulcrum becomes dirty—gets gummed up, and eventually wears. Increased friction, decreased sensitivity and inaccuracy result. (In time even small amounts of dirt in the atmosphere will have this effect.)

On the other hand, with a Torsion Balance based on fulcra which twist instead of roll, this cannot happen. There are no friction pivots or knife-edge fulcrum; thus no metal-to-metal wear, and the weighing mechanism cannot be affected by foreign material. The balance will not become sluggish, it retains its initial accuracy and sensitivity, and because of its virtually one-piece construction, adjustment is permanent.

The Torbal DWL2 shown above is a 120-gram capacity balance with a dial accuracy of 5 mg.; silicon fluid damping for fast weighing; dials with 9 g x 1 g, and 1 g x 0.01 g graduations, to eliminate use of small loose weights. Write today for literature.

The Torsion Balance Company TORBAL

Department A
Main Office and Factory: Clifton, N. J.; Sales Offices: Birmingham, Ala.; Chicago, Ill.; San Mateo, Cal.; Pittsburgh, Pa.; Plants and Offices in Montreal, Quebec; London, England and Waterford, Ireland

Circle No. 87 on Readers' Service Card

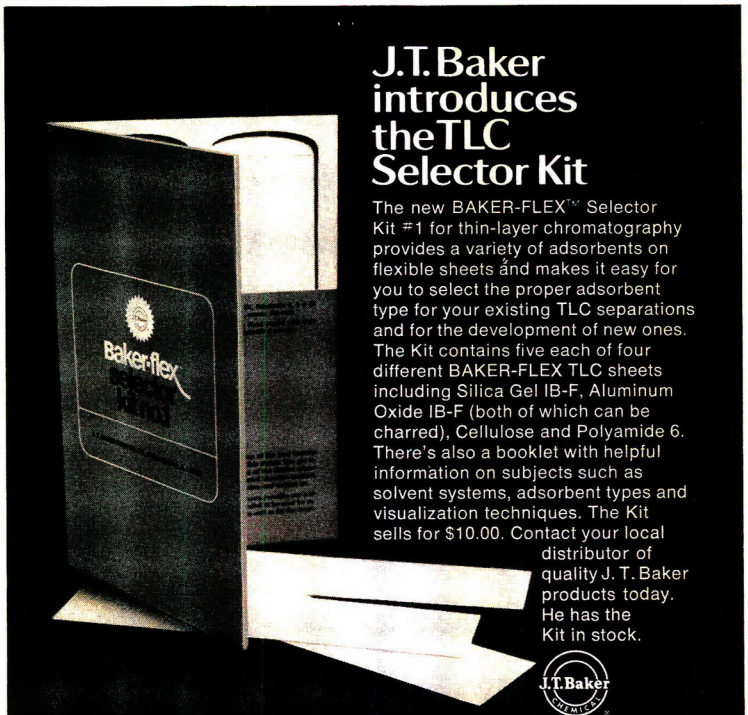

J.T. Baker introduces the TLC Selector Kit

The new BAKER-FLEX™ Selector Kit #1 for thin-layer chromatography provides a variety of adsorbents on flexible sheets and makes it easy for you to select the proper adsorbent type for your existing TLC separations and for the development of new ones. The Kit contains five each of four different BAKER-FLEX TLC sheets including Silica Gel IB-F, Aluminum Oxide IB-F (both of which can be charred), Cellulose and Polyamide 6. There's also a booklet with helpful information on subjects such as solvent systems, adsorbent types and visualization techniques. The Kit sells for $10.00. Contact your local distributor of quality J. T. Baker products today. He has the Kit in stock.

J.T.Baker CHEMICAL

J. T. BAKER CHEMICAL COMPANY, PHILLIPSBURG, NEW JERSEY 08865

Circle No. 81 on Readers' Service Card

Manufacturers' Literature

Spectrometer. Model 750 Atomcounter, a desk-size direct-reading spectrometer unaffected by temperature, vibration, or shock, is detailed in Bulletin No. 38, 12 pages. Fisher Scientific Co., J-308 Fisher Bldg., Pittsburgh, Pa. 15219 **615**

Laboratory Safety. The topics included in this 1969 manual of laboratory safety are accident prevention in the laboratory, laboratory first aid, fires and firefighting, safety equipment, and references on laboratory safety. Fisher Scientific Co., 312 Fisher Bldg., Pittsburgh, Pa. 15219 **616**

pH Meters. Two Accumet pH meters for research and general purpose use are introduced in an eight-page bulletin. Fischer Scientific Co., 312 Fisher Bldg., Pittsburgh, Pa. 15219 **617**

Filters. A new standard filter catalog, eight pages, carries information on monopass narrowband filters, laser line very narrowband filters, neutral density filters, long and shortwave pass filters, and laser beamsplitters and attenuators. Optics Technology Inc., 901 California Ave., Palo Alto, Calif. 94304 **618**

IR Sampling Accessory Kits. Data Sheet D-463 describes and illustrates the Liquid and Mull Sampling Kit, the Basic Infrared Accessory Kit, and the Infrared Microsampling Kit. Perkin-Elmer Corp., Norwalk, Conn. 06852 **619**

Gas Chromatograph. Model 900 is described and illustrated in Bulletin L-142, 12 pages. The injectors, column oven, detectors, and amplifiers are among the components discussed. Perkin-Elmer Corp., Norwalk, Conn. 06852 **620**

Radioactive Products. Over 140 new products and services are offered in this 216-page, 1969/70 catalog. Many carbon-14 and tritium labelled compounds are offered at higher specific activity than before. The Radiochemical Centre, Amersham, Buckinghamshire, England **621**

Laboratory Equipment. A 30-page catalog presents a selected list of testing and laboratory equipment for industry. Testing Machines Inc., 400 Bayview Ave., Amityville, L. I., N. Y. 11701 **622**

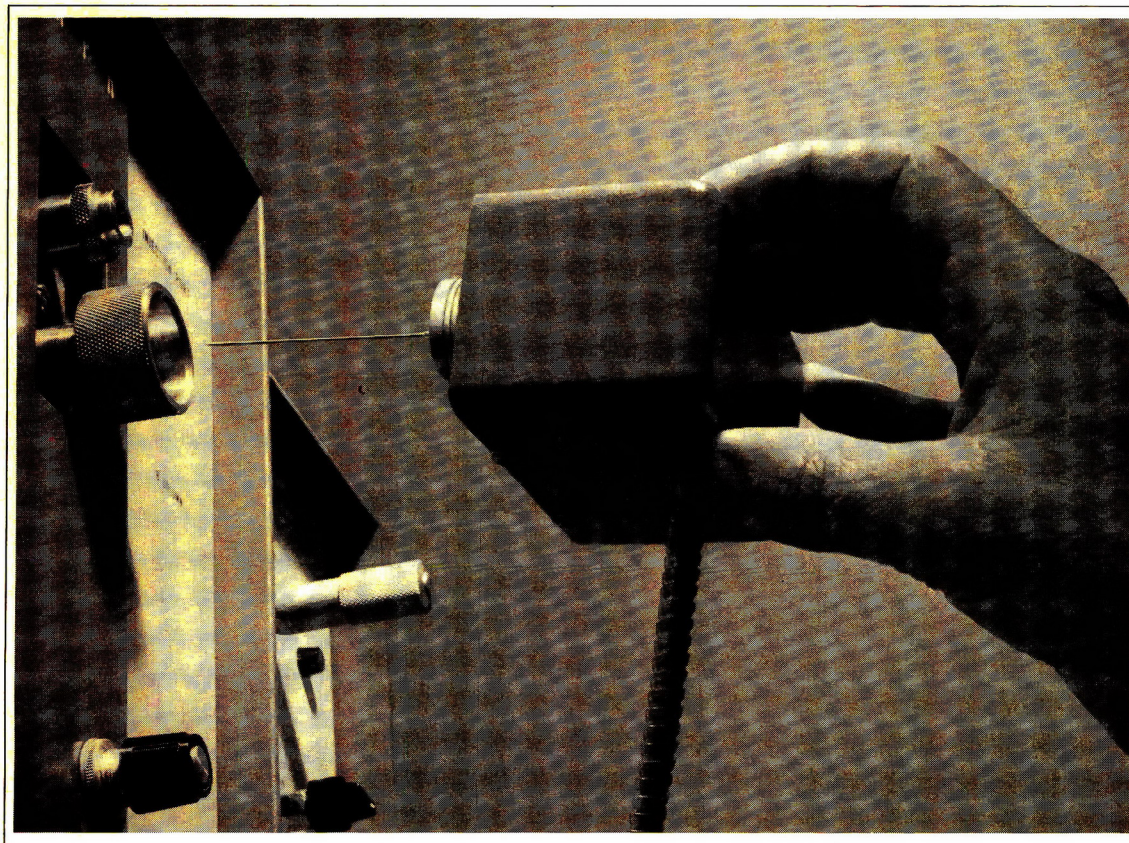

Automate your Analytical GC for prep work in less than one hour—for less than $3000

If you already own a good analytical gas chromatograph, here's a sensible way to add automatic preparative gc, reliably and economically. Install the new H-P Model 5795A Preparative Attachment on your analytical gc. It'll take less than one hour to do the job, and you'll benefit in many ways.

First, you'll gain a fully automatic prep gc capable of unattended operation during overnight or weekend runs, or of semi-automatic and manual operation when desired.

Second, you'll retain full use of your analytical gc because the 5795A does not interfere with its performance in any way.

Third, you'll enjoy a higher level of reliability and performance than is possible with previously designed small-scale prep gc's. New standards of mechanical simplicity and solid state circuitry introduced by the 5795A eliminate the serious problems of unreliable automation and uncertain purity that have plagued other small-scale prep gc's.

The 5795A can be installed on any H-P Series 5750, 810, 720 or 700 Gas Chromatograph. It can also be adapted to many competitive instruments. Basic price of the complete attachment is $2800. For full information, call the nearest H-P sales office or write for Bulletin 5795.

Hewlett-Packard, Route 41, Avondale, Pennsylvania 19311. In Europe: 1217 Meyrin-Geneva, Switzerland.

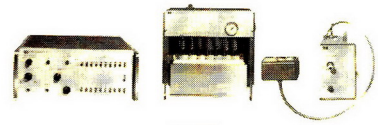

HEWLETT hp PACKARD

ANALYTICAL INSTRUMENTS

43901

Circle No. 107 on Readers' Service Card

now...contamination-free pumping plus cool, noiseless operation!

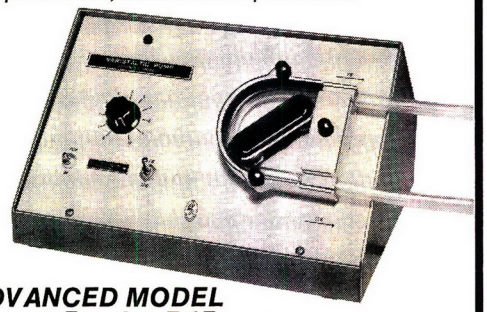

ADVANCED MODEL

varistaltic pump®

Produces peristaltic effect to pump acids, bases, toxic and sterile liquids and gases—safely and quietly through flexible tubing — without the liquid coming in contact with pumping mechanism. Gearless direct-drive permanent-magnet motor is solid-state controlled . . . for reproducibly adjusted speeds from 24 to 400 R.P.M., with ±3% stability . . . and a delivery volume range from 50 ml to 5,000 ml per minute. Switch action reversibility.

Unit weighs approx. 18 lbs., is housed in handsome 2-tone lightweight metal cabinet—12½" long x 9½" deep x 7½" high. Available in 115-volt or 220-volt A.C. models.

Advanced Model Varistaltic Pump (115-volt A.C.) $210.00

For information on our full line of Varistaltic Pumps-Rheostat Controlled, Generator Feed-Back Controlled, Solid State and Air Driven Explosion Proof Model, write for Complete Bulletin.

Available through your laboratory supply dealers

MANOSTAT *Corporation*

20 N. Moore St., Dept. 521, N.Y., N.Y. 10013

Circle No. 110 on Readers' Service Card

NEW

BETHLEHEM GLASS TUBING SCORER!



A radical departure from the conventionally designed glass knife. For scoring borosilicate glass tubing. The handle is of solid clear plastic. A tungsten carbide cutting blade, triangular in design with three cutting edges is inserted and clamped into the handle. The blade is reversible and actually provides six usable cutting edges in all. Blades are replaceable. Cutting edge 1½"—overall length 6"—shipping weight 1 lb. KN3 Knife $24.00

BETHLEHEM APPARATUS COMPANY, INC.

Hellertown, Pa. 18055 Phone 215 838-7034

Circle No. 16 on Readers' Service Card

Manufacturers' Literature

EPR Spectrometer Systems. Control console modules, the microwave bridge, magnet systems, cavities, accessories, and performance and physical specifications for the E-line electron paramagnetic resonance spectrometer systems are described in a 12-page brochure. Varian, Analytical Instrument Division, 611 Hansen Way, Palo Alto, Calif. 94303 **623**

Acid Digestion Bomb. Product Sheet 4745 presents a Teflon (Du Pont) lined bomb for dissolving silicates and other refractory materials in strong acids. Parr Instrument Co., Inc., 211 Fifty-third St., Moline, Ill. 61265 **624**

Multichannel Analyzer. Bulletin 900P, 12 pages, describes the 900 Series multichannel analyzers which feature built-in optional functions and accessories. Packard Instrument Co., Inc., 2200 Warrenville Rd., Downers Grove, Ill. 60515 **625**

Company Periodicals

Requests for copies of the following publications, catalogs, etc., should be sent directly to the address shown. Business or professional letterheads are requested.

The Laboratory, Vol. 37, No. 1. Among the new instruments discussed in this issue is a desk-size direct-reading spectrometer for multi-element analysis. Fisher Scientific Co., 312 Fisher Bldg., Pittsburgh, Pa. 15219

Laboratory Instrument Mart, April/May 1969. Spectrophotometers, gas chromatographs, oscilloscopes, and computers are among the instruments listed. Included are tips on how the items may be bought, sold, traded, and leased. Laboratory Instrument Exchange, Inc., 301 E. Erie St., Chicago, Ill. 60611

Current Laboratory Practice, Vol. 1, No. 2. A method for separating DNP amino acids in urine and serum is offered in this issue. Gelman Instrument Co., P. O. Box 1448, Ann Arbor, Mich. 48106

Givaudanian, April 1969. The physical and chemical testing of aerosol cosmetics is discussed in this issue. Givaudan Corp., 321 W. 44 St., New York, N. Y. 10036

Gas-Chrom Newsletter, Vol. 10, No. 2. A list of basic columns for several areas of gas chromatographic analysis is offered. Applied Science Laboratories, Inc., State College, Pa. 16801

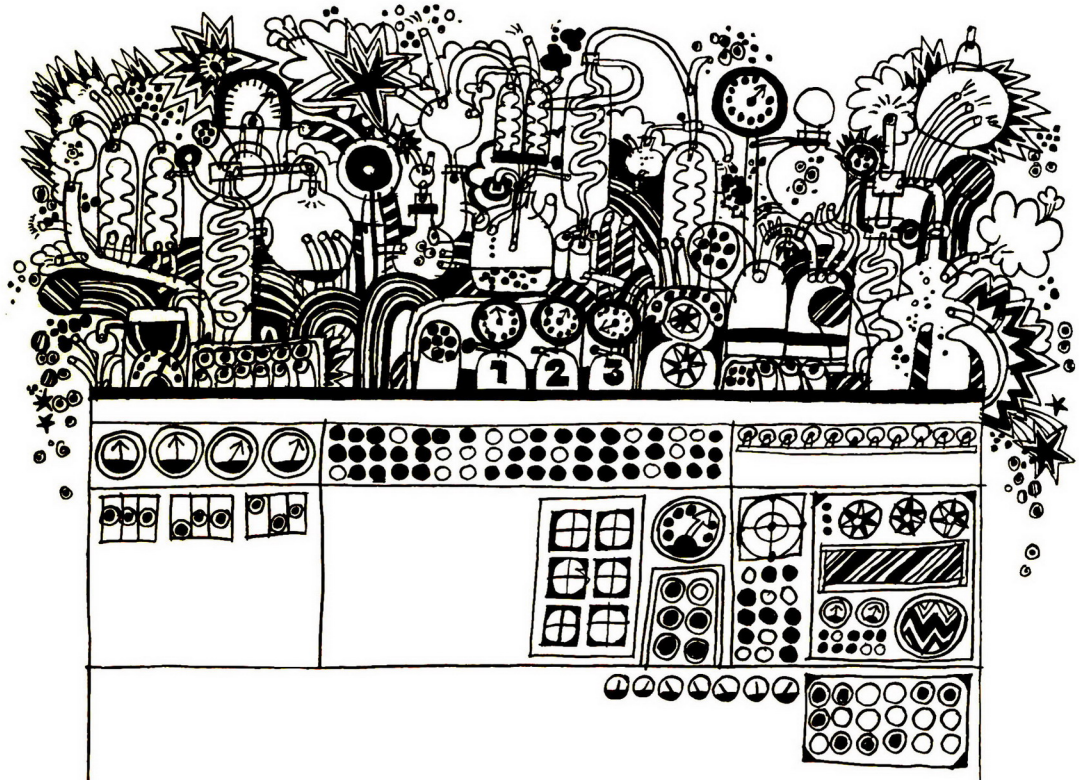

To what extent is your laboratory automated?

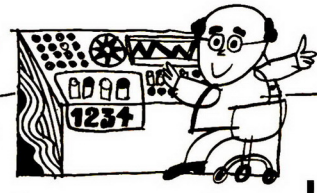

A good many things have not yet been developed which you need in order to completely automate your laboratory. The 120 researchers in our laboratory are of the opinion that this will still take a few years.

We made the first contribution to automation in 1946 with the first substitution balance which weighed samples ten to twenty times faster than the old two-pan balance. Innovations have been continuously added to Mettler balances. For example, the Mettler level-matic automatically compensates for level errors, the compact digital indicator speeds up the process of reading the results, the taring system shortens the weighing time.

If your time is still too expensive for reading off the result and writing it down, you can buy our printer balance. It prints out the result on an adhesive strip (accurate to five places). Or you can combine the Mettler with a recording device or a computer.

Some of the other Mettler measurement devices operate even more automatically than the balances. The Thermoanalyzer carries out TGA/DTG/DTA measurements simultaneously. All defining magnitudes and measurement values are drawn in colored curves.

The Mettler FP1 automatically determines melting and boiling points with an hourly capacity of more than 30 samples. It stores the measurement values digitally. The FP2 is for microthermal studies, and the FP3 automatically determines dropping points. (A bright note for the fat and oil industry.)

We have a few very new thermal and volumetric measurement devices in the research stage. A few are already in the torture chamber where we test every new measurement device with difficult endurance tests. After all, when one automates measurement processes, the automated measurement device has to really operate more dependably than the human being.

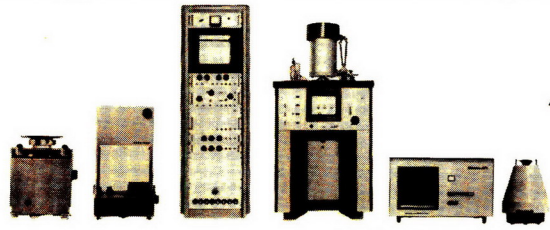

Mettler

Princeton, New Jersey
Zurich, Switzerland
Giessen, West Germany

Circle No. 48 on Readers' Service Card

COOL?

You bet we do! . . . to —10, —20, —30, or even —40° C. with the widest range of refrigerated chillers and immersion coolers available from any single source. Specially designed ⅛, ¼, and ½ HP units provide low temperature capability for circulators without refrigeration, any water bath where low temperatures are required or those requiring additional cooling capacity. A perfect choice for any laboratory requiring a reliable, economically priced, high capacity, low temperature cooling source.

FEATURES

- 7 MODELS — 3 COMPRESSOR SIZES
- OPERATE DOWN TO —40° C.
- HIGH COOLING CAPACITY up to 5600 BTU/HR.
- ELIMINATES NEED FOR ICE OR DRY ICE
- FAST "PULL-DOWN"
- QUIET OPERATION
- GUARANTEED ONE FULL YEAR 5 years on compressors
- PORTABLE

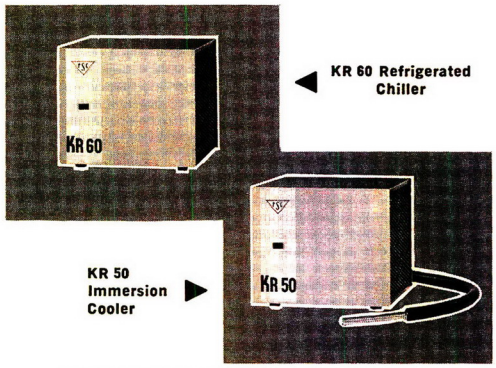

THE MOST COMPLETE LINE OF REFRIGERATED CHILLERS & IMMERSION COOLERS

Model	Rating	Unit Type	Operating Range (in 2L Methanol)	Price
KR 10	⅛ HP	Standard	—13° C.	$225
KR 30	¼ HP	Standard	—23° C.	$295
KR 40	¼ HP	Standard w/Pump	—23° C.	$375
KR 50	¼ HP	Standard w/Probe	—35° C.	$295
KR 60	½ HP	Standard	—25° C.	$395
KR 70	½ HP	Standard w/Pump	—25° C.	$495
KR 80	½ HP	Standard w/Probe	—40° C.	$395

Ask for BULLETIN 49

Another quality product from....

PSC **PolyScience Corporation**

2101 DEMPSTER STREET EVANSTON, ILLINOIS 60201
(312) 475-2909

Circle No. 122 on Readers' Service Card

Oxygen analyzers — 4 models, all with solid state electronics.

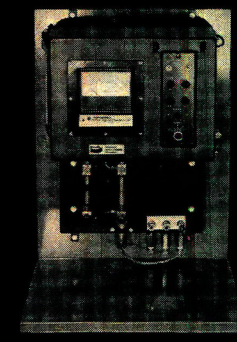

Bendix oxygen analyzers are available to handle your measurement problems from the ppm range to the 100% range. Our trace oxygen analyzer can measure as low as 0-10 ppm full scale. Percentage measurements are handled by the Servomex line of analyzers. Available in two portable and two standard models. All Servomex units use the "magnetic-susceptibility" principle and solid state electronics. Priced from $495.00. Write: The Bendix Corporation, Process Instruments Division, Ronceverte, West Virginia 24970.

Bendix

Circle No. 13 on Readers' Service Card

TRACE INORGANICS IN WATER
ADVANCES IN CHEMISTRY SERIES No. 73

Twenty-one papers from a symposium by the Division of Water, Air, and Waste Chemistry of the American Chemical Society, chaired by Robert A. Baker. Includes:

Five surveys on broad topics—

- **Transport properties of electrolytes**
- **Anions in aqueous solution**
- **Effects of trace inorganics on the ice/water system**
- **Aluminum species in water**
- **The role of hydrous Mn and Fe oxides in fixation of metals in soils and sediments**

Eleven papers on analytical developments, such as:

- **Atomic absorption** (3 papers)
- **Atomic fluorescence**
- **Flame emission**
- **Neutron activation**

And five research reports.

396 pages with index Cloth bound (1968) $12.50
Postpaid in U.S. and Canada; plus 20 cents elsewhere.

Set of L.C. cards free with library orders.

Order from

SPECIAL ISSUES SALES
DEPT. B
AMERICAN CHEMICAL SOCIETY
1155 SIXTEENTH ST., N.W.
WASHINGTON, D.C. 20036

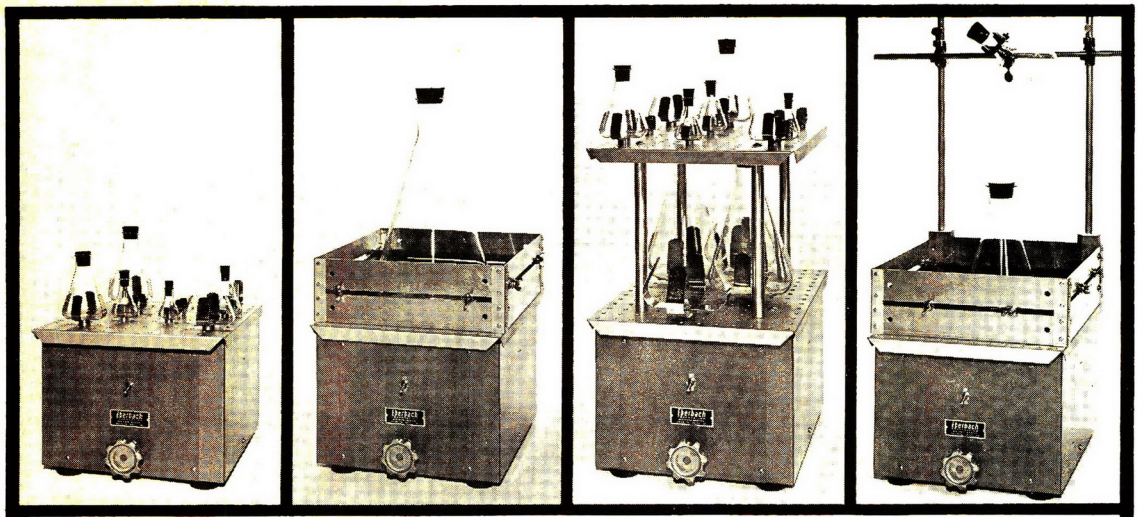

Power unit with platform | With utility box carrier | With platform & tiering posts | With utility box & vertical rods

- 20-240 excursions per minute
- Minimum space required—14″ x 12″ x 9⅜″ high

SMALL TABLE TOP RECIPROCATING SHAKER

This exceptionally wide speed range readily adapts this Shaker to low speed motion studies, as well as violent agitation. Stroke can be adjusted to ½″, 1″ or 1½″. 115 volt, 50/60 cycle. Shaker Power Unit with platform, Catalog No. 5850..... $215.00
Write for Bulletin No. 750

Eberbach CORPORATION P.O. Box 1024 Ann Arbor, Mich. 48106

Circle No. 3 on Readers' Service Card

See ACS Laboratory Guide for All Products/Sales Office

TIME CONSECUTIVE NUMBER LABELS

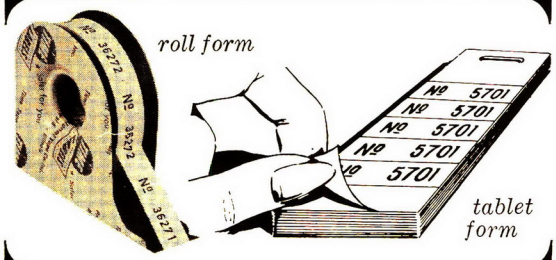

self-sticking numbers for use on test tubes, requisition forms, specimen containers.

Available in roll or tablet form, Time Consecutive Number Labels stick to any surface in temperatures ranging from —70°F to +250°F. Numbers can be repeated from 1 to 8 times in roll form, up to 10 times in tablet form. Supplied with standard "No." prefix or your choice of 5 special prefixes. Write for free literature and order instructions.

TIME LABELS

All Time Tape products are Bacteriostatic for your Safety

AVAILABLE THROUGH LABORATORY AND HOSPITAL DEALERS

PROFESSIONAL TAPE CO., INC.
363 EAST BURLINGTON ROAD
RIVERSIDE, ILLINOIS 60546

Circle No. 61 on Readers' Service Card

SAVE up to 30% in cost

plus 75% in inventory
WITH NEW 4-IN-1 LAB STOPPER

TWiSTiT®

Pat. No. 3282457

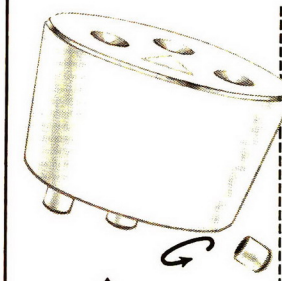

Simply twist off the seals for one, two, or three holes.

Versatile white, natural rubber stoppers.

- **Unit priced to save you more!**
- **Unit packed for easy ordering and stock taking!**

Sizes 3 to 10 (plus assortment) for most of your needs.

Order from your dealer now.

mp molded products COMPANY
EASTHAMPTON, MASS. 01027
Dept. of United Elastic Company — Division of J. P. Stevens & Co., Inc.

Circle No. 77 on Readers' Service Card

LABORATORY SUPPLY CENTER

N-Acetyl-Thiourea • Adenosine-5′-triphosphate, Disodium Salt
5-Bromosalicylaldehyde • o-Bromotoluene • 2,6-Dichlorophenol
2,6-Dichloroquinone-4-chloroimide • Diethyl Adipate • DMG
Diglycolic Acid • Dimethyl Dihydroresorcinol • p-Dinitrobenzene
N,N′-Diphenylbenzidine • 2-Furylmethyl Ketone • Hippuric Acid
Menadione • Methyl Cyclohexanol • Naphthalhydroxamic Acid, Na
Oxamic Acid • Phenyl-thiourea • Purine • Sodium Thioglycolate
Taurine • Triphenyl Stibine • Uracil • Urea Nitrate • Xylitol

Write for list K-68 of other chemicals

Tel: 201 696-1700 TWX: 710 988-5831 Zip Code 07440

EASTERN CHEMICAL CORPORATION BOX K PEQUANNOCK, N. J.

CLEAR FUSED QUARTZ

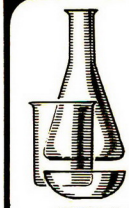

- STOCK
  Rods, tubes, plates, discs, ingots
- LABWARE
  Test tubes, flasks, beakers, dishes, joints, seals, stop cocks, quartz-to-metal
- APPARATUS
  Fabrication or repairs quickly made per your drawings or instructions

FREE CATALOG!

QUARTZ SCIENTIFIC, INC.

34602 Lakeland Blvd. Eastlake, Ohio 44094 • 989 Commercial St. Palo Alto, Calif. 94303

MASS SPECTROMETRIC ANALYSIS

Thin films-solid state materials.
Bulk and trace analysis of all solid materials.
Concentration gradients of diffused impurities.
Resolution 5000.
Sensitivity to parts per billion.
GCA Technology Division, division of GCA Corporation, Bedford, Mass., Tel. (617) 275-9000.
Attn: Director of Marketing

Your specialist in AGATE



Mortars with pestles

Ø	2″	3″	4″	5″	6″	8″
ccm	10	25	50	100	250	500
$	3–	7–	13–	24–	55–	150–

Orders over 150—free any U.S. place.
For further data about agate parts (balls, ball mills a.s.o.) please contact:

C. GIESE KG. establ. 1890
P. O. B. 2556c
658 Idar-Oberstein, Germany

ANALYTICAL AND CONSULTING SERVICES

- Mass Spectrometric Analysis of Inorganic Solids and H/D, C^{13}/C^{12}, N^{15}/N^{14}, O^{18}/O^{16}, and S^{34}/S^{32}
- Radiochemical and Atomic Absorption Analyses at Trace Levels
- Gas Chromatographic Analysis of Trace Radioactive and Stable Gases

ISOTOPES
A TELEDYNE COMPANY

50 Van Buren Avenue, Westwood, N. J. 07675
Phone: (201) 664-7070

---

now even better for Fluoride
AMADAC-F™

Convenience-packaged mixture of lanthanum chelate of 3-aminomethylalizarin-NN-diacetic acid, buffers and stabilizers, affords accurate, sensitive and convenient quantitative colorimetric method for fluoride.

50 g. (for 100 detns.), with bibliography and complete instructions.....$15

BURDICK & JACKSON LABORATORIES, INC. 616 722-2310
MUSKEGON, MICHIGAN 49442

LaMotte Chemical

Chestertown, Maryland 21620

Manufacturers of chemical testing equipment and accessories since 1919

Write Dept. AC for free catalog

DIRECT READING X-RAY FLUORESCENT AND OPTICAL EMISSION SPECTROMETERS

Applied Research Laboratories
Direct Reading Spectrochemical
Including:

Model 25,000 Vacuum X-Ray Quantometer
Model 29,000 Optical emission Quantometer
Model 24,500 Recording Console
Model 12,350 X-Ray Power Supply
Model 5,700 Controlled Multisource unit
Currently in operation. Available due to Laboratory Consolidation

For information contact: **J. Paul Wentz, ALLVAC, A Teledyne Co. P. O. Box 759, Monroe, North Carolina 28110, phone 704 289-4511.**

DEUTERATED POLYETHYLENE

1 Gram $100 5 Grams $300

BIO-RAD Laboratories

32nd and Griffin Avenue
Richmond, California 94804
Phone (415) 234-4130

NMR SPECTROSCOPY

Spectratec, Inc.

Jeolco C-60HL Spectrometer
Variable Temperature Operation
Spin Decoupling, Interpretation
24 Hour Service on Routine 60 MHz Spectra
Write for Brochure

P.O. Box 17081
Dulles International Airport
Washington, D.C. 20041
(703) 471-1835

Rates Available on Request

Analytical Chemistry

Anne Forrest, Production Manager

600 Summer St.
Stamford, Conn. 06904
203-348-7531

CABLE ADDRESS: SACTEX **PROMPT SHIPMENT**

POLAROGRAPHIC SPECIALTIES

Quaternary ammonium compounds.
Highly purified salts and solutions.
Cells designed for use above -2.0 volts.

SOUTHWESTERN ANALYTICAL CHEMICALS BOX 485 — AUSTIN, TEX AREA 512 444-3626
—literature on request

LABORATORY SUPPLY CENTER

Specialists in Distillation
PODBIELNIAK
Custom Glassblowing
Distillation Columns — Vacuum Jacketed
Heli-Pak Packings — Corrosion resistant metals
Evacuated Vessels — Dewars
Podbielniak, Inc.
203 Gateway Road, Bensenville, Ill. 60106
Tel.: (312) 766-1816

STOP BUMPING
in BOILING LIQUIDS
Prevent superheating and boiling loss.
Speed distillation. Safe. Efficient.
WRITE FOR LITERATURE
HENGAR GRANULES
A division of Henry Troemner, Inc.
6815 Greenway Ave., Phila., Pa. 19142
Phone (215) 724-0800

ANALYTICAL SERVICES
MASS SPECTROMETRY
Organics — Gas Analysis — N^{15}, O^{18}, H^2, He^3 Isotopes
COMBINED GC-MS
THERMAL ANALYSIS-DTA-TGA-DSC
WEST COAST TECHNICAL SERVICE
1049 S. San Gabriel Blvd.
San Gabriel, California 91776
(213) 287-0926

Rates Available on Request

Analytical Chemistry

Anne Forrest
Production Manager

600 Summer St.
Stamford, Conn. 06904
203-348-7531

INDEX TO ADVERTISERS IN THIS ISSUE

°**Ace Glass, Inc.** 44
Heller Creative Advertising

Air Reduction Co., Inc. 35:100
Fuller & Smith & Ross, Inc.

Amersham/Searle, Div. of G. D. Searle & Co. 46
Frank J. Corbett, Inc.

°**Analabs, Inc.** ..... OBC
Kenyon Hoag Associates

Applied Coatings, Inc. 106
Gallard Advertising Agency, Inc.

Applied Research Laboratories 101
Jordan Advertising & Marketing Services, Inc.

Applied Science Laboratories, Inc. 111
Science Advertising Associates

J. T. Baker Chemical Co. 43:120
DeMartin, Merona & Associates, Inc.

°**Bausch & Lomb, Inc.** 77:79
Wolff Associates, Inc.

°**Beckman Instruments, Inc.**
Cedar Grove Operations 98
Lescarboura Advertising, Inc.
Scientific Instruments Div. 62
Hixson & Jorgensen, Inc.
Spinco Div. 1
N. W. Ayer /Jorgensen/MacDonald, Inc.

°**Bell & Howell, CEC/Analytical Instruments** 39
N. W. Ayer/Jorgensen/MacDonald, Inc.

°**Bendix Corp., Process Instruments Div.** 6:116:118:124
MacManus, John & Adams, Inc.

°**Bethlehem Apparatus Co., Inc.** 122
Beaumont, Heller & Sperling, Inc.

°**James G. Biddle Co.** 116
The Michener Co.

°**Bio-Rad Laboratories** 50
Bonfield Associates, Inc.

°**Brinkmann Instruments, Inc.** 41:103
The Shaller-Rubin Co., Inc.

°**Buchler Instruments, Inc.** 104
Selvin & Jaffe

°**Carle Instruments, Inc.** 72
Cochrane Chase & Co., Inc.

°**Fred S. Carver, Inc.** 100
J. C. Bull, Inc.

°**Cary Instruments, A Varian Subsidiary** 42
Chiat/Day, Inc.

Chemical Materials Catalog 109
Persons Advertising, Inc.

°**Chemtrix, Inc.** 110
Hugh Dwight Advertising, Inc.

°**Chromatronix, Inc.** 102
Bonfield Associates, Inc.

Coleman Instruments Corp. 96:108
Mandabach and Simms, Inc.

°**Cosmos Scientific Co.** 63
Valerie Taylor Associates

Culligan, Inc. 115
Alex T. Franz, Inc.

°**W. H. Curtin & Co.** 70
Robinson-Gerrard, Inc.

Delmar Scientific Glass Products of Coleman Instruments 112
Mandabach and Simms, Inc.

Harry W. Dietert & Co. 29
Watkins-Rogers, Inc.

°**Digital Equipment Corp.** 86
Kalb & Schneider, Inc.

°**duPont Co.** 59
Rumrill-Hoyt, Inc.

°**Eastman Kodak Co., Eastman Organic Chemicals** 68:69
Rumrill-Hoyt, Inc.

Eberbach Corp. 125
Drury, Lacy, Inc.

Electron Technology 119
Kniep Associates

Carlo Erba, S.p.A. 78
Publicitas

Esterline Angus, Div. of Esterline Corp. 113
Caldwell-Van Riper, Inc.

°**Fabri-Tek Instruments, Inc.** 31
Ralph Timmons, Inc.

°**Farrand Optical Co., Inc.** 82:113
Taube/Violante, Inc.

Fluoroware 103
Colle & McVoy Advertising Agency, Inc.

°**Gilford Instrument Laboratory, Inc.** ... 66
Garber-Evans Advertising, Inc.

Glas-Col Apparatus Co. 40
Fensholt Advertising, Inc.

Gulf General Atomic, Inc. 117
Barnes-Champ Advertising

°**Hamilton Co.** 19
Swain/Mealer, Inc.

°**Heath Co.** 27
Advance Advertising Service, Inc.

°**G. K. Heller Corp.** 112
Feeley & Wheeler, Inc.

°**Hellma Cells, Inc.** 83

°**Hewlett-Packard Co., Avondale Div.** .. 16:121
Richardson, Thomas & Bushman, Inc.

°**Hewlett-Packard Co., Palo Alto** 45
Lennen & Newell, Inc.

°**Hoke, Inc.** 109:116
Tek-Mark, Inc.

Illinois Water Treatment Co. 118
Cummings, Brand, McPherson Associates, Inc.

Infotronics Corp. 80
Robinson-Gerrard, Inc.

°**Instrumentation Laboratory, Inc.** 21
Pazolt & Co.

°**Instrumentation Specialties Co., Inc.** . 28
Graham Printing & Advertising Service

°**Instruments for Research & Industry** . 53
Richardson, Thomas & Bushman, Inc.

International Plasma Corp. 51
Hal Lawrence, Inc.

°**Jarrell-Ash Div., Fisher Scientific Co.** 76
Fuller & Smith &, Ross, Inc.

°**Johns-Manville** 30
Cunningham & Walsh, Inc.

Johnson Reprint Corp. 8
Turner & Feeney, Inc.

°**Kewaunee Mfg. Co.** 52
Phillipps Associates, Inc.

°**Klett Mfg. Co., Inc.** 4

°**Kontes Glass Co.** 73
Garceau, Hallahan & McCullough, Inc.

°*See ad in ACS Laboratory Guide*

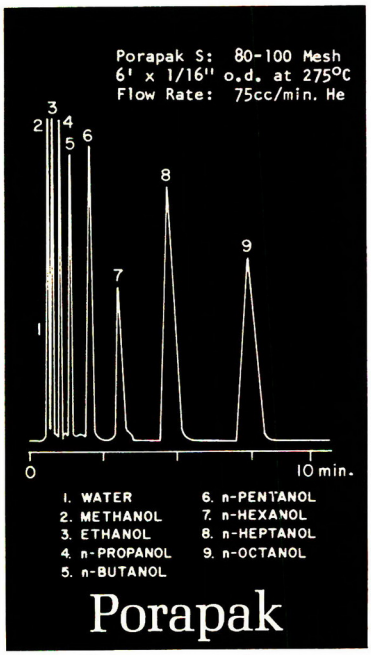

... still just a word to you?

Find out why it's already *the* word to thousands of

GAS CHROMATOGRAPHERS

If you haven't yet tried Porapak®, treat yourself to the original porous polymer column packings that revolutionized GC resolution and speed just three years ago.

- Water elutes as a sharp peak.
- Needs no liquid coating, but produces quality separations you'd expect from liquid-coated packings.
- No bleed, no need for compensating temperature programming.
- Highly reproducible peaks and retention times.
- Now 8 types, including two silanized versions, for separating the widest range of polar and non-polar materials.
- Temperature-stable up to 250° and above.
- Very fast overload recovery.
- Won't fracture; easy to pack, perfect for high-pressure systems.

Porapak is manufactured only by Waters. Write or call for complete information, including the name of your nearest distributor. Waters Associates, Inc., 61 Fountain St., Framingham, Mass. 01701. Phone (617) 879-2000.



4410

WATERS ASSOCIATES

Circle No. 12 on Readers' Service Card

INDEX TO ADVERTISERS IN THIS ISSUE

°Labindustries 48
Bonfield Associates, Inc.
E. Leitz, Inc. 64
L. W. Frohlich & Co.

Manostat Corp. 122
Fairfax, Inc.
Matheson, Coleman and Bell 114
Cooper, Strock & Scannell, Inc.
Matheson Gas Products (A Div. of Will Ross, Inc.) 56
Cooper, Strock & Scannell, Inc.
McKee-Pedersen Instruments 91
Dave Comstock Advertising
°Mettler Instrument Corp. 10:60:95:123
Mort Barish Associates, Inc.
Milton Roy Co. 74:75
Beaumont, Heller & Sperling, Inc.
Molded Products, United Elastic Div. of J. P. Stevens Co., Inc. 125
Albert L. Gibney Co.

°Nalgene Labware Div., Nalge Co., Div. of Sybron Corp. 55
Wolff Associates, Inc.
Norton Plastics & Synthetics Div. 74
Northlich, Stolley of Akron, Inc.
°Nuclear-Chicago Corp., A Subsidiary of G. D. Searle & Co. 18
Sidney Clayton Associates, Inc.
Nuclear Data, Inc. 9
Sang & Wardrop, Inc.
Nuclear Diodes, Inc. 119
Nupro Co. ..... IBC
Falls Advertising Co.

°Orion Research, Inc. 95:96
Visual Research & Design Corp.
Orlando Research Corp. 25
Neals & Hickok, Inc.
Owens-Illinois, Inc. 33
Meldrum & Fewsmith, Inc.

°Packard Instrument Co., Inc. A Subsidiary of Ambac Industries, Inc. 12
Ross Llewellyn, Inc.
Peninsular Chemresearch, Inc. 116
Advertising Associates of Jacksonville, Inc.
°Perkin-Elmer Corp. 34:61:107
Gaynor & Ducas, Inc.
°Pharmacia Fine Chemicals, Inc. 36
Cummins, MacFail & Nutry, Inc.
°Photovolt Corp. 5
Michel-Cather, Inc.
°Pierce Chemical Co. 115
Advertising Design
Pitchford Mfg. Corp. 130
°Polyscience Corp. 124
Precision Scientific Co. 57
Tri-State Advertising Co., Inc.
Precision Sampling Corp. 108
William U. Stracener
Princeton Applied Research Corp. 89
Mort Barish Associates, Inc.
Professional Tape Co., Inc. 125
Robert Peterson Advertising Agency

°Sadtler Research Laboratories, Inc. 105
Product Promotions Agency, Inc.
°Sage Instruments, Inc. 83
Mohr & Co., Inc.
°Sargent-Welch Scientific Co. 58:97
Sidney Clayton & Associates, Inc.

°See ad in ACS Laboratory Guide

WHY TAKE "SECONDS"

..when you can have First Editions?

Order your own supply of these important I&EC "originals"...Reprints of several recent I&EC Annual Reviews are available separately or in sets as described below:

Materials of Construction
1967 **$1.00**
deals with protective coatings..stainless steels and other ferrous alloys..plastics technology..aluminum..elastomers..adhesives..
01067

Unit Operations
1967 **$1.00**
deals with mixing..drying..size-reduction..crystallization..distillation..liquid-liquid extraction..ion exchange
01167

Fundamentals
1967 **$1.00**
deals with mass transfer..heat transfer..computers and process control..kinetics and reaction engineering..mathematics
01267

. . For only $1.00 more you can buy a complete set of

Materials of Construction—1966
Unit Operations —1966
Fundamentals —1966
01966

☐ 01067 ☐ 01167 ☐ 01267 ☐ 01966

To: **Reprint Dept. B**
American Chemical Society
1155 16th St. N.W.
Washington, D.C. 20036

From:

Name_____

Address_____

City_____

State_____ Zip Code

Amount enclosed_____

INDEX TO ADVERTISERS IN THIS ISSUE

*Schleicher & Schuell Co. 26
Wildrick & Miller, Inc.
*Schoeffel Instrument Corp. 47
J. S. Lanza & Associates
*Scientific Glass Apparatus Co., Inc. ... 20
Steelmet, Inc. 54
S. Lawrence Rothman

T & T Technology, Inc. 103
Marshall Smith and Associates
Techne, Inc. 129
Harrison Wright Associates, Ltd.
*Technicon Corp. 7
Mediad, Inc.
*Thermolyne Corp. 102
E. R. Hollingsworth & Associates
*Arthur H. Thomas Co. 94
*The Torsion Balance Co. 120
Michel-Cather, Inc.
*Tracor, Inc. ..... IFC
Winn-McLane Associates, Inc.

*Ultra Carbon Corp. 38
The Jaqua Co.

*Varian Associates 65
Botsford, Constantine & McCarty, Inc.

*Wang Laboratories, Inc. 81
Impact Advertising, Inc.
*Waters Associates, Inc. 14:128
Thomas R. Sundheim, Inc.
*Wilkens-Anderson Co. 129
Mandabach and Simms, Inc.
*Wilks Scientific Corp. 71
A. B. W. Toft & Co.
Wilmad Glass Co., Inc. 17
George F. Walsh Advertising Agency
M. Woelm 109
Linder Presse Union GMBH

*Carl Zeiss, Inc. 37
Michel-Cather, Inc.

Laboratory Supply Center 126:127

Allvac, A Teledyne Co.
Bio-Rad Laboratories
Burdick & Jackson Laboratories, Inc.
Eastern Chemical Corp.
GCA Corp., Technology Div.
C. Giese KG.
Isotopes, Inc., A Teledyne Co.
LaMotte Chemical Products Co.
Podbielniak, Inc.
Pure Aire Corp.
Quartz Scientific, Inc.
Southwestern Analytical Chemicals
Spectratec, Inc.
Troemner, Inc.
West Coast Technical Service

▼ ▼ ▼

Advertising Management for the American Chemical Society Publications

REINHOLD PUBLISHING CORP., a Subsidiary of Litton Publications, Inc., Division of Litton Industries, Inc. Thomas N. J. Koerwer, Advertising Sales Director, ACS Publications; Alfred E. Gall, Corporate Production Director, 600 Summer St., Stamford, Conn. 06904. Phone: 203-348-7531. Cable Address: REINPUB STAMFORD-CONNECTICUT

SALES DEPARTMENT

J. Barry Stanford
Advertising Sales Manager

SALES REPRESENTATIVES

Stamford Connecticut 06904 . . . J. Barry Stanford, Frank Ryan, Murray Strelitz, Reinhold Publishing Corp., 600 Summer St., 203-348-7531

Philadelphia 19107 . . . James A. Byrne, Reinhold Publishing Corp., 12 So. 12th St., 215-922-0346

Chicago 60603 . . . Eugene P. Eldridge, Reinhold Publishing Corp., 10 So. La Salle St., 321-726-1282

Cleveland 44114 . . . Michael Hayes, Reinhold Publishing Corp., East Ohio Bldg., 1717 East 9th St., 216-771-4011

Los Angeles 90045 . . . Clay H. Holden, Lynn Gaskill, Reinhold Publishing Corp., 8939 So. Sepulveda Blvd., 213-776-0552

San Francisco 94109 . . . Clay S. Holden, Lynn Gaskill, Reinhold Publishing Corp., 415-421-8080

Denver 80203 . . . Robert H. Heidersbach, Roy McDonald Associates, Inc., 846 Lincoln St., 303-825-3325

Houston 77006 . . . Frank N. Vickrey, Roy McDonald Associates, Inc., 3130 Southwest Freeway, 713-529-6711

Tulsa 74114 . . . Max C. Nelson, Roy McDonald Associates, Inc., 2570 South Harvard Ave., 918-742-9961

Great Britain and Western Europe . . . Brayton Nichols, The American Magazine Group, 44 Conduit Street, London, W. 1, England

Japan . . . Sumio Oka, International Media Representatives, Ltd., 2-4, 6-chome, Akasaka, Minatoku, Tokyo, Japan

PRODUCTION DEPARTMENT

Anne Forrest
Advertising Production Manager
Analytical Chemistry

See ad in ACS Laboratory Guide

More than likely you already have a Tecam thermostatic water bath – its so quiet, so well made, so efficient, so economical – you probably take it for granted.

If you haven't got one or need another – write to us and we will tell you all about this full range and the accessories. If you have any special requirements, then don't hesitate to call on Techne's accumulated know-how.

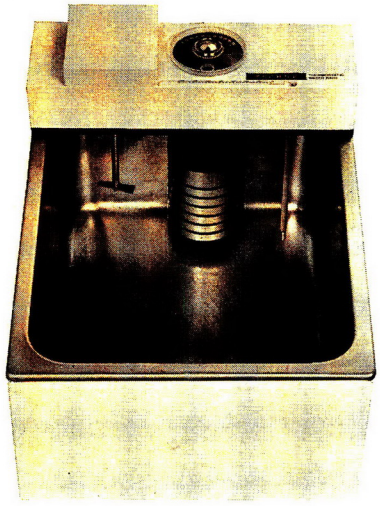

and it comes in five sizes

Techne Incorporated
661 Brunswick Pike Princeton New Jersey 08540 USA
Telephone (609) 452-9275
Circle No. 68 on Readers' Service Card

HIGH TORQUE STIRRER

ONLY $39.40 COMPLETE

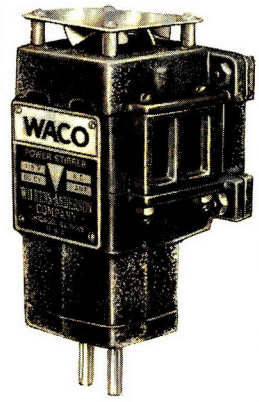

Designed specifically for laboratories where long, continuous use is required. Sparkless, induction type motor provides continuous 24 hour service for months at a time! A built-in cooling fan eliminates overheating or burning out.

No. 86100—WACO Power Stirrer, complete with tubular brass mounting rod and 6 foot cord . . . only **$39.40**
Stirrer chucks and rods available.

Order direct or write for descriptive folder.

Laboratory Supplies and Equipment

wilkens-anderson co.
4525 W. Division St., Chicago, Ill. 60651
Circle No. 74 on Readers' Service Card

FUTURE ARTICLES

High-Frequency Titrimetric Determination of the Total Base Number of Lubricating Oils

B. P. Caughley and M. V. Joblin

Polarographic Studies of Chloroacetones

M. E. Hall and E. M. Harris

Solvent Extraction in the Presence of Emulsion Forming Residues. Application to the Atomic Absorption Determination of Gold in Low Grade Ores

Stephen L. Law and Thomas E. Green

High Frequency Excitation of Independently Vaporized Samples in Emission Spectrometry

Imrich Kleinmann and Vratislav Svoboda

Solvation of Aluminum(III) Ion in Dimethylsulfoxide Water Solutions by Proton Magnetic Resonance Spectrometry

D. P. Olander, R. S. Marianelli, and R. C. Larson

Metal Complexing Properties and Proton Magnetic Resonance Spectra of 5-Halo-8-Quinolinols

R. G. Beimer and Quintus Fernando

Determination of Samarium and Gadolinium in Rare Earth Ores by Neutron Capture Gamma-Ray Activation Analysis

S. M. Lombard and T. L. Isenhour

Determination of Major Constituents by Atomic Absorption Spectrometry

Fredric J. Feldman, Jane A. Blasi, and Stanley B. Smith, Jr.

Fractionation of Low Temperature Coal Tar by Gel Permeation Chromatography

B. C. B. Hsieh, R. E. Wood, L. L. Anderson, and G. R. Hill

Direct Determination of Fluoride in Phosphate Rock Samples Using the Specific Ion Electrode

C. R. Edmond

The Detection of Thioureido Groups in Open Chain and Heterocyclic Compounds by Hydrazinolysis

R. G. Dickinson and N. W. Jacobsen

Effects of Organic Solvents on Tin Absorbance in an Air–Hydrogen Flame

W. W. Harrison and P. O. Juliano

Determination of Potassium-40 by Gamma Ray Spectrometry for Potassium-40–Argon-40 Geochronology

Lucia Civetta, Paolo Gasparini, and John A. S. Adams

PORTABLE AND LABORATORY X-RAY SPECTROGRAPH

PORTASPEC®

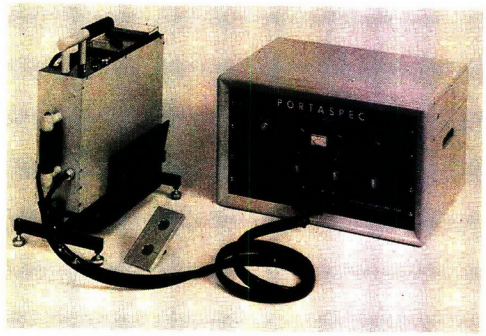

An inexpensive portable X-ray spectrograph for accurate quantitative analysis and material sorting.

Elemental range #22 through #98.

Employs conventional dispersive technique.

Applicable for solids, liquids, powders, coating thickness measurements, low cost on-line or on-stream control.

Operates on 115V commercial line or optional power generator on handling cart.

Norelco® PITCHFORD AUTHORIZED DEALERS

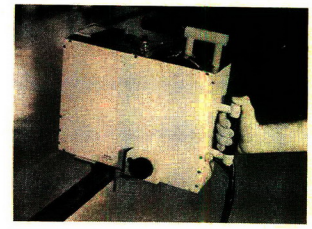

PHILLIPS ELECTRONIC INSTRUMENTS: Mt. Vernon, N.Y. ● Chicago, Ill. ● Atlanta, Ga. ● Houston, Tex. ● Cleveland, Ohio ● Dayton, Ohio ● Philadelphia, Pa. ● Rochester, N.Y.
VAN WATERS & ROGERS, INC.: Anchorage, Alaska ● Phoenix, Ariz. ● Los Angeles, Calif. ● San Diego, Calif. ● West Sacramento, Calif. ● Honolulu, Hawaii ● Portland, Ore. ● Salt Lake City, Utah ● Seattle, Wash. ● Spokane, Wash.
TECHNICAL EQUIPMENT CORP.: Denver, Colo. ● Albuquerque, N. Mex.
LICO, INC.: Burlington, Mass.
PITCHFORD SCIENTIFIC INSTRUMENTS CORP.: Pittsburgh, Pa.

Mfd. by: Pitchford Manufacturing Corp., 1901 Painters Run Rd., Pittsburgh, Pa. 15241

Circle No. 18 on Readers' Service Card

NUPRO®

BELLOWS SEALED VALVES

- PRESSURES—Ultra-high vacuum to 2600 p.s.i.
- TEMPERATURES—Cryogenic to 1500°F
- SIZES—⅛" through ¾" tubing
- MATERIALS—Brass, 316 stainless steel and Monel
- CAPACITIES—Cv=0.019 to 1.2
- OPERATION—Hand; Toggle; Air Operated

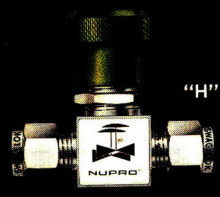

"H" SERIES

Hermetically sealed; Vacuum; High purity, rare and hazardous fluids; Instruments; Counters; Gas analysis.



"B" SERIES

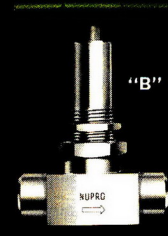

"B" SERIES



"B" SERIES DOUBLE ACTING CYLINDER

The versatile Bellows Valve! Positive stem retraction; All welded, metal gasketed and plastic stem tip models; Used with corrosives, tough solvents, high vacuum, thin gases, and high temperatures; Sampling systems, pilot plants, research and instrumentation; Remote control with air operated models.



"BK" SERIES AIR OPERATED

Miniature; Normally Open or Closed fail-safe Air Operated Valves; Vacuum; Instruments; Toxic fluids.



"BKT" SERIES TOGGLE OPERATED

Flip open; Cannot be over-tightened; Soft seat; Vacuum; hazardous gases and liquids; Instruments; Test boards.

BELLOWS VALVE TESTING

All NUPRO Bellows Valves are **100%** helium leak-tested to a rate of 4.14×10^{-9} atmosphere cc/sec. at all seals, around the entire bellows assembly and for shut-off as a standard procedure. Air Operated Valves are tested at the seat for shut-off to a rate of 8.28×10^{-8} atmosphere cc/sec.

"T" SERIES

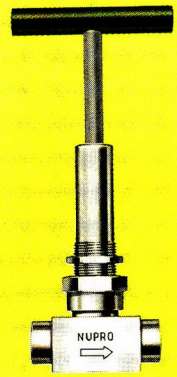

Temperature extremes; High pressures; Liquid metals; Steam sampling; Double Acting and Normally Closed Air Operators available for remote control.

"BM" SERIES BELLOWS METERING

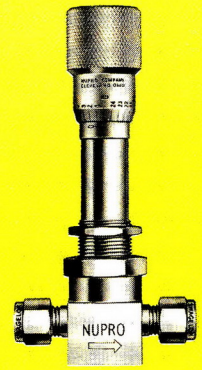

0.055 inch orifice; Micrometer control of dangerous fluids; High temperatures; Vacuum bleed.

"U" SERIES

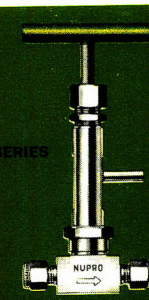

Ultimate in Bellows Valves! Secondary enclosure seals; Monitored bonnets available; Cryogenics; Liquid metals; High and cycling temperatures; Radioactive, toxic, hazardous and expensive fluids.

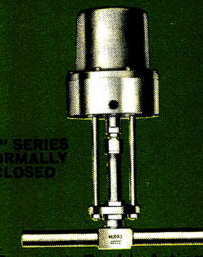

"U" SERIES NORMALLY CLOSED

Compact, Double Acting and Normally Closed Air Operators are available for remote control of "U" Series Valves in the most difficult fluid containment systems.

NUPRO COMPANY/ 15635 SARANAC ROAD, CLEVELAND, OHIO 44110

NUPRO®...*where greater things are happening!*

©1969 by Nupro Company/all rights reserved Monel-Reg. T.M. International Nickel

Circle No. 54 on Readers' Service Card

New from Analabs, a 350 Plus Page Catalog of High Quality Chemicals

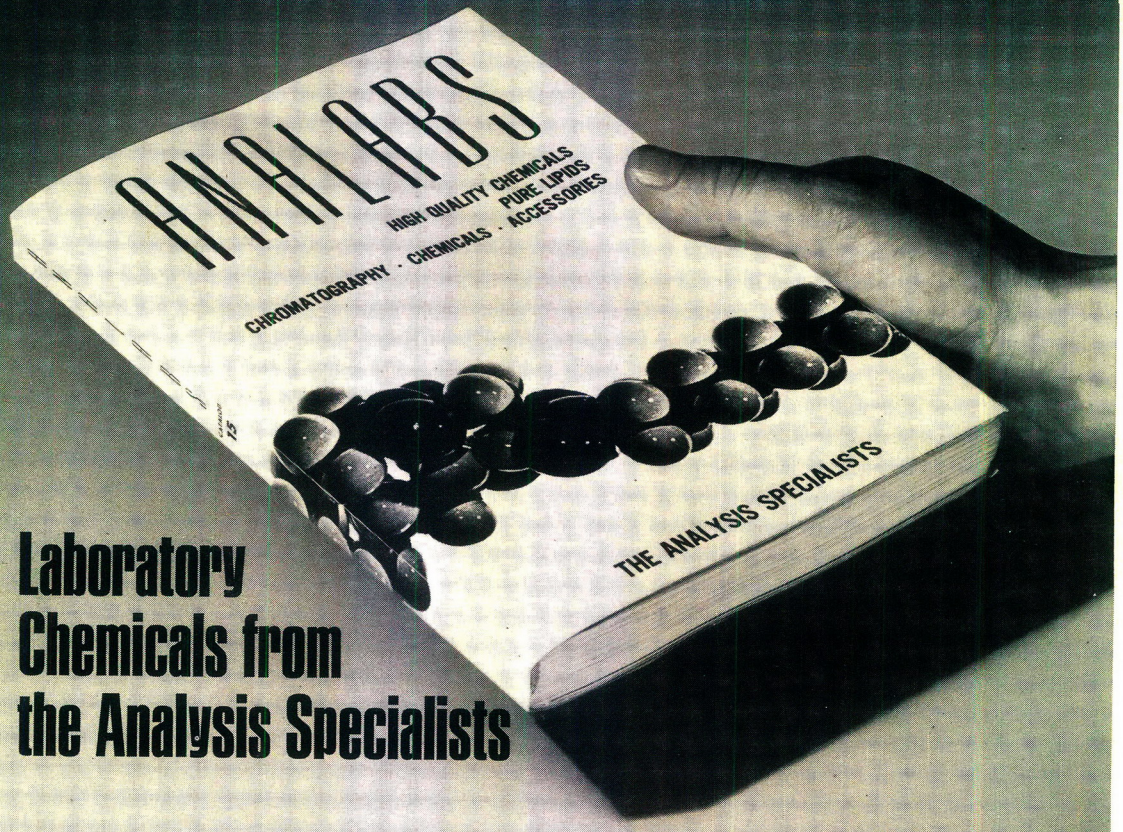

Laboratory Chemicals from the Analysis Specialists

We at Analabs have been working hard for the last year not only on our Gas Chromatography chemicals and our Lipid Standards, but we have now expanded into a full-fledged line of High Purity Laboratory Chemicals. We have more than 5000 for starters, all available, all of Analabs-type purity. Why are we a new factor in the Laboratory Chemical field with a great plus on our side? — because we know more about chemical purity analysis than our competitors.

If you're looking for high purity, large selection, good prices and dependable delivery, come to Analabs.

But most important, if you use, have to store or just contemplate using, Laboratory Chemicals, you really should have our new, 300 plus page catalog. It's sensational. Just let us know you want it and we'll send it right out.

ANALABS

ANALABS, INC.
80 Republic Drive
North Haven, Conn. 06473
203/288-3400, 288-8463-4
"The Analysis Specialists"

Circle No. 137 on Readers' Service Card